DESIGN AND DEVELOPMENT OF SITE SPECIFIC CHEMICAL DELIVERY SYSTEMS FOR ANTI-ARTHRITIC AGENTS

A thesis submitted to
THE MAHARAJA SAYAJIRAO UNIVERSITY OF BARODA
For the award of the degree of

Doctor of Philosophy

in
PHARMACY

By
VIJAY A. PAWAR

Under the guidance of
PROF. M. R. YADAV

सत्यं शिवं सुन्दरम्

Pharmacy Department
Faculty of Technology and Engineering
The M. S. University of Baroda
Vadodara-390 001

JULY 2013

DECLARATION

In accordance with University ordinance number ACED-309 Ph.D., I, the undersigned state that, the work presented in this thesis entitled **"Design and Development of Site Specific Chemical Delivery Systems for Anti-arthritic Agents"** comprises independent investigations carried out by me. Wherever references have been made to the work of others, it has been clearly indicated with the source of information under the title of references at end of each chapter. The result of this work has not been previously submitted for any degree/fellowship

Date: 16.07.2013   **Vijay A. Pawar**

Place: Vadodara   Pharmacy Department

                                                 Faculty of Technology and Engineering

                                                 The M. S. University of Baroda

                                                 Vadodara-390 001

Date: 16-07-2013

CERTIFICATE

This is to certify that the thesis entitled **"Design and Development of Site Specific Chemical Delivery Systems for Anti-arthritic Agents"** submitted for the Ph. D. Degree in Pharmacy by Mr. Vijay Arjun Pawar incorporates the original research work carried out by him under my supervision and no part of this work has been previously submitted for any degree. Wherever references have been made to the work of others, it has been clearly indicated with the source of information under the chapters of references.

Guide   **Head**

Prof. M. R. Yadav   Pharmacy Department

DEAN
Faculty of Technology & Engineering
The M.S. University of Baroda
Vadodara -390 001

INDEX

LIST OF ABBREVIATIONS

RA   : Rheumatoid arthritis

BPA   : Biphenylacetic acid

CRP   : C-reactive protein

COSY   : Correlation spectroscopy

COX   : Cycloxygenase

CDS   : Chemical delivery systems

DSC   : Differential scanning calorimetry

DMARDs   : Disease modifying anti-rheumatic drugs

ESR   : Erythrocyte sedimentation rate

EDC   : Ethyl dimethylaminopropyl carbodiimide

ESI   : Electro spray ionization

GAGs   : Glucosaminoglycans

HETCOR   : Heteronuclear correlation spectroscopy

IA   : Intra-articular

IR   : Infrared

ITLC   : Instant thin layer chromatography

i.v.   : Intravenous

IL   : Interleukin

MTT   : 3-(4,5-Dimethylthiazol-2-yl)-2,5-diphenyltetrazolium bromide

NSAIDs   : Non-steroidal anti-inflammatory drugs

OA   : Osteoarthritis

PLGA   : Poly-lactide-co-glycolide

PLA   : Poly-*L*-lactic acid

PMR   : Proton nuclear magnetic resonance spectroscopy

SEM   : Scanning electron microscopy

^{99m}Tc : Technetium^{99m}

TEM   : Transmission electron microscopy

TLC   : Thin layer chromatography

TNF   : Tumor necrosis factor

ROI   : Region of interest

SF   : Synovial fluid

Acknowledgements

INTRODUCTION

1. Introduction

Autoimmunity is the failure of an organism in recognizing its own constituent parts as self, which allows an immune response against its own cells and tissues.[1-2] Any disease that results from such an aberrant immune response is termed an autoimmune disease and prominent examples include Coeliac disease, diabetes mellitus type-1 (IDDM), Hashimoto's thyroiditis, Graves' disease and rheumatoid arthritis (RA).[3-4]

2. Arthritis

Arthritis (from Greek *arthro*-, joint + -*itis*, inflammation; plural: arthritides) is a chronic autoimmune disease of which the main characteristic is irreversible joint destruction.[5-6] It is a group of conditions involving damage to the joints of the body. Rheumatic diseases are estimated to affect up to 1.1 % of world's population and these patients are often treated with steroids, Non-Steroidal Anti-Inflammatory agents (NSAIDs), Disease Modifying Anti-Rheumatic Drugs (DMARDs) and/or immunosuppressive drugs.[7] Currently available therapy for the arthritis focuses on reducing inflammation of the joints with NSAIDs and steroids.

3. Types of arthritis

There are over 150 different forms of arthritides but the most common of them includes rheumatoid arthritis (RA), osteoarthritis (OA), spinal disorders and septic arthritis.[8]

3.1 Rheumatoid arthritis

RA is a chronic immune inflammatory disease characterized by synovial hyperplasia, joint destruction and extra-articular manifestations with a significant impact on both morbidity and mortality. It affects 0.5-1 % of the population in the industrialized world and commonly leads to significant disability and a consequent reduction in quality of life.[9] It is two to three times more frequent in women than in men and can start at any age with a peak incidence between the fourth and sixth decade of life.[10]

3.1.1 Etiology and pathogenesis of RA

The etiopathology of this condition is not fully understood. Many consider it to be an autoimmune disorder, although its exact cause is unknown. It is known that neutrophils, macrophages, synovial fibroblasts, T cells and B cells are involved in the mechanisms that drive the onset of RA.[11] T cells, B cells and macrophages infiltrate the synovium and form discrete lymphoid aggregates, sometimes with ectopic germinal centers while

macrophage-like and fibroblast-like synoviocytes accumulate in the intima causing hyperplasia and secrete degradative enzymes. [12] The difference between anatomy of normal and arthritic joints is shown in **Fig. 1.1** below.
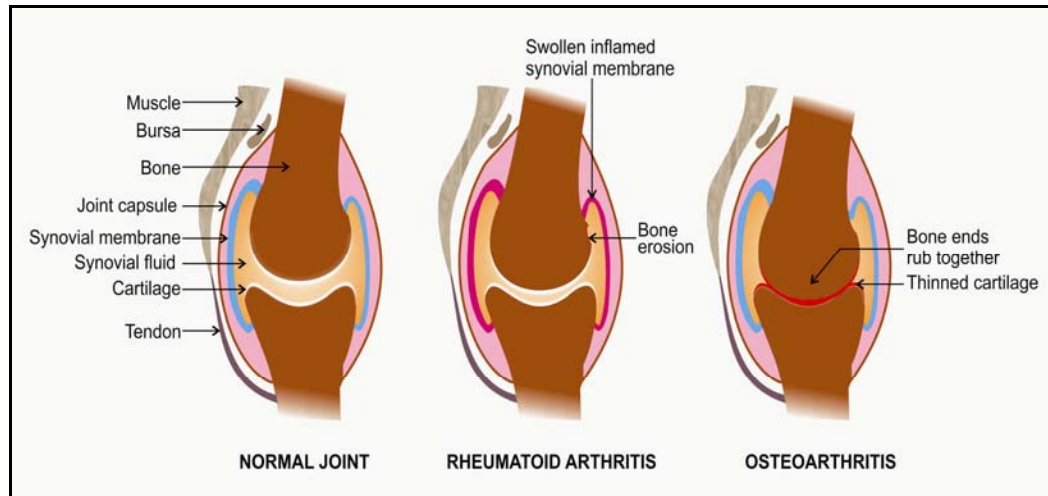
Fig. 1.1: Anatomy of normal and arthritic joints OA/RA

3.2. Osteoarthritis

In contrast to RA, OA is relatively noninflammatory degenerative joint disease occurring mostly in older persons and is characterized by the degeneration of articular cartilage, hypertrophy of bone at the margins and changes in the synovial membrane. OA is the most common joint disease affecting over 50 % of the population over 65 years of age and 80 % of the population over 75 years of age. The most common symptom of OA is pain often worsening with joint movements and improving at rest.

3.2.1 Etiology and pathogenesis of OA

OA usually has a slow and insidious onset. Clinically, OA manifests in the form of gradual development of joint pain, joint stiffness and crepitus with motion, joint effusions and limitation of movement in the joints.[13] Risk factors for the development and progression of OA include local biomechanical factors like obesity, joint injury, joint deformity and extensive sport participation as well as systemic factors including age, gender, ethnic characteristics, bone density and estrogen deficiency.[14]

OA affects only one single or a few joints. The joints most frequently affected by OA, based on radiographic evidence in Caucasian populations are the knees (33 % prevalence) followed by the hands (29.5 %), feet (20.8 %) and the hips (4.7 %).

4. Arthritis and cartilage damage

4.1. Structure of articular cartilage

Articular cartilage is a specialized connective tissue resting on subchondral bone that covers the surfaces of diarthrodial joints. A mature articular cartilage is a heterogeneous tissue with four distinct regions: the superficial tangential (or gliding) zone, middle (or transitional) zone, the deep (or radial) zone and the calcified cartilage zone located immediately below the tidemark and above the subchondral bone.[15] Joint cartilage, a connective tissue that consists of chondrocytes and their surrounding extracellular matrices plays an essential role in the mechanical cushioning of joints in postnatal locomotion.
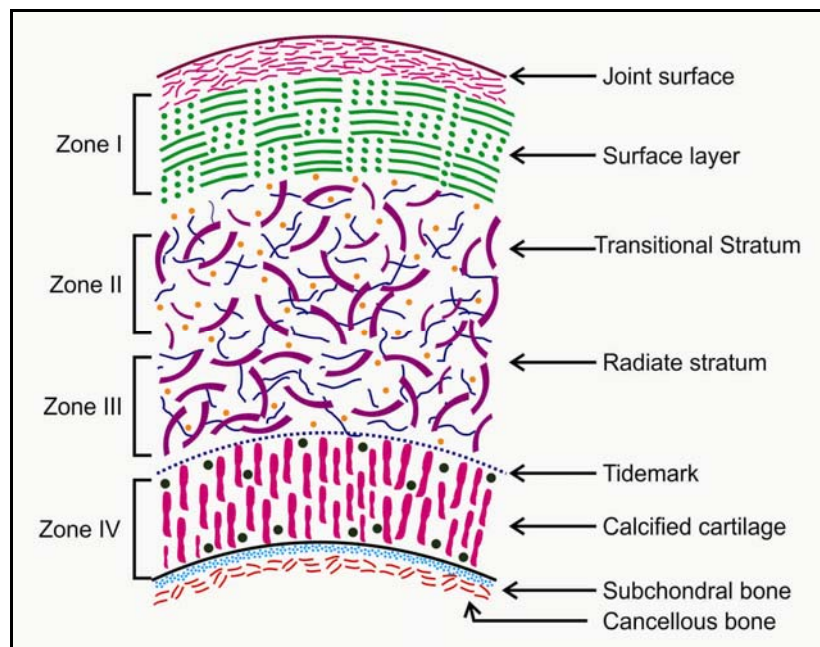
Fig. 1.2: Articular cartilage anatomy and collagen arrangement

Damage to joint cartilage is likely to lead to long term joint problems. This is largely because cartilage does not have a direct supply of blood (avascular tissue) and thus cannot be quickly repaired naturally by the body. Joints are also particularly vulnerable to degeneration because it is common for the needs of their repair to outstrip the body's ability to produce new cartilage.[16]

4.2. Biochemistry of cartilage

Cartilage is made up of water (70 %) and type II collagen (20 %) with proteoglycans and glycosaminoglycans (consisting mainly of aggrecan and chondroitin) produced by chondrocytes. Healthy joint cartilage distributes static and dynamic joint

loading and decreases friction. Sparsely distributed cartilage cells maintain the cartilage matrix rich in collagen and proteoglycans. The quality of this matrix is critical for maintaining the functional properties of the cartilage. Changes in the joint cartilage associated with OA include gradual proteolytic degradation of the matrix associated with increased synthesis of the same (or slightly altered) matrix components by the chondrocytes.[17]

The major collagen in articular cartilage is type-II collagen, which accounts for >50 % of its dry weight. As the second component of cartilage, aggrecan is a multidomain proteoglycan with several well-characterized functional regions. The core protein of aggrecan comprises of two *N*-terminal globular domains G1 and G2 separated by the E1 domain followed by a more extended E2 domain and terminated by the third globular domain G3. The negatively charged groups in aggrecan are keratan sulfate and chondroitin sulfate in the E2 domain. A large amount of negative charges in this domain contributes to the stiffness of cartilage[18]

4.2.1. Proteoglycans

Proteoglycans are huge complex molecules composed of proteins and sugars. They interlink with the collagen fibers forming a dense matrix or network inside the cartilage making it resilient so that it can stretch when we move and spring back into place. Proteoglycans also trap water from the tissues acting like a sponge giving cartilage the flexibility. [17-19]

4.2.2. Glucosaminoglycans

The most abundant heteropolysaccharides in the body are the GAGs. These molecules are long unbranched polysaccharides containing a repeating disaccharide unit. The disaccharide units contain either of the two modified sugars *N*-acetylgalactosamine (GalNAc) or *N*-acetylglucosamine (GlcNAc) and an uronic acid such as glucuronate or iduronate. GAGs are highly negatively charged molecules, with extended conformation that imparts high viscosity to the solution. [17]

The specific GAGs of physiological significance are hyaluronic acid, dermatan sulfate, chondroitin sulfate, heparin and heparan sulfate and keratan sulfate. Hyaluronic acid is unique among the GAGs in that it does not contain any sulfate and is not found covalently attached to proteins as a proteoglycan. Hyaluronic acid polymers are very large (molecular weights of 100,000-10,000,000) and can displace a large volume of water. This property makes them excellent lubricators and shock absorbers[20] The composition of

various GAGs and the linkage they contains have been shown in **Table 1.1** below and in **Table 1.2** the location of various GAGs has been given.

Table 1.1: Composition of GAGs and linkage

Sr. No	Type of sugar	Composition	Linkage
1	Hyaluronates	D-glucuronate + GlcNAc	**(1, 3)**
2	Dermatan sulfates	L-iduronate (many are sulfated) + GalNAc-4-sulfate	**(1, 3)**
3	Chondroitin sulfates	D-glucuronate + GalNAc-4- or 6-sulfate	**(1, 3)**
4	Heparan sulfates	D-glucuronate-2-sulfate (or iduronate-2-sulfate) + *N*-sulfo-D-glucosamine-6-sulfate	**(1, 4)**
5	Keratan sulfates	Galactose + GlcNAc-6-sulfate	**(1, 4)**

*GlNAc= Glucosamine *N*-acetyl, **GalNAc**=Galactosamine *N*-acetyl

Table 1.2: Types of GAGs and their location

Sr.No	GAGs	Localization
1	Hyaluronates	Synovial fluid, ECM of loose connective tissue
2	Dermatan sulfates	Skin, blood vessels, heart valves
3	Chondroitin sulfates	Cartilage, bone, heart valves
4	Heparan sulfates	Basement membranes, components of cell surface
5	Keratan sulfates	Cornea, bone, cartilage,
6	Heparin	Component of intracellular granules of mast cells lining the arteries of the lungs, liver and skin

4.3. Cartilage damage and repair

A large range of motion and the demands of constant use especially bearing weight can damage the cartilage of the joints. Not just age, but sports and accidents can lead to similar damage.

In a person with joint issues, cartilage is destroyed faster than it is synthesized. The key limiting step on the synthesis side is production of GAGs for which glucosamine is the basic building block.[21] Glucosamine is a natural substance found in the body and made from the combination of a sugar (glucose) and an amine derived from the amino acid glutamine. Chondrocytes are cells responsible for the repair and regeneration of cartilage tissues, both its removal when damaged and its synthesis.

Enzymes produced by the chondrocytes tear down damaged or old cartilage, just as proteoglycans synthesized by the chondrocytes renew cartilage. Both steps are necessary for joint health and a balance needs to be maintained. Various molecules involved in the catabolic and anabolic processes of the chondrocytes are shown in **Table 1.3**

A balance between anabolic and catabolic signals maintains the homeostasis of cartilage. In normal cartilage the balance between anabolism and catabolism is equivalent. In OA cartilage, catabolism becomes more dominant than anabolism leading to the degradation of the cartilage.[17] **Fig. 1.3** and **1.4** provides diagramatic and schematic view of the signaling factors affecting cartilage homeostasis respectively.

Table 1.3: Molecules involved in the catabolic and anabolic processes of the chondrocytes

No	Source	Process		
		Catabolism	**Anabolism**	**Ref.**
1	Proteolytic Enzymes	Collagenases-I, II, III Stromelysin, Aggrecanase Cathepsin-K, COX	TIMPs	19, 69, 72
2	Cytokines and Growth Factors (GF)	IL-1, IL-17 TNF-α	TGF-β IGF, bFGF BMPs	35, 56-57
3	Nitric oxide and Prostaglandins	NO Prostaglandin E2	--	19,35

*TIMPs: Tissue inhibitors of metalloproteinase

As the most abundant bone cell type, osteocytes are mature osteoblasts located in the bone matrix. Normally bone resorption by osteoclasts and bone formation by osteoblasts are well balanced to maintain the function of the skeleton. However, under pathological conditions (e.g., RA and OA) such balance is disturbed. Bone resorption however is mostly mediated by osteoclasts.

It is believed that various cytokines released during development of the disease help to recruit osteoclasts to the sites of destruction. As osteoclasts start the bone resorption process they will secrete cathepsin-K to cleave the type-I collagen triple helix fibrils and other bone proteins.[24]
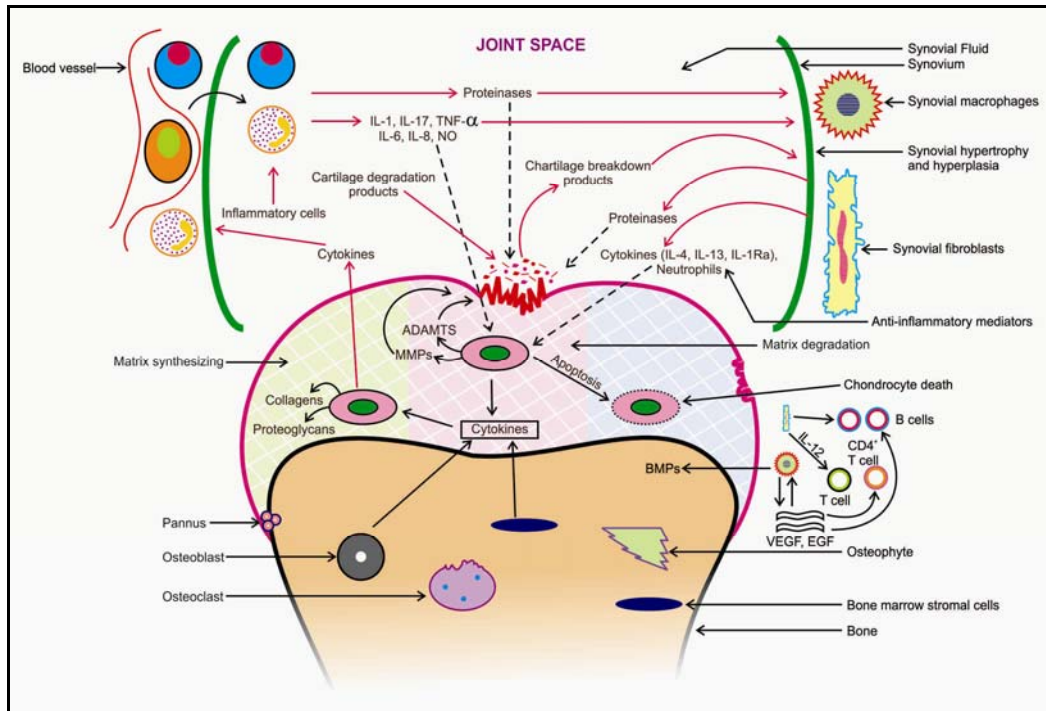
Fig. 1.3: Anabolic and catabolic signaling factors affecting cartilage homeostasis,[27] involvement of the synovium in OA pathophysiology and products of cartilage breakdown that are released into synovial fluid.[28]

*(**Abbreviations: ADAMTs**: a disintegrin and metalloproteinase with thrombospondin motifs, **CCL2**: CC chemokine ligand-2, **CXCl-13**: CXC chemokine ligand 13, **EGF**: Endothelial growth factor, **GM-CSF**: Granulocyte macrophage colony stimulating factor, **LIF**: Leukemia inhibitory factor, **LTB4**: Leukotriene B4, **NAMPT**: Nicotinamide Phosphoribosyl transferase, **NGF**: nerve growth factor, **TIMP**: Tissue inhibitor of metalloproteinase's, **VCAM-1**: Vascular cell adhesion molecule-1, **VEGF**: Vascular endothelial growth factor)*
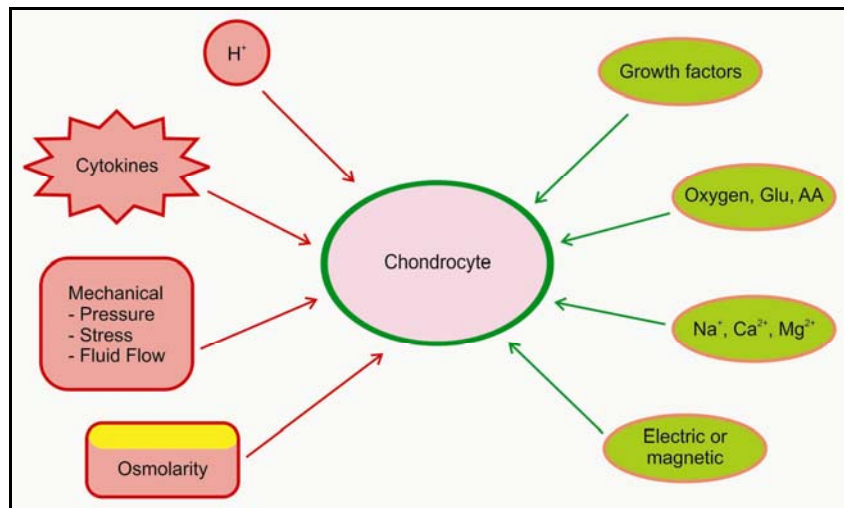
Fig. 1.4: Regulators of cartilage metabolism

5. Diagnosis of arthritis

Arthritis is a complicated disease and an accurate diagnosis is required for proper treatment of arthritis. As mentioned earlier with over 150 types of arthritis, early symptoms can overlap and diagnosis can be difficult but this is beyond the scope of this chapter. Here, diagnosis of RA and OA mainly has been focused.

5.1. Diagnosis of RA

RA can be difficult to diagnose. Many other conditions resemble it and its symptoms can develop insidiously. In a clinical diagnosis patients commonly report pain and stiffness in multiple joints. One third of the patients initially experience symptoms at just one location or a few scattered sites.

Table 1.4: Summary of the tests and findings associated with RA.[25-26]

SR. No	Laboratory Test*	Associated Findings
1	C-Reactive protein	Typically increased to >0.7 pg/ml.
2	ESR	Often increased to >30 mm per hour.
3	Hemoglobin/hematocrit	Slightly decreased; Hb average 10 g per dL normochromic, normocytic or microcytic anemia.
4	Liver function	Normal or slightly elevated alkaline phosphatase
5	Platelets	Usually increased
6	Radiographic findings of involved joints	May be normal or show osteopenia or erosions near joint spaces in early disease.
7	Rheumatoid factor	Negative in 30 % of patients early in illness; can be positive in other processes e.g., lupus; scleroderma

* Recommended for initial evaluation for RA

In RA, antibodies that collect in the synovium of the joint are known as rheumatoid factor. **Table 1.4** enlists various major tests and findings associated with RA.

5.2. Diagnosis of OA

OA requires some special mention because it is the most common form of arthritis. It differs from RA in several important respects as described below:

- OA usually occurs in older people
- It is located in only one or a few joints. (In fact OA is probably most often confused with RA if it affects multiple joints in the body)
- The joints are less inflamed
- Progression of pain is almost always gradual

The diagnosis of OA is largely made by obtaining a detailed history and conducting a complete physical examination. Clinically indicated laboratory tests may include tests for erythrocyte sedimentation rate and rheumatoid factor. Synovial fluid analysis may be conducted to help exclude other diagnoses.[27] Radiographs can provide objective evidence of the disease.

6. Arthritis treatment

Arthritis causes significant morbidity and mortality and must be treated aggressively from the time of its diagnosis. There is no known cure for arthritis or means of preventing it. Optimal management requires early diagnosis and timely introduction of agents that reduce the probability of irreversible joint damage. Other studies suggest that early aggressive treatment may alter the course of the disease and most rheumatologists favor aggressive treatment early in the course of the disease.[28]

6.1. Treatment of RA

The principles of management of RA are to relieve pain, prevent deformity and maintain normal functions. Therapeutic goals include preservation of functions and quality of life, minimization of pain and inflammation, joint protection and control of systemic complications. Drug therapy for RA rests on two principal approaches, symptomatic treatment with NSAIDs and DMARDs.[29] **Fig. 1.5** outlines possible approaches to the treatment of a patient with RA.
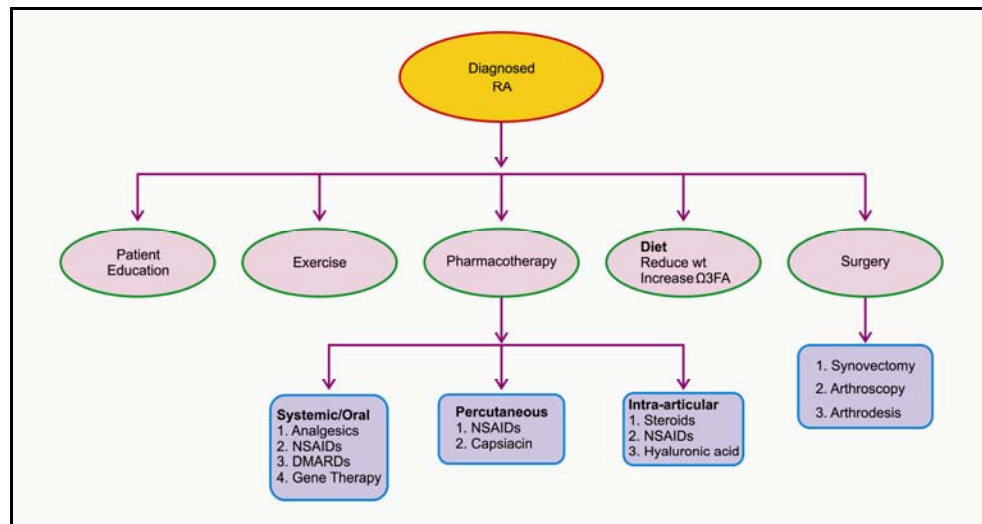
Fig. 1.5: Approaches to the treatment of RA

Joint destruction in RA begins within a few weeks of onset of symptom and early treatment decreases the rate of disease progression. Therefore it is imperative to diagnose the disease and initiate the treatment as soon as possible. If not treated on time RA may develop various complications such as anemia, cancer, cardiac complications, fistula formation rheumatic nodules etc. [25] Patients with RA must be managed by a multidisciplinary team in which the general practitioner and rheumatologist are pivotal. Patient's involvement in decisions on therapeutic options is increasingly important.[30]

6.1.1. Education

Education has an important role; it provides information on the disease and its therapies giving patients a realistic outlook and allowing them to be involved in therapeutic decisions.

6.1.2. Exercise

Much of the pain and stiffness in RA arises from periarticular tissues such as muscles and tendons. These symptoms are amenable to exercise to some extent and it is important that all patients with RA regularly perform a general exercise programme to improve and maintain general fitness and maintain muscle bulk around the joints.

6.1.3. Dietary advice

Dietary advice is often sought and should be provided appropriately. Dietary issues include weight reduction and the addition of fish oils or evening primrose oil. Fish oil substitutes have enabled reduction or discontinuation of NSAIDs in RA patients.

6.1.4. Pharmacotherapy

Once the diagnosis of RA has been confirmed, treatment with drugs that retard joint destruction and reduce disability should be commenced promptly in almost all cases. Pharmacotherapy for rheumatoid arthritis generally involves an NSAID for control of pain, with selective use of low-dose oral or intra-articular (IA) glucocorticoids and initiation of a DMARD. Other analgesics also may be used; NSAIDs have no effect on long-term disability but provide symptom relief.

6.1.4.1. Analgesics and NSAIDs

Analgesics reduce pain and NSAIDs lessen pain and stiffness. Both groups of drugs are used widely to control symptoms of rheumatoid arthritis. Evidence for use of analgesics is modest but uncontroversial support for use of NSAIDs is considerably stronger. NSAIDs have lost their historical role as first-line treatment because of concerns about their limited effectiveness, inability to modify the long-term course of disease and gastrointestinal and cardiac toxic effects.

NSAIDs interfere with a small segment of the inflammatory cascade only, namely prostaglandin generation by cyclooxygenases (COXs), but do not interfere with the underlying immuno-inflammatory events or retard joint destruction. Combinations of two or more NSAIDs should be avoided since they are no more effective and may have additive adverse effects.[31] Since the present work pertains to site specific chemical delivery of some NSAIDs it is in order to discuss NSAIDs, their classification, mechanism of action and adverse effects etc. in detail as discussed in **Section-7**

6.1.4.2. DMARDs

In contrast to NSAIDs, DMARDs 'modify' the disease process in all these respects and once DMARDs are effective no further symptomatic therapies are needed. All patients whose RA remains active despite adequate treatment with NSAIDs are candidates for DMARD therapy. Active RA may lead to irreversible joint damage even in the early months of the disease; while NSAIDs and glucocorticoids may alleviate symptoms; joint damage may occur and progress.[30]

Currently DMARDs such as adalimumab, methotrexate, azathioprine, infliximab, etanercept etc. are used for the treatment of arthritis.

6.1.4.3. Glucocorticoids

Low-dose oral glucocorticoids (<10 mg prednisone daily or equivalent) and local injections of glucocorticoids are highly effective for relieving symptoms in patients with active RA. Low dose glucocorticoids appear to slow the rate of joint damage.[32] The adverse effects of systemic glucocorticoids, especially when taken in higher doses for extended periods of time limit their use, however when administered by an experienced physician glucocorticoid injection of joints and periarticular structures is safe and effective. Injecting one or a few of the most involved joints in a patient early in the course of RA may provide local and even systemic benefits. The effects are sometimes dramatic but may be temporary. Prompt improvement from IA glucocorticoids helps to instill confidence in the patients impressing that the treatment can be effective. A patient who has flare in one or a few joints can be treated successfully by injection of the flaring joint or joints without requiring a major change in the prescribed regimen.[28]

6.1.4.4 Biological agents for RA

Most of the biologic agents have been evaluated as single agent therapy (monotherapy) and thus have not yet been tested in combination with one another (e.g., anti-CD4 MAb combined with anti-TNF agents) or with currently used DMARDs.[33] TNF inhibitors were the first licensed biological agents followed by abatacept, rituximab, and

tocilizumab. Various biological agents developed or under development are shown in **Table 1.5**

Table 1.5: Biologic agents that inhibit T cell function and have been evaluated in clinical trials in patients with RA

No	Biologic Agent	Target Antigen
1	Murine anti-CD4 MAb*	CD4+ T Cell
2	Chimeric anti-CD4 (depleting) MAb	CD4+ T Cell
3	CAMPATH-1H MAb	CDw 52
4	Murine anti-CD5 ricin toxin	CD5
5	Anti-CD7 MAb	CD7
6	Anti-IL-2 MAb	IL-2 receptor
*MAb: monoclonal antibody		

6.1.4.5 Gene Therapy

Gene therapy provides another avenue for treating autoimmune disorders. The goal is to increase local expression of anti-inflammatory molecules involved in synovial tissue. Candidate molecules to date have included cytokine antagonists such as IL-lRa, sTNFR, IL-10, IL-4, and sIL-1R. The feasibility of this approach has been tested in animal models using IL-1Ra.[34]

6.1.4.6 Surgery

Even if joint inflammation is successfully controlled or eliminated with medication, patients with chronic RA have unacceptable pain and/or limitation of function because of structural joint damage or functional impairment is severe, then surgery should be considered.[25] Synovectomy and arthroplasty have significant roles in the overall management of RA. Hip and knee arthroplasty and forefoot reconstruction can significantly improve mobility in patients with damaged joints. Arthrodesis may be helpful for unstable joints (e.g. wrist, atlantoaxial joint).[28]

6.2. Treatment of OA

The aims of treatment of OA are patient education, pain control and improvement of function. The treatment interventions in OA include non-drug therapy, drug therapy, and surgical treatment as shown in **Fig. 1.6**.[17] Though each therapy has respective

advantages and efficacy to some degree, there is no fundamental therapy aimed at repairing the underlying molecular problem.
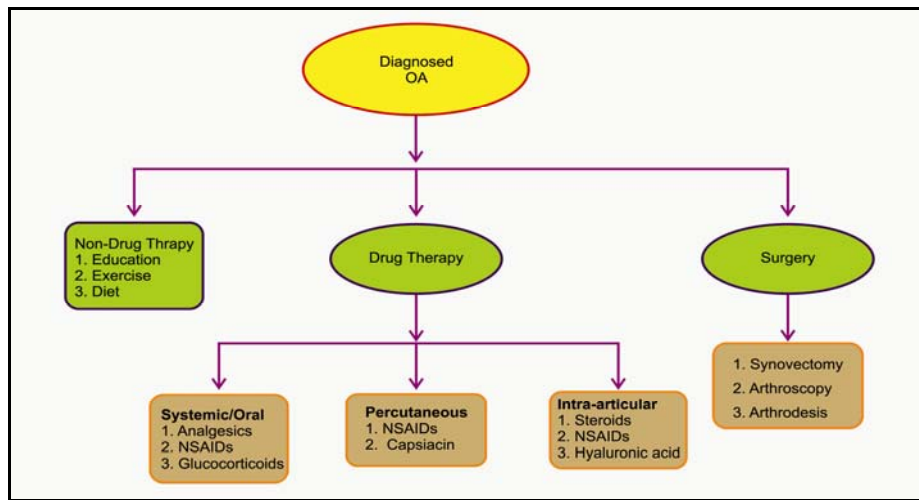
Fig. 1.6: Approaches to the treatment of OA

6.2.1. Non-drug therapy

Formal patient education by any member of a multidisciplinary team should be an initial part of management of OA. Physical therapy is another mainstay in the treatment of OA; the mechanisms of which have not been clarified yet. Physiotherapists use two major approaches: muscle strengthening programs specific for certain joints and general aerobic conditioning.

6.2.2. Drug therapy

Paracetamol is a common first choice drug among several analgesics. Use of this medication is supported by the excellent safety record and low cost of paracetamol relative to NSAIDs. Especially in the elderly it is safe and well tolerated.[35] Paracetamol/opiate combinations such as coproxamol may be used if paracetamol alone is unhelpful. Stronger opiates should be avoided if at all possible.

Both the ACR and European League against Rheumatism guidelines (ELR) recommend paracetamol alone as an initial therapy. NSAIDs have been found to have equal efficacy to paracetamol in most patients with OA.[42] However recent data suggest that NSAIDs may be better than paracetamol for symptomatic relief of OA in large joints. Novel therapeutic agents have been developed that act as specific inhibitors of the cyclooxygenase-2 isoform (COX-2 inhibitors). Topical treatment is an additional option for patients with OA who have inadequate pain relief or who cannot tolerate systemic

therapy. The two types of topical agents in the treatment of this disorder are NSAIDs and capsaicin.[37] a recent meta-analysis concluded that both agents are well tolerated and have significantly greater analgesic effects than placebo.

IA corticosteroids are widely used in the management of patients with OA of the knee, most commonly in those patients who have active inflammation. Patients with a painful flare of OA of the knee may benefit from IA injection of a corticosteroid such as methylprednisolone (Medrol) or triamcinolone (Aristocort).[38] When a joint is painful and swollen, short term pain relief can be achieved with aspiration of joint fluid followed by IA injection of a corticosteroid. A joint should not be injected with more than three or four times in one year because of the possibility of cartilage damage from repeated injections.[39]

Other choice is use of hyaluronic acid, a high molecular weight polysaccharide and a major component of synovial fluid and cartilage. Several studies suggest that IA hyaluronic acid shows superior pain relief to placebo and equivalent relief to corticosteroid injections but with a greater duration of action.[40]

6.2.3. Surgical treatment

In majority cases surgical treatment of OA is considered only after failure of non-surgical treatments. Four categories of non-biological procedures are considered in surgical management: osteotomy, arthroscopy, arthrodesis and arthroplasty.[41] For most patients, especially in the elderly ones total joint arthroplasty is highly successful and the therapeutic effects will last for the remainder of the patient's expected lifespan.

6.2.4. Future direction for OA treatment

An approach that incorporates tissue engineering is one of the most promising of OA therapies.[42] Use of viral vectors is a viable method to induce anabolic genes into sampled cells to achieve cartilage development with high efficiency.[26] Scaffolding of natural polymers has been used to shape cartilage appropriately.

7. Non-Steroidal Anti-inflammatory Drugs (NSAIDs)

NSAIDs, is an important therapeutic class of drugs used to suppress pain and inflammation in cases of RA and other inflammatory diseases.[43] In 1970s a scientific breakthrough occurred with the elucidation of the molecular mechanism of aspirin and other NSAIDs.[44] Since then heterogeneous groups of compounds often unrelated chemically (although most of them are organic acids) have been introduced as NSAIDs. These anti-inflammatory substances block the biosynthesis of prostaglandins which contribute to a variety of physiological and pathophysiological functions.

7.1. Classification of NSAIDs

NSAIDs can be broadly classified on the basis of their selectivity for COX enzyme.[45]

7.1.1. Non-selective acidic COX inhibitors: There can be further sub-classified on the basis of chemical structure e.g. aspirin, paracetamol, indomethacin, ibuprofen, naproxen etc.

7.1.2. Selective COX-2 inhibitors: e.g. etodolac, nimesulide, celecoxib, etoricoxib etc.

7.2. Pharmacological actions and therapeutic uses of NSAIDs

All NSAIDs including selective COX-2 inhibitors are anti-inflammatory, antipyretic and analgesic. One important exception is acetaminophen which is antipyretic and analgesic but is largely devoid of anti-inflammatory effect. Other uses of NSAIDs include treatment of cancer. Prostaglandin E_2 has been implicated in the humoral hypocalcaemia associated with some neoplasm and treatment with NSAIDs can effectively suppress serum calcium levels in some cancer patients. Excessive production of renal PGs has been implicated in the pathogenesis of some of the metabolic abnormalities in the Bartter's syndrome and NSAIDs have been found to be useful in the treatment of this disorder.[44]

7.3. Mechanism of action of NSAIDs

The major mechanism by which NSAIDs elicit their therapeutic effect is inhibition of PG synthesis. NSAIDs work by interfering with the cyclooxygenase pathway. The normal process begins with arachidonic acid; this acid is converted by the enzyme cyclooxygenase (COX) to synthesize different prostaglandins (PGs).[44]

7.4. Side effects of NSAIDs

Side effects of NSAIDs are due to the inhibition of COX-1 enzyme. The widespread use of NSAIDs has meant that the adverse effects of these relatively safe drugs have become increasingly prevalent. Some major adverse effects of NSAIDs include gastrointestinal toxicity, renal ADRs, photosensitivity, blockade of platelet aggregation, hepatic complications and inhibition of uterine motility etc.[46]

8. Approaches used to reduce toxicity of NSAIDs

There are several ways in which the risk of side effects of NSAIDs can be reduced. Some of these are given below:

- By prodrug approach

- Using selective COX-2 inhibitors

- Using lower-risk NSAIDs such as ibuprofen at doses of less than 1,600 mg per day

- Using enteric-coated aspirin (has a lower risk of side effects)

- Using misoprostol which protects the stomach lining when taken in addition to NSAIDs

- Incorporating proton pump inhibitors: Omeprazole, Ranitidine, Cimetidine, Famotidine etc.

- By parentral administration of NSAIDs

- By targeted drug delivery of NSAIDs

9. Cartilage targeted drug delivery in arthritis

It has been first shown by Freudenberg *et al.*[47] that dried preparations of cartilage can take up certain cations from solution and this observation was further proved by Boyd *et al.*[48] who showed that the equivalent capacity of the cartilage to bind sodium, calcium, and barium ions *in vitro* and the mechanism involved is the same in each case and that it may be regarded as a stoichiometric chemical reaction. The binding of calcium by cartilage was shown to be an ion exchange reaction.

The close correlation between binding capacity and sulphate content in both preparations implicates chondroitin sulphate as the principal binding agent. Since sulfate is present as the ester sulfate it can account for only one half of the total binding capacity for the cations. Although the protein carboxyl groups have been shown to bind cations and could conceivably account for the total binding capacity of the cartilage.[49] The experiment from Klotz *et. al.* shows no binding of phosphate unless cartilage contains appreciable amounts of calcium in which case phosphate is taken up by the cartilage until the Ca: P ratio is approximately that of hydroxyapatite. [49]

These findings suggest that conflicting results obtained by Roche and Deltour *et al.*[50] that cartilage first binds phosphate followed by a binding of calcium was clear from the experiment done by Klotz *et. al.* and it could be concluded that when mineral content (cations) is high in cartilage then mineral itself may absorb the ions (anions), and this phenomenon may be responsible for the results obtained by Roche and Deltour *et al.*[48]

This finding was further supported by the fact that quaternary ammonium compounds like hexamethonium **(1)** and decamethonium **(2)** accumulated preferentially in certain avascular cartilaginous tissues on intramuscular injection[51], whereas little of them

were found in blood rich bone marrow. It has been postulated that these quaternary ammonium compounds are localized in the cartilage tissues, probably by virtue of ionic interactions with cartilaginous tissues. Thus it is concluded that both the mono and diquaternary compounds which exist exclusively in the charged form in blood are localized in the cartilage by ionic interactions with polyanionic acid mucopolysaccharides. However diquaternary compounds achieved higher concentrations in cartilage than the monoquaternary compounds; because energy of interaction of dicationic compounds is double than monocationic compounds.
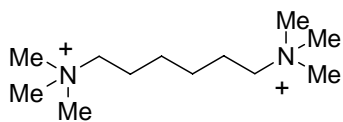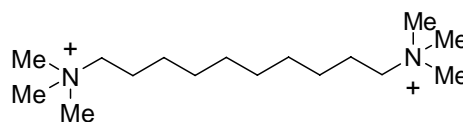
(1)   **(2)**
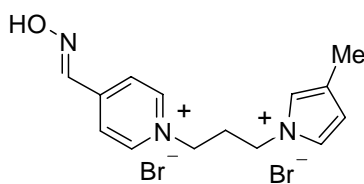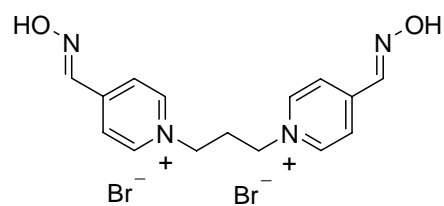
(3)   **(4)**
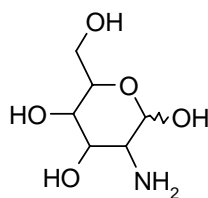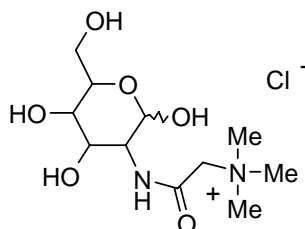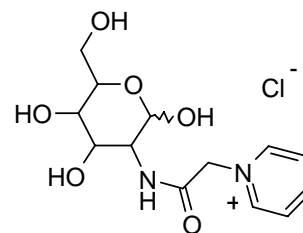
(5)   **(6)**   **(7)**

These observations have been further supported by Maurizis *et al.*[52] and it was concluded that localization of quaternary ammonium compounds such as pyrimidoxime **(3)** and *N,N*-trimethylene bis(pyridinium-4-aldoxime) dibromide (TMB4) **(4)** in the cultured proteoglycan suspension was due to ionic interaction. This factor together with their poor lipophilicity can explain their high selectivity for the cartilaginous tissues as opposed to other proteoglycan containing tissues such as skin.

This idea has been further extended to the site specific delivery of antirheumatic agent *D*-glucosamine **(5)** to the cartilaginous tissues by conjugating it with some

quaternary ammonium groups. ^{14}C-Labeled quaternary ammonium-glucosamine conjugates (**6** and **7**) were prepared by Giraud *et al.* and their biodistribution in rats were studied.[53]

It was reported that introduction of a quaternary ammonium moiety in *D*-glucosamine (**5**) a compound which already exhibited a special tropism for cartilage, allowed the molecule to be carried more selectively to the cartilagenous tissues soon after intravenous injection in rodents. Both the compounds (**6** and **7**) have been reported to have higher affinity for cartilaginous tissues than for the unconjugated [14]C-*D*-glucosamine (**5**)
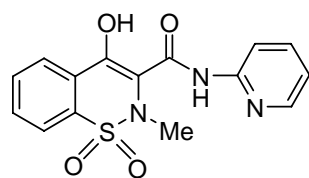
(8)
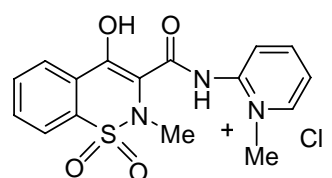
(9)
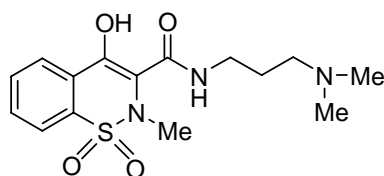
(10)
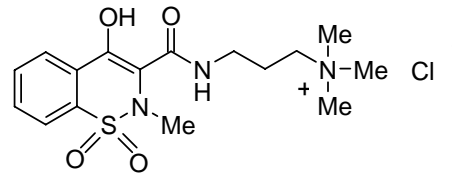
(11)
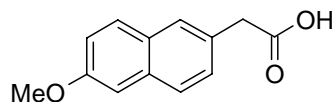
(12)
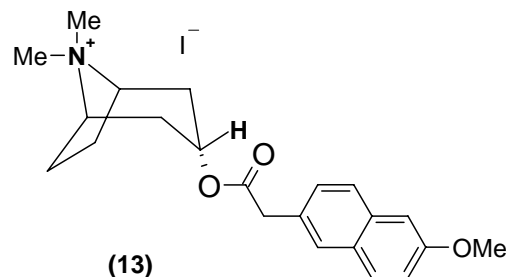
(13)

Literature survey also revealed that introduction of a quaternary ammonium function on oxicam structures greatly increased their affinity for the cartilaginous tissues. Analog of oxicam NSAIDs like piroxicam (**8**) and propoxicam (**10**), in which the active group was linked to quaternary ammonium function [piroxicam-N$^+$ (**9**) and propoxicam-N$^+$ (**11**)] were synthesized and labeled with radioactive probes. Pharmacokinetic study conducted on rats showed that these molecules were able to highly concentrate in joint cartilage.[54]

Previous work from this laboratory[55] also reported selectivity of NSAIDs such as 6-MNA (**12**) towards cartilage increased when cationic group was present in structure (**13**). The above compound (**13**) was also evaluated for site specificity and it was found

that it was localized in inflammed areas and intensely accumulated in the cartilage as compared to parent NSAIDs **(12)** following i.v. administration. So from the above literature reports we can conclude that cationic molecules possess affinity towards anionic cartilage hence advantage could be taken of this property to develop various chemical delivery systems of NSAIDs or their delivery systems for the treatment of arthritis.

References

1. Halldorsdottir H.D., Jonsson T., Thorsteinsson J. and Valdimarsson H. A., Prospective study on the incidence of rheumatoid arthritis among people with persistent increase of rheumatoid factor. *Ann. Rheum. Dis.* **2000**, 59, 149-51.

2. Kurki P., Aho K., Palosuo T. and Heliovaara M., Immunopathology of rheumatoid arthritis. Antikeratin antibodies precede the clinical disease. *Arthritis Rheum.* **1992**, 35, 914-17.

3. Silman A.J., Hennessy E. and Ollier B., Incidence of rheumatoid arthritis in a genetically predisposed population. *Br. J. Rheumatol.* **1992**, 31, 365-68.

4. www.wikipedia.org

5. Harris E.D., DiBona D.R. and Krane S.M., A mechanism for cartilage destruction in rheumatoid arthritis. *Trans. Assoc. Am. Phys.* **1970**, 83, 267-76.

6. Scott D.L., Shipley M., Dawson A., Edwards S. and Woolf A.D., The clinical management of Rheumatoid arthritis and Osteoarthritis: Strategies for improving clinical effectiveness. *Br. J. Rheumatol.* **1998**, 34, 546-54

7. Achira M., Totsuka R. and Kume T., Differences in pharmacokinetics and hepatobilliary transport of novel anti-inflammatory agents between normal and adjuvant arthritis rats. *Xenobiotica.* **2002**, 32, 1139-49

8. World Health Organization. Chronic rheumatic conditions: (Available at http://www.who.int/chp/topics/rheumatic/en/) Accessibility verified November 2, **2012**

9. Wolfe F.E. and Hawley D.J., The long term outcome of rheumatoid arthritis. Work disability: a prospective 18 year study of 816 patients. *J. Rheumatol.* **1998,** 25, 2108-17

10. Pugner K.M., Scott D. I., Holmes J.W. and Hieke K., The costs of rheumatoid arthritis: an international long-term view. *Semin. Arthritis Rheum.* **2000**, 29, 305-20

11. Cascão R., Rosário H.S., Souto-Carneiro M.M. and Fonseca J.E., Neutrophils in rheumatoid arthritis: More than simple final effectors. *Autoimmun. Rev.* **2010**, 9, 531-35.

12. Smolen J.S. and Steiner G., Therapeutic strategies for rheumatoid arthritis. *Nat Rev Drug. Discov.* **2003**, 2, 473-88

13. Gerwin N., Hops C. and Lucke A., Intraarticular drug delivery in osteoarthritis *Adv. Drug. Deliv. Rev.* **2006,** 58, 226-42

14. Creamer P. and Hochberg M.C., Osteoarthritis. *Lancet.* **1997**, 350, 503-09

15. Wang D. and Bromme D., Drug delivery strategies for cathepsin inhibitors in joint diseases. *Expert. Opin. Drug. Deliv.* **2005**, 2, 1015-28

16. Smith G.N., Myers S.L., Brandt K.D., Mickler E.A. and Albrecht M.E., Diacerhein treatment reduces the severity of osteoarthritis in the canine cruciate-deficiency model of osteoarthritis *Arthritis Rheum.* **1999**, 42, 545-54.

17. Hashimoto M., Nakasa T., Hikata T. and Asahara H., Molecular Network of Cartilage homeostasis and osteoarthritis *Med. Res. Rev.* **2008**, 28, 464-81.

18. Kiani C., Chen L., Wu Y.j., Yee A.J. and Yang B.B., Structure and function of aggrecan. *Cell Res.* **2002**, 12, 19-32

19. Block A. and Bettelheim F., Water vapor sorption of hyaluronic acid. *Biochim. Biophys. Acta,* **1970,** 201-69

20. Laurent T. and Gergely J., Light Scattering Studies on Hyaluronic Acid. *J. Biol. Chem.* **1955**, 212-25

21. Vajaradul Y., Double-blind clinical evaluation of intra-articular glucosamine in outpatients with gonarthosis. *Clin. Ther.* **1981**, 3,336-43

22. Goldring M.B., The role of cytokines as inflammatory mediators in osteoarthritis: Lessons from animal models. *Connect. Tissue. Res.* **1999,** 40, 1-11.

23. Sellam J. and Berenbaum F., The role of synovitis in pathophysiology and clinical symptoms of osteoarthritis. *Nat. Rev. Rheumatol.* **2010,** 6, 625-35

24. Everts V., Delaisse J.M., Korper W. and Beertsen W., Cysteine proteinases and matrix metalloproteinases play distinct roles in the subosteoclastic resorption zone. *J. Bone Miner. Res.* **1998,** 13, 1420-30

25. Rindfleisch J.A. and Muller D., Diagnosis and management of rheumatoid arthritis. *Am. Fam. Physician.* **2005**, 72, 1037-47

26. Boers M., Rheumatoid arthritis. Treatment of early disease. *Rheum. Dis. Clin. North Am.* **2001**, 27, 405-14

27. Hinton R., Moody R.L., Davis A.W. and Thomas S.F., Osteoarthritis: Diagnosis and therapeutic considerations. *Am. Fam. Physician.* **2002**, 65, 841-48

28. Kent Kwoh C., Guidelines for the management of rheumatoid arthritis. American College of Rheumatology Ad. Hoc. Committee on Clinical Guidelines. *Arthritis Rheum.* **1996**, 39, 713-22

29. Smolen J. S. and Steiner G., Therapeutic strategies for rheumatoid arthritis. *Nat. Rev. Drug discov.* **2003**, 2, 473-88

30. Brooks P. M., Management of Rheumatoid Arthritis. *Medicine*, **2002**, 30, 50-53

31. Scott D. L., Wolfe F. and Huizinga T. W. J., Seminar Rheumatoid arthritis. *The Lancet*, **2010**, 376, 1094-08

32. Kinvan J.R., The effect of glucocorticoids on joint destruction in rheumatoid arthritis. The Arthritis and Rheumatism Council Low-Dose Glucocorticoid Study Group. *N. Engl. J. Med.* **1995**, 333, 142-46

33. Moreland L.W., Heck L.W. and Koopman W.J., Biologic agents for treating rheumatoid arthritis. Concepts and progress. *Arthritis Rheum.* **1997**, 40, 397-09

34. Roessler F.J., Allen E.D., Wilson J.M., Hartman J.W. and Davidson B.L., Adenoviral mediated gene transfer to rabbit synovium *in vivo*. *J. Clin. Invest.* **1993,** 92, 1085-92

35. Courtney P. and Doherty M., Key questions concerning paracetamol and NSAIDs for osteoarthritis. *Ann. Rheum. Dis.* **2002,** 61,767-73

36. Recommendations for the medical management of osteoarthritis of the hip and knee: 2000 update. American College of Rheumatology Subcommittee on Osteoarthritis Guidelines. *Arthritis Rheum.* **2000**, 43, 1905-15 (No authors listed)

37. Moore R.A., Tramer M.R., Carroll D., Wiffen P.J. and McQuay H.J., Quantitative systematic review of topically applied non-steroidal anti-inflammatory drugs. *BMJ.* **1998**, 316, 333-38

38. Freidman D.M. and Moore M.E., The efficacy of intra-articular steroids in osteoarthritis: a double-blind study. *J Rheumatol.* **1980**, 7, 850-56

39. Manek N. J. and Lane N.E., Osteoarthritis: current concepts in diagnosis and management. *Am. Fam. physician.* **2000**, 61, 1795-04

40. Jones A.C., Pattrick M., Doherty S. and Doherty M., Intra-articular hyaluronic acid compared to intra-articular triamcinolone hexacetonide in inflammatory knee osteoarthritis. *Osteoarthritis Cartilage.* **1995**, 3, 269-273

41. Felson D.T., Lawrence R.C., Hochberg M.C., McAlindon T., Dieppe P.A., Minor M.A., Blair S.N., Berman B.M., Fries J.F., Weinberger M., Lorig K.R., Jacobs J.J. and Goldberg V., Osteoarthritis: New insights. Part 2: Treatment approaches. *Ann Intern Med.* **2000**, 133, 726-37

42. Nesic D., Whiteside R., Brittberg M., Wendt D., Martin I. and Mainil-Varlet P., Cartilage tissue engineering for degenerative joint disease. *Adv. Drug. Deliv. Rev.* **2006**, 58, 300-22

43. Ahmed S. M., NSAIDs: Chemistry and Pharmacological Actions. *American Journal of Pharmaceutical Education.* **2003**, 67, 1-7

44. Vane J.R., Inhibition of prostaglandin synthesis as a mechanism of action for aspirin-like drugs. *Nat. New. Biol.* **1971,** 231-32

45. F.S.K.Barar, Non-narcotic analgesics and antipyretics Essentials of Pharmacot-herapeutics. S. Chand and company Ltd, New-Delhi, third ed.; **2005**, 117

46. Amanda R., Deirdre D., John H. and Tanya P. NSAID Prescribing Precautions. *Am. Fam. Physician.* **2009**, 80, 1371-78

47. Freudenburg E. and Gyorgy P., *Biochem. Z.* **1921**, 116, 96

48. Boyd E.S. and Newman W.F., Ion binding properties of cartilage. *J. Biol. chem.* **1951**, 193, 243

49. Klotz I. M. and Curme I. G., *J. Am. Chem. Soc.*, **1948**, 70, 939

50. Roche J. and Deltour G., *Bull. Soc. chim. biol.* **1943**, 26, 1260

51. Khursheed A. and Lloyd J.R., Distribution of hexamethonium and other quaternary ammonium compounds in cartilage. *J. Pharmacol. Exp. Ther.* **1971**, 176, 83-92

52. Maurizis J.C., Ollier M., Nicolas C., Madelmont J.C., Garrigue H. and Veyre A., *In vitro* binding of oxime acetylcholinesterase reactivators to proteoglycans synthesized by cultured chondrocytes and fibroblasts. *Biochem. Pharmacol.* **1992.** 44, 1927-33

53. Giraud I., Rapp M., Maurizis J.C. and Madelmont J.C., Application to a Cartilage Targeting Strategy. *Bioconjugate Chem.* **2000**, 11, 212-18

54. Nicolas C., Verny M., Giraud I., Ollier M., Rapp M., Maurizis J. and Madelmont J., New Quaternary Ammonium Oxicam Derivatives Targeted toward Cartilage. *J. Med. Chem.* **1999**, 42, 5235-40

55. Yadav M.R., Pawar V.A., Marvaniya S.D., Halen P.K., Giridhar R. and Mishra A.K., Site specific chemical delivery of NSAIDs to inflamed joints: synthesis, biological activity and gamma-imaging studies of quaternary ammonium salts of tropinol esters of some NSAIDs or their active metabolites. *Bioorg. Med. Chem.* **2008**, 16, 9443-49

AIMS AND OBJECTIVES

Aims and Objectives

Literature Survey revealed that treatment of arthritis (RA or OA) requires lifelong therapies thereby various strategies were developed to treat arthritis including development of drugs from different chemical classes and various drug delivery systems.

Oral drug delivery is a widely accepted delivery system but it produces side effects during treatment due to widespread distribution of the drug throughout the body, while and arthritis may be associated only with one or more joints. So in order to avoid these side effects delivery systems with ability to deliver the drug to the required site is essential. Percutaneous delivery systems are used for mild to moderate pain associated with joints and produce negligible side effects due to local application but the drugs may have varying (<1 %) skin permeability as skin is the main barrier for this. In IA delivery systems drug is directly instilled into the joint cavity hence these are used only where cartilage damage occurs very fast. IA administered drugs have very low joint residence time so there is need to develop delivery systems which will have long residence time within the joint cavity and release the drug over a prolonged periods of time.

The present work was undertaken with the aim of developing various drug delivery systems of NSAIDs having long half life for the treatment of arthritis mainly RA and OA. The present work is classified mainly into the following four types as shown in **Fig. 2.1**

1. Intra-Articular Chemical Delivery Systems (IA-CDS)
2. Percutaneous Drug Delivery Systems (PDDS)
3. Intra-Articular Liposomal Drug Delivery Systems (IA-LDDS)
4. Oral Drug Delivery Systems (ODDS)

1. Intra-Articular Chemical Delivery Systems (IA-CDS)

The aim of this work was to develop cationic chemical delivery systems (CDS) of various NSAIDs to improve drug residence time in joints on IA administration.

2. Percutaneous Drug Delivery Systems (PDDS)

The objective of this study was to investigate the usefulness of the salt formation and prodrug approaches to improve the percutaneous delivery of some NSAIDs such as 6-methoxy-2-naphthylacetic acid (6-MNA) and biphenylacetic acid (BPA) for the treatment of rheumatic diseases.

3. Intra-Articular Liposomal Drug Delivery Systems (IA-LDDS)

The aim of the current work was to develop cationic liposomal formulations containing NSAIDs having long half life, selectivity towards COX-II enzyme and affinity towards joint cavity so as to improve the overall therapeutic efficacy of these agents after encapsulating them into liposomal formulation.
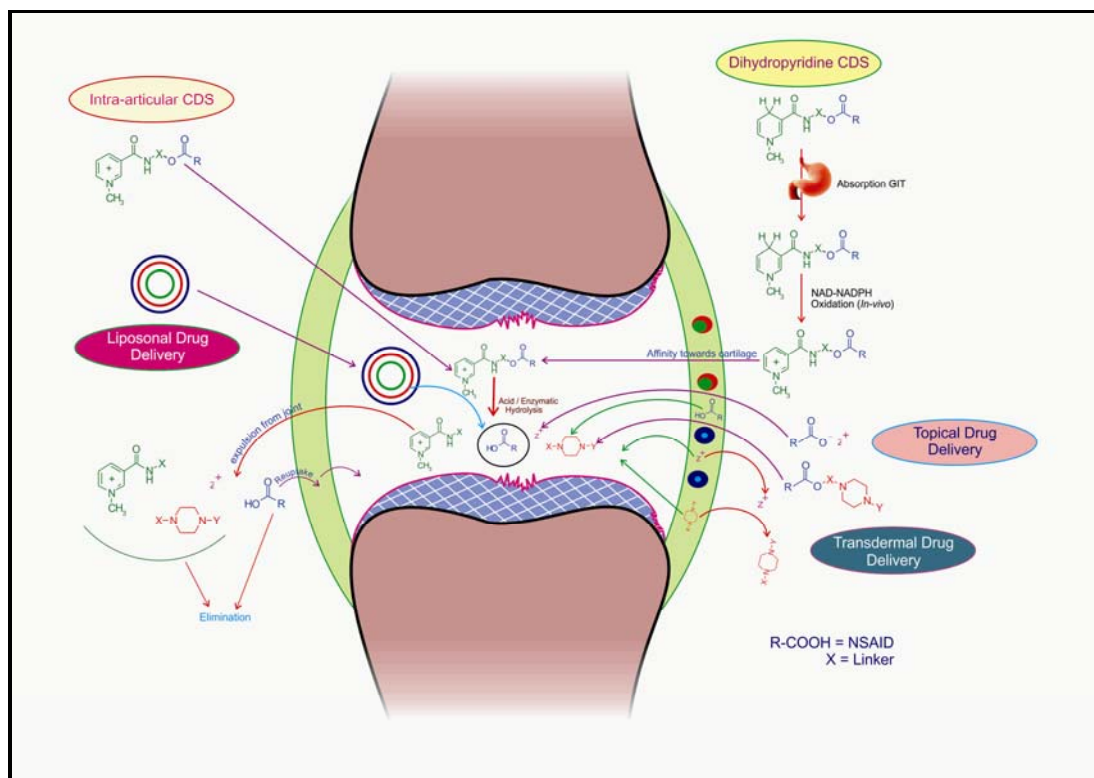
Fig. 2.1: Strategies for delivery of NSAIDs and their fate after administration

4. Oral Drug Delivery Systems (ODDS)

The aim of this work was to prepare dihydropyridine derivatives of some NSAIDs. These derivatives would be initially non-ionic in nature but would get oxidized *in vivo* by NAD-NADPH co-enzyme system to generate pyridinium ion. Such derivatives would retain the advantages of quaternary ammonium compounds i.e. their site specificity but would solve the oral bioavailability problems of these agents when taken orally.

The basic principle behind the development of these CDS is further discussed in detail in the respective section.

Section-I

INTRA-ARTICULAR DRUG DELIVERY

Introduction

Local drug action within the joint cavity is essential for the treatment of arthritic disorders and for relief from the associated pain and inflammation.[1] Intra-articular (IA) injection is one of the methods to deliver drugs within the joint cavity and corticosteroids were the first substances to be injected locally into the IA space.[2] Hydrocortisone was first used for IA injection in 1951 and was found to lower indicators of the inflammation response, including IA leukocyte count.[3] Since then various corticosteroid suspensions have been used to combat pain and inflammation associated with osteoarthritis (OA) or active rheumatoid arthritis (RA), but the use of corticosteroids in arthritis has been controversial. Animal studies have suggested that multiple corticosteroid injections might alter cartilage protein synthesis and consequently damage the cartilage.[4] These deleterious effects curbed early enthusiasm for IA corticosteroid therapy in arthritis. However other studies suggest that primate joints respond differently than those of rodents and corticosteroids may be useful when used appropriately.[5] IA deliveries provide advantages as compared to other routes for the treatment of active arthritis or OA using corticosteroids or other therapeutic agents such as non-steroidal anti-inflammatory agents (NSAIDs), visco-supplementation etc.

Development of long acting IA delivery system is not an easy task as it has to be based on adequate knowledge of chemical, pharmaceutical and biological disciplines and it is multidisciplinary in nature. There are various factors which influence the fate of drug molecules once they are released from the immobilized depot in the joint cavity, so it is important to understand anatomy and physiology of synovial joints in detail. [1]

1. Synovial joints: The primary role of joints is to provide mobility and stability to the skeleton. The bones of synovial joints are held together by fibrous capsule and accessory ligaments. The inner surface of the capsule is lined by the synovium and the articular surfaces are covered by the hyaline cartilage; further their contact is facilitated by synovial fluid (SF) acting as lubricant.[6] Various components of synovial joints are synovium, synovial fluid, cartilage and bone as shown in **Fig. 1.1**

1.1. Synovium: The synovium consists of two layers, the inner intima layer and a deep subintima. Within the intima are the synovial lining cells of type A and B. One third of the synovial membrane cells are comprised of type-A synviocytes that are macrophages which clear debris within the membrane. Type-B synoviocytes are the most prevalent cells

closely resembling fibroblasts and they synthesize hyaluronic acid (HA), a very long chain glycosaminoglycan.[6]
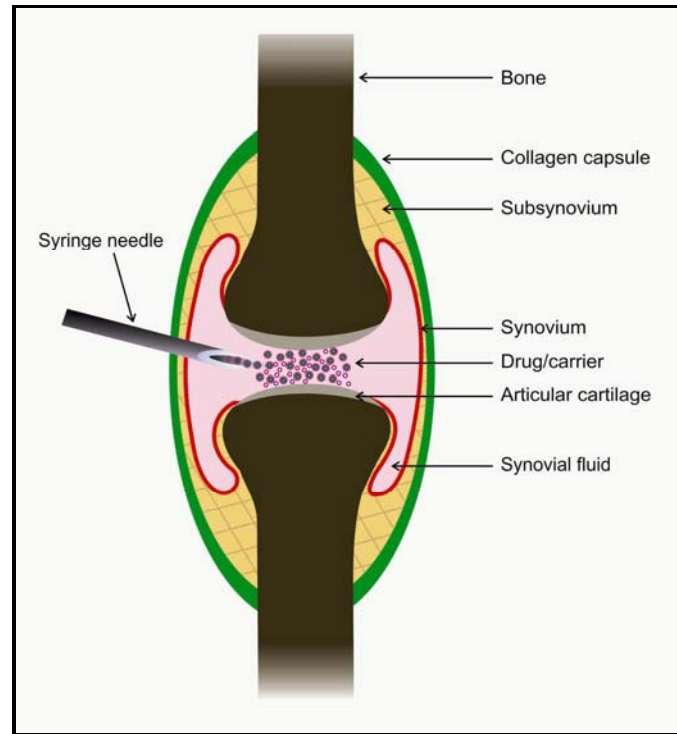
Fig. 1.1: Synovial joint

The synovium performs several functions such as ultra-filtration of plasma and synthesis of HA by type-B synoviocytes from the SF which is essential for the preservation of the low coefficient of friction between the surfaces of articular cartilages and provides the nutrients.[6]

1.2.   Synovial fluid

The synovial fluid (SF) is present in the cavity of synovial joint. It is a viscous, non-Newtonian fluid exhibiting thixotropic properties. The average volume of SF in normal human adult knee joint is about 2 ml.[6] This volume can increase up to several hundred milliliters under pathological conditions.[7] SF can be distinguished from plasma by the presence of HA (0.35 g/100 ml) and lubricin (0.005 g/100 ml approx.). These two molecules are the major contributors of SF viscosity and are also important for one of its main functions i.e. to act as lubricant of the joint surfaces.

1.3.   Articular cartilage

Articular cartilage provides each moving bony portion of a joint with a smooth, frictionless surface. It is capable of reversible compression, distributing an applied load

homogeneously and minimizing contact stress to the underlying bone. The structure and function of cartilage and its matrix components have been maintained throughout the life by the resident chondrocytes as described earlier in detail in introductory part.

2. Drug transport and distribution process in synovial joints

In the joint cavity, the solute drug molecule, once released from the immobilized depot, may take part in a number of reactions and distribution (equilibrium) processes before it is eventually cleared from the synovial space. These processes, the relative importance of which is determined by the physicochemical properties of the drug substance and the barrier properties of the synovium are shown in schematic diagram **(Fig. 1.2)**. Concomitant to binding of the drug to components of the SF, its transport and distribution into the synovium and articular cartilage and subsequent uptake by synoviocytes and chondrocytes may occur.[1]
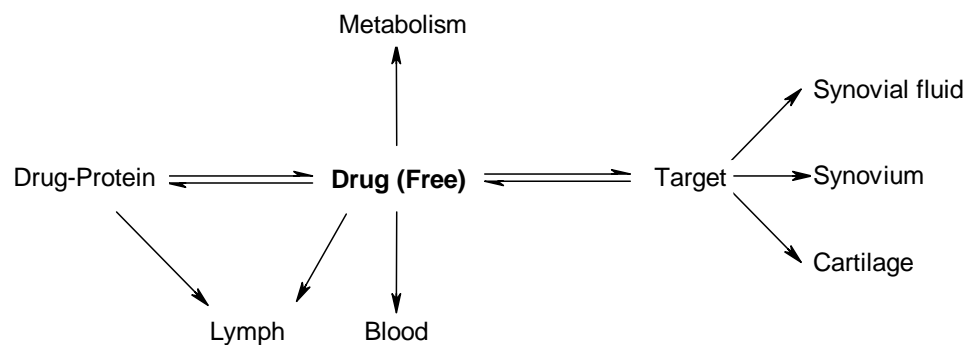
Fig.1.2: Schematic representation of drug transport and distribution processes in the joint.

2.1. Trans-synovial transport

The synovium constitutes the main barrier for drug transport out of the joint cavity due to its complex architecture. The healthy synovial lining is thin (60 μm) and discontinuous without intercellular junctions. Together with the ECM, the synoviocytes function as a permeable, inhomogeneous matrix.[1] The healthy joint is penetrated by capillaries close to the surface of the synovium (modal depth 35 μm in man).

Upon oral drug administration, observed joint C_{max} and T_{max} values are usually lower and occur at later time points respectively, than the corresponding parameters in plasma.[8] For many NSAIDs, plasma/SF drug concentration ratios have been found to reflect plasma/synovial protein concentration ratios. Further, free NSAID concentrations have been found to be similar in the two compartments after attainment of steady state conditions. Often the SF concentrations are more sustained than plasma concentrations

after oral or i.v. administration.[8] Due to continuous drug entrance from the blood compartment, IA elimination half-lives ($t_{1/2}$) estimated from pharmacokinetic profiles obtained following oral administration may tend to underestimate the ''true'' rate of drug disappearance from the SF after IA administration. By appropriate corrections, however, reasonable estimates of rates of disappearance from joints relevant to IA administration can be extracted from oral pharmacokinetic data as shown in **Table 1.1** below.

As apparent, relatively fast disappearance from the joint is observed for small solutes with $t_{1/2}$ values in the range of about 0.1 to 6 h. In this connection disappearance kinetics from the joint cavity has often been described by simple first-order kinetics.

Table 1.1: Synovial disappearance half-lives ($t_{1/2}$) and molecular weights (MW) of various solutes.[1]

No	Compound	$t_{1/2}$ (h)	MW (g/mol)
1	Albumin	1.23*	6.7×10^4
2	Procaine	0.80*	236
3	Diclofenac	5.2	296
4	Salicylic acid	2.4	138
5	Paracetamol	1.1	151
6	Etodolac	4.1	287
7	Ibuprofen	1.9	206
8	Indomethacin	3.3	358
9	Tenoxicam	2.6	337
10	Flurbiprofen	3.4	244
11	Ketoprofen	1.9	254
12	Naproxen	1.6	230
13	Tiaprofenic acid	1.5	260
14	Tolmetin	2.2	257
15	^{14}C-Cortisone	1.3	360

*Values relate to IA administration in animal model (other values from oral dosing)

2.2. Drug transport into cartilage

After IA administration drugs are likely to distribute from the SF into various joint tissues. Calculations on glucose transport, to feed the chondrocytes of the articular cartilage, have revealed that diffusion of this nutrient in the relatively viscous SF might be too slow for reaching the center of larger joints. Instead joint motion is suggested to generate additional solute transport by convection.[9] Upon attainment of a uniform glucose concentration in the SF, diffusion into cartilage is sufficiently fast to supply the chondrocytes with this nutrient. Similar considerations may be of relevance for drug distribution in the joint cavity. At the SF-cartilage interface two major parameters govern the efficiency of solute transport into the cartilage ECM, that is, the size and the charge of the solute.

3. Pharmacokinetic fate of IA administered drugs[10]

IA injection of aqueous solutions of relatively high doses of drugs for example corticosteroids, local anaesthetics, and NSAIDs results in diffusion of drug rapidly into the blood and consequently duration of drug action is relatively short[8,10,11] First-order transfer rate constants for drug transport out of the synovial space have been reported for various NSAIDs, including diclofenac, etodolac, ibuprofen, indomethacin and tenoxicam.[12] Almost identical transfer rate constants were found with a mean value of 0.32 ± 0.12 h^{-1} and hence, corresponding half-lives of approximately 2 h. Thus, prolongation of drug residence time within the joint has to be accomplished by transient immobilization of the injected dose in the form of depot formulations.

Rational design of IA depot formulations requires an in-depth understanding of **(i)** the physicochemical and enzymatic events, which are likely to be operating for drugs injected into the synovial space and **(ii)** the time dependence of these interrelated events each of which influences drug residence time in the joint.

4. Residence time of drug in synovial joints

The short half-life of IA administered drugs can be explained by the synovial ultra-structure which offers little barrier to the diffusion of molecules in and out of the joint. As a consequence of the synovial ultra-structure there is free trans-synovial flux of water and solutes such that the volume of fluid in a joint cavity is completely replaced many times over in 24 h.[6] Small molecules (MW < 10,000 Da) such as lactate, cytokines and most

drugs, including NSAIDs, local anaesthetics (LA), diffuse easily through the interstitium and across capillary walls and therefore exist in equilibrium between SF and plasma.[13]

Albumin also diffuses easily through the interstitium; the reflection of albumin by the synovium is negligible for practical purposes.[14] SF is therefore a dialysate of plasma plus HA secreted by type-B synoviocytes. Even with HA, multiple (3-5) weekly injections are needed in order to achieve efficacious OA treatment. There is a need for sustained release delivery systems if the potential of IA drug administration for the anti-arthritics is to be realised.[15]

4.1. Factors affecting performance of IA drug delivery

The direct delivery of a drug to an affected joint offers the possibility of reaching high drug concentration at the site of action with minimum systemic exposure. Besides the minimum systemic toxicity there are other factors that may contribute to show adverse effects or decreased efficacy of IA delivery as described below:

   4.1.1. Size

   4.1.2. Shape

   4.1.3. Quantity

   4.1.4. Charge

   4.1.5. Rate of drug release

   4.1.6. Number of injections

4.1.1. Size

Concerning the size of the IA administered particles, the discussion on the work done in the field will focus on liposomes, microparticles (microsphere), and nanoparticles emphasizing aspects such as joint retention and phagocytosis as a function of size. Drugs are cleared from SF by lymph drainage, which is largely dependent on the size of the molecule.

The clearance of albumin from SF in knees of OA patients is about 0.04 ml/min, corresponding to a turnover of about 1 h. In other studies the residence time of NSAIDs in SF was shown to be as short as 1-5 h.[1] Bonanomi *et al*. reported that increasing the size of liposomes, ranging from 160 nm to 750 nm in diameter, resulted in a 2.6-fold increase in retention to 48 h post-injection.[16-17] A similar observation was described for liposomes containing methotrexate, for which a mean diameter of 1.2 μm ensured a higher retention, and thus anti-inflammatory action, than 100 nm sized liposomes.[18-19] There is an upper limit (40-250 nm radius) to the size of particles that can escape freely from the joint

cavity. Albumin possesses a hydrated molecular domain of 3.55 nm and HA has a radius of gyration of 100-200 nm.[20] Possibly the simplest means of prolonging drug residence time within joints is to formulate a microsphere (MS) of size >250 nm and thereby exploit size inclusion. The fate of biocompatible MS is size dependent, those <10 μm (optimally between 1 and 4 μm) in diameter are phagocytosed by the SF and synovial resident and recruited macrophages, without evoking a neutrophil response. Larger MS (>4 μm) are not phagocytosed, but are sequestered as subsynovial granulation plaques, surrounded by giant cells.[15,21]

4.1.2. Shape

Not only the size, but also the shape of the particles injected into the joint is important for triggering an immune response. Irregularly shaped microparticles have been demonstrated to promote tissue inflammation in comparison to the round shaped drug delivery systems. In this respect, Liggins *et al*. showed that irregularly, milled chitosan particles induced joint inflammation despite the known articular biocompatibility of this biomaterial.[22] Similar histological observations showing marked inflammation in the synovial membrane and the subsynovial lining were made by Ratcliffe *et al*. for poly-*L*-lactic acid (PLA) and poly(butyl cyanoacrylate) microparticles obtained by simple polymer grinding.[24] Thus, to avoid inflammatory reactions subsequent to the administration of irregularly shaped particles, round-shaped particles are to be preferred for IA drug delivery.[19] This fact was also supported by evidence obtained by injecting IA suspensions. Due to the crystalline nature drugs generate inflammatory conditions leading to crystal induced arthritis.[19]

4.1.3. Quantity

Apart from size and shape the quantity of IA injected drug delivery system, is also important to the appearance of an immune response, as shown in the studies conducted by Nishide *et al*. They demonstrated an enhanced number of white blood cells with increasing amounts of injected microparticles, from 5 to 40 mg per knee.[25] In contrast, no significant dose dependent inflammatory effect was observed for paclitaxel embedded small Poly-Lactide-co-glycolide (PLGA) microparticles after IA administration of 15 to 75 mg of particles per joint in healthy rabbit knees.[19,26]

4.1.4. Charge

Little information is available on the effect of charge on disappearance rates through the synovium. In the study performed by Simkin and Pizzorno, it was found that synovial permeability of magnesium and calcium was lower than for other small neutral

molecules investigated.[1,27] Literature survey also revealed that introduction of a quaternary ammonium function on oxicam structures greatly increased their affinity for the cartilaginous tissues.[28] These findings suggest that positively charged molecules may interact with negatively charged sugars present in cartilage and may improve drug residence time with joint cavity.

4.1.5. Release profile

If the drug is released rapidly then efficacy is likely to be approximately to that of free drug and hence it offers no therapeutic advantage. A worse scenario is that the drug is released too slowly resulting in target tissues being exposed to sub-therapeutic dose levels thus having little or no efficacy. Achieving the middle ground, sustained drug release at levels within the therapeutic range *in vivo* may be possible through rational drug delivery design for which rigorous *in vitro* characterization of release kinetics required to be done.[15]

4.1.6. Number of injections

An obvious drawback of IA injection is discomfort, pain and possible risk of infection. Therefore the number of IA injections per year should be reduced to a minimum. These complications coupled with short residence time of the drug in joint cavity underscores the need for the development of sustained release formulations for IA delivery.[1]

5. Drug delivery strategies in joint disease

In RA, the local inflammatory reaction in and around joint tissues promotes an acidic environment. This is partially due to the low levels of oxygen in the synovial tissue and fluid, which appears to induce a shift towards anaerobic glycolysis and lactate formation.[30] In some cases, *p*H values of SF have been reported to be as low as 6.[31-32] Considering the buffering capacity of SF, a much lower *p*H value in the synovial tissue may be expected. In addition, there seems to be a direct correlation between the low *p*H of the joint tissues and indices of disease severity. The low *p*H has also been associated with local osteoclast activity and bone destruction.[33] For OA, cartilage damage of the joint has been associated with a significant drop of *p*H at the articular cartilage surface, which may contribute to high activities of cathepsins in cartilage destruction.[30] The drug delivery strategies based on the low *p*H value of synovial joint of the RA and OA (such as *p*H

sensitive and temperature sensitive gel) and the negative charge of the cartilage (cationic colloidal delivery systems), are in the developmental stage.

6. Literature review

It has been reported that first-order transfer rate constants operate for various NSAIDs, in synovial space.[10] These half-lives vary between 1 and 2 h for cortisone, naproxen or ketoprofen and up to 22-26 h for hyaluronan.[19] In other studies the residence time of NSAIDs in SF has been shown to be as short as 1-5 h.[23] The clearance of albumin from SF in knees of OA patients was estimated to be about 0.04 ml/min, corresponding to a turnover of about 1 h. So in terms of absorption and distribution into the systemic circulation, the IA route is equivalent to other non-i.v. parenteral routes of administration.[19]

Derendorf *et al.*[34] investigated the pharmacokinetics of glucocorticoid formulations following IA injection. These studies showed that the residence time of poorly soluble glucocorticoids administered as suspension formulations (e.g., rimexolone, triamcinolone acetonide) in the knee joint was longer than for the soluble glucocorticoids administered as solution formulations (e.g. betamethasone hydrogen phosphate disodium).[34] This is due to the fact that the dissolved molecules rapidly undergo clearance from the knee joint, while the solid particles of suspension formulations need to dissolve prior to being cleared from the joint. Thus, the residence time of an IA injected compound in the knee joint depends mainly on its solubility and dissolution rate.[6]

In some cases formulations are available as suspensions or dry powders due to solubility or stability issues related to the drugs. But due to the crystalline nature, these drugs can generate inflammatory conditions upon IA injection, leading to crystal-induced arthritis which is observed in 10 % of the patients, but disappearing within a few days.[35] Along with this, controlled growth of crystals also bears the risk of poor biocompatibility of the suspension formulation upon IA injection.

In case of LipotalonR® a liposomal formulation containing modified dexamethasone i.e. dexamethasone-21-palmitate the solubility of the dexamethasone derivative is reduced due to the covalent bonding of the fatty acid chain, thereby enabling the inclusion of the compound into a liposomal formulation from which the drug is slowly released following IA injection.[6]

The potential of liposomes to increase the IA residence time of drugs was first suggested in 1976 by Shaw *et al.*[36] which represented an important drug delivery system

with valuable clinical utility for IA drugs. Bonanomi *et al*. reported that the encapsulation of dexamethasone palmitate in liposomes resulted in improved retention compared to microcrystalline triamcinolone acetonide.[16] Additionally, follow up study showed that increasing the size of these liposomes ranging from 160 nm to 750 nm in diameter, resulted in a 2.6-fold increase in retention to 48 h post-injection.[17]

Hydrocortisone encapsulated liposomes remarkably improved subjective and objective indices of inflammation after 48 h, with a slow return to the pre-injected state after 2 weeks. So, liposomes have been shown to be very efficient systems in the local treatment of joint diseases in laboratory animals and also in humans.

In the early studies, liposomes showed limited efficacy following IA injection due to rapid release of the drug and its leakage into the circulation. However, Williams *et al*.[18] were able to demonstrate efficacy of liposomes in a rat antigen induced arthritis model by using liposomally conjugated MTX to reduce the rapid loss of MTX from the liposomes and the joint.[18,37]

Williams *et al*. reported that encapsulation of methotrexate in 1.2 μm sized liposomes reduced joint swelling by 26.5 % compared to only 3.5 % of the 100 nm sized liposomes after day 1 of their injection. Moreover, the effect was still notable 20 days after the injection of the liposomes.[18-19] **Fig. 1.3** Shows various treatment strategies for arthritis with their limitations and benefits

Niosomes, which are non-ionic surfactant-based liposomes, were studied for the local delivery of diclofenac sodium to treat arthritis. Radiolabelling study showed that lipogelosomes injected in rabbit arthritic joints showed the longest retention times compared to other formulations. The radioisotope was slowly released in such a way that 67 % of the initially injected radioactivity still remained present 24 h post-injection.[38]

Together with liposomes, another drug delivery system i.e microsphere represents one of the most widely studied means to decrease IA drug clearance. In this respect, Lu *et al*. reported that the mean residence time of flubiprofen got doubled compared to injection of the drug suspension.[40] Similar observations were made for a celecoxib solution compared to the celecoxib embedded chitosan microspheres, where the chitosan microspheres showed a 10-fold increase in the concentration of celecoxib in the joints after IA injection.[41]

Wigginton *et al*. studied pharmacokinetics of methotrexate (MTX), wherein the elimination of MTX (5 mg) from the joint was found to be biexponential over 24 h and the second dose was given after 24 h and the half-life was found to be 0.54 and 2.9 h

respectively. However, the authors concluded that MTX was clinically ineffective, primarily because the IA half-life of methotrexate was too short relative to the probable synovial cell cycle generation time. Repeated IA MTX doses produced better results.

Liang *et al.* formulated methotrexate embedded PLA microparticles and tested their pharmacokinetics after IA injection in healthy rabbits. As expected, the concentration of methotrexate in the synovial tissues following IA injection was found to be significantly higher in the group treated with microparticles compared to the one treated with the drug solution.[42]

Horisawa *et al.*[21] showed PLGA nanoparticles (mean diameter 265 nm) were extensively phagocytosed and subsequently transported through the synovial membrane within 3-7 days. In contrast, microspheres (mean diameter 26 μm) were neither phagocytosed nor transported to the underlying synovial membrane, but they triggered a granulation reaction with multinuclear giant cells.[19]

Nishide *et al.* also supported these findings using poly-*D,L*-lactic acid (PDLLA) microspheres. The authors concluded that microspheres with diameters larger than 20 μm were neither internalised into macrophages, nor did they produce important inflammatory responses when injected IA into healthy rabbit joints.[43]
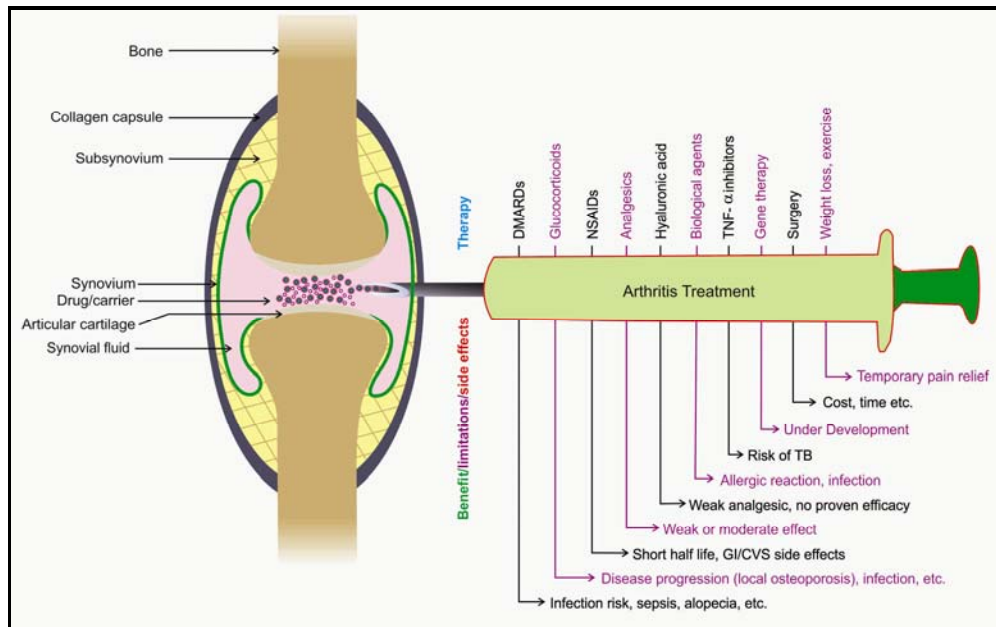

Fig. 1.3: Benefits, limitations and adverse effects of various anti-arthritic agents.

Liggins *et al.* have conducted studies to observe of the effect of size and dose of microspheres on biocompatibility or tolerability in rabbit joints.[45] They have shown that

PLGA microspheres of a smaller size range of 1-20 µm produced a greater inflammatory response in rabbit joints than larger sized microspheres (35-105 µm).[37] The phagocytosis of microspheres by synovial macrophages improved the retention of microspheres in the joint and also ensured an increased drug concentration in inflammatory cells and delayed clearance from the joint minimizing drug exposure to cartilage.[28,44]

Ramesh *et al.* pointed out that no drug was detected in the serum of healthy rabbits 7 h after the IA injection of dexamethasone encapsulated in PLA microparticles, thus concluding that dexamethasone release is localised in the joint.[46] In contrast, a small quantity of methotrexate was detected in rabbit plasma 5 min post-injection of PLA microparticles, mostly due to a burst release of the drug from the particles.[47] Moreover, the microparticles, whose size was in the range of 30-100 µm, did not induce acute inflammatory reactions. From the above studies it can be concluded that the most suitable size for microsphere is between 5 and 10 µm. This particle size range ensures capture of the particles by the synovial macrophages, a process that results in a prolonged retention time in the joint and also limits the inflammatory reactions.[19]

Rothenfluh *et al.* demonstrated that in order to achieve efficient carrier penetration into the cartilage, the carrier size plays important role. He coated nanoparticles with collagen-II binding peptide. Fluorescence measurement studies showed 14.9 fold preferential accumulation of 38 nm mean diameter nanoparticles within the cartilage relative to 96 nm diameter nanoparticles. This significant difference was attributed to the 60 nm pore size of the dense collagen network.[48] Rothenfluh *et al.*[48] demonstrated that the peptide decorated nanoparticles concentrated up to 72-fold more in the articular cartilage than nanoparticles displaying scrambled peptide sequence following IA injection in mice. Various drug delivery systems and their benefits or limitations or adverse effects are shown in **fig. 1.4**

Alternative approaches that might also benefit from an IA administration in terms of limitation of non-specific systemic binding, are targeting of the folic acid receptor FRb, which is up-regulated in activated synovial macrophages and targeting of E-selectin, which is an adhesion molecule that is up-regulated on the vascular endothelium of inflammed tissue.[19]

Amongst the physical methods the use of a magnetic field may improve the accumulation of magnetic drug delivery systems at the targeted site. In this respect, Tanaka *et al.*[49] used a 0.2 T permanent magnet implanted into the femur to increase the IA retention time of magnetic liposomes containing TGFb1. It was demonstrated that the

presence of a magnet leads to a more efficient retention of the liposomes in the joint and to a significant diminution of cartilage defects up to 12 weeks.[49] Butoescu *et al.* incorporated superparamagnetic iron oxide nanoparticles (SPIONs) in PLGA microparticles loaded with dexamethasone and achieved a joint residence time of at least 3 months.[50] Regarding the possible toxicity of the SPIONs, Schulze *et al.* demonstrated that 30-40 nm PVA-coated SPIONs were biocompatible with articular and periarticular tissues in sheep.[51]

Other studies on magnetic nanoparticles were conducted by Hellstern *et al.*[51] The authors observed that the nanoparticles are taken up by the reticuloendothelial system, and that the main organs in which the nanoparticles are detected after IA administrations are the liver and the spleen. Magnetic drug delivery systems need further investigation before the initiation of clinical trials to confirm the delivery of sufficient payloads to the joint, long-term retention and efficacy in arthritis or OA animal models.[19]

Thermally responsive elastin like polypeptide gels that can spontaneously aggregate after IA injection represent a simple and innovative way to prolong the IA half-life of a drug. These aggregating elastin like polypeptides form a drug depot resulting in a 25-fold longer half-life than drugs administered with the non-aggregating protein.[47] Research is going on to chemically couple the elastin like polypeptide to proteins, such as the IL-1 receptor antagonist, in order to achieve higher residence times.[47]
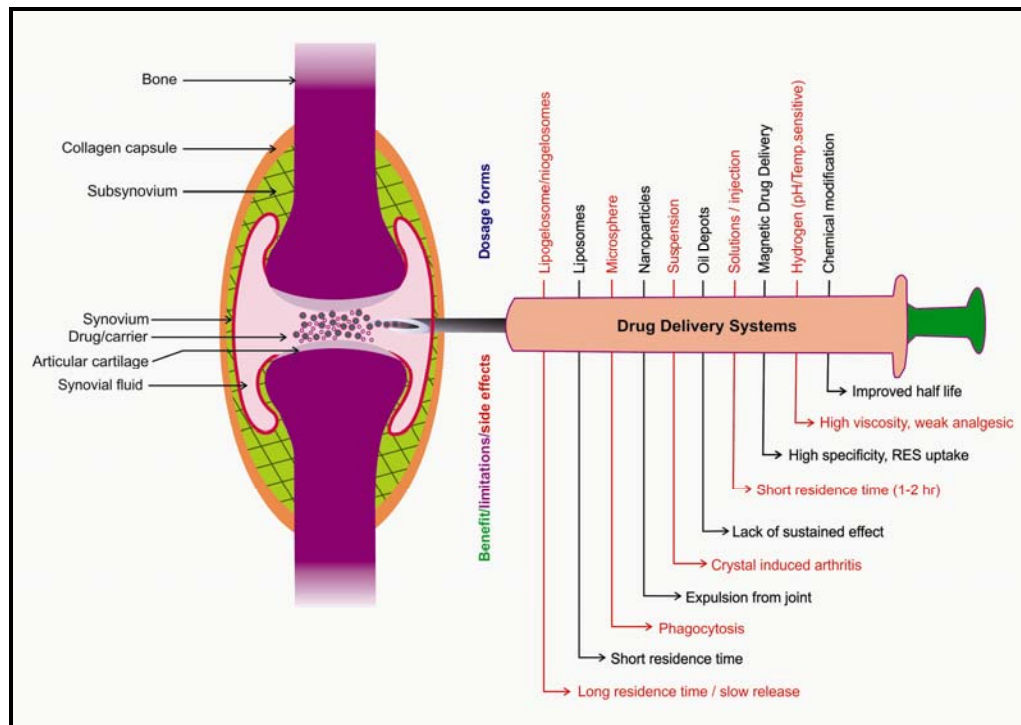
Fig. 1.4: Benefits, limitations and adverse effects of various drug delivery systems

As a possibility, a positively charged colloidal delivery system may be more specific in directing drugs to RA joints because of the EPR (enhanced permeability and retention) effect. The positive charge may help to prolong the retention time of the delivery system to allow complete release of the payload in the joint. The neutralisation of aggrecan negative charges by a positively charged delivery system may further weaken the mechanical strength of the cartilage. Therefore, it would be ideal if the positive charge of the delivery system resides temporarily in the cartilage only and eventually be cleared from the cartilage or degraded.[30]

Currently available therapy for IA injection includes (i) Celestone®/Soluspan® injection which contains 3 mg/ml betamethasone as betamethasone sodium phosphate and 3 mg /ml betamethasone acetate available as suspension (Mfg By: Schering Corporation), (ii) Depo-Medrol® contains methylprednisolone acetate 20/40/80 mg available in injection, suspension dosage form. (Mfg. by Pharmacia And Upjohn Co), (iii) Lipotalon® contains dexamethasone-21-palmitate manufactured by Merckle Pharmaceuticals.

References

1. Larsen C., Ostergaard J., Larsen S.W., Jensen H., Jacobsen S., Lindegaard C. and Andersen P.H., Intra-Articular Depot Formulation Principles: Role in the Management of Postoperative Pain and Arthritic Disorders. *J. Pharm. Sci.* **2008**, 97, 4622-54.

2. William L., Elizabeth D.L. and Lori L., Intra-Articular Injections. *Anaesthesiology Clin.* **2007**, 25, 853-62

3. David H. N., Intra-articular injections for osteoarthritis of the knee. *Cleveland clinic. Journal. of medicine.* **2006**, 73, 897

4. Chandler G.N. and Wright V., Deleterious effect of intra-articular hydrocortisone. *Lancet.* **1958**, 2, 661-63

5. Gibson T., Burry H., Poswillo D. and Glass J., Effect of intra-articular corticosteroid injections on primate cartilage. *Ann. Rheum. Dis.* **1977**, 36, 74-79

6. Gerwin N., Hops C. and Lucke A., Intraarticular drug delivery in osteoarthritis. *Adv. Drug. Deliv. Rev.* **2006**, 58, 226-42

7. Evans C.H., Gouze E., Gouze J.N., Robbins P.D. and Ghivizzani S.C., Gene therapeutic approaches transfer in vivo. *Adv. Drug. Deliv. Rev.* **2006**, 58, 243-58

8. Wallis W.J. and Simkin P.A., Antirheumatic drug concentrations in human synovial fluid and synovial tissue. Observations on extravascular pharmacokinetics. *Clin. Pharmacokinet.* **1983**, 8, 496-22

9. Maroudas A., Bullough P., Swanson S. and Freeman M., The permeability of articular cartilage. *J. Bone. Joint. Surg.* **1968**, 50B, 166-77

10. Pedersen B.T., Ostergaard J., Larsen S.W. and Larsen C., Characterization of the rotating dialysis cell as an in vitro model potentially useful for simulation of the pharmacokinetic fate of intra-articularly administered drugs. *Eur. J. Pharm. Sci.* **2005**, 25, 73-79.

11. Okuyama S. and Aihara H., 1984. The mode of action of analgesic drugs in adjuvant arthritic rats as an experimental model of chronic inflammatory pain: possible central analgesic action of acidic nonsteroidal antiinflammatory drugs. *Jpn. J. Pharmacol.* **1984**, 35, 95-103.

12. Elmquist W.F., Chan K.K. and Sawchuk R.J., Transsynovial drug distribution: Synovial mean transit time of diclofenac and other nonsteroidal antiinflammatory drugs. *Pharm. Res.* **1994**, 11, 1689-97

13. Divine J.G., Zazulak B.T. and Hewett T.E., Viscosupplementation for knee osteoarthritis: a systematic review. *Clin Orthop. Relat. Res.* **2007**, 455, 113-22.

14. Levick J.R., A method for estimating macromolecular reflection by human synovium, using measurements of intra-articular half lives. *Ann Rheum Dis.* **1998**, 57, 339-44

15. Edwards S.H., Intra-articular drug delivery: The challenge to extend drug residence time within the joint. *Vet. J.* **2011**, 190, 15-21.

16. Bonanomi M.H., Velvart M., Stimpel M., Roos K.M., Fehr K. and Weder H.G., Studies of pharmacokinetics and therapeutic effects of glucocorticoids entrapped in liposomes after intraarticular application in healthy rabbits and in rabbits with antigen-induced arthritis. *Rheumatol. Int.* **1987**, 7, 203-12.

17. Bonanomi M.H., Velvart M. and Weder H.G., Fate of different kinds of liposomes containing dexamethasone palmitate after intra-articular injection into rabbit joints. *J. Microencapsul.* **1987**, 4, 189-200.

18. Williams A.S., Camilleri J.P., Goodfellow R.M. and Williams B.D., A single intraarticular injection of liposomally conjugated methotrexate suppresses joint inflammation in rat antigen-induced arthritis. *Br. J. Rheumatol.* **1996**, 35, 719-24.

19. Butoescu N., Jordan O. and Doelker E., Intra-articular drug delivery systems for the treatment of rheumatic diseases: A review of the factors influencing their performance. *Eur. J. Pharm. Biopharm.* **2009**, 73, 205-18

20. Hirota K., Hasegawa T., Hinata H., Ito F., Inagawa H., Kochi C., Soma G., Makino K. and Terada H., Optimum conditions for efficient phagocytosis of rifampicin-loaded PLGA microspheres by alveolar macrophages. *J. Control. Rel.* **2007**, 119, 69-76

21. Horisawa E., Kubota K., Tuboi I., Sato K., Yamamoto H., Takeuchi H. and Kawashima Y., Size-dependency of *DL*-lactide/glycolide copolymer particulates for intra-articular delivery system on phagocytosis in rat synovium. *Pharm. Res.* **2002**, 19, 132-39.

22. Holland T.A. and Mikos A.G., Advances in drug delivery for articular cartilage *J. Control. Rel.* **2003**, 86, 1-14.

23. Owen S.G., Francis H.W. and Roberts M.S., Disappearance kinetics of solutes from synovial fluid after intra-articular injection. *Br. J. Clin. Pharmacol.* **1994**, 38, 349-55

24. Ratcliffe J.H., Hunneyball I.M., Smith A., Wilson C.G. and Davis S.S., Preparation and evaluation of biodegradable polymeric systems for the intra-articular delivery of drugs. *J. Pharm. Pharmacol.* **1884**, 36, 431-36

25. Nishide M., Kamei S., Takakura Y. and Tamai S., Fate of biodegradable *D,L*-lactic acid oligomer microspheres in the articulus. *J. Bioact. Compat. Polym.* **1999**,14, 385-98

26. Liggins R.T., Cruz T., Min W., Liang L., Hunter W.L. and Burt H.M., Intra-articular treatment of arthritis with microsphere formulations of paclitaxel: biocompatibility and efficacy determinations in rabbits. *Inflamm. Res.* **2004**, 53, 363-72

27. Simkin P.A. and Pizzorno J.E., Transsynovial exchange of small molecules in normal human subjects. *J. Appl. Physiol.* **1974**, 36, 581-87.

28. Nicolas C., Verny M., Giraud I, Ollier M., Rapp M., Maurizis J.C. and Madelmont J.C., New quaternary ammonium oxicam derivatives targeted toward cartilage: synthesis, pharmacokinetic studies, and antiinflammatory potency. *J. Med Chem.* **1999**, 42, 5235-40.

29. Yadav M.R., Pawar V.A., Marvaniya S.M., Halen P.K., Giridhar R. and Mishra A.K., Site specific chemical delivery of NSAIDs to inflamed joints. *Bioorg. Med. Chem.* **2008**, 16, 9443-49.

30. Wang D. and Brömme D., Drug delivery strategies for cathepsin inhibitors in joint diseases. *Expert Opin. Drug Deliv.* **2005**, 2, 1015-28

31. Goldie I. and Nachemson A., Synovial *p*H in rheumatoid knee joints. I. The effect of synovectomy. *Acta Orthop. Scand.* **1969,** 40, 634-41

32. Levick J.R., Hypoxia and acidosis in chronic inflammatory arthritis; relation to vascular supply and dynamic effusion pressure. *J. Rheumatol.* **1990**, 17**,** 579-82

33. Nordström T., Shrode L.D., Rotstein O.D., Romanek R., Goto T., Heersche J.N., Manolson M.F., Brisseau G.F. and Grinstein S., Chronic extracellular acidosis induces plasmalemmal vacuolar type H+ ATPase activity in osteoclasts. *J. Biol. Chem.* **1997**, 272, 6354-60.

34. Derendorf H., Möllmann H., Grüner A., Haack D. and Gyselby G., Pharmacokinetics and pharmacodynamics of glucocorticoid suspensions after intra-articular administration. *Clin. Pharmacol. Ther.* **1986**, 39, 313-17.

35. Ellman M.H. and Becker M.A., Crystal-induced arthropathies: recent investigative advances. *Curr. Opin. Rheumatol.* **2006**, 18, 249-55

36. Shaw I.H., Knight C. G. and Dingle J.T., Liposomal retention of a modified anti-inflammatory steroid. *Biochem. J.* **1976**, 158, 473-76

37. Burt H.M., Tsallas A., Gilchrist S. and Liang L.S., Intra-articular drug delivery systems: Overcoming the shortcomings of joint disease therapy. *Expert Opin Drug Deliv.* **2009**, 6, 17-26.

38. Türker S., Erdoğan S., Ozer A.Y., Ergün E.L., Tuncel M., Bilgili H. and Deveci S., Scintigraphic imaging of radiolabelled drug delivery systems in rabbits with arthritis. *Int. J. Pharm.* **2005**, 296, 34-43.

39. Schwendener R.A., Lagocki P.A. and Rahman Y.E., The effects of charge and size on the interaction of unilamellar liposomes with macrophages. *Biochim. Biophys. Acta.* **1984**, 772, 93-101.

40. Lu Y., Zhang G., Sun D., Zhong Y., Preparation and evaluation of biodegradable flurbiprofen gelatin micro-spheres for intra-articular administration. *J. Microencapsul.* **2007**, 24, 515-24.

41. Thakkar H., Sharma R.K., Mishra A.K., Chuttani K. and Murthy R.S., Efficacy of chitosan microspheres for controlled intra-articular delivery of celecoxib in inflamed joints. *J. Pharm. Pharmacol.* **2004**, 56, 1091-99.

42. Liang L.S., Jackson J., Min W., Risovic V., Wasan K.M. and Burt H.M. Methotrexate loaded poly (*L*-lactic acid) microspheres for intra-articular delivery of methotrexate to the joint. *J. Pharm. Sci.* **2003**, 93, 943-56.

43. Nishide M., Kamei S., Takakura Y. and Tamai S., Fate of biodegradable *D, L*-lactic acid oligomer microspheres in the articulus. *J. Bioact. Compat. Polym.* **1999**, 14, 385-98.

44. Ratcliffe J.H., Hunneyball I.M., Wilson C.G., Smith A. and Davis S.S., Albumin microspheres for intra-articular drug-delivery: investigation of their retention in normal and arthritic knee joints of rabbits. *J. Pharm. Pharmacol.* **1986**, 39, 290-95.

45. Hellstern D., Schulze K., Schöpf B., Petri-Fink A., Steitz B., Kamau S., Hilbe M., Koch-Schneidemann S., Vaughan L., Hottiger M., Hofmann M., Hofmann H. and von Rechenberg B., Systemic distribution and elimination of plain and with Cy3.5 functionalized poly (vinyl alcohol) coated superparamagnetic maghemite nanoparticles after intraarticular injection in sheep in vivo. *J. Nanosci. Nanotechnol.* **2006**, 6, 3261-68.

46. Ramesh D.V., Tabata Y. and Ikada Y., Bioabsorbable microspheres for local drug release in the articulus. *J. Bioact. Compat. Polym*. **1999**, 14, 137-49

47. Betre H., Liu W., Zalutsky M.R., Chilkoti A., Kraus V.B. and Setton L.A., Thermally responsive biopolymer for intra-articular drug delivery. *J. Control. Release.* **2006**, 115, 175-82.

48. Rothenfluh D.A., Bermudez H., O'Neil C.P. and Hubbell J.A., Biofunctional polymer nanoparticles for intra-articular targeting and retention in cartilage. *Nat. Mater.* **2008**, 7, 248-54.

49. Tanaka H., Sugita T., Yasunaga Y., Shimose S., Deie M., Kubo T., Murakami T. and Ochi M., Efficiency of magnetic liposomal transforming growth factor-beta 1 in the repair of articular cartilage defects in a rabbit model. *J. Biomed. Mater. Res. A.,* **2005**, 73, 255-63.

50. Butoescu N., Jordan O., Petri-Fink A., Hofmann H. and Doelker E., Coencapsulation of dexamethasone 21-acetate and spions into biodegradable polymeric microparticles designed for intra-articular delivery. *J. Micoencapsul.* **2008**, 25, 339-50

51. Schulze K., Koch A., Schopf B., Petri A., Steitz B., Chastellain M., Hofmann M., Hofmann H. and Von Rechenberg B., Intraarticular application of superparamagnetic nanoparticles and their uptake by synovial membrane an experimental study in sheep. *J. Magn. Magn. Mater.* **2005**, 293, 419-32

Aims and Objectives

Literature survey revealed that a drug in solution form is rapidly expelled from the joint cavity upon IA administration; so various drug delivery systems such as suspension, liposomes, microspheres etc. have been developed and tested, and have been found to be more effective than simple injection with improved residence time.[1] Cartilage tissue contains negatively charged polysaccharides so drug residence time could be improved upon IA administration if positive charge is present either on the drug moiety or on the drug carrier system. But little information is available on the effect of charge on disappearance rates through the synovium.[1]

In a study by Simkin and Pizzorno, it was found that synovial permeability of magnesium and calcium was lower than that of other neutral and small molecules investigated.[1,2] Literature survey also proved that introduction of a quaternary ammonium function on oxicam structure greatly increased its affinity for the cartilaginous tissues.[3] Quaternary ammonium tropinol esters also show affinity towards cartilage on i.v. administration. These findings suggest that positively charged molecules may interact with negatively charged polysaccharides present in cartilage and may improve drug residence time in the joint cavity.[4]

A positively charged colloidal delivery system may be more specific in directing drugs to RA joints because of the EPR effect. The positive charge may help to prolong the retention time of the delivery system to allow complete release of the payload in the joint. But the neutralisation of aggrecan negative charges by a positively charged delivery system may further weaken the mechanical strength of the cartilage. Therefore, it would be ideal if the positive charge of the delivery system resides only temporarily in the cartilage and get eventually cleared from the cartilage or gets degraded. Enhanced cell penetration of the positively charged delivery system may also raise the undesirable toxicity issues.[5]

The aim of the current work was to develop cationic chemical delivery systems (CDS) of various non-steroidal anti-inflammatory drugs (NSAIDs) to improve drug residence time in joints on IA administration for the treatment of active RA or OA. To develop an ideal chemical delivery system the carrier should be non-toxic, releases drug over a prolonged time and after complete release of the drug must get excreted from the joint without any adverse effects. To fulfill the above requirements it was planned to synthesize CDS of various NSAIDs using nicotinic acid (**1**) as carrier. Ackermann has

demonstrated that ingested nicotinic acid is partly excreted by the dog as trigonelline (**1A**) which has also been isolated by Linneweh and Reinwein from normal human urine.[6-7]

(1)   **(1A)**
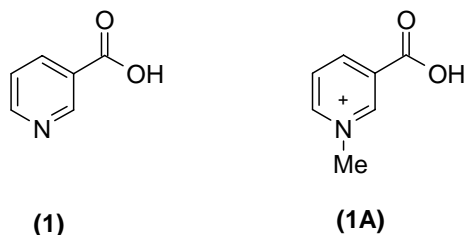
Herbert P. *et al.* have shown that normal human subjects excrete only 1-3 milligram of nicotinic acid and its derivatives (amide, glycine conjugate) daily compared to 30-50 mg. of trigonelline.[6] So trigonelline is a major excretory product of nicotinic acid metabolism with proven safety profile. Hence it was planned to develop CDS of various NSAIDs using this carrier. The general structure of the designed CDS is shown in F**ig. 2.1.**
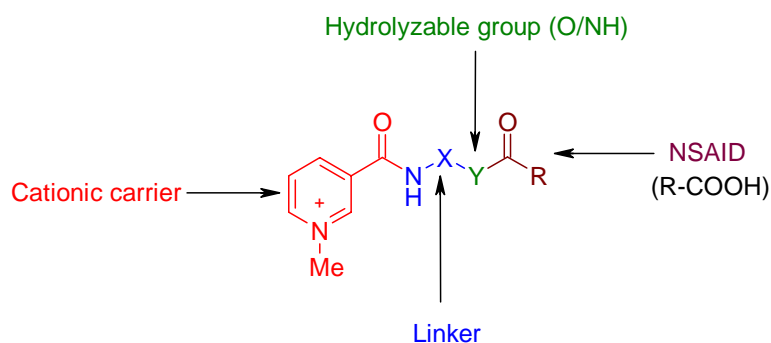
Fig.2.1: Schematic representation of cationic CDS.

The designed CDS contains positively charged pyridinium head linked to the drug through a suitable linker (X). This cationic group will interact with negatively charged polysaccharides present in the cartilage and will improve localization of the drug. Further, the designed CDS contains hydrolyzable functional groups such as ester/amide (Y=O/NH) which will undergo enzymatic and/or acid catalyzed hydrolysis to release the free drug (R-COOH) in a controlled manner.

As shown in **Fig. 2.2** once the CDS is injected by IA route it may adopt two pathways **(i)** it may be expelled from the joint as such and gets excreted or hydrolyzed in blood (*p*H 7.4) to liberate the active drug which might be again available to cartilage tissue by reuptake mechanism. **(ii)** The CDS remains in the joint space and slowly undergoes enzymatic or acidic hydrolysis, as synovial joint contains many enzymes and the *p*H of synovial fluid also gets decreased in inflammatory conditions (*p*H 6). So it was necessary

to study hydrolysis kinetics of the synthesized CDS in phosphate buffers of pH 6 and 7.4, and in human serum *in vitro*.
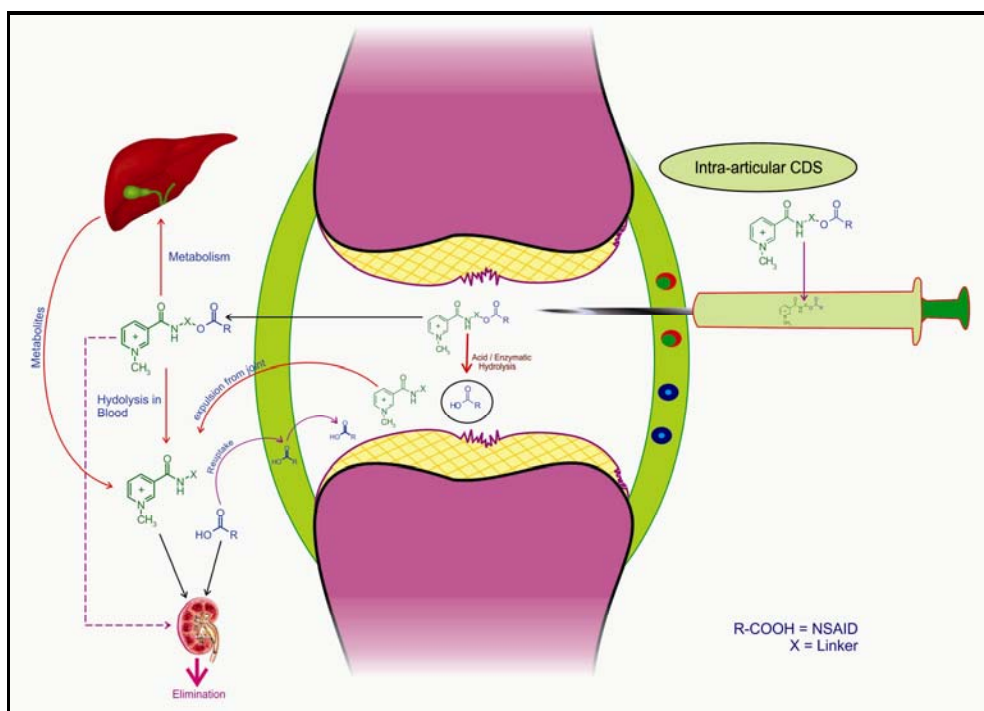
Fig. 2.2: Fate of IA administered CDS

Besides cartilage, the positively charged CDS and cationic metabolites of CDS may be deposited in the liver and gets cleared by the kidney. Therefore, liver and renal toxicity issues are important in development of these systems.[5] So it was planned to study *in vitro* cell cytotoxicity of the developed CDS and compare their relative toxicity with the parent NSAIDs.

Further it was also planned to evaluate joint localization and residence time (half life) of the synthesized CDS and the parent drugs using standard radiolabeling techniques using [99m]Technetium as radiolabeling agent.

References

1. Larsen C., Ostergaard J., Larsen S.W., Jensen H., Jacobsen S., Lindegaard C. and Andersen P.H., Intra-Articular Depot Formulation Principles: Role in the Management of Postoperative Pain and Arthritic Disorders. *J. Pharm. Sci.* **2008**, 97, 4622-54.

2. Simkin P.A. and Pizzorno J.E., Transsynovial exchange of small molecules in normal human subjects. *J. Appl. Physiol.* **1974**, 36, 581-87

3. Nicolas C., Verny M., Giraud I., Ollier M., Rapp M., Maurizis J.C. and Madelmont J.C., New quaternary ammonium oxicam derivatives targeted toward cartilage: synthesis, pharmacokinetic studies, and antiinflammatory potency. *J. Med. Chem.* **1999**, 42, 5235-40.

4. Yadav M.R., Pawar V.A., Marvaniya S.M., Halen P.K., Giridhar R. and Mishra A.K., Site specific chemical delivery of NSAIDs to inflamed joints: synthesis, biological activity and gamma-imaging studies of quaternary ammonium salts of tropinol esters of some NSAIDs or their active metabolites. *Bioorg. Med. Chem.* **2008**, 16, 9443-49.

5. Wang D. and Brömme D., Drug delivery strategies for cathepsin inhibitors in joint diseases. *Expert. Opin. Drug. Deliv.* **2005**, 2, 1015-28

6. Herbert P. S., William A. P. and Edward D. L., Synthesis and excretion of trigonelline. *J. Biol. Chem.* **1940**, 135, 483-85

7. Linneweh W. and Reinwein H., Isolation of trigonelline from human urine. *Z. physiol. Chem.* **1932**, 207, 48.

3. Results and Discussion

The work carried out towards achieving the proposed plan has been discussed under the following four main headings:

3.1. Chemical studies

3.2. Hydrolyses kinetics

3.3. Cytotoxicity studies

3.4. Biodistribution and gamma imaging studies

3.1. Chemical studies

To synthesize the envisaged CDS, a scheme was planned as given in general **Scheme-1**, wherein nicotinic acid **(1)** was reacted with ethanol in presence of sulphuric acid to obtain ethyl nicotinate[1] **(2)**. Ethyl nicotinate was further treated with aminoalcohols[2] **(3a-3e)** and diamines **(3f-3g)** to obtain various hydroxyalkylnicotinamide **(4a-4e)** and aminoalkylnicotinamide **(4f-4g)** derivatives. These nicotinamide derivatives **(4a-4g)** were coupled with various NSAIDs **(5I-5V)** to get ester **(6aI-6eV)** and amide **(6fI-6gV)** derivatives. The derivatives so obtained were quaternized using methyl iodide in acetonitrile or acetone as a solvent to obtain quaternary ammonium chemical delivery systems **(7aI-7gV)**. The two NSAIDs which were not available commercially but required for the development of CDS i.e. 6-methoxy-2-naphthylacetic acid (6-MNA) **(8)** and biphenylacetic acid (BPA) **(9)** were synthesized as per the reported procedures.[3]

The synthesis of the chemical delivery systems of various NSAIDs has been discussed under the following subheadings:

3.1.1. Chemical delivery systems of ibuprofen **(7aI-7gI)**

3.1.2. Chemical delivery systems of naproxen **(7aII-7gII)**

3.1.3. Chemical delivery systems of indomethacin **(7aIII-7gIII)**

3.1.4. Chemical delivery systems of 6-MNA **(7aIV-7eIV)**

3.1.5. Chemical delivery systems of BPA **(7aV-7eV)**

3.1.1. Chemical delivery systems of ibuprofen (7aI-7gI)

Ibuprofen **(5I)** is a clinically used NSAID belonging to the arylpropionic acid class; hence ibuprofen was chosen as one of the NSAIDs for the present work. The CDS of ibuprofen **(7aI-7gI)** were synthesized as depicted in **Scheme-1**. These CDS fall into two main types, one which contains suitable aminoalcohol moiety **(3a-3e)** as a linker to give hydrolyzable ester derivatives **(7aI-7eI)** and another contains diamine **(3f-3g)** as linker to give amide derivatives **(7fI-7gI)**.

In order to execute **Scheme-1**, various hydroxyalkylnicotinamide (**4a-4e**) and aminoalkylnicotinamide (**4f-4g**) derivatives were synthesized from ethyl nicotinate (**2**) using suitable linkers (**3a-3g**). Ethyl nicotinate (**2**) was treated with aminoalcohols (**3a-3e**) at 80-90°C under stirring for 10-12h and the excess aminoalcohol removed under vacuum
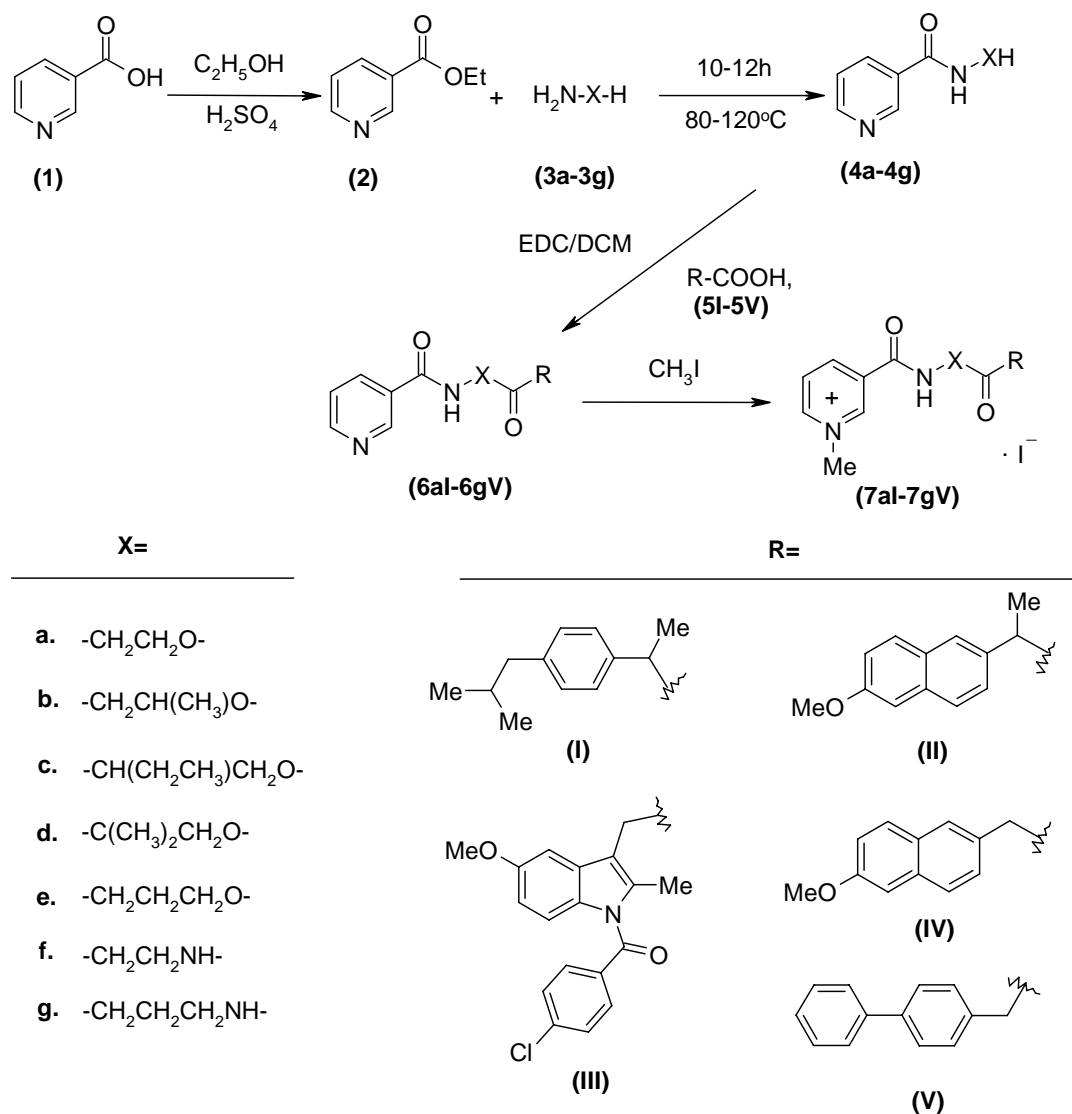
Scheme-1

to gave hydroxyalkylnicotinamide intermediates (**4a-4e**). It was observed that majority of these esters were low melting and probably due to this reason, compounds (**4a-4e**) were isolated as liquids. Another series of compounds (**4f-4g**) were synthesized in the same manner using excess of diamines (**3f-3g**) to give aminoalkylnicotinamide intermediates (**4f-4g**). Spectral data of these intermediates (**4a-4g**) is given in **Table 3.1**

Table 3.1: Spectral data of derivatives **(4a-4g)**

Comp.	IR Peaks (cm^{-1})	PMR Peaks (δ)
4a	3270, 1635, 1310, 1064,	9.07 (s, 1H), 8.67-8.65 (d, 1H), 8.45-8.43 (t, 1H), 8.22-8.19 (d, 1H), 7.41-7.37 (m, 1H), 4.74 (s, 1H), 3.70- 3.68 (t, 2H), **3.52-3.47 (m, 2H)**
4b	3285, 1639, 1301, 1122, 702	9.0 (s, 1H), 8.58-8.55 (d, 1H), 8.18-8.12 (m, 2H), 7.33-7.29 (m, 1H), 4.05-3.99 (m, 1H), 3.65 (s, 1H), 3.58-3.25 (m, 2H), **1.19-1.18 (d, 3H)**
4c	3278, 2964, 1638, 1302, 703	9.07 (s, 1H), 8.66-8.65 (d, 1H), 8.22-8.19 (d, 1H), 8.01-7.99 (d, 1H), 7.40-7.36 (m, 1H), 4.04 (bs, 1H), 3.63-3.62 (d, 2H), 3.55 (s, 1H), **1.74-1.53, (m, 2H), 0.97-0.94 (t, 3H)**
4d	3274, 1645, 1372, 702	8.90 (s, 1H), 8.60-8.58 (d, 1H), 8.07-8.04 (d, 1H), 7.32-7.29 (m, 1H), 6.97 (s, 1H), 4.62 (s, 1H), 3.66 (s, 2H), **1.41 (s, 6H)**
4e	3282, 1637, 1305, 702	9.0 (s, 1H), 8.61-8.60 (d, 1H), 8.45-8.43 (m, 1H), 8.17 -8.14 (d, 1H), 7.37-7.34 (t, 1H), 4.44 (s, 1H), 3.72-3.69 (t, 2H), 3.58-3.53 (q, 2H), **1.15-1.79 (m, 2H)**
4f	3348, 3281, 1644, 1307, 825, 706	9.05-9.04 (s, 1H), 8.65-8.63 (d, 1H), 8.22 (bs, 1H), 8.17-8.14 (m, 1H), 7.36-7.32 (m, 1H), 3.50-3.46 (q, 2H), 2.93-2.90 (t, 2H), **2.70 (s, 2H)**
4g	3279, 1644, 1590, 1308, 708	8.81 (s, 1H), 8.35-8.33 (d, 1H), 7.87-7.84 (d, 1H), 7.05-7.02 (m, 1H), 3.22-3.14 (m, 1H), 2.52-2.49 (t, 2H), 2.42-2.40 (t, 2H), 1.54-1.39 (m, 2H), **1.28-1.23 (m, 2H)**

The first member of the ibuprofen series, **(7aI)** was synthesized as per **Scheme-1**. Ibuprofen **(5I)** was coupled with *N*-(2-hydroxyethyl)nicotinamide **(4a)** using ethyl-(dimethylaminopropyl)carbodimide (EDC) as coupling agent in dichloromethane to give the derivative **(6aI)** which on quaternization using methyl iodide in acetonitrile gave a crude yellow semisolid product, which was crystallized from ethyl acetate to give **(7aI)** as a white product.

The IR spectrum (**Fig. 3.1 A**) of compound **(7aI)** showed carbonyl stretching of ester and amide groups as sharp intense bands at 1730 cm^{-1} and 1679 cm^{-1} respectively. N-H Stretching of amide was observed at 3272 cm^{-1} and the peaks due to C-O stretching came at 1205 and 1174 cm^{-1}.

(7aI)
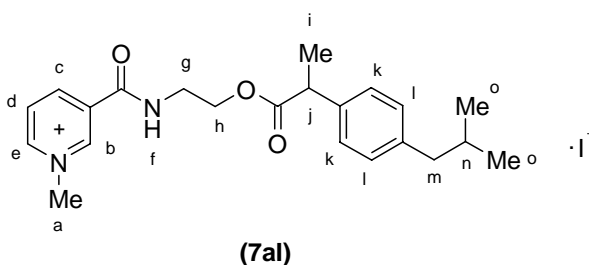
The PMR spectrum (**Fig. 3.1 B**) of the compound **(7aI)**, showed singlet at δ 9.80 for the single proton of pyridinium-H_b, multiplet at δ 8.89-8.87 due to NH_f and -H_e protons with coupling constants equal to 8.0 Hz. Another proton of pyridinium ring (-H_c) was observed at 8.72-8.69 as a multiplet (*J=8.0* Hz) single proton of pyridinium ring appeared at δ 8.0-7.97 as a multiplet (-H_d), (*J=8.0* Hz). The protons of 1,4-disubstituted phenyl ring appeared at δ 7.15-6.97 as a multiplet. Methyl protons (C$H_{3/a}$) of quaternary nitrogen appeared at δ 4.50 as a singlet, The single proton (-CH_n) appeared at δ 1.77-1.70 as a multiplet and methyl protons (-C$H_{3/i}$) at δ 1.43-1.41 as a doublet (*J=7.16* Hz). The six methyl protons (C$H_{3/o}$) appeared at δ 0.81-0.79 as a doublet.

^{13}C-NMR spectrum (**Fig. 3.1 C**) shows peaks at δ 175.0, and 161.35 for *C*=O carbon of ester and amide groups respectively, aromatic carbons appear at 146.82, 144.76, 144.76, 140.51, 137.45, 133.93, 129.29, 128.23, 127.32 and aliphatic carbons appear at 62.40, 49.42, 44.92, 44.89, 38.95, 30.15, 22.37 and 18.65. The H-H coupling was also confirmed using COSY spectrum as shown in **Fig. 3.1 E**

(A)

(B)

(C)

MF: $C_{22}H_{23}N_2O_3$ / I
MW: 369.2

(D)

61
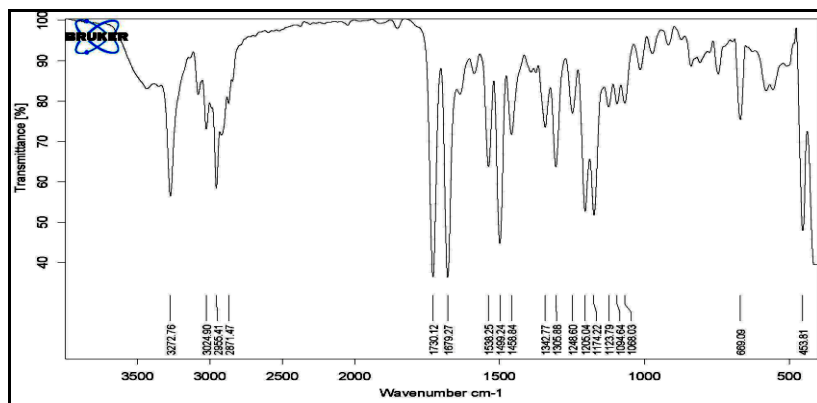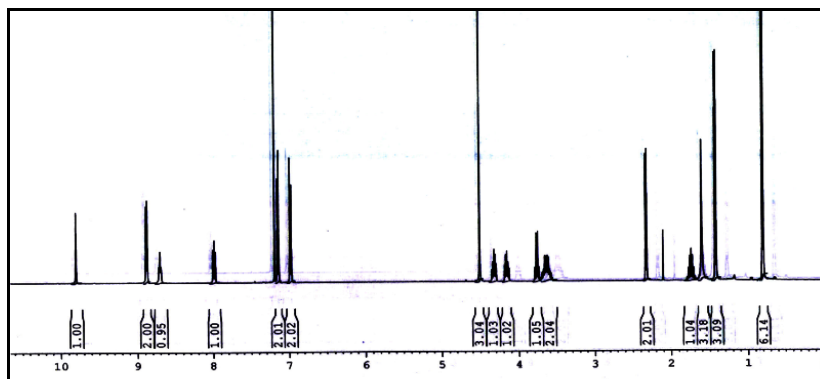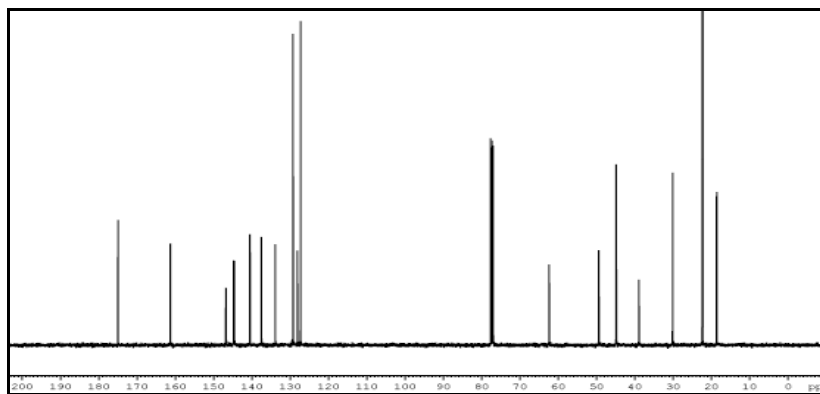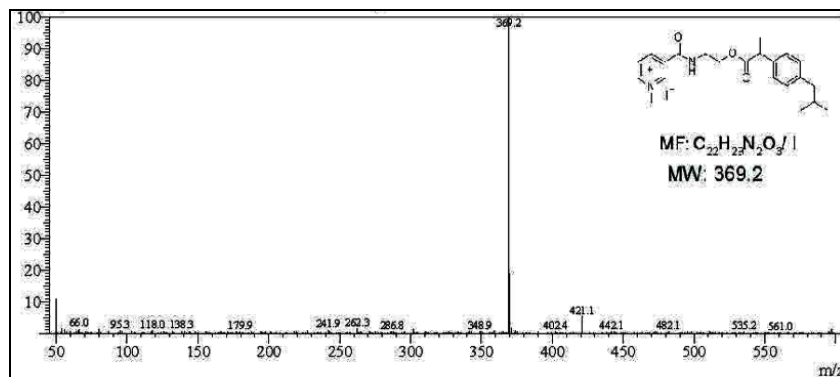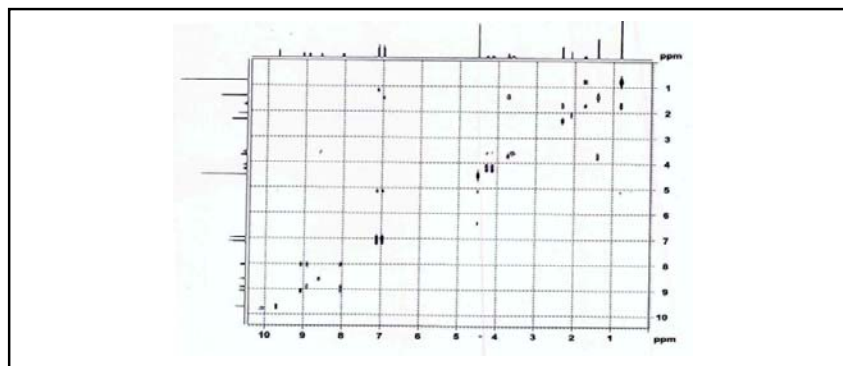
(E)
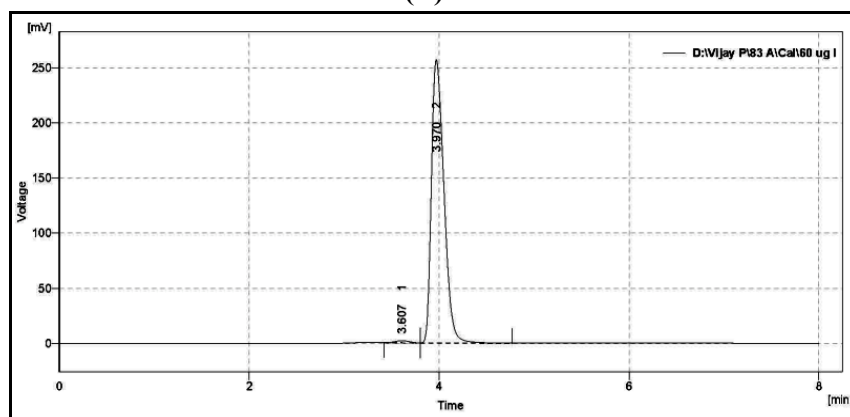
(F)

Fig. 3.1: Spectra of derivative **(7aI)**; IR spectrum **(A)**, ^{1}H-NMR **(B)**, ^{13}C-NMR **(C)**, Mass spectrum **(D)**, COSY **(E)** and HPLC chromatogram **(F)**.

Another series of CDS **(7fI-7gI)** containing diamine moiety **(3f-3g)** as a linker have been synthesized as per the procedure given for compound **(7aI)**. Ibuprofen **(5I)** was coupled with *N*-(2-aminoethyl)nicotinamide **(4f)** using EDC. HCl as coupling agent in dichloromethane to give the intermediate **(6fI)** which on quaternization using methyl iodide in acetonitrile gave a crude yellow semisolid product, which was crystallized from ethyl acetate to give **7fI** as a yellow solid.

The IR spectrum of compound **(7fI)** showed single carbonyl stretching of diamide groups as a sharp intense band at 1645 cm^{-1}, N-H stretching of amide at 3337 cm^{-1} and the peak due to C-N stretching came at 1236 cm^{-1}.

(7fI)
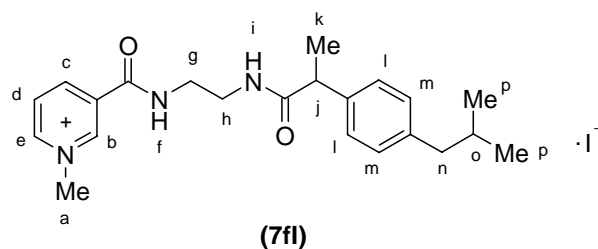
The PMR spectrum **(Fig. 3.2 A)** of the compound **(7fI)**, showed signals at δ 9.64 as a singlet for pyridinium-H_b, multiplet at δ 9.12-9.11 due to pyridinium-H_e, another pyridinium proton-H_c and NH_f at δ 8.88-8.83 as a multiplet with coupling constant equal to 8.0 Hz, triplet due to pyridinium-H_d at δ 8.05-8.03 (*J=8.0* Hz) and broad singlet at δ 7.44 due to NH_i. The protons of phenyl ring (Ar-$H_{2/l}$, *J=8.0* Hz) appeared at 7.21-7.19 and at 6.95-6.93 (Ar-$H_{2/m}$, *J=8.0* Hz) as doublets. Singlet due to methyl protons (-$CH_{3/a}$) of quaternary nitrogen appeared at δ 4.50, quartet due to methine proton (-CH_j) at 3.66-3.64 (*J=7.08* Hz) and methylene protons of ethylenediamine moiety ($CH_{2/g-h}$) at 3.50-3.33 as a multiplet. Doublet due to (-$CH_{2/n}$) appeared at 2.31-2.29 and multiplet at 1.74-1.71 for -CH_o, protons (*J=6.70* Hz), Signal at 1.38-1.37 due to methyl protons (-$CH_{3/k}$) with coupling constant equal to *7.08* Hz and six protons of dimethyl group ($CH_{3/p}$) at 0.80-0.79 as a doublet (*J=6.66* Hz) were also observed.

^{13}C-NMR spectrum of **7fI (Fig. 3.2 B)** shows peaks at 174.32, 160.97 for *C*=O carbons, aromatic carbons at 146.73, 145.25, 142.94, 139.13, 139.0, 133.61, 128.53, 127.34, 126.79 and aliphatic carbons at 48.37, 45.0, 44.32, 39.86, 39.02, 37.92, 29.65, 22.03 and 18.37. The mass spectrum **(Fig. 3.2 C)** of **7fI** shows peak at 368.1 (M[+]) which is also the base peak. The compound also showed high chromatographic purity (>99%) by HPLC.
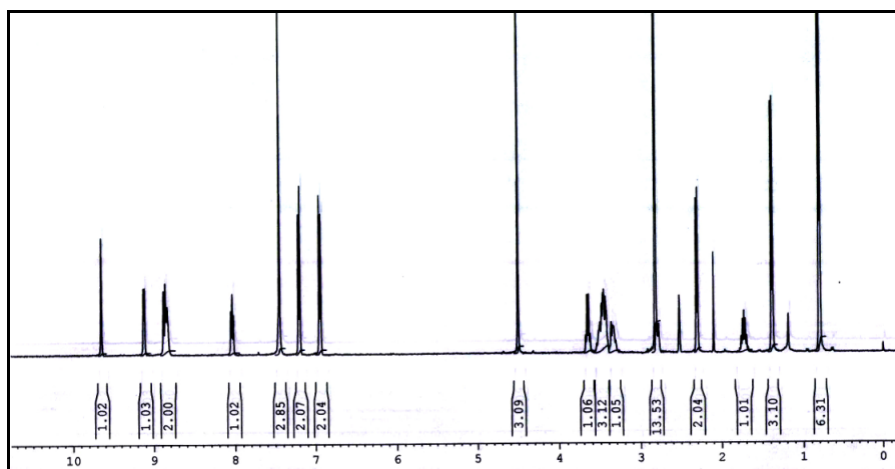
(A)
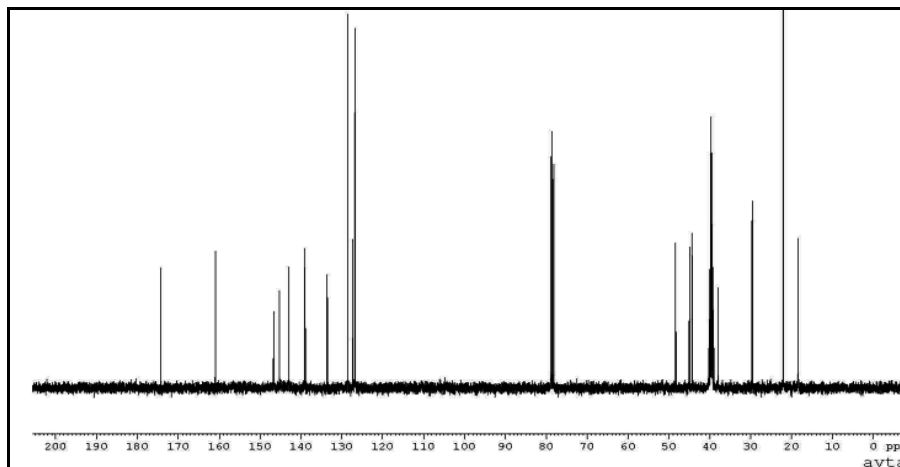
(B)
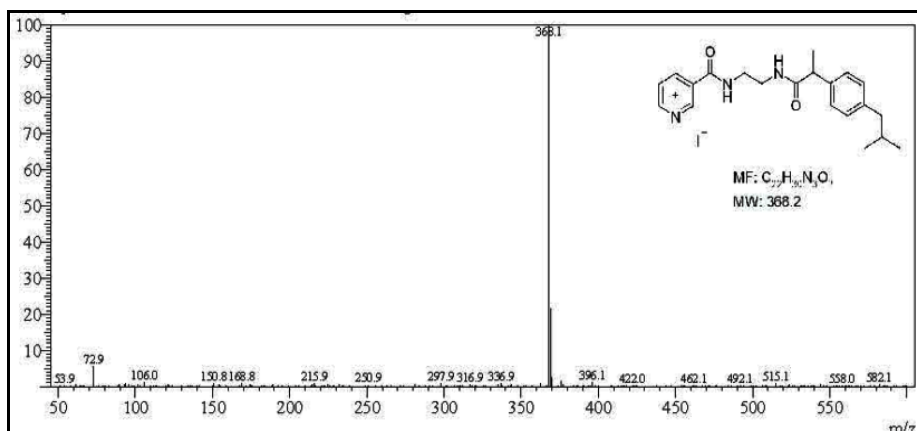
(C)

Fig. 3.2: Spectra of derivative **(7fI)**; ^{1}H-NMR **(A)**, ^{13}C-NMR **(B)**, and Mass
spectrum **(C)**.

Spectral data of the remaining ibuprofen derivatives **(7bI-7eI)** and **(7gI)** is given in **Table-3.1.**

Table 3.1: Spectral data of derivatives **(7bI-eI)** and **(7gI)**

Comp.	IR Peaks (cm^{-1})	PMR Peaks (δ)
7bI	3260, 1725, 1669, 847	9.80 (s, 1H) 8.89-8.87 (d, 2H) 8.72-8.69 (t, 1H), 8.00-7.97 (t,1H) 7.15-7.13 (d, 2H), 6.99-6.97 (d, 2H), 4.50 (s, 3H), 4.35-4.12 (m, 2H), 3.79-3.74 (q, 1H) 3.68-3.60 (m, 2H), 2.33-2.31 (d, 2H), 1.77-1.70 (m,1H), 1.43-1.41 (d,3H), 0.81-0.79 (d,6H)

7cI	3238, 1729, 1668, 834	9.80 (s, 1H), 9.06 (s, 1H) 8.92-8.90 (d, 1H), 8.45-8.43(d, 1H), 8.06-8.03 (t, 1H) 7.20-7.01 (dd, 4H), 4.58 (s, 3H), 4.34-4.29 (m, 2H), 4.22-4.19 (m, 1H), 3.80-3.65 (q, 1H), 1.82-1.73 (m, 2H), 1.72-1.67 (m, 1H), 1.49-1.44 (d, 3H), 0.96-0.93 (t, 3H), 0.89-0.87 (d, 6H)
7dI	3244, 1729, 1670, 746	9.59 (s, 1H), 9.08-9.06 (d, 1H), 8.76-8.74 (d, 1H), 8.05-8.01 (t, 1H), 7.97 (bs, 1H), 7.21-7.03 (dd, 4H), 4.57 (s, 3H), 4.33 (s, 2H), 3.80-3.78 (q, 1H), 2.40-2.38 (d, 2H), 1.82-1.78 (m, 1H), 1.50-1.48 (d, 3H), 1.46 (s, 6H), 0.90 (s, 6H).
7eI	3230, 1725, 1669, 735	10.10 (s, 1H), 9.02-9.0 (d, 1H), 8.90-8.87 (t, 1H), 8.85-8.84 (d, 1H), 8.06-8.03 (t, 1H), 7.21-7.07 (dd, 4H), 4.59 (s, 1H), 4.25-4.13 (m, 2H), 3.76-3.70(q, 1H), 3.54-3.49 (t, 2H), 3.22 (s, 1H), 2.43-2.42 (d, 2H), 2.08-2.02 (m, 2H), 1.86-1.80 (m, 1H), 1.53-1.44 (d, 3H), 0.90-0.87 (d, 6H)
7gI	3268, 1658 850	9.84 (s, 1H), 9.14-9.12 (d, 1H), 9.03-9.00 (d, 1H), 8.81-8.78 (d, 1H), 8.12-8.08 (t, 1H), 7.27-7.06 (dd, 4H), 6.69-6.66 (t, 1H), 4.60 (s, 3H), 4.12-4.09 (q, 1H), 3.75-3.67 (q, 2H), 3.46-3.34 (m, 2H), 2.43-2.40 (d, 3H), 1.85-1.77 (m, 2H), 1.49-1.44 (d, 2H), 1.27-1.21 (m, 1H), 0.89-0.86 (d, 6H)

3.1.2. Chemical delivery systems of naproxen (7aII-7gII)

Another member of the NSAIDs class chosen for developing suitable delivery systems was naproxen **(5II)**. Chemical delivery systems of naproxen were synthesized as per the previously described **Scheme-1**. Naproxen **(5II)** was coupled with *N*-(2-hydroxyethyl)nicotinamide **(4a)** using EDC.HCl as coupling agent in dichloromethane to give the derivative **(6aII)** which on quaternization using methyl iodide in acetonitrile gave a crude yellow semisolid product, which was crystallized from ethyl acetate to give **7aII** as a white solid.

The IR spectrum **(Fig. 3.3 A)** of the compound **(7aII)** showed carbonyl stretching of ester and amide groups as sharp intense bands at 1721 cm^{-1} and 1671 cm^{-1} respectiv-

ely. N-H stretching of amide was observed at 3284 cm^{-1} and the peaks due to C-O stretching came at 1273 and 1175 cm^{-1}.
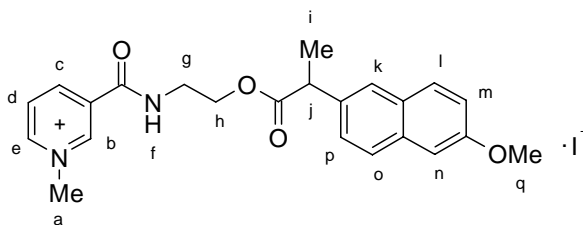
(7aII)

The PMR spectrum **(Fig. 3.3 B)** of the compound **(7aII)** shows singlet of pyridinium-H_b at δ 9.34, doublet of another pyridinium-H_e at δ 9.15-9.13 with coupling constant equal to 8.0 Hz, multiplet at δ 9.04-9.02 due to pyridinium-H_d, singlet at δ 8.74-8.72 due to pyridinium-H_c (*J=8.0* Hz) and peak at δ 8.09-8.03 due to NH_f proton. Naphthalene protons (Ar-H_{k-p}) were observed at δ 7.66-7.07 as multiplets. The signal for methyl protons (-C$H_{3/a}$) of quaternary nitrogen appeared at δ 4.44 as a singlet. The methylene protons (C$H_{2/h}$) appeared at δ 4.28-4.25 as a triplet. Quartet appeared at δ 3.91-3.86 due to methine proton (CH_j) and multiplet at δ 3.67-3.56 due to methylene protons (-C$H_{2/g}$). The singlet at δ 3.33 equivalent to three protons and doublet at 1.52-1.51 for three protons were due to (-C$H_{3/q}$) and (-C$H_{3/i}$) protons respectively.

^{13}C-NMR spectrum **(Fig. 3.3 C)** of **7aII** shows peaks at 172.73 and 160.01 for carbonyl carbons of ester and amide functional group respectively, peaks at 155.85, 145.75, 143.94, 141.18, 134.28, 131.94, 127.82, 126.16, 124.97, 117.41, 104.33 appeared due to aromatic carbons and the aliphatic carbons appeared at 61.09, 54.14, 47.23, 43.29, 39.06, 38.85, 38.44, 38.02, 37.33 and 17.20.

(A)

(B)

(C)

MF: $C_{23}H_{25}N_2O_4 \cdot I$

MW: 393.38
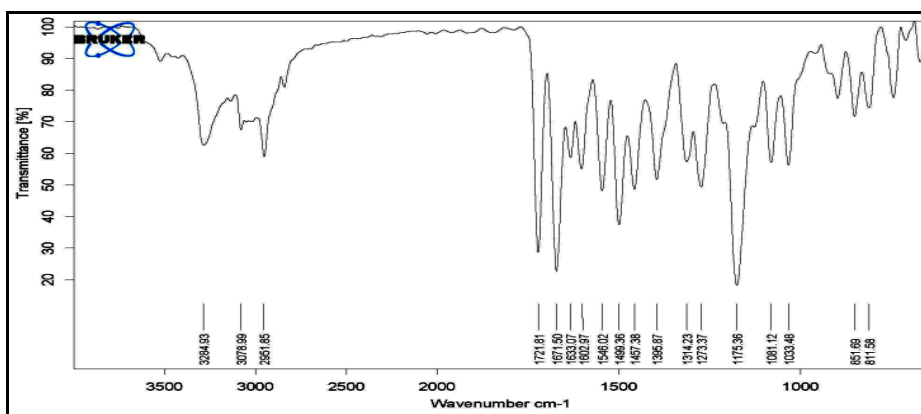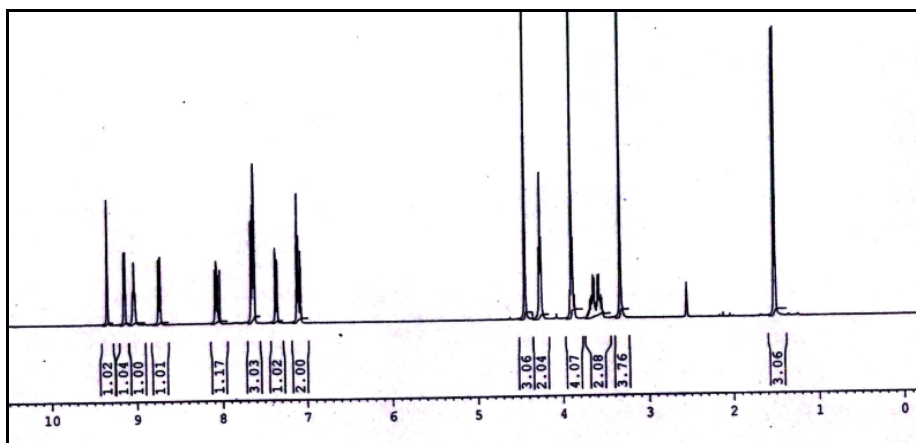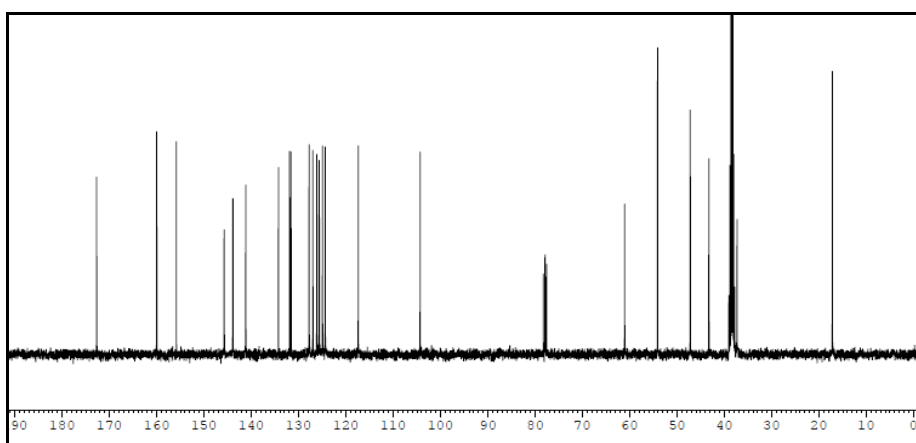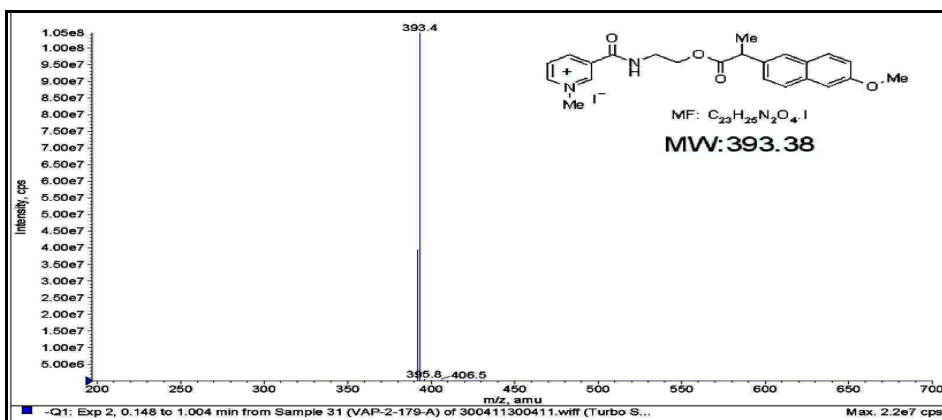
(D)
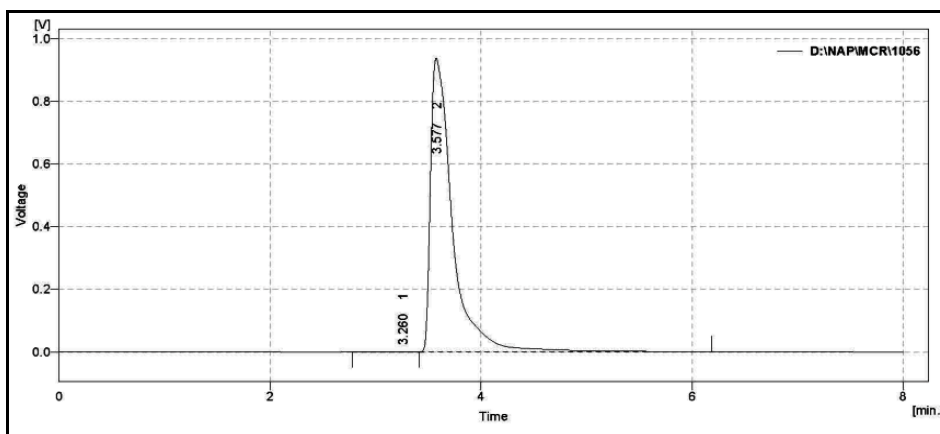
(E)

Fig. 3.3: Spectra of derivative **(7aII)**; IR spectrum **(A)**, ^{1}H-NMR **(B)**, ^{13}C-NMR **(C)**, Mass spectrum **(D)** and HPLC chromatogram **(E)**.

The mass spectrum of compound **(7aII)** shows peak at 393.4 (M^+) which is also the base peak. The compound showed high chromatographic purity (>98.5%) by HPLC. Other derivatives of the series have been synthesized and characterized in the same manner as discussed for compound **(7aII)**. Spectral data of the remaining naproxen derivatives (**7bII-7gII**) is given in **Table-3.2**

Table 3.2: Spectral data of derivatives **(7bII-7gII)**

Comp.	IR Peaks (cm^{-1})	PMR Peaks (δ)
7bII	1721, 1666, 1187, 892	δ 9.08 (s, 1H), 9.02-9.01(d, 1H), 8.81 (bs, 1H), 8.45-8.43 (d, 1H), 7.83-7.79 (m, 1H), 7.59-7.05 (m, 6H), 5.16-5.13 (m, 1H), 4.35 (s, 3H), 3.92 (s, 3H), 3.84-3.82 (q, 1H), 3.37-3.33 (t, 2H), 1.50-1.49 (d, 3H), 1.33-1.32 (d, 3H)
7cII	1727,1668, 1239, 854	9.23 (s, 1H), 8.94-8.87 (dd, 1H), 8.61-8.57 (m, 1H) 8.18-8.13 (dd, 1H), 7.85-7.75 (m, 1H), 7.61-6.97 (m, 6H), 4.40 (s, 3H), 4.34 (s, 3H), 3.91-3.88 (d, 4H), 1.74-1.65 (m, 1H), 1.54-1.51 (d, 3H), 1.27-1.23 (q, 1H), 0.95-0.90 (t, 3H)
7dII	1730,1658, 1372, 854	9.29 (s, 1H) 9.11-9.10 (d, 1H), 8.65-8.63 (d, 1H), 8.28 (s, 1H), 8.05-8.01 (m, 1H), 7.66-7.07 (m, 6H), 4.40 (s, 3H), 3.90 (s, 3H), 3.37-3.34 (m, 1H), 3.02 (s, 2H), 1.51-1.48

68

		(d, 3H), 1.38-1.35 (d, 6H)
7eII	1716,1667, 1266	9.44 (s, 1H), 9.15-9.13 (d, 1H), 9.06-9.03 (m, 1H), 8.91-8.89 (d, 1H), 8.23-8.19 (m, 1H), 7.76-7.11 (m, 6H), 4.44 (s, 3H), 4.15-4.11 (q, 2H), 3.91-3.89 (q, 1H), 3.88 (s, 3H), 3.40-3.35 (t, 2H), 1.89-1.85 (p, 2H), 1.52-1.50 (d, 3H)
7fII	1665, 1210, 857	δ 9.17 (s, 1H), 9.01-8.99 (d, 1H), 8.88-8.85 (m, 1H), 8.61-8.59 (d, 1H), 8.10-8.07 (m, 1H), 7.99-7.94 (m, 1H), 7.77-7.07 (m, 6H), 4.36 (s, 3H), 3.89 (s, 3H), 3.74-3.72 (q, 1H), 3.53-3.39 (m, 2H), 3.31-3.24 (t, 2H), 1.50-1.44 (d, 3H)
7gII	1673, 1269, 857	δ 9.52 (s, 1H), 9.15-9.14 (d, 1H), 8.95-8.93 (d, 2H), 8.14-8.10 (m, 1H), 7.84-7.81 (m, 1H), 7.70-7.65 (m, 3H), 7.47-7.44 (d, 1H), 7.11-7.09 (d, 2H), 4.49 (s, 3H), 3.90 (s, 3H), 3.79-3.77 (q, 1H), 3.38-3.37 (m, 2H), 3.24-3.17 (m, 2H), 1.78-1.75 (p, 2H), 1.52-1.50 (d, 3H)

3.1.3. Chemical delivery systems of indomethacin (7aIII-7gIII)

In order to synthesize quaternary ammonium derivatives of indomethacin **Scheme-1** was employed. Indomethacin **(5III)** was coupled with various hydroxyl- and aminoalkyl nicotinamide derivatives **(4a-4g)** using EDC as a coupling agent to give the derivatives **(6aIII-gIII)** which on quaternization by methyl iodide gave quaternary ammonium derivatives **(7aIII-7gIII)** of indomethacin. Derivative **(7aIII)** was synthesized using *N*-(2-hydroxyethyl)nicotinamide **(4a)** and indomethacin **(5III)** to give **6aIII** as an intermediate which on quaternization by methyl iodide gave yellow semisolid which was further crystallized from ethanol to obtain **7aIII** as a yellow solid.

In the IR spectrum **(Fig. 3.4 A)** of compound **(7aIII)** the *C=O* stretchings were observed at 1728, 1683 and at 1662 cm^{-1} for the ester and amide carbonyl groups respectively. *N-H* stretching was observed at 3276 cm^{-1} and the peaks due to *C-O* stretching appeared at 1228 and 1173 cm^{-1}.
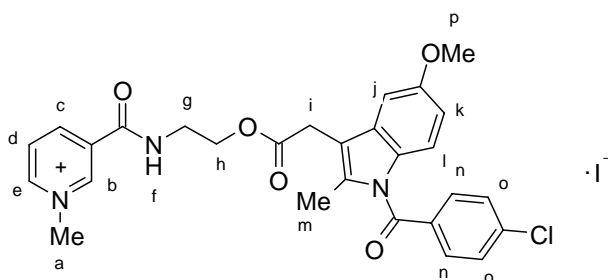
(7aIII)

PMR Spectrum (**Fig. 3.4. B**) showed signal at δ 9.41 as a singlet for pyridinium-H_b, multiplet at δ 9.18-9.16 due to pyridinium-H_e with coupling constant equal to 8.0 Hz, multiplet at δ 9.08 due to pyridinium-H_d, (*J=8.0*) and a signal at δ 8.81-8.79 due to pyridinium-H_c, (*J=8.0* Hz). The NH_f proton appeared at δ 8.15-8.11 as a triplet. The aromatic protons of phenyl ring appeared at δ 7.69-7.55 (Ar-H_n), and at δ 7.57-7.55 (Ar-H_o), as doublets and multiplets due to indole protons (Ar-H_{j-l}) appeared at δ 6.95-6.56. The methyl protons on quaternary nitrogen (-C$H_{3/a}$) appeared at δ 4.49 as a singlet. Signals at δ 4.31-4.28 were observed due to methylene protons (-C$H_{2/h}$) as triplet. Methoxy protons (-C$H_{3/p}$) showed signal at δ 3.77 as a singlet and the methylene (-C$H_{2/i}$) protons appeared as singlet at δ 3.71. Other methylene protons (-C$H_{2/g}$) appeared at δ 3.67-3.63 as multiplet and the methyl protons (-C$H_{3/m}$) appeared as a singlet at δ 2.25.

^{13}C-NMR spectrum **(Fig. 3.4 C)** shows peaks at δ 170.17, 167.63, 160.93 due to C=O carbons, aromatic carbons appear at 155.32, 146.84, 145.19, 142.58, 138.16, 135.25, 133.61, 130.88, 130.07, 128.80, 127.30, 114.26, 112.21, 111.03, 101.27 and aliphatic carbons appear at 62.31, 55.33, 48.29, 40.25, 40.04, 39.83, 39.20, 38.55, 29.59 and 13.20. The mass spectrum of compound **(7aIII)** shows peak at 520.60 (M$^+$) which is also the base peak. The compound also showed high chromatographic purity by HPLC.

(A)

(B)

(C)

MF: C$_{26}$H$_{27}$ClN$_3$O$_5$· I

MW: 520.84

(D)

(E)

71
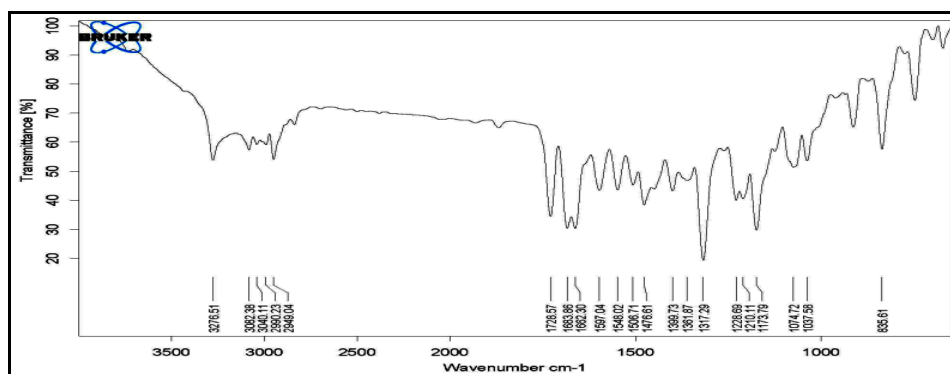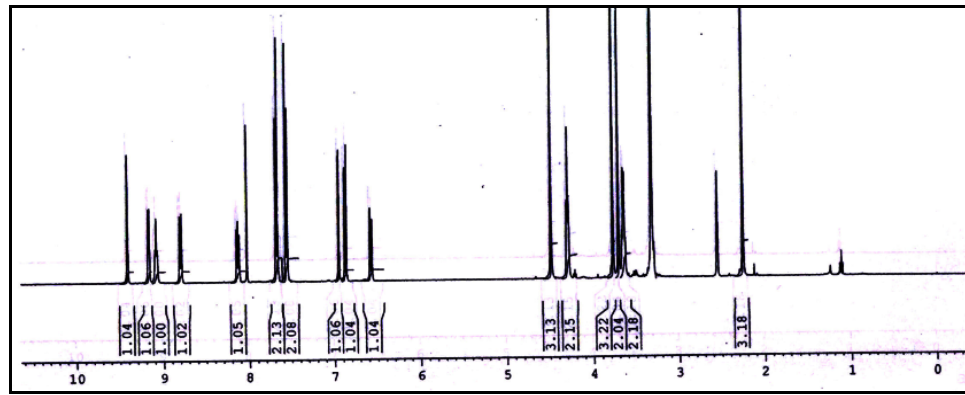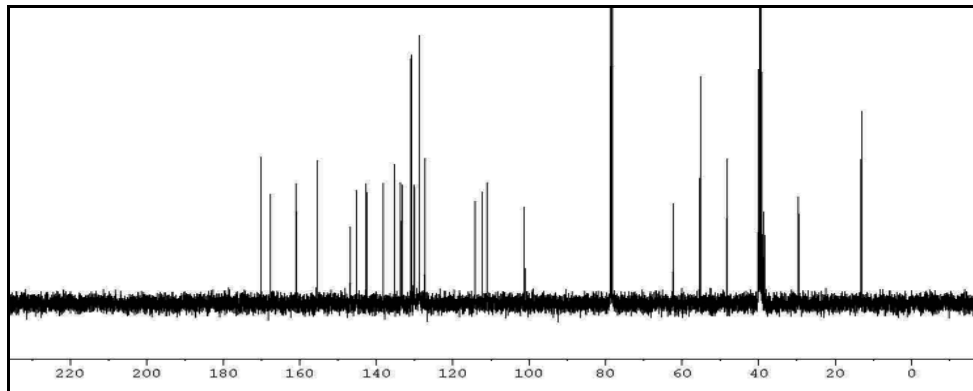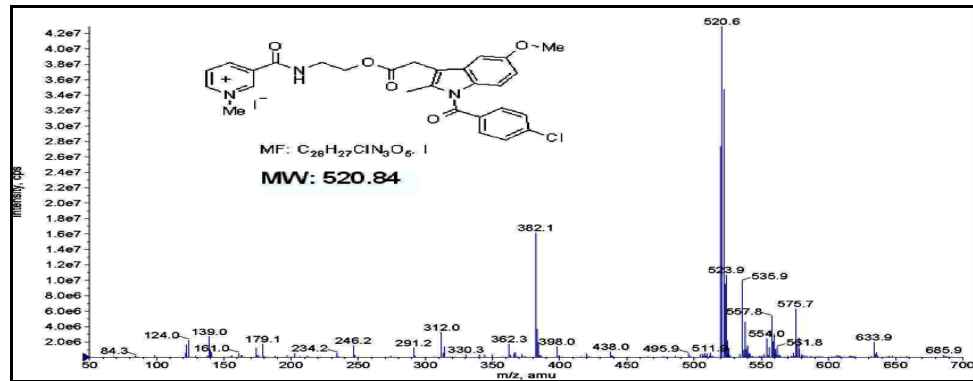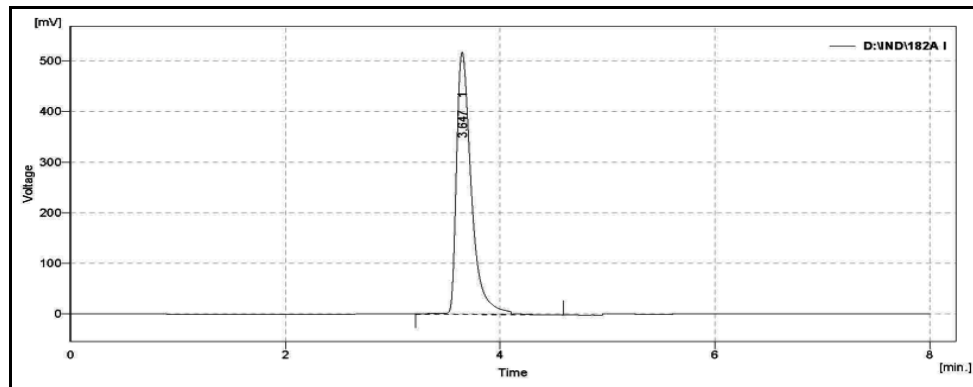
Fig. 3.4: Spectra of derivative **(7aIII)**; IR spectrum **(A)**, ^{1}H-NMR **(B)**, ^{13}C-NMR **(C)**, Mass spectrum **(D)** and HPLC chromatogram **(E)**.

Other derivatives of the series have been synthesized and characterized in the same manner as compound **(7aIII)**. Spectral data of the remaining indomethacin derivatives **(7bIII-7gIII)** is given in **Table 3.3.**

Table 3.3: Spectral data of the derivatives **(7bIII-7gIII)**

Comp.	IR Peaks (cm^{-1})	PMR Peaks (δ)
7bIII	3439, 1729, 1675,1323, 754	9.54 (s, 1H) 8.95-8.93 (d, 1H), 8.73-8.71 (d, 1H), 8.61-8.58 (m, 1H), 7.92-7.88 (m, 1H), 7.67-7.63 (d, 2H), 7.48-7.45 (d, 2H), 6.97-6.96 (d,1H), 6.89-6.87 (d, 1H), 6.55-6.52 (dd, 1H), 4.47 (s, 3H), 3.80 (s, 3H), 1.36-1.30 (d, 3H)
7cIII	3436, 1733, 1672, 1322,754	9.51 (s, 1H), 8.97-8.95 (d, 1H), 8.74-8.72 (d, 1H), 8.28 (bs, 1H), 7.93-7.89 (m, 1H), 7.67-7.65 (d, 2H), 7.48-7.46 (d, 2H), 6.94-6.93 (dd, 2H), 6.48-6.45 (dd,1H), 4.48 (s, 3H), 4.33 (s, 3H), 3.83 (s, 3H), 1.27-1.24 (m,1H)
7dIII	3436, 1733, 1675, 1322,752	9.53 (s, 1H), 9.0-8.98 (d, 1H), 8.70-8.68 (d, 1H), 7.69-7.93 (t, 1H), 7.87 (s, 1H), 7.64-7.62 (d, 2H), 7.47-7.44 (d, 2H), 6.95 (s,1H), 6.88-6.86 (d,1H), 6.56-6.54 (d,1H), 4.50 (s, 3H), 3.78 (s, 3H), 1.49 (s, 6H)
7eIII	3288, 1711, 1630, 1316, 827	9.53 (s, 1H), 9.20-9.18 (d, 1H), 9.07-9.04 (m, 1H), 8.98-8.96 (d, 1H), 8.21-8.17 (m, 1H), 7.67-7.66 (d, 2H), 7.55-7.54 (d, 2H), 6.98 (s, 1H), 6.92-6.89 (d, 1H), 6.67-6.64 (d, 1H), 4.50 (s, 3H), 3.80 (s, 3H), 1.99-1.93 (p, 2H)

7fIII	3273,1663, 1312,751	9.34 (s, 1H), 9.14-9.13 (d, 1H), 8.83 (s, 1H), 8.73-8.71 (d, 1H), 8.04-8.02 (m, 1H), 7.71-7.52 (d, 2H), 7.54-7.52 (d, 2H), 6.99 (s, 1H), 6.92-6.90 (d, 1H), 6.55-6.53 (d, 1H), 4.45 (s, 3H), 3.77 (s, 3H), 2.26 (s, 3H)
7gIII	3299, 2929, 1668, 754	9.5 (s, 1H), 9.18-9.17 (d, 1H), 9.0-8.98 (m,1H), 8.95-8.93 (d, 1H), 8.19-8.15 (m, 1H), 7.97-7.95 (t, 1H), 7.70-7.52 (dd, 4H), 7.09-6.62 (m, 3H), 4.48 (s, 3H), 3.79 (s, 3H), 3.33 (s, 3H), 3.26-3.22 (q, 2H), 1.81-1,75 (m, 2H)

3.1.4. Chemical delivery systems of 6-MNA (7aIV-7eIV)

Nabumetone is a non-acidic, NSAID devoid of local gastric irritation. But as such this is not active biologically. It gets metabolized to 6-methoxy-2-naphthylacetic acid (6-MNA) **(5IV)**, which acts as anti-inflammatory agent. So, it was planned to prepare CDS of 6-MNA the active metabolite of nabumetone. The required NSAID i.e. 6-MNA **(5IV)** was synthesized as per the reported procedure.[3] Synthesis of 6-MNA has been described in Section-III (Section 3.1). As discussed earlier in **Scheme-1**, same procedure has been adopted for the synthesis of CDS **(7aIV-7eIV)** of 6-MNA **(5IV)**. The first derivative **(7aIV)** was synthesized by coupling 6-MNA **(5IV)** with *N*-(2-hydroxyethyl)nicotinamide **(4a)** using EDC.HCl as the coupling agent to give the derivative **(6aIV)** as an ester which on quaternization using methyl iodide gave the final compound **(7aIV)** as yellow solid.

In the IR spectrum **(Fig. 3.5 A)** of the synthesized derivative **(7aIV)** strong bands at 1735 and 1672 cm^{-1} due to *C=O* stretching of ester and amide groups respectively were observed.
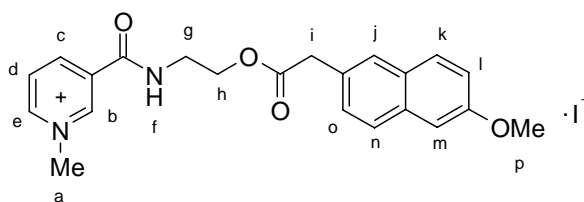
(7aIV)

The PMR spectrum **(Fig. 3.5 B)** of the compound **(7aIV)** showed signal at δ 9.38 as a singlet due to pyridinium-H_b proton. Another pyridinium proton (-H_e) merged with amide proton (NH$_f$) was observed at δ 9.11-9.08 as a multiplet with coupling constant equal to 8.0Hz. Multiplets at δ 8.80-8.78 and δ 8.09-8.06 appeared due to pyridinium-H_c

and pyridinium-H_d respectively. Naphthalene protons (Ar-H_{j-o},) were observed at δ 7.62-7.04 as multiplet. Methyl protons on quaternary nitrogen (-$CH_{3/a}$) appeared at δ 4.41 as a singlet and methylene protons (-$CH_{2/g}$) at δ 4.26-4.23 as a triplet. Peaks were observed at δ 3.85 as singlet due to methoxy protons (-$CH_{3/p}$) and at δ 3.73 and 3.64-3.60 due to methylene protons (Ar-C$H_{2/i}$) and (-$CH_{2/h}$) respectively.

^{13}C-NMR spectrum (**Fig. 3.5** C) shows peaks at 171.17 and 161.22, due to carbonyl carbons. Peaks at 157.03-105.44 were observed for aromatic carbons. Aliphatic carbons appeared at 62.28-38.60. Mass spectrum **(Fig. 3.5 D)** shows peak at 379.0 (M+) which is also the base peak. The compound also showed high chromatographic purity.

(A)

(B)

74
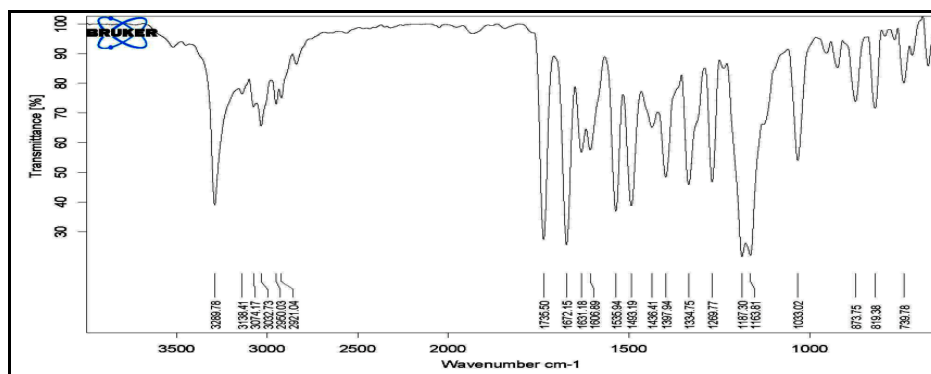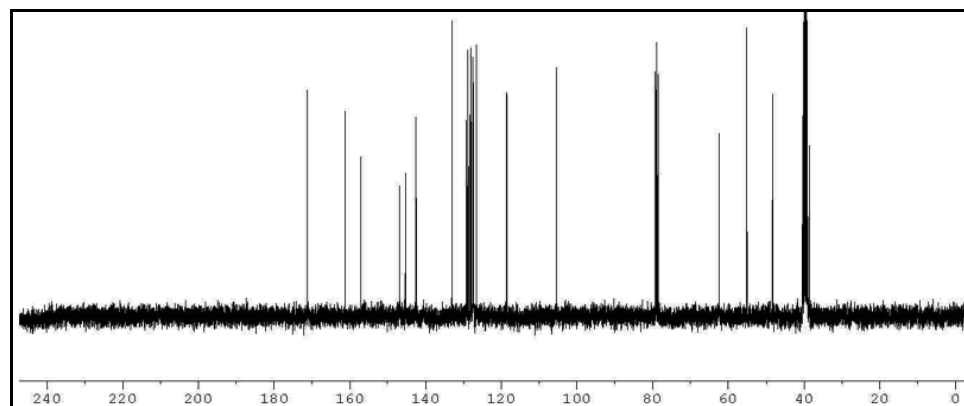
(C)
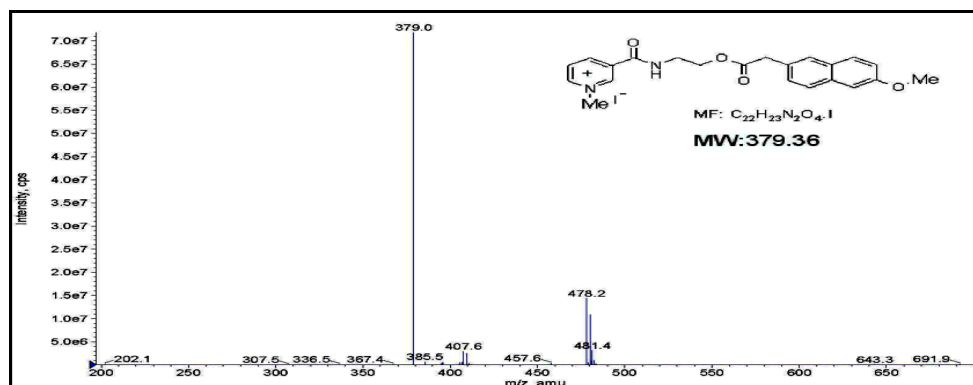
(D)

Fig. 3.5: Spectra of derivative **(7aIV)**; IR spectrum **(A)**, ^{1}H-NMR **(B)**, ^{13}C-NMR **(C)**, mass spectrum **(D)**.

Other derivatives of the series have been synthesized and characterized in the same manner as compound **(7aIV)**. Spectral data of the remaining 6-MNA derivatives (**7bIV-7eIV)** is given in **Table-3.4.**

Table 3.4. Spectral data of derivatives **(7bIV-7eIV)**

Comp. No.	IR Peaks (cm^{-1})	PMR Peaks (δ)
7bIV	1724,1668, 1264, 852	9.26 (s, 1H), 74-8.73 (d, 1H), 8.61-8.59 (d, 1H), 8.55-8.53 (m, 1H), 7.72-7.69 (m, 1H), 7.58-7.00 (m, 3H), 7.35-7.32 (m, 1H), 7.06-7.0 (m, 2H), 5.26-5.22 (m,1H), 4.27 (s, 3H), 3.88 (s, 3H), 3.74 (s, 2H), 3.64-3.53 (m, 2H), 1.32-1.30 (d, 3H)
7cIV	3246, 1727, 1667, 1264, 850,	9.30 (s, 1H), 8.76-8.74 (d, 1H), 8.62-8.60 (d, 1H), 8.27-8.25 (m, 1H), 7.73-7.70 (m, 1H), 7.58-7.53 (m, 3H), 7.37-7.27 (m, 1H), 7.14-7.0 (m, 2H), 4.41-4.31 (m, 2H), 4.29 (s, 3H), 3.90-3.89 (m, 1H), 3.88 (s, 3H), 3.77 (s, 2H), 1.84-1.69 (m, 2H), 0.99-0.95 (t, 3H)
7dIV	3267, 1737, 1660, 1329, 857	9.36 (s, 1H), 9.12-9.10 (d, 1H), 8.75-8.73 (d, 1H), 8.34 (s, 1H), 8.10-8.05 (t, 1H), 7.66-7.08 (d, 3H), 7.35-7.33 (d, 1H), 7.17-7.08 (m, 2H), 4.41 (s, 3H), 4.33 (s, 2H), 3.90 (s, 3H), 3.78 (s, 2H), 1.42 (s, 6H)

7eIV	1724,1666, 1265, 850	9.45 (s, 1H), 9.15-9.13 (d, 1H), 9.13-9.10 (m, 1H), 8.93-8.91 (d, 1H), 8.23-8.19 (m, 1H), 7.75-7.73 (d, 2H), 7.68 (s, 1H), 7.38-7.36 (d, 1H), 7.23 (s, 1H), 7.14-7.12 (d, 1H), 4.44 (s, 3H), 4.17-4.14 (t, 2H), 3.88 (s, 3H), 3.78 (s, 2H), 3.46-3.41 (q, 2H), 1.94-1.91 (m, 2H)

3.1.5. Chemical delivery systems of BPA (7aV-7eV)

Fenbufen is a potent anti-inflammatory agent that is metabolized into 4-hydroxy-4-biphenylbutanoic acid and 4-biphenylacetic acid (5V). 4-Biphenylacetic acid (BPA) (5V) is an active metabolite of fenbufen with three times more anti-inflammatory activity than the parent drug.[4] Synthesis of 4-biphenylacetic acid has been described in Section-3 (Section 3.1). The chemical delivery systems of BPA were prepared according to Scheme-1, in which N-(2-hydroxyethyl)nicotinamide (4a) was coupled with BPA (5V) using EDC. HCl as coupling agent to give the derivative (6aV) which on quaternization using methyl iodide gave a residue which was crystallized from chloroform: methanol to give (7aV) as a yellow solid.
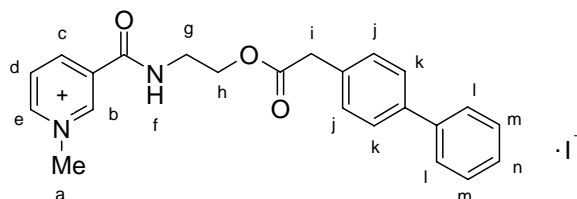
(7aV)

IR spectrum (Fig. 3.6 A) of compound (7aV) showed C=O stretching at around 1721 and 1672 cm^{-1} due to ester and amide carbonyl functional groups respectively. The N-H stretching and deformation peaks were observed around 3271 and 1495 cm^{-1}.

The PMR spectrum (Fig. 3.6 B) of the compound (7aV) showed singlet at δ 9.53 due to proton of pyridinium (-H_b) ring. Other signal appeared at δ 9.19-9.16 as a multiplet due to pyridinium-H_e merged with NH_f, proton with coupling constant equal to 8.0 Hz. The multiplet at δ 8.96-8.94 was due to pyridinium-H_c. Other proton of pyridinium-H_d appeared at δ 8.19-8.16 as mltiplet. Nine biphenyl ring protons were observed at 7.57-7.32 as a multiplet (Ar-H_{j-n}). The methyl protons of quaternary nitrogen (-C$H_{3/a}$) appeared at δ 4.47 as a singlet, methylene protons (-C$H_{2/h}$) at δ 4.30-4.28 as a triplet (J=4.0 Hz) and a peak at δ 3.72 due to methylene protons (Ar-C$H_{2/i}$) appeared as singlet. Other methylene protons (-C$H_{2/g}$) appeared at δ 3.72-3.65 as a multiplet (J=4.0 Hz)

^{13}C-NMR shows (**Fig. 3.6 C**) peaks at δ 170.95 and 160.84 for carbonyl carbons of ester and amide functional groups. Aromatic carbons appeared at 146.41-126.18 and the aliphatic carbons appeared at 62.24, 48.41, 40.29, 39.87, 39.10, 38.89 and 38.45. The mass spectrum of compound (**7aV**) shows peak at 375.90 (M^+) which is also the base peak. The derivative (**7aV**) was found to be pure and chromatographic purity by HPLC was more than 98.90 %.
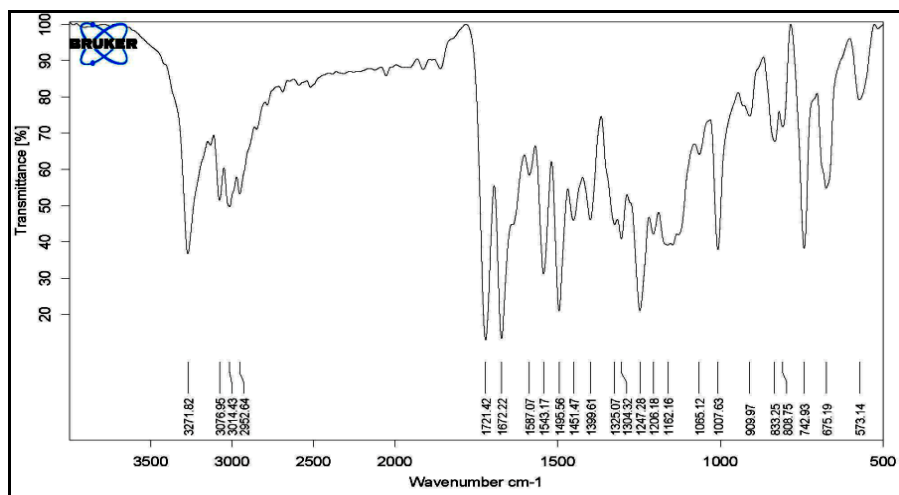
(A)
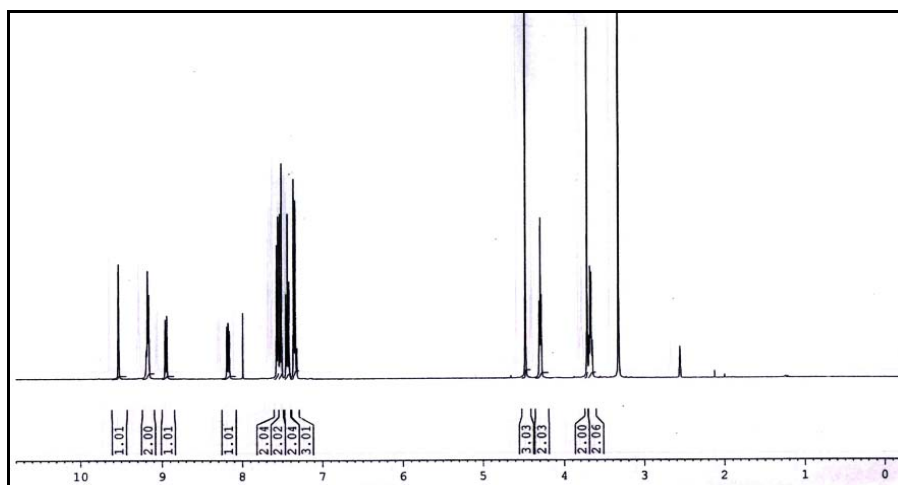
(B)
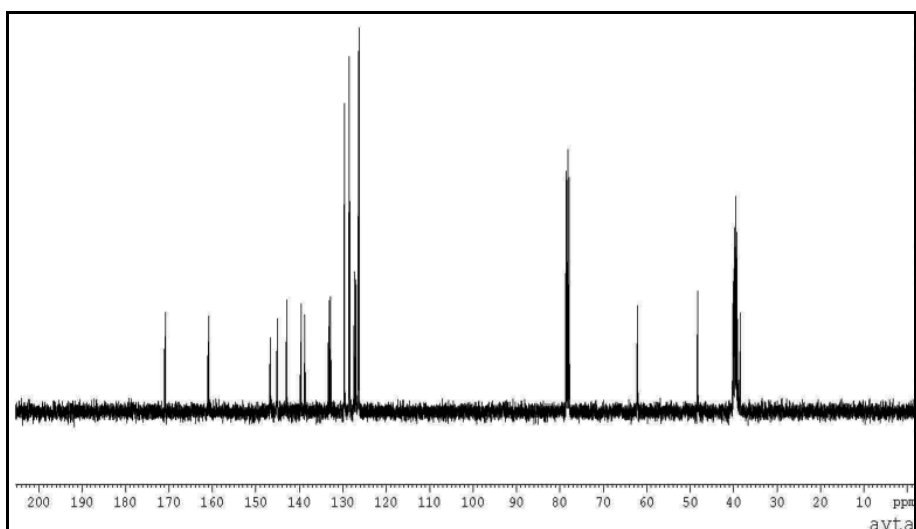
(C)
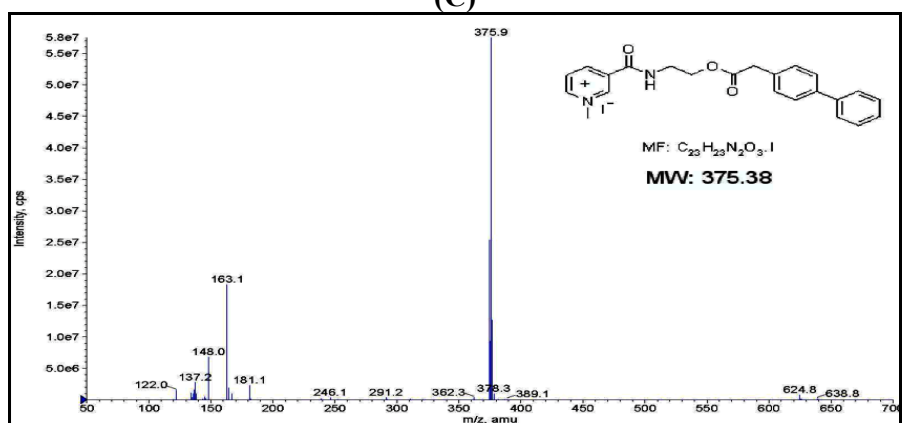
(D)

Fig. 3.6: Spectra of derivative **(7aV)**; IR spectrum **(A)**, ^{1}H-NMR **(B)**, ^{13}C-NMR **(C)**, Mass spectrum **(D)**.

Other derivatives of the series have been synthesized and characterized in the same manner as compound **(7aV)**. Spectral data of the remaining BPA derivatives (**7bV-7eV**) is given in **Table 3.5.**

Table 3.5: Spectral data of derivatives **(7bV-7eV)**

Comp.	IR Peaks (cm^{-1})	PMR Peaks (δ)
7bV	3236, 1725, 1667,744	9.46 (s, 1H), 8.79-8.73 (m, 2H), 8.75-8.73 (d, 1H), 8.62-8.59 (d, 1H), 7.87-7.85 (t, 1H), 7.48-7.19 (m, 9H), 5.17-5.12 (m, 1H), 4.30 (s, 3H), 3.48-3.46 (t, 2H), 1.99 (s, 2H) 1.24-1.23 (d, 3H)

7eV	3247, 1727, 1665,743	9.54 (s, 1H), 8.79-8.76 (m, 2H), 8.32-8.30 (d, 1H), 7.86-7.82 (t, 1H), 7.49-7.19 (m, 9H), 4.33 (s, 3H), 4.29-4.18 (m, 2H), 3.65 (s, 2H), 1.97-1.1.94 (d, 2H), 1.79-1.64 (m, 1H), 0.92-0.89 (t, 3H)
7fV	3436, 1728, 1668,743	9.52 (s, 1H), 8.84-8.82 (d, 1H), 8.70-8.68 (d, 1H), 7.93 (bs, 1H), 7.89-7.86 (t, 1H), 7.53-7.31(m, 9H), 4.41 (s, 3H), 4.37 (s, 2H), 3.74 (s, 2H), 1.52 (s, 6H)
7gV	3391, 1725, 1660,741	9.93 (s, 1H), 8.98-8.96 (m, 2H), 8.86-8.85 (d, 1H), 8.01-7.97 (t, 1H), 7.57-7.26 (m, 9H), 4.51 (s, 3H), 4.23-4.20 (t, 2H), 3.70 (s, 2H), 3.58-3.53 (q, 2H), 3.09 (bs, 1H), 2.08-2.05 (m, 2H)

3.2. Hydrolyses kinetics study

The synthesized chemical delivery systems (CDS) have to be injected by IA route, so once they are deposited into the joint cavity they must be hydrolyzed enzymatically or non-enzymatically to liberate the active NSAID to elicit the desired pharmacological action. As mentioned previously the administered CDS contain hydrolysable ester and amide groups which either undergo hydrolysis in the joint cavity or expelled in the intact form from joints which will be ultimately hydrolyzed in the systemic circulation and generate free NSAIDs. The free NSAID again appear in the joint cavity by reuptake mechanism or get excreted from the body. Hence, it is important to study the hydrolysis kinetics of synthesized CDS at various *p*H conditions and in serum. This *in vitro* study will give idea about the fate of CDS upon IA administration.

The *p*H of joint cavity gets decreased up to *p*H 6 in inflammatory conditions while the *p*H of normal human blood is around 7.4. All the synthesized CDS were evaluated *in vitro* for their stability at 37$\pm$1 °C in buffers of *p*H 6.0 and 7.4 which simulated the *p*H of the joint cavity and the blood. To get an idea about the enzymatic susceptibility of CDS towards serum esterase, *in vitro* hydrolyses studies were performed in pooled human serum (80/90 %) at 37$\pm$1 °C for all the CDS.

The studies so performed are discussed under the following five headings:

3.2.1. Hydrolyses studies of CDS of ibuprofen (7aI-7gI)

3.2.2. Hydrolyses studies of CDS of naproxen (7aII-7gII)

3.2.3. Hydrolyses studies of CDS of indomethacin (7aIII-7gIII)

3.2.4. Hydrolyses studies of CDS of 6-MNA (7aIV-7eIV)

3.2.5. Hydrolyses studies of CDS of BPA (7aV-7eV)

3.2.1. Hydrolyses studies of CDS of ibuprofen (7aI-7gI)

High performance liquid chromatography (HPLC) methods were developed for the analysis of CDS. The CDS **(7aI-7gI)** were analyzed using a mobile phase consisting of acetonitrile and monobasic potassium phosphate buffer (KH_2PO_4) (15 mM). The ratio of mobile phase was adjusted for each of these CDS to obtain retention time of 3-6 min. Analytical method was validated for linearity, precision, accuracy, limit of detection (LOD) and limit of quantification (LOQ) as described in literature.[5-7] A stock solution of CDS in buffer solution or in water was prepared. Dilutions were made representing samples from 60 ng/ml to 60 μg/ml and analyses of the samples were performed at 220 nm. Each experiment was repeated thrice, and LOD and linearity determined as shown in **Fig. 3.2.1** Analysis of the data within this range offered Equation-1. Graphical representation of the data proved the linearity of data as shown in **Fig. 3.2.2**
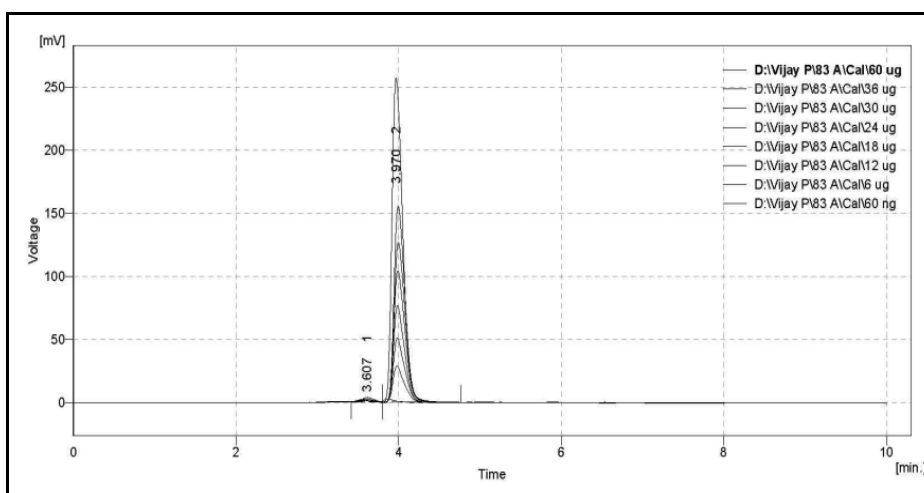
Fig. 3.2.1: Calibration and linearity chromatogram of derivative **(7aI)**

Table 3.2.1: The absorbance readings of **(7aI)** for the studies in buffers

Concentration (µg/ml)	Mean area (mV) ±SD*
6	269.0±7.07
12	481.0±12.82
18	718.5±14.12
24	969.5±16.26
30	1172.5±16.36
36	1437.0±22.82

*n=3

$$A = 38.88x + 24.7\ldots\ldots\ldots\ldots\ldots\textbf{(1)}$$

$(R^2=0.999)$

Where, A=concentration (µg/ml). X= area

For the determination of half life of disappearance of CDS, the derivative **(7aI)** in phosphate buffer solution was kept at 37±1°C at *p*H 6.0 and 7.4. After different time intervals aliquots (1.0 ml) were withdrawn from the test solution and appropriate dilutions were made using mobile phase and injected into HPLC system (20 µl) and analyzed at 220 nm in triplicate and area (mV) was measured. There are various methods used for the determination of order of the reaction but graphical method is the most common one.[8]
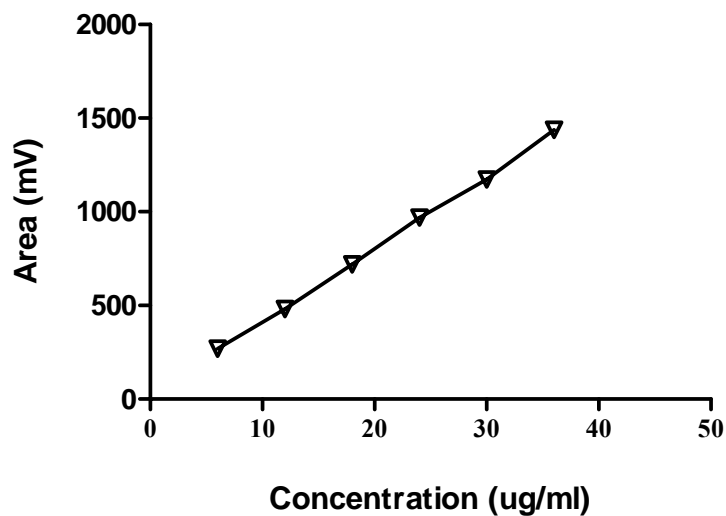
Fig. 3.2.2: Calibration plot for the estimation of **(7aI)**

According to this method, on plotting the concentration factor (y-x) versus t, if a straight line is obtained then the reaction is of zero order, if log (y-x) versus t gives a straight line then reaction is first order, if 1/(y-x) against t offers a straight line then the reaction is second order and if a straight line is obtained by plotting $1/(y-x)^2$ against t then the reaction is of third order.

The areas obtained from the study were plotted according to the above given criteria and correlation coefficients were determined. These were found to be 0.989, 0.995, 0.961 and 0.900 for zero, first, second and third order kinetics respectively as shown in **Fig. 3.2.3**

From these values it has been concluded that the synthesized CDS followed first order kinetics and as the overall concentration of the CDS is very small in the medium, so it is pseudo-first order kinetics. Comparing the above obtained linear equation with the general equation for the psuedo-first order kinetics, $\log Z_0 / (Z_0 - Z) = -k \times t/2.303$ (Z_0 is initial concentration of a substance, Z is the constant fraction degrading from it in time interval 't', k is the rate constant and t is time), we get the rate constant k for Sample **(7aI)** as given below:

$$k = m \times 2.303$$
$$= -0.051 \times 2.303,$$
$$= -0.1174$$

Table 3.2.2: Data presentation of (7aI) for calculation of rate constant (k) at pH 6.0

Time (days)	Area (mV) mean±SD (n=3)	Conc. (µg/ml) y	Amt. Degraded (µg/ml) x	y-x (µg/ml)	y-x (mol/lit)
1	824.33±26.10	20.56	0	20.56	4.14×10^{-05}
2	731.66±22.54	18.18	2.38	18.18	3.66×10^{-05}
4	615.33±23.45	15.19	5.37	15.19	3.06×10^{-05}
6	490.33±15.03	11.97	8.59	11.97	2.41×10^{-05}
8	368.66±12.03	8.847	11.71	8.84	1.78×10^{-05}
10	298.66±14.26	7.04	13.52	7.046	1.41×10^{-05}

Time (days)	Area (mV) mean±SD (n=3)	y-x (µg/ml)	Log (y-x) (mol/lit)	1/(y-x)	1/(y-x)^2
1	824.33±26.10	20.56	-4.38	24131.2	582316751.3
2	731.66±22.54	18.18	-4.43	27294.3	744977554.7
4	615.33±23.45	15.19	-4.51	32670.3	1067345826
6	490.33±15.03	11.97	-4.61	41440.6	1717326761
8	368.66±12.03	8.84	-4.74	56098.9	3147084090
10	298.66±14.26	7.046	-4.84	70432.5	4960730244

x= Concentration of derivative **(7aI)** at various time intervals which got hydrolyzed

y= initial concentration of the derivative at 0 h, i.e. 20.56 µg/ml

y-x= Concentration of derivative left intact in the solution at various time intervals
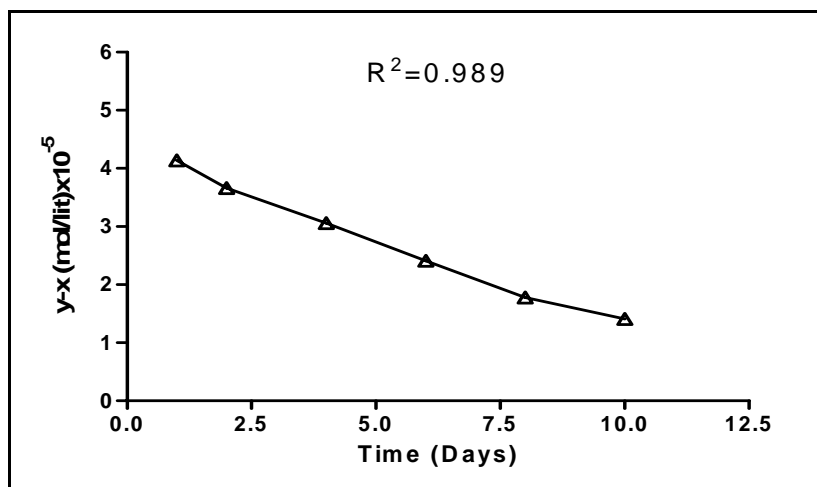
(A)
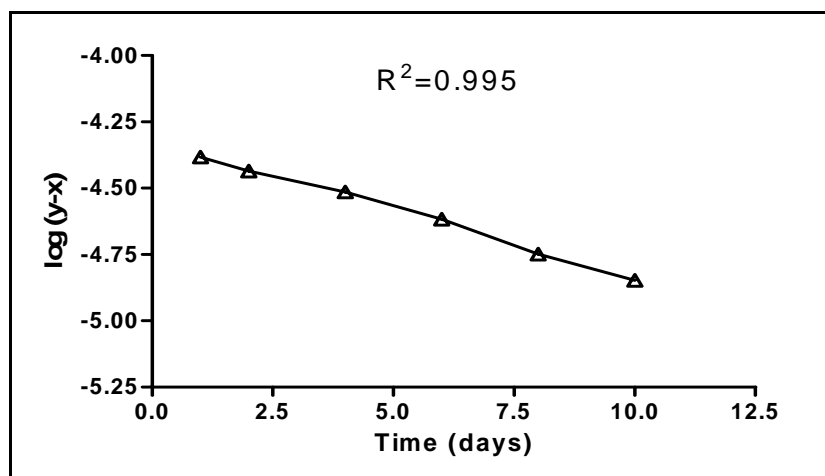
(B)
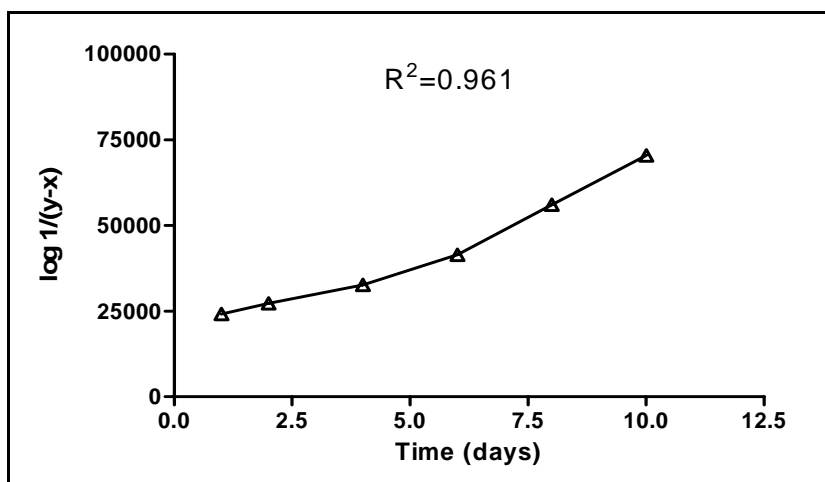
(C)
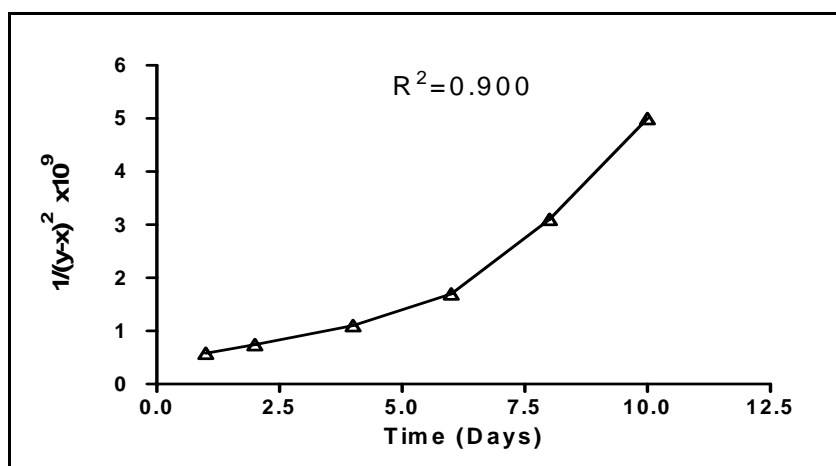
(D)

Fig. 3.2.3: Graphical presentation for calculated (y-x) vs t **(A)**, log (y-x) vs t **(B)**, 1/(y-x) vs t **(C)**, and $1/(y-x)^2$ vs t **(D)** for sample **(7aI)** at pH 6.0

Further calculations were done to find out half-life using first order half-life equation as given below:

$$t_{1/2} = 0.693/k \ldots\ldots\ldots\ldots\ldots\ldots (2)$$

The same procedure as described above was followed for rest of the derivatives **(7bI-7fI)**, and the calibration and chromatographic conditions have been shown in **Fig. 3.2.4** and **Table 3.2.3**

Stability study in human serum has been carried out using the same calibration curve as used in stability study determination in phosphate buffers. Working solutions of test compounds were prepared by dissolving the compounds in water and small amount of DMSO (20-40 μl). Whenever required followed by sonication for 2 min. Human serum samples were kept at 37 ^{o}C for 5 min before the addition of the test compound to initiate the reaction. Aliquots of the incubation mixtures (100 μL) were transferred to another tube containing 400 μL of cold acetonitrile/1 N HCl (90/10, v/v) to stop the reaction.[9] Samples were then centrifuged at 2800 rpm for 10 min.

Control incubations in the absence of the test compound were also performed. The analyses of test compounds were performed by the same method as indicated above and additionally guard column has been used. In all experiments, the stability of the synthesized CDS was determined as the percentage of the remaining compound at the given time point of interest (assuming 100 % of the compound is present at time 0). The slope of the linear regression from log (y-x) versus time plot (-k) was determined and the *in vitro* human serum half-life was determined using the above given equation (2) and the data obtained has been shown in **Table 3.2.4**.
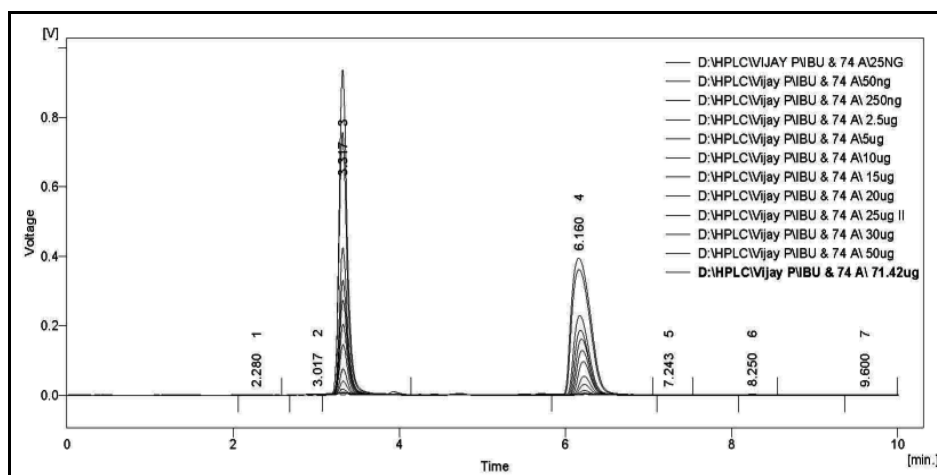
Fig. 3.2.4: Calibration and linearity chromatogram of **7fI**, (RT=3.31 min**)**
and the parent drug **5I** (RT=6.16)
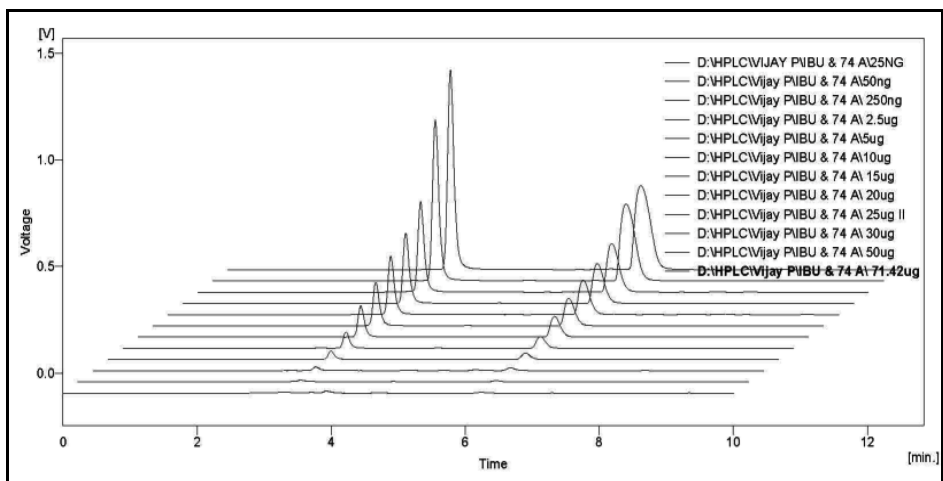
Fig. 3.2.5: 3D Calibration and linearity chromatogram of CDS **(7fI)**
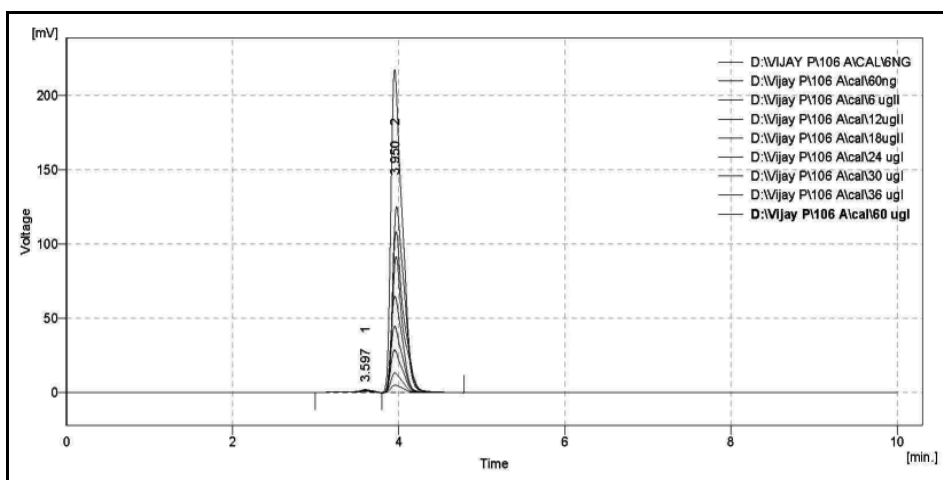
Fig. 3.2.6: Calibration and linearity chromatogram of CDS **(7bI)**
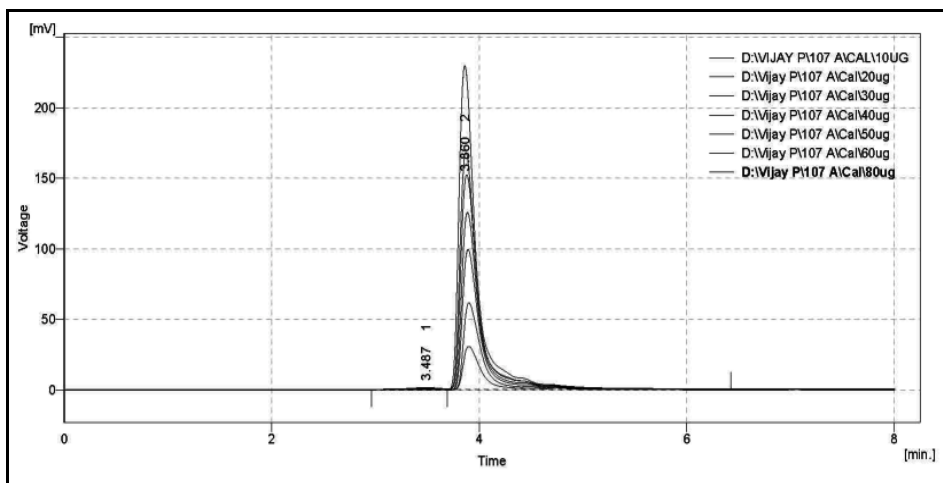
Fig. 3.2.7: Calibration and linearity chromatogram of CDS **(7dI)**

Table 3.2.3: Chromatographic data for CDS **(7aI-gI)**

Compound	RT (min)	Linearity (µg)	λ max (nm)	Mobile phase PB:ACN*	Flow rate (ml/min)
7aI	3.90±0.1	6-60	220	9:1	0.75
7bI	3.97±0.1	6-60	220	9:1	0.75
7cI	3.60±0.1	5-50	220	8:2	0.75
7dI	3.64±0.1	5-50	220	8:2	0.75
7eI	3.50±0.1	6-36	220	9:1	0.75
7fI	3.33±0.1	2.5-50	220	2:8	0.75
7gI	3.60±0.1	6-48	220	2:8	0.75

*PB= Phosphate buffer (15 mM): ACN= Acetonitrile

Table 3.2.4: Half lives of disappearance for CDS **(7aI-7gI)** in phosphate buffers pH 6.0, 7.4 and in the human serum.

Compound	Half life of disappearance of various CDS		
	pH 6.0 (h)	pH 7.4 (h)	Human serum (min)
7aI	141.01	156.87	8.45
7bI	167.76	133.68	15.30
7cI	164.33	177.63	12.84
7dI	137.28	184.55	18.47
7eI	85.37	92.55	10.88
7fI	432.0	446.40	38.10
7gI	384.0	412.80	28.44

The studies in buffers (*p*H 6.0 and 7.4) indicated that all of the drug derivatives **(7aI-7gI)** showed very high stability in both the *p*H conditions with the CDS having diamide bond found to be more stable as compared to CDS with ester bond. The half-lives ranged from 85.37-446.4 hours. The long half-lives of the derivatives (7**aI-7gI**) assured that these CDS would be hydrolyzed slowly giving prolonged release of the parent NSAID but a very long half life also is not described as it would adversely contribute to the therapeutic effect of the parent NSAID due to insufficient therapeutic concentration at the site of action.

On the other hand stability studies in human serum showed very fast hydrolysis of CDS and the half-lives varied from 8.45-38.10 min. This could be due to enzyme catalyzed hydrolysis of the CDS. Interestingly CDS without ester bond **(7fI-7gI)** showed moderate stability over the CDS with ester bond.

From the above studies it could be concluded that the synthesized CDS upon IA administration may release active drug in a controlled manner due to the coupled action of *p*H and enzymes (synovial fluid has *p*H 6.0 and increased activity of hydrolyzing enzymes during inflammation) and may show improved therapeutic effect.

3.2.2. Hydrolyses studies of CDS of naproxen (7aII-7gII)

Hydrolysis study of CDS of naproxen has been carried out in the same way as discussed for CDS of ibuprofen **(7aI-7gI)**. HPLC method has been developed to determine half life of disappearance of the synthesized CDS in phosphate buffers of *p*H 6 and 7.4, and in human serum. Half-lives of disappearance of CDS **(7aII-7gII)** were calculated and given in **Table 3.2.7.** The chromatographic conditions used for all the CDS were listed in **Table 3.2.6** below. For calibration plot and linearity determination, mobile phase composition was adjusted for each CDS so that the retention time (RT) of each CDS would fall in the range of 3-6 min as shown in **Fig. 3.2.8** below. Calibration curve shows linearity with r^2=0.999 as shown in **Fig. 3.2.9** and **Table 3.2.5**
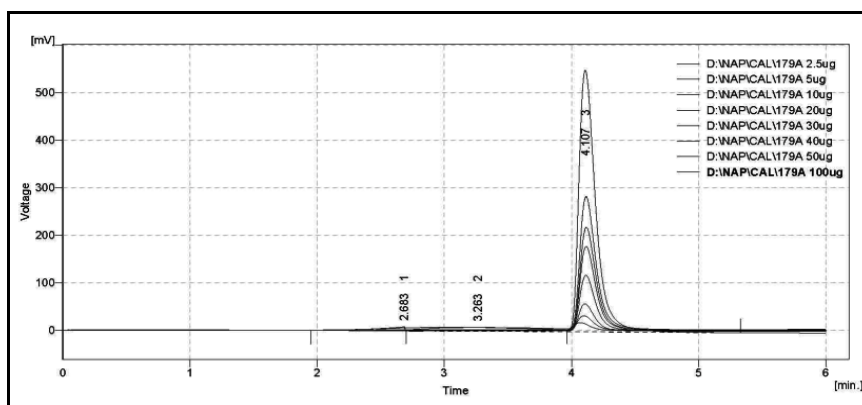
Fig. 3.2.8: Calibration and linearity chromatogram of derivative **(7aII)**

Table 3.2.5: The absorbance readings of **7aII** for the studies in buffers

Concentration (µg/ml)	Mean area (mV) ±SD*
5.0	264±08
10.0	504±14
20.0	1026±19
30.0	1563±16
40.0	2038±22
50.0	2609±26

*n=3,   A= 51.92x + 7.40…….……**(3)**, (R^2=0.999)

From these results it could be concluded that pyridinium salts were quite stable in phosphate buffer pH 6 as well as 7.4; the primary route of hydrolysis of these compound may be ester/amide bond cleavage.
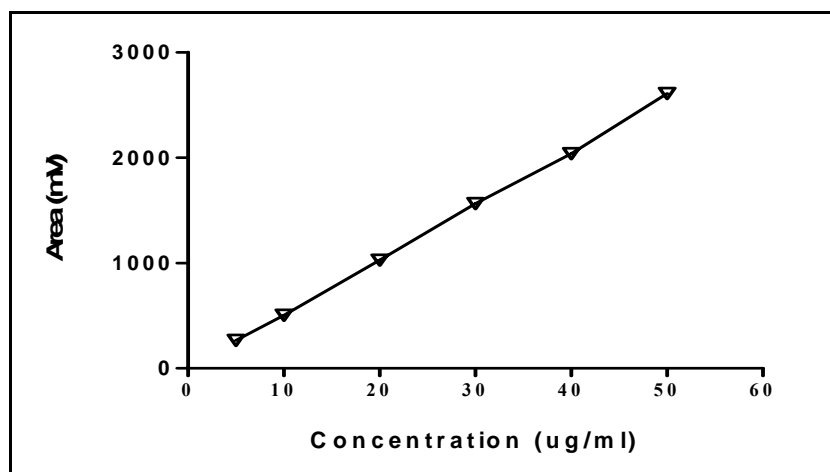
Fig. 3.2.9: Calibration plot for the estimation of **7aII**

89

Table 3.2.6: Chromatographic data of CDS **(7aII-7gII)**

Compound	RT (min)	Linearity (μg)	λ max (nm)	Mobile phase PB (15mM):ACN*	Flow rate (ml/min)
7aII	4.11±0.1	5-50	229.0	8:2	0.75
7bII	3.73±0.1	5-50	229.0	8:2	0.75
7cII	3.68±0.1	5-50	229.0	8:2	0.75
7dII	3.71±0.1	5-50	229.0	8:2	0.75
7eII	3.77±0.1	5-50	229.0	8:2	0.75
7fII	3.66±0.1	5-50	229.0	8:2	0.75
7gII	3.64±0.1	5-50	229.0	8:2	0.75

Table 3.2.7: Half lives of disappearance of CDS in various conditions

Compound	Half life of disappearance of CDS 7aII-7gII		
	*p*H 6.0 (h)	*p*H 7.4 (h)	Human serum (min)
7aII	52.58 h	72.58	8.10
7bII	144.88	192.36	6.40
7cII	168.40	204.18	5.30
7dII	132.50	228.31	10.12
7eII	491.41	578.35	4.06
7fII	127.2	134.4	14.18
7gII	276.1	252.97	11.36

All the synthesized CDS have shown rapid enzymatic hydrolysis in human serum to cleave ester/amide bond present in CDS **(7aII-7gII).** Again from the above studies it could be concluded that the synthesized CDS upon IA administration will release the active drug in a controlled manner over a long period of time.

3.2.3. Hydrolyses studies of CDS of indomethacin (7aIII-7gIII)

Hydrolysis study of a CDS of indomethacin has been carried out in the same way as discussed for CDS **(7aI-7gI)**. HPLC method has been developed to determine half-lives of disappearance of the synthesized CDS in phosphate buffers of *p*H 6 and 7.4 and in human serum. The chromatographic conditions used for all the CDS have been listed in **Table 3.2.9** below. Calibration plot and linearity were determined as shown in **Fig. 3.2.11**
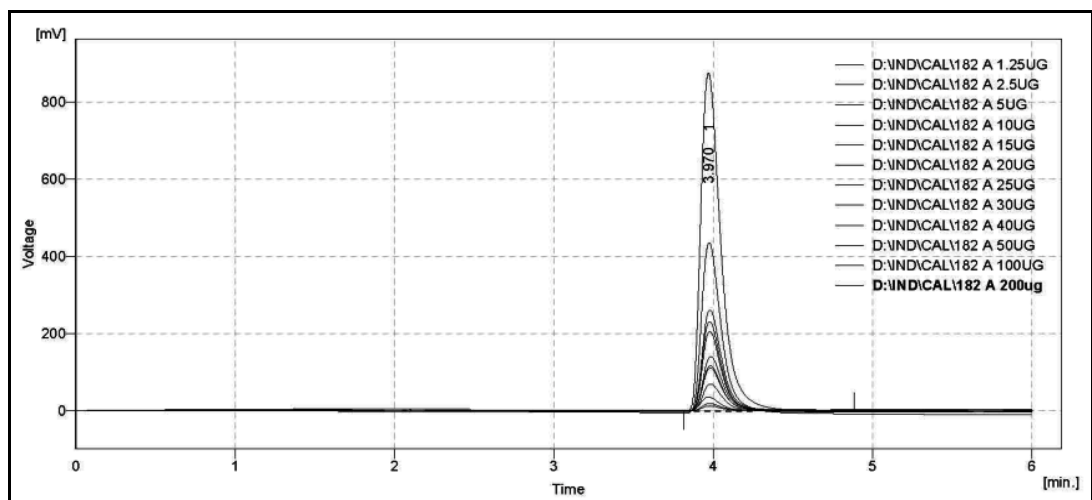
Fig. 3.2.10: Calibration and linearity chromatogram of derivative **(7aIII)**

Table 3.2.8: The absorbance readings of **7aIII** for the studies in buffers

Concentration (µg/ml)	Mean area (mV) ±SD*
2.5	158±08
5.0	297±11
10.0	593±14
20.0	1113±21
30.0	1689±24
40.0	2288±31

*n=3,

$$A= 56.35x + 13.25…………(4), (R^2=0.999)$$
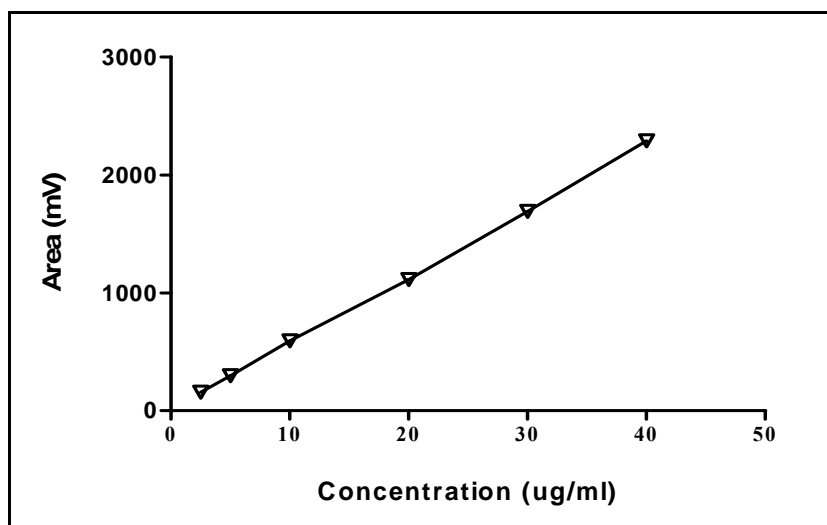
Figure 3.2.11: Calibration plot for the estimation of **7aIII**

Table 3.2.9: Chromatographic conditions for CDS **(7aIII-7gIII)**

Compound	RT (min)	Linearity (μg)	λ max (nm)	Mobile phase PB(15mM):ACN*	Flow rate (ml/min)
7aIII	3.98±0.1	2.5-40	229.0	8:2	0.75
7bIII	3.73±0.1	2.5-40	229.0	8:2	0.75
7cIII	3.76±0.1	2.5-40	229.0	8:2	0.75
7dIII	3.74±0.1	2.5-40	229.0	8:2	0.75
7eIII	3.71±0.1	2.5-40	229.0	8:2	0.75
7fIII	3.81±0.1	2.5-40	229.0	8:2	0.75
7gIII	3.78±0.1	2.5-40	229.0	8:2	0.75

*ACN=Acetonitrile

From these results it could be concluded that indomethacin CDS were quite stable in phosphate buffer of pH 6.0 as well as 7.4, but interestingly compared to CDS of ibuprofen **(7aI-7gI)** and naproxen **(7aII-7gII)** these CDS showed significantly low stability in phosphate buffer at pH 6.0 and 7.4, except for **7fIII-7gIII**.

This instability may be due to presence of extra hydrolysable groups in indomethacin CDS **(7aIII)** which may contribute to the low stability of these CDS. Suspected sites (**I-III**) which are prone to hydrolysis are shown in the structure given below.

Table 3.2.10: Half lives of disappearance of CDS **(7aIII-7gIII)** in phosphate buffers of pH 6.0 and 7.4 and in human serum (80 %).

Compound	Half life of disappearance of various CDS		
	pH 6.0 (h)	pH 7.4 (h)	Human serum (min)
7aIII	29.11	38.35	18.40
7bIII	76.85	81.47	16.10
7cIII	41.84	52.70	22.55
7dIII	56.37	69.74	39.50
7eIII	32.44	49.61	46.74
7fIII	135.88	147.53	55.80
7gIII	141.7	129.20	34.19

(7aIII)
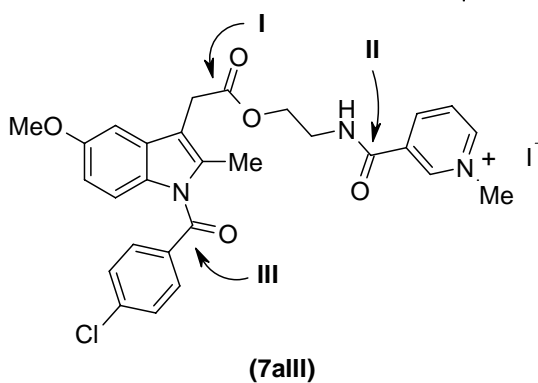
The primary route of hydrolysis of these CDS may be ester bond cleavage. Indomethacin CDS were also prone to hydrolysis in human serum but are more stable than CDS of ibuprofen and naproxen, may be due to steric hinderance due to bulky indomethacin moiety.

3.2.4. Hydrolyses studies of CDS of 6-MNA (7aIV-7eIV)

Hydrolysis study of a CDS of 6-MNA **(5IV)** has been carried out in the same way as discussed for CDS **(7aI-7gI)**. HPLC method has been developed to determine half-lives of disappearance of the synthesized CDS in phosphate buffers of *p*H 6.0 and 7.4, and in human serum. The chromatographic conditions used for all the CDS have been listed in **Table 3.2.12** below. Calibration plot and linearity were determined and mobile phase composition adjusted for each CDS so that RT should fall in the range of 3-6 min as shown in **Fig. 3.2.13** below.
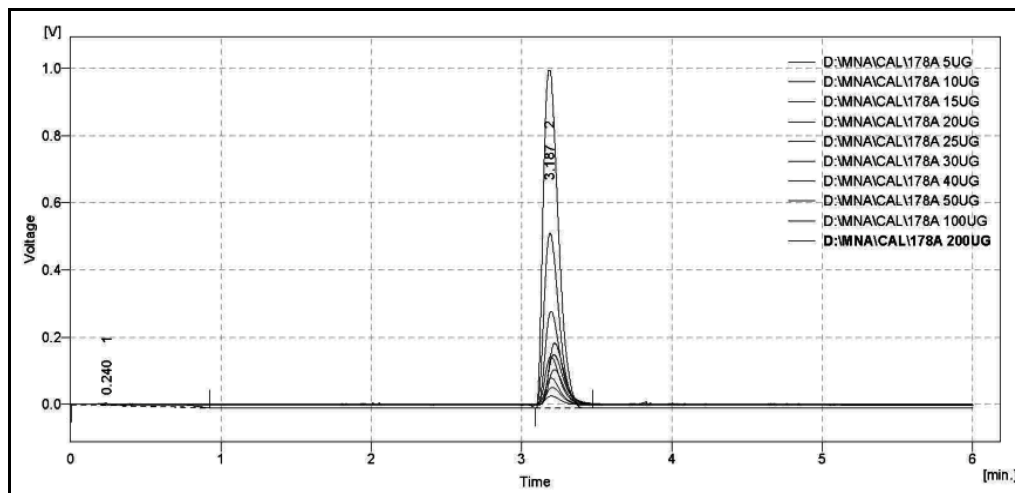
Fig. 3.2.12: Calibration and linearity chromatogram of derivative **(7aIV)**

Table 3.2.11: The absorbance readings of **(7aIV)** for the studies in buffers

Concentration (µg/ml)	Mean area (mV) ±SD*
10.0	358±09
15.0	551±11
20.0	746±14
30.0	1111±19
40.0	1520±23
50.0	1973±26

*n=3,

A= 39.93x–55.03…………**(5)**

R^2=0.998)

94
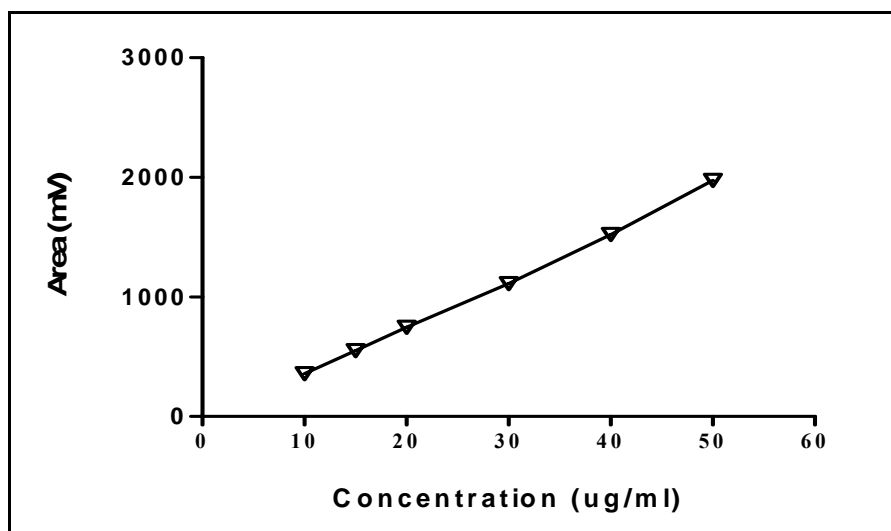
Fig. 3.2.13: Calibration plot for the estimation of **(7aIV)**

Table 3.2.12: Chromatographic conditions for CDS **(7aIV-7gIV)**

Compound	RT (min)	Linearity (μg)	λ max (nm)	Mobile phase PB:ACN*	Flow rate (ml/min)
7aIV	3.18±0.1	10-50	226.0	8:2	1.0
7bIV	3.65±0.1	10-50	226.0	8:2	0.75
7cIV	3.63±0.1	10-50	226.0	8:2	0.75
7dIV	3.64±0.1	10-50	226.0	8:2	0.75
7eIV	3.66±0.1	10-50	226.0	8:2	0.75

Table 3.2.13: Half life of disappearance of CDS **(7aIV-gIV)** in phosphate buffers of *p*H 6.0 and 7.4 and in human serum (80 %).

Compound	Half life of disappearance of various CDS		
	*p*H 6.0 (h)	*p*H 7.4 (h)	Human serum (min)
7aIV	252.11	276.30	18.41
7bIV	220.40	271.50	34.80
7cIV	204.30	283.56	22.63
7dIV	271.12	148.80	32.41
7eIV	180.48	218.40	16.09

3.2.5. Hydrolyses studies of CDS of BPA (7aV-7eV)

Hydrolysis study of a CDS of BPA **(5V)** has been carried out in the same way as discussed for CDS **(7aI-7gI)**. HPLC method has been developed to determine half-lives of disappearance of the synthesized CDS in phosphate buffers of *p*H 6 and 7.4, and in human serum.

The chromatographic conditions used for all the CDS have been listed in **Table 3.2.15** below. Calibration plot and linearity were determined and mobile phase composition adjusted for each CDS so that RT should fall in the range of 3-6 min as shown in **Fig. 3.2.15** below.
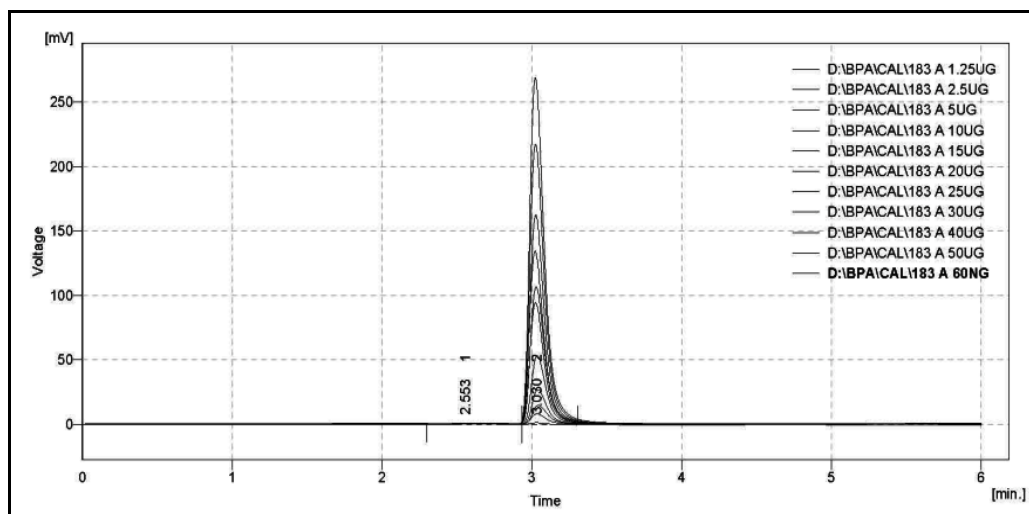
Fig. 3.2.14: Calibration and linearity chromatogram of derivative **(7aV)**

Table 3.2.14: The absorbance readings of **(7aV)** for the studies in buffers

Concentration (µg/ml)	Mean area (mV) ±SD*
2.5	99±06
5	184±10
10	367±16
20	741±19
30	1125±22
40	1504±26
50	1865±33

*n=3,

$$A = 37.43x - 1.43 \ldots \ldots \ldots \ldots (4),$$

$$(R^2 = 0.999)$$
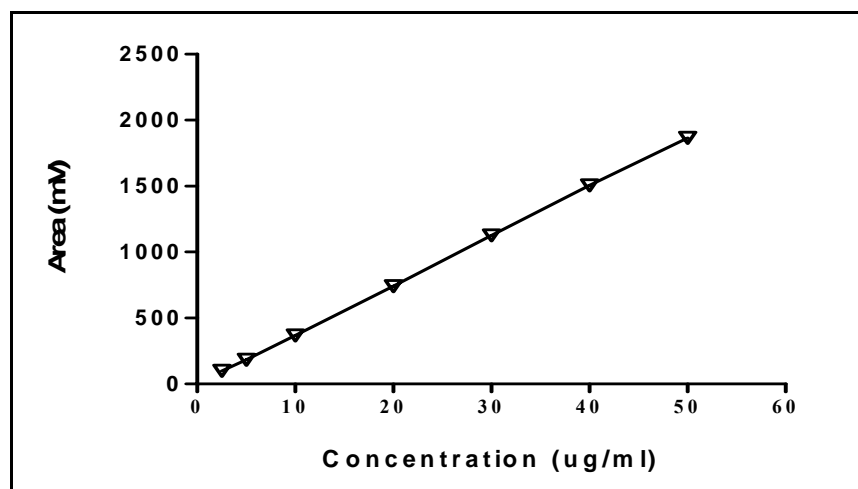
Fig. 3.2.15: Calibration plot for the estimation of **(7aV)**

Table 3.2.15: Chromatographic conditions for CDS **(7aV-gV)**

Compound	RT (min)	Linearity (µg)	λ max (nm)	Mobile phase PB(15mM):ACN*	Flow rate (ml/min)
7aV	3.02±0.1	2.5-50	228.0	8:2	1.0
7bV	4.18±0.1	2.5-50	228.0	8:2	0.75
7cV	4.13±0.1	2.5-50	228.0	8:2	0.75
7dV	4.15±0.1	2.5-50	228.0	8:2	0.75
7eV	4.22±0.1	2.5-50	228.0	8:2	0.75

Table 3.2.16: Half life of disappearance of CDS **(7aV-gV)** in phosphate buffer pH 6.0, 7.4 and in human serum (80 %).

Compound	$t_{1/2}$ in Phosphate buffer and human serum		
	pH 6.0 (h)	pH 7.4 (h)	Human serum (90%) (min)
7aV	180.12	276.03	26.88
7bV	218.11	230.40	34.51
7cV	244.8	304.8	18.55
7dV	224.81	324.10	30.77
7eV	194.4	267.81	44.07

The studies in buffers (*p*H 6.0 and 7.4) indicated that all the CDS **(7aI-7gV)** showed very high stability in phosphate buffer at both the *p*H conditions. CDS having diamide bond were found to be more stable as compared to CDS with ester bond. The minimum and maximum values of half life of disappearance were shown in **Table 3.2.17** below.

The long half-lives of the CDS **(7aI-7gV)** in phosphate buffers assured that these CDS would be hydrolyzed slowly giving prolonged release of the parent drug but a very long half life is also not desirable. On the other hand stability studies in human serum showed very fast hydrolysis of CDS and the half-life values fall in the range of 4.06-55.80 min. This could be due to enzyme catalyzed hydrolysis of the CDS. Interestingly CDS without ester bond **(7fI-7gIII)** showed moderately high stability over the CDS with ester bond **(7aI-7eV)**. This may be due to highly specific hydrolyzing nature of esterase enzymes towards ester bond.

Table 3.2.17: Comparison of half lives of disappearance of CDS **(7aI-7gV)**

CDS	Series	Half life of disappearance in PB		Human serum
		*p*H 6 (min-max h)	*p*H 7.4 (min-max h)	(min-max, min)
7aI-7eI	Ester	85.37-167.76	92.55-184.55	8.45-18.47
7fI-7gI	Amide	384-432	412.80-446.40	28.44-38.10
7aII-7eII	Ester	52.58-491.41	72.58-578.35	4.06-10.12
7fII-7gII	Amide	127.2-276.1	134.4-252.97	11.36-14.18
7aIII-7eIII	Ester	29.11-76.85	38.35-81.47	16.10-46.74
7fIII-7gIII	Amide	135.88-141.7	129.20-147.53	34.19-55.80
7aIV-7eIV	Ester	180.48-271.12	148.80-283.56	16.09-34.80
7aV-7eV	Ester	180.12-244.8	230.40-324.10	18.55-44.07

From the above studies it could be concluded that all the synthesized CDS upon IA administration might release active drug in a controlled manner due to the coupled action of *p*H and enzymes.

3.3. Cytotoxicity studies (MTT assay)

As mentioned earlier cationic molecules get accumulated in the liver also along with cartilage and cleared by the kidney. Therefore, liver and renal toxicity issues have to

be addressed in order to develop these CDS.[10] Hence, this study was undertaken to evaluate the *in vitro* cellular response to CDS on exposure. *In vitro* assays for xenobiotic toxicity are recently carefully considered by key government agencies (e.g. NIH, FDA etc), mainly to reduce the use of animals in research and to assess human risks. Rat Liver cell line (BRL-3A) has been chosen for the present study.[11]

The MTT assay is a <u>colorimetric assay</u> for measuring the activity of enzymes that reduce MTT to <u>formazan</u> dyes giving a purple color. Its application allows assessing the viability (cell counting) and the proliferation of <u>cells</u> (<u>cell culture assays</u>). It can also be used to determine <u>cytotoxicity</u> of potential <u>medicinal</u> agents and toxic materials, since these agents would stimulate or inhibit cell viability and growth. The assay is based on the reduction of soluble yellow tetrazolium salt (MTT Br) to insoluble Purple formazan crystals by metabolically active cells as shown below. Only live cells can take up tetrazolium salt. The enzyme, NADPH dehydrogenase present in the mitochondria of live cells can convert internalized tetrazolium salt to purple coloured formazan crystals, which is directly proportional to the number of live cells.

MTT Br **(8)**   Formazan **(9)**
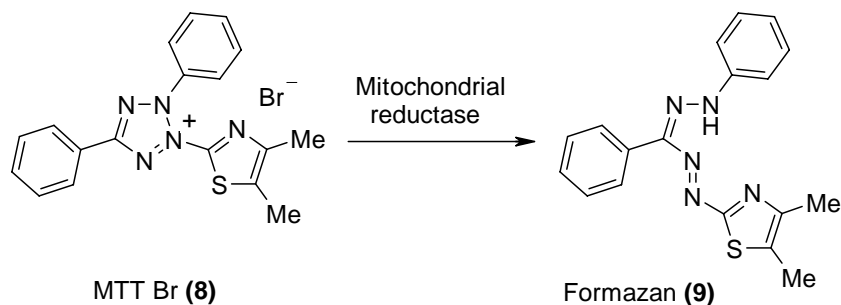
The compound can be quantified by measuring its absorbance at a fixed <u>wavelength</u> (between 500 and 600 nm, usually 570nm) by a microplate reader (<u>spectrophotometer</u>). The percent viability of the cells can be calculated using the formula given below.

$$\text{Cell viability (\%)} = At/Ac \times 100 \dots\dots\dots\dots\text{(1)}$$

Where:

At= absorbance of sample (test) at 570 nm;

Ac= absorbance of control at 570 nm

MTT assay was performed on the synthesized CDS and their IC_{50} concentration compared with parent drugs as shown in **Fig. 3.3.1**

Table 3.3.1: MTT assay result of compound **(5I)**

Sample Concentration (µg/ml)	% Cell viability ± SD	% Cell Death
Control	100±3.01	--
46.87	79.10±5.04	20.90
93.75	79.03±5.08	20.97
187.5	71.53±4.11	28.47
375	62.14±3.20	37.86
750	37.01±3.05	62.99
1500	27.98±2.08	72.01
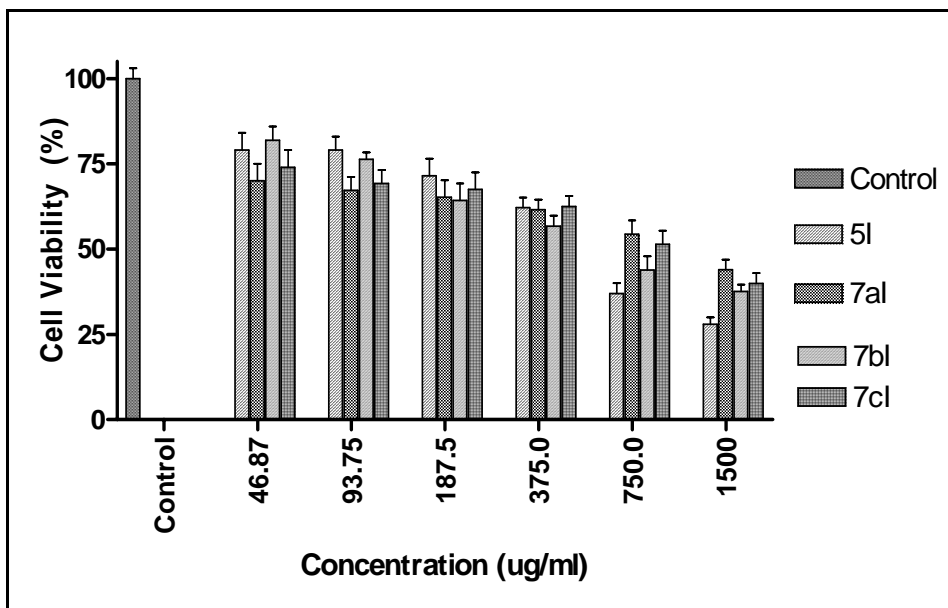
Fig. 3.3.1: Effect of various concentrations of compounds on cell viability
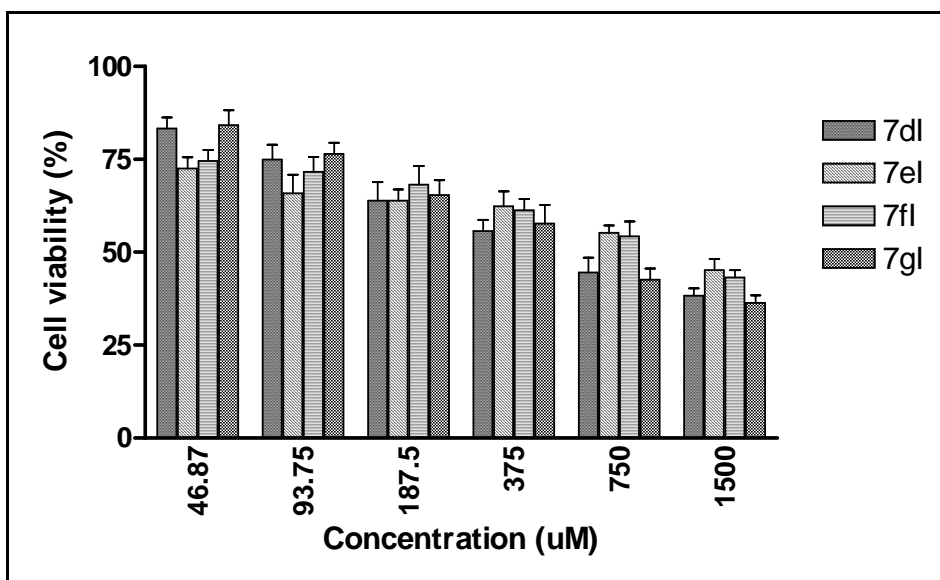
Fig. 3.3.2: Effect of various concentrations of compounds **(7dI-7gI)** on cell viability

Along with cell viability, morphology of the cells was also studied to check whether any cell necrosis occurred or not. The photograph of normal cells and drug treated cells shows slight cell necrosis in CDS treated cells at high concentration as compared to normal cells.
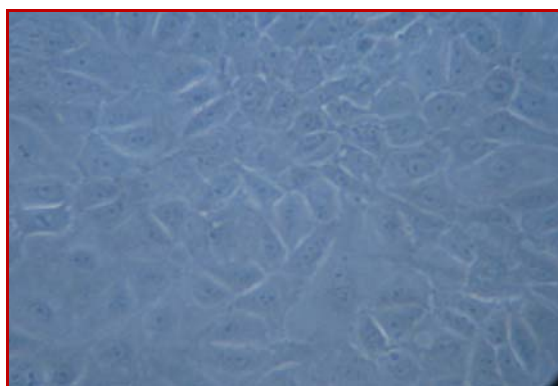
Fig. 3.3.3: Photograph of normal rat Liver cell line (BRL-3A)
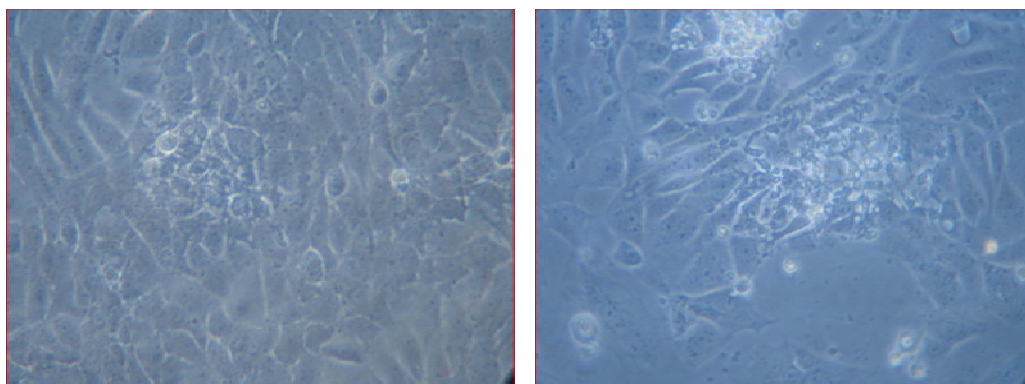
Fig. 3.3.4: Photograph of rat Liver cell line (BRL-3A) treated with CDS **(7aI)**.

(A)   at low concentration (46.48 μM), **(B)** at high concentration (1500 μM)
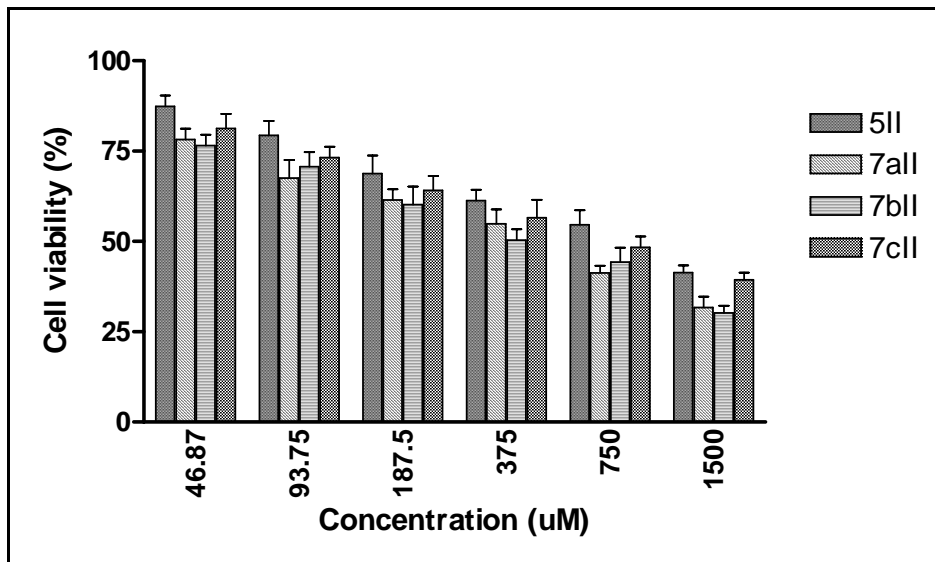
Fig. 3.3.5: Effect of various concentrations of compounds **(5II, 7aII-7cII)** on cell
Viability
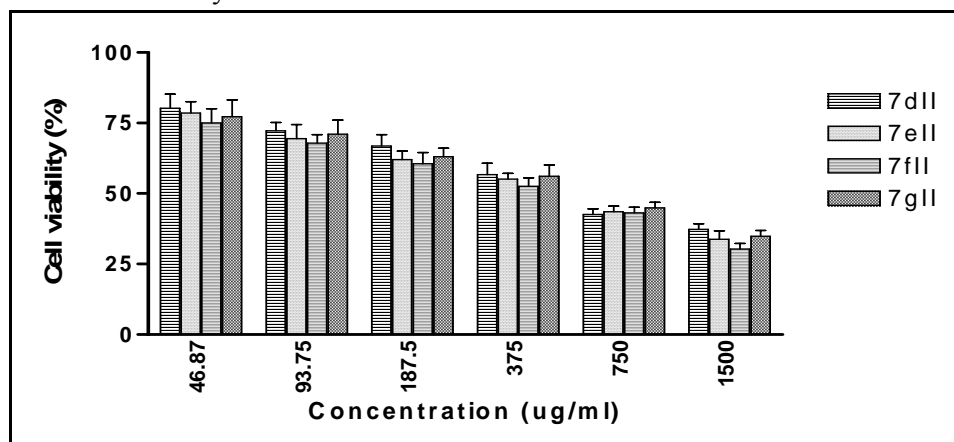
Fig. 3.3.6: Effect of various concentrations of compounds **(5II, 7dII-7gII)** on cell
viability
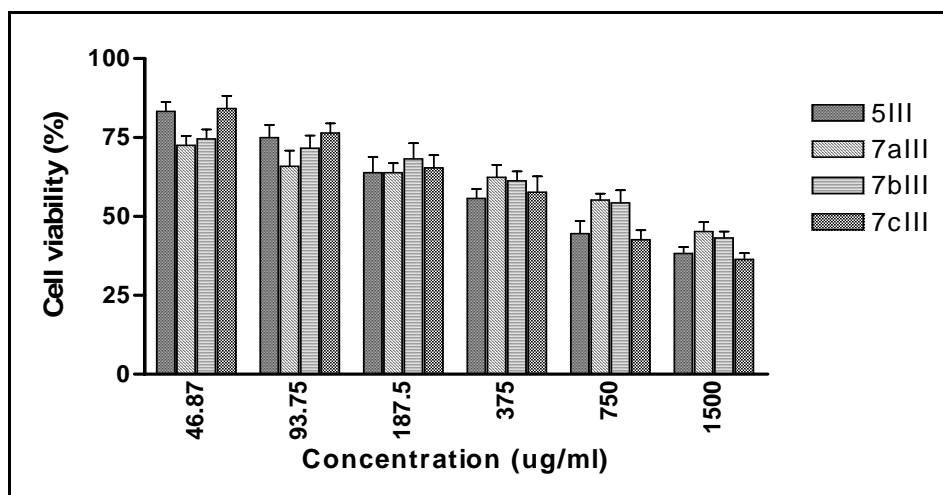
Fig. 3.3.7: Effect of various concentrations of compounds **(5III, 7aIII-7cIII)** on cell viability.
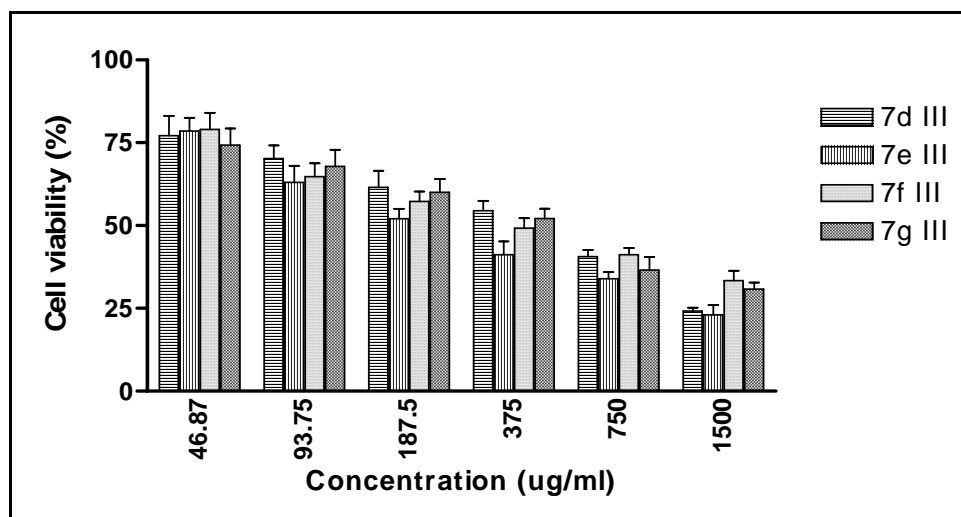
Fig. 3.3.8: Effect of various concentrations of compounds **(7dIII-7gIII)** on cell viability
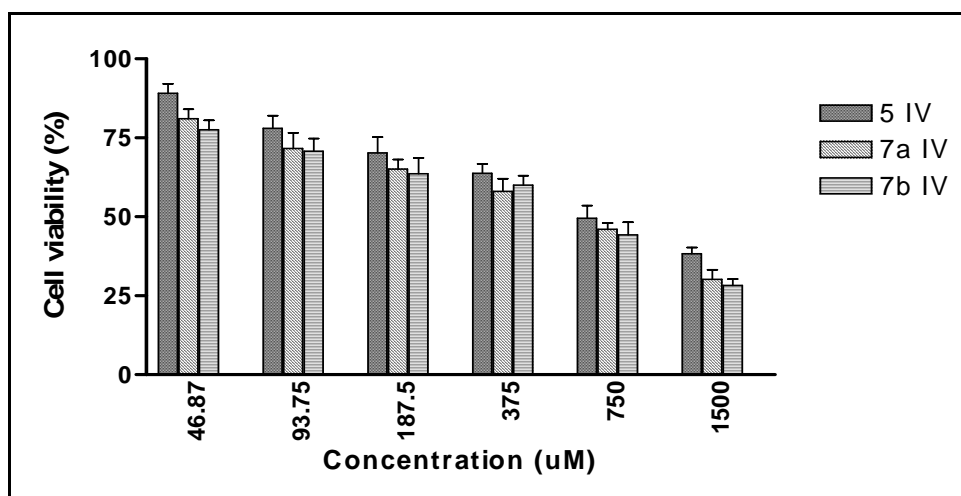
Fig. 3.3.9: Effect of various concentrations of compounds **(5IV, 7aIV-7bIV)** on cell

viability
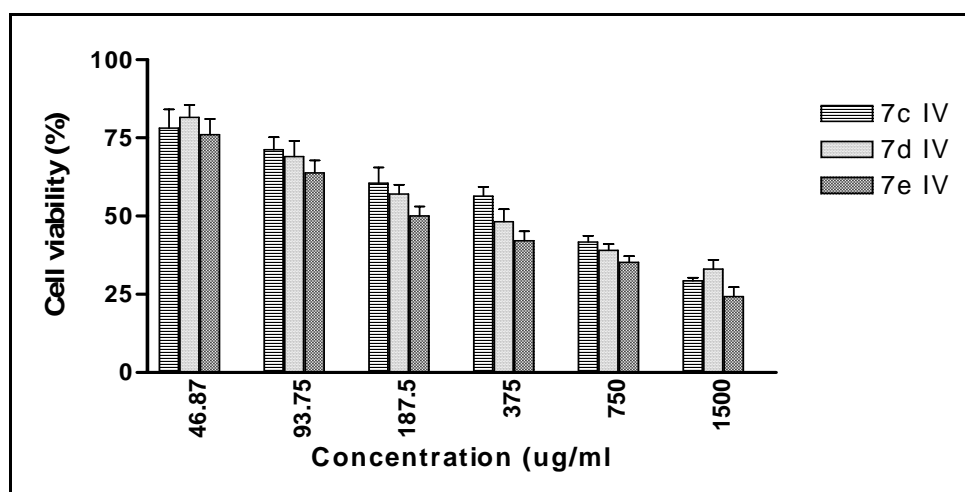
Fig. 3.3.10: Effect of various concentrations of compounds **(7cIV-7eIV)** on cell viability
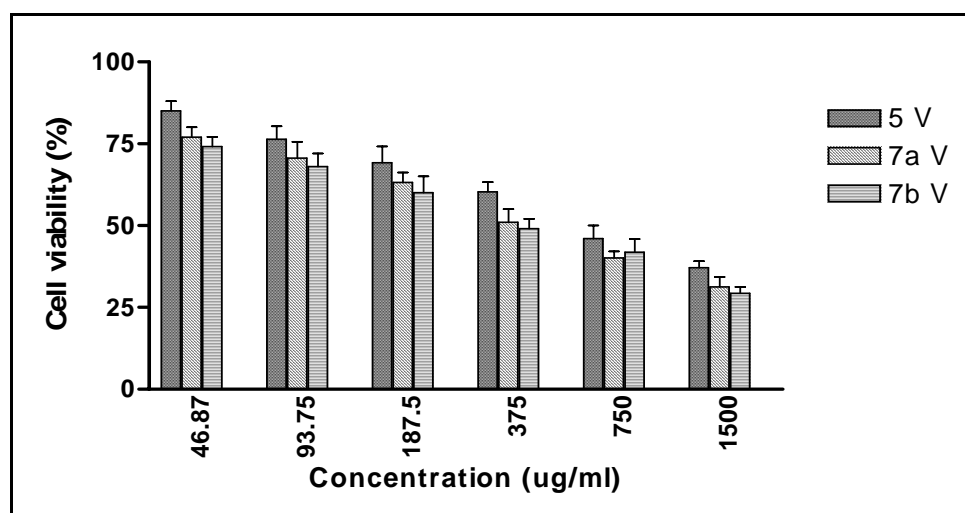
Fig. 3.3.11: Effect of various concentrations of compounds **(5V, 7aV-7bV)** on cell viability
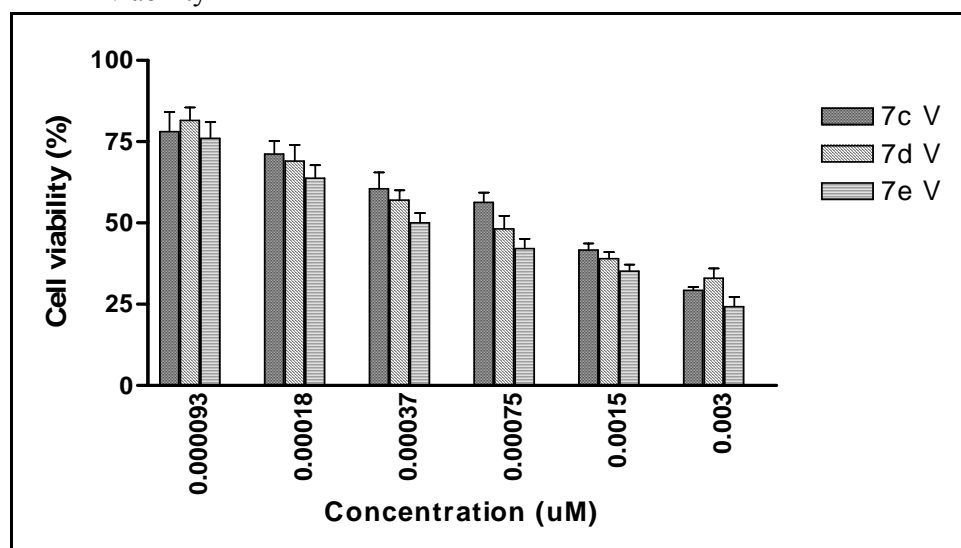
Fig. 3.3.12: Effect of various concentrations of compounds **(7cV-7eV)** on cell viability

From the *in vitro* cell line studies it was concluded that there is no significant effect of pyridinium carrier system on cell toxicity. But as compared to the parent drugs all the synthesized CDS showed higher cell death which may be due to charge on the CDS. All the cell membranes have negative charge and they may interact with positively charged molecules affecting the cell permeability which may result in cell death or retardation of cell growth. Such type of interaction may also result in cell necroses which occurs at higher concentrations of CDS but the parent NSAIDs lack this effect as shown in **Fig. 3.3.4**.

3.4. Bio-distribution and gamma imaging studies

This study was carried out with the aim to assess the residence time of NSAIDs and synthesized CDS in joint cavity upon IA administration. Little information is available in the literature on the effect of charge on residence time of drugs in joint cavity. For such a study to be performed, radiolabeling of the synthesized derivatives was required to be done for their localization/quantification in the joint cavity. To study these aspects the NSAID and the CDS were labeled using ^{99m}Tc. Nearly 80 % of all radiopharmaceuticals, used in nuclear medicine are ^{99m}Tc-labeled compounds. The reason for such a predominant position of ^{99m}Tc in clinical use is its extremely favorable physical and radiation characteristics. It has a 6-hour (approximately) half-life and emits soft monochromatic γ-rays of 140 keV power which do not affect the patient adversely. ^{99m}Tc is readily available in a sterile, pyrogen free and carrier free state from ^{99}Mo-^{99m}Tc generators.

Technetium can exist in eight oxidation states namely, -1 to +7, and the stability of these oxidation states depends on the type of ligands and chemical environment. The +7 and +4 states are the most stable states. The lower oxidation states are normally stabilized by complexation with ligands. The radioactive form of technetium (^{99m}Tc) is available as sodium pertechnetate salt (^{99m}Tc-NaTcO$_4$). In this salt, technetium is present in a stable state so, it does not easily complex with various ligands. To make a complex, the oxidation state has to be reduced to +5 or less from its original +7 state. For this purpose various reducing agents like stannous chloride, stannous citrate, stannous tartrate and sodium borohydride with concentrated hydrochloric acid and ferrous sulphate with dithionite are used. Among these, stannous chloride in acidic medium is the most widely

used reducing agent. After reduction of technetium to lower oxidation state, the pH of the medium has to be raised because complexes in general are less stable in acidic media and more stable in neutral/alkaline media. But, the pH of the medium cannot be raised to a more basic side otherwise the stannic form of tin (which gets formed in the medium) and the reduced forms of technetium precipitate out. So, a compromise has to be made and a proper pH adjustment of the solution has to be done so that there is no precipitation and the complex also remains stable.

The reduced ^{99m}Tc can combine with different ligands like -COO-, -CONH, -OH, -NH$_2$, -CO-, -COOR and -SH to afford complexes which may be stable depending on the medium and the complexing agent. For a new compound acting as a complexing agent for ^{99m}Tc, its labeling efficiency has to be evaluated. If the new compound is a good complexing agent then it would give a stable complex under the given conditions and the labeling efficiency would be approximately 100 % but, if the complex is not very stable then this efficiency would be much less.[12-13]

To assess the stability, the solution of the complex is run on ascending instant thin layer chromatography (ITLC) in three different solvent systems separately, as mobile phases i.e. acetone (100 %), saline (0.9 %) and a mixture of pyridine-acetic acid-water (PAW) (3.5:5:1), and detection of the complex is carried out using γ-camera. In acetone (100 %) and saline (0.9 %) solvent systems the ^{99m}Tc-bound complex would remain at the base of application of the spot and the uncomplexed ^{99m}Tc would travel along with the solvent front while in the PAW solvent system the complex would travel along with the solvent front while the uncomplexed ^{99m}Tc would remain at the base. By subtracting the activity obtained from acetone/saline run ITLC from the activity of PAW-run ITLC (activity of the solvent front region) the net amount of activity obtained from the labeled compound could be obtained which would provide the labeling efficiency. Stability of the labeled complex in human serum could also be determined based on the above said principle. After incubating the labeled complex with serum, samples were withdrawn at different time intervals and run on ITLC using the above described three mobile phases separately. Any increase in reduced/hydrolysed ^{99m}Tc activity is an indication of breakdown of the complex in human serum. 6-MNA **(5IV)** was chosen as the parent NSAID for all the studies as it has a long half-life. Due to its long half life it would be easy to find out its concentration in the whole body if the drug would leave the joint.

3.4.1. Optimization of radiolabeling of CDS and parent drug

The radiolabling of the compounds with reduced ^{99m}Tc was carried out as per the direct labeling method. The radiolabeling was optimized by taking three factors into account i.e. effect of pH on complex formation, incubation time and stannous chloride concentration.[14]

Table 3.4.1: Effect of pH on radiolabeling efficiency of compounds **(5IV, 7aI-7bI, 7aIV)**

pH	% Radiolabeled compound			
	5IV	**7aI**	**7bI**	**7aIV**
5.5	63.08±3.1	67.18±5.0	61.29±2.1	72.80±4.1
6.0	71.06±4.0	77.04±4.1	75.11±4.3	84.05±3.0
6.5	84.38±4.3	88.05±4.3	90.01±3.0	96.51±5.1
7.0	**94.44±5.1**	**95.88±5.0**	**94.86±5.1**	**95.61±4.2**
7.5	89.01±4.7	91.07±3.7	91.76±4.0	94.46±5.0
8.0	80.36±3.0	84.53±4.1	85.60±4.1	90.47±3.1

The pH of the labeled complex was increased from 5.5 to 8 and its effect on labeling efficiency was studied. The radiolabeled complexes were incubated for various time periods (5-40 min) and the effect of incubation time on labeling efficiency was determined keeping other variables constant. The effect of stannous chloride dihydrate (SnCl$_2$.2H$_2$O) concentration (50-200 μg) on the labeling efficiency was also studied to obtain the optimum concentration needed for maximum labeling. From the data it was concluded that maximum radiolabeling efficiency was obtained at pH 7.0, with incubation time of 30 min and at 150 μg stannous chloride concentration.
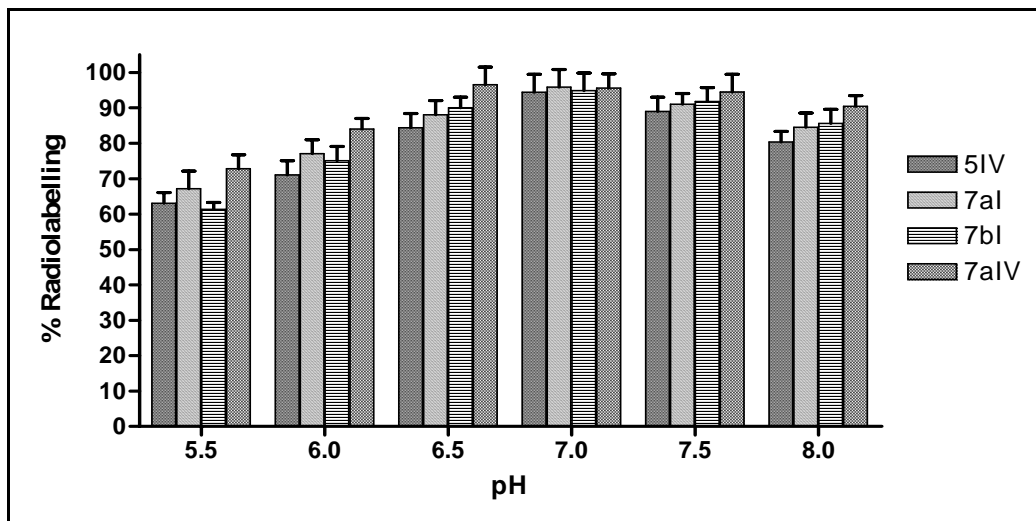
Fig. 3.4.1: Effect of *p*H on radiolabeling efficiency of compounds (**5IV, 7aI-7bI, 7aIV**)

Table 3.4.2: Effect of incubation time on radiolabeling efficiency of derivatives

(**5IV, 7aI-7bI, 7aIV**)

Incubation Time (min)	% Radiolabeled compound			
	5IV	**7aI**	**7bI**	**7aIV**
5.0	60.12±3.0	63.17±2.3	59.01±3.1	64.05±3.0
10	68.06±4.1	82.51±3.1	78.56±2.0	84.15±2.1
20	88.33±3.2	89.06±4.1	87.96±3.3	89.96±3.4
30	95.06±2.0	94.08±4.3	**96.86±4.3**	**94.57±4.2**
40	**96.40±3.0**	**95.09±5.0**	96.63±5.1	91.05±4.3
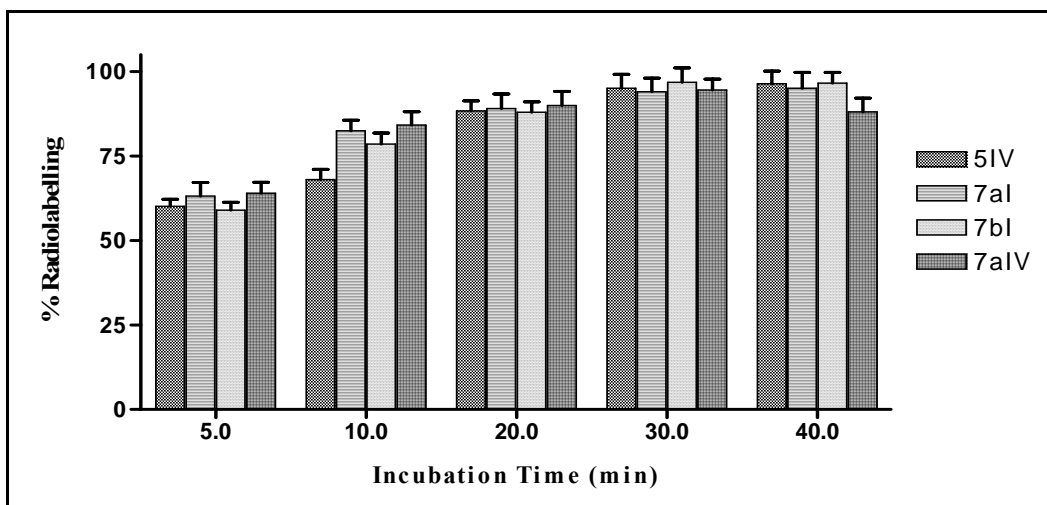
Fig. 3.4.2: Effect of incubation time on radiolabeling efficiency of compounds **(5IV, 7aI-7bI, 7aIV)**

Table 3.4.3: Effect of $SnCl_2 \cdot 2H_2O$ concentration on radiolabeling efficiency of derivatives **(5IV, 7aI-7bI, 7aIV)**

$SnCl_2$ (µg)	5 IV			7aI			7bI		
	% B	% F	% C	% B	% F	% C	% B	% F	% C
50	79.89	18.13	1.88	78.77	19.33	1.9	81.54	15.87	2.41
100	84.55	14.33	1.11	83.78	13.87	1.76	87.71	11.64	0.58
150	94.87	4.61	0.51	**96.04**	3.37	0.39	93.84	5.06	0.69
200	**95.01**	4.1	0.88	95.1	3.77	1.12	**94.88**	4.09	1.02

$SnCl_2$ (µg)	7aIV		
	% B	% F	% C
50	84.1	14.67	1.23
100	89.55	8.46	1.97
150	**94.91**	4.36	0.72
200	93.45	5.45	1.04

% B= % bound; % F= % Free; % C= % colloid
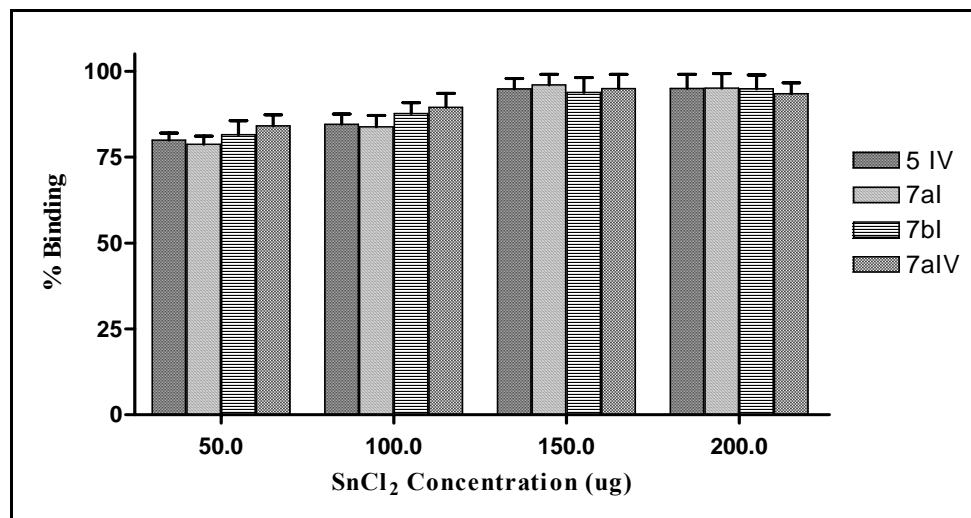
Fig. 3.4.3: Effect of $SnCl_2 \cdot 2H_2O$ concentration on radiolabeling efficiency of compounds **(5IV, 7aI-7bI, 7aIV)**

3.4.2. *In vitro* **stability study of** ^{99m}**Tc- labeled complexes in saline.**

The *in vitro* stability study[15] of radiolabeled complexes was determined in sodium chloride (0.9 %) by ascending thin layer chromatography. The ^{99m}Tc-labeled compound solution (0.1 ml) was prepared and mixed with normal saline (1.9 ml) and incubated (37$\pm$ 1°C). ITLC was performed at different time intervals (2.0, 4.0, 6.0 and 24 hours) as described above, in acetone to assess the stability of the complex. Any decrease in percentage of ^{99m}Tc-labeled complex was considered as its degree of degradation. As shown in **Table 3.4.4.** the complexes of the parent drug (5IV) and the CDS **(7aI-7bI, 7aIV)** were reasonably stable up to 24 h in normal saline.

Table 3.4.4: Stability study of compounds **(5IV, 7aI-7bI, 7aIV)** in saline

Compound	% Radiolabeling Efficiency (in saline)			
	5 min	**02 h**	**06 h**	**24 h**
5 IV	96.16±2.0	93.38±4.2	88.52±5.2	86.75±4.0
7aI	94.47±4.3	93.24±3.3	91.30±3.3	85.53±4.6
7bI	95.63±4.3	93.35±2.1	90.16±2.4	87.17±3.4
7aIV	94.89±4.2	91.22±3.8	86.11±4.9	79.19±3.2

3.4.3. *In vitro s*tability study of ^{99m}**Tc- labeled complexes in human serum.**

The *in vitro* stability of radiolabelled complexes was tested in human serum. The study was accomplished by incubating an aliquot of 0.1ml of labeled complex prepared in saline (0.9 %) and mixed with 1.9 ml of serum and incubated at 37$\pm$1°C. ITLC was performed at different time intervals (0, 2, 6, and 24 h) as described above, in acetone to assess the stability of the complex. Any decrease in percentage of ^{99m}Tc-labeled complex was considered as its degree of degradation. It is evident from **Table 3.4.5.** that the complexes of the parent drug **(5IV)** and the CDS **(7aI-7bI, 7aIV)** were sufficiently stable up to 6 hours and reasonably stable up to 24 hours.

Table 3.4.5: Stability study of compounds **(5IV, 7aI-7bI, 7aIV)** in human serum

Compound	% Radiolabeling Efficiency (in human serum)			
	5 min	**02 h**	**06 h**	**24 h**
5IV	96.56±2.0	92.38±4.1	89.52±5.2	81.70±4.0
7aI	94.48±4.3	91.29±3.5	89.30±3.3	82.03±4.3
7bI	94.06±4.3	92.37±2.3	88.16±2.4	83.77±3.4
7aIV	94.37±4.2	91.82±3.7	90.11±4.1	80.11±3.8

3.4.4. Gamma imaging studies

IA residence time of synthesized CDS and parent drug were studied in inflammatory condition. Animals were divided into two groups, Group-A (standard) was administered by IA the parent NSAID i.e 6-MNA **(5IV)**. Another group, Group-B (Test) was administered by IA the synthesized CDS, 3 h after induction of inflammation in the rat paw. Inflammation was induced in the right hind paw of the rats by injecting carrageenan (0.1 ml, 1 % w/v in normal saline) into the subplantar region of the paw. The animals were anaesthetized, fixed on a board and images were taken 2 h, 6 h and 24 h after the administration of the radiolabeled complexes by IA route.

Table 3.4.6: Percentage of radioactivity in knee after IA administration

Time (h)	% Radioactivity in ROI*			
	5IV	**7aIV**	**7bIV**	**7aIV**
1	100±4.0	100±5.1	100±3.0	100±4.3
2	58.47±3.1	78.14±4.0	76.54±3.1	81.09±4.1
6	42.06±4.3	63.57±4.1	60.78±3.0	64.37±3.0
24	13.44±3.0	43.41±4.0	40.96±4.1	42.05±3.1

*Radioactivity counts converted in to percentage and initial counts taken as 100 %; (ROI=Region of interest)

The gamma images obtained are shown in **Fig. 3.4.7-3.4.11** below and radioactivity was measured for whole body as well as for the region of interest (ROI) i.e. knee. Initially, injection was given in both the knees of the animal for the estimation and validation of radioactivity. Subsequently, after establishing the experiment, only one knee

in all the remaining animals was injected with the radiolabelled complex for the purpose of localization of the derivatives.
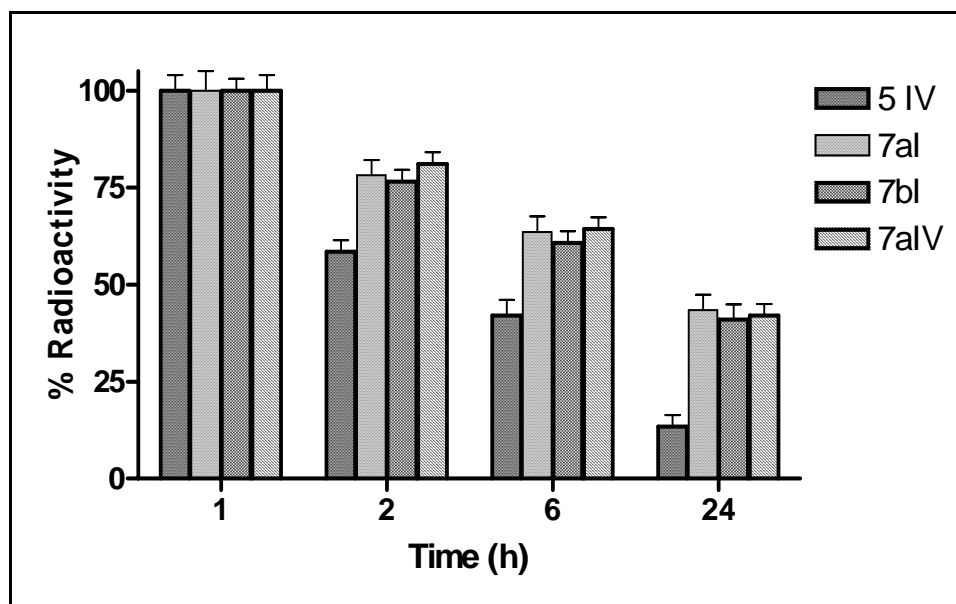
Fig. 3.4.4: Effect of time on Radioactivity after IA injection in knee

(A)   (B)
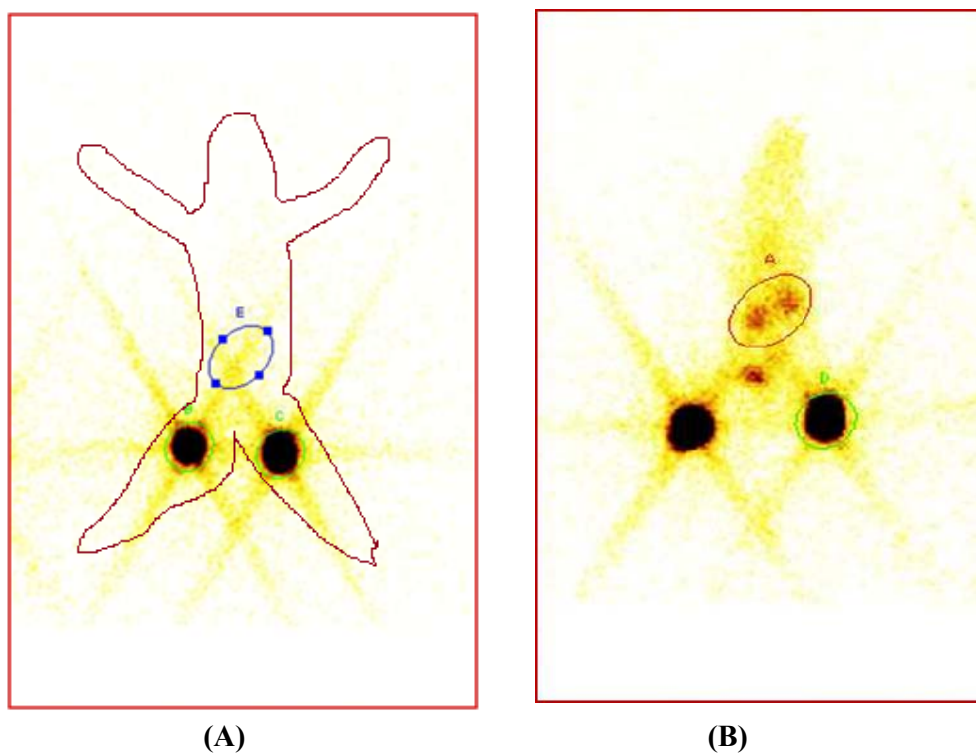
Fig. 3.4.5: A: Gamma camera image of rats after IA injection of **(5IV)** 1h

B: Gamma camera image of rats after IA injection of **(5IV)** 6h
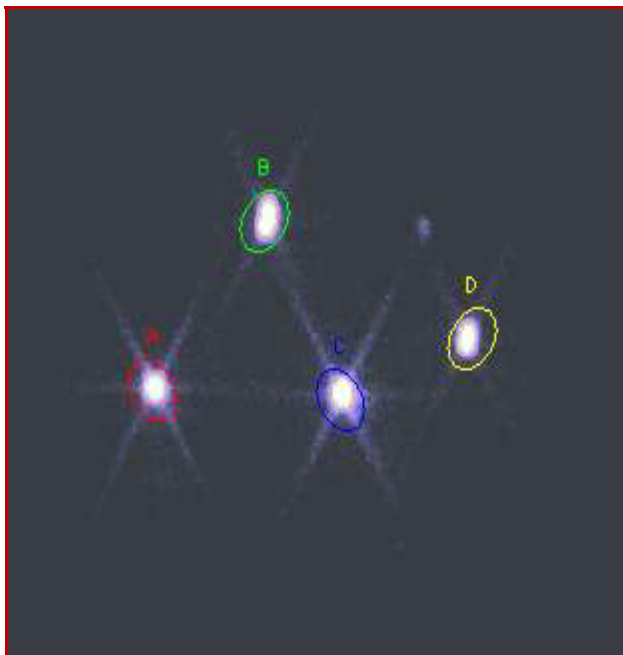
Fig. 3.4.6: Gamma camera image of rats after IA injection of compounds (A=**5IV**, B=**7aI**, C=**7bI** and D=**7fI**) ***** 2 h (In figure there are total four animals **A-D** injected drug on right knee.
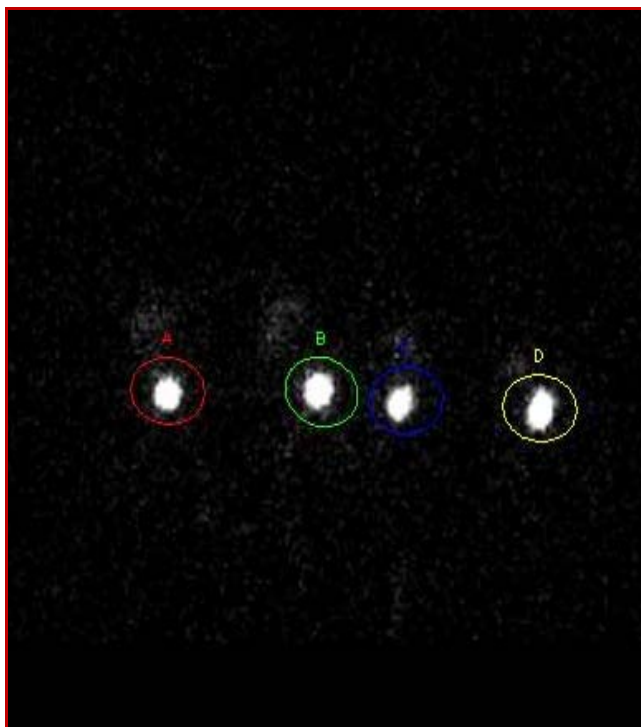
Fig. 3.4.7: Gamma camera image of rats after IA injection of compounds after 6 h (IA injection of CDS, A=**5IV**, B=**7aI**, C=**7bI** and D=**7fI**)
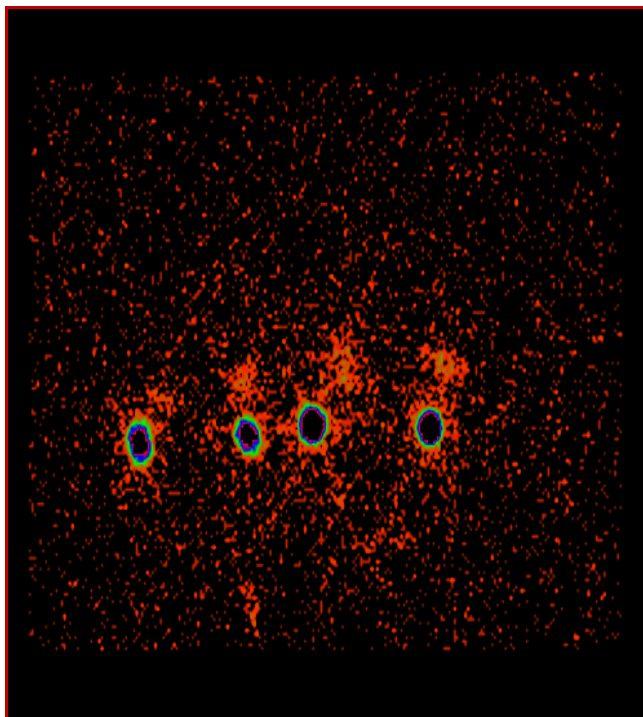
Fig. 3.4.8: Gamma camera image of rats after IA injection of **(5IV, 7aI-7bI, 7aIV)** after 24 h

From the obtained data and figures it is clear that all the synthesized CDS **(7aI-7bI, 7aIV)** showed high retention time in joints after IA administration as compared to the parent drug **(5IV)**. Further, radioactivity obtained for the synthesized CDS after 24 h was about 4 times higher in ROI compared to the parent drug. So it can be concluded that cationic molecules are retained for a longer period of time in joint cavity by ionic interaction and hence in the initial phase we can extend residence time of the drug by these CDS. Other representative derivatives from each CDS class have been evaluated and found to be similar in their retention behavior.

As per the proposed mechanism these CDS will deliver active drug slowly by hydrolysis of the ester or amide groups. Taking into consideration the rate of hydrolysis of the synthesized CDS in human serum it could be assumed that in the joint cavity the synthesized CDS will undergo rapid hydrolysis, as in inflammatory conditions level of various hydrolyzing enzymes is increased in joint cavity.

After hydrolysis the free drug can be slowly expelled from the joint and again reabsorbed in to joints. Further NSADs which have long half life coupled with joint affinity

such as 6-MNA, BPA may have significant impact with respect to improved joint retention time when modified into quaternary derivatives.

4. Experimental

The experimental work has been divided into four parts:

4.1. Chemical studies

4.2. Hydrolyses kinetics

4.3. Cytotoxicity study (MTT assay)

4.4. Radiolabeling studies

4.1. Chemical studies

All the reagents and solvents required for syntheses were purified by general laboratory techniques before use. Melting points were determined using silicon oil bath type melting point apparatus (Veego) and are uncorrected. The completion of the reaction was monitored by thin layer chromatography (TLC) on silica gel pre-coated plates (60 F_{254}, Merck, 0.25 mm thickness), visualizing in ultraviolet light (254 nm) or iodine vapors. The yields reported here are un-optimized. Ultraviolet spectra (UV, λ_{max} in nm) were recorded on Shimadzu UV-1800 spectrophotometer. IR spectra (wave numbers in cm^{-1}) were recorded on a BRUKER ALPHA-T (Germany) FT-IR spectrophotometer using potassium bromide discs.

PMR spectra were recorded using Bruker Advance-II 400 MHz spectrometer in $CDCl_3$ or DMSO-d_6 solvents and expressed as δ ppm, coupling constant (J) has been expressed in Hz. Mass spectra were recorded using Thermo Fisher mass spectrometer using EI as ion source for all the compounds except pyridinium salts where ESI was used as ion source. HPLC analysis was performed using Shimadzu prominence system (Kyoto, Japan) consisting of LC-20AT Pump, and SPD 20 A detector. The chromatographic column used was phenomenex C-18, 250 mm length X 4.6 mm diameter with 0.5 μ particle size and Column temperature was maintained at 25-28 °C. Separation of analytes was performed under isocratic conditions at a flow-rate of 0.5-1.0 ml/min. The mobile phase consisted of phosphate buffer (PB, 15 mM) - acetonitrile.

Chromatographic separations were performed on columns using silica gel 100–200 mesh and neutral alumina, activity grade I. All reagents used were of analytical reagent grade obtained from S. d. fine chemicals, Spectrochem, Qualigens and Sigma-Aldrich.

4.1.1. Ethyl 3-pyridinecarboxylate (ethyl nicotinate) (2)

Nicotinic acid **(1)** (5 g, 40.65 mM) was refluxed with sulphuric acid (3.98 g, 40.65 mM) and absolute alcohol (3.73 g, 81.30 mM) for 10 h and the mixture was cooled to

room temperature and poured on to the crushed ice. The mixture was made alkaline by the addition of ammonia solution. The resulting mixture was extracted with ethyl acetate (3 x 20 ml). The solvent was dried and removed under vaccum to get the titled compound as an oil[1]. (5.5 g, 89.60 %).

Anal.:

TLC : R_f 0.74 (Chloroform: Methanol, 1:0.3)

UV (MeOH) : 217 nm, (log ε 3.99).

IR (Neat, cm^{-1}): 1717, 1588, 1276, 1107, 738 and 699

MS (m/z) : 151.07 (M$^+$)

4.1.2. *N*-(2-Hydroxyethyl)nicotinamide (4a)

A neat mixture of ethyl nicotinate **(2)** (5 g, 33.11 mM) and 2-aminoethanol **(3a)** (2.25 g 33.11 mM) was heated at 80-85 °C overnight. As the mixture was cooled, it solidified into a low melting white solid which was crystallized from isopropanol to get a hygroscopic white solid. (4.8 g, 87.32 %,). m.p. 88-90 °C (lit.[2] m.p. 88.5-89.5 °C)

Anal.:

TLC : R_f 0.69 (Methanol)

UV (MeOH) : 256.5 nm, (log ε 4.45).

IR (KBr, cm^{-1}): 3270, 1635, 1594, 1545, 1310, 1064, and 1027

PMR (CDCl$_3$): 9.07 (s, 1H, pyridine-*H*), 8.67-8.65 (d, 1H, pyridine-*H*), 8.45-8.43 (t, 1H, N*H*), 8.22-8.19 (d, 1H, pyridine-*H*), 7.41-7.37 (m, 1H, pyridine-*H*), 4.74 (s, 1H, O*H*), 3.70-3.68 (t, 2H, O-C*H$_2$*) and 3.52-3.47 (m, 2H, N-C*H$_2$*)

MS (m/z) : 167.10 (M+1)

4.1.3. *N*-(2-Hydroxypropyl)nicotinamide (4b)

The title compound was prepared from ethyl nicotinate **(2)** (5 g, 33.11 mM) and 1-amino-2-propanol **(3b)** (3.22 g, 43.0 mM). The neat mixture was heated and stirred at 80-85 °C for overnight. Excess of aminoalcohol was removed under vaccum to get a yellow oil of the product[2] (5.80 g, 97.31 %)

Anal.:

TLC : R_f 0.53 (Ethyl acetate)

UV (MeOH) : 240 nm, (log ε 3.56).

IR (Neat, cm^{-1}): 3285, 3074, 1639, 1593, 1301, 1122 and 702.

PMR (CDCl$_3$) : 9.0 (s, 1H, pyridine-*H*), 8.58-8.55 (d, 1H, pyridine-*H*), 8.18-8.12 (m, 2H, pyridine-*H*, N*H*), 7.33-7.29 (m, 1H, Pyridine-*H*), 4.05-3.99 (m, 1H, O-C*H*), 3.65 (s, 1H, O-*H*), 3.58-3.25 (m, 2H, N-C*H*$_2$), and 1.19-1.18 (d, 3H, C*H*$_3$)

MS (m/z)   : 181.13 (M+1)

4.1.4. *N*-(1-Hydroxybutan-2-yl)nicotinamide (4c)

The title compound was prepared from ethyl nicotinate **(2)** (5.0 g, 33.11 mM) and 2-amino-1-butanol **(3c)** (3.83 g, 43.04 mM) following the method described for the synthesis of compound **(4b)** to give yellow oil of the desired product **(4c)** (6 g, 93.45 %).

Anal.:

TLC   : R$_f$ 0.48 (Methanol)

UV (MeOH)   : 237 nm, (log ε 4.1).

IR (Neat, cm^{-1}): 3278, 1638, 1540, 1302 and 703

PMR (CDCl$_3$) : 9.07 (s, 1H, pyridine-*H*), 8.66-8.65 (d, 1H, pyridine-*H*), 8.22-8.19 (d, 1H, pyridine-*H*), 8.01-7.99 (d, 1H, N*H*), 7.40-7.36 (m, 1H, pyridine-*H*), 4.04 (bs, 1H, N-C*H*), 3.63-3.62 (d, 2H, O-C*H*$_2$), 3.55 (s, 1H, O-*H*), 1.74-1.53(m, 2H, -C*H*$_2$) and 0.97-0.94 (t, 3H, -C*H*$_3$)

MS (m/z)   : 195.1 (M+1)

4.1.5. *N*-(1-Hydroxy-2-methylpropan-2-yl)nicotinamide (4d)

The title compound was prepared from ethyl nicotinate **(2)** (5.0 g, 33.11 mM) and 2-amino-2-methyl-1-propanol **(3d)** (3.83 g, 43.04 mM) following the method described for the synthesis of compound **(4b)** to give yellow oil of the desired product **(4g)** (5.90 g, 91.85 %).

Anal.:

TLC   : R$_f$ 0.55 (Methanol)

UV (MeOH)   : 262 nm, (log ε 3.91)

IR (Neat, cm^{-1}): 3274, 3059, 1645, 1540, 1372 and 702

PMR (CDCl$_3$) : 8.90 (s, 1H, pyridine-*H*), 8.60-8.58 (d, 1H, pyridine-*H*), 8.07-8.04 (d, 1H, pyridine-*H*), 7.32-7.29 (m, 1H, Pyridine-*H*), 6.97(s,1H,N*H*), 4.62 (s, 1H, -OH), 3.66 (s, 2H, O-C*H*$_2$) and 1.41 (s, 6H,C(C*H*$_3$)$_2$)

MS (m/z)   : 195.13 (M+1)

4.1.6. *N*-(3-Hydroxypropyl)nicotinamide (4e)

The title compound was prepared from ethyl nicotinate **(2)** (5.0 g, 33.11 mM) and 3-amino-1-propanol **(3e)** (2.73 g, 36.42 mM) following the method described for the synthesis of compound **(4b)** to give yellow oil of the desired product **(4e)** (5.60 g, 93.96 %).

Anal.:

TLC : R_f 0.39 (Methanol)

UV (MeOH) : 262 nm, (log ε 3.8)

IR (Neat, cm^{-1}): 3282, 1637, 1541, 1305 and 702

PMR (CDCl$_3$) : 9.0 (s, 1H, pyridine-*H*), 8.61-8.60 (d, 1H, pyridine-*H*), 8.45-8.43 (t, 1H, N*H*), 8.17-8.14 (d, 1H, pyridine-*H*),7.37-7.34 (m, 1H, pyridine-*H*), 4.44 (s, 1H, O-*H*), 3.72-3.69 (t, 2H, O-C*H$_2$*), 3.58-3.53 (m, 2H, N-C*H$_2$*) and 1.15-1.79 (m, 2H, -C*H$_2$*),

MS (m/z) : 180.1 (M+1)

4.1.7. *N*-(2-Aminoethyl)nicotinamide (4f)

In a 250 ml RBF fitted with dropping funnel, ethylenediamine **(3f)** was added and the contents were heated at 120 ^{0}C with vigorous stirring followed by slow addition of ethyl nicotinate **(2)** (5.0 g, 33.11 mM) in to the above solution over 30-45 min and the reaction continued for 10-12 h. Excess of ethylenediamine was removed under vaccum to give yellow oil of the desired product **(4f)** (4.1 g, 75.04 %) (Note: Product contained *N*, *N*-dinicotinoyl ethylenediamide (dimer) as an impurity in minor amounts and used further without purification).

Anal.:

TLC : R_f 0.47 (Ethyl acetate)

UV (MeOH) : 215 nm, (log ε 3.99)

IR (Neat, cm^{-1}): 3348, 3281, 3051, 1644, 1544, 1307, 825 and 706

PMR (CDCl$_3$) : 9.05 (s, 1H, pyridine-*H*), 8.65-8.63 (d, 1H, pyridine-*H*), 8.22 (bs, 1H, N*H*), 8.17-8.14 (m, 1H, pyridine-*H*), 7.36-7.32 (m, 1H, pyridine-*H*), 3.50-3.46 (m, 2H, N-C*H$_2$*), 2.93-2.90 (t, 2H, N-C*H$_2$*) and 2.70 (s, 2H, N*H$_2$*)

MS (m/z) : 166.0 (M+1)

4.1.8. *N*-(3-Aminopropyl)nicotinamide (4g)

The title compound was prepared from ethyl nicotinate **(2)** (5.0 g, 33.11 mM) and 1,3-diaminopropane **(3g)** (68.97 ml) following the method described for the synthesis of compound **(4f)** to give yellow oil of the desired product **(4g)** (5.1 g, 86.04 %).

Anal.:

    TLC   : R_f 0.41 (Ethyl acetate)

    UV (MeOH) : 239 nm, (log ε 3.76)

    IR (KBr, cm^{-1}): 3279, 3047, 1644, 1590, 1308 and 708

    PMR (CDCl$_3$): 8.81 (s, 1H, pyridine-*H*), 8.35-8.33 (d, 1H, pyridine-*H*), 7.87-7.84
                     (d, 1H, pyridine-*H*), 7.05-7.02 (m, 1H, pyridine-*H*), 3.22-3.14 (m,1H,
                     CON*H*), 2.52-2.49 (t, 2H, N*H*$_2$), 2.42-2.40 (t, 2H, N-C*H*$_2$), 1.54-1.39
                     (m, 2H, -C*H*$_2$) and 1.28-1.23 (m, 2H, -C*H*$_2$)

    MS (m/z)   : 180.02 (M+1)

4.1.9. 2-Nicotinamidoethyl 2-(4-isobutylphenyl)propanoate (6aI)

Ibuprofen **(5I)** (2.97 g, 14.45 mM) was dissolved in dichloromethane (DCM, 25 ml) and the reaction mixture was cooled to 0-3°C. Ethyl(dimethylaminopropyl) carobod-imide (EDC.HCl) (3.0 g, 15.66 mM) was added into the above reaction mixture and stirring continued for 10-15 min. Dimethylaminopyridine (DMAP) was added in catalytic amount (50 mg). In a separate conical flask the alcohol **(4a)** (2.0 g, 12.04 mM) was dissolved in anhydrous DCM (10 ml) and this solution was added dropwise with stirring to the previously chilled reaction mixture and stirring was continued till the reaction completed (12-18 h) at room temperature. Once the reaction was completed then the reaction mixture was diluted with dichloromethane and washed with chilled water (3 X 20 ml) followed by washing with sodium bicarbonate solution (10 %) (3 X 20 ml). Organic layer was separated, dried, and solvent removed under reduced pressure to afford the desired compound **(6aI)** as yellow oil. (3.1 g, 72.68 %)

Anal.:

    TLC   : R_f 0.65 (Ethyl acetate)

    UV (MeOH)   : 220 nm, (log ε 4.21)

    IR (Neat, cm^{-1}): 3307, 1730, 1649, 1595, 1161 and 849

    MS (m/z)   : 354.18 (M$^+$)

4.1.10. 1-Nicotinamidopropan-2-yl 2-(4-isobutylphenyl)propanoate (6bI)

The title compound was prepared from ibuprofen (5I) (3.31 g, 16.01 mM), EDC. HCl (3.35 g, 17.55 mM) and the alcohol (4b) (2.63 g, 14.63 mM) following the method described for the synthesis of compound (6aI) to give yellow colored oil of the desired product (6bI) (3.50 g, 65.09 %).

Anal.:

TLC : R_f 0.68 (Chloroform: Methanol, 1:0.3)

UV (MeOH) : 219 nm, (log ε 3.34)

IR (Neat, cm^{-1}): 3308, 1728, 1651, 1536, 1164 and 733

MS (m/z) : 368.30 (M$^+$)

4.1.11. 2-Nicotinamidobutanyl 2-(4-isobutylphenyl)propanoate (6cI)

The title compound was prepared from ibuprofen (5I) (3.07 g, 13.55 mM), EDC. HCl (3.07 g, 14.91 mM) and the alcohol (4c) (2.630 g, 13.55 mM) following the method described for the synthesis of compound (6aI) to give yellowish oil of the desired product (6cI) (3.80 g, 73.37 %).

Anal.:

TLC : R_f 0.65 (Chloroform: Methanol, 1:0.3)

UV (MeOH) : 220 nm, (log ε 3.20)

IR (Neat, cm^{-1}): 3303, 1730, 1647, 1535, 1161 and 733

MS (m/z) : 382.2 (M$^+$)

4.1.12. 2-Methyl-2-nicotinamidopropanyl 2-(4-isobutylphenyl)propanoate (6dI)

The title compound was prepared from ibuprofen (5I) (3.07 g, 13.55 mM), EDC. HCl (3.07 g, 14.91 mM) and the alcohol (4d) (2.63 g, 13.55 mM) following the method described for the synthesis of compound (6aI) to give yellow oil of the desired product (6dI) (3.70 g, 71.44 %).

Anal.:

TLC : R_f 0.63 (Chloroform: Methanol, 1:0.3)

UV (MeOH) : 220 nm, (log ε 3.90)

IR (Neat, cm^{-1}): 3307, 1730, 1658, 1522, 1162 and 734

MS (m/z) : 382.2 (M$^+$)

4.1.13. 3-Nicotinamidopropyl 2-(4-isobutylphenyl)propanoate (6eI)

The title compound was prepared from ibuprofen (5I) (3.61 g, 17.63 mM), EDC. HCl (3.62 g, 18.99 mM) and the alcohol (4e) (2.63 g, 14.61 mM) following the method described for the synthesis of compound (6aI) to give yellow oil of the desired product (6eI) (3.57 g, 66.39 %).

Anal.:

      TLC   : R_f 0.65 (Chloroform: Methanol, 1:0.3)

      UV (MeOH)   : 219 nm, (log ε 3.50)

      IR (Neat, cm^{-1}): 3312, 1727, 1649, 1539, 1163 and 733

      MS (m/z)   : 368.2 (M$^+$)

4.1.14. *N*-[2-(2-(4-Isobutylphenyl)propanamido)ethyl]nicotinamide (6fI)

The title compound was prepared from ibuprofen (5I) (2.74 g, 13.33 mM), EDC. HCl (2.77 g, 14.54 mM) and the amine (4f) (2.0 g, 12.12 mM) following the method described for the synthesis of compound (6aI) to give yellow oil of the desired product (6fI) (3.10 g, 72.45 %).

Anal.:

      TLC   : R_f 0.70 (Chloroform: Methanol, 1:0.3)

      UV (MeOH)   : 220 nm, (log ε 4.01)

      IR (Neat, cm^{-1}): 3327, 1627, 1534, 1346 and 1088

      MS (m/z)   : 353.20 (M$^+$)

4.1.15. *N*-[3-(2-(4-Isobutylphenyl)propanamido)propyl]nicotinamide (6gI)

The title compound was prepared from ibuprofen (5I) (2.53 g, 12.29 mM), EDC. HCl (2.56 g, 12.29 mM) and the amine (4g) (2.0 g, 11.17 mM) following the method described for the synthesis of compound (6aI) to give yellow oil of the desired product (6gI) (2.5 g, 60.96 %).

Anal.:

      TLC   : R_f 0.66 (Chloroform: Methanol, 1:0.3)

      UV (MeOH)   : 257, 262 nm, (log ε 4.10)

      IR (Neat, cm^{-1}): 3306, 2956, 1640, 1594, 1550 and 709

      MS (m/z)   : 367.16 (M$^+$)

4.1.16. 2-Nicotinamidoethyl 2-(6-methoxy-2-naphthyl)propanoate (6aII)

The title compound was prepared from naproxen **(5II)** (1.52 g, 6.62 mM), EDC. HCl (1.38 g, 7.22 mM) and the alcohol **(4a)** (1.0 g, 6.02 mM) following the method described for the synthesis of compound **(6aI)** to give pink oil of the desired product[2] **(6aII)** (2.10 g, 92.22 %).

Anal.:

TLC : R_f 0.65 (Chloroform: Methanol 3 drop)

UV (MeOH) : 226 nm

IR (Neat, cm^{-1}): 3317.60, 3061, 2939, 1719.31, 1636.96, 1265 and 1168

4.1.17. 1-Nicotinamidopropan-2-yl 2-(6-methoxy-2-naphthyl)propanoate (6bII)

The title compound was prepared from naproxen **(5II)** (1.40 g, 6.11 mM), EDC. HCl (1.27 g, 6.66 mM) and the alcohol **(4b)** (1.0 g, 5.55 mM) following the method described for the synthesis of compound **(6aI)** to give oil of the desired product **(6bII)** (1.60 g, 73.46 %).

Anal.:

TLC : R_f 0.65 (Chloroform: Methanol 3 drop)

UV (MeOH) : 229 nm

IR (Neat, cm^{-1}): 3056, 1725, 1632, 1603, 1262 and 851

4.1.18. 2-Nicotinamidobutanyl 2-(6-methoxy-2-naphthyl)propanoate (6cII)

The title compound was prepared from naproxen **(5II)** (1.30 g, 5.67 mM), EDC. HCl (1.18 g, 6.18 mM) and the alcohol **(4c)** (1.0 g, 5.15 mM) following the method described for the synthesis of compound **(6aI)** to give white solid of the desired product **(6cII)** (1.30 g, 62.04 %). m.p. 98-100 ^{o}C

Anal.:

TLC : R_f 0.65 (Chloroform: Methanol 3 drop)

UV (MeOH) : 229 nm

IR (KBr, cm^{-1}): 3339, 1733, 1639, 1605, 1265 and 850

4.1.19. 2-Methyl-2-nicotinamidopropyl 2-(6-methoxy-2-naphthyl)propanoate (6dII)

The title compound was prepared from naproxen **(5II)** (1.30 g, 5.67 mM), EDC. HCl (1.18 g, 6.18 mM) and the alcohol **(4d)** (1.0 g, 5.15 mM) following the method

described for the synthesis of compound (6aI) to give white solid of the desired product (6dII) (1.50 g, 71.58 %). m.p. 102-104 $^{\circ}$C

Anal.:

TLC : R_f 0.65 (Chloroform: Methanol 3 drop)

UV (MeOH) : 230 nm

IR (KBr, cm^{-1}) : 3310, 1634, 1262 and 1156

4.1.20. 3-Nicotinamidopropanyl 2-(6-methoxy-2-naphthyl)propanoate (6eII)

The title compound was prepared from naproxen (6) (1.40 g, 6.11 mM), EDC.HCl (1.27 g, 6.66 mM) and N-(3-hydroxypropyl)nicotinamide (4e) (1.0 g, 5.55 mM) following the method described for the synthesis of compound (6aI) to give white solid of the desired product[2] (1.30 g, 59.69 %) m.p. 108-111 $^{\circ}$C (lit.[2] m.p. 100-102 ^{0}C)

Anal.:

TLC : R_f 0.65 (Chloroform: Methanol 3 drop)

UV (MeOH) : 230 nm

IR (KBr, cm^{-1}) : 3310, 1634, 1603, 1262 and 1174

4.1.21. *N*-[2-(2-(6-Methoxy-2-naphthyl)propanamido)ethyl]nicotinamide (6fII)

The title compound was prepared from naproxen (6) (1.53 g, 6.01 mM), EDC.HCl (1.38 g, 7.27 mM) and N-(2-aminoethyl)nicotinamide (4f) (1.0 g, 6.06 mM) following the method described for the synthesis of compound (6aI) to give yellow solid of the desired product (1.60 g, 69.94 %). m.p. 150-152 $^{\circ}$C

Anal.:

TLC : R_f 0.63 (Chloroform: Methanol 3 drop)

UV (MeOH) : 230 nm

IR (KBr, cm^{-1}) : 3291, 1643, 1603, 1025 and 854

4.1.22. N-(3-Nicotinamidopropanyl)-2-(6-methoxy-2-naphthyl)propanamide (6gII)

The title compound was prepared from naproxen (6) (1.41 g, 6.14 mM), EDC.HCl (1.28 g, 6.70 mM) and N-(3-aminopropyl)nicotinamide (4g) (1.0 g, 5.58 mM) following the method described for the synthesis of compound (6aI) to give white solid of the desired product (6gII) (1.30 g, 59.44 %). m.p. 102-104 ^{0}C

Anal.:

TLC : R_f 0.65 (Chloroform: Methanol 3 drop)

UV (MeOH)   : 230 nm

IR (KBr, cm^{-1})   : 3310, 1638, 1213 and 851

4.1.23. 2-(Nicotinamido)ethyl 1-(4-chlorobenzoyl)-5-methoxy-2-methylindol-3-acetate (6aIII)

The title compound was prepared from indomethacin **(5III)** (2.37 g, 6.62 mM), EDC.HCl (1.38 g, 7.22 mM) and the alcohol **(4a)** (1.0 g, 6.02 mM) following the method described for the synthesis of compound **(6aI)** to give yellow oil, which on crystallization by ethanol gave yellow solid and recrystallization from methanol to offered white solid of the desired product[2] **(6aIII)** (1.90 g, 62.33 %). m.p. 122-124 °C

Anal.:

TLC   : R$_f$ 0.72 (Chloroform: Methanol 3 drop)

UV (MeOH)   : 222, 320 nm

IR (KBr, cm^{-1}): 3312, 1730, 1668, 1642, 1596 and 1024

4.1.24. 1-(Nicotinamido)propan-2-yl 2-(1-(4-chlorobenzoyl)-5-methoxy-2-methylindol)-3-acetate (6bIII)

The title compound was prepared from indomethacin **(5III)** (2.17 g, 6.11 mM), EDC. HCl (1.27 g, 7.22 mM) and the alcohol **(4b)** (1.0 g, 5.55 mM) following the method described for the synthesis of compound **(6aI)** to give yellow semisolid, which on crystallization by 2-propanol gave white solid of the desired product **(6bIII)** (1.70 g, 58.84 %). m.p. 112-114 °C

Anal.:

TLC   : R$_f$ 0.77 (Chloroform: Methanol 3 drop)

UV (MeOH)   : 316 nm

IR (KBr, cm^{-1}): 3389, 1726, 1708, 1671, 1594, 753 and 705

4.1.25. 2-(Nicotinamido)butan-2-yl 2-(1-(4-chlorobenzoyl)-5-methoxy-2-methylindol)-3-acetate (6cIII)

The title compound was prepared from indomethacin **(5III)** (2.02 g, 5.67 mM), EDC. HCl (1.18 g, 6.18 mM) and the alcohol **(4c)** (1.0 g, 5.15 mM) following the method described for the synthesis of compound **(6aI)** to give yellow solid, which on crystallization by 2-propanol gave white solid of the desired product **(6cIII)** (0.90 g, 71.10 %). m.p. 157-159 °C

Anal.:

TLC : R_f 0.58 (Chloroform: Methanol 3 drop)

UV (MeOH) : 317 nm

IR (KBr, cm^{-1}): 3319, 1736, 1661, 1592, 1148, 853 and 753

4.1.26. 2-(Nicotinamido)-2-methylpropan-2-yl 2-(1-(4-chlorobenzoyl)-5-methoxy-2-methylindol)-3-acetate (6dIII)

The title compound was prepared from indomethacin **(5III)** (2.02 g, 5.67 mM), EDC. HCl (1.18 g, 6.18 mM) and the alcohol **(4d)** (1.0 g, 5.15 mM) following the method described for the synthesis of compound **(6aI)** to give yellow oil of the desired product **(6dIII)** (1.90 g, 69.02 %).

Anal.:

TLC : R_f 0.67 (Chloroform: Methanol 3 drop)

UV (MeOH) : 316 nm

IR (KBr, cm^{-1}): 3370, 1731, 1681, 1592 and 753

4.1.27. 3-Nicotinamidopropanyl 2-(1-(4-chlorobenzoyl)-5-methoxy-2-methylindol-3-acetate (6eIII)

The title compound was prepared from indomethacin **(5III)** (2.18 g, 6.11 mM), EDC. HCl (1.27 g, 6.66 mM) and the alcohol **(4e)** (1.0 g, 5.55 mM) following the method described for the synthesis of compound **(6aI)** to give yellow oil which on recrystallization by 2-propanol gave white solid of the desired product[2] **(6eIII)** (1.90 g, 65.77 %). m.p. 120-122 ^{o}C (lit.[2] m.p. 119-121 ^{o}C)

Anal.:

TLC : R_f 0.66 (Chloroform: Methanol 3 drop)

UV (MeOH) : 316 nm

IR (KBr, cm^{-1}) : 2967, 1731, 1677, 1591, 1311 and 753

4.1.28. N-(2-Nicotinamido)ethyl-2-(1-(4-chlorobenzoyl)-5-methoxy-2-methylindol)-3-acetamide (6fIII)

The title compound was prepared from indomethacin **(5III)** (2.38 g, 6.66 mM), EDC.HCl (1.38 g, 7.27 mM) and amine **(4f)** (1.0 g, 6.06 mM) following the method described for the synthesis of compound **(6aI)** to offer yellow solid which on recrystall-

ization with 2-propanol-chloroform gave pure yellow solid of the desired product **(6fIII)** (1.70 g, 55.54 %). m.p. 195-196 ^{o}C

Anal.:

TLC : R_f 0.74 (Chloroform: Methanol 3 drop)

UV (MeOH) : 316 nm

IR (KBr, cm^{-1}) : 3286, 1673, 1593 and 753

4.1.29. 3-(Nicotinamido)propyl-2-(1-(4-chlorobenzoyl)-5-methoxy-2-methylindol)-3-acetamide (6gIII)

The title compound was prepared from indomethacin **(5III)** (2.19 g, 6.14 mM), EDC. HCl (1.28 g, 6.70 mM) and amine **(4g)** (1.0 g, 5.58 mM) following the method described for the synthesis of compound **(6aI)** to give yellow solid which was crystallized from methanol to yield pure yellow solid of the desired product **(6gIII)** (1.80 g, 62.08 %). m.p. 171-173 ^{o}C

Anal.:

TLC : R_f 0.75 (Chloroform: Methanol 3 drop)

UV (MeOH) : 316 nm

IR (KBr, cm^{-1}) : 3299, 1668, 1636, 1222 and 1151

4.1.30. 2-Nicotinamidoethyl 2-(6-methoxy-2-naphthyl)acetate (6aIV)

The title compound was prepared from 6-MNA **(5IV)** (1.43 g, 6.62 mM), EDC. HCl (1.38 g, 7.22 mM) and the alcohol **(4a)** (1.0 g, 6.02 mM) following the method described for the synthesis of compound **(6aI)** to yield yellow solid which on crystallization by ethyl acetate-methanol or chloroform-methanol offered white solid of the desired product **(6aIV)** (1.50 g, 68.40 %). m.p. 53-55 ^{o}C

Anal.:

TLC : R_f 0.53 (Chloroform: Methanol 3 drop)

UV (MeOH) : 229 nm

IR (KBr, cm^{-1}): 322, 1722, 1622, 1591, 1248 and 1029

4.1.31. 1-Nicotinamidopropan-2-yl 2-(6-methoxy-2-naphthyl)acetate (6bIV)

The title compound was prepared from 6-MNA **(5IV)** (1.31 g, 6.11 mM), EDC. HCl (1.27 g, 6.11 mM) and the alcohol **(4b)** (1.0 g, 5.55 mM) following the method

described for the synthesis of compound **(6aI)** to give yellow semisolid of the desired product **(6bIV)** (1.60 g, 76.10 %).

Anal.:

      TLC   : R_f 0.61 (Chloroform: Methanol 3 drop)

      UV (MeOH) : 227 nm

      IR (KBr, cm^{-1}): 3131, 1730, 1636, 1607, 1397 and 816

4.1.32. 2-Nicotinamidobutanyl 2-(6-methoxy-2-naphthyl)acetate (6cIV)

The title compound was prepared from 6-MNA **(5IV)** (1.31 g, 6.11 mM), EDC. HCl (1.27 g, 6.11 mM) and the alcohol **(4c)** (1.0 g, 5.55 mM) following the method described for the synthesis of compound **(6aI)** to give yellow semisolid which was further recrystallized from acetonitrile to get white solid of the desired product **(6cIV)** (1.70 g, 84.03 %). m.p. 69-71 ^{0}C

Anal.:

      TLC   : R_f 0.71 (Chloroform: Methanol 3 drop)

      UV (MeOH) : 227 nm

      IR (KBr, cm^{-1}): 3319, 1720, 1638, 1606, 1302, 852 and 745

4.1.33. 2-Methyl-2-nicotinamidopropanyl 2-(6-methoxy-2-naphthyl)acetate (6dIV)

The title compound was prepared from 6-MNA **(5IV)** (1.22 g, 5.67 mM), EDC. HCl (1.18 g, 6.18 mM) and the alcohol **(4d)** (1.0 g, 5.15 mM) following the method described for the synthesis of compound **(6aI)** to give yellow solid of the desired product **(6dIV)** (1.60 g, 79.18 %). m.p. 78-81 ^{0}C

Anal.:

      TLC   : R_f 0.68 (Chloroform: Methanol 3 drop)

      UV (MeOH) : 227 nm

      IR (KBr, cm^{-1}): 3341, 1735, 1637, 1606, 1316 and 853

4.1.34. 3-Nicotinamidopropanyl 2-(6-methoxy-2-naphthyl)acetate (6eIV)

The title compound was prepared from 6-MNA **(5IV)** (1.31 g, 6.11 mM), EDC. HCl (1.27 g, 6.11 mM) and the alcohol **(4e)** (1.0 g, 5.55 mM) following the method described for the synthesis of compound **(6aI)** to give yellow solid of the desired product **(6eIV)** (1.50 g, 71.42 %). m.p. 80-82 ^{0}C

Anal.:

TLC   : R_f 0.68 (Chloroform: Methanol 3 drop)

UV (MeOH)   : 227 nm

IR (KBr, cm^{-1}): 3285, 1729, 1630, 1607, 1268 and 853

4.1.35. 2-Nicotinamidoethyl 4-biphenylacetate (6aV)

The title compound was prepared from BPA **(5V)** (1.40 g, 6.62 mM), EDC (1.38 g, 7.22 mM) and the alcohol **(4a)** (1.0 g, 6.02 mM) following the method described for the synthesis of compound **(6aI)** to give yellow solid, which on crystallization by chloroform-methanol offered white solid of the desired product **(6aV)** (1.80 g, 82.50 %). m.p.111-113 ^{o}C

Anal.:

TLC   : R_f 0.62 (Chloroform: Methanol 3 drop)

UV (MeOH)   : 251 nm

IR (KBr, cm^{-1}): 3299, 1727, 1638, 1544, 1166 and 822

4.1.36. 1-Nicotinamidopropan-2-yl 4-biphenylacetate (6bV)

The title compound was prepared from BPA **(5V)** (1.29 g, 6.11 mM), EDC. HCl (1.27 g, 6.66 mM) and the alcohol **(4b)** (1.0 g, 5.55 mM) following the method described for the synthesis of compound **(6aI)** to give yellow oil of the desired product **(6bV)** (1.30 g, 62.49 %).

Anal.:

TLC   : R_f 0.71 (Chloroform: Methanol 3 drop)

UV (MeOH)   : 251 nm

IR (Neat, cm^{-1}): 3285, 1727, 1630, 1590 and 742

4.1.37. 2-Nicotinamidobutyl 4-biphenylacetate (6cV)

The title compound was prepared from BPA **(5V)** (1.20 g, 5.67 mM), EDC. HCl (1.18 g, 6.18 mM) and the alcohol **(4c)** (1.0 g, 5.15 mM) following the method described for the synthesis of compound **(6aI)** to give white solid of the desired product **(6cV)** (1.30 g, 64.93 %). m.p. 110-112 ^{0}C

Anal.:

TLC   : R_f 0.67 (Chloroform: Methanol 3 drop)

UV (MeOH)   : 251 nm

IR (KBr, cm^{-1}): 3305, 1717, 1638, 1590 and 748

4.1.38. 2-Methyl-2-nicotinamidopropyl 4-biphenylacetate (6dV)

The title compound was prepared from BPA **(5V)** (1.20 g, 5.67 mM), EDC (1.18 g, 6.18 mM) and the alcohol **(4d)** (1.0 g, 5.15 mM) following the method described for the synthesis of compound **(6aI)** to gave yellow oil of the desired product **(6dV)** (1.40 g, 69.92 %).

Anal.:

TLC   : R_f 0.64 (Chloroform: Methanol 3 drop)

UV (MeOH)   : 251 nm

IR (Neat, cm^{-1}): 3029, 1730, 1651, 1590 and 741

4.1.39. 3-Nicotinamidopropyl 4-biphenylacetate (6eV)

The title compound was prepared from BPA **(5V)** (1.29 g, 6.11 mM), EDC. HCl (1.27 g, 6.66 mM) and the alcohol **(4e)** (1.0 g, 5.55 mM) following the method described for the synthesis of compound **(6aI)** to give white solid of the desired product **(6eV)** (1.10 g, 52.87 %). m.p. 129-131 ^{o}C

Anal.:

TLC   : R_f 0.53 (Chloroform: Methanol 3 drop)

UV (MeOH)   : 251 nm

IR (KBr, cm^{-1}): 3285, 1727, 1630, 1590 and 742

4.1.40. 2-(1-Methylpyridinium-3-carboxamido)ethyl 2-(4-isobutylphenyl)propanoate iodide (7aI)

A reaction mixture containing ester **(6aI)** (2.5 g, 7.06 mM) and methyl iodide (2 g, 14.12 mM) in acetonitrile (20 ml) was refluxed for 2-3 h and the solvent and excess reagent removed under reduced pressure to afford yellow semisolid which on crystallization in ethyl acetate gave white solid of the desired product[17] **(7aI)** (3.1 g, 88.64 %). m.p. 148-150 ^{o}C (lit[17] m.p. 144-146 ^{o}C).

Anal.:

TLC   : R_f 0.35 (Methanol: 1 drop glacial acetic acid (GAA))

UV (MeOH)   : 219 nm, (log ε 4.52)

IR (KBr, cm^{-1}): 3272, 1730, 1679, 1205 and 1174

PMR (CDCl$_3$): 9.80 (s, 1H, pyridinium-*H*), 8.89-8.87 (d, 2H, pyridinium-*H*), 8.00 -7.97 (m,1H, pyridinium-*H*), 8.72-8.69(m,1H, N*H*),7.15-7.13 (d, 2H , Ar-*H$_2$*), 6.99-6.97 (d, 2H,Ar-*H$_2$*), 4.50 (s, 3H, N-C*H$_3$*), 4.35-4.12

(m, 2H,-OCH_2), 3.79-3.74 (q, 1H,-CH), 3.68-3.60 (m, 2H,-CH_2), 2.33-2.31 (d, 2H,-CH_2), 1.77-1.70 (m, 1H, -CH), 1.43-1.41 (d, 3H -CH_3) and 0.81-0.79 (d, 6H, (CH_3)$_2$)

^{13}CMR (CDCl$_3$):175.0, 161.35, 146.82, 144.76, 144.76, 140.51, 137.45, 133.93, 129.29, 128.23, 127.32, 62.40, 49.42, 44.92, 44.89, 38.95, 30.15, 22.37 and 18.65

MS (m/z)   : 369.2 (M$^+$)

HPLC   : > 99.10 %

4.1.41. 1-(1-Methylpyridinium-3-carboxamido)propan-2yl 2-(4-isobutylphenyl) propanoate iodide (7bI)

The title compound was prepared from ester **(6bI)** (2.5 g, 6.79 mM) and methyl iodide (2.89 g, 20.35 mM) following the method described for the synthesis of compound **(7aI)** to give yellow oil of the desired product **(7bI)** (2.80 g, 80.82 %)

Anal.:

TLC   : R$_f$ 0.32 (Methanol: 1 drop GAA)

UV (MeOH) : 219 nm, (log ε 3.6)

IR (KBr, cm^{-1}): 3260, 1725, 1669, 1166 and 847

PMR (CDCl$_3$) :9.80 (s, 1H, pyridinium-H), 8.89-8.87 (d, 2H, pyridinium-H), 8.72-8.69 (m, 1H, NH), 8.00-7.97(m, 1H, pyridinium-H),7.15-7.13 (d,2H, Ar-CH_2), 6.99-6.97 (d, 2H, Ar-CH_2), 4.50 (s, 3H, N-CH_3),4.35-4.12 (m, 2H,-OCH_2), 3.79-3.74 (q, 1H,-CH), 3.68-3.60 (m,2H,-CH_2), 2.33-2.31 (d, 2H, -CH_2), 1.77-1.70 (m, 1H,-CH), 1.43-1.41 (d, 3H,-CH_3) and 0.81-0.79 (d, 6H, -(CH_3)$_2$).

MS (m/z)   : 383.2(M$^+$)

HPLC   : > 99.40 %

4.1.42. 2-(1-Methylpyridinium-3-carboxamido)butanyl 2-(4-isobutylphenyl) propanoate iodide (7cI)

The title compound was prepared from ester **(6cI)** (2.5 g, 6.54 mM) and methyl iodide (2.78 g, 19.57 mM) following the method described for the synthesis of compound **(7aI)** to give yellow oil of the desired product **(7cI)** (2.90 g, 84.56 %).

Anal.:

TLC   : R$_f$ 0.29 (Methanol: 1 drop GAA)

UV (MeOH)   : 220 nm, (log ε 4.3)

IR (KBr, cm^{-1}): 3238, 1729, 1668, 1163 and 734

PMR (CDCl$_3$):9.80 (s, 1H, pyridinium-*H*), 9.06 (s, 1H, N*H*), 8.92-8.90 (d,1H,pyridinium-*H*, *J=8.12*), 8.45-8.43(d, 1H, pyridinium-*H*, *J=8.0*), 8.06 -8.03 (m, 1H, pyridinium-*H*, *J=6.96*), 7.20-7.01 (dd,4H, phenyl-*H*,*J=8.04,8.04*), 4.58 (s, 3H, N-C*H₃*), 4.34-4.29 (m,2H, -C*H₂*), 4.22-4.19(m, 1H, N-C*H*), 3.80-3.65 (q, 1H, Ar-C*H*),1.82-1.73 (m, 2H,-C*H₂*),1.72-1.67 (m, 1H,-C*H*), 1.49-1.44 (d, 3H,-C*H₃*), 0.96-0.93 (t, 3H,-C*H₃*) and 0.89-0.87 (d, 6H, (C*H₃*)$_2$)

MS (m/z)   : 397.2 (M$^+$)

HPLC   : > 98.89 %

4.1.43. 2-(1-Methylpyridinium-3-carboxamido)-2-methylpropanyl 2-(4-isobutyl phenyl)propanoate iodide (7dI)

The title compound was prepared from ester **(7dI)** (2.5 g, 6.54 mM) and methyl iodide (2.78 g, 19.57 mM) following the method described for the synthesis of compound **(7aI)** to give yellow oil of the desired product **(7dI)** (3.10 g, 90.40 %).

Anal.:

TLC   : R$_f$ 0.24 (Methanol: 1 drop GAA)

UV (MeOH)   : 220 nm, (log ε 3.5)

IR (KBr, cm^{-1}): 3244, 1729, 1670, 1163, and 746

PMR (CDCl$_3$): 9.59 (s, 1H, pyridinium-*H*), 9.08-9.06 (d, 1H, pyridinium-*H*,*J=6.08*), 8.76-8.74 (d, 1H, pyridinium-*H*, *J=8.08*), 8.05-8.01 (t,1H, pyridinium-*H*, *J=6.12*), 7.97 (bs, 1H, N*H*), 7.21-7.03 (dd,4H, phenyl-*H*, *J=8.06*), 4.57 (s, 3H, N-C*H₃*), 4.33 (s, 2H, O-C*H₂*), 3.80-3.78 (q, 1H, Ar-C*H*), 2.40-2.38 (d, 2H, -C*H₂*), 1.82-1.78 (m, 1H, -C*H*), 1.50-1.48 (d, 3H, -C*H₃*), 1.46 (s, 6H, (C*H₃*)$_2$) and 0.90-0.85 (s, 6H, (-C*H₃*)$_2$)

^{13}CMR (CDCl$_3$):174.81, 61.22, 161.48-127.09, 68.53, 60.66, 55.46, 50.32, 49.45, 45.04, 30.14, 24.21, 22.36-18.31 and 14.10.

MS (m/z)   : 397.25 (M$^+$)

HPLC   : > 99.55 %

4.1.44. 3-(1-Methylpyridinium-3-carboxamido)propanyl 2-(4-isobutylphenyl)propa noate iodide (7eI)

The title compound was prepared from ester **(6eI)** (2.5 g, 6.54 mM) and methyl iodide (2.89 g, 19.62 mM) following the method described for the synthesis of compound **(7aI)** to give yellow oil of the desired product **(7eI)** (2.67 g, 77.06 %).

Anal.:

TLC : R_f 0.35 (Methanol: 1drop glacial acetic acid)

UV (MeOH) : 219 nm, (log ε 4.10)

IR (KBr, cm^{-1}): 3230, 2955, 1725, 1669, 1163 and 735

PMR (CDCl$_3$):10.10 (s, 1H, pyridinium-*H*), 9.02-9.0 (d, 1H, pyridinium-*H*,*J=8.08*), 8.90-8.87 (m, 1H, N*H*), 8.85-8.84 (d, 1H, pyridinium-*H*,*J=6.08*), 8.06-8.03 (t, 1H, pyridinium-*H*, *J=6.16*), 7.21-7.07 (dd,4H, phenyl-*H*, *J=8.08, 8.08*), 4.59 (s, 1H, N-C*H*), 4.25-4.13 (m, 2H, -C*H*$_2$), 3.76-3.70 (q, 1H, -C*H*), 3.54-3.49 (t, 2H, -C*H*$_2$), 3.22 (s, 1H, N*H*), 2.43-2.42 (d, 2H, Ar-C*H*$_2$), 2.08-2.02 (m, 2H, -C*H*$_2$),1.86-1.80 (m, 1H, C*H*), 1.53-1.44 (d, 3H, C*H*$_3$) and 0.90-0.87 (d, 6H, C*H*$_3$)$_2$)

MS (m/z) : 383.2 (M$^+$)

HPLC : > 99.55 %

4.1.45. *N*-[2-(2-(4-Isobutylphenyl)propanamido)ethyl]-1-methyl-3-carboxamido pyridinium iodide (7fI)

The title compound was prepared from amide intermediate **(6fI)** (2.0 g, 5.66 mM) and methyl iodide (2.41 g, 16.99 mM) following the method described for the synthesis of compound **(7aI)** to give yellow oil of the desired product **(7fI)** (2.30 g, 82.01 %).

Anal.:

TLC : R_f 0.32 (Methanol: 1drop glacial acetic acid)

UV (MeOH) : 219 nm, (log ε 3.15)

IR (KBr, cm^{-1}): 3337, 1645, 1548, 1236 and 671

PMR (CDCl$_3$) : 9.64 (s, 1H, Ar-*H*), 9.11-9.12 (d, 1H, Ar-*H*), 8.83-8.88 (t, 2H, Ar-*H*, N*H*), 8.02-8.05 (t, 1H, Ar-C*H*), 7.19-7.21(d, 2H, Ar-C*H*$_2$), 6.93-6.95 (d, 2H, Ar-C*H*$_2$), 4.50 (s, 3H,-C*H*$_3$), 3.64-3.66 (q, 1H,-C*H*$_2$), 3.43-3.50 (q, 3H,-C*H*$_2$, -N*H*), 3.33-3.36 (q, 1H,-C*H*$_2$), 2.29-2.31 (d,

2H,-CH_2), 1.71-1.74 (m, 1H, -CH), 1.37-1.38 (d, 3H,-CH_3) and 0.79-0.80 (d, 6H, (CH_3)$_2$)

^{13}CMR (CDCl$_3$): 174.32, 1160.97, 146.73, 145.25, 142.94, 139.13, 139.0, 133.61, 128.53, 127.34, 126.79, 48.37, 45.0, 44.32, 39.86, 39.02, 37.92, 29.65, 22.03 and 18.37

MS (m/z)   : 368.1 (M$^+$)

HPLC   : > 99.19 %

4.1.46. *N*-[3-(2-(4-Isobutylphenyl)propanamido)propyl]-1-methyl-3-carboxamido pyridinium iodide (7gI)

The title compound was prepared from amide intermediate **(6gI)** (2.0 g, ,5.44 mM) and methyl iodide (2.32 g, 16.34 mM) following the method described for the synthesis of compound **(7aI)** to give yellow semisolid of the desired product **(7gI)** (2.20 g, 79.31 %).

Anal.:

TLC   : R$_f$ 0.35 (Methanol: 1 drop GAA)

UV (MeOH)   : 220 nm, (log ε 3.90)

IR (KBr, cm^{-1}): 3268, 3050, 1658, 1510 and 850

PMR (CDCl$_3$) : 9.84 (s, 1H, pyridinium-H), 9.14-9.12 (d, 1H, pyridinium-H, *J=6.08*), 9.03-9.00 (d, 1H, pyridinium -H, *J=8.12*), 8.81-8.78 (d,1H, pyridinium-H, *J=5.84*), 8.12-8.08 (t, 1H, NH), 7.27-7.06 (dd,4H, phenyl-H, *J=8.08*), 6.69-6.66 (t, 1H, NH), 4.60 (s, 3H, N-CH_3), 4.12-4.09 (q, 1H, Ar-CH), 3.75-3.67 (q, 2H, -CH_2), 3.46-3.34 (m, 2H, -CH_2), 2.43-2.40 (d, 3H, -CH_3), 1.85-1.77 (m, 2H,-CH_2), 1.49-1.44 (d, 2H, Ar-CH_2), 1.27-1.21 (m, 1H, CH) and 0.89-0.86 (d, 6H, (CH_3)$_2$).

^{13}CMR (CDCl$_3$):175.49, 161.17, 154.99, 146.85, 144.87, 140.98, 138.66, 137.65, 134.20, 130.01, 129.88, 128.19, 127.30, 53.77, 49.56, 46.32, 44.94, 37.12, 30.15, 28.64, 22.38, 18.56 and 14.67

MS (m/z)   : 382.2 (M$^+$)

HPLC   : > 99.19 %

4.1.47. 2-(1-Methylpyridinium-3-carboxamido)ethyl 2-(6-methoxy-2-naphthyl) propionate iodide (7aII)

A reaction mixture containing ester **(6aII)** (1.0 g, 2.64 mM) and methyl iodide (1.11 g, 7.92 mM) in acetonitrile/acetone (20 ml) were refluxed for 2-3 h. Solvent and the excess reagent were removed under reduced pressure to afford yellow semisolid which on crystallization in ethyl acetate gave light yellow solid of the desired product[2] which was found to be hygroscopic in nature **(7aII)** (1.1 g, 79.91 %) m.p. 168-170 $^{\circ}$C. (lit.[2] m.p. 169-170)

Anal.:

TLC   : R_f 0.35 (Methanol: 1 drop GAA)

UV (MeOH) : 226, 266 nm

IR (KBr, cm^{-1}): 3284, 1721, 1671, 1602 and 1175

PMR (CDCl$_3$): 9.34 (s, 1H, pyridinium-*H*), 9.15-9.13 (d, 1H, pyridinium-*H*, *J=8.0*), 9.04-9.02 (m, 1H, pyridinium-*H*, *J=8.0*), 8.74-8.72 (d,1H, pyridinium-*H*, *J=8.0*), 8.09-8.03 (m, 1H, N*H*), 7.66-7.07 (m,6H, naphthalene-*H*), 4.44 (s, 3H, N-C*H*$_3$), 4.28-4.25 (t, 2H,-C*H*$_2$),3.91-3.86 (q, 1H, C*H*), 3.67-3.56 (m, 2H, N-C*H*$_2$), 3.33 (s, 3H,O-C*H*$_3$) and 1.52-1.51 (d, 3H, -C*H*$_3$)

^{13}CMR (CDCl$_3$):172.73, 160.01, 155.85, 145.75, 143.94, 141.18, 134.28, 131.94, 127.82, 126.16, 124.97, 117.41, 104.33, 61.09, 54.14, 47.23, 43.29, 39.06, 38.85, 38.44, 38.02, 37.33 and 17.20

MS (m/z)   : 393.40 (M$^+$)

HPLC   : > 99.10 %

4.1.48. 1-(1-Methylpyridinium-3-carboxamido)-2-propanyl 2-(6-methoxy-2-naphthyl) propanoate iodide (7bII)

The title compound was prepared from ester **(6bII)** (1.0 g, 2.54 mM) and methyl iodide (1.07 g, 7.64 mM) following the method described for the synthesis of compound **(7aII)** to give yellow solid of the desired product **(7bII)** (0.90 g, 66.17 %). 188-190 $^{\circ}$C

Anal.:

TLC   : R_f 0.35 (Methanol: 1 drop GAA)

UV (H$_2$O)   : 228 nm

IR (KBr, cm^{-1}): 3349, 1721, 1666, 1602, 1187 and 892

PMR (CDCl$_3$): 9.08 (s, 1H, pyridinium-*H*), 9.02-9.01(d, 1H, pyridinium-*H*, *J=4.0*) 8.81 (bs, 1H, N*H*), 8.45-8.43 (d, 1H, pyridinium-*H*,*J=4.0*), 7.83-7.79 (t, 1H, pyridinium-*H*, *J*=4.0), 7.59-7.05 (m,6H, naphthalene-

H), 5.16-5.13 (m, 1H, OC*H*, *J*=2.92), 4.35 (s, 3H, N-C*H₃*), 3.92 (s, 3H, O-C*H₃*), 3.84-3.82 (q, 1H, Ar-C*H*,*J*=8.0), 3.37-3.33 (t, 2H, N-C*H₂*), 1.50-1.49 (d, 3H,-C*H₃*, *J*=7.2) and 1.33-1.32 (d, 3H, -C*H₃*, *J*=6.28)

MS (m/z)   : 407.41(M$^+$)

HPLC   : > 98.69 %

4.1.49. 2-(1-Methylpyridinium-3-carboxamido)butanyl 2-(6-methoxy-2-naphthyl) propanoate iodide (7cII)

The title compound was prepared from ester **(6cII)** (1.0 g, 2.46 mM) and methyl iodide (1.04 g, 7.38 mM) following the method described for the synthesis of compound **(7aII)** to give yellow oil of the desired product **(7cII)** (0.88 g, 65.23 %).

Anal.:

TLC   : R$_f$ 0.35 (Methanol: 1 drop GAA)

UV (H₂O)   : 228 nm

IR (KBr, cm^{-1}): 2971, 1727, 1668, 1604, 1239 and 854

PMR (CDCl₃) : 9.23 (s, 1H, pyridinium-*H*), 8.94-8.87 (dd, 1H, pyridinium-*H*, *J=8.0,8.0*), 8.61-8.57 (m, 1H, pyridinium-*H*, *J=8.0*), 8.18-8.13 (dd,1H, pyridinium-*H*, *J=8.0*), 7.85-7.75 (m, 1H, N*H*), 7.61-6.97 (m, 6H, naphthalene-*H*), 4.40 (s, 3H, N-C*H₃*), 4.34 (s, 3H, O-C*H₃*), 3.91-3.88 (d, 4H, (C*H₂*)₂, *J=4.0*), 1.74-1.65 (m, 1H, N-C*H, J=4.0*), 1.54-1.51 (d, 3H, -C*H₃*, *J*=1.76), 1.27-1.23 (q,1H,-C*H*) and 0.95-0.90 (t, 3H, -C*H₃*, *J= 4.0*)

^{13}CMR (CDCl₃): 174.95, 174.62, 171.21, 161.09, 157.52, 146.11, 145.94, 144.12-105.44, 65.78 60.40 55.71 51.62 49.12 45.07, 24.19 and 10.66

MS (m/z)   : 421.2 (M$^+$)

HPLC   : > 99.58 %

4.1.50. 2-Methyl-2-(1-methylpyridinium-3-carboxamido)propanyl 2-(6-methoxy-2-naphthyl)propanoate iodide (7dII)

The title compound was prepared from ester **(6dII)** (1.0 g, 2.46 mM) and methyl iodide (1.04 g, 7.38 mM) following the method described for the synthesis of compound **(7aII)** to give yellow colored hygroscopic solid of the desired product **(7dII)** (0.95 g, 70.42 %).

Anal.:

TLC : R_f 0.35 (Methanol: 1 drop GAA)

UV (H_2O) : 228 nm

IR (KBr, cm^{-1}): 3448, 1730, 1658, 1605, 1372 and 854

PMR (CDCl$_3$): 9.29 (s, 1H, pyridinium-*H*), 9.11-9.10 (d, 1H, pyridinium-*H,J=8.0*), 8.65-8.63 (d, 1H, pyridinium-*H, J=8.0*), 8.28 (s, 1H,N*H*), 8.05-8.01 (m, 1H, pyridinium-*H, J=8.0*), 7.66-7.07 (m, 6H,naphthalene-*H*), 4.40 (s, 3H, N-C*H₃*), 3.90 (s, 3H, O-C*H₃*), 3.37-3.34(m, 1H, C*H*-CO), 3.02 (s, 2H, O-C*H₂*), 1.51-1.48 (d, 3H, C-C*H₃, J=4.0*) and 1.38-1.35 (d, 6H, C(C*H₃*)₂)

HPLC : > 99.58 %

4.1.51. 3-(1-Methylpyridinium-3-carboxamido)propanyl 2-(6-methoxy-2-naphthyl)propanoate iodide (7eII)

The title compound was prepared from ester **(6eII)** (0.5 g, 1.27 mM) and methyl iodide (0.53 g, 3.82 mM) following the method described for the synthesis of compound **(7aII)** to give a white solid of the desired product[2] **(7eII)** (0.55 g, 80.62 %). m.p. 98-101°C (lit.[2] m.p. 100-102°C)

Anal.:

TLC : R_f 0.35 (Methanol: 1 drop GAA)

UV (H_2O) : 228, 264 nm

IR (KBr, cm^{-1}): 3470, 1716, 1667, 1599 and 1266

PMR (CDCl$_3$): 9.44 (s, 1H, Pyridinium-*H*), 9.15-9.13 (d, 1H, pyridinium-*H,J=8.0*), 9.06-9.03 (m, 1H, pyridinium-*H, J=8.0*), 8.91-8.89 (d, 1H,pyridinium-*H, J=8.0*), 8.23-8.19 (t, 1H, N*H*), 7.76-7.11 (m, 6H,naphthalene-*H*), 4.44 (s, 3H, N-C*H₃*), 4.15-4.11 (q, 2H, N-C*H₂*),3.91-3.89 (q, 1H, -COC*H, J=7.12*), 3.88 (s, 3H, O-C*H₃*), 3.40-3.35 (t, 2H, O-C*H₂, J=6.6*), 1.89-1.85 (m, 2H, -C*H₂, J=6.6*) and 1.52-1.50 (d, 3H, -C*H₃, J=7.12*)

^{13}CMR (CDCl$_3$):173.74, 160.65, 157.11-135.33, 133.58-105.19 (10C, Ar), 61.85, 54.90, 48.23, 44.65, 39.84, 27.87 and 18.28

MS (m/z) : 407.8 (M$^+$)

HPLC : > 99.58 %

4.1.52. *N*-[2-(2-(6-Methoxy-2-napthhyl)propanamido)ethyl]-1-methyl-3-carboxamido pyridinium iodide (7fII)

The title compound was prepared from amide intermediate **(6fII)** (1.0 g, 2.64 mM) and methyl iodide (1.83 g, 7.94 mM) following the method described for the synthesis of compound **(7aII)** to give yellow oil of the desired product **(7fII)** (0.78 g, 56.69 %).

Anal.:

TLC : R_f 0.35 (Methanol: 1 drop GAA)

UV (H_2O) : 228 nm

IR (KBr, cm^{-1}) : 3393, 1665, 1603, 1210 and 857

PMR (CDCl$_3$) : 9.17 (s, 1H, pyridinium-*H*), 9.01-8.99 (d, 1H, pyridinium-*H*,*J=8.0*), 8.88-8.85 (m, 1H, pyridinium-*H*, *J=8.0*), 8.61-8.59 (d,1H, pyridinium-*H*, *J=8.0*), 8.10-8.07 (m, 1H, N*H*), 7.99-7.94 (m,1H, N*H*), 7.77-7.07 (m, 6H, naphthaene-*H*), 4.36 (s, 3H, N-C*H₃*),3.89 (s, 3H, O-C*H₃*), 3.74-3.72 (q, 1H, -C*H*, *J=7.04*), 3.53-3.39(m, 2H, N-C*H₂*), 3.31-3.24 (t, 2H, N-C*H₂*) and 1.50-1.44 (d, 3H,-C*H₃*, *J=7.04*)

^{13}CMR (CDCl$_3$):174.11, 161.08, 157.20, 146.58, 144.97, 142.42, 137.08, 133.23, 128.98, 127.07, 126.38, 125.68, 118.77, 105.46, 55.12, 52.12, 48.19, 45.20, 39.78, 39.15, 37.84, 35.00 and 18.19

MS (m/z) : 391.8 (M$^+$)

HPLC : > 99.90 %

4.1.53. *N*-[3-(2-(6-Methoxy-2-naphthyl)propanamido)propanyl)-1-methyl-3-carbox-amido pyridinium iodide (7gII)

The title compound was prepared from amide intermediate **(6gII)** (1.0 g, 2.55 mM) and methyl iodide (0.54 g, 7.92 mM) following the method described for the synthesis of compound **(7aII)** to give yellow oil which was further crystallized using ethyl acetate and methanol to give white solid of the desired product **(7gII)** (0.86 g, 62.99 %). m.p. 192-194 ºC

Anal.:

TLC : R_f 0.35 (Methanol: 1 drop GAA)

UV (H_2O) : 229 nm

IR (KBr, cm^{-1}): 3276, 1673, 1631, 1604, 1269 and 857

PMR (CDCl$_3$) :9.52 (s, 1H, pyridinium-*H*), 9.15-9.14 (d, 1H, pyridinium-*H*,*J=8.0*), 8.95-8.93 (d, 2H, pyridinium-*H*, N*H*, *J=8.0*), 8.14-8.10(m, 1H, pyridinium-*H*, *J=8.0*), 7.84 (m, 1H, N*H*), 7.70-7.65 (m,3H, Ar-*H*, 7,8, *J=8.0*),7.47-7.44 (d, 1H, Ar-*H*, *J=8.0*), 7.11-7.09 (d, 2H, Ar-*H*, *J=8.0*), 4.49 (s, 3H, N-C*H*$_3$), 3.90 (s, 3H, O-C*H*$_3$),3.79-3.77 (q, 1H, -C*H*, *J=6.96*), 3.38-3.37 (m, 2H, N-C*H*$_2$), 3.24-3.17 (m, 2H, N-C*H*$_2$), 1.78-1.75 (m, 2H, -C*H*$_2$, *J=6.36*) and 1.52-1.50(d, 3H,-C*H*$_3$, *J=6.96*)

^{13}CMR (CDCl$_3$): 173.78, 160.64, 156.89-137.17 (5C, pyridinium), 133.54-105.25 (10C, Ar), 54.92, 48.20, 45.27, 39.63, 37.29, 36.30 and 18.39

MS (m/z)   : 406.6 (M$^+$)

HPLC   : > 99.58 %

4.1.54. 2-(1-Methylpyridinium-3-carboxamido)ethyl 1-(4-chlorobenzoyl)-5-methoxy-2-methylindol-3-acetate iodide (7aIII)

A reaction mixture containing ester intermediate **(6aIII)** (1.0 g, 1.97 mM) and methyl iodide (0.83 g, 5.92 mM) in acetonitrile/acetone (20 ml) was refluxed for 2-3 h. The solvent and the excess reagent were removed under reduced pressure to afford yellow solid which on crystallization in ethanol and small amount of ether gave light yellow solid of the desired product[2] **(7aIII)** (0.8 g, 62.48 %) m.p. 176-179 ^{o}C (lit.[2] m.p. 178-179 ^{o}C)

Anal.:

TLC   : R$_f$ 0.35 (Methanol: 1 drop GAA)

UV (MeOH) : 220, 320 nm

IR (KBr, cm^{-1}): 3276, 3040, 2949, 1728, 1683, 1662, 1597, 1228 and 1173

PMR (CDCl$_3$): 9.41 (s, 1H, pyridinium-*H*), 9.18-9.16 (d, 1H, pyridinium-*H*,*J=8.0*), 9.08 (m, 1H, pyridinium-*H*, *J=8.0*), 8.81-8.79 (d, 1H,pyridinium-*H*, *J=8.0*), 8.15-8.11 (t, 1H, N*H*), 7.69-7.55 (d, 2H,phenyl-*H*, *J=8.0*), 7.57-7.55 (d, 2H, phenyl-*H*, *J=8.0*), 6.95-6.56 (m, 3H, indol-*H*), 4.49 (s, 3H, N-C*H*$_3$), 4.31-4.28 (t, 2H, O-C*H*$_2$), 3.77-3.74 (m, 3H, O-C*H*$_3$), 3.71 (s, 2H, CO-C*H*$_2$), 3.67-3.63 (m, 2H, N-C*H*$_2$), 2.25 (s, 3H, Ar-C*H*$_3$)

^{13}CMR (CDCl$_3$): 170.17, 167.63, 160.93, 155.32, 146.84, 145.19, 142.58,138.16, 135.25, 133.61, 130.88, 130.07, 128.80, 127.30, 114.26, 112.21,

111.03, 101.27, 62.31, 55.33, 48.29, 40.25, 40.04, 39.83, 39.20, 38.55, 29.59 and 13.20

MS (m/z)   : 520.60 (M$^+$)

HPLC   : > 99.31 %

4.1.55. 1-(1-Methylpyridinium-3-carboxamido)propan-2-yl 1-(4-chlorobenzoyl)-5-methoxy-2-methylindol-3-acetate iodide (7bIII)

The title compound was prepared from ester intermediate **(6bIII)** (1.0 g, 1.92 mM) and methyl iodide (0.81 g, 5.76 mM) following the method described for the synthesis of compound **(7aIII)** to give yellow solid. The product was purified by column chromatography using neutral alumina as stationary phase and ethyl acetate as eluent followed by 50 % methanol in ethyl acetate to get a yellow hygroscopic solid of the desired product **(7bIII)** (0.80 g, 62.83 %). m.p. 96-98 ^{o}C

Anal.:

TLC   : R$_f$ 0.39 (Methanol: 1 drop GAA)

UV (MeOH) : 315 nm

IR (KBr, cm^{-1}): 3439, 1729, 1675, 1590, 1323 and 754

PMR (CDCl$_3$):9.54 (s, 1H, Pyridinium-*H*) 8.95-8.93 (d, 1H, Pyridinium-*H*, *J=8.0,8.0*), 8.73-8.71 (d, 1H, Pyridinium-*H*, *J=8.0*) , 8.61-8.58 (m, 1H, Pyridinium-*H*, *J=8.0*), 7.92-7.88 (t, 1H, N*H*, *J*=6.08), 7.67-7.63 (d, 2H, Phenyl-*H*, *J*=8.0), 7.48- 7.45 (d, 2H, Phenyl-*H,J*=8.0), 6.97-6.96 (d,1H, Indo-*H*, *J*=2.48), 6.89 (5, 1H, Indol-*H*), 6.55-6.52 (dd, 1H, Indol-*H*, *J* =2.52), 5.26-5.21 (m, 1H, OC*H*), 4.47-4.44 (s, 3H, N-C*H₃*), 3.80 (s, 3H,-OC*H₃*), 3.58-3.54 (t, 2H, -CON*H*), 2.23 (s, 3H, Indol-C*H₃*), 2.13 (s, 2H, Indol-C*H₂*) and 1.36-1.30 (d, 3H, -C*H₃,* *J=8.0*).

HPLC   : > 99.0%

4.1.56. 2-(1-Methylpyridinium-3-carboxamido)butanyl 1-(4-chlorobenzoyl)-5-methoxy-2-methylindol-3-acetate iodide (7cIII)

The title compound was prepared from ester intermediate **(6cIII)** (1.0 g, 1.87 mM) and methyl iodide (0.79 g, 5.61 mM) following the method described for the synthesis of compound **(7aIII)** to afford a yellow semisolid which was recrystallized from ethyl

acetate-methanol to obtain yellow hygroscopic solid of the desired product **(7cIII)** (0.60 g, 47.40 %). m.p. 48-50 $^{\circ}$C

Anal.:

TLC   : R$_f$ 0.41 (Methanol: 1 drop GAA)

UV (MeOH)   : 228 nm

IR (KBr, cm^{-1}): 3436, 1733, 1672, 1590, 1322 and 754

PMR (CDCl$_3$) : 9.51 (s, 1H, Pyridinium-*H*) 8.97-8.95 (d, 1H, 1H, Pyridinium-*H*,*J=8.0,8.0*), 8.74-8.72 (d, 1H, Pyridinium-*H*, *J=8.0*), 8.28(bs,1H, N*H*), 7.93-7.89 (m, 1H, Pyridinium-*H*, *J=8.0*), 7.67-7.65 (d, 2H, Phenyl-*H*, *J=8.0*), 7.48- 7.46 (d, 2H, Phenyl-*H*, *J=8.0*), 6.94-6.93 (dd, 2H, Indol, *H*-6,7, *J=2.48*), 6.48-6.45 (dd,1H, Indol *H*-4, *J=2.48*), 4.48 (s, 3H, N-C*H*$_3$), 4.33 (s, 3H,-OC*H*$_3$), 3.83 (s, 3H, indol-C*H*$_3$), 3.69 (s, 2H, Indol-C*H*$_2$-), 2.20 (s, 2H, O-C*H*$_2$), 1.80-1.66 (m, 2H, C-C*H*$_2$-), 0.96-0.92 (t, 3H, C-C*H*$_3$) and 1.27-1.24 (m, 1H, N-C*H*).

HPLC   : >98.6%

4.1.57. 2-Methyl-2-(1-methylpyridinium-3-carboxamido)propanyl 1-(4-chloro benzoyl)-5-methoxy-2-methylindol-3-acetate iodide (7dIII)

The title compound was prepared from ester intermediate **(6dIII)** (1.0 g, 1.87 mM) and methyl iodide (0.79 g, 5.61 mM) following the method described for the synthesis of compound **(7aIII)** to give yellow semisolid which was recrystallized from ethyl acetate-methanol to yield yellow hygroscopic solid of the desired product **(7dIII)** (0.80 g, 63.20 %). m.p. 86-88 $^{\circ}$C

Anal.:

TLC   : R$_f$ 0.35 (Methanol: 1 drop GAA)

UV (MeOH)   : 318 nm

IR (KBr, cm^{-1}): 3436, 1733, 1675, 1591, 1322 and 752

PMR (CDCl$_3$): 9.53 (s, 1H, Pyridinium-*H*) 9.0-8.98 (d, 1H, 1H, Pyridinium-*H*,*J=8.0*), 8.70-8.68 (d, 1H, Pyridinium-*H*, *J=8.0*), 7.69-7.93 (m,1H, Pyridinium-*H*, *J=8.0*), 7.87 (s, 1H, N*H*), 7.64- 7.62 (d, 2H,Phenyl-*H*, *J=8.0*), 7.47- 7.44 (d, 2H, Phenyl-*H*, *J=8.0*), 6.95 (s,1H, Indol *H*-4), 6.88- 6.86 (d,1H, Indol *H*-6, *J=8.96*), 6.56-6.54 (d, 1H, Indol *H*-7, *J=8.96*), 4.50 (s, 3H, N-C*H*$_3$), 4.38 (s, 2H,O-

CH_2-), 3.78 (s, 3H,-OCH_3), 3.76 (s, 2H, indol -CH_2), 2.28 (s,3H,

Indol-CH_3), 1.49 (s, 6H, (CH_3)$_2$)

^{13}CMR (CDCl$_3$):170.93, 168.44, 160.97, 155.85, 148.11, 144.57 139.31, 135.79-129.18, 127.69, 114.79, 122.66, 111.54, 101.69, 68.92, 56.10, 55.38, 49.23, 30.52, 24.33, 13.75

MS (m/z)　　　: 548.3 (M$^+$)

HPLC　　　　: >96.4 %

4.1.58. 3-(1-Methylpyridinium-3-carboxamido)propanyl 1-(4-chlorobenzoyl)-5-methoxy-2-methylindol-3-acetate iodide (7eIII)

The title compound was prepared from ester intermediate **(6eIII)** (1.0 g, 1.91 mM) and methyl iodide (0.81 g, 5.76 mM) following the method described for the synthesis of compound **(7aIII)** to give yellow solid which on crystallization in ethanol and small amount of ether yielded light yellow solid of the desired product[2] **(7eIII)** (1.10 g, 86.40 %), m.p. 166-168 ^{o}C.

Anal.:

TLC　　　　: R$_f$ 0.35 (Methanol: 1 drop GAA)

UV (MeOH)　: 222, 320, 315 nm

IR (KBr, cm^{-1}): 3288, 1711, 1630, 1594, 1316, 827

PMR (CDCl$_3$): 9.53 (s, 1H, pyridinium-H), 9.20-9.18 (d, 1H, pyridinium-H, $J=8.0$), 9.07-9.04 (m, 1H, pyridinium-H, $J=8.0$), 8.98-8.96 (d,1H,pyridinium-H, $J=8.0$), 8.21-8.17 (t, 1H, CONH), 7.67-7.66 (d,2H, phenyl-H, $J=4.0$), 7.55-7.54 (d, 2H, $J=4.0$), 6.98-6.97 (s, 1H,indole-H), 6.92-6.89 (d, 1H, indole-H, $J=9.04$), 6.67-6.64 (d, 1H,indole-H, $J=9.04$), 4.50 (s, 3H, N-CH_3), 4.19-4.16 (t, 2H, O-CH_2,$J=6.4$), 3.80 (s, 3H, O-CH_3), 3.71 (s, 2H, indole-CH_2), 3.49-3.44 (q, 2H, N-CH_2, $J=6.56$), 2.32 (s, 3H, indole-CH_3) and 1.99-1.93 (m,2H, O-C-CH_2, $J=6.56$)

MS (m/z)　　　: 535.8 (M$^+$)

^{13}CMR (CDCl$_3$):171.23, 168.43, 161.10, 155.99-101.63, 62.43, 56.06, 49.23, 36.73, 30.25 and 13.22

HPLC　　　　: >99.8 %

4.1.59. N-[2-(1-Methylpyridinium-3-carboxamido)ethyl-2-[1-(4-chlorobenzoyl)-5-methoxy-2-methylindole]-3-acetamide iodide (7fIII)

The title compound was prepared from amide intermediate **(6fIII)** (1.0 g, 1.98 mM) and methyl iodide (0.83 g, 5.94 mM) following the method described for the synthesis of compound **(7aIII)** to offer yellow semisolid of the desired product **(7fIII)** (0.8 g, 62.44 %).

Anal.:

  TLC   : R_f 0.38 (Methanol: 1 drop GAA)

  UV (MeOH) : 258, 316 nm

  IR (KBr, cm^{-1}): 3273, 1663, 1590, 1312 and 751

  PMR (CDCl$_3$) : 9.34 (s, 1H, pyridinium-*H*), 9.14-9.13 (d, 1H, pyridinium-*H*, *J=6.04*), 8.83 (s, 1H, CO*NH*), 8.73-8.71 (d, 1H, pyridinium-*H*, *J=8.0*), 8.04-8.02 (m, 1H, pyridinium-*H*, *J=8.0*), 7.71-7.52 (d, 2H, phenyl-*H*, *J=8.0*), 7.54-7.52 (d, 2H, phenyl-*H*, *J=8.0*), 6.99 (s, 1H, indole-*H*), 6.92-6.90 (d, 1H, indole-*H*, *J=2.24*), 6.55-6.53 (d, 1H, indole-*H*, *J=2.24*), 4.45 (s, 3H, N-*CH₃*), 4.08-4.06 (t, 1H, CO*NH*), 3.77 (s, 3H, -O*CH₃*), 3.57-3.48 (m, 4H, N(*CH₂*)₂) and 3.44 (s, 2H, indole-*CH₂*), 2.26 (s, 3H, indole-*CH₃*)

  ^{13}CMR (CDCl$_3$): 171.15, 168.67, 161.39, 155.97-155.85, 146.08-144.24, 139.23, 56.25, 53.83, 49.12, 39.97-32.27 and 14.64

  MS (m/z) : 519.0 (M$^+$)

  HPLC   : >95.2 %

4.1.60. N-[3-(1-Methylpyridinium-3-carboxamido)propyl]-2-[1-(4-chlorobenzoyl)-5-methoxy-2-methylindol]-3-acetamide iodide (7gIII)

The title compound was prepared from amide intermediate **(6gIII)** (1.0 g, 1.92 mM) and methyl iodide (0.83 g, 5.78 mM) following the method described for the synthesis of compound **(7aIII)** to give yellow semisolid which was recrystallized from methanol: chloroform: ethyl acetate (1:1:1) to yield light yellow solid of the desired product **(7gIII)** (0.90 g, 70.67 %). m.p. 170-172 ^{o}C

Anal.:

  TLC   : R_f 0.35 (Methanol: 1 drop GAA)

  UV (MeOH) : 255 nm

  IR (KBr, cm^{-1}): 3299, 1668, 1591 and 754

PMR (CDCl$_3$): 9.5 (s, 1H, Pyridinium-*H*), 9.18-9.17 (d, 1H, Pyridinium-*H*, *J=4*), 9.0-8.98 (m, 1H, Pyridinium-*H*, *J=4.0*), 8.95-8.93 (d,1H, pyridinium-*H*, *J=8.0*), 8.19-8.15 (t, 1H, CONH, *J=6.16*), 7.97-7.95 (t, 1H, CON*H*, *J=5.76*), 7.70-7.52 (dd, 4H, phenyl-H), 7.09-6.62 (m, 3H, indol-*H*), 4.48 (s, 3H, N-C*H*$_3$), 3.79 (s, 3H, -OC*H*$_3$), 3.55 (s, 2H, indol-C*H*$_{2-}$), 3.41-3.38 (q, 2H, N-C*H*$_2$, *J=6.12*), 3.33 (s, 3H, Indol-C*H*$_3$), 3.26 (q, 2H,N-C*H*$_2$, *J=6.12*) and 1.81-1,75 (m, 2H, -C*H*$_2$-, *J=6.12*).

^{13}CMR (CDCl$_3$): 169.65, 167.64, 160.85, 155.45, 146.85, 145.29, 142.66, 137.92, 135.05, 133.86, 133.42, 130.94, 130.21, 127.32, 114.37, 114.02, 111.07, 101.53, 55.38, 48.26, 40.21, 40.01, 39.80, 39.17, 37.28, 36.39, 31.30, 28.71, 13.35

MS (m/z)　　：533.3 (M$^+$)

HPLC　　　：>99.8 %

4.1.61. 2-(1-Methylpyridinium-3-carboxamido)ethyl 2-(6-methoxy-2-naphthyl) acetate iodide (7aIV)

A reaction mixture containing ester intermediate **(6aIV)** (1.0 g, 2.74 mM) and methyl iodide (1.16 g, 8.23 mM) in acetonitrile (20 ml) were refluxed for 2-3 h. The solvent and excess reagent were removed under reduced pressure to afford yellow solid which on crystallization in chloroform-methanol yielded yellow solid of the desired product **(7aIV)** (1.2 g, 86.27 %). m.p. 132-134 ^{o}C

Anal.:

TLC　　　　：R$_f$ 0.35 (Methanol: 1 drop GAA)

UV (MeOH)　：229 nm

IR (KBr, cm^{-1}): 3289, 2950, 1735, 1672, 1606 and 1187

PMR (CDCl$_3$): 9.38 (s, 1H, pyridinium-*H*), 9.11-9.08 (d, 2H, pyridinium-*H*, N*H*, *J=8.0*), 8.80-8.78 (d, 1H, pyridinium-*H*, *J=8.0*), 8.09-8.06 (m, 1H, pyridinium-*H*), 7.62-7.58 (m, 3H, naphthalene-*H*, *J=8.0*), 7.32-7.04 (m, 3H, naphthalene-*H*, *J=8.0*), 4.41 (s, 3H, N-C*H*$_3$), 4.26-4.23 (m,2H, N-C*H*$_2$, *J=4.0*), 3.85 (s, 3H, O-C*H*$_3$), 3.73 (s, 2H, Ar-C*H*$_2$) and 3.64-3.60 (m, 2H, O-C*H*$_2$)

^{13}CMR　　：171.17, 161.22, 157.03, 146.94, 145.26, 142.51, 133.0, 129.11, 128.75, 127.99, 127.32, 126.56, 118.57, 105.44, 62.28, 55.11,

48.29, 40.35, 40.01, 39.80, 39.17 and 38.60

MS (m/z)   : 379.0(M$^+$)

HPLC   : >99.5 %

4.1.62. 1-(1-Methylpyridinium-3-carboxamido)propan-2-yl 2-(6-methoxy-2-naphthyl-2-yl)acetate iodide (7bIV)

The title compound was prepared from ester intermediate **(6bIV)** (0.5 g, 1.32 mM) and methyl iodide (0.55 g, 3.96 mM) following the method described for the synthesis of compound **(7aIV)** to yield a yellow oil but it contained some impurity. The crude oil was purified by column chromatography using neutral alumina as stationary phase and ethyl acetate as mobile phase followed by ethyl acetate: methanol (1:1) mixture to get pure yellow oil of the desired product **(7bIV)** (0.45 g, 64.44 %).

Anal.:

TLC   : R$_f$ 0.43 (Methanol: 1 drop GAA)

UV (MeOH)   : 226 nm

IR (Neat, cm^{-1}): 3245, 1724, 1668, 1605, 1264 and 852

PMR (CDCl$_3$) : 9.26 (s, 1H, Pyridinium-*H*), 8.74-8.73 (d, 1H, Pyridinium-*H*, *J*=6.08), 8.61-8.59 (d,1H, Pyridinium-*H*, *J=8.0*), 8.55-8.53 (m, 1H, Pyridinium-*H*, *J=8.0*), 7.72-7.69 (m, 1H, N*H*, *J=4.0*), 7.58-7.00 (m, 3H, Ar-*H*, *J=4*), 7.35-7.32 (m, 1H, Ar-*H*, *J=4.0*) 7.06-7.0 (m, 2H, Ar-*H, J=4*), 5.26-5.22 (m,1H, O-C*H*), 4.27 (s, 3H, N-C*H*$_3$), 3.88 (s, 3H,-OC*H*$_3$,), 3.74 (s, 2H, Ar-C*H*$_2$), 3.64-3.53 (m,2H, N-C*H*$_2$, *J=4.0*), 1.32-1.30 (d, 3H, -C*H*$_3$, *J=4.0*)

^{13}CMR   : δ172.18, 161.40, 157.57, 69.68, 55.60, 49.15, 44.45, 41.46 and 17.96

HPLC   : >99.90 %

4.1.63. 2-(1-Methylpyridinium-3-carboxamido)butanyl 2-(6-methoxy-2-naphthyl) acetate iodide (7cIV)

The title compound was prepared from ester intermediate **(6cIV)** (0.5 g, 1.27 mM) and methyl iodide (0.53 g, 3.82 mM) following the method described for the synthesis of compound **(7aIV)** to give brown oil of the desired product **(7cIV)** (1.10 g, 80.70 %).

Anal.:

TLC   : R$_f$ 0.45 (Methanol: 1 drop GAA)

UV (H$_2$O)   : 226 nm

IR (Neat, cm^{-1}): 3246, 1727, 1667, 1605, 1264, 850 and 742

PMR (CDCl$_3$) : δ 9.30 (s, 1H, Pyridinium-*H*), 8.76-8.74 (d, 1H, Pyridinium-*H*, *J=8.0*), 8.62-8.60 (d, 1H, Pyridinium-*H*, *J=8.0*), 8.27-8.25 (m, 1H, N*H*), 7.73-7.70 (m, 1H, Pyridinium-*H*, *J=8.0*), 7.58-7.53 (m, 3H, Ar-*H*, *J=8.0*), 7.37-7.27 (m, 1H, Ar-*H*, *J=8.0*), 7.14-7.0 (m, 2H, Ar-*H*, *J=8.0*), 4.41-4.31 (m, 2H, O-C*H*$_2$), 4.29 (s, 3H, N-C*H*$_3$), 3.90-3.89 (m, 1H, N-C*H*), 3.88 (s, 3H, O-C*H*$_3$) 3.77 (s, 2H, Ar-C*H*$_2$), 1.84-1.69 (m, 2H, -C*H*$_2$) and 0.99-0.95 (t, 3H, -C*H*$_3$, *J=7.44*)

^{13}CMR   :172.14, 161.21, 157.57, 145.80, 144.26, 133.83, 129.38-105.50 (10C, Ar), 65.69, 55.58, 51.93, 49.06, 41.27, 23.97 and 10.78

MS (m/z)   : 407.20 (M$^+$)

HPLC   : >95.9 %

4.1.64. 2-Methyl-2-(1-methylpyridinium-3-carboxamido)propyl 2-(6-methoxy-2-naphthyl)acetate iodide (7dIV)

The title compound was prepared from ester intermediate **(6dIV)** (0.5 g, 1.32 mM) and methyl iodide (0.55 g, 3.96 mM) following the method described for the synthesis of compound **(7aIV)** to give light pink colored solid of the desired product **(7dIV)** (0.54 g, 79.32 %). m.p. 210-212 ^{0}C

Anal.:

TLC   : R$_f$ 0.48 (Methanol: 1 drop GAA)

UV (H$_2$O)   : 226 nm

IR (KBr, cm^{-1}): 3267, 1737, 1660, 1607, 1329 and 857 and 751

PMR (CDCl$_3$): 9.36 (s, 1H, Pyridinium-*H*), 9.12-9.10 (d, 1H, Pyridinium-*H*,*J=8.0*), 8.75-8.73 (d, 1H, Pyridinium-*H*, *J=8.0*), 8.34 (s, 1H, N*H*), 8.10-8.05 (m, 1H, Pyridinium-*H*, *J=8.0*), 7.66-7.08 (d, 3H, Ar-*H* , *J=8.0*), 7.35-7.33 (d, 1H, Ar-*H*, *J=8.0*), 7.17-7.08 (m, 2H, Ar-*H*, *J=8.0*), 4.41 (s, 3H, N-C*H*$_3$), 4.33 (s, 2H, -C*H*$_2$), 3.90 (s, 3H, -OC*H*$_3$), 3.78 (s, 2H, O-C*H*$_2$) and 1.42 (s, 6H, C(C*H*$_3$)$_2$)

MS (m/z)   : 407.2 (M$^+$)

HPLC   : >99.2 %

4.1.65. 3-(1-Methylpyridinium-3-carboxamido)propanyl 2-(6-methoxy-2-naphthyl) acetate iodide (7eIV)

The title compound was prepared from ester intermediate **(6eIV)** (0.5 g, 1.32 mM) and methyl iodide (0.55 g, 3.96 mM) following the method described for the synthesis of compound **(7aIV)** to give yellowish brown oil of the desired product **(7eIV)** (0.50 g, 72.72 %).

Anal.:

TLC : R_f 0.45 (Methanol: 1 drop GAA)

UV (H_2O) : 226 nm

IR (Neat, cm^{-1}): 3248, 2950, 1724, 1666, 1605, 1265 and 850

PMR ($CDCl_3$): 9.45 (s, 1H, pyridinium-*H*), 9.15-9.13 (d, 1H, pyridinium-*H*, *J=8.0*), 9.13-9.10 (m, 1H, Pyridinium-*H*, *J=8.0*), 8.93-8.91 (d, 1H, pyridinium-*H*, *J=8.0*), 8.23-8.19 (t, 1H, CO*NH*), 7.75-7.73 (d, 2H, Ar-*H*, *J=8.0*), 7.68 (s, 1H, Ar-*H*), 7.38-7.36 (d, 1H, Ar-*H*, J=8.0), 7.23 (s, 1H, Ar-*H*), 7.14-7.12 (d, 1H, Ar-*H*, *J=8.0*), 4.44 (s, 3H, N-*CH₃*), 4.17-4.14 (t, 2H, O-*CH₂*, *J=8.0*), 3.88 (s, 3H, -O*CH₃*), 3.78 (s, 2H, Ar-*CH₂*-), 3.46-3.41 (q, 2H, N-*CH₂*, *J=8.0*) and 1.94-1.91 (p, 2H, -*CH₂*, *J=8.0*)

^{13}CMR : 171.05, 160.79, 157.08, 146.69-145.20 (2C), 142.81-133.39 (2C), 133.02-105.32 (10C, Ar), 61.99, 54.98, 48.31, 39.65, 36.43 and 27.90

MS (m/z) : 393.6 (M^+)

HPLC : >99.7%

4.1.66. 2-(1-Methylpyridinium-3-carboxamido)ethyl 4-biphenylacetate iodide (7aV)

A reaction mixture containing ester intermediate **(6aV)** (1.0 g, 2.74 mM) and methyl iodide (1.17 g, 8.32 mM) in acetonitrile (20 ml) were refluxed for 2-3 h. The solvent and excess reagent were removed under reduced pressure to afford a yellow solid which on crystallization in chloroform-methanol yielded yellow solid of the desired product **(7aV)** (1.10 g, 78.93 %). m.p. 140-142 ^{o}C

Anal.:

TLC : R_f 0.39 (Methanol: 1 drop GAA)

UV (MeOH) : 250 nm

IR (KBr, cm^{-1}) : 3271, 1721, 1672, 1543, and 1007

PMR ($CDCl_3$): 9.53 (s, 1H, pyridinium-*H*), 9.19-9.16 (m, 2H, pyridinium-*H*, N*H*, *J=8.0*), 8.96-8.94 (d, 1H, pyridinium-*H*), 8.19-8.16 (t, 1H,

pyridinium-*H*), 7.57-7.32 (m, 9H, biphenyl-*H*), 4.47 (s, 3H, N-C*H*$_3$), 4.30-4.28 (t, 2H, O-C*H*$_2$, *J=4.0*), 3.72 (s, 2H, Ar-C*H*$_2$) and 3.72-3.65 (q, 2H, N-C*H*$_2$, *J=4.0*)

^{13}CMR (CDCl$_3$):170.95, 160.84, 146.41, 145.03, 143.01, 139.71, 139.57, 138.57, 138.66, 133.27, 132.75, 129.54, 128.57, 127.26, 126.44, 126.18, 62.24, 48.41, 40.29, 39.87, 39.10, 38.89 and 38.45

MS (m/z)   : 375.90 (M$^+$)

HPLC   : >98.9 %

4.1.67. 1-(1-Methylpyridinium-3-carboxamido)propan-2-yl 4-biphenylacetate iodide (7bV)

The title compound was prepared from ester intermediate **(6bV)** (1.0 g, 2.67 mM) and methyl iodide (1.12 g, 8.01 mM) following the method described for the synthesis of compound **(7aV)** to give yellow semisolid. This semisolid mass was triturated with hexane first and then with hexane-ethyl acetate mixture. The solvent was decanted to leave pure product as a yellow oil of the desired product **(7bV)** (0.9 g, 65.27 %).

Anal.:

TLC   : R$_f$ 0.40 (Methanol)

UV (MeOH)   : 252 nm

IR (KBr, cm^{-1}) : 3236, 1725, 1667, 1590 and 744

PMR (CDCl$_3$) : 9.46 (s, 1H, pyridinium-*H*), 8.79-8.73 (m, 2H, pyridinium-*H*, N*H*), 8.75-8.73 (d, 1H, CO-N*H*, *J=8.2*), 8.62-8.59 (d, 1H, pyridinium-*H*, *J=4*), 7.87-7.85 (m, 1H, pyridinium-*H*, *J=6.16*), 7.48-7.19 (m, 9H, biphenyl-*H*), 5.17-5.12 (m, 1H, CH-O, *J=4.0*), 4.30 (s, 3H, N-C*H*$_3$), 3.48-3.46 (t, 2H, N-C*H*$_2$, *J=6.4*), 1.99 (s, 2H, Ar-C*H*$_2$) and 1.24-1.23 (d, 3H, C-C*H*$_3$, *J=6.44*)

^{13}CMR   :171.93, 161.47, 145.98-126.80 (17C, Ar), 69.75, 49.23, 44.59, 41.26 and 17.97

MS (m/z)   : 389.2 (M$^+$)

HPLC   : >97.8 %

4.1.68. 2-(1-Methylpyridinium-3-carboxamido)butanyl 4-biphenylacetate iodide (7cV)

The title compound was prepared from ester intermediate **(6cV)** (1.0 g, 2.57 mM) and methyl iodide (1.08 g, 7.72 mM) following the method described for the synthesis of

compound **(7aV)** to yield yellow semisolid. This semisolid mass was triturated with hexane and then with hexane-ethyl acetate mixture. The solvent was decanted to leave pure product as a yellow oil of the desired product **(7cV)** (0.80 g, 58.58 %).

Anal.:

TLC : R_f 0.42 (Methanol)

UV (MeOH) : 252 nm

IR (KBr, cm^{-1}) : 3247, 3058, 1727, 1665, 1590 and 743

PMR (CDCl$_3$) : 9.54 (s, 1H, pyridinium-*H*), 8.79-8.76 (m, 2H, pyridinium-*H*, N*H*,), 8.32-8.30 (d, 1H, pyridinium-*H*, *J=8.0*), 7.86-7.82 (m, 1H, pyridinium-*H*, *J=8.0*), 7.49-7.19 (m, 9H, biphenyl-*H*), 4.33 (s, 3H, N-C*H*$_3$), 4.29-4.18 (m, 2H, -C*H*$_2$), 3.65 (s, 2H, Ar-C*H*$_2$), 1.97 (d, 2H, O-C*H*$_2$), 1.79-1.64 (m, 1H, N-C*H*, *J=7.04*) and 0.92-0.89 (t, 3H, -C*H*$_3$).

^{13}CMR : 171.87, 161.19, 145.89-126.76, 65-67, 52.03, 46.16, 41.01, 23.99 and 10.81

MS (m/z) : 403.2 (M$^+$)

HPLC : >97.5 %

4.1.69. 2-Methyl-2-(1-methylpyridinium-3-carboxamido)propanyl 4-biphenylacetate iodide (7dV)

The title compound was prepared from ester intermediate **(6dV)** (1.0 g, 2.74 mM) and methyl iodide (1.17 g, 8.32 mM) following the method described for the synthesis of compound **(7aV)** to give yellow semisolid. This semisolid mass was triturated with hexane first and then with hexane-ethyl acetate mixture. The solvent was decanted to leave pure product as a yellow oil of the desired product **(7dV)** (0.85 g, 62.25 %).

Anal.:

TLC : R_f 0.39 (Methanol)

UV (MeOH) : 252 nm

IR (KBr, cm^{-1}) : 3436, 1728, 1668, 1590, 743

PMR (CDCl$_3$) : 9.52 (s, 1H, pyridinium-*H*), 8.84-8.82 (d, 1H, pyridinium-*H*, *J=8.0*), 8.70-8.68 (d, 1H, pyridinium-*H*, *J=8.0*), 7.93 (bs, 1H, N*H*), 7.89-7.86 (m, 1H, pyridinium-*H*, *J=8.0*), 7.53-7.31(m, 9H, biphenyl-*H*), 4.41 (s, 3H, N-C*H*$_3$), 4.37 (s, 2H, O-C*H*$_2$), 3.74 (s, 2H, Ar-C*H*$_2$) and 1.52 (s, 6H, (C*H*$_3$)$_2$)

HPLC : >98.7 %

4.1.70. 3-(1-Methylpyridinium-3-carboxamido)propanyl 4-biphenylacetate iodide (7eV)

The title compound was prepared from ester intermediate **(6eV)** (0.50 g, 1.33 mM) and methyl iodide (0.56 g, 4.0 mM) following the method described for the synthesis of compound **(7aV)** to give yellow semisolid. This semisolid mass purified by column chromatography using neutral alumina as stationary phase and ethyl acetate as eluent followed by ethyl acetate: methanol (1:1) to give pure yellow oil of the desired product **(7eV)** (0.49 g, 71.07 %).

Anal.:

TLC $\quad\quad$: R_f 0.39 (Methanol)

UV (MeOH) $\quad$: 252 nm

IR (KBr, cm^{-1}): 3391, 2948, 1725, 1660, 1589 and 741

PMR (CDCl$_3$) : 9.93 (s, 1H, pyridinium-*H*), 8.98-8.96 (m, 2H, pyridinium-*H*, N*H*, *J=8.0*), 8.86-8.85 (d, 1H, pyridinium-*H*), 8.01-7.97 (m, 1H, pyridinium-*H*, *J=8.0*), 7.57-7.26 (m, 9H, biphenyl-*H*, 4.51 (s, 3H, N-C*H$_3$*), 4.23-4.20 (t, 2H, O-C*H$_2$*, *J=8.0*), 3.70 (s, 2H, Ar-C*H$_2$*), 3.58-3.53 (q, 2H, N-C*H$_2$*, *J=8.0*), 3.09 (bs, 1H, N*H*) and 2.08-2.05 (m, 2H, O-C-C*H$_2$*, *J=8.0*)

MS (m/z) $\quad$: 389.2 (M$^+$)

HPLC $\quad\quad$: >96.3 %

4.2. Hydrolyses studies

All the synthesized CDS were evaluated for their stability in buffers (*p*H 6.0 and 7.4), which simulate the *p*H conditions existing in the synovial fluid and blood. The enzymatic susceptibility towards serum esterases of all the CDS was evaluated *in vitro* in pooled human serum (90 %). HPLC analysis was performed using shimadzu prominence system (Kyoto, Japan) consisting of LC-20AT Pump, and SPD 20 A detector.

The chromatographic column used was phenomenex C-18, 250 mm length X 4.6 mm diameter with 0.5 µ particle size and Column temperature was maintained at 25-28 °C. Separation of analyte was performed under isocratic conditions at a flow-rate of 0.5-1.5 ml/min. The mobile phase consisted of phosphate buffer (PB, *p*H 5-5.5, 15 mM) acetonitrile. 20 µl of sample was loaded using syringe through rheodyne injector. The solutions and the buffers used in the study were prepared in distilled water. The buffers used were prepared according to the procedure as given in USP. All the chemicals used

were of analytical reagent grade. Human Plasma was obtained from SSG Hospital and Indu Blood Bank, Vadodara, India. The absorbance measurements were made on a UV-visible spectrophotometer (UV-1800, Shimadzu Corporation, Japan).

Solutions and buffers

1. Sodium hydroxide (0.2 M): Sodium hydroxide (8.0 g) was dissolved in distilled water and volume made up to 1000 ml with distilled water.

2. Potassium dihydrogen phosphate (0.2 M): Potassium dihydrogen phosphate (27.22 g) was dissolved in distilled water and diluted to 1000 ml in a standard volumetric flask.

3. Phosphate buffer *p*H 6.0: Potassium dihydrogen phosphate (0.2 M, 50 ml) and sodium hydroxide solution (0.2 M, 5.6 ml) were taken in volumetric flask (200 ml) and the final volume was made up to 200 ml with distilled water.

4. Phosphate buffer *p*H 7.4: Potassium dihydrogen phosphate (0.2 M, 50 ml) and sodium hydroxide solution (0.2 M, 39.1 ml) were taken in volumetric flask (200 ml) and the final volume was made up to 200 ml with distilled water.

5. Mobile phase: The mobile phase was prepared from potassium dihydrogen phosphate solution (15 mM) by dissolving 2.041 g into 1000 ml water. The resulting solution was filtered through Whatman filter paper (0.22 μ) and appropriate amount of acetonitrile was added and the final solution sonicated for 10 min before use.

4.2.1. Analytical method validation

The method was validated for linearity. Linearity of an analytical method is its ability within a definite range to obtain results directly proportional to the concentrations (quantities) of the analyte in the sample[5-6] Linearity in light absorption is examined to ensure that Beer's law operates over the range of interest.

For evaluation of the linearity of the HPLC method for the synthesized CDS, the standard solutions were prepared in the range of 1-100 μg/ml concentrations (n=3) and absorbance were recorded at respective λ max (nm). The method was said to be linear for estimation of CDS if its R^2 was near to 1. Least square regression method was used to determine the regression coefficient, r and the equation for the best fitting line.

4.2.2. General procedure for the preparation of calibration curve for estimating CDS in buffers and in human serum

A stock solution (1000 μg/ml) of CDS **(7aI-7gV)** was prepared in double distilled water and DMSO was used in small quantity if required followed by sonication for 5 min.

From this stock solution appropriate dilutions were prepared in double distilled water to give solutions of concentrations in the range of 1-200 μg/ml. Aliquots (0.1 ml) were withdrawn individually from these solutions, and transferred in to Eppendorf tube containing 0.9 ml of mobile phase. And from the above solution 20 μl of the sample was injected using 100 μl syringe and absorbance measured (mV) at the specified λ max (nm). Retention time of CDS was kept in between 3-6 min by adjusting phosphate buffer-acetonitrile ratio or controlling flow rate of mobile phase. Samples were analyzed in triplicate and calibration curve was plotted using concentration (μg) versus absrbance (mV) and the linearity was determined.

4.2.3. General procedure for the stability studies of CDS in phosphate buffer pH 6 and 7.4.

Phosphate buffer (pH 6 or 7.4) was equilibrated in a water bath at 37 °C. A stock solution was freshly prepared for each CDS by dissolving it in water and if required small amount of DMSO was used. 10 μl of the stock solution was added per milliliter of the buffer solution used in the study in each experiment. Aliquots of 100 μl were withdrawn at various time points and pipetted in to 400 μl portion of the mobile phase. The samples were centrifuged for 3 min at 4000 rpm and the supernatant was sampled to determine the rate of disappearance of the CDS using HPLC.

4.2.4. General procedure for the stability study of CDS in human serum

Human serum was incubated at 37±0.5 °C before use. A stock solution of CDS was freshly prepared by dissolving it in water and if required small amount of DMSO was used. In each experiment stock solution of CDS (100 μl) was added to serum (3ml) in the study. Aliquots of 100 μl were withdrawn at various time points and pipetted in to 400 μl portion of ice cold acetonitrile containing 5 % DMSO by volume. Samples were vortexed for 5 sec and centrifuged for 5 min at 4000 rpm and the supernatant was sampled to determine the half life of disappearance of CDS using HPLC. The first order equation ($t_{1/2}$ = 0.693/k) was used to calculate the half-lives.

4.3. Cytotoxicity study (MTT assay)

All the synthesized CDS were evaluated for their *in vitro* cytotoxicity on normal rat Liver cell line (BRL-3A) or mouse embryonic fibroblasts (NIH 3T3). These cell lines were procured from NCCS Pune and ACTRACT Mumbai. All the chemicals and media required for the study were purchased from Himedia Chemicals, Mumbai. Plates (96 well) and cultured flask were purchased from Tarson. All the compounds were perfectly dried

and UV treatment given before use. Stock solutions of all the derivatives were prepared in double distilled water and small amount of DMSO (20 μl) added if required with sonication for 3 min.

Reagents

1. 3-(4,5-Dimethythiazol-2-yl)-2,5-diphenyltetrazolium bromide (MTT) solution: Prepared by dissolving appropriate quantities to get final concentration of 0.5 mg/ml of serum-free Dulbecco's Modified Eagle Medium (DMEM) medium.

2. Solubilization solution: DMSO 150 μl per well

3. Phosphate Buffered Saline (PBS; pH 7.4): Sodium phosphate monobasic (NaH_2PO_4) (0.63 g) and sodium phosphate dibasic (Na_2HPO_4) (0.17 g) and sodium chloride (NaCl) (4.5 g) were dissolved in sterile double distilled water (500 ml). The pH was then adjusted to 7.4 with sodium hydroxide solution and the solution filtered through Whatman filter paper (0.22 μ) under aseptic conditions and stored in refrigerator.

4.3.1. General Procedure

Cells are plated in 96 well plates at a concentration of 1 x 10^4 cells/well. Twenty four hours after plating, cells were washed twice with serum-free medium (100 μl) and starved by incubating the cells in serum-free medium for an hour at 37 ^{o}C. After starvation, cells were treated with synthesized CDS or standard drugs (NSAIDs) of different concentrations for 24 hours. At the end of treatment, the medium from all the wells was discarded and MTT (0.5 mg/ml) 100 μl containing DMEM was added to each well. The cells were then incubated for 4 h at 37 ºC in the CO_2 incubator. The MTT containing medium was then discarded and the cells were washed with PBS (200 μl). The crystals were then dissolved by adding 100 μl of solubilization solution (DMSO) and mixed properly by pipeting up and down. Absorbance of the purple blue formazan dye was measured in microplate reader at 570 nm. The OD of each sample was then compared with the control OD and the graph was plotted.

4.4. Radiolabeling study

Silica gel coated fiber sheets (Gelman Sciences. Inc., Ann Arbor, MI) were used for performing the instant TLC (ITLC). A well type gamma ray spectrophotometer (Type GRS23C, Electronics Corporation of India ltd., Mumbai) was used for the gamma rays counting. The solutions were prepared in distilled water and all the chemicals and solvents used were of analytical grade. Sprague-Dawley rats (3 in each group) were used for the

studies. Carrageenan (1 % w/v in normal saline) was used for inducing inflammation. Imaging was performed using a Single Photon Emission Computerized Tomography (SPECT, LC 75-005, Diacam, Siemens, USA) gamma camera. Ketamine/diazepam in combination was used to induce anesthesia in animals. Radiolabeling study was performed at Institute of Nuclear Medicine and Allied Sciences (INMAS), New Delhi.

4.4.1. Chemicals and reagents

1. Sodium bicarbonate solution (1 %): Accurately weighed Sodium bicarbonate (1 g) was dissolved in sufficient quantity of water and volume was made up to 100 ml with water.

2. Stannous chloride solution (1 mg/ml.): Accurately weighed stannous chloride (100 mg) was dissolved in sufficient quantity of acetic acid (10 %) and volume was made up to 100 ml with acetic acid (10 %).

4. Acetic acid (10 %): Glacial acetic acid (11.4 ml) was dissolved in water and volume was made up to 100 ml with water.

5. Sodium chloride solution (0.9 %): Accurately weighed Sodium chloride (0.9 g) was dissolved in sufficient quantity of water and volume was made up to 100 ml with water.

6. Mobile Phase (PAW): Pyridine, acetic acid and water in 3:5:1.5 proportions was mixed.

7. Carrageenan (1 %): Carrageenan (10 mg) was dissolved in 1 ml of water.

4.4.2. Radiolabeling of compounds

The radiolabeling of the compounds with reduced ^{99m}Tc was carried out as per the direct labeling method.[15] ^{99m}Tc-NaTcO$_4$ (1.0 ml, 2 mCi/ml) was mixed well with stannous chloride solution (0.1 ml, 1 mg/ml, in acetic acid (10 %)). The pH was adjusted to 7.0 using sodium bicarbonate solution (0.5 M). To this mixture, solution of the compound (1.0 ml, 2 mg/ml) was added and the reaction mixture incubated for 15 minutes (37±1°C). The above experiment was repeated by varying the conditions one at a time i.e. using different moles of stannous chloride (50 μl-200 μl), changing the pH of the medium between 6 and 8 at various values and varying the incubation time period (15, 30 and 45 minutes) of the reaction mixture. The procedure was repeated exactly in the same manner for all of the CDS and the parent drugs.

4.4.3. Evaluation of the labeling efficiency

Ascending instant thin layer chromatography (ITLC) was performed using acetone (100 %) or saline (0.9 %) as the mobile phase. Radiolabeled complex (2-3 μl) was applied

at a point 1.0 cm away from one end of an ITLC-SG strip. The strip was developed in acetone or saline and the solvent front was allowed to rise upto 8 cm from the origin. The strip was cut one cm below the solvent front and the radioactivity in each segment was determined in the gamma ray counter. The free pertechnetate which moved with the solvent ($R_f = 0.9$) and the reduced/hydrolysed (R/H) technetium along with the labeled complex remaining at the point of application were determined. ITLC was also run in pyridine-acetic acid water (3: 5: 1.5 v/v) mobile phase to determine the amount of reduced/hydrolysed (R/H) ^{99m}Tc (radio-colloids). The R/H ^{99m}Tc remained at the point of application while both the free pertechnetate and the labeled complex moved away with the solvent front in this solvent system (PAW). The difference between the activity for the spots which moved along with the solvent front using either acetone or saline from that obtained in the PAW system (at the point of application) gave the net amount of ^{99m}Tc-labeled complex. This procedure was repeated for the radiolabeling of all the CDS and the parent NSAIDs and for all the experiments conducted for optimization of labeling parameters like *p*H, incubation time and quantity of the reducing agent used.

4.4.4. *In vitro* stability study of ^{99m}Tc- labeled complex in saline and human serum

The *in vitro* stability study[15] of radiolabeled complex was determined in sodium chloride (0.9 %) and in human serum separately by ascending thin layer chromatography. The ^{99m}Tc-labeled compound solution (0.1 ml) prepared in saline (0.9 %) as described above was mixed separately with human serum (1.9 ml) or normal saline (1.9 ml) and incubated (37 ± 1 °C). ITLC was performed at different time intervals (0, 0.25, 0.5, 1.0, 2.0, 4.0 and 24 hours) as described above, in acetone to assess the stability of the complex. Any decrease in percentage of ^{99m}Tc-labeled complex was considered as its degree of degradation.

4.4.5. Gamma imaging studies

IA residence time of synthesized CDS and parent drugs were studied in normal and inflammatory conditions. The parent drug used for the study was 6-MNA **(5IV)**. Animals were divided into three groups **(A-C)** as follow:

   Group A-Consisted of animals which were administered with 6-MNA by IA route.

   Group B-Consisted of normal animals (without inducing inflammation) which
         were administered with individual CDS by IA route.

   Group C-Consisted of animals (in which inflammation was induced) which were
         administered with individual CDS by IA route.

For group **C**, inflammation was induced 3 h prior to IA administration of parent drug or CDS. Three hour after injection the animals were anaesthetized, fixed on a board using the adhesive tapes and gamma imaging photographs were taken 1, 2, 6 and 24 h hour after injecting the complex (IA). Radioactivity counts were measured for region of interest (ROI) as well as for whole body and percent activities remaining after a particular time interval were calculated. The above described procedure was followed for studying the biodistribution of the complexes of the remaining CDS.

References

1. Sharma M.C., Sahu N.K., Kohli D. V., Chaturvedi S.C. and Sharma S., Synthesis characterization and biological activities of some 1-(nicotinylamino)-2-substituted azitidine-4-ones as potential anti-bacterial agents. *Digest J. of nanomaterials and biostructures* **2009**, 4, 361-67

2. Phelan M.J. and Bodor N., Improved Delivery through Biological Membranes. XXXVII. Synthesis and Stability of Novel Redox Derivatives of Naproxen and Indomethacin. *Pharm. Res.* **1989**, 6, 667-76

3. Harrison I.T., Lewis B., Nelson P., Rooks W., Roszkowski A., Tomolonis A. and Fried J.H.*,* Non-steroidal anti-inflammatory Agents. 6- Substituted 2-naphthylacetic acids. *J. Med. Chem.,***1970**, 13, 203

4. Schwenk E. and Papa D., *J. Org. Chem.*, **1946**, 11, 798

5. Hubert P.H., Chiap P., Crommen J., Boulanger B., Chapuzet E., Mercier N., Bervoas M.S., Chevalier P., Grandjean D., Lagorce P., Lallier M., Laparra M.C., Laurentie M. and Nivet J.C., Validation of the quantitative analytical procedures. Harmonization of the steps. STP *Pharma. practice* **2003**, 13, 101-38

6. Hubert P.H., Nguyen-Huu J.J., Boulanger B., Chapuzet E., Cohen N., Compagnon P.A., Dewé W., Feinberg M., Laurentie M., Mercier N., Muzard G., Valat L. and Rozet E., Harmonization of strategies for the validation of quantitative analytical procedures. A SFSTP proposal-part III. *J. Pharm. Biomed. Anal.* **2007**, 45, 82-96

7. Guidance for industry: Bioanalytical Method Validation, U.S. Department of Health and Human Services, Food and Drug Administration, Center for Drug Evaluation and Research (CDER), Center for Biologics Evaluation and Research (CBER), May **2001**

8. Patrick J.S. Martins Physical Pharmacy and Pharmaceutical Sciences. Lippincott Williams and wilkins, fifth ed., Philadelphia USA. **2006**, 397-50

9. Prat M., Fernández D., Buil M.A., Crespo M.I., Casals G., Ferrer M., Tort L., Castro J., Monleón J.M., Gavaldà A., Miralpeix M., Ramos I., Doménech T., Vilella D., Antón F., Huerta J.M., Espinosa S., López M., Sentellas S., González M., Albertí J., Segarra V., Cárdenas A., Beleta J. and Ryder H., Discovery of novel quaternary ammonium derivatives of (3R)-quinuclidinol esters as potent and long-acting muscarinic antagonists with potential for minimal systemic exposure after inhaled administration. *J. Med. Chem.* **2009**, 52, 5076-92.

10. Wang D. and Brömme D., Drug delivery strategies for cathepsin nhibitors in joint diseases. *Expert Opin. Drug Deliv.* **2005**, 2,1015-28

11. Hussain S.M., Hess K.L., Gearhart J.M., Geiss K.T. and Schlager J.J., In vitro toxicity of nanoparticles in BRL 3A rat liver cells. *Toxicol. In Vitro.* **2005**, 19, 975-83.

12. Saha G. B., Methods of Radiolabeling., In: Physics and Radiobiology of Nuclear Medicine, Saha G. B., Ed., 5th edition Springer-Verlag, New York, **1993**, 100-106

13. Chauhan U.P.S., Mishra P., and Chander J., "99mTcdiethylmonoiodo-IDA: a radiopharmaceutical for hepatobiliary scintigraphy," *Appl. Radiat. Isot.*, **1993**, 44, 843-48

14. Yadav M.R., Pawar V. A., Marvaniya S.M., Halen P.K., Giridhar R. and Mishra A.K., Site specific chemical delivery of NSAIDs to inflamed joints: synthesis, biological activity and gamma-imaging studies of quaternary ammonium salts of tropinol esters of some NSAIDs or their active metabolites. *Bioorg. Med. Chem.* **2008**, 16, 9443-49.

15. Saha G. B., Methods of Radiolabeling., In: Physics and Radiobiology of Nuclear Medicine, Saha G. B., Ed., 5th edition Springer-Verlag, New York, **1993**, 100-106

16. Lovesey A.C., Ross W.C.J., Potential Coenzyme Inhibitors. Part-II, Reduction of 4-Methylnicotinamide Derivatives by Sodium Dithionite and Sodium borohydride. *J. Chem. Soc. (B),* **1969**, 193

17. Perioli L, Ambrogi V, Bernardini C, Grandolini G, Ricci M, Giovagnoli S, Rossi C., Potential prodrugs of non-steroidal anti-inflammatory agents for targeted drug delivery to the CNS. *Eur. J. Med. Chem.* **2004**, 39, 715-27.

Section-II

PERCUTANEOUS DRUG DELIVERY

Introduction

Non-steroidal anti-inflammatory drug (NSAIDs) is a class of drugs used for the treatment of rheumatoid arthritis (RA) and osteoarthritis (OA). Oral therapy of these agents is very effective, but their clinical use is often limited due to potential adverse effects.[1] The well known side effects of NSAIDs such as ulceration and irritation of gastrointestinal (GI) mucosa have accelerated the development of alternative delivery systems such as topical formulations that allow local absorption at the target tissue without systemic side effects. But to deliver the drug through skin is not an easy task due to the protective function of skin which poses physicochemical limitations to the permeant crossing the barrier. Special physicochemical requirements of the drugs for percutaneous delivery have limited the number of commercially available products based on topical drug delivery.

Various strategies have been developed over the years to improve percutaneous delivery of NSAIDs, and chemical modification of the drugs is one of them.[2] The present work is related to the development of novel percutaneous chemical drug delivery systems of some NSAIDs for the treatment of rheumatic diseases, So, it is in order to explain the principles of percutaneous delivery system in brief.

1. Percutaneous drug delivery systems

Percutaneous drug delivery means drug delivery through skin. It is a convenient route of drug administration which is acceptable by the patients. Ideally, drugs which need low doses or have high potency can be administered through the skin. Percutaneous drug delivery is mainly classified into two types:

1.1 Topical drug delivery

1.2 Transdermal drug delivery

1.1 Topical drug delivery

Topical delivery can be defined as application of a drug or drug containing formulation for the treatment of dermal, local soft tissue, and joint disorders. Topical approach is useful when the disease is associated with the skin or joint and for that the drug need to permeate into the skin and not to penetrate into blood circulation.[3]

1.2 Transdermal drug delivery

Transdermal drug delivery is the delivery of drugs through the skin to achieve a systemic effect. Objective of transdermal delivery is to avoid first pass metabolism and avoid side effects when administered by oral route.

1.3 Benefits of percutaneous drug delivery[4]

Percutaneous drug delivery possesses many advantages such as it avoids first pass metabolism and other variables such as low pH of the stomach, gastric emptying time etc. It provides sustained and controlled delivery of the drug, reduces systemic toxicity of the drug due to direct access to the target site, provides large surface area and a convenient route of administration of the drug. It is painless administration and has improved patient acceptance.

1.4 Limitations of percutaneous drug delivery[5]

Percutaneous delivery of drugs suffers from certain drawbacks such as the drug should have molecular weight less than 500 Da, its partition coefficient should be in between 1-3, may lead to pre-systemic metabolism of the drug due to presence of enzymes in the skin and may lead to side effects like skin irritation and sensitization reactions. Further, skin acts as an efficient barrier against absorption of large number of drugs.

2. Percutaneous drug delivery and skin

The major problem associated with percutaneous drug delivery is the excellent barrier property of the skin. In order to utilize successfully the phenomenon of percutaneous absorption it is necessary to understand the structure of the skin and its functions.

2.1 Structure of the skin

The skin is the largest organ in the body, comprising about 15% of the body weight. The total skin surface of an adult ranges from 12 to 20 square feet. In terms of chemical composition, the skin has about 70 % water, 25 % protein and 2 % lipids. The remainder includes trace minerals, nucleic acids, glycosoaminoglycans, proteoglycans and numerous other chemicals. The skin consists of three main layers: epidermis, dermis and subcutaneous tissue.[6] Cross section of the skin showing all the layers are shown in **Fig. 1.1.**

2.1.1 Epidermis

The epidermis is the topmost layer of the skin. Epidermis is classified in to two types, non-viable epidermis (stratum corneum) and viable epidermis (aqueous nature). The stratum corneum (SC) consists of multilayers of dead cells, hardened proteins (keratins), and lipids. Cells are flattened, compacted, dehydrated and keratinized forming a protective crust. Dead cells from stratum corneum continuously slough off and are replaced by new ones coming from below.[7]

The epidermis consists of three types of cells, keratinocytes, melanocytes and Langerhans cells. Keratinocytes, the cells that make the protein keratin, are the predominant type of cells in the epidermis. The skin completely renews itself every 3-5 weeks. Another significant group of cells in the epidermis is melanocytes, the cells producing melanin. The aqueous nature of the viable epidermis becomes the main barrier to percutaneous absorption of highly lipophilic drugs that have poor partitioning affinity towards an aqueous environment.[16]
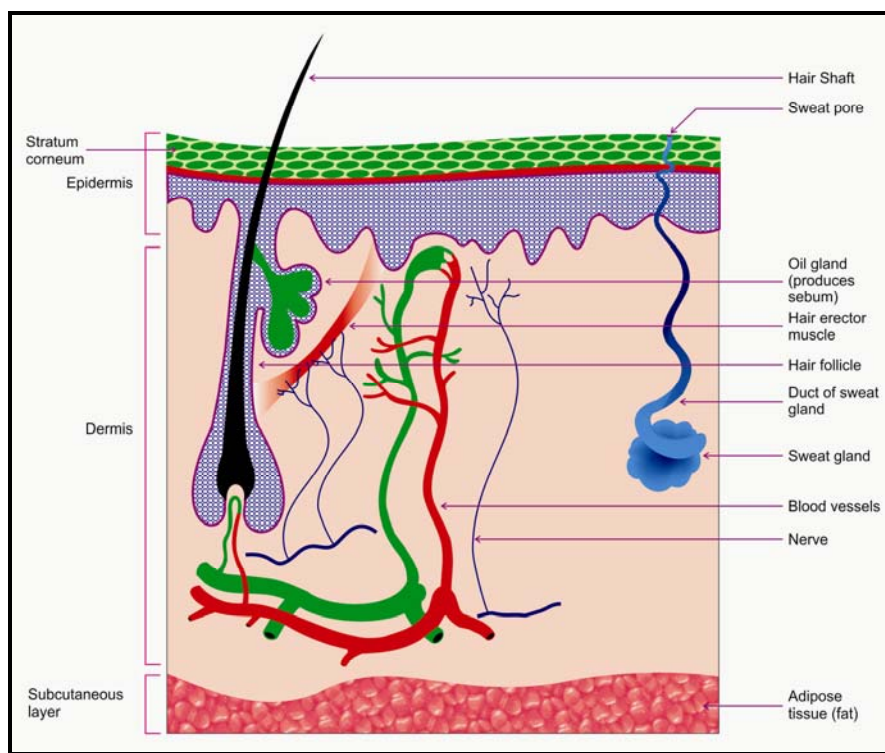
Fig.1.1: Cross section of human Skin

2.1.2 Dermis

The dermis is the middle layer of the skin located between the epidermis and subcutaneous tissue. It is the thickest layer of the skin (0.2-0.3 cm) and comprises a tight, sturdy mesh of collagen and embedded in amorphous colloidal ground substances such as elastin fibers. The key cells in the dermis are fibroblasts, which synthesize collagen, elastin and other structural molecules. The proper functioning of fibroblasts is highly important for overall skin health.[8]

The dermis also contains blood vessels, sensory nerves and lymph nodes. These are important for oxygenating and nourishing the skin and protecting it from invading microorganisms etc. It also contains segments of sebaceous glands, sweat glands, hair

follicles as well as a relatively small number of nerve and muscle cells. Sebacious glands, located around hair follicles, is of particular importance for skin health as they produce sebum, an oily protective substance that lubricates and waterproofs the skin and hair. The dermis is the layer responsible for the skin's structural integrity, elasticity and resilience.[9]

2.1.3 Subcutaneous tissue

Subcutaneous (hypodermis) tissue is the innermost layer of the skin located under the dermis and consists mainly of fat. The predominant type of cells in the subcutaneous tissue is adipocytes or fat cells.[10] Subcutaneous fat acts as a shock absorber and heat insulator, protecting underlying tissues from cold and mechanical trauma and provides cushioning to epidermis and dermis.

2.1.4 Skin appendages

There are various types of appendages on skin surface that include hair follicles with sebaceous gland, eccrine and apocrine sweat glands. There are about 40-70 hair follicles and 200-250 sweat ducts/cm^2 of the skin. The eccrine sweat glands (2-5 million) produce sweat (*p*H 4-6.8) and excrete several drugs, proteins and also control heat.

2.2 Functions of the skin[11-12]: Skin performs many functions as given below:

- It causes protection from water loss, injury, chemicals and microorganisms.
- It is responsible for excretion of urea and uric acid.
- It regulates body temperature,
- Skin helps in vitamin-D synthesis for body, has large blood reservoir and performs immunity functions against various allergens.

3. Drug permeation routes through skin

The process of percutaneous absorption is defined as the movement of substance(s) from the skin surface to the target tissue or general circulation. It involves penetration through the stratum corneum, diffusion through layers of skin, uptake by capillary network and finally transportation to the target tissues to achieve therapeutic action.

As shown in **Fig. 1.2.** there are four routes by which drugs can permeate the skin, which includes:[13-15]

3.1. Transappendageal (follicular) route: permeation through hair follicles

3.2. Transcellular (intracellular) route: permeation through cells

3.3. Paracellular route (intercellular route): It is the major route for the drug permeation and involves permeation of drug in between cells.

3.4. Appendageal route (eccrine): permeation through sweat gland, eccrine gland.
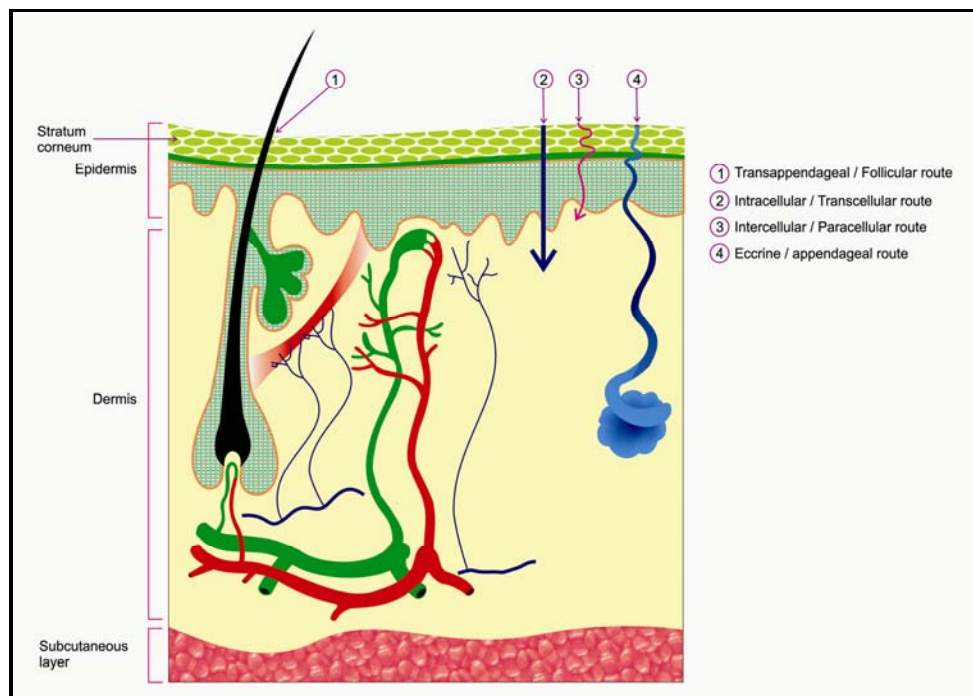
Fig. 1.2: Possible drug permeation routes across human skin

4. Pharmacokinetics of drugs through skin

The phenomenon of permeation by diffusion of the permeant into and through the skin and finally into the blood stream is known as percutaneous absorption.[16] Before a topically applied drug can act either locally or systemically, it must permeate the skin. The process of percutaneous absorption is complicated and involves a large number of processes occurring either consequently or simultaneously.[17] However, the current knowledge of percutaneous absorption involves mainly six steps which must occur before a drug can be absorbed from a topically applied formulation and ultimately appear in the cutaneous circulation or deeper tissues:[18]

1) The drug transports (dissolution) within the delivery system to vehicle-skin surface interface.

2) Partitioning of the drug takes place from the vehicle in to the SC.

3) There occurs diffusion of the drug through the SC.

4) Partitioning of the drug from the lipophilic SC into the aqueous viable epidermis takes place.

5) Diffusion of the drug takes place through the viable epidermis and upper dermis.

6) Ultimately there is drug uptake by cutaneous circulation.

Passive diffusion is the primary process for the drug permeability through skin. Therefore the general phenomenon of skin permeation can be described by the Fick's law of diffusion, which offers the basis for the development of the equation for drug absorption.[16, 19-20] *In vitro* skin permeation studies are often carried out by using diffusion models where a membrane is placed between two compartments; the drug formulation is placed in one compartment while the other compartment has a receptor solution providing sink conditions. After sufficient time, steady state diffusion across the membrane prevails and Fick's law of diffusion is expressed as follow:

$$J_{ss} = DCo/h \text{---------------- (1)}$$

Where J_{ss} is the steady state rate of the skin permeation; D is diffusion coefficient of permeation within the membrane; Co is the concentration of the permeation in the first layer of the membrane on the donor side and h is effective thickness of membrane.

The concentration Co within the membrane is difficult to measure, but the Co is related to C, the concentration of permeant in the donor phase that baths the membrane, in accordance with the partition coefficient P. Thus, the steady state transport of a drug through a membrane per unit area can be expressed as an expanded form of Fick's law i.e.:

$$J_{ss} = DPC/h \text{-------------- (2)}$$

Where Jss = Steady state rate of skin permeation (rate of movement of permeant
across the skin)

D= Diffusion coefficient of the permeant within the membrane

C= dissolved concentration of drug in vehicle (effective, donor side)

P= partition coefficient of permeant between the membrane and the vehicle

h= effective thickness of the membrane

. As complications and uncertainties remains upon exact determination of the vehicle/membrane partition coefficient and thickness of the membrane, it is useful to determine the permeability coefficient Kp according to equation given below:

$$Kp = DP/h \text{--------------- (3)}$$

This can be substituted into equation (2) to give equation (4)

$$J_{ss} = KpC \text{---------------- (4)}$$

Where the rate of movement of the permeant (J_{ss}) across the skin is directly proportional to the concentration gradient. The permeability coefficient (**Kp)** obtained experimentally, provides a means of expressing absorption measurements for comparing different concentrations.

Extrapolation of the pseudo steady state portion of the graph is given by equation (2) to the intercept on the axis providing a measure of lag time (t_L). The lag time is the time required for a permeant to establish a uniform concentration gradient with the membrane of thickness **h** having diffusion coefficient D as shown in equation (5)

$$t_L = h^2/6D \text{--------------- (5)}$$

It should be noted that the Fick's law of diffusion is applied only to a simple, inert membrane and thus, it may be an over simplification of complex permeation processes actually taking place in SC as it excludes binding and metabolism of drugs in the skin.

5. Physicochemical properties of the drug affecting skin permeation

5.1 Partition coefficient (*P*)

Partition coefficient is defined as the ratio of the concentrations of the compound in organic phase (hydrophobic phase) and aqueous phase (hydrophilic phase). It is a useful parameter for determining the drug permeation into skin. Normally for determining partition coefficient 1-octanol is chosen as hydrophobic phase and water as hydrophilic phase.[21] The logarithm of the ratio of the concentrations of the solute in these two phases is called log*P*. For effective permeation through the skin the drug should have partition coefficient (log*P*) in between 1-3.

5.2 Diffusion coefficient (*D*)

Fick's first law of diffusion states that flux of the solute goes from the higher concentration to lower concentration. Magnitude of the flux is directly proportional to the concentration gradient. Fick's first law relates with the assumption of flux of the solute in steady state.[22]

5.3 Balanced hydrophilic-lipophilic characteristics

Very lipophilic compounds may be retained in the SC which results in limited permeation into the aqueous viable epidermis. So ideally a compound must possess balanced hydrophilic and lipophilic properties.[23]

5.4 Drug concentration

Increase in concentration of the drug in vehicle increases its percutaneous absorption. At a constant drug concentration, the amount absorbed is directly proportional to the surface area. However this is not applicable to all drugs; few drugs produce significant decrease in absorption rates with increase in concentration.[24,28]

5.5 Interaction between skin, drug and vehicle

Rate of drug permeation through skin is influenced by interactions between drug-skin, drug-vehicle and vehicle-skin. A drug-skin interaction may result in increase or decrease in penetration rate of the drug, Vehicle-skin interaction may change hydration state of the SC and may change skin permeability. Drug-vehicle interaction results in slow diffusion of the drug from the vehicle on to the skin surface and decrease in skin permeability.[25,28]

5.6 Solubility and molecular characteristics of drug

Aqueous solubility of a drug strongly influences the rate of transport across the absorption site. Increase in solubility increases the skin permeation rates but there should be a balance between hydrophilic and lipophilic properties of molecules. It has been proved that skin permeation rate increases in presence of fatty acids and amines.[26]

5.7 Degree of ionization

Lipophilic nature of biological membranes allows unionized molecules to permeate easily. Ionized species were 10^4 times less permeable than unionized species. However it has been suggested that ionized species can permeate the lipid membranes through pores (like GIT). Various *in vitro* studies have shown that both ionized and unionized species of a drug can permeate a lipid membrane.[27]

5.8 Other factors

Other parameters which affect permeability through skin include effect of vehicle/solvent, degree of skin hydration, skin temperature, skin age and regional sites, species variation, pathological injuries to the skin, cutaneous drug metabolism, polymorphism, viscosity, surface tension, volatility of solvent, particle size etc. All these parameters affect skin permeation. Further, compounds with lower melting points have better skin permeation.[28]

6. Percutaneous drug delivery of NSAIDs

Various guidelines for percutaneous NSAIDs were developed through a regimented process of systematic review of the literature and are evidence based. **Table 1.1** enlists current OA guidelines. These guidelines reflect the expertise of US, European and international physicians and researchers from a variety of medical disciplines.[29] All guidelines recommend use of topical NSAIDS except AHA scientific statement. The AHA scientific statement is focused more narrowly on minimizing cardiovascular risks and therefore differs from these guidelines in recommending paracetamol or NSAIDs.[29]

Table 1.1: Guideline with recommendations for topical NSAIDs [29]

No	Guideline	Recommendation
1	AGS	All patients with other localized non-neuropathic persistent pain may be candidates for topical NSAIDs
2	AAOS	Patients with symptomatic OA of the knee, history of ulcer, GI bleeding receive one of the following for pain 1. Acetaminophen (<4 g/day), 2. Topical NSAIDs, 3. NSAIDs plus gastroprotective agent, Cycloxygenase-2 inhibitors
3	AHA	None
4	OARSI	Topical NSAIDs and capsaicin can be effective and alternatives to oral analgesics/NSAIDs in knee OA
5	NICE	Consider topical NSAIDs for pain relief in addition to core treatment
6	EULAR	Local treatment is preferred over systemic treatments for mild-to-moderate pain and when only few joints are affected

AAOS: *American academy of orthropaedic surgeons;* **AGS**: *American geriatrics society;* **AHA**: *American heart association;* **EULAR**: *European league against rheumatism;* **NICE**: *National institute for health and clinical excellence;* **OARSI**: *Osteoarthritis research society international.*

The OARSI, EULAR and AGS guidelines recommend that physicians initial pharmacologic treatment with paracetamol and topical NSAIDs are appropriate candidates for second line therapy in patients who do not tolerate or respond to paracetamol. EULAR recommends that topical NSAIDs are safe and effective.

7. Strategies to improve percutaneous drug delivery

NSAIDs are widely used for the treatment of rheumatic diseases and related painful conditions but bioavailability of topically applied NSAIDs is only 1-2 %. To improve the percutaneous delivery of NSAIDs, various strategies have emerged over recent years and these can be categorized as shown in **Fig**.**1.3**.[30] Formulation and chemical

modifications of the drugs are the two major approaches which are useful in targeting the drugs to cross the skin barrier function.

7.1 Formulation approach

Conventional formulation approach includes various types of formulations used for the topical drug delivery. Most commonly they incorporate the chemical permeation enhancers such as menthol, ethanol, isopropyl alcohol, limonene etc. which increase the permeability of drugs through skin but simultaneously increase skin irritation also. While newer formulations like liposomes, niosomes, ethosomes, transferosomes are also gaining importance, but they are much more expensive and not suitable for all the drugs.
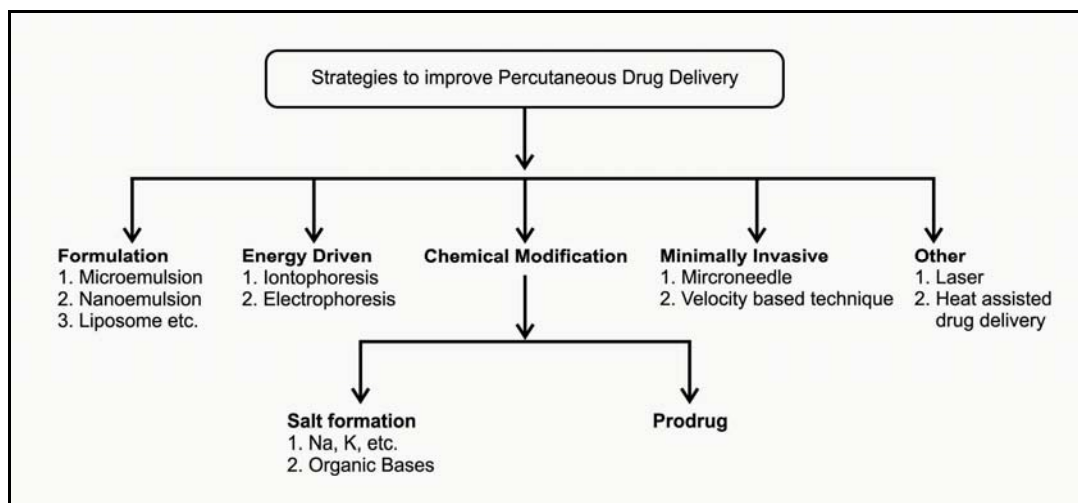
Fig. 1.3: Strategies for improving skin permeation of drugs

7.1.1 Microemulsions

A transdermal preparation containing ketoprofen was developed by Yun-Seok Rhee *et al.*[31] using o/w microemulsion system. The optimum formulation of the microemulsion consisted of 3% ketoprofen, 6 % oleic acid, 30 % Labrasol/ Cremophor (1:1) and water. Various terpenes (5 %) were added to the microemulsion and their effect on the skin permeation of ketoprofen from the microemulsion was evaluated. Limonene resulted 3-fold increase in enhancing activity over the control.

7.1.2 Nanoemulsions

Various o/w nanoemulsions of aceclofenac were prepared by Shakeel *et al.* [32] by the spontaneous emulsification method. A significant increase in permeability parameters

such as steady-state flux (J_{ss}) and permeability coefficient (Kp), were observed in optimized nanoemulsion formulation.

7.1.3 Liposomes

Liposomal formulation of naproxen was prepared for percutaneous drug delivery using different lipids such as stratum corneum lipids (SCL) and phosphatidylcholine/cholesterol (PC/CHOL). *In vitro* diffusion was studied by Franz diffusion cell on liposome dispersions viscosized by carbomer. The *in vitro* study showed a lower naproxen flux for stratum corneum lipids with respect to PC/CHOL liposomes. So, it is concluded that PC/CHOL liposome promoted naproxen permeation through the skin.[33]

2.2. Salt formation approach

For the percutaneous delivery of piroxicam (**1**), various ethanolamine salts (PX-EAs, **1a-1c**) were prepared to improve physicochemical properties for transdermal application. Piroxicam monoethanolamine salt (**1a**) and piroxicam diethanolamine salts (**1b**) had higher solubility than piroxicam in most of the vehicles tested and a higher permeation rate across the skin.[34]

The preparation of mefenamic acid alkanolamine salts (**2a-2d**) (monoethanolamine, diethanolamine, triethanolamine and propanolamine) was attempted to increase the transdermal flux of mefenamic acid.[35] A lipophilic enhancer system consisting of isopropyl myristate (IPM) and ethanol (9:1) produced a marked enhancement of mefenamic flux from the alkanolamine complexes through hairless rat skin membrane.

(1a-1c)   **(2a-2d)**
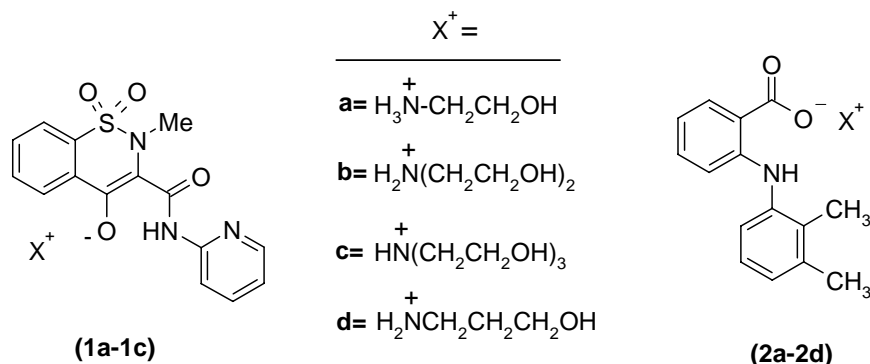
Among the alkanolamines examined, the propanolamine complex had the greatest enhancing effect on the permeation of mefenamic acid. So, the salt formation results in increased permeability as salts are more soluble in aqueous system than the drug alone.

2.3 Prodrug approach

K. B. Sloan *et al.* have synthesized *N,N*-dialkylhydroxylamine derivatives of indomethacin (**3a-3b**) to improve the delivery of indomethacin through mouse skin as compared to indomethacin by a factor of two[37] which was found to be more effective than indomethacin in inhibiting thermal inflammation (two to three times) in animal models, but as effective as indomethacin in inhibiting UV radiation erythema in human volunteers. A series of acyloxyalkyl esters of ketoprofen (**4**) and naproxen (**5**) were synthesized by Rautio *et al.*[36] and investigated as topical prodrugs with the aim of improving the dermal delivery of these drugs.
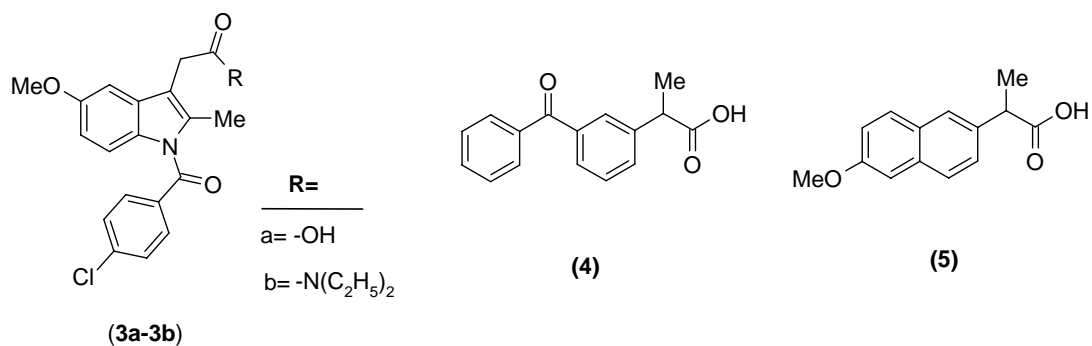
All acyloxyalkyl ester prodrugs (**6a-6h, 7a-7h**) were found to be much more lipophilic than their parent molecules, proved to be highly stable in aqueous solutions and hydrolyzed readily to the parent drugs both in human serum and human skin homogenate. However, the fluxes through excised human skin *in vitro* were still low, most probably due to poor aqueous solubility of the prodrugs and to high partition coefficients that were above the optimal range for skin permeation. Only the acetyloxyethyl ester prodrug of naproxen (**7e**), which was the most hydrophilic member of the series, exhibited a slight enhancement of *in vitro* skin permeability compared to naproxen (**5**) itself.

(6)   **(7)**
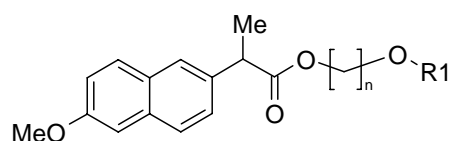
	n	R1			n	R1
(6a)	2	-H		**(7a)**	2	-H
(6b)	3	-H		**(7b)**	3	-H
(6c)	4	-H		**(7c)**	4	-H
(6d)	1	-COCH$_3$		**(7d)**	1	-COCH$_3$
(6e)	2	·COCH$_3$		**(7e)**	2	-COCH$_3$
(6f)	3	·COCH$_3$		**(7f)**	3	-COCH$_3$
(6g)	4	-COCH$_3$		**(7g)**	4	-COCH$_3$
(6h)	1	-COC(CH$_3$)$_3$		**(7h)**	1	-COC(CH$_3$)$_3$

Further, novel morpholinyl **(9a)** and piperazinylalkyl **(8, 9b** and **10a-10b)** esters of naproxen (**5**) were synthesized and evaluated *in vitro* for their properties as bioreversible topically administered dermal prodrugs **(5)** by Rautio *et. al.*[38]

Among the prodrugs, two piperazinyl derivatives (**9b**) and (**10b**) resulted in 4 and 9-fold enhancement of permeation compared to naproxen at *p*H 7.4. Further, novel polyoxyethylene esters of various NSAIDs were synthesized and evaluated as potential dermal prodrugs by Bonnia *et al.*[39]
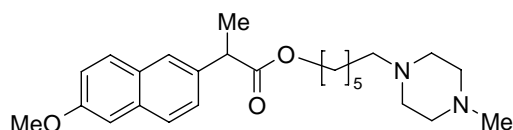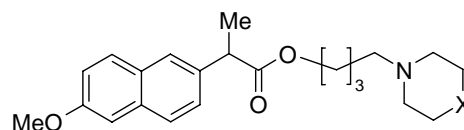
(8)   **(9a)** X= O
                                        (9b) X= NCH$_3$
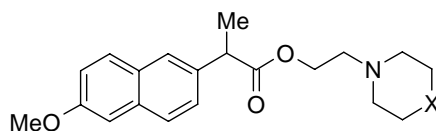
(10a) X= NH
(10b) X= NCH$_3$

Six 1-alkylazacycloalkan-2-one esters of ketoprofen (**14a-14c** and **15a-15c**) were synthesized and evaluated as potential dermal prodrugs of ketoprofen. Esters (**14a-14c** and **15a-15c**) showed increased lipophilicity compared with the parent drug ketoprofen (**4**), and good stability in phosphate buffer (*p*H 7.4), and were readily hydrolyzed by porcine esterases.

n=
(14a) = 1
(14b) = 2
(14c) = 3

n=
(15a) = 1
(15b) = 2
(15c) = 3
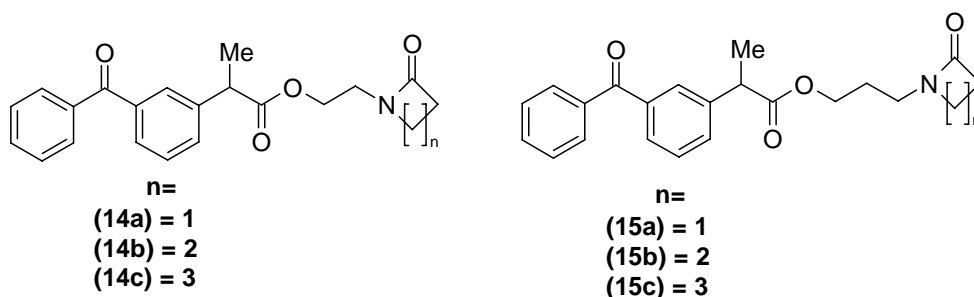
Results from *in vitro* percutaneous absorption studies showed that, amongst all of the synthesized esters, only esters (**14a**) and (**15b**) showed higher cumulative amount of drug penetration through the skin, compared with that obtained after topical application of ketoprofen (**4**). *In vivo* results showed an interesting delayed and sustained activity of ester (**15b**), compared to the parent drug.[40]

From the literature survey it is concluded that dermal administration currently holds a high level of interest in pharmaceutical research. Literature also suggests that chemical modification i.e. salt formation and prodrug approach has big impact on permeability of NSAIDs as compared to other strategies to deliver NSAIDs by topical route.

References

1. Jelena D., Bozena M. and Kathryn E. U., Amphiphilic star like macromolecules as novel carriers for topical delivery of non-steroidal anti-inflammatory drugs. *AAPS Pharm. Sci.,* **2003**, 5, 1

2. Swarbrick J., Lee G., Brom J., Drug permeation through human skin. *J. Pharm. Sci.,* **1984**, 73, 1352-55

3. Marc B. B., Dermal and transdermal drug delivery systems. *Drug Deliv.* **2006**, 13, 175-187

4. Kim B.S., Won M., Lee K.M. and Kim C.S., *in vitro* Permeation studies of nanoemulsions containing ketoprofen as a model drug. *Drug. Deliv.,* **2008**, 15, 465-69

5. Rautio J., Synthesis and *in vitro* evaluation of topical prodrugs of some NSAIDs Ph.D. Thesis, Synthesis, University of kuopio, **2000**, P-16

6. Breathnach A.S. Aspects of epidermal ultrastructure. *J. Invest. Dermatol.*, **1975**, 65, 2-15

7. Odland G.F. Structure of the skin. In Goldsmith LA Ed. *Physiology, Biochemistry, and Molecular Biology of the Skin*, **1991**, 3-62

8. Lavker R.M. and Matoltsy A.G., Substructure of keratohyalin granules of the epidermis as revealed by high resolution electron microscopy. *J.Ultrastruct. Res.,* **1971**, 35, 575-81

9. Lynley A.M. and Dale B.A., The characterisation of human epidermal filaggrin, a histidine rich keratin filament-aggregating protein. *Biochim. Biophys. Acta.* **1983**, 744, 28-35

10. Rice R.H. and Green H., The cornified envelope of terminally differentiated human epidermal keratinocytes consists of cross-linked protein. *Cell.,* **1977**, 11, 417-22

11. Buxman M.M., Wuepper K.D., Cellular localization of epidermal trans-glutaminase: a histochemical and immunochemical study. *J. Histochem. Cytochem.,* **1978**, 26, 340-48

12. Handgraft J. Structure activity relationships and percutaneous absorption. *J. Control. Rel.,* **1991**, 15, 221-26

13. Cullander C., What are the pathways of iontophoretic current flow through mammalian skin? *Adv. Drug Del. Rev.,***1992**, 9, 119-35

14. Barry B. W., Lipid protein partitioning theory of skin penetration enhancement. *J. control. Rel.,* **1991**, 15, 237-48.

15. Guy R.H. and Handgraft J., Mathematical models of percutaneous absorption: In percutaneous absorption mechanism-methodology drug delivery. Marcel Dekker Inc, New York. **1989**, 13-26.

16. Scheuplein R.J. and Blank I.H., Permeability of the skin. *Physiol. Rev.,* **1971**, 51, 702-47

17. Guy R.H., Hadgraft J. and Bucks D.A., Transdermal drug delivery and cutaneous metabolism. *Xenobiotica.,* **1987**, 17, 325-43.

18. Guy. R.H. Transdermal drug delivery: The ground rules are emerging. *Pharm. Int.,* **1985**, 5, 112-116.

19. Idron B., Percutaneous absorption. *J. Pharm. Sci.,* **1975**, 64, 901-924

20. Barry B.W., Mode of action o permeation enhancers in human skin. *J. Control. Rel.* **1987**, 6, 85-97

21. Kerr D. Roberts W., 7-Alkylcarbonyloxymethyl prodrugs of theophylline. *Int. J. Pharm.,* **1998**, 167, 37-48

22. Guy R.H. and Handgraft J., Percutaneous penetration enhancement: Physicochemical considerations and implications for prodrug design in prodrugs: Topical and ocular drug delivery. Marcel Dekker Inc, New York. **1992**, 1-16.

23. Guy R.H., Handgraft J., Selection of drug candidate for transdermal drug delivery. In: Developmental issues and research initiative, Marcel Dekker Inc, New York. **1989**, 59-81.

24. Singh P. and Roberts M.S., Skin permeability and local tissue concentrations of nonsteroidal anti-inflammatory drugs after topical application. *J. Pharmacol. Exp. Ther.* **1994**, 268, 144-151

25. Moddaresi M., Brown M.B., Zhao Y., Tamburic S. and Jones S.A., The role of vehicle-nanoparticle interactions in topical drug delivery. *Int J Pharm.* **2010**, 400, 176-82

26. Montagna W., In The Evaluation of therapeutic agents and cosmetics, T. H. Stemberg and V. D. Newcomer, Eds., McGraw Hill, New York, **1964**

27. Copper E. R. Molecular modifications for dermal and transdermal drug delivery. *Pharm. Int.,* **1986**, 12, 308-10

28. Singh S. and Singh J., Transdermal drug delivery by passive diffusion and iontophoresis: A Review. *Med. Res. Rev.*, **1993**, 13, 569-621.

29. Roy D. A., New guidelines for topical NSAIDs in the osteoarthritis treatment paradigm. *Curr. Med. Res. Opin.*, **2010,** 26, 2871–76

30. Schuetz Y.B., Naik A., Guy R.H. and Kalia Y.N., Emerging strategies for the transdermal delivery of peptide and protein drugs. *Expert Opin. Drug Deliv.,* **2005**, 2, 533-38

31. Rhee Y.S., Choi J.G., Park E.S. and Chi S.C., Transdermal delivery of ketoprofen using microemulsions. *Inter. J. Pharm.*, **2001**, 228, 161-170

32. Faiyaz S., Sanjula B., Alka A., Javed A., Mohammed A. and Sheikh S., Nanoemulsions as vehicles for transdermal delivery of aceclofenac. *AAPS Pharm SciTech.*, **2007**, 8, 191-99

33. Puglia C., Bonina F., Rizza L., Cortesi R., Merlotti E., Drechsler M., Mariani P., Contado C., Ravani L. and Esposito E., Evaluation of Percutaneous Absorption of Naproxen from Different Liposomal Formulations. *J. Pharm. Sci.*, **2010**, 99, 2819-29

34. Hyun-Ah Cheong and Hoo-Kyun Choi., Enhanced percutaneous absoption of piroxicam via salt formation with ethanolamines. *Pharm. Res.,* **2002**, 19, 1375-80

35. Fang L., Numajiri S., Kobayashi D. and Morimoto Y., The use of complexation with alkanolamines to facilitate skin permeation of mefenamic acid. *Inter. J. Pharm.*, **2003**, 262, 13-22

36. Rautio J., Taipale H., Gynther J., Vepsalainen J., Nevalainen T. and Jarvinen T., *In Vitro* Evaluation of acyloxyalkyl esters as dermal prodrugs of ketoprofen and naproxen. *J. Pharm. Sci.*, **1998**, 87, 1622-28

37. K. B. Sloan et.al., Acyloxyamines as prodrugs of anti-inflammatory carboxylic acids for improved delivery through skin. *J. Pharm. Sci.* **1984**, 73, 1734-37

38. Rautio J., Nevalainen T., Taipale H., Vepsäläinen J., Gynther J., Laine K. and Järvinen T., Piperazinylalkyl prodrugs of naproxen improve *in vitro* skin permeation. *Eur. J. Pharm. Sci.*, **2000**, 11, 157-63

39. Bonina F.P., Puglia C., Barbuzzi T., de Caprariis P., Palagiano F., Rimoli M.G. and Saija A., *In vitro* and *in vivo* evaluation of polyoxyethylene esters as dermal prodrugs of ketoprofen, naproxen and diclofenac. *Eur. J. Pharm.Sci.*, **2001**, 14, 123-34

40. Bonina F., Santagati N.A. and Puglia C., Ketoprofen 1-alkylazacycloalkan-2-one esters as dermal prodrugs: i*n vivo* and i*n vitro* evaluations. *Drug. Dev. Ind. Pharm.* **2003**, 29, 181-90

2. Aims and Objectives

For the treatment of rheumatic diseases mainly RA and OA the percutaneous application of drugs has recently received considerable importance due to its advantages over other drug delivery methods.[1] In joint diseases the percutaneous delivery of drugs to underlying muscle and joints is of considerable importance. Evidence also supports that local application of NSAIDs induces less adverse effects than orally administered anti-inflammatory agents.[2-5] The bioavailability of topically applied NSAIDs is only up to 1-2% in humans.[1] This limitation has led to the development of various strategies to enhance permeation of drugs through skin that include salt formation, prodrug designing and formulation approaches. Besides low permeability, all NSAIDs have short half life (3-4 h) and other unsuitable physicochemical properties (log$P$, pKa, molecular weight etc.)[5]

The objective of the present study was to investigate the usefulness of the salt formation and prodrug approaches to improve the percutaneous delivery of some NSAIDs such as 6-methoxy-2-naphthylacetic acid (6-MNA) **(16)** and biphenylacetic acid (BPA) **(17)** for the treatment of rheumatic diseases.
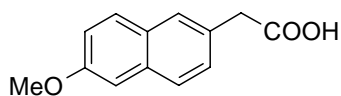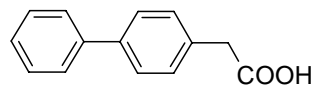
(16) **(17)**

6-MNA and BPA are active metabolites of nabumetone and fenbufen respectively having long half life.[6-8]

Specific aims of the current work have been listed below:

1) Design of salts and prodrugs of 6-MNA and BPA to modify pharmacokinetic characteristics and thereby enhance the skin permeation.

2) Syntheses of the designed novel salts and prodrug derivatives of 6-MNA and BPA. These salts and derivatives are designed to release the parent drug via ionic bond cleavage (salts) or enzymatic and/or chemical hydrolysis of covalent bonds.

3) To evaluate the effects of promoieties on the physicochemical and kinetic properties of the prodrugs and salts; such as aqueous solubility, lipophilicity, chemical degradation or enzymatic hydrolysis and release of the parent drug.

4) To evaluate the effects of the physicochemical and kinetic properties of the synthesized prodrugs and salts for the *in vitro* skin permeation model.

5) To improve the skin permeation of 6-MNA and BPA through these prodrug and salt formation approaches.

References

1. Rautio J., Nevalainen T., Taipale H., Vepsäläinen J., Gynther J., Laine K. and Järvinen T., Synthesis and in vitro evaluation of novel morpholinyl and methyl piperazinyl acyloxyalkyl prodrugs of 2-(6-methoxy-2-naphthyl)propionic acid (Naproxen) for topical drug delivery. *J. Med. Chem.* **2000**, *43,* 1489-94

2. Suh H., Jun H.W., Dzimianski M.T. and Lu G.W., Pharmacokinetic and local tissue disposition studies of naproxen-following topical and systemic administration in dogs and rats. *Biopharm. Drug Dispos.* **1997**, 18, 623-33.

3. Underwood M., Advice to use topical or oral ibuprofen for chronic knee pain in older people: randomized controlled trial and patient preference study. *BMJ.* **2008**, 336, 138-42.

4. Altman R.D. New guidelines for topical NSAIDs in the osteoarthritis treatment paradigm. *Curr. Med. Res. Opin.* **2010**, 26, 2871-76

5. Rautio J., Nevalainen T., Taipale H., Vepsäläinen J., Gynther J., Laine K. and Järvinen T., Piperazinylalkyl prodrugs of naproxen improve in vitro skin permeation. *Eur. J. Pharm. Sci.* **2000**, 11, 157-63.

6. Roberts M.S. and Cross S.E., Percutaneous absorption of topically applied NSAIDS and other compounds: role of solute properties, skin physiology and delivery systems. *Inflammopharmacology.* **1999**, 7, 339-50.

7. Nobilis M., Kopecký J., Kvetina J., Svoboda Z., Pour M., Kunes J., Holcapek M. and Kolárová L., Comparative Biotransformation and Disposition Studies of Nabumetone in Humans and Mini pigs Using HPLC with Ultraviolet, Fluorescence and Mass-spectrometric Detection. *J. Pharm. Biomed. Anal*. **2003**, 32, 641-56

8. Brogden R.N., Heel R.C., Speight T.M. and Avery G.S., Fenbufen: a review of its pharmacological properties and therapeutic use in rheumatic diseases and acute pain. *Drugs.* **1981**, 21, 1-22.

3. Results and Discussion

The work carried out towards achieving the proposed plan has been classified in to the following two main headings:

3.1. Salt formation approach

3.2. Prodrug approach

3.1 Salt formation approach

The work has been discussed under the following three main headings:

3.1.1. Design of salts

3.1.2. Syntheses and characterization of salts

3.1.3. Physicochemical evaluation of the salts

   3.1.3.1. Determination of aqueous solubility

   3.1.3.2. Determination of Log *P*

   3.1.3.3. *In vitro* skin permeation study

3.1.1 Design of salts

Salts are usually considered alternatives of the parent drugs for drug delivery systems if physicochemical properties of the parent drug molecules are not suitable for a formulation. As mentioned earlier all NSAIDs have very low permeability through skin (<1 %), short half life (3-4 h), and lack of affinity towards joints etc. Attempts have been made to improve their permeability by salt formation; however, none of the long acting salts of NSAIDs coupled with their specific affinity towards joints have been investigated till date.

In the current study various salts of active metabolites of nabumetone and fenbufen i.e 6-MNA **(16)** and BPA **(17)** respectively, have been designed, prepared and evaluated to improve their transdermal delivery for the treatment of arthritis. Considering the presence of acidic functional group we have designed some salts of these agents with organic and inorganic bases.

Alkanolamines such as ethanolamine, diethanolamine, triethanolamine and diethylamine (DEA) have been chosen for this purpose along with sodium salt. These agents are weak bases, and contain basic amino functional group and one or more polar hydroxyl groups except for the DEA and sodium salts. Amino group will react with acidic functional group present in the NSAIDs resulting into salt formation imparting aqueous solubility which is further enhanced by polar hydroxyl group. Structures of the designed salts are shown in **Fig. 3.1.1**
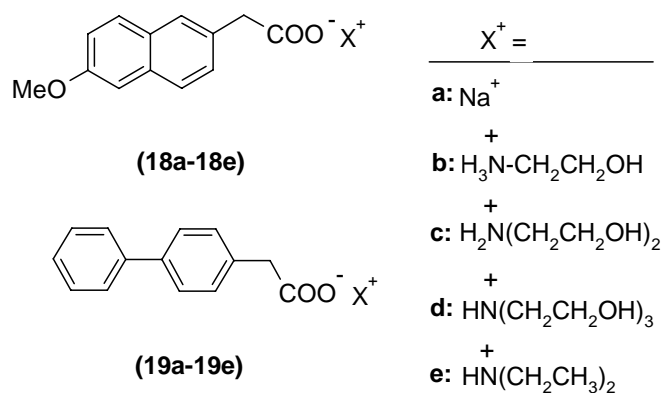
Fig. 3.1.1: The general structure of the designed salts of 6-MNA **(16)** and BPA **(17)**

3.1.2 Syntheses and characterization of the salts

6-MNA **(16)** and BPA **(17)** were dissolved separately in dichloromethane (wherever required small amount of methanol was added to make the solution clear) and an equimolar amount of base was added and the reaction mixtures were stirred for 6-8 h. The precipitated salts were collected by filtration and recrystallized from ethyl acetate to yield pure salts **(18a-18e)** and **(19a-19e)** of 6-MNA and BPA respectively.

Table 3.1.1: Physicochemical and spectral data of compounds **(16, 18a-18e)**

Compound	Physical State	Melting point (^{o}C)	DSC (endotherm ^{o}C)	IR (cm^{-1})
16	White Solid	171-173	171.55	1693, 1416, 1265
18a	White Solid	>275	281.12	1707, 1267, 1028
18b	Yellow Solid	156-158	157.15	3285, 1704, 1263
18c	White Solid	72-74	80.01/117.38	3385, 1706, 1387
18d	White Solid	94-97	106.17	3354,1709, 1227
18e	White Solid	136-139	114.84	3389, 1707, 1264

Prepared salts were characterized by using IR and DSC. Physicochemical and spectral data of the compounds are listed in **Table 3.1.1** above, and the surface morphology was studied by SEM.

Regarding the interaction between 6-MNA and alkanolamine bases, important information was gathered from IR spectroscopy. The FT-IR spectra of 6-MNA and its salts are shown in **Fig. 3.1.2.** 6-MNA showed a strong sharp signal at $1693cm^{-1}$, characteristic of the carbonyl stretching vibrations.

The carbonyl peak of the 6-MNA in salt form was shifted to higher wavenumber (1707 cm^{-1}). Other signs of interaction were reflected by shifts in the range of 3389-3285 cm^{-1} due to N-H stretching which were absent in **16** and **18a**. However **18b** shows signals at 3285 cm^{-1} whereas **18c** and **18d** show peaks around 3385 cm^{-1} suggesting that the intermolecular hydrogen bonding of the salts might have shifted the N-H or O-H stretching bands.

──── **(16),** ──── **(18a)** ──── **(18b),** ──── **(18c),** ──── **(18d),** ──── **(18e)**
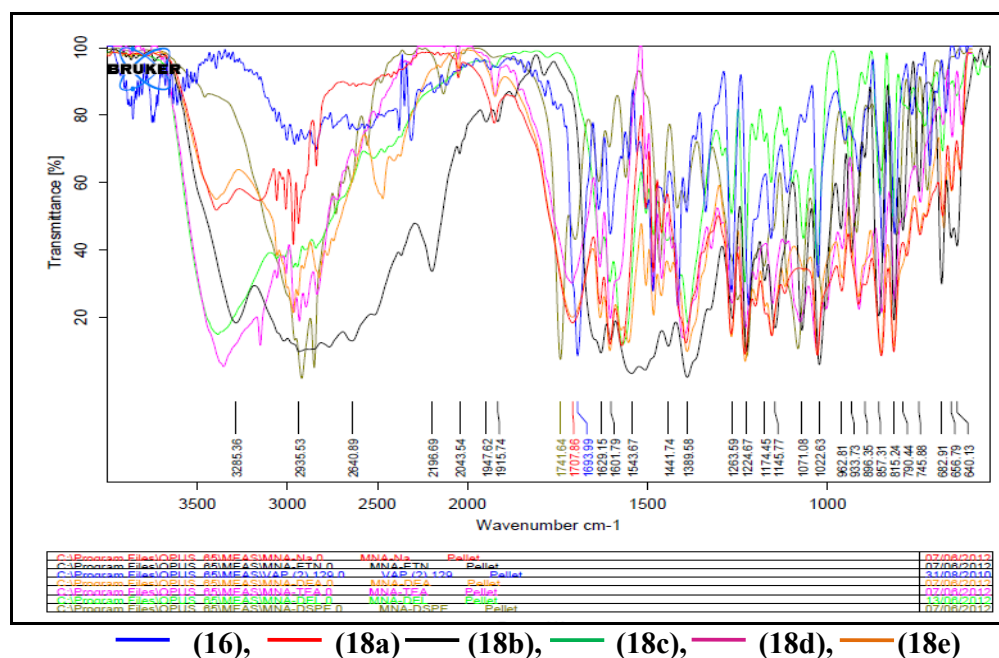
Fig. 3.1.2: Overlaid FT-IR Spectra of 6-MNA **(16)** and its salts **18a-18e)**

Fig. 3.1.3. and **3.1.4.** Show DSC curve of 6-MNA **(16)** and its salts **(18a-18e).** **Table 3.1.1** summarizes melting point and endothermic peaks of 6-MNA and its salts and these values are in good agreement with each other. Melting points of the salts decreased remarkably compared to the parent drug except for the sodium salt **(18a)** which showed higher melting point. All these shifts in melting points are indication of salt formation.

Surface morphology of the compounds vary from each other and to evaluate this parameter SEM of the prepared salts were performed. From this study we can conclude that each salt has a different surface morphology as shown in **Fig. 3.1.5.**
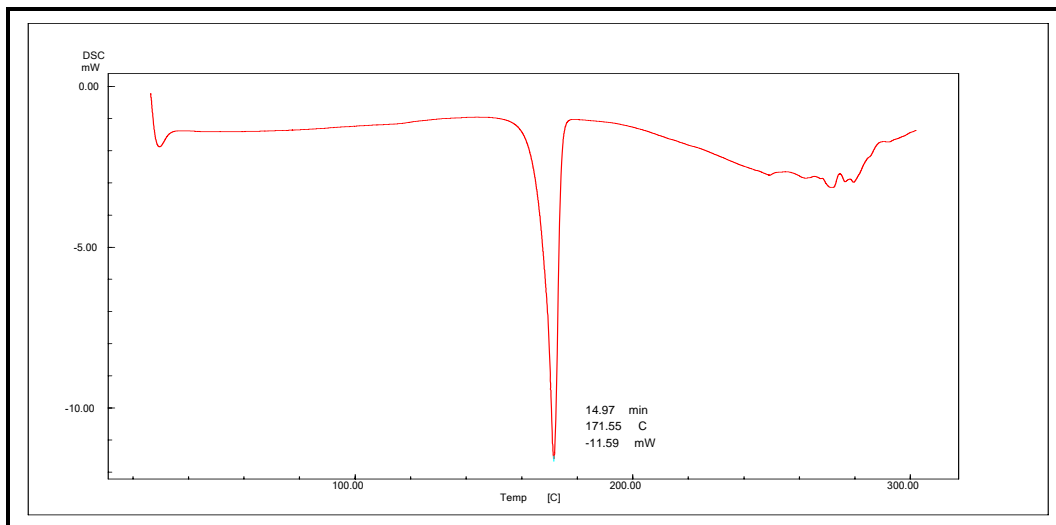

Fig. 3.1.3: DSC thermogram of 6-MNA **(16)**
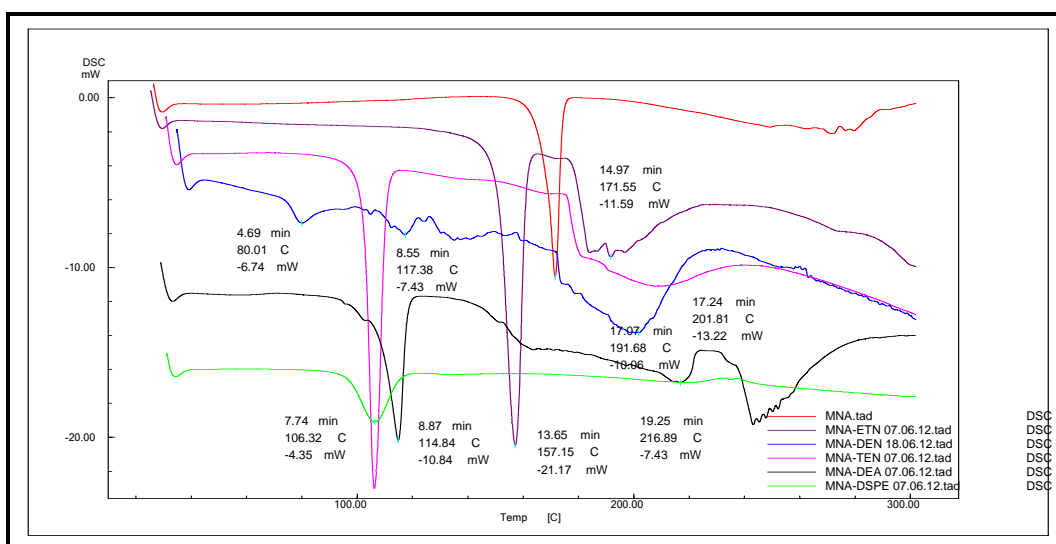
Fig. 3.1.4: Overlaid DSC thermograms of 6-MNA **(16)** and its salts **(18a-18e)**

(16)

(18a)
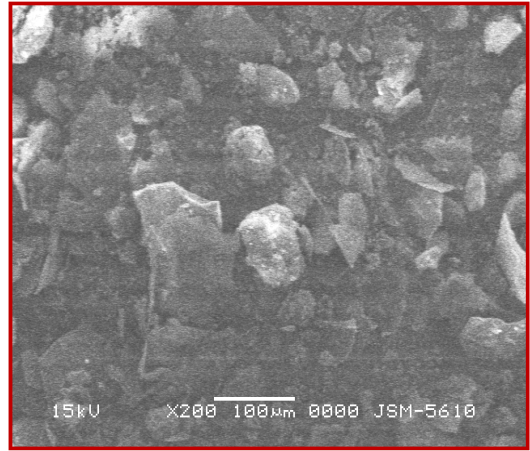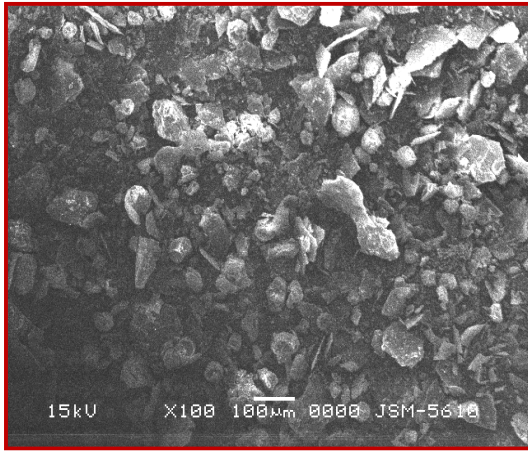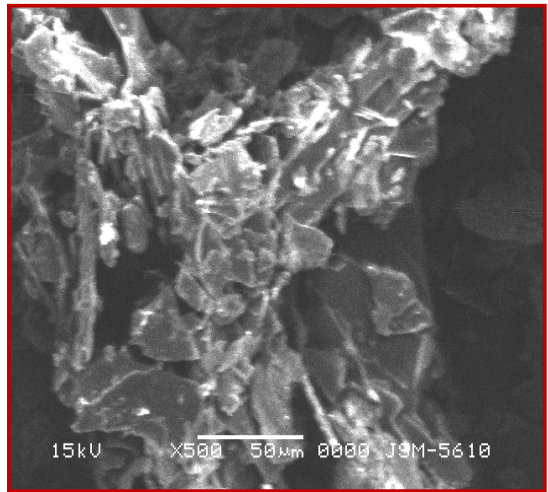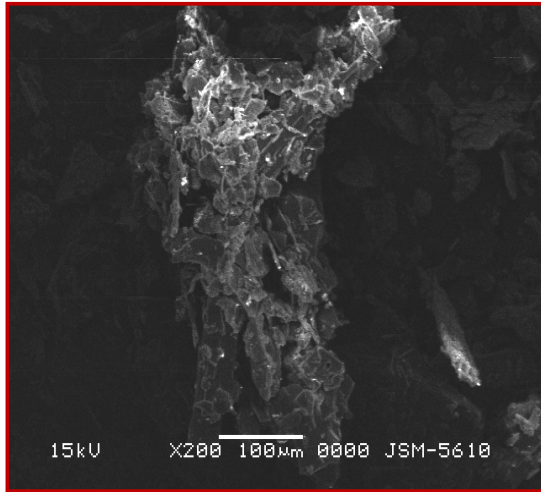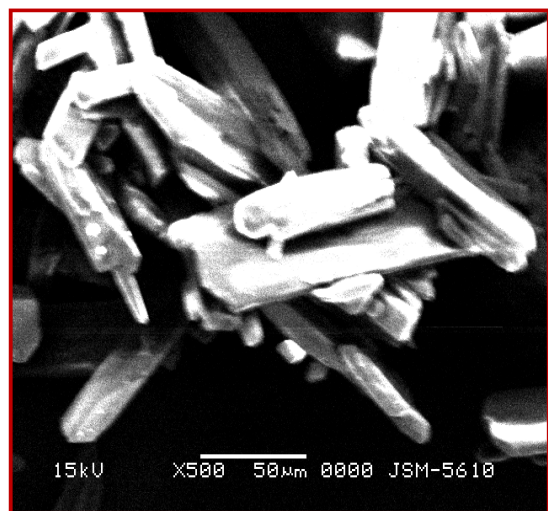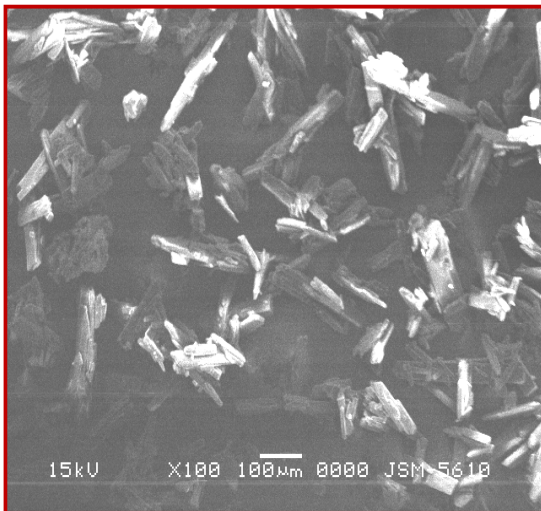
(18b)
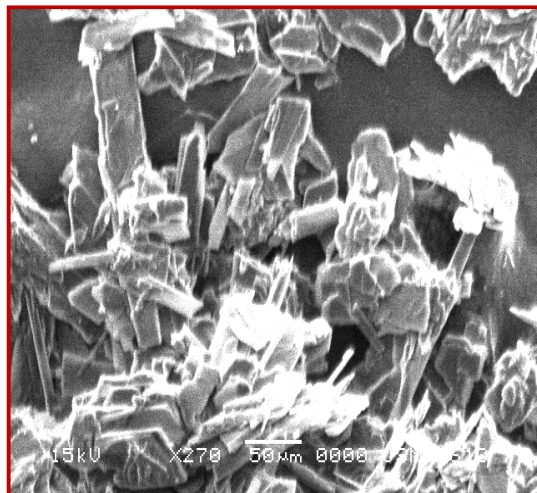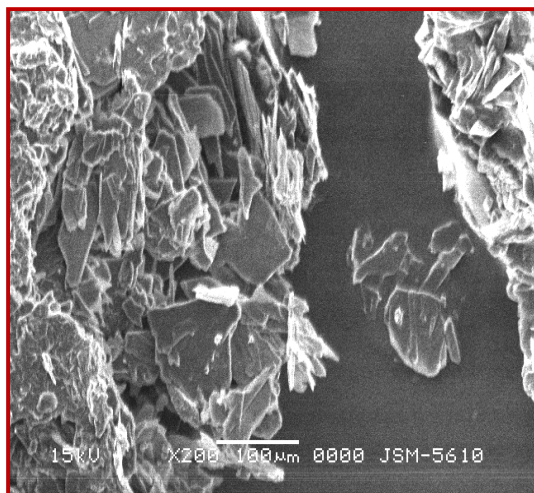
(18c)
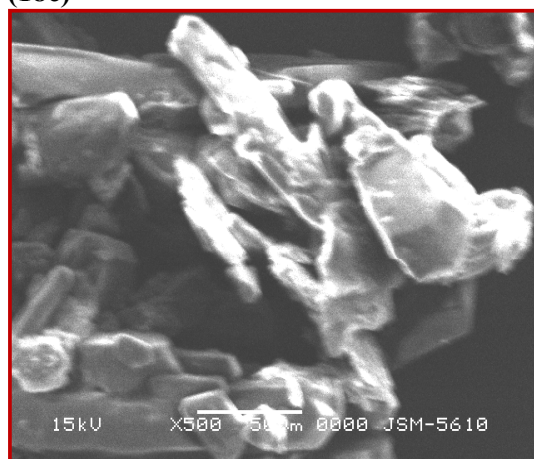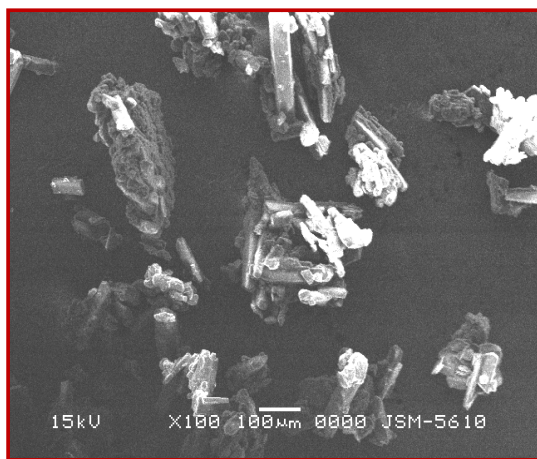
(18d)
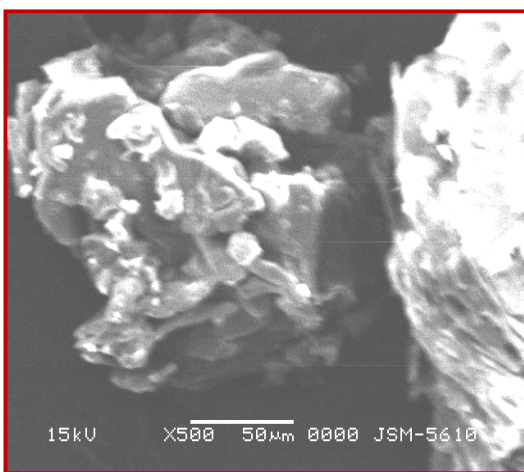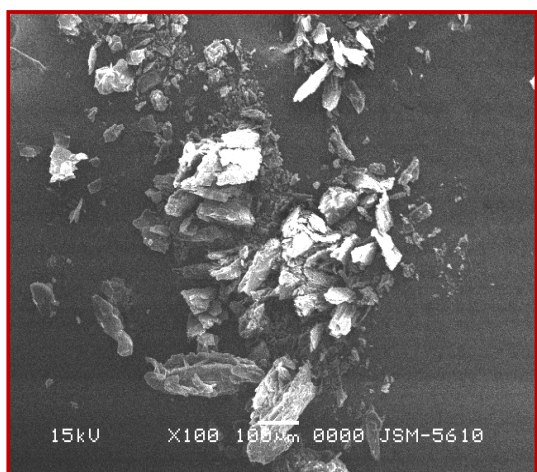
(18e)

Fig. 3.1.4: Scanning electron microscope images of compounds **(16, 18a-18e)**

Salts of BPA also show same features as described under 6-MNA **(16)**. The physicochemical and spectral data of compounds **(17, 19a-19e)** are shown in **Table 3.1.2.**

Table 3.1.2: Physicochemical and spectral data of compounds **(17, 19a-19e)**

Compound	Physical State	Melting point (^{o}C)	DSC (Endotherm^{o}C)	IR (cm^{-1})
17	White Solid	163-165	153.89	1685, 1413, 1249,
19a	White Solid	>275	--	1684, 1557, 1294,
19b	Yellow Solid	116-119	137.62	3263, 1674, 1391,
19c	Semisolid	--	--	3248, 1679, 1374,
19d	White Solid	82-84	87.91	3354, 1681, 1077,
19e	Semisolid	--	--	3407, 1699, 1571,
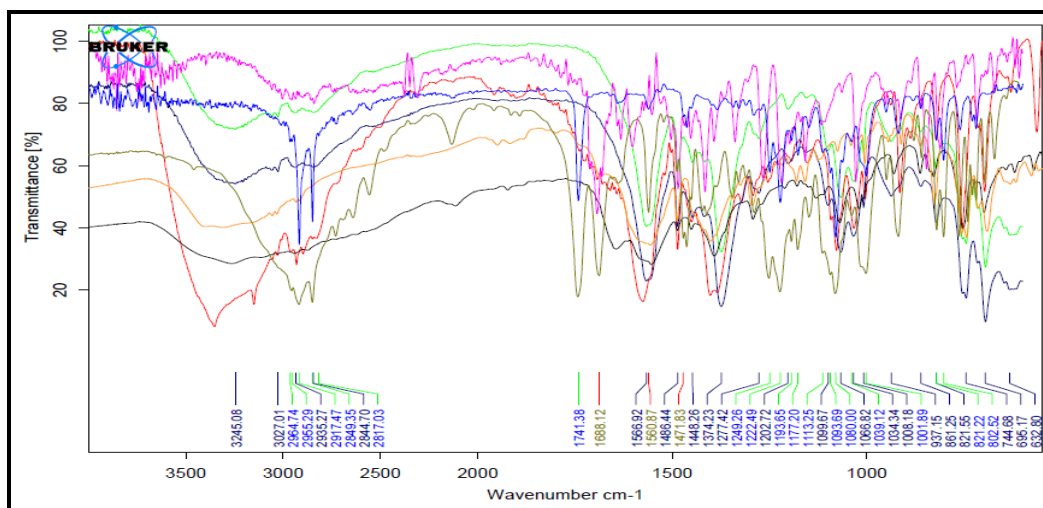
Fig. 3.1.6: Overlaid FT-IR Spectra of BPA **(17)** and its salts **19a-19e)**
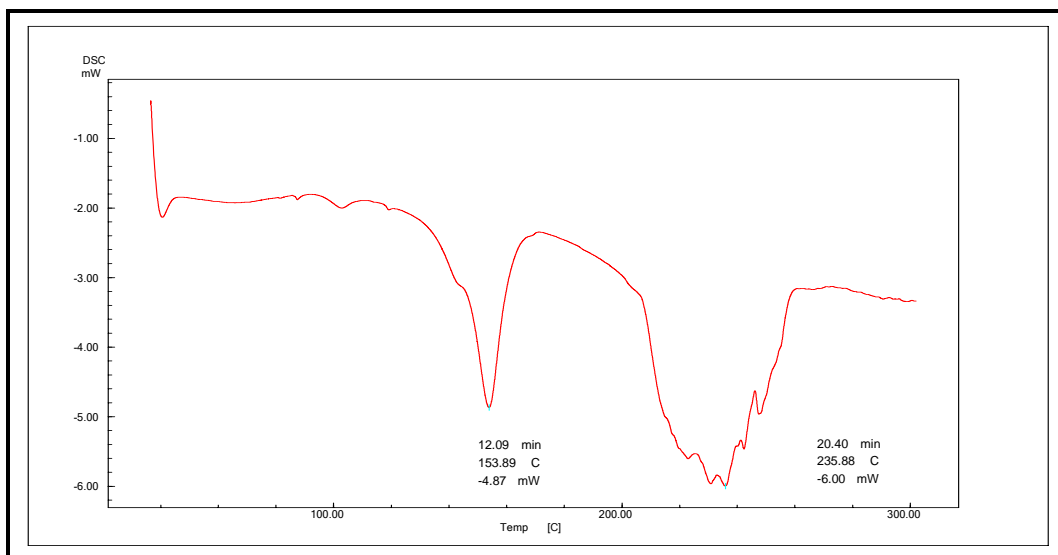
Fig. 3.1.7: DSC thermogram of BPA

(17)
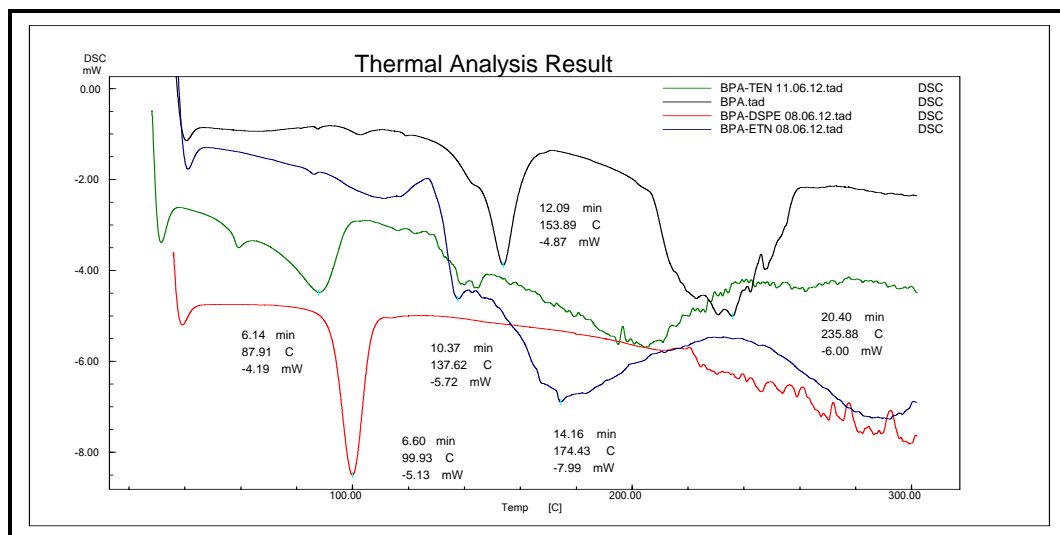
Fig. 3.1.8: Overlaid DSC thermograms of BPA **(17)** and its salts **19a-19e)**

(17)

(19a)

(19b)

186
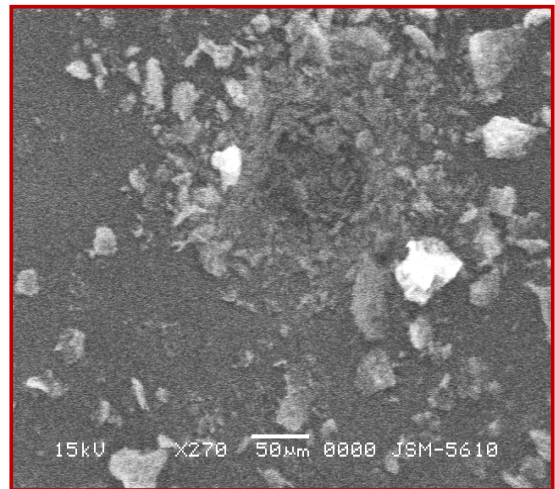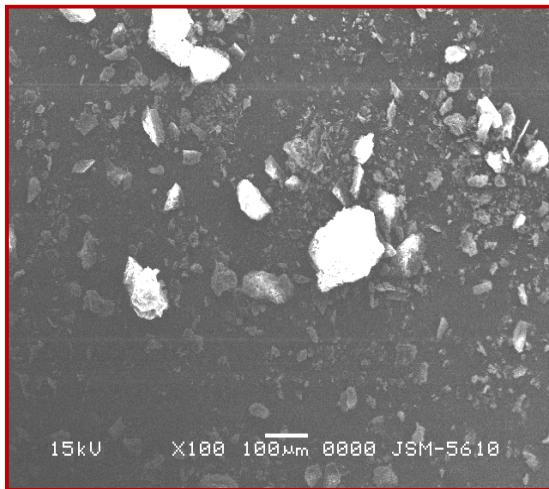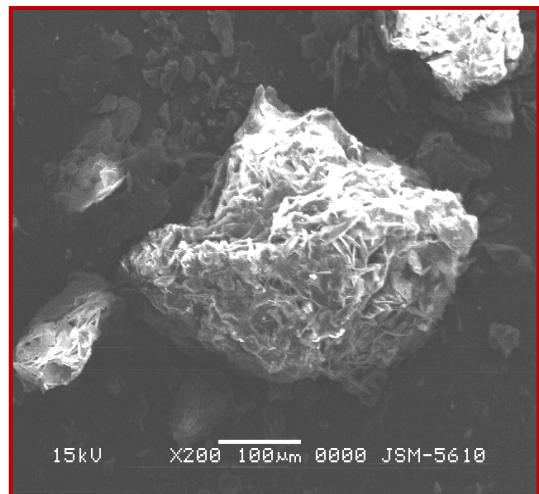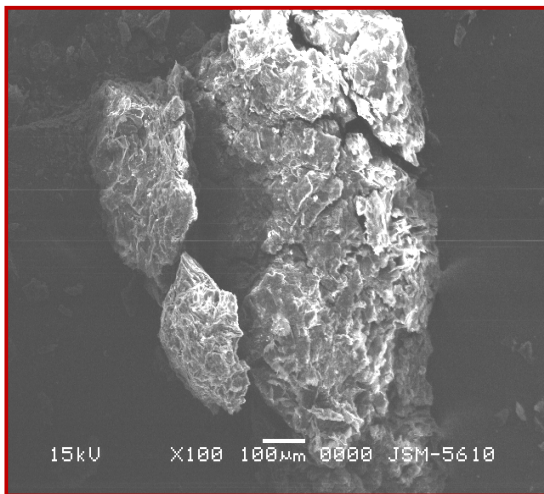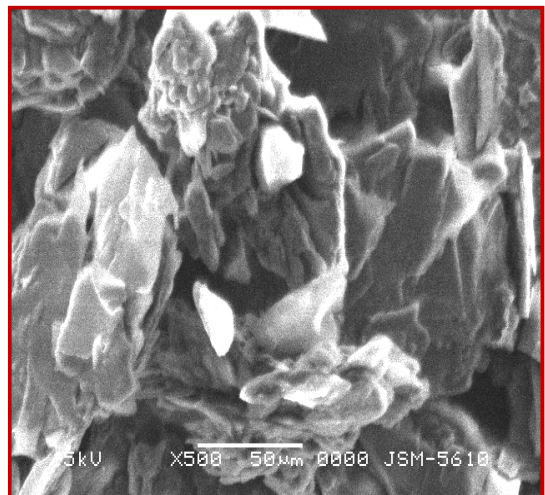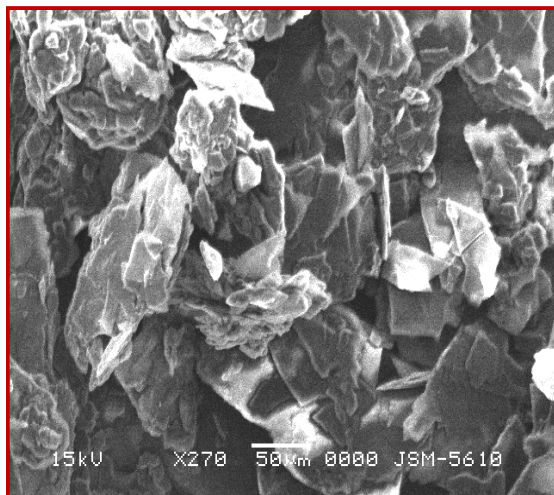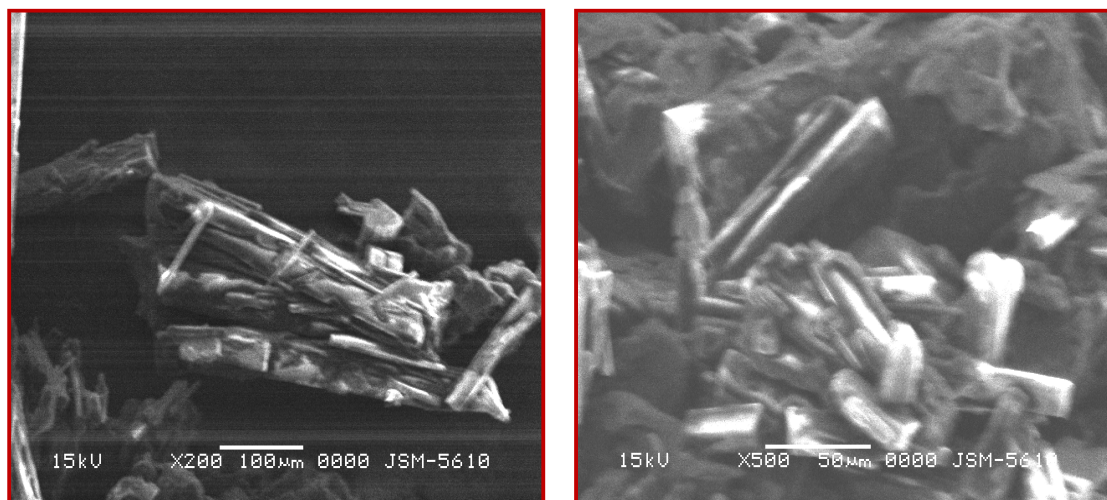
(19d)

Fig. 3.1.9: Scanning electron microscope images of compounds **(17, 19a-19d)**

3.1.3. Physicochemical evaluation

For the evaluation of various physicochemical parameters such as aqueous solubility, partition coefficient and *in vitro* skin permeability, HPLC method as developed earlier (Section-I) has been used. Calibration curves for 6-MNA **(16)** and BPA **(17)** were plotted and linearity range calculated.

3.1.3.1. Determination of aqueous solubility

Due to biphasic nature of skin, the ideal salt form should exhibit adequate lipid solubility as well as aqueous solubility. Aqueous solubility of 6-MNA and its salts were determined in phosphate buffer at the physiological *p*H 7.4 and at *p*H 5.0 as the environment of the outer surface of the skin is acidic (*p*H 4.2-6.5).[1,8] **Table 3.1.3** shows aqueous solubility of 6-MNA **(16)** and its salts **(18a-18e)**.

3.1.3.2. Determination of Log *P*

Lipid solubility plays a crucial role in determining skin permeability of a compound because the SC (stratum corneum) the major barrier to drug permeation is essentially lipoidal in nature and generally favors permeation of lipophilic drugs.[1] The apparent partition coefficients of 6-MNA **(17)** and salts **(18a-18e)** were determined by partitioning them between phosphate buffer (0.16 M) and saturated n-octanol at both *p*H 5.0 and *p*H 7.4 using shake flask method. **Table 3.1.4** shows Log P_{app} values of 6-MNA **(16)** and its salts **(18a-18e)**.

Table 3.1.3: Aqueous solubility of 6-MNA **(16)** and salts at pH 5.0 and at pH 7.4

Compound	Aqueous Solubility (mM)	
	pH 5.0	pH 7.4
16	0.78 ± 0.18	63.34 ± 0.24
18a	17.01 ± 0.19	24.08 ± 0.27
18b	34.81 ± 0.24	27.13 ± 0.29
18c	36.02 ± 0.31	31.09 ± 0.41
18d	21.92 ± 0.42	25.40 ± 0.72
18e	08.10 ± 0.29	06.09 ± 0.29
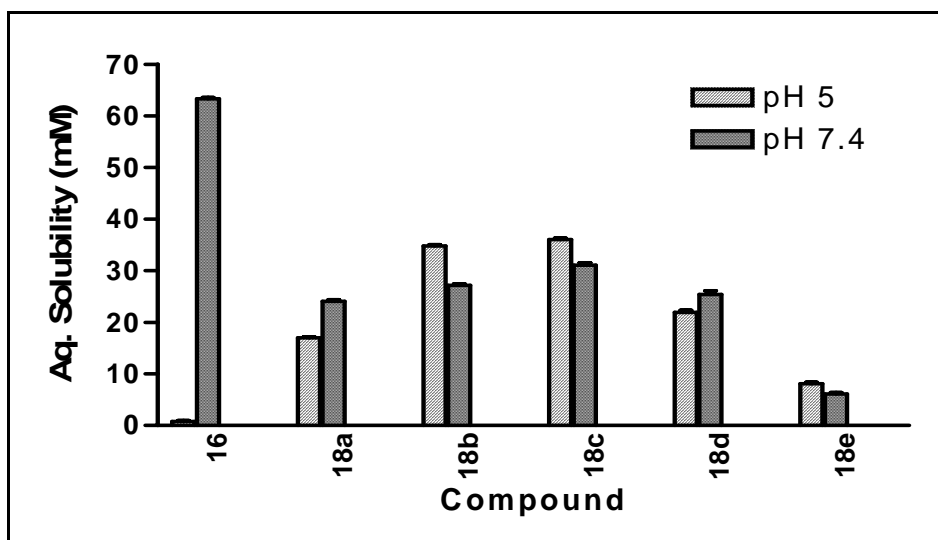
Fig. 3.1.10: Aqueous solubility of the 6-MNA **(16)** and salts **(18a-18e)** at pH 5.0 and at pH 7.4

Table 3.1.4: Partition coefficient (Log P_{app}) values of 6-MNA **(16)** and its salts

Compound	Log P_{app}	
	pH 5.0	pH 7.4
16	1.823 ± 0.020	0.233 ± 0.037
18a	0.807 ± 0.031	0.704 ± 0.061
18b	1.491 ± 0.041	1.063 ± 0.043
18c	0.917 ± 0.043	1.011 ± 0.031
18d	1.101 ± 0.015	1.061 ± 0.017
18e	2.310 ± 0.032	2.010 ± 0.019
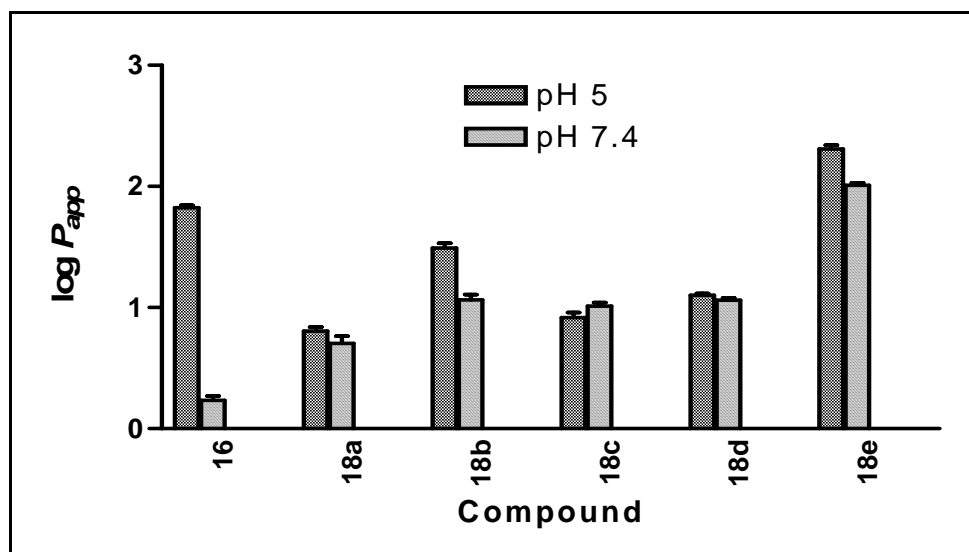
Fig. 3.1.11: Partition coefficient (Log P_{app}) values of 6-MNA **(16)** and its salts **(18a-18e)**

Table 3.1.5: Aqueous solubility of BPA **(17)** and salts at pH 5.0 and at pH 7.4

Compound	Aqueous Solubility (mM)	
	pH 5.0	pH 7.4
17	0.57 ± 0.14	54.08 ± 0.14
19a	14.23 ± 0.31	17.05 ± 0.21
19b	28.96 ± 0.28	24.10 ± 0.34
19c	41.05 ± 0.43	37.08 ± 0.33
19d	24.27 ± 0.22	21.30 ± 0.52
19e	07.20 ± 0.37	05.18 ± 0.45
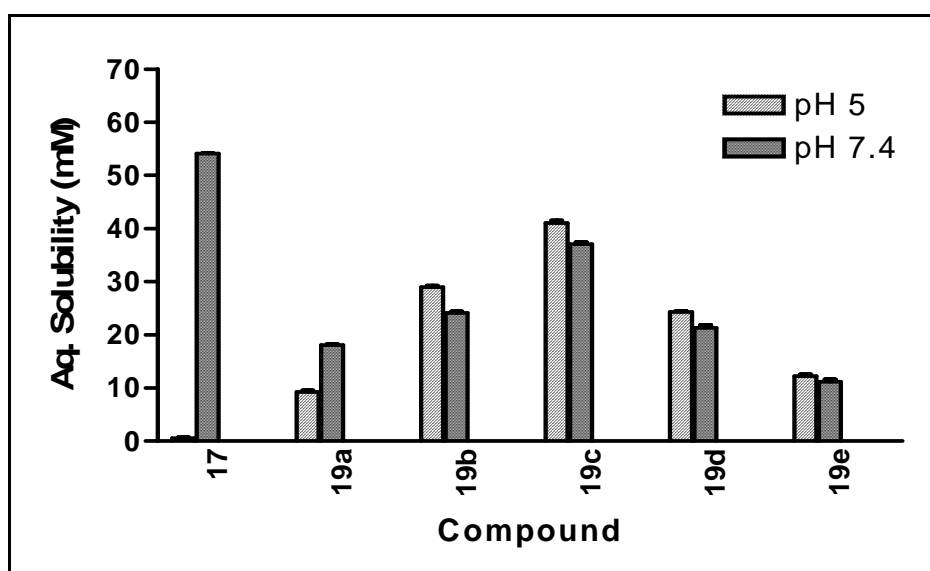
Fig. 3.1.12: Aqueous solubility of BPA **(17)** and its salts **(19a-19e)**

189

Table 3.1.6: Partition coefficient (Log P_{app}) values of BPA **(17)** and its salts

Compound	Log P_{app}	
	*p*H 5.0	*p*H 7.4
17	1.207 ± 0.060	0.433 ± 0.041
19a	0.687 ± 0.043	0.507 ± 0.052
19b	2.0340 ± 0.039	1.463 ± 0.076
19c	1.019 ± 0.073	0.911 ± 0.031
19d	1.208 ± 0.047	1.141 ± 0.047
19e	1.410 ± 0.031	1.010 ± 0.090
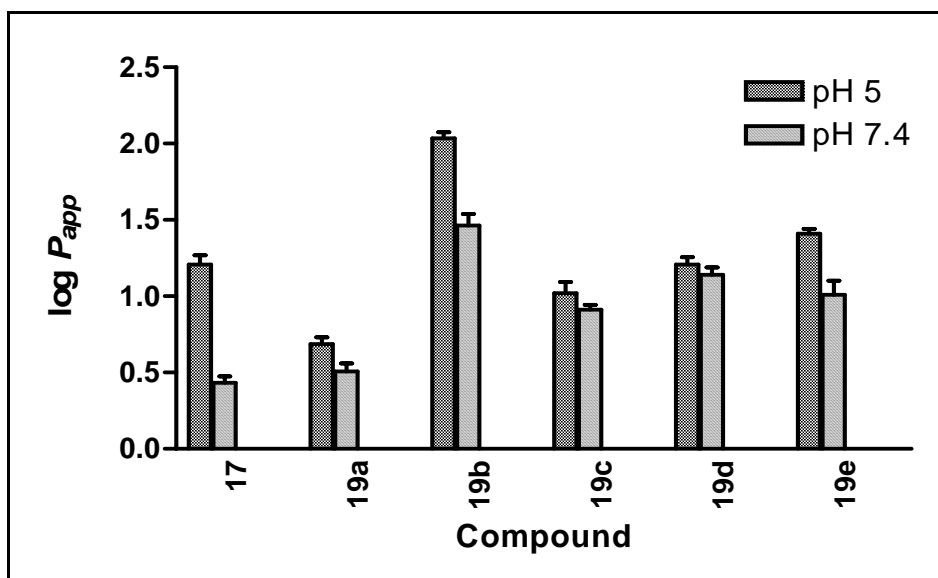
Fig. 3.1.13: Partition coefficient (Log P_{app}) values of BPA **(17)** and its salts **(19a-19e)**

3.1.3.3 *In vitro* skin permeation study

In vitro skin permeation study was performed by using rat skin. The *in vitro* diffusion experiments showed that salts of both 6-MNA **(16)** and BPA **(17)** were able to permeate rat abdominal skin. For each salt and parent drug the cumulative amounts permeated through skin were plotted against time. A steady state flux (*J*ss) was obtained by dividing the slope of that graph by surface area of the diffusion cell (4.906 cm^2).[1,8]

Table 3.1.7: *In vitro* skin permeation of 6-MNA **(16)** and its salts **(18a-18e)**

Time (h)	Cumulative amount permeated ($\mu g/cm^2$)					
	16	**18a**	**18b**	**18c**	**18d**	**18e**
1	3.85±2.0	9.87±3.0	15.55±2.0	7.69±3.0	6.04±2.0	5.34±2.0
2	6.81±2.0	19.13±3.0	36.88±4.0	18.55±2.0	11.08±2.0	9.01±3.0
4	16.01±3.0	45.75±4.0	109.4±5.0	64.61±5.0	29.88±4.0	19.44±4.0
8	29.49±4.0	84.66±5.0	215.1±7.0	164.06±9.0	67.4±5.0	61.7±8.0
24	52.96±5.0	252.62±9.0	450.4±14.0	356.4±16.0	176.8±11.0	148.6±10.0

Table 3.1.8: *In vitro* skin permeation of BPA **(17)** and its salts **(19a-19e)**

Time (h)	Cumulative amount permeated ($\mu g/cm^2$)					
	17	**19a**	**19b**	**19c**	**19d**	**19e**
1	3.46±2.0	12.05±3.0	28.47±2.0	22.14±3.0	18.7±2.0	9.58±2.0
2	6.66±2.0	23.45±3.0	61.51±4.0	57.44±2.0	38.1±2.0	19.45±3.0
4	18.51±3.0	56.81±4.0	157.89±5.0	145.69±5.0	91.56±4.0	61.04±4.0
8	31.14±4.0	120.1±5.0	310.4±7.0	256.1±9.0	189±5.0	107.4±8.0
24	54.06±5.0	215.31±9.0	514.3±14.0	467.8±16.0	376.4±11.0	197.5±10.0

The steady-state flux (Jss) of 6-MNA **(16)**, BPA **(17)** and their salts **(18a-19e)** were given in **Table 3.1.9** All the salts have shown higher flux values than the parent NSAIDs. Amongst all the salts, salts **(18b** and **19b)** have shown highest steady state flux from 6-MNA and BPA series respectively.

Table 3.1.9: Steady state flux of 6-MNA **(16)**, BPA **(17)** and their salts

Derivative	Jss (μg/cm^{2}h)	Derivative	Jss (μg/cm^{2}h)
16	0.489	**17**	0.42
18a	2.15	**19a**	1.75
18b	4.03	**19b**	4.14
18c	3.13	**19c**	3.76
18d	1.52	**19d**	3.11
18e	1.29	**19e**	1.60
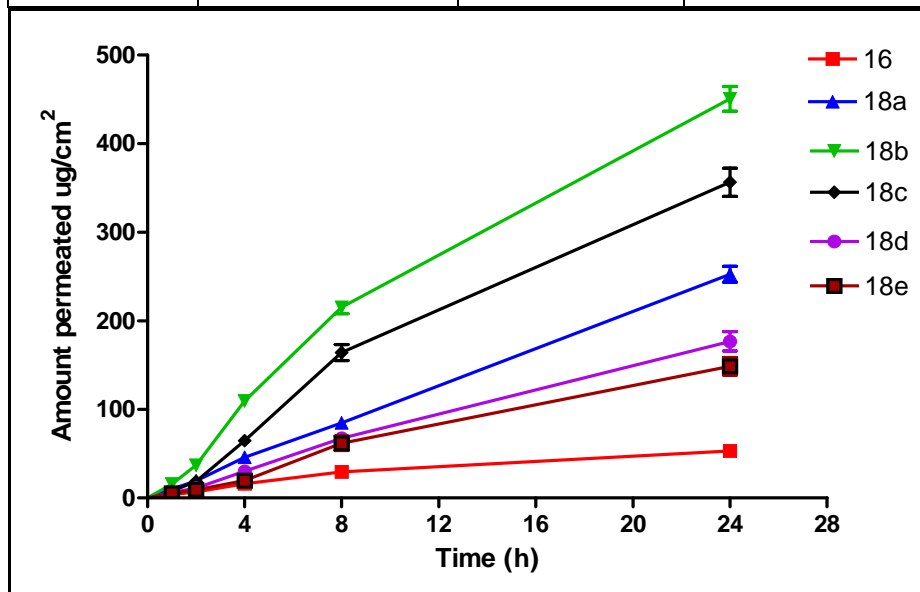
Fig. 3.1.14: Permeation profiles (mean SEM, n=3) for **16** and its salts **(18a-18e)**
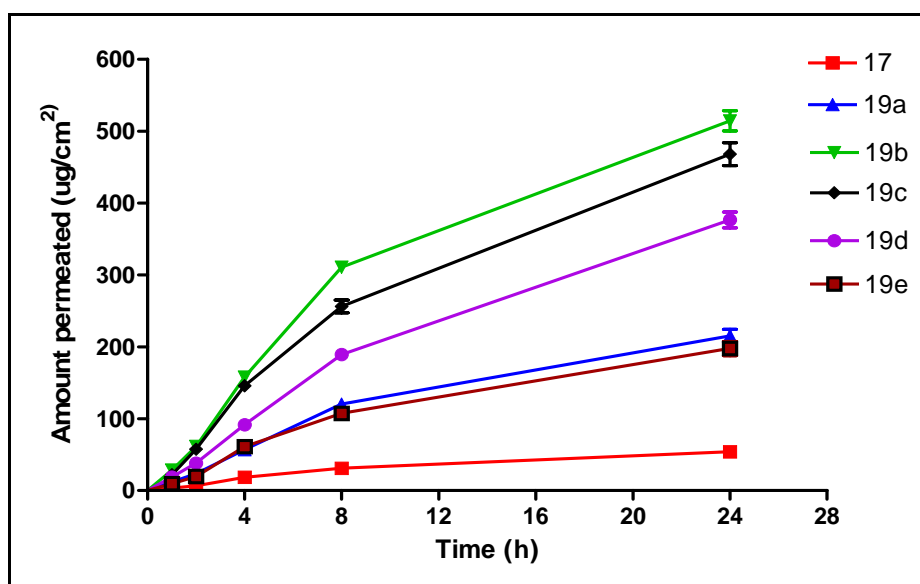
Fig. 3.1.15: Permeation profiles (mean SEM, n=3) for **17** and its salts **(19a-19e)**

The ethanolamine salts **(18b, 19b)** displayed 9-10 times higher flux than the parent NSAIDs. The result also showed that salts with higher flux have a balance between solubility and partition coefficient. Further, except for sodium salt all the salts have lower melting points than the parent drugs and higher permeability through the skin, which support previous, reports[28] indicating that a decrease in melting point or conversion of solid state to liquid state improves the permeability of drugs through skin.

3.2 Prodrug approach

The work carried out towards achieving the proposed plan has been discussed under the following three main headings.

3.2.1. Design of prodrugs

3.2.2. Syntheses and characterization of prodrugs

3.2.3. Physicochemical evaluation of the prodrugs

    3.2.3.1. Determination of aqueous solubility

    3.2.3.2. Determination of Log *P*

    3.2.3.3. Hydrolyses kinetics study

    3.2.3.4. *In vitro* skin permeation study

3.2.1 Design of prodrugs

In order to improve the permeability of 6-MNA **(16)** the first essential requirement is to improve the aqueous solubility with balanced log*P*. To achieve this it was planned to synthesize piperazine derivatives of **16** as shown in **Fig. 3.2.1.** The designed prodrug derivatives would contain piperazine ring moiety with various electron withdrawing or electron donating substituents to modify the *p*Ka, suitable linker to impart lipophilicity and hydrolysable ester grouping. Piperazine is freely soluble in water and ethylene glycol. It is a weak base with a pK_b of 4.19; the *p*H of a 10% aqueous solution of piperazine is 10.8-11.8.
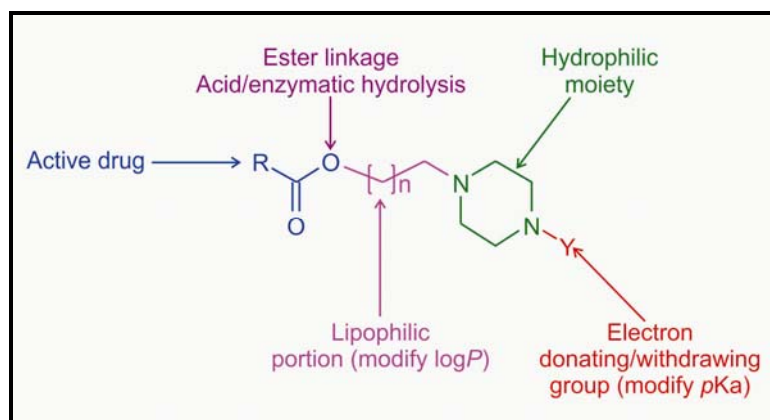
Fig. 3.2.1: General structure of designed prodrugs of 6-MNA **(16)**

In order to know the structural properties of the designed prodrugs at pH 5 and 7.4 QikProp 3.2 software was used.[2] QikProp is quick, accurate, easy-to-use software designed by Professor William L. Jorgensen which predicts absorption, distribution, metabolism, and excretion (ADME) parameters. QikProp software predicts physically significant descriptors and pharmaceutically relevant properties of organic molecules, either individually or in batches. For each successfully processed molecule, QikProp produces the following descriptors and properties.

Table 3.2.1: Various descriptors used in QikProp 3.2 software.

Property or descriptor	Description	Recommen- ded value
MW	Molecular weight of the molecule	130-725
Dipole	Computed dipole moment of the molecule	1.0-12.25
SASA	Total solvent accessible surface area (SASA) in square angstroms using a probe with a 1.4 Å radius	300-1000
FOSA	Hydrophobic component of the SASA (saturated carbon and attached-H).	0-750
FISA	Hydrophilic component of the SASA (SASA on N, O, and H on heteroatoms)	7-330
PISA	∏ (Carbon and attached hydrogen) component of	0-450

	the SASA.	
QPlogPo/w	Predicted octanol/water partition coefficient	-2.0-6.5
QPlogS	Predicted aqueous solubility, log S. S in mol dm^{-3} concentration of the solute in a saturated solution that is in equilibrium with the crystalline solid.	-6.5-0.5
QPlogKp	Predicted skin permeability, log Kp.	-8.0- -1.0)
QPlogKhsa	Prediction of binding to human serum albumin.	-1.5-1.5

The molecules were built within Maestro using the build module and prepared for analysis by using LigPrep module at physiological pH of Schrödinger 2009 by keeping all other parameters to their standard values. Structural properties were calculated by using QikProp as given in **Table 3.2.4-3.2.5**. pKa values for structures were calculated using Epik at physiological pH 7.4 using H_2O solvent.[3] The obtained results are given in **Table 3.2.6.**

Table 3.2.2: Various protonated forms obtained for twelve derivatives at pH 5.0
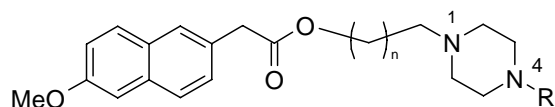
Entry ID	n	R	Protonation of Nitrogen at pH 5	
			N^1	N^4
TD1	1	-CH$_3$	+	+
TD2	1	-CH$_2$CH$_3$	+	+
TD3	1	-COCH$_3$	+	--
TD4	1	-Ph	+	--

TD4A	1	-Ph	+	+
TD5	1	-CH$_2$CH$_2$CH$_3$	+	+
TD6	1	-CH$_2$CH$_2$CH$_2$CH$_3$	+	+
TD7	2	-CH$_3$	+	+
TD8	2	-CH$_2$CH$_3$	+	+
TD9	2	-COCH$_3$	+	--
TD10	2	-Ph	+	+
TD10A	2	-Ph	+	--
TD11	2	-CH$_2$CH$_2$CH$_3$	+	+
TD12	2	-CH$_2$CH$_2$CH$_2$CH$_3$	+	+

+ = Protonated, -- = Not protonated

Table 3.2.3: Various protonated forms obtained for tweleve derivatives at pH 7.4
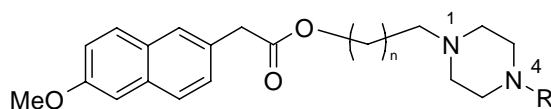
Entry ID	n	R	Protonation of Nitrogen at pH 5	
			N^1	N^4
TD1	1	-CH$_3$	--	--
TD1A	1	-CH$_3$	+	--
TD1B	1	-CH$_3$	--	+
TD1C	1	-CH$_3$	+	+
TD2	1	-CH$_2$CH$_3$	--	--
TD2A	1	-CH$_2$CH$_3$	+	--
TD2B	1	-CH$_2$CH$_3$	--	+
TD2C	1	-CH$_2$CH$_3$	+	+
TD3	1	-COCH$_3$	+	--

TD4	1	-Ph	+	--
TD5	1	-CH$_2$CH$_2$CH$_3$	--	--
TD5A	1	-CH$_2$CH$_2$CH$_3$	+	--
TD5B	1	-CH$_2$CH$_2$CH$_3$	--	+
TD5C	1	-CH$_2$CH$_2$CH$_3$	+	+
TD6	1	-CH$_2$CH$_2$CH$_2$CH$_3$	--	--
TD6A	1	-CH$_2$CH$_2$CH$_2$CH$_3$	+	--
TD6B	1	-CH$_2$CH$_2$CH$_2$CH$_3$	--	+
TD6C	1	-CH$_2$CH$_2$CH$_2$CH$_3$	+	+
TD7	2	-CH$_3$	--	--
TD7A	2	-CH$_3$	+	--
TD7B	2	-CH$_3$	--	+
TD7C	2	-CH$_3$	+	+
TD8	2	-CH$_2$CH$_3$	--	--
TD8A	2	-CH$_2$CH$_3$	+	--
TD8B	2	-CH$_2$CH$_3$	--	+
TD8C	2	-CH$_2$CH$_3$	+	+
TD9	2	-COCH$_3$	+	--
TD10	2	-Ph	+	--
TD11	2	-CH$_2$CH$_2$CH$_3$	--	--
TD11A	2	-CH$_2$CH$_2$CH$_3$	+	--
TD11B	2	-CH$_2$CH$_2$CH$_3$	--	+
TD11C	2	-CH$_2$CH$_2$CH$_3$	+	+
TD12	2	-CH$_2$CH$_2$CH$_2$CH$_3$	--	--
TD12A	2	-CH$_2$CH$_2$CH$_2$CH$_3$	+	--
TD12B	2	-CH$_2$CH$_2$CH$_2$CH$_3$	--	+
TD12C	2	-CH$_2$CH$_2$CH$_2$CH$_3$	+	+

+ = Protonated, -- = Not protonated

197

Table 3.2.4: Design parameters and structural properties of various protonated forms at *p*H 5.0

Entry ID	MW	Dipole	SASA	FOSA	FISA	PISA	QPlogPo/w	QPlogS	QPlogKp	QPlogKhsa
MNA	216.236	4.352	444.137	136.445	100.097	207.596	3.212	-3.832	-2.345	-0.191
TD1	342.437	3.885	674.199	432.612	36.132	205.454	2.694	-2.043	-5.011	0.006
TD2	356.464	3.803	703.38	463.954	33.96	205.466	3.068	-2.433	-4.875	0.123
TD3	370.447	6.281	697.287	419.979	71.832	205.476	2.23	-2.023	-3.606	-0.419
TD4	404.508	4.647	753.889	338.856	23.969	391.063	5.104	-5.296	-2.07	0.761
TD4A	404.508	3.567	764.033	341.77	30.995	391.268	5.126	-5.489	-2.199	0.792
TD5	370.491	3.774	736.49	497.364	33.673	205.453	3.466	-2.898	-4.773	0.257
TD6	384.517	3.767	769.175	530.063	33.657	205.455	3.86	-3.355	-4.677	0.39
TD7	356.464	3.428	720.827	462.441	52.747	205.639	3.045	-2.764	-5.22	0.171
TD8	370.491	2.112	764.115	499.389	57.084	207.642	3.454	-3.421	-5.197	0.323
TD9	384.474	5.784	751.772	451.368	94.771	205.634	2.565	-2.895	-3.932	-0.242
TD10	418.535	4.397	807.847	369.905	46.609	391.333	5.441	-6.156	-2.39	0.937
TD10A	418.535	3.238	807.484	371.096	45.007	391.381	5.494	-6.149	-2.361	0.956
TD11	384.517	3.371	783.035	526.995	50.403	205.637	3.818	-3.617	-4.985	0.423
TD12	398.544	3.365	815.766	559.76	50.373	205.634	4.212	-4.075	-4.889	0.555

Table 3.2.5: Design parameters of various protonated forms at *p*H 7.4

Entry ID	MW	Dipole	SASA	FOSA	FISA	PISA	QPlogPo/w	QPlogS	QPlogKp	QPlogKhsa
MNA	216.236	4.352	444.137	136.445	100.097	207.596	3.212	-3.832	-2.345	-0.191
TD1	342.437	3.592	685.361	427.866	51.84	205.656	2.621	-2.255	-5.3	0.022
TD1A	342.437	3.293	665.391	419.957	39.965	205.469	2.566	-1.876	-5.081	-0.039
TD1B	342.437	3.511	685.503	429.624	50.219	205.66	2.636	-2.257	-5.27	0.024
TD1C	342.437	3.885	674.199	432.612	36.132	205.454	2.694	-2.043	-5.011	0.006
TD2	356.464	3.504	716.004	461.585	48.764	205.655	3.016	-2.673	-5.147	0.146
TD2A	356.464	3.25	694.709	452.651	36.577	205.48	2.953	-2.269	-4.923	0.08
TD2B	356.464	3.436	714.667	462.323	46.684	205.66	3.033	-2.647	-5.109	0.147
TD2C	356.464	3.803	703.38	463.954	33.96	205.466	3.068	-2.433	-4.875	0.123
TD3	370.447	6.281	697.287	419.979	71.832	205.476	2.23	-2.023	-3.606	-0.419
TD4	404.508	4.647	753.889	338.856	23.969	391.063	5.104	-5.296	-2.07	0.761
TD5	370.491	3.469	748.968	494.501	48.812	205.655	3.411	-3.134	-5.052	0.279
TD5A	370.491	3.252	727.377	485.437	36.462	205.478	3.347	-2.725	-4.825	0.213
TD5B	370.491	3.409	747.891	495.741	46.492	205.658	3.428	-3.114	-5.009	0.279
TD5C	370.491	3.774	736.49	497.364	33.673	205.453	3.466	-2.898	-4.773	0.257
TD6	384.517	3.46	781.854	527.402	48.798	205.654	3.805	-3.595	-4.956	0.412
TD6A	384.517	3.244	760.269	518.393	36.416	205.461	3.743	-3.186	-4.728	0.346
TD6B	384.517	3.404	780.518	528.383	46.478	205.657	3.821	-3.57	-4.913	0.412

TD6C	384.517	3.767	769.175	530.063	33.657	205.455	3.86	-3.355	-4.677	0.39
TD7	356.464	3.481	720.644	461.057	53.952	205.636	3.009	-2.761	-5.243	0.159
TD7A	356.464	3.614	710.961	447.778	57.542	205.64	2.905	-2.577	-5.309	0.123
TD7B	356.464	2.915	731.703	465.735	58.326	207.641	3.059	-2.97	-5.316	0.193
TD7C	356.464	3.428	720.827	462.441	52.747	205.639	3.045	-2.764	-5.22	0.171
TD8	370.491	3.029	764.472	500.012	56.81	207.65	3.438	-3.428	-5.192	0.315
TD8A	370.491	3.546	740.351	480.748	53.962	205.641	3.295	-2.971	-5.147	0.243
TD8B	370.491	2.958	760.903	498.462	54.79	207.65	3.456	-3.361	-5.155	0.317
TD8C	370.491	2.112	764.115	499.389	57.084	207.642	3.454	-3.421	-5.197	0.323
TD9	384.474	5.784	751.772	451.368	94.771	205.634	2.565	-2.895	-3.932	-0.242
TD10	418.535	4.397	807.847	369.905	46.609	391.333	5.441	-6.156	-2.39	0.937
TD11	384.517	3.043	797.314	532.949	56.717	207.648	3.833	-3.888	-5.094	0.448
TD11A	384.517	3.519	772.451	512.966	53.855	205.629	3.685	-3.417	-5.049	0.374
TD11B	384.517	2.949	794.134	531.885	54.605	207.645	3.851	-3.828	-5.056	0.449
TD11C	384.517	3.371	783.035	526.995	50.403	205.637	3.818	-3.617	-4.985	0.423
TD12	398.544	3.048	830.194	565.846	56.697	207.652	4.227	-4.348	-4.998	0.581
TD12A	398.544	3.515	805.395	545.934	53.841	205.62	4.08	-3.878	-4.953	0.507
TD12B	398.544	2.957	826.759	564.526	54.589	207.644	4.244	-4.283	-4.959	0.582
TD12C	398.544	3.365	815.766	559.76	50.373	205.634	4.212	-4.075	-4.889	0.555

Table 3.2.6: pKa of 6-MNA **(16)** and its derivatives at physiological pH 7.4 using H_2O as solvent.

Title	pKa 1	pKa 2
MNA	4.316	-
TD1	3.572	7.719
TD2	3.657	7.863
TD3	6.335	-
TD4	3.49	7.324
TD5	3.675	7.892
TD6	3.678	8.079
TD7	4.214	7.749
TD8	4.299	7.893
TD9	6.592	-
TD10	3.681	7.581
TD11	4.317	7.922
TD12	4.32	8.109

3.2.2 Syntheses and characterization of prodrugs (25a-25d and 26a-26d)

Considering the optimum values for ideal prodrug design from the above studies and feasibility of their synthesis it was planned to synthesize eight derivatives **(25a-25d and 26a-26d)** as shown below. **Scheme-1** was employed to synthesize piperazinylalkyl ester prodrugs of 6-MNA **(16)**.
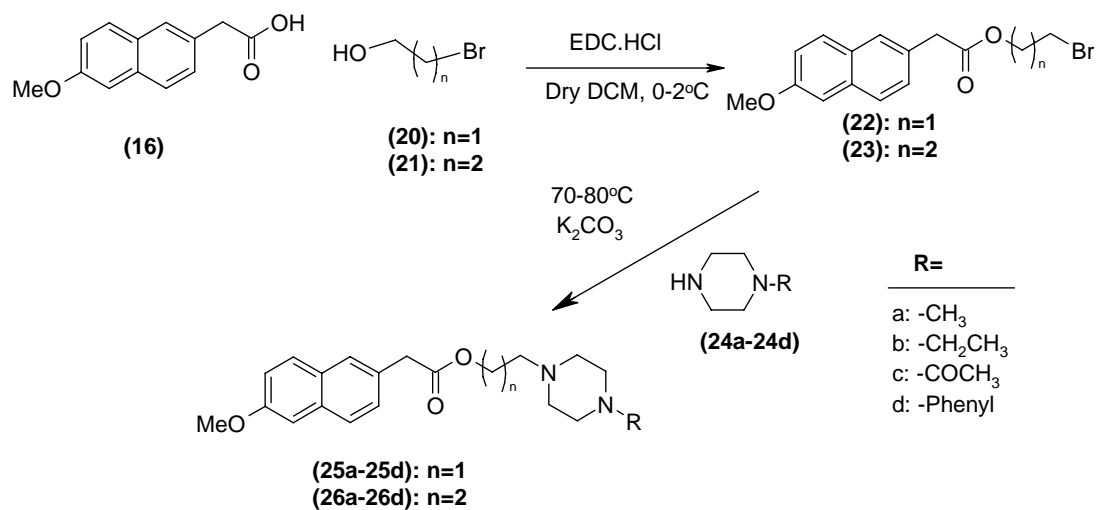
Scheme-1: Synthesis of prodrugs of 6-MNA **(16)**

6-MNA **(16)** was coupled with 2-bromoethanol **(20)** using 1-ethyl-3-(3-dimethylaminopropyl)carbodiimide (EDC) as coupling agent and dimethylaminopyridine (DMAP) as catalyst in dry dichloromethane (DCM) at 0-2 ^{0}C to obtain the desired intermediate 2-bromoethyl 2-(6-methoxy-2-naphthyl)acetate **(22).**

(22)
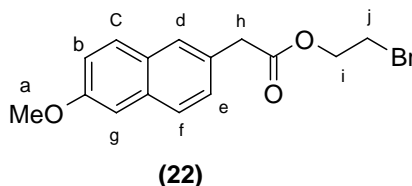
The structure was confirmed by IR spectroscopy which showed strong absorption peak at 1727 cm^{-1} due to carbonyl stretching of ester group. PMR spectrum showed multiplet at δ 7.71-7.11 of six naphthalene protons (Ar-H_{b-g}), a triplet at δ 4.42-4.39 due to methylene protons (-CH_{2i}) with coupling constant equal to 6.08 Hz. Methoxy protons (-O$CH_{3/a}$) appeared at δ 3.91 as singlet and methylene protons attached to aromatic ring (-$CH_{2h)}$ appeared at δ 3.79. A triplet due to methylene protons (-$CH_{2/j}$) was observed at δ 3.51-3.48 with coupling constant equal to 6.08 Hz.

Similarly another intermediate **(23)** required for synthesis of the final derivatives was prepared according to the same procedure as adopted for **22** using 6-MNA **(16)** and 3-bromo-1-propanol **(21)** to give 3-bromopropyl 2-(6-methoxy-2-naphthyl)acetate **(23)** as a white solid.

(23)
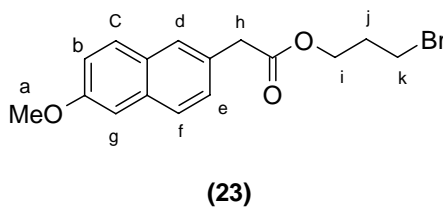
It was confirmed by IR spectroscopy which showed strong absorption peak at 1735 cm^{-1} due to carbonyl stretching of ester group. The PMR spectrum of compound **(23)** showed multiplet at δ 7.71-7.11 for the six naphthalene protons (Ar-H_{b-g}) and methylene protons (-$CH_{2/i,}$) appeared at δ 4.25-4.22 as a triplet with coupling constant equal to 6.4 Hz. Methoxy protons (-O$CH_{3/a}$) showed singlet at δ 3.91 and a singlet of methylene protons attached to aromatic ring (Ar-C$H_{2/h}$) appeared at δ 3.75. Other methylene protons (-$CH_{2/k}$) appeared at δ 3.40-3.36 as a triplet with coupling constant equal to 6.04 Hz. Multiplet at δ 2.18-2.11 appeared due to methylene protons (-$CH_{2/j}$) with coupling constant equal to J=6.0 Hz.

3.2.2.1 Syntheses of substituted piperazinethyl esters (25a-25d) of 6-MNA (16)

Synthesis of substituted piperazinethyl esters **(25a-25d)** of 6-MNA **(16)** were carried out by using synthetic route shown in **Scheme-1**. The reaction of 2-bromoethyl 2-(6-methoxy-2-naphthyl)acetate **(22)** with substituted piperazines **(24a-24d)** was accomplished by refluxing the reagents in dry acetone with two drops of DMF and potassium carbonate at 70-80 ^{0}C till the reaction got completed.

The synthesis of 2-(4-methylpiperazin-1-yl)ethyl 2-(6-methoxy-2-naphthyl)acetate **(25a)** was carried out in the same fashion as described above by reacting 2-bromoethyl 2-(6-methoxy-2-naphthyl)acetate **(22)** and *N*-methylpiperazine **(24a)** to get brown oily product **(25a)**.

(25a)
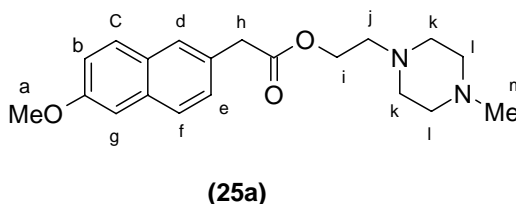
The IR spectrum **(Fig. 3.2.2.A)** of the ester **(25a)** showed absorption peak at 1730 cm^{-1} due to carbonyl stretching of ester group. The peaks at 1264 cm^{-1} and 1148 cm^{-1} are due to C-O and C-N stretching vibration's respectively. Its PMR spectrum **(Fig. 3.2.2.B)** showed multiplet at δ 7.63-7.03 for six naphthalene protons (Ar-H_{b-g}) and a triplet at δ 4.16-4.13 due to methylene (-C$H_{2/i}$) protons with coupling constant equal to 5.8 Hz. A singlet due to methoxy protons (-C$H_{3/a}$) appeared at δ 3.83 and of methylene (Ar-C$H_{2/h}$) at δ 3.68. The other methylene protons (N-C$H_{2/j}$) showed triplet at δ 2.54-2.51 with coupling constant equal to 5.8 Hz. The piperazine protons appeared as multiplet at δ 2.38-2.27 (-$H_{k,l}$) and *N*-methyl protons (-C$H_{3/m}$) at δ 2.16 as a singlet.

^{13}C-NMR spectrum **(Fig. 3.2.2.C)** shows peak at 171.67 for carbonyl carbon. Aromatic carbons of naphthalene ring (10C) appear in the range of δ 157.62-105.56. Methoxy carbon appears at δ 56.2 and -OCH_2 at δ 62.31. Four piperazine carbons were observed at δ 52.12-55.3. Other aliphatic carbons appeared at δ 52.93 (N-CH_2), δ 52.12-52.64 (2C, piperazine, *C*-2,6), δ 45.70 (Ar-CH_2-) and δ 41.20 (1C, N-CH_3). Mass spectrum **(Fig. 3.2.2.D)** shows molecular ion peak at 342.5 (M$^+$) and also M+2 peak at 344.0 which is base peak. The compound showed high chromatographic purity (>98.2 %) by HPLC **(Fig. 3.2.2.E)**.

Other compounds **(25b-25d)** of the series were prepared in the same fashion as described for derivative **(25a)**; their analytical data are given in **Table 3.2.7.**

(A)

(B)

(C)

204
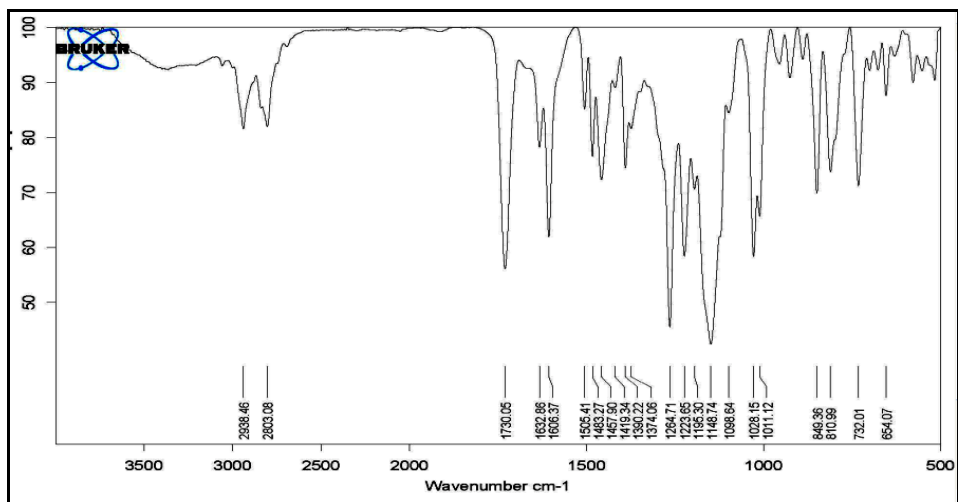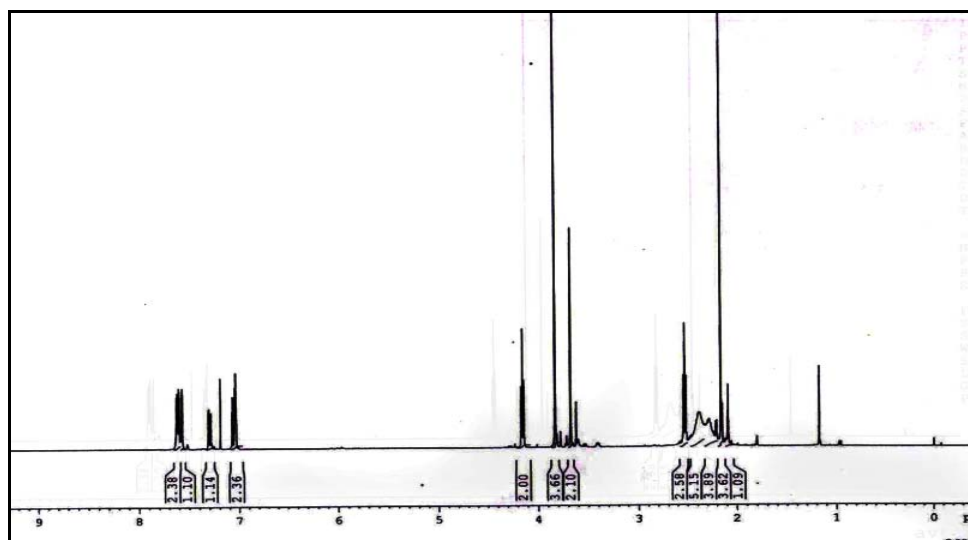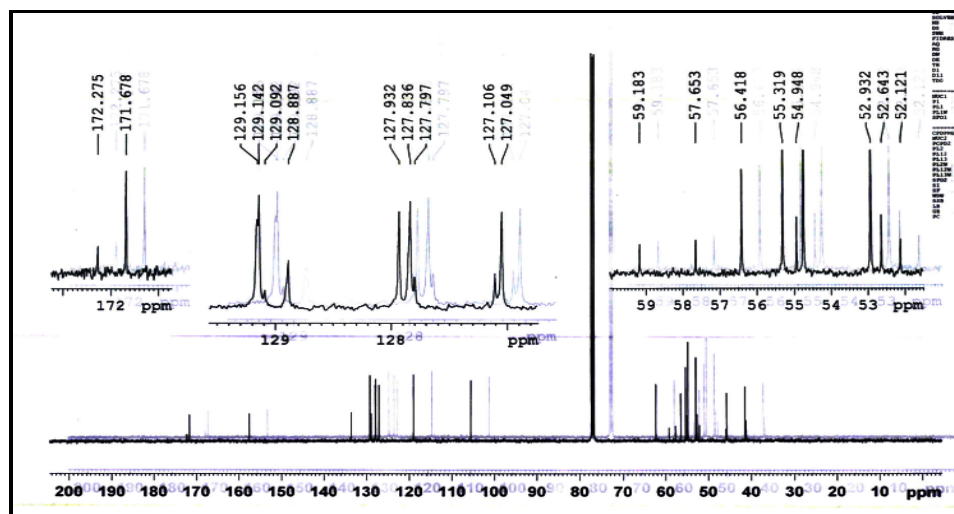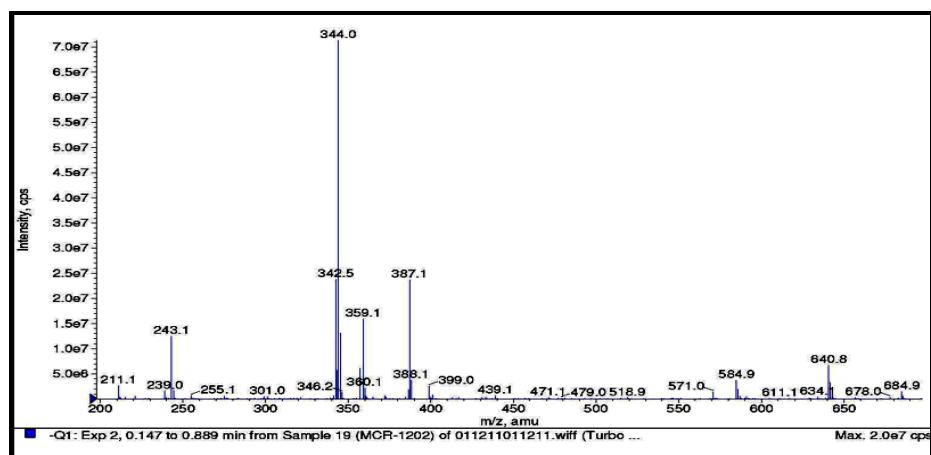
(D)
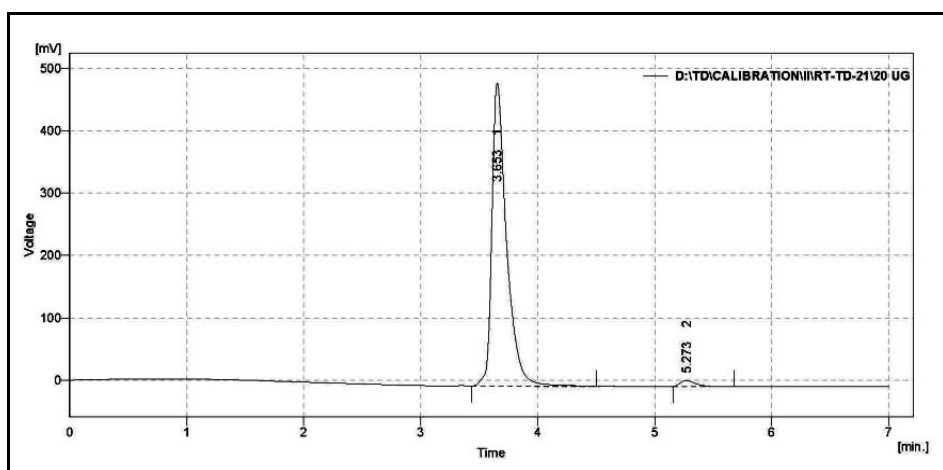
(E)

Fig. 3.2.2: Spectra of derivative **(25a)**; IR spectrum **(A)**, ^{1}H-NMR **(B)**, ^{13}C-NMR **(C)**, Mass spectrum **(D)** and HPLC chromatogram **(E)**.

3.2.2.2 Synthesis of substituted piperazinpropyl esters (26a-26d) of 6-MNA

Synthesis of substituted piperazinylalkyl esters **(26a-26d)** of 6-MNA were carried out as per the synthetic route shown in **Scheme-1**. The reaction of 3-bromopropyl 2-(6-methoxy-2-naphthyl)acetate **(23)** with substituted piperazines **(24a-24d)** was accomplished by refluxing both the reactants in dry acetone with two drops of DMF and potassium carbonate at 70-80 ^{0}C till the reaction got completed.

The product was isolated and purified by column chromatography to get a brown oily product. IR spectrum **(Fig. 3.2.3. A)** of the compound **(26a)** showed a strong absorption peak at 1732 cm^{-1} due to carbonyl stretching of ester group. The peaks at 1398 cm^{-1} and 1163 cm^{-1} are due to C-O and C-N stretching vibrations respectively. The PMR signals of compound **(26a)** appeared at δ 7.62-7.02 (m, 6H, Ar-*H*b-g), 4.07-4.04 (t, 2H, -

C$H_{2/i}$), 3.81 (s, 3H, -OC$H_{3/a}$), 3.64 (s, 2H, Ar-C$H_{2/h}$), 2.34-2.28 (m, 8H, N-CH_2/$_{l-m}$), 2.27-2.23 (t, 2H, -C$H_{2/k}$), 2.16 (s, 3H, -C$H_{3/n}$) and 1.75-1.74 (m, 2H, -C$H_{2/j}$) **(Fig. 3.2.3. B)**
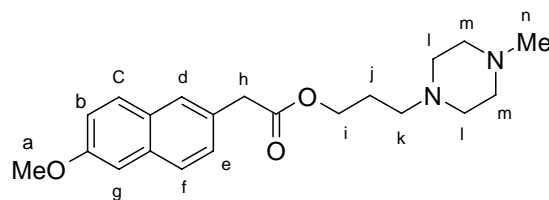
(26a)

^{13}C-NMR spectrum **(Fig. 3.2.3. C)** shows peaks at 17.76, 168.92, 157.65, 133.59-105.56, 62.94, and 55.32-21.31. The mass spectrum **(Fig. 3.2.3. D)** of compound **(26a)** shows peak at 356.03 (M$^+$) which is also the base peak. The compound also showed high chromatographic purity (>98 %) by HPLC.

(A)

(B)

206
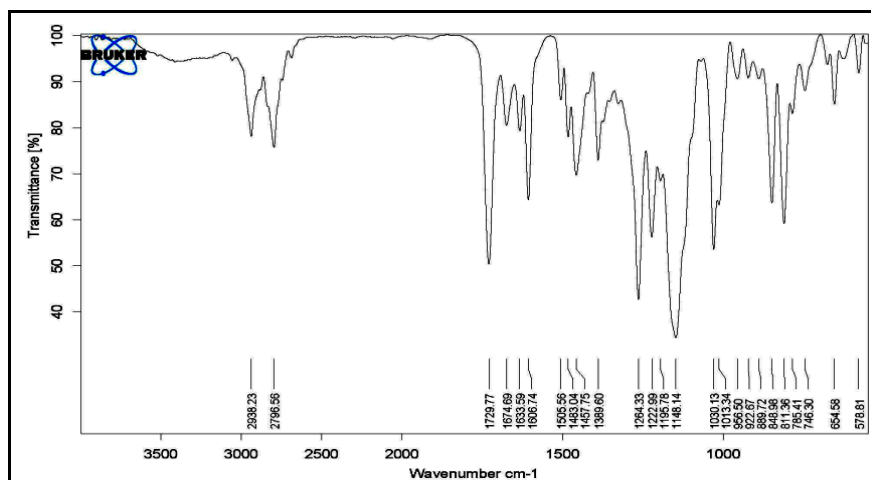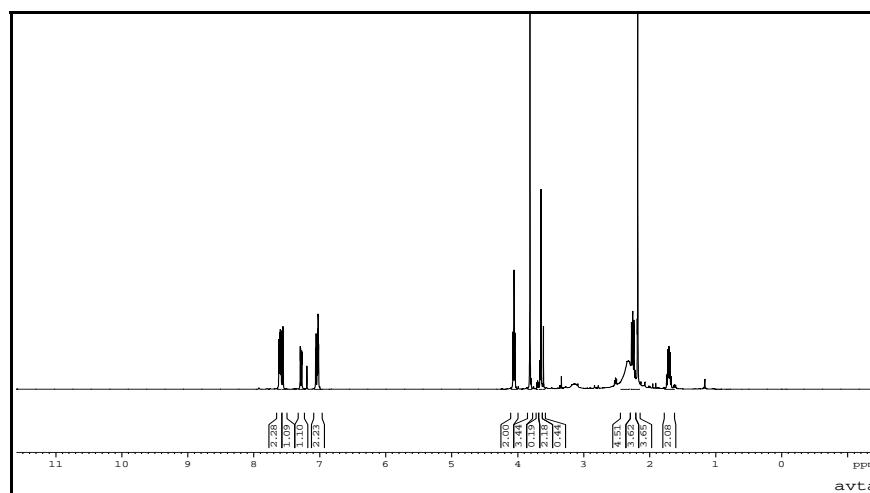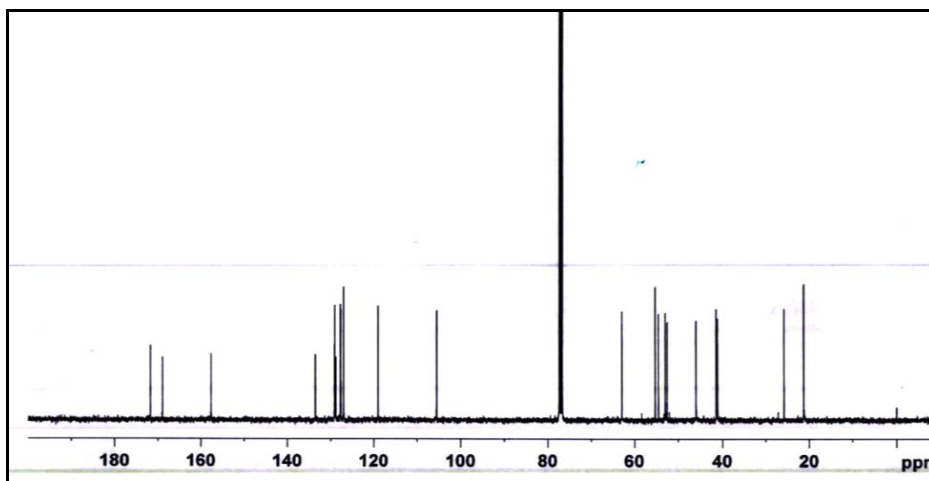
(C)
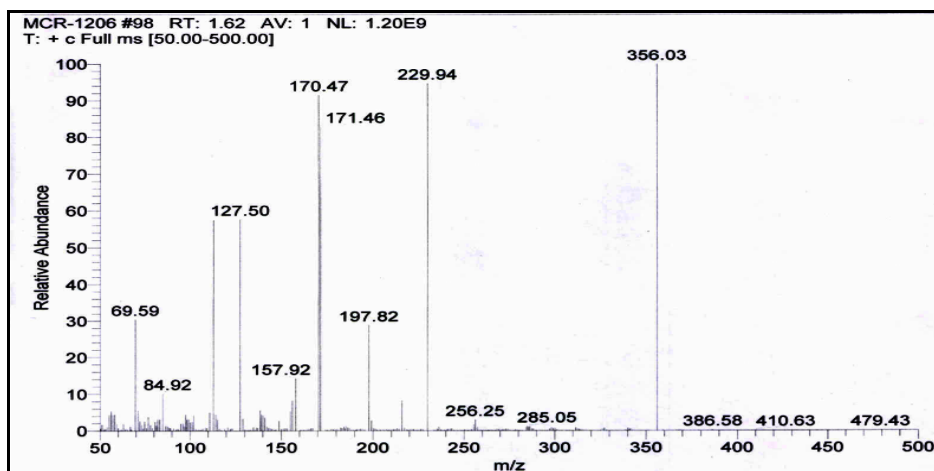
(D)
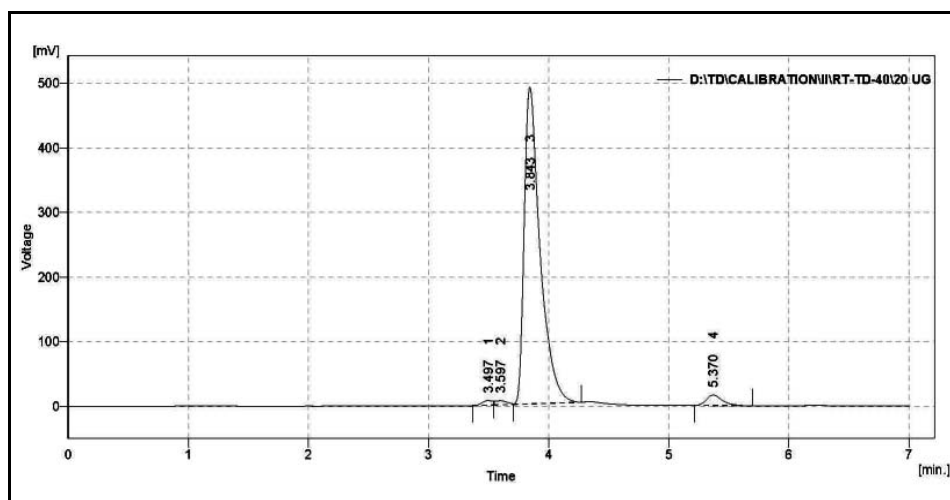
(E)

Fig. 3.2.3: Spectra of derivative **(26a)**; IR spectrum **(A)**, ^{1}H-NMR **(B)**, ^{13}C-NMR **(C)**, Mass spectrum **(D)** and HPLC chromatogram **(E)**.

Syntheses of other derivatives **(26b-26d)** from this series were carried out by the procedure as described above and their spectral data is given in **Table 3.2.7**

Table 3.2.7: Spectral data of derivatives **(25b-25d** and **26b-26d)**

Compound No.	IR Peaks (cm^{-1})	PMR Peaks (δ)
25b	1731, 1264,1151	7.03-7.63 (m, 6H), 4.14-4.17 (t, 2H), 3.83 (s, 3H), 3.68 (s, 2H), 2.52-2.54 (t, 2H), 2.34-2.38 (m, 8H), 2.26-2.31 (q, 2H), 0.95-0.99 (t, 3H)
25c	1730, 1263, 1150	7.03-7.63 (m, 6H), 4.13-4.16 (t, 2H), 3.82 (s, 3H), 3.67 (s, 2H), 3.40-3.43 (t, 2H), 3.11-3.13 (t, 2H), 2.50-2.52 (t, 2H), 2.27-2.29 (t, 2H), 2.19-2.21 (t, 2H), 1.90 (s, 3H)
25d	1720, 1234, 1147	7.22-7.70 (m, 6H), 6.80-7.15 (m, 5H), 4.27-4.29 (t, 2H), 3.90 (s, 3H), 3.77 (s, 2H), 2.95-3.02 (t, 4H), 2.64-2.67 (t, 2H), 2.49-2.52 (t, 4H)
26b	1732, 1265,1156	6.95-7.55 (m, 6H), 3.96-3.99 (t, 2H), 3.75 (s, 3H), 3.54 (s, 2H), 2.47-2.50 (t, 2H), 2.26-2.42 (m, 8H), 2.19-2.21 (m, 2H), 1.55-1.58 (m, 2H), 0.94-0.97 (m, 3H)
26c	1728, 1263, 1150	7.11-7.70 (m, 6H), 4.13-4.17 (t, 2H), 3.91 (s, 3H) 3.73 (s, 2H), 3.54-3.57 (t, 2H), 3.35-3.38 (t, 2H), 2.27-2.33 (m, 6H), 2.05 (s, 3H), 1.77-1.80 (m, 2H)
26d	1736, 1267, 1155.	7.15-7.63 (m, 6H), 6.75-7.07 (m, 5H), 4.07-4.11 (t, 2H), 3.81 (s, 3H), 3.66 (s, 2H), 3.04-3.06 (t, 4H), 2.40-2.43 (t, 4H), 2.28-2.32 (t, 2H), 1.73-1.77 (m, 2H)

3.2.3 Physicochemical evaluation of 6-MNA and the synthesized prodrugs (25a-25d and **26a-26d)**

For the evaluation of various physicochemical parameters such as aqueous solubility, partition coefficient and hydrolysis kinetics study, HPLC method has been developed. Calibration curve for 6-MNA **(16)** and its different prodrugs were plotted and their linearity calculated.

Chromatographic conditions

Chromatography was performed under isocratic conditions at a flow-rate of 0.9 ml/min. The mobile phase consisted of phosphate buffer (PB, 15 mM): acetonitrile (1:1)

and methanol:acetonitrile (9:1). Solution of the prodrug was filtered through Whatman filter paper (0.2 μ) and degassed for 10 min in an ultrasonic bath. An aliquot of sample solution (20 μl) was injected onto the analytical column with a manual injection, the column effluent was monitored at 227 nm.

Table 3.2.8: Chromatographic conditions for **(16)** and derivatives **(25a-26d)**

Derivative	Linearity range (µg)	Mobile phase composition	Flow rate (ml/min.)	Retention time (R_t Min.)	λ_{max}
16				4.73 ± 0.2	230
25a				3.65 ± 0.2	
25b	0.5-40	PB:ACN (1:1)	0.9	3.88 ± 0.2	
26a				3.84 ± 0.2	
26b				4.14 ± 0.2	227
25c	0.5-30			3.17 ± 0.2	
25d		MeOH:ACN (9:1)	1.0	3.69 ± 0.2	
26c	0.5-45			3.15 ± 0.2	
26d				3.60 ± 0.2	

PB=Phosphate buffer (15 mM), MeOH=Methanol, ACN=Acetonitrile
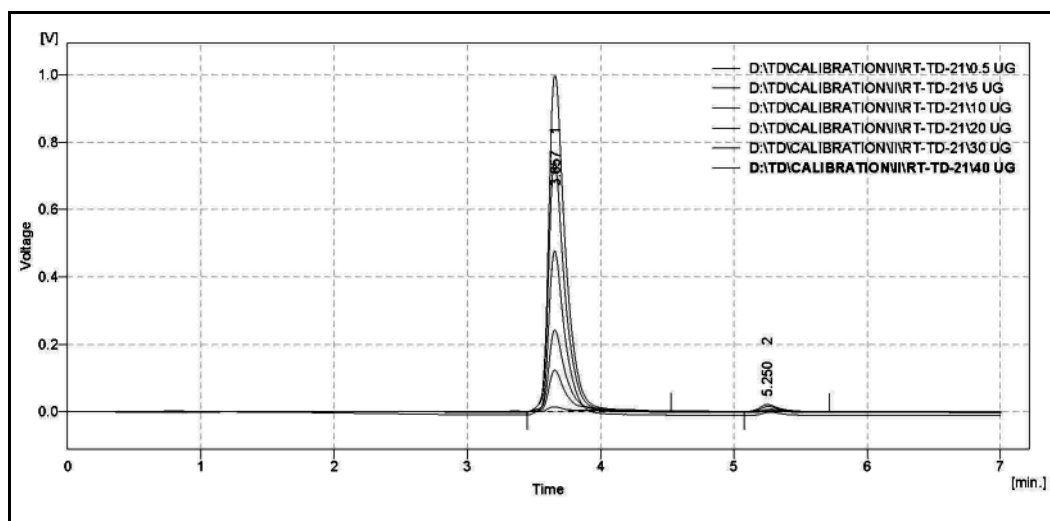
Fig. 3.2.12: Retention time and linearity plot for prodrug **(25a)**
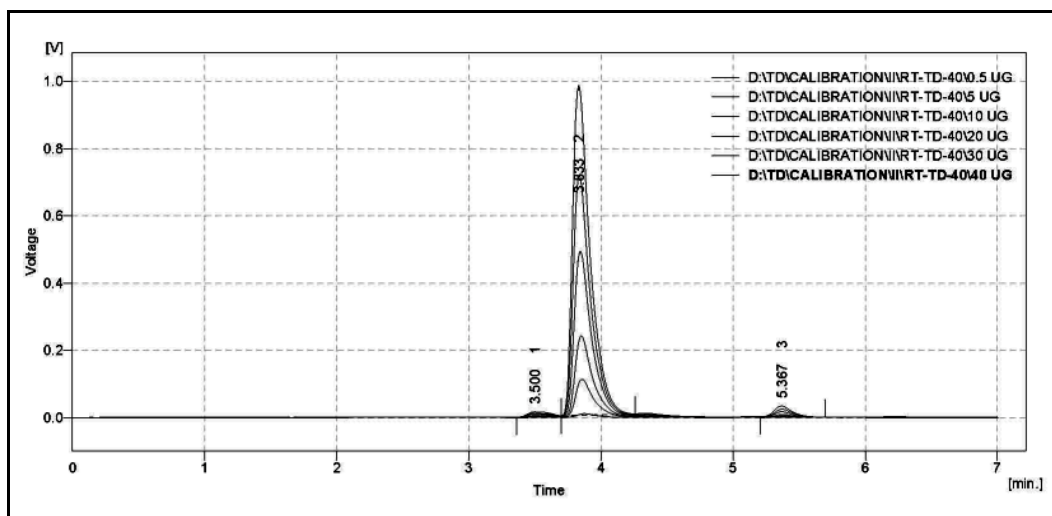
Fig. 3.2.13: Retention time and linearity plot for prodrug **(26a)**

Table 3.2.9: Data for preparation of calibration curve for estimation of **(25a-25b** and **26a-26b)**

Conc. (µg/ml)	Area (mVs) for 25a-25b	Area (mVs) for 26a-26b
0.5	257±5	128±6
5	1209±11	1120±10
10	2166±19	2233±18
20	4224±28	4479±34
30	6410±35	6720±55
40	8735±5	9027±64

Table 3.2.10: Data for preparation of calibration curve for estimation of **(25c-25d and 26c-26d)**

Conc. (µg/ml)	Area (mVs) for 25c-25d	Area (mVs) for 26c-26d
0.5	118 ±8.0	124±9
5	915 ±15.0	1266±15
10	1712±23.0	2712±28
15	2398±36	--
20	3184±45	5720±39
25	4038±67	--

30	4884±74	8615±57
45	--	12450±84
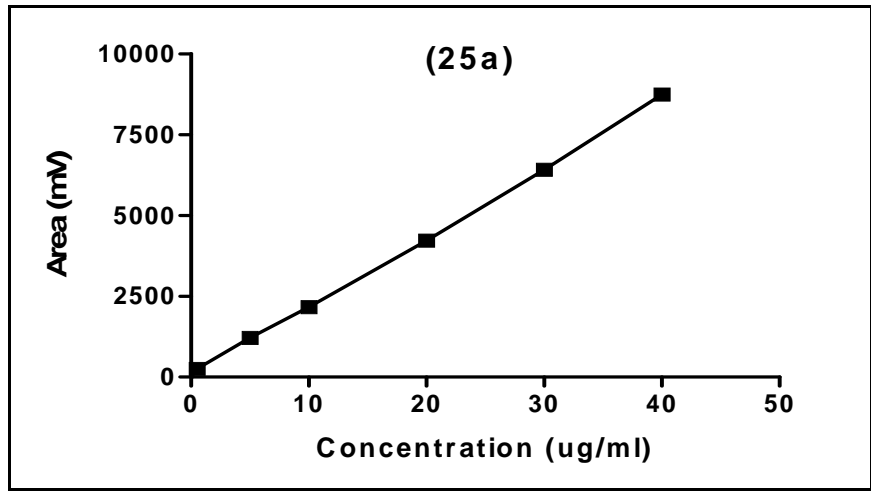
(A): y=216.1x+83.36 (R^2=0.999)
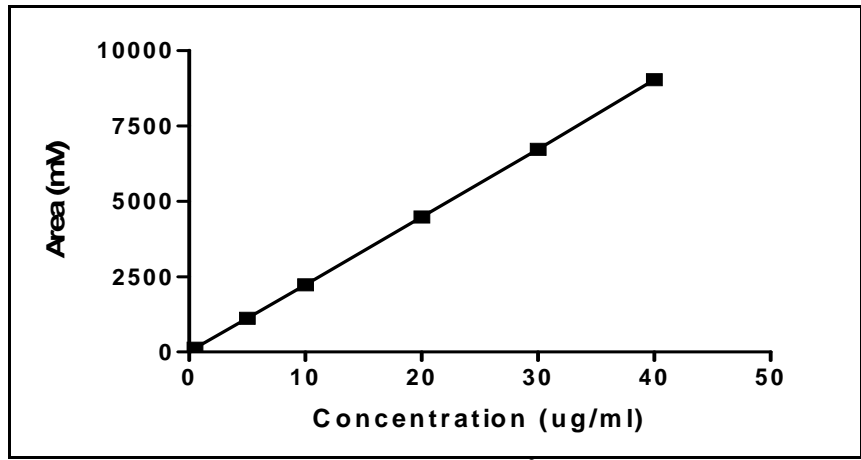
(B): y=224.8x-6.70 (R^2=1.00)
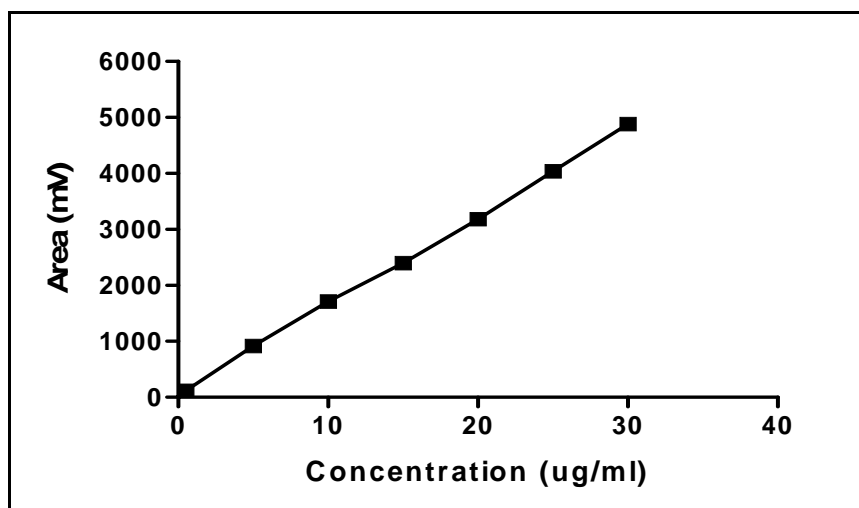
(C): $y=162.1x-68.71$ ($R^2=0.998$)
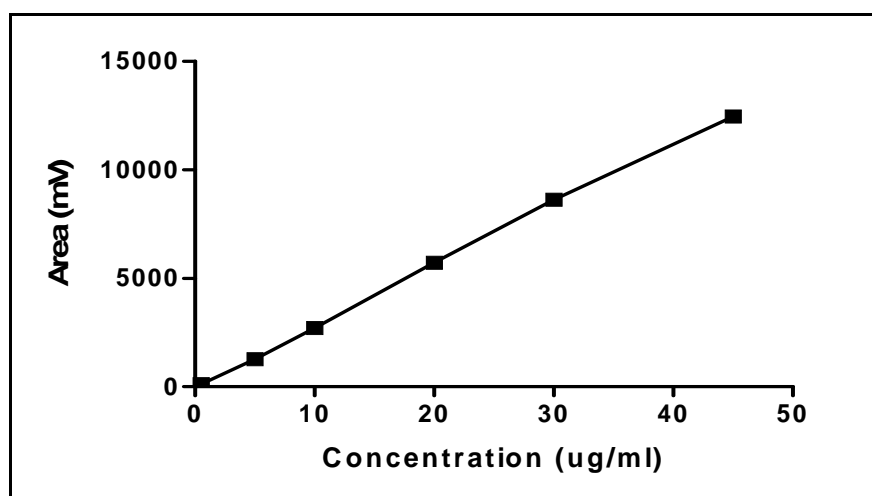
(D): $y=281.1x-28.58$ ($R^2=0.999$)

Fig. 3.2.17: Calibration plot for estimation of **A: 25a-25b; B: 26a-26b; C: 25c-25d; D:** 26c-26d

3.2.2.1 Determination of aqueous solubility of the prodrugs

Due to biphasic nature of skin, the ideal topical prodrug should exhibit adequate lipid solubility as well as aqueous solubility. Aqueous solubility of 6-MNA and its prodrugs were determined at the physiological pH 7.4 and at pH 5.0 the pH of of the outer surface of the skin (pH 4.2-6.5).[4]

Table 3.2.11: Aqueous solubility of 6-MNA and prodrugs at pH 5.0 and pH 7.4

Compound	Aqueous Solubility (mM)	
	pH 5.0	pH 7.4
16	0.78 ± 0.18	63.34 ± 0.24
25a	23.41 ± 0.16	21.58 ± 0.23
25b	26.01 ± 0.23	12.10 ± 0.17
25c	1.22 ± 0.01	1.49 ± 0.01
25d	0.292 ± 0.002	0.314 ± 0.002
26a	28.41 ± 0.19	20.09 ± 0.16
26b	16.30 ± 0.14	6.20 ± 0.03
26c	6.07 ± 0.02	3.11 ± 0.01
26d	0.267 ± 0.001	0.019 ± 0.0002

Generally an ionized molecule is more water soluble than its unionized form. Because of the acidic character of 6-MNA (pKa 4.16) it is more soluble in aqueous medium at pH 7.4 than at pH 5.0. On the other hand piperazinyl prodrugs **(25a-25b** and **26a-26b)** which possess basic ionizable group (N^1 and/or N^4) get more ionized at pH 5.0 than at pH 7.4. Piperazinyl prodrugs **(25c-25d** and **26c-26d)** with electron withdrawing groups at N^4 have only one basic ionizable group that makes them less soluble at pH 5.0 with no significant differences observed at pH 7.4. The aqueous solubility of 6-MNA is higher at pH 7.4 and for piperazinyl prodrugs **(25a-25b** and **26a-26b)** it is higher at pH 5.0 Overall, substituted piperazinylalkyl prodrugs exhibited higher aqueous solubility as compared to 6-MNA **(16)** at pH 5.0. Aqueous solubility of all piperazinylalkyl prodrugs of 6-MNA at pH 7.4 was found to be comparatively lesser than 6-MNA.
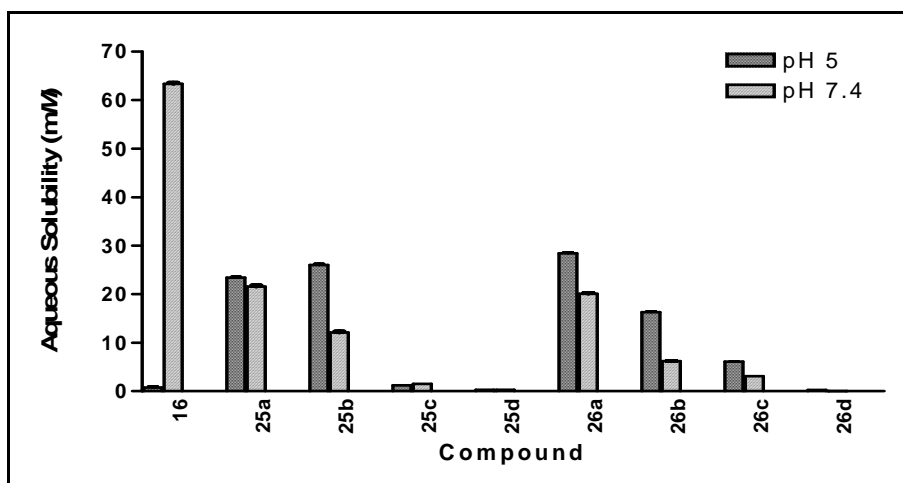
(A)
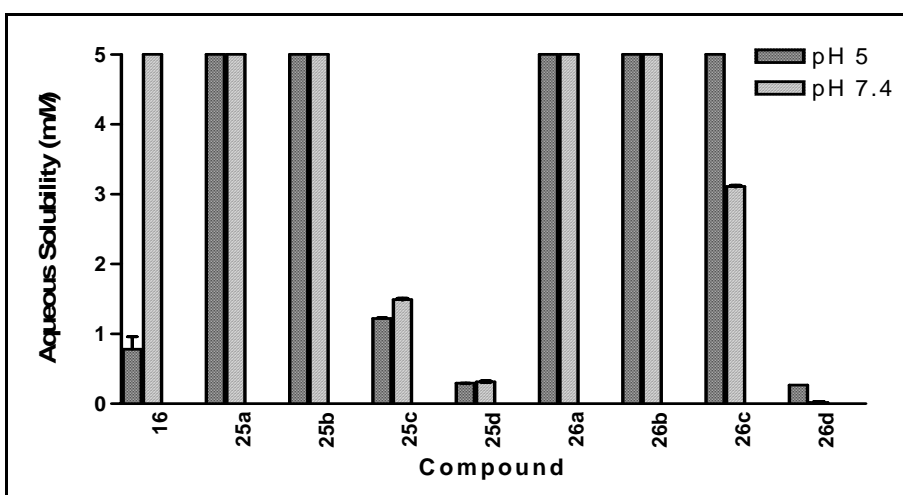
(B)

Fig. 3.2.18: A-Comparison of aqueous solubility at *p*H 5.0 and *p*H 7.4, **B**-expanded view
scale 0-5 m*M* (Y axis). P<0.0001 compared to 6-MNA **(16)** (Bonferroni's test
one way ANOVA)

The data showed that aqueous solubility of piperazinyl prodrugs was *p*H dependent
and lowering the *p*H generally increased aqueous solubility of the prodrugs. Substituted
piperazinyl promoieties seemed to be suitable for maintaining or increasing the aqueous
solubility of 6-MNA at *p*H range 5.0 and *p*H 7.4.

3.2.2.2 Determination of apparent partition coefficient (Log *P*app)

Lipid solubility plays a crucial role in determining skin permeability of a particular
compound because stratum corneum (SC) the major barrier to drug permeation is
essentially lipoidal in nature and generally favors permeation of lipophilic drugs. The
apparent partition coefficients of 6-MNA **(16)** and prodrugs were determined by

214

partitioning them between phosphate buffer (0.16 M) and saturated *n*-octanol at *p*H 5.0 and *p*H 7.4 using shake flask method.

Although the partition domain of human SC lipids is more polar than octanol.[5-6] octanol is often used to estimate skin/water partition coefficient because the partionating in 1-octanol/water system mimics the partition in skin/water system.[7] The apparent partition coefficients of 6-MNA **(16)** and prodrugs are listed in **Table 3.2.12.**

All of the prodrugs of 6-MNA **(16)** have retained more or less comparable lipophilicity at pH 5.0 except derivative **(25d,** log P_{app}=2.171±0.005) which is more lipophilic than 6-MNA **(16)** (log P_{app}=1.823±0.002). At *p*H 7.4 all the prodrugs showed increased log P_{app} values as compared to 6-MNA with a maximum increase in lipophilicity of about 10 fold for prodrug **(26d)**

Table 3.2.12: Log P_{app} values of 6-MNA **(16)** and its prodrugs **(25a-25d and 26a-26d)**

Compound	Log P_{app}	
	*p*H 5.0	*p*H 7.4
16	1.823 ± 0.002	-0.233 ± 0.012
25a	0.104 ± 0.001	0.235 ± 0.001
25b	0.041 ± 0.001	0.434 ± 0.003
25c	1.217 ± 0.001	0.911 ± 0.001
25d	2.171 ± 0.005	1.164 ± 0.010
26a	0.119 ± 0.002	0.220 ± 0.007
26b	0.069 ± 0.005	0.539 ± 0.006
26c	0.372 ± 0.002	0.670 ± 0.001
26d	1.147 ± 0.003	2.04 ± 0.01
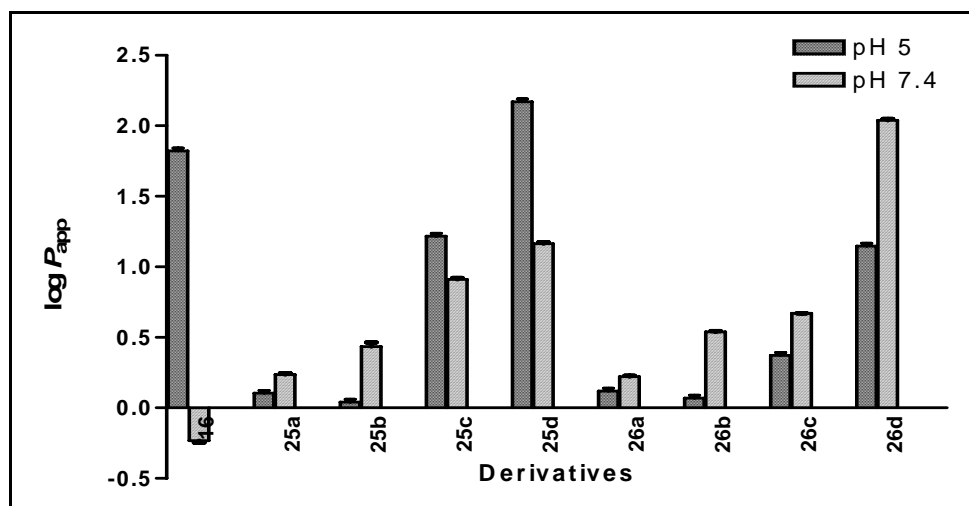
Fig. 3.2.19: Comparison of log P_{app} values at pH 5.0 and pH 7.4, P <0.0001 compared with 6-MNA **(16)** (Bonferroni's test one way ANOVA)

Although the lipophilicity of most of the prodrugs were lower at pH 5.0 than at pH 7.4 but some of them maintained good lipophilicity (logP_{app} = 0.04-2.17) at this pH (5.0). The lipophilicity of all the prodrugs of 6-MNA **(16)** varied widely due to changes in promoieties. For an effective dermal penetration, prodrugs should possess not only high lipophilicity but also adequate aqueous solubilities which is improved in this case by piperazinyl promoieties.

3.2.3 Hydrolyses kinetics studies

In addition to suitable aqueous and lipid solubility, percutaneous prodrugs should be stable chemically in bulk form and in dosage formulations. Thus, degradation of prodrugs was studied both at physiological pH 7.4 and in acidic pH 5.0 at constant temperature 37±1 ^{0}C. To determine the order of reaction three main methods are generally employed i.e. substitution method, half-life method and graphical method, The most commonly used method is graphical method, which is used here for determining the order of reaction.

3.2.3.1 Determination of order of reaction for derivative (25a) at pH 5.0

The data obtained for determining the order of reaction for prodrug (25a) at pH 5.0 is showed in **Tables 3.2.13-3.2.15**

Table 3.2.13: Data representation for calculation of rate constant (K) of derivative **(25a)** at pH 5.0 using zero order. Initial concentration **(y)** at 0 hours=**36.55 µg/ml**

Time (hrs)	Area (mVs)	Amt. degraded (x)	(y-x) (µg/ml)	(y-x) (mol/lit.)
0	7880	0	36.555	1.06×10^{-4}
12	7492	1.819	34.736	1.01×10^{-4}
48	5940	9.096	27.759	8.02×10^{-5}
60	5214	12.50	24.055	7.03×10^{-5}
72	4404	16.297	20.258	5.92×10^{-5}
84	3745	19.387	17.168	5.02×10^{-5}

Where, x = Concentration of the derivative (**25a**) which got hydrolysed at

various time intervals.

(y-x) = Concentration of the derivative (mol/lit) (**25a**) left in the solution

at various time intervals.

Table 3.2.14: Data representation for calculation of rate constant (K) of derivative **(25a)**

at pH 5.0 using first (log y-x); second 1/(y-x) and third $1/(y-x)^2$ order.

Time (hrs)	Area (mVs)	(y-x) (µg/ml)	Log (y-x)	1/(y-x)	$(y-x)^2$	$1/(y-x)^2$
0	7880	36.555	-3.971	9355	1.142×10^{-8}	8.75×10^{7}
12	7492	34.736	-3.993	9845	1.031×10^{-8}	9.69×10^{7}
48	5940	27.459	-4.095	12454	6.446×10^{-9}	1.55×10^{8}
60	5214	24.055	-4.152	14216	4.947×10^{-9}	2.02×10^{8}
72	4404	20.258	-4.227	16882	3.508×10^{-9}	2.85×10^{8}
84	3745	17.168	-4.299	19920	2.519×10^{8}	3.97×10^{8}

Where, Log (y-x) = Logarithmic value of concentration of the derivative (**25a**)

left in the solution at various time intervals.

Table 3.2.15: Order of reaction for derivative **(25a)** at pH 5.0

Order of reaction	R^2
Zero order	0.9489
First order	**0.9598**
Second order	0.9091
Third order	0.8422

217

So, from the value of R^2 it is apparent that the degradation kinetics of the compound (25a) followed first order because R^2 of first order is nearest to 1.

For first order half-life $t_{1/2}$ = 0.693/K, where K = rate constant
From first order equation, LogC = -Kt/2.303 + LogC$_0$
From the first order graph, slope = -K/2.303 = -0.0038

$$K = 0.00875$$

$$t_{1/2} = 0.693/K = 0.693/0.00875 = 79.18 \text{ hr}$$

3.2.3.2 Determination of order of reaction for derivative (25a) at *p*H 7.4

In a similar manner as described for derivative (25a) at *p*H 5.0, calculations were done at *p*H 7.4 for the reaction kinetics. The order of the reaction was determined and found out to be first order as shown in **Table 3.2.16.**

Table 3.2.16: Order of reaction for derivative (25a) at *p*H 7.4

Order of reaction	R^2
Zero order	0.6005
First order	**0.8685**
Second order	0.8038
Third order	0.5910

For the first order, half-life $t_{1/2}$ = 0.693/K, where K = rate constant
From first order equation, LogC = -Kt/2.303 + LogC$_0$
From the first order graph, slop = -K/2.303 = -0.0173

$$K = 0.03984$$

$$t_{1/2} = 0.693/K = 0.693/0.00875 = 17.39 \text{ hr}$$

Considering that the hydrolysis of the piperazinylalkyl ester derivatives followed first order degradation kinetics, further calculations were done for finding the rate constant (K) and hence half-life for other derivatives **(Table 3.2.17)** according to the first order kinetic equation i.e. LogC = -Kt/2.303 + LogC$_0$

The aqueous stability of piperazinyl prodrugs was *p*H dependent and stabilities were substantially greater at *p*H 5.0 than at *p*H 7.4. The reason for high instability at *p*H

7.4 is quite obvious as the esters are more prone to hydrolysis in alkaline medium due to higher concentration of hydroxide nucleophile.

3.2.3.3 Stability study in human serum

An essential prerequisite for the successful development of a percutaneous prodrug is its bioconversion to the drug in the skin. Distribution of esterases that are capable of hydrolyzing ester prodrugs are widespread in the body and several types of specific and non-specific esterases are found in blood and skin.[5-6] In the present study, the enzymatic hydrolysis kinetics study of prodrugs was carried out in human serum.

All prodrugs were found to be highly susceptible to enzymatic hydrolysis in human serum *in vitro*. They exhibited first order degradation kinetics and hydrolyzed quantitatively to the corresponding parent drugs. Half-life ($t_{1/2}$) values of prodrugs were summarized in **Table 3.2.17**

3.2.4 *In-vitro* skin permeation study

The diffusion experiments showed that both 6-MNA **(16)** and its prodrugs were able to permeate rat abdominal skin *in vitro*. For different prodrugs and for 6-MNA the cumulative amounts permeated through skin were plotted against time. A steady state flux (*J*ss) was obtained by dividing the slope of that graph by surface area of the diffusion cell.[1,8] The steady-state flux (*J*ss) of 6-MNA **(16)** and prodrugs were given in **Table 3.2.18.** All the prodrugs have shown higher flux values than the parent NSAID **(16).**

Table 3.2.17: Half-lives of the prodrugs in phosphate buffer at *p*H 5.0, 7.4 and in human Serum

| Compound | Half-life ($t_{1/2}$) | | |
| | Phosphate buffer ($t_{1/2 \text{ in}}$ hr) | | Human serum (90%) |
	*p*H 5.0	*p*H 7.4	($t_{1/2}$ in min)
25a	79.18	17.39	46.29
25b	250.76	21.96	37.61
25c	27.60	27.86	< 10*
25d	< 6*	< 6*	ND
26a	376.14	23.50	60.18
26b	601.82	45.59	29.79
26c	158.3	30.39	< 10*
26d	< 6*	< 6*	ND

*complete disappearance of derivatives within this time interval, ND: Not done

Amongst all of the prodrugs, prodrug **(26b)** has shown the highest steady state flux and **(25b)** the lowest. Prodrugs **(25a)** and **(26a)** have shown intermediate flux values but both have shown 5-fold and 7-fold higher values than the parent NSAID. Prodrug **(26b)** having the highest flux was 12-fold higher than the parent NSAID. The results showed that lipophilic piperazinyl prodrugs with adequate aqueous solubility increased the flux of 6-MNA **(16)**.

Table 3.2.18: Steady state flux and permeability coefficient of 6-MNA **(16)** and prodrugs **(25a-25b** and **26a-26b)**

Compound	Permeability coefficient K_p	Steady state flux Jss ($\mu g/cm^2 h$)
16	1.953	0.46
25a	0.356	2.23
25b	0.244	1.37
26a	0.286	2.98
26b	0.655	5.46

Table 3.2.19: Permeation profile data of **16** and derivatives **(25a-25b** and **26a-26b)**

Time (h)	Cumulative amount (μg)				
	16	**25a**	**25b**	**26a**	**26b**
1	3.85±0.60	21.33±0.80	13.11±0.90	25.28±1.60	37.52±1.40
2	5.81±0.90	30.54±1.10	18.79±1.30	43.67±2.40	95.95±4.50
4	16.01±1.10	85.46±1.60	51.43±2.30	109.56±4.70	196.35±8.90
8	29.49±1.50	148.97±3.10	96.54±4.50	201.04±5.90	310.45±12.30
12	31.80±1.80	178.69±5.60	104.55±5.30	235.81±9.60	384.14±18.99
24	37.96±10.0	210.33±12.31	131.65±6.10	283.61±18.47	560.44±32.13

The results clearly demonstrated that those prodrugs of 6-MNA **(16)** which possessed adequate lipid and aqueous solubility, permeated the skin better than those prodrugs which had low lipophilicity and poor aqueous solubility.
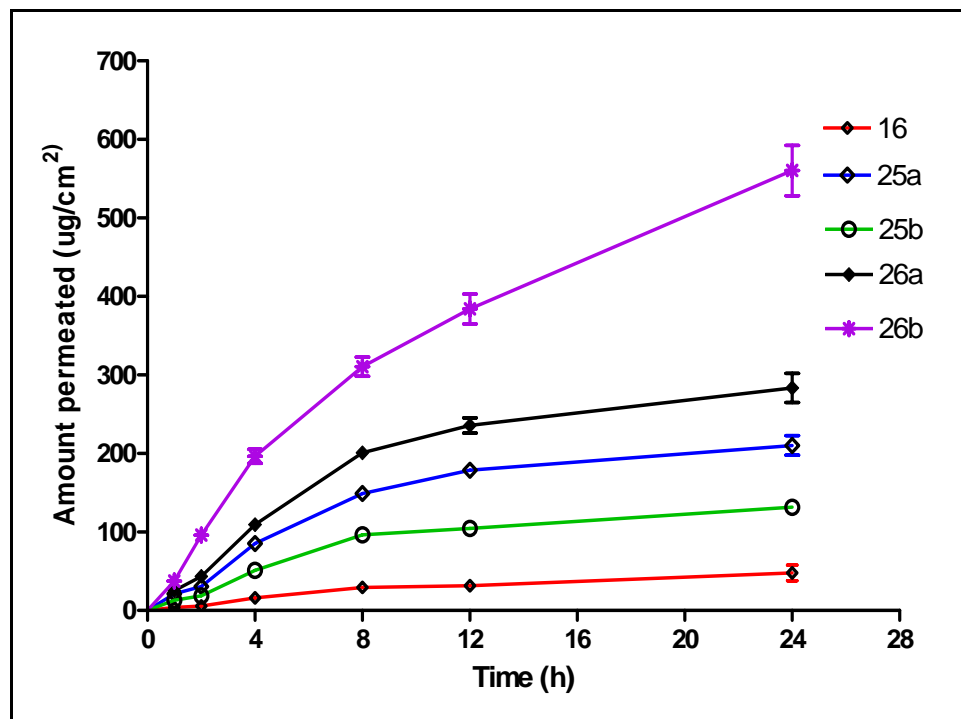
Fig. 3.2.20: Permeation profiles (mean SEM, n=3) for **16** and prodrugs

(25-25a-b and 26a-26b)
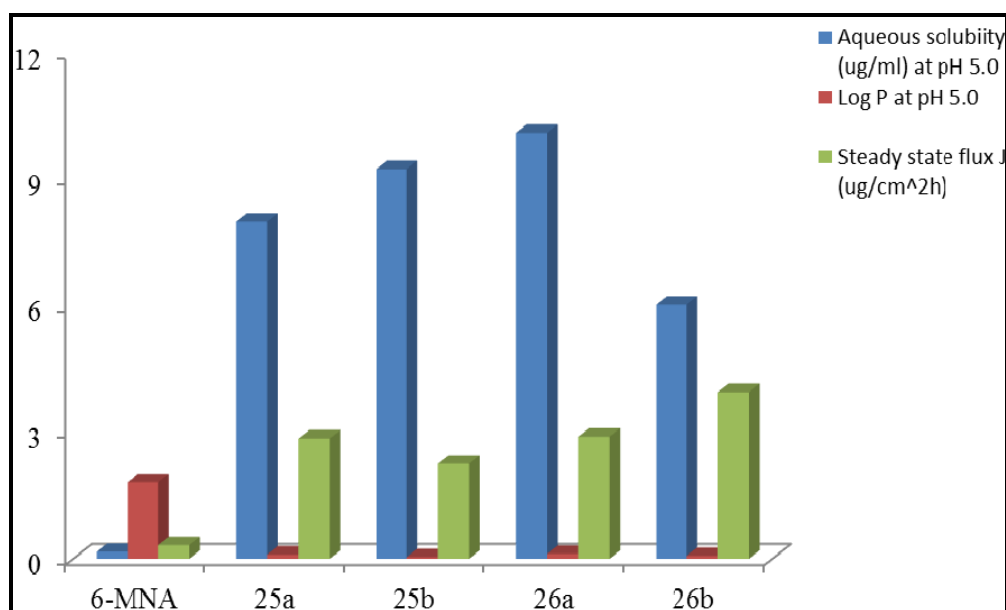
Fig. 3.2.21: Comparison of aqueous solubility, Log P_{app} and steady state flux (Jss) of 6-MNA **(16)** and derivatives **(25-25a-b and 26a-26b)**

4. Experimental

All the reagents and solvents required for synthesis were purified by general laboratory techniques before use. Purity of the compounds and completion of reactions were monitored by thin layer chromatography (TLC) on silica gel plates (60 F_{254}; Merck), visualizing with ultraviolet light or iodine vapors. The yields reported here are un-optimized. Compounds were purified by column chromatography wherever required using neutral aluminum oxide (active) as stationary phase and suitable solvent as eluent.

Melting points were determined using a Veego make silicon oil bath-type melting point apparatus and are uncorrected. The IR spectra were recorded using KBr disc method in cm^{-1} on a Bruker FT-IR, Model 8300. The PMR and ^{13}C NMR (ppm) spectra were recorded in $CDCl_3$ on a Bruker 400 MHz spectrometer (chemical shifts in δ ppm, coupling constant J in MHz). λ_{max} was determined on Shimadzu 1800 UV spectrophotometer. HPLC analysis was performed by using Shimadzu prominence UV/VIS (pump LC-20AT, detector SPD 20 A), column purospher 5μ (e) C-18, 4.6 X 250 mm, Column temperature was 25-28 °C. Chromatography was performed under isocratic conditions, at a flow-rate of 0.9 ml/min. The mobile phase consisted of phosphate buffer (PB, 15 mM)-acetonitrile.

Mass of the compounds was determined in LCMS. *In vitro* skin permeation study was conducted using Franz type diffusion cell and Wistar rats were used as source of skin. Scanning electron microscope (SEM) model ESEM-EDAX XL-30, Philips (Netherlands) was used for surface morphology study.

The work carried out has been discussed under the following heads:

4.1 Chemical studies

4.1.1 Syntheses of salts

4.1.2 Syntheses of prodrugs

4.2 Physicochemical evaluation studies

4.2.1 Determination of aqueous solubility

4.2.2 Determination of partition coefficient (Log P_{app})

4.2.3 Hydrolysis kinetics studies

4.2.4 *In vitro* skin permeation studies

4.1 Chemical studies

4.1.1 Synthesis of salts

Equimolar amounts of the parent NSAID and amine/base were dissolved in dichloromethane under stirring and the stirring was continued for 2-4 h till the salts

precipitated out. Solvent was removed in *vacuo* and the residue was crystallized from methanol or ethyl acetate to get pure solid.

4.1.2 Synthesis of prodrugs

4.1.2.1. 2-Bromoethyl 2-(6-methoxy-2-naphthyl)acetate (22)

In a round bottom flask (250 ml), 6-MNA **(16)** (5.0 g, 23.14 mM) was dissolved in dry DCM (100 ml). The solution was cooled to 0-2 $^{\circ}$C followed by the addition of EDC (5.30 g, 27.77 mM) in to it with stirring. DMAP (50 mg) was added into the reaction mixture as a catalyst followed by the slow addition of 2-bromothanol (4.90 ml, 69.44 mM). Stirring was continued till the reaction got completed.

After completion of the reaction (18 h), the reaction mixture was washed with chilled water (2 x 100 ml) to remove EDC and then with acetic acid (10 %, 2 x 50 ml) followed by washing with saturated solution of sodium bicarbonate (2 x 100ml) and again with chilled water (1 x 100 ml). DCM layer was separated and dried over anhydrous sodium sulphate, filtered and the solvent removed on rota evaporator to get a yellow product. Crude product so obtained was given charcoal treatment in methanol and recrystallized from methanol to get a fluffy white product. The solid product was dried in vacuum at 40 ^{0}C/300 mmHg (3.5 g, 46.79 %) m.p. 81-84 ^{0}C.

Anal.:

      TLC (R$_f$)   : 0.74 (Chloroform)

      UV (MeOH) : 225 nm

      IR (KBr, cm^{-1}): 1727 and 1214

      PMR (CDCl$_3$): δ 7.71-7.67 (m, 3H, Ar-*H*), 7.39-7.37 (dd, 1H, Ar-*H*, *J*=1.76), 7.15-7.11 (m, 2H, Ar-*H*), 4.42-4.39 (t, 2H, -OC*H*$_2$, *J*=6.08), 3.91 (s, 3H, -OC*H*$_3$), 3.79 (s, 2H, -COC*H*$_2$) and 3.51-3.48 (t, 2H, -C*H*$_2$Br, *J*=6.08).

4.1.2.2. 2-(4-Methylpiperazin-1-yl)ethyl 2-(6-methoxy-2-naphthyl)acetate (25a)

Intermediate 2-bromoethyl 2-(6-methoxy-2-naphtyl)acetate **(22)** (0.5 g, 1.54 mM) was dissolved in dry acetone (20 ml) with DMF (two drop) in a pressure tube *N*-Methylpiperazine (0.46 g, 4.64 mM) and potassium carbonate (0.5 g, 3.62 mM) were added in the above reaction mixture. The tube was sealed and heated on oil bath at 70-80 ^{0}C with stirring. The reaction was monitored till completion (10 days) and the reaction mixture was filtered to remove K$_2$CO$_3$ and acetone recovered under vacuum to get brown

oily product which was purified by column chromatography using hexane: ethyl acetate (1:1) as the mobile phase and active neutral aluminium oxide as the stationary phase to yield yellowish brown oil which failed to crystallize. The oily product so obtained was dried in vacuum oven at 40 ^{0}C/300 mmHg (0.44 g, 83 %).

Anal.:

      TLC (R_f)   : 0.43 (Chloroform: Methanol; 9:1)

      UV (H_2O)   : 226 nm

      IR (KBr, cm^{-1})   : 1730, 1264 and 1148

      PMR (CDCl$_3$)   : 7.63-7.03 (m, 6H, Ar-*H*), 4.16-4.13 (t, 2H, -OC*H*$_2$, *J*=5.8), 3.83 (s, 3H, -OC*H*$_3$), 3.68 (s, 2H, -OC*H*$_2$), 2.54-2.51 (t, 2H, N-C*H*$_2$, *J*=5.8), 2.38-2.27 (m, 8H, piperazine-*H*) and 2.16 (s,3H, -C*H*$_3$).

      ^{13}CNMR (CDCl$_3$): 171.67(1C, *C*O), 157.62-105.56 (10*C*, Ar-*C*), 62.31 (1C, O*C*H$_2$), 56.2 (O-*C*H$_3$), 55.3-54.94 (2C, piperazine), 52.93 (1C, -*C*H$_2$-N), 52.64-52.12 (2C, piperazine), 45.70 (Ar-*C*H$_2$-) and 41.20 (1C,-N-*C*H$_3$).

      Mass (m/z)   : 342.5 (M$^+$)

      HPLC   : > 98.9 %

4.1.2.3. 2-(4-Ethylpiperazin-1-yl)ethyl 2-(6-methoxy-2-naphthyl)acetate (25b)

Derivative (**25b**) was synthesized by the same procedure as mentioned for derivative (**25a**) using 2-bromoethyl 2-(6-methoxy-2-naphthyl)acetate **(22)** (0.5 g, 1.54 mM) and *N*-ethylpiperazine (0.21 g, 1.85 mM) to get an oily product which was purified by column chromatography using hexane: ethyl acetate (1:1) as the mobile phase and active neutral aluminium oxide as stationary phase. Yellowish green oily product so obtained was dried in vacuum oven at 40 ^{0}C/300 mmHg (0.25 g, 45.45 %).

Anal.:

      TLC (R_f)   : 0.53 (Chloroform: Methanol; 9:1)

      UV (Distilled H_2O): 226 nm

      IR (KBr, cm^{-1})   : 1731, 1264 and 1151

      PMR (CDCl$_3$)   :7.63-7.03 (m, 6H, Ar-*H*), 4.17-4.14 (t, 2H, -OC*H*$_2$, *J*=5.76), 3.83 (s, 3H, -OC*H*$_3$), 3.68 (s, 2H, -COC*H*$_2$), 2.54-2.52 (t, 2H, -C*H*$_2$N, *J*=5.76), 2.38-2.37 (m, 8H, piperazine-*H*), 2.31 -2.26 (q, 2H, -C*H*$_2$, *J*=7.2) and 0.99-0.95 (t, 3H, -C*H*$_3$, *J*= 7.16)

      HPLC   :> 96 %

4.1.2.4. 2-(4-Acetylpiperazin-1-yl)ethyl 2-(6-methoxy-2-naphthyl)acetate (25c)

Derivative (**25c**) was synthesized by the procedure as mentioned for derivative (**25a**) using 2-bromoethyl 2-(6-methoxy-2-naphthyl)acetate (**22**) (0.5 g, 1.54 mm) and *N*-acetylpiperazine (0.23 g, 1.84 mM) to get an oily product which was purified by column chromatography using hexane:ethyl acetate (1:1) as the mobile phase and active neutral aluminium oxide as stationary phase. The red brown oily product so obtained was dried in vacuum oven at 40 ^{0}C/300 mmHg (0.17 g, 34.88 %).

Anal.:

TLC (R_f)	: 0.56 (Chloroform: Methanol; 9:1)
UV (H_2O)	: 225 nm
IR (KBr, cm^{-1})	: 1730, 1626, 1263 and 1150
PMR (CDCl$_3$)	: 7.63-7.03 (m, 6H, Ar-*H*), 4.16-4.13 (t, 2H, -OC*H$_2$*, *J*=5.44), 3.82 (s, 3H, -OC*H$_3$*), 3.67 (s, 2H, -COC*H$_2$*), 3.13-3.11 (t, 2H, N-C*H$_2$*, *J*=5), 2.52-2.50 (m, 4H, piperazine-*H*), 2.29-2.19 (m, 4H, piperazine-*H*) and 1.90 (s, 3H, -COC*H$_3$*)
HPLC	:> 96 %

4.1.2.5. 2-(4-Phenylpiperazin-1-yl)ethyl 2-(6-methoxy-2-naphthyl)acetate (25d)

Derivative (**25d**) was synthesized by the same procedure as mentioned for derivative (**25a**) using 2-bromoethyl 2-(6-methoxy-2-naphthyl)acetate (**22**) (0.5 g, 1.54 mM) and *N*-phenylpiperazine (0.30 g, 1.85 mM to get a crude solid product which was successively recrystallized from methanol to yield white solid. The product was dried in vacuum oven at 60 ^{0}C/300 mmHg (0.3 g, 47.91 %) m.p. 91-93 ^{0}C.

Anal.:

TLC (R_f)	: 0.69 (Chloroform: Methanol; 9:1)
UV (H_2O)	: 226 nm
IR (KBr, cm^{-1})	: 1720, 1234 and 1147
NMR (CDCl$_3$)	: 7.70-7.22 (m, 6H, Ar-*H*), 7.15-6.80 (m, 5H, phenyl-*H*), 4.29-4.27 (t, 2H, -OC*H$_2$*, *J*=5.56), 3.90 (s, 3H, -OC*H$_3$*), 3.77 (s, 2H, -COC*H$_2$*), 3.02-2.95 (t, 4H, piperazine-*H*, *J*=5.08), 2.67-2.64 (t, 2H, N-C*H$_2$*, *J*=5.56) and 2.52-2.49 (t, 4H, piperazine-*H*, *J*=5.12)
HPLC	:> 90 %

4.1.2.6. 3-Bromoproyl 2-(6-methoxy-2naphthyl)acetate (23)

In a round bottom flask (250 ml), 6-MNA **(16)** (1.0 g, 4.62 mM) was dissolved in dry DCM (100 ml). The solution was cooled to 0-2 ^{o}C followed by the addition of EDC (1.06 g, 5.55 mM) in to it with stirring. DMAP (50 mg) was added into the reaction mixture as a catalyst followed by the slow addition of 3-bromo-1-propanol (0.62 ml, 6.94 mM). Stirring was continued till the reaction was completed.

After completion of the reaction (18 h), the reaction mixture was washed with chilled water (2 x 50ml) to remove EDC and then with acetic acid (10 %, 2 x 25 ml) followed by washing with saturated solution of sodium bicarbonate (2 x 50 ml) and again with chilled water (1 x 50 ml). DCM layer was dried over anhydrous sodium sulphate and the solvent removed on rota evaporator to get a yellow product. The crude product so obtained was given charcoal treatment in methanol and recrystallized from methanol to get a fluffy white product. The solid product was dried in vacuum at 40 ^{0}C/300 mmHg (0.8 g, 51.25 %) m.p. 44-46 ^{0}C

Anal.:

TLC (R_f)   : 0.81 (Chloroform)

UV (MeOH)   : 225 nm

IR (KBr, cm^{-1}): 1735 and 1267

PMR (CDCl$_3$) : 7.71-7.68 (dd, 2H, Ar-*H*, *J*=4.28), 7.64 (s, 1H, Ar-*H*) 7.38-7.35
              (m, 1H, Ar-*H*,), 7.15- 7.11 (m, 2H, Ar-*H*), 4.25-4.22 (t, 2H, -
              OC*H*$_2$, *J*=6.56), 3.91 (s, 3H, -OC*H*$_3$), 3.75 (s, 2H, -COC*H*$_2$), 3.40-
              3.36 (t, 2H, -C*H*$_2$Br, *J*=6.04) and 2.18-2.11 (m, 2H, -C*H*$_2$, *J*=6.56).

4.1.2.7. 3-(4-Methylpiperazin-1-yl)propyl 2-(6-methoxy-2-naphthyl)acetate (26a)

Derivative **(26a)** was synthesized by the same procedure as mentioned for derivative **(25a)** using intermediate 3-bromoproyl 2-(6-methoxy-2-naphthyl)acetate **(23)** (0.3 g, 0.890 mM) and *N*-methylpiperazine (0.106 g, 1.068 mM) to get brown oily product. The oily product was purified by column chromatography using hexane: ethyl acetate (1:1) as the mobile phase and active neutral aluminium oxide as the stationary phase to yield a brown oily product which failed to crystallize. The product so obtained was dried in vacuum oven at 40 ^{0}C/300 mmHg (0.15 g, 48.31 %).

Anal.:

TLC (R_f)   : 0.60 (Chloroform: Methanol; 10:0.5)

UV (H$_2$O)   : 226 nm

IR (KBr, cm^{-1}) : 1732, 1398 and 1163

PMR (CDCl$_3$)   :7.63-7.03 (m, 6H, Ar-H), 4.07-4.04 (t, 2H, -OCH_2, J=6.48), 3.81 (s, 3H, -OCH_3), 3.64 (s, 2H, -COCH_2), 2.34-2.28 (m, 8H, piperazine-H), 2.27-2.23 (t, 2H, -NCH_2, J=7.24), 2.16 (s, 3H, N-CH_3) and 1.75-1.69 (m, 2H, -C-CH_2, J=7.04).

HPLC   :> 97.5 %

4.1.2.8. 3-(4-Ethylpiperazin-1-yl)propyl 2-(6-methoxy-2-napthyl)acetate (26b)

Derivative (**26b**) was synthesized by the same procedure as mentioned for derivative (**25a**) using intermediate 3-bromoproyl 2-(6-methoxy-2naphthyl)acetate (**23**) and *N*-ethylpiperazine (0.12 g, 1.0 mM) to get brown oily product. The product was purified by column chromatography using hexane: ethyl acetate (1:1) as the mobile phase and active neutral aluminium oxide as stationary phase to yield brown oily product which failed to crystallize. The product so obtained was dried in vacuum oven at 40 ^{0}C/300 mmHg (0.20 g, 62.50 %).

Anal.:

TLC (R$_f$)   : 0.40 (Chloroform: Methanol; 10:0.5)

UV (H$_2$O)   : 226 nm

IR (KBr, cm^{-1})   : 1732, 1265 and 1156

NMR (CDCl$_3$)   : 7.55-6.95 (m, 6H, Ar-H), 3.99-3.96 (t, 2H, -OCH_2, J=6.4), 3.75 (s, 3H, -OCH_3), 3.54 (s, 2H, -CH_2), 2.50-2.47 (t, 2H, N-CH_2), 2.42-2.26 (m, 8H, piperazine-H), 2.21-2.19 (m, 2H, -N-CH_2), 1.58-1.55 (m, 2H, -CH_2-, J=4.88) and 0.97-0.94 (m, 3H, -CH_3).

HPLC   :> 90 %

4.1.2.9. 3-(4-Acetylpiperazin-1-yl)propyl 2-(6-methoxy-2-napthyl)acetate (26c)

Derivative (**26c**) was synthesized by the same procedure as mentioned for derivative (**25a**) using intermediate 3-bromoproyl 2-(6-methoxy-2-naphthyl)acetate (**23**) and *N*-acetylpiperazine (0.22 g, 1.78 mM) to get brown oily product which was purified by column chromatography using hexane: ethyl acetate (1:1) as the mobile phase and active neutral aluminium oxide as stationary phase to yield brown oily product which failed to crystallize. The product thus obtained was dried in vacuum oven at 40 ^{0}C/300 mmHg (0.51 g, 89.47 %).

Anal.:

TLC (R_f)   : 0.51 (Chloroform: Methanol; 19:1)

UV (H_2O)   : 226 nm

IR (KBr, cm^{-1})   : 1728, 1632, 1263 and 1150

NMR ($CDCl_3$)   : 7.70-7.11 (m, 6H, Ar-*H*), 4.17-4.13 (t, 2H, -OC*H*$_2$, *J*=6.4), 3.91 (s, 3H, -OC*H*$_3$), 3.73 (s, 2H, -COC*H*$_2$), 3.57-3.54 (t, 2H, N-C*H*$_2$, *J*=5.12), 3.38-3.35 (t, 2H, piperazine -*H*), 2.33-2.27 (m, 6H, piperazine-*H*) 2.05 (s, 3H, -COC*H*$_3$), 1.80-1.77 and (m, 2H, -C*H*$_2$, *J*=5.12)

^{13}C NMR ($CDCl_3$):   δ 171.76 (1C, -*C*O), 168.92 (1C, -*C*O), 157.65-105.56 (10C, Ar-*C*), 62.94 (1C, -O*C*H$_2$), 55.32 (1C, -O*C*H$_3$), 54.57 (1C, N-*C*H$_2$), 53.05-52.60 (2C, piperazine-*C*), 46.04 (1C, -*C*H$_2$CO), 41.50-41.18 (2C, piperazine-*C*), 25.80 (1C, -*C*H$_2$) and 21.31 (1C, -*C*H$_3$).

HPLC   :> 92.8 %

4.1.2.10. 3-(4-Phenylpiperazin-1-yl)propyl 2-(6-methoxy-2-naphthyl)acetate (26d)

Derivative (**26d**) was synthesized by same procedure as mentioned for derivative (**25a**) using intermediate 3-bromoproyl 2-(6-methoxy-2-naphthyl)acetate (**23**) and *N*-phenylpiperazine (0.28 g, 1.78 mM) to get crude solid product which was successively recrystallized from methanol to yield light brown solid. The product was dried in vacuum oven at 60 ^{0}C/300 mmHg (0.3 g, 48.32 %) m.p. 78-80 ^{0}C.

Anal.:

TLC (R_f)   : 0.73 (Chloroform: Methanol; 1:0.05)

UV (H_2O)   : 227 nm

IR (KBr, cm^{-1})   : 2959, 1736, 1267 and 1155

NMR ($CDCl_3$)   :δ 7.63-7.15 (m, 6H, Ar-*H*), 7.07-6.75 (m, 5H, phenyl-*H*), 4.11-4.07 (t, 2H, -OC*H*$_2$, *J*=6.44), 3.81 (s, 3H, -OC*H*$_3$), 3.66 (s, 2H, -C*H*$_2$CO), 3.06-3.04 (t, 4H, piperazine-*H*, *J*=4.88), 2.43-2.40 (t, 4H, piperazine-*H*, *J*=5.04), 2.32-2.28 (t, 2H, N-C*H*$_2$, *J*=7.2) and 1.77-1.73 (m, 2H, -C*H*$_2$, *J*=7.64).

Mass (m/z)   : 418 (M$^+$)

HPLC   :> 99.6 %

4.2. Physicochemical evaluation

Chemicals and Reagents

1. Phosphate buffer (15 mM): Monobasic potassium dihydrogen phosphate (KH_2PO_4, 1.026 g) was dissolved in distilled water to make the volume up to 500 ml. (Molecular weight of KH_2PO_4 = 136.08 g/mol).

2. Phosphate buffer pH 5.0 (0.16 M): Monobasic potassium dihydrogen phosphate (KH_2PO_4, 2.177 g) was dissolved in distilled water to make the volume up to 100 ml. and the pH of the solution was adjusted with 0.2 M sodium hydroxide.

3. Phosphate buffer pH 7.4 (0.16 M): Monobasic potassium dihydrogen phosphate (KH_2PO_4, 2.177 g) was dissolved in distilled water to make the volume up to 100 ml and adjusted the pH of the solution with 0.2 M sodium hydroxide to pH 5.0.

4. Phosphate buffer saline pH 7.4: Dibasic disodium hydrogen phosphate (Na_2HPO_4, 1.38 g), monobasic potassium dihydrogen phosphate (KH_2PO_4, 0.27 g) and sodium chloride (8.0 g) were dissolved in distilled water to make the volume up to 1000 ml.

4.2.1 Aqueous solubility

The aqueous solubility of 6-MNA, BPA and their salts or prodrugs were determined in phosphate buffer (0.16 M) at both pH 5.0 and 7.4 at room temperature. Excess amounts of each prodrug were added to phosphate buffer (0.5 ml). The mixtures were stirred and centrifuged at 6000 rpm for 5 min. The concentrations of each of the salt or prodrugs in their saturated solutions were analyzed by the HPLC. The pH of the solutions was held constant throughout the experiment.[1,8]

4.2.2 Apparent partition coefficient (Log P_{app})

The apparent partition coefficients (log P_{app}) of 6-MNA, BPA and their salts or prodrugs were determined at room temperature between 1-octanol and phosphate buffer (0.16 M) at pH 5.0 and 7.4 using shake flask method. 1-Octanol was saturated with phosphate buffer for 24 h by stirring vigorously before use. A known concentration of the compound in phosphate buffer was shaken with a suitable fixed volume of 1-octanol. After shaking, both the phases were separated by centrifugation at 6000 rpm for 5 min. The concentrations of the compounds in the buffer phase and in the 1-octanol phase were determined by HPLC. [1,8]

4.2.3 Hydrolysis kinetics study

Stability Study or the rates of chemical hydrolysis of prodrugs were studied in aqueous phosphate buffer solutions of pH 5.0 and pH 7.4 (0.16 M) at $37\pm1\ ^0$C. An

appropriate amount of prodrug was dissolved in phosphate buffer (5 ml) and the solutions were maintained at temperature 37 ± 1 ^{0}C. At appropriate time intervals, samples were taken and analyzed for the remaining quantity of the prodrug by the HPLC. Prodrugs were found to degrade by first-order degradation kinetics. Half-lives ($t_{1/2}$) for the hydrolysis of the different prodrugs were calculated from the slope of the linear portion of the plotted logarithm of the remaining concentration of the prodrugs versus time.[1,8] The first order equation ($t_{1/2} = 0.693/k$) was used to calculate the half-lives.

4.2.4 *In vitro* skin permeation studies

In vitro skin permeation studies were performed by using rat skin. Samples of rat skin were obtained from the abdominal region of Wistar rat. Abdominal region of the rat was shaved using depilatory cream (*Anne French*, Wyeth pharmaceuticals Ltd.). Animal was euthanized by high dose of anesthetic ether and the abdominal skin was excised and thoroughly washed with phosphate buffer saline solution (*p*H 7.4). The skin surface (epidermal side) was cleaned with the aid of cotton impregnated with aqueous sodium lauryl sulphate (1 % w/v, 0.5 ml). The remaining fat in the dermal side was entirely removed by cotton impregnated with ether. The skin was washed with distilled water and dried well with clean and dry cotton.[1,8]

The *in vitro* skin permeation studies were carried out using the Franz-type diffusion cell. Skin specimens were rehydrated before being mounted in the diffusion cell. The receptor medium (0.05 M phosphate buffer saline solution of *p*H 7.4) was stirred and kept at 37 ± 1 ^{0}C throughout the study. The compounds were applied as solutions in phosphate buffer of *p*H 5.0. At specified time intervals aliquots (0.5 ml) were withdrawn from the receptor compartment and replaced with fresh buffer. The drug concentrations were analyzed by HPLC.

The steady-state flux for 6-MNA **(16),** BPA **(17)** and their salts or prodrugs were determined by plotting the cumulative amount of the parent drug and the intact prodrug as measured in the receptor phase against time, and dividing the slope of the steady-state position by the surface area of the diffusion cell (4.906 cm^2).[1,8] The permeability coefficients (*K*) for the steady-state delivery were obtained by dividing the steady-state flux by the solubilities of the compounds in the applied corresponding vehicle.

References

1. Rautio J., Nevalainen T., Taipale H., Vepsäläinen J., Gynther J., Laine K. and Järvinen T., Piperazinylalkyl prodrugs of naproxen improve *in vitro* skin permeation. *Eur.J. Pharm. Sci.*, **2000**, 11, 157-63

2. QikProp, version 3.2, Schrödinger, LLC, New York, NY, **2009**

3. Epik, version 2.0, Schrödinger, LLC, New York, NY, **2009**

4. Siddiqui O., Physicochemical physiological and mathematical consideration in optimizing percutaneous absorption of drugs. *Crit. Rev. Ther. Drug Carr. Syst.* **1989**, 6, 1-38

5. Anderson B.D., Higuchi W.I. and Raykar P.V., Heterogeneous effects on permeability partition coefficient relationship in human stratum corneum. *Pharm. Res.* **1988**, 5, 566-72

6. Raykar P.V., Fung M.C. and Anderson B.D., The role of protein and lipid domains in the uptake of solutes by human stratum corneum. *Pharm. Res.* **1988**, 5, 140-50

7. Williams F.M., Clinical significant of esterase in man. *Clin. Pharmacokin.* **1985**, 10, 392-403

8. Amjad Q. and Soraya A. Synthesis of piperazinylalkyl ester prodrugs of ketorolac and their i*n vitro* evaluation fo,r transdermal delivery. *Drug. Dev. Ind. Pharm.* **2008**, 34, 1054-63

9. Singh S. and Singh J., Transdermal drug delivery by passive diffusion and iontophoresis: A Review. *Med. Res. Rev.*, **1993**, 13, 569-621.

Section-III
IA-Liposomal Drug Delivery

1. Introduction

1.1 Liposomes

A liposome is defined as a structure consisting of one or more concentric spheres of lipid bilayers separated by water or aqueous buffer compartment as shown in **Fig. 1.1.**[1-2] A liposome is an artificially prepared vesicle composed of a lipid bilayer, formed spontaneously when the lipids are dispersed in aqueous media giving rise to population of vesicles, which may range in size from tens of nanometers to tens of microns in diameter.[3]
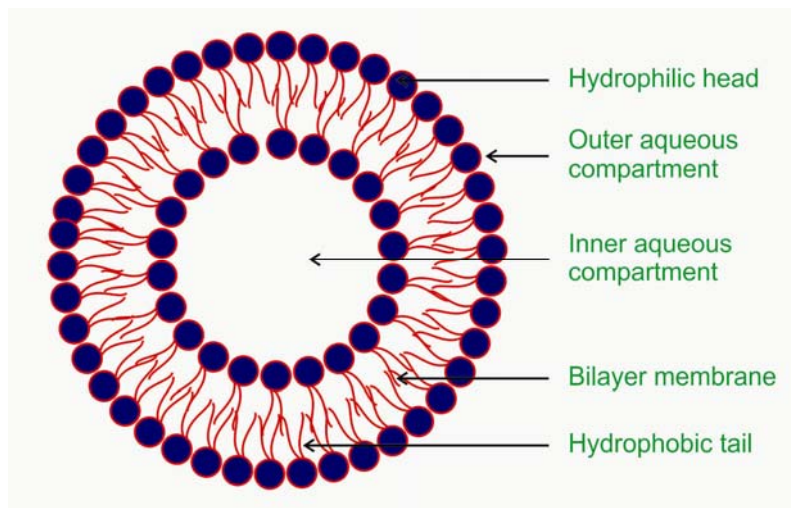
Fig. 1.1: General structure of liposome

Liposomes were brought in attention to the scientific world by A.D. Bangham in 1960's.[4] From 1969 to 1979, various method for preparation of liposome were developed to study biological process of membranes and membrane bound proteins. By 1979, liposomes were proposed as drug carriers to modify the therapeutic index of a drug by reducing toxicity or increasing efficacy of the parent drug. The potential use of liposome as a biodegradable or biocompatible drug carrier to enhance the potency and reduce the toxicity of the therapeutic agent was recognized only in late 80's and early 90's. Only then series of liposome-based therapeutics were approved for human use by U.S. Food and Drug Administration (FDA).

The modern era of liposomes is characterized by scale-up of liposomal production and a better selection of lipid raw materials for liposome preparation. Many sophisticated lipids, allowing control over the physicochemical and biological fate of liposomes became available. This includes lipids that change the integrity of liposomes in response to change

in temperature and pH, polymerizable lipids and lipids that reduce or prevent the uptake of liposomes by mononuclear phagocytes system (MPS) etc.

1.2 Classification of liposomes

Liposomes are mainly classified on the basis of their structural properties, method of preparation or their composition and applications as shown in **Table 1.1-1.3**[5-6]

Table 1.1: Liposome classification based on structure (size and lamellarity).

No	Type of liposome	Abbreviation	Size range (Diameter)	No of lipid bilayers
1	Unilamellar vesicle	UV	All size range	one
2	Small unilamellar vesicle	SUV	20-100 nm	one
3	Medium unilamellar vesicle	MUV	>100 nm	one
4	Large unilamellar vesicle	LUV	>100 nm	one
5	Giant unilamellar vesicle	GUV	>1 µm	one
6	Oligo lamellar vesicle	OLV	0.1-1 µm	Approx. 5
7	Multi lamellar vesicle	MLV	>0.5 µm	5-25
8	Multi vesicular vesicle	MV	>1 µm	multicompartmental

Table 1.2: Liposome classification based on method of preparation

No	Abbreviation	Type
1	REV	Single or OLV made by the reverse phase evaporation method.
2	MLV-REV	MLV made by the reverse phase evaporation method
3	SPLV	Stable plurilamellar vesicles
4	FATMLV	Frozen and thawed MLV
5	VET	Vesicles prepared by extrusion methods
6	FUV	Vesicles prepared by fusion
7	DRV	Dehydration rehydration vesicles

Table 1.3: Liposome classification based on Composition and Application

No	Type of liposome	Composition	Abbreviation
1	Conventional liposome	Phospholipid and cholesterol	CL
2	Fusogenic liposome	Reconstituted sendai virus envelops	RSVE
3	*p*H Sensitive liposomes	Phospholipid such as PER or DOPE	-
4	Cationic liposome	Cationic lipid with DOPE	-
5	Long circulating liposome	Cholesterol, 5-10% PEG, DSP	LCL
6	Immunoliposome	CL or LCL with attached monoclonal antibody	IL

1.3. Components of liposomes

Liposome are generally composed of the following classes of materials[5,7]

    1.3.1. Phospholipids

    1.3.2. Sphingolipids and steroids

    1.3.3. Other substances

1.3.1 Phospholipids

Phospholipids are one of the major components of liposomes. Four groups of phospholipids that can be used for liposome preparation have been described. These include phospholipids from natural sources [e.g. egg phoshatidylcholine (PC), egg phosphatidylethanolamine], modified natural semi synthetic phospholipids (e.g. phospholipids obtained from the natural sources whose acyl chains are removed and chemically replaced by defined acyl chains), fully synthetic phospholipids (e.g. phospholipids made by complete synthetic pathway) and phospholipids with non-natural head groups (e.g. polyethylene glycol-phosphatidyl ethanolamine).

1.3.2 Sphingolipids and steroids

Important member of sphingolipids group include sphingomyelin and gangliosides and sterols such as cholesterol and derivatives included as components of liposomal membranes.[1] Cholesterol is a major component of natural membrane and its incorporation into lipid bilayer causes major changes in the property of vesicles. Cholesterol itself does not form bilayer structure but can be incorporated into phospholipid membrane in high concentrations. These lipids tend to increase vesicle stability on shelf and increase the

fluidity or micro viscosity of the bilayer, decrease the permeability of the membrane to water soluble molecules and stabilize the membrane in the presence of biological fluids[8-10]

1.3.3 Other substances

A variety of other lipids and surfactants can be used to form liposomes such as single chain surfactants in combination with cholesterol, non-ionic lipids such as a variety of polyglycerol and polyethoxylated mono and dialkyl amphiphiles for topical pharmaceutical preparations. Some recently prepared single and double chain lipids having fluorocarbon chains which can form very stable liposomes, stearylamine and dicetyl phosphate which impart either a positive or a negative surface charge to liposomes and number of other compounds having a single long-chain hydrocarbon and an ionic head such as quaternary ammonium salt and dialkyl phosphate have been found to be capable of forming vesicles.[1-2] Antioxidants such as α-tocopherol or BHT are often included as components of liposomal membranes to minimize lipid degradation by oxidation.[3] A chelating agent (EDTA) is also included to sequester heavy metals which act as catalysts for the oxidation-reduction processes.[3]

1.4 Preparation of liposomes[11]

Formation of liposomes is not a spontaneous process. Lipid vesicles are formed when phospholipids are placed in water and consequently form one bilayer or a series of bilayers, each separated by water molecules, once enough energy is supplied. Liposomes can be created by sonicating phospholipids in water. In different preparation procedures, a general pattern is involved as follows:

- Dissolution of lipid and formation of film
- Hydration of the lipid or film
- Sizing of the liposomes
- Removal of the non-encapsulated drug

Commonly used methods for preparation of liposomes are as given below:

1.4.1 Thin film hydration

1.4.2 Reverse phase evaporation

1.4.3 *p*H induced vesiculation

1.4.4 Injection of water miscible solvents

1.4.5 Injection of water immiscible solvents

1.4.6. Detergent dialysis method

1.4.1 Thin film hydration

In the laboratory, a mixture of lipids in volatile organic solvent is deposited on the surface of a round bottom flask as the solvent is removed by rotary evaporation under reduced pressure. MLVs ranging in tens of micrometers to several tenths of a micrometer form spontaneously when an excess volume of aqueous buffer is added to the dry lipid and the flask are agitated.

1.4.2 Reverse phase evaporation

LUVs can be prepared by forming water in oil emulsion of phospholipids and a buffer in excess organic phase followed by removal of the organic phase under reduced pressure. Removal of the organic phase under the vaccum causes the phospholipid coated droplets of water to coalesce and eventually form a viscous gel.

1.4.3 pH induced vesiculation

SUVs can be prepared from mixed depression of PC and phosphatidic acid (PA) provided that the molar proportion of PC is 70 % or less. These liposomes are formed when the phospholipid mixtures are dispersed directly in sodium hydroxide at pH 10 or in water the pH of which is rapidly increased. However, the technique is limited to charged phospholipids and their mixtures with neutral phospholipids.

1.4.4 Injection of water miscible solvents

Water miscible solvents like ethanol, glycerin and polyglycols have been employed in preparation of liposomes. The solvent containing the lipid is diluted by an excess amount of the aqueous phase rather than being vaporized. As the solvent concentration is reduced by diafiltration or ultrafiltration liposomes are formed.

1.4.5 Injection of water immiscible solvents

The lipid mixture is injected into an aqueous solution of the material to be encapsulated at reduced pressure. Vaporization of the solvents leads to formation of single layer vesicles

1.4.6 Detergent dialysis method

Removal of detergent molecules from aqueous dispersion of phospholipid-detergent mixture is another approach to produce liposomes. As the detergent is removed, the micelles become progressively richer in the phospholipid contents and coalesce to form closed single bilayer vesicles.

1.5 Separation of un-entrapped drug from liposomal suspension

Many lipophilic drugs exhibit a high affinity to the lipid bilayer and are associated with liposomes completely. However, for other compounds encapsulation efficiency is less than 100 % so un-entrapped material has to be removed using various techniques such as dialysis and ultrafiltration[5], ultracentrifugation[3,5], gel permeation chromatography[3,5], ion-exchange resins[13], protamine aggregation[3] etc.

1.6 Mechanism of liposome formation

The exact mechanism involved in liposome formation is still not fully understood. It has been suggested that the large free energy change between water and hydrophobic environment is responsible for the preference of a typical lipid to assemble in bilayer structure excluding water as much as possible from the hydrophobic core in order to achieve the lowest free energy level and hence the highest stability for the aggregate structure (thermodynamic basis of bilayer assembly or the hydrophobic effect).

1.7 Basic properties of liposomes

Variations in liposome size, charge, surface hydration, membrane fluidity and clearance of lipid-associated drug are responsible for liposomal stability and for various cellular interactions.

1.7.1 Surface charge

Based on the head group composition of the lipid and pH, liposomes bear a negative, neutral or positive charge on the surface. The nature and density of charge on the surface of the liposomes influence stability, kinetics and extent of biodistribution, as well as interaction with and uptake of liposomes by target cells. Liposomes with a neutral surface charge have a lower tendency to be cleared by cells of the reticuloendothelial system (RES) after systemic administration and the highest tendency to aggregate. Although negatively charged liposomes reduce aggregation and have increased stability in suspension, their non-specific cellular uptake is increased *in vivo*. Negatively charged liposomes containing phosphatidylserine (PS) or phosphatidylglycerol (PG) were observed to be endocytosed at a faster rate and to a greater extent than neutral liposomes.[14-15]

Negative surface charge is recognized by receptors located on a variety of cells, including macrophages.[16] Inclusion of some glycolipids, such as the ganglioside GM1 or phosphatidyl inositol (PI), inhibit uptake of such liposomes by macrophages and RES cells and result in longer circulation times. It has been suggested that a small amount of

negatively charged lipid stabilizes neutral liposomes against an aggregation-dependent uptake mechanisms. [17] High doses of positively charged liposomes have been shown to produce varying degrees of tissue inflammation.[18]

1.7.2 Surface hydration or steric effect

The surface of the liposome membrane can be modified to reduce aggregation and avoid recognition by RES using hydrophilic polymers. This strategy is often referred to as surface hydration or steric modification. Surface modification is often done by incorporating gangliosides, such as GM1 or lipids that are chemically conjugated to hygroscopic or hydrophilic polymers, usually polyethylene glycol (PEG); this technology is similar to protein PEGylation.

1.7.3 Fluidity of lipid bilayer

Lipid bilayers and liposome membranes exhibit a well ordered or gel phase below the lipid phase transition temperature (Tc) and a disordered or fluid phase above the Tc. The lipid phase transition is measured and expressed as Tc, the temperature at which equal proportion of the two phases coexist. At temperature corresponding to Tc, a maximum leakiness is observed in liposomes.[20]

1.7.4 Liposome size

Early research has demonstrated that liposome size affects vesicle distribution and clearance after systemic administration. The rate of liposome uptake by RES increases with the size of the vesicles.[10] Whereas *in vivo* RES uptake can be saturated at high doses of liposomes or by pre-dosing with large quantities of control liposomes, this strategy may not be practical for human use because of the adverse effects related to the impairment of physiological functions of RES. The general observation for liposomes of similar composition is that increasing size results in rapid uptake by RES.[20] Most recent investigations have used unilamellar vesicles, 50-100 nm in size, for systemic drug delivery applications.

1.8. Characterization of liposomes

Once liposomes are prepared by suitable method it is important to determine physical and chemical characteristics of the prepared liposomes which influence their behavior *in vivo* and *in vitro*. Several examples demonstrating the importance of proper selection of liposomal structure to obtain optimum and reproducible therapeutic effects have been published.[20-22] The types of the characterization of liposomes can be divided into three broad categories as summarized below:[23]

- Physical characterization
- Chemical characterization
- Biological characterization

Physical, chemical and biological characterization of liposomes includes evaluation of the parameters as given in **Tables 1.4-1.6**

Table 1.4: Physical characterization methods of liposomes

No	Parameter	Instrumental method for analysis
1	Vesicle shape and surface morphology	TEM, SEM
2	Vesicle size and size distribution	TEM, Dynamic light scattering
3	Surface charge	Free flow electrophoresis
4	Electrical surface potential	Zeta potential measurement
5	Lamellarity	P^{31}-NMR
6	Phase behavior	DSC, Freeze fracture electron microscopy
7	Drug entrapment	HPLC
8	Drug release	Diffusion cell/dialysis

Table 1.5: Chemical characterization of liposomes

No	Parameter	Instrumental method for analysis
1	Phospholipid concentration	HPLC/Barrlet assay
2	Cholesterol concentration	HPLC/cholesterol oxide assay
3	Drug concentration	Assay
4	Anti-oxidant degradation	HPLC/TLC
5	pH	pH meter
6	Osmolarity	Osmometer

Table 1.6: Biological characterization of liposomes

No	Parameter	Method for analysis
1	Sterility	Aerobic/anaerobic culture
2	Pyrogenicity	Rabbit fever response
3	Animal toxicity	Monitoring of survival of rats

1.9 Stability of liposomes

The stability of liposomes should meet the same standard as conventional pharmaceutical formulations and can be discussed under the following headings:

1.9.1 Physical Stability

Changes in the size of the liposomes can take place over a period of time. These changes can be a result of aggregation and sedimentation or fusion (irreversible formation of new colloidal structures). The methods used to characterize the size of liposomes can be used to follow these changes in size. However, to differentiate between aggregation and fusion, fluorescent markers such as terbium citrate, sodium dipicolinate, calcein cobalt complex in association with EDTA etc. are used. Liposome membrane fusion may also be detected through fluorescence resonance energy transfer between two lipids originally present in different sets of liposomes.[24]

1.9.2 Chemical stability

As phospholipids usually form the backbone of the bilayer, their chemical stability is important. Two types of chemical degradation reactions can affect the performance of phospholipid bilayers which include hydrolysis of the ester bonds and peroxidation of the unsaturated acyl chains (if present). Oxidation of cholesterol can be monitored through gas liquid chromatography using a silica capillary column to separate cholesterol from its oxidation products.[3]

1.10 Approaches to improve liposomal stability[6]

To be commercially feasible, liposomes should have a satisfactory shelf life. Various approaches to improve the physical and chemical stability of liposomes are discussed below.

A) Selection of bilayer components

Stability of liposome can be improved by minimum use of unsaturated phospholipids. If unsaturated lipids are used, addition of antioxidants such as α-tocopherol (<15 mg/day, adult) or butylated hydroxyltoluene (0.02 %) and use of argon or nitrogen to minimize exposure of oxygen are recommended. Oxidation of unsaturated phospholipids, catalyzed by heavy metals may be inhibited by addition of metal chelators such as EDTA (<2 %) and use of light resistance containers. Processing and storage of liposomes at low temperature can add stability to the liposomes. With aqueous liposome dispersion, the selection of a proper pH range (pH 6-7) will reduce hydrolysis and lipid peroxidation-mediated damage.

Addition of substantial fraction of cholesterol decreases the rate of leakage during storage by rendering the bilayer structure more rigid. Use of saturated phospholipids is a useful technique to improve the stability. To reduce the probability for liposome aggregation or fusion, a charge inducing agent is often included in the bilayer. Conversion of small vesicles to large structures as a result of fusion process can be markedly reduced by the presence of trace amount of the phospholipid 1,3-diacyl-2-phosphatidyl choline[6]

B. Freeze drying of liposomes

Freeze drying of liposomes is an excellent method to increase the shelf life of liposomes. Cryoprotectants such as sucrose, maltose, trehalose, lactose, proteins, amino acids, and polyalcohols have been used as additives.[6]

C. Proliposome approach

Lipids dissolved in organic solvents and deposited on finely powdered sodium chloride or sorbitol, upon hydration form liposome dispersion. This approach can only be used for those compounds that are fully liposome associated upon hydration and when a wide particle size distribution is acceptable in the clinical situation.

1.11 Applications of liposomes[6]

The literature concerning the applications of liposomes is so vast that a detailed review in this thesis is not possible. An idea of the varied applications of liposomes can be obtained from **Table 1.7.** which shows the developed liposomal products or products under development.

Table 1.7: Liposomal formulations commercially available or under development

No	Drug/Application	Liposome Utility	Trade Name/Company	Disease States Treated
1	Amphotericin-B	Solublization	Ambisone/Gilead Sciences	Fungal infections
2	Doxorubicin	Site avoidance	Myocet/Zeneus	Metastatic breast Cancer
3	Morphine	Prolonged action	DepoDur/Skyepharma	Postsurgical analgesia
4	Estradiol	--	Estrasorb/Novavx	Menopausal therapy
5	Corticosteroids, Drug depot	Sustained Release	--	Cancer, Biotherapeutics
6	Cytosine arabinoside, IL	Drug Protection	--	Cancer etc.
7	Immunomodulators, Vaccines	RES Targeting	--	Cancer, Tropical Parasites

References

1. Lasic D., Weiner N., Riaz M. and Martin F., Liposomes in pharmaceutical dosage forms: Disperse systems. Lieberman H.A., Rieger M.M., and Banker G.S. Eds. Vol 3, Marcel Dekker Inc. New York. **1998**, 43-86

2. Lasic D.D., The mechanism of vesicle formation. *Biochim. J.* **1998**, 256, 1-11

3. New RRC., "Introduction, Preparation and Characterization of liposomes: A practical Approach, New RCC ed. Oxford University Press, Oxford, **1990**,1-161

4. Bangham A.D., Standish M. M. and Watkins J. C., Diffusion of univalent ions across the lamellae of swollen phospholipids. *J. Mol. Biol.* **1965**, 13, 238-52

5. Crommelin D.J.A. and Schreir H., Liposomes in colloidal Drug delivery systems. Kreuter J. Ed. Marcel Dekker Inc. New York, **1994**, 73-190

6. Lasic D.D., Chapter-10, Applications of Liposomes. Handbook of Biological Physics. Elsevier Science BV Ltd. **1995**, 1, 494

7. Bangham Y. and Crommelin D.J.A., "Liposomes as pharmaceutical dosage forms to microencapsulation "in Encyclopedia of pharmaceutical Technology, Marcel Dekker Inc. New York, **1994**, 9, 1-39

8. Gabizon A.A. and Barenholz Y., liposomes as Drug Carriers. Gregoriadis G Ed. John Wiley and Sons, New York, **1988**, 365-79

9. Gabizon A.A. and Papahadjopoulous D., Liposomes formulations with prolonged circulation time in blood and enhanced uptake by tumors. *Proc. Natl. Acad. Sci.* USA, **1988**, 85, 6949-53

10. Hwang K.J., In liposomes: From biophysics to Therapeutics. Ostro MJ (Ed.) Marcel Dekker Inc. New York, **1987**, 109-156

11. Kathleen M. M., Efstathios K., Ananth V. A. and Ravi V. B., Masking and triggered unmasking of targeting ligands on nanocarriers to improve drug delivery to brain tumors. *Biomaterials,* **2009**, 30, 3986–95

12. Shinitzky M. and Barcnholz Y., Fluidity parameters of lipid regions determined by fluorescence polarization. *Biochim. Biophys. Acta.* **1978**, 515, 367-94

13. Storm G., Van-Bloois L., Brouwer M. and Crommelin D.J.A., The interaction of cytosatic drugs with adsorbents in aqueous media. The potential implications for liposome preparation. *Biochim. Biophys. Acta.,* **1985**, 818, 343-51

14. Allen T.M., Hansen C., Martin F., Redemann C. and Yau-young A., Liposome containing synthetic lipid derivatives of poly (ethylene glycol) show prolonged circulation half-life *in vivo. Biochim. Biophys*., **1991**, 1066, 29-36

15. Lee R.J. and Low P.S., Folate mediated tumor cell targeting of liposomes entrapped doxorubicin in vitro. *Biochim. Biophys. Acta.,* **1995**, 1233, 134-44

16. Lee R.J. and Low P.S., Delivery of liposomes into cultured KB cells via folate receptor mediated endocytosis. *J. Bio. Chem.,* **1994**, 269, 3198-04

17. Israelachvili J., Marcelja S. and Horn R.G., Physical principles of membrane organization. Q. *Rev. Biophys.* **1980**, 13, 121-200

18. Scheule R.K., St. George J.A., Bagley R.G., Marshall J., Kaplan J.M., Akita G.Y., Wang K.X., Lee E.R., Harris D.J., Jiang C., Yew N.S., Smith A.E. and Cheng S.H., Basis of pulmonary toxicity associated with cationic lipid-mediated gene transfer to the mammalian lung. *Hum. Gene. Ther.* **1997**, 8, 689-707

19. Nassander U.K., Strom G., Peeters PAM. and Crommelin D.J.A. Liposomes in Bio-degradable polymers as Drug Delivery Systems, Mchasin, Langer R ed. Macel Dekker Inc. New York, **1990**, 261-3338

20. Senior J., Crawley J.C. and Gregoriadis G., Tissue distribution of liposome exhibiting long half lives in the circulation after the intravenous injection. *Biochim. Biophys. Acta.,* **1985**, 839, 1-8

21. Goren D., Gabizon A. and Barenholz Y., The influence of physical characteristics of liposomes on their pharmacological behavior. *Biochim. Biophys. Acta.*, **1990**, 1029, 285-94

22. Storm G., Van Bloois L., Steerenberg P.A., Van Etten E., Degroot G. and Crommelin D.J.A. Liposome encapsulation of doxorubicin: Pharmaceutical and Therapeutic aspects. *J. Control. Rel.*, **1989**, 9, 215-229

23. Samad A., Sulatana Y. and Aqil M., Liposomal drug delivery systems: An Update Review, *Curr. Drug. Deliv.* **2007**, 4, 297-305.

24. Jones G.R. and Cossins A.R., Physical methods of study in Liposomes: A Practical Approach. New RRC ed. Oxford University press, Oxford, **1990**, 183-220

2. Aims and Objectives

Liposomes have long been proposed as ideal carriers for the delivery of drugs and to improve their therapeutic effect.[1] Liposomal physicochemical properties can be changed as per the requirements from therapeutic point of view to get maximum benefits, such as passage through biological barriers, retention at the target site, avoiding toxicity to non-target sites and to prevent premature degradation.[2-3] These formulations can be applied locally or systemically. As the present work is concerned about arthritis so it was planned to use liposome formulations to deliver the drug locally.

From the study of intra-articularly (IA) administered cationic chemical delivery systems (CDS) in previous section and literature survey it was concluded that introduction of positive charge on drug carrier system improves the residence time of drugs within the joint cavity. The NSAID diclofenac sodium in particular has attracted more attention due to quick onset of analgesic effects and anti-inflammatory properties.[4] However diclofenac has very short plasma half life (1.2-2 h), undergoes enterohepatic circulation (35 %), lacks affinity towards joints (synovial disappearance half life 1.5h), shows non-selectivity towards cycloxygenase enzymes (COX) and can evoke adverse gastrointestinal side effects.[5]

The aim of the present work was to develop cationic liposomal formulations of NSAIDs with long half life, selectivity towards COX-II enzyme and affinity towards joint cavity producing less gastrointestinal side effects (ideally without undergoing enterohepatic circulation). The encapsulation of NSAIDs possessing all these ideal features in to liposomes with further modifications of liposomal properties such as size, lammelarity, charge etc. was expected to improve the overall therapeutic efficacy of these agents after IA injection in patients with OA.

The specific aims of the present work were as follows:

1. **Syntheses of NSAIDs:** It was planned to prepare liposomes of 6-methoxy-2- naphthyl acetic acid (6-MNA) **(1)** and biphenylacetic acid (BPA) **(2)**, as these molecules fulfill

| (1) | (2) |

the above criteria required for ideal NSAIDs. 6-MNA and BPA are the active metabolites of nabumetone[6] and fenbufen[7] with half lives of 23-33 h and 10-12 h

respectively. So, it was planned to synthesize both these molecules in the laboratory as these are not available commercially.

2. **Preparation of cationic liposomes:** Cationic liposomes may increase the retention time of the drug delivery system within joint cavity. Further, multilammellar liposomes also provide lubricating effect which is beneficial during this diseased condition.

3. **Characterization of liposomes:** It was planned to characterize the prepared liposomes for their size, charge, lamellarity, entrapment efficiency, stability etc.

4. **Release study:** It was planned to study release of the drug from liposomes. Sustained release of active medicament is an essential criterion for the development of long acting drug delivery systems which could be injected IA.

5. ***In vivo* efficacy in animal model:** It was planned to evaluate efficacy of these drug delivery systems using Freunds adjuvant induced arthritis model.[6]

References

1. Van den Hoven J.M., Van Tomme S.R., Metselaar J.M., Nuijen B., Beijnen J.H. and Storm G., Liposomal Drug Formulations in the Treatment of Rheumatoid Arthritis *Mol. Pharm.* **2011**, 8, 1002-15.

2. De Silva M., Page Thomas D. P., Hazleman B. L. and Wraight P., Liposomes in arthritis: a new approach. *Lancet* **1979**, 313, 1320–22.

3. Fendler J.H. and Romero A. Liposomes as drug carriers. *Life Sci.* **1977**, 20, 1109.

4. Saravanan M., Bhaskar K., Maharajan G. and Pillai K.S., Development of gelatin microspheres loaded with diclofenac sodium for intra-articular administration. *J Drug Target.* **2011**, 19, 96-103.

5. Larsen C., Ostergaard J., Larsen S.W., Jensen H., Jacobsen S., Lindegaard C. and Andersen P.H., Intra-Articular Depot Formulation Principles. *J. Pharm. Sci.* **2008**, 97, 4622-54.

6. Nobilis M., Kopecký J., Kvetina J., Svoboda Z., Pour M., Kunes J., Holcapek M. and Kolárová L., Comparative biotransformation and disposition studies of nabumetone in humans using HPLC. *J. Pharm. Biomed. Anal.* **2003**, 32, 641-56.

7. Chiccarelli F.S., Eisner H.J. and Van Lear G.E., Metabolic and pharmacokinetic studies with fenbufen in man. *Arzneimittelforschung.* **1980**, 30, 728-35.

3. Results and Discussion

The work carried out towards achieving the proposed plan has been discussed under the following four main headings:

3.1. Syntheses of the selected NSAIDs

3.2. Salt formation and characterization

3.3. Formulation of liposomes

3.4. Characterization of liposomes

3.5. Stability testing of liposomes

3.6. Biodistribution and gamma imaging studies

3.7. *In vivo* studies in arthritis model

3.1 Syntheses of NSAIDs

The primary aim of this drug delivery approach was to improve the residence time of the drug within the joint cavity after IA administration. The half life of the drug contributes equally for long duration of action along with the nature and type of drug delivery system. As majority of the clinically used NSAIDs have short half lives (<2-4 h) it was planned to synthesize active metabolites of nabumetone and fenbufen i.e. 6-MNA **(1)** and BPA **(2)** respectively which have long half lives (21-27 and 10-12 h respectively) and other favorable properties such as affinity towards joint, COX-II selectivity etc.

3.1.1 Synthesis of 6-MNA (1)

Nabumetone **(3)** was synthesized in the laboratories of Beecham Pharmaceuticals in 1978 and is a non-acidic NSAID devoid of local gastric irritation side effect. But as such this is not active biologically, it undergoes rapid and extensive first-pass biotransformation in the liver to form the principal active compound 6-MNA **(1)**, which acts as an anti-inflammatory agent.[1]

(3)   **(1)**

6-MNA is more than 99 % bound to plasma proteins[2], with the volume of distribution being small (7.5 L) after intravenous administration[2]. 6-MNA penetrates well into the synovial fluid, and does not undergo enterohepatic circulation.[3] The average terminal phase elimination half-life of 6-MNA is approximately 21-27 h. The mode of

action of 6-MNA consists of potent and relatively selective inhibition of cyclooxygenase-2 (COX 2). The biotransformation pathway of nabumetone **(3)** is shown in **Fig. 3.1.**

Fig. 3.1: Biotransformation pathway of nabumetone **(3)** and ideal features of the active metabolite 6-MNA **(1)**

It was planned to synthesize 6-MNA by the reported procedure as shown in **Scheme-1**. β-Naphthol **(4)** was methylated to naroline[4] **(5)** using dimethyl sulphate under basic conditions. Naroline **(5)** was acetylated with acetyl chloride under controlled conditions to offer 6-acetyl-2-methoxynaphthalene **(6)** as per the reported method.[5]
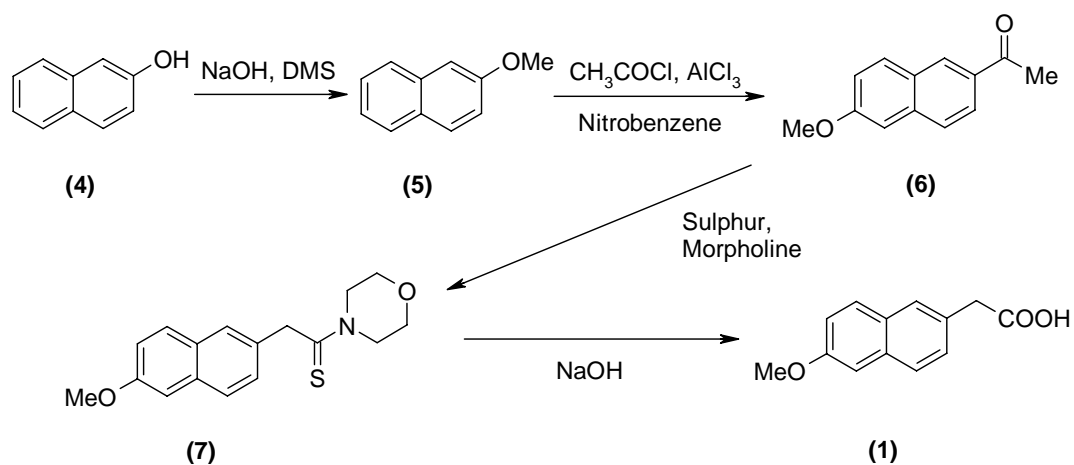
Scheme 3.1: Synthesis of 6-MNA **(1)**

The acetylated product **(6)** was subjected to Kindler-modified Wilgerodt reaction by refluxing it in morpholine containing sulphur. The thiomorpholide **(7)** so formed was isolated and hydrolysed under basic conditions. Hydrolysis of the thioamide **(7)** was performed by refluxing it in aqueous solution of sodium hydroxide to get acid **(1)** which was isolated and recrystallized to get pure acid[6] **(1)** as white powder.

6-MNA **(1)** gave a broad band at 3003 cm^{-1} (O-H*str*) and a strong characteristic peak at 1693 cm^{-1} (C=O*str*) in its IR spectrum. In the NMR spectrum (**Fig. 3.2. A**) aromatic protons appeared at δ 7.70-7.08, It yielded singlets at δ 3.87 (3H; OCH_3) and 3.68 (2H; -CH_2) in the PMR spectrum. Mass spectrum showed a molecular ion peak at 215.91 (M$^+$) which was also the base peak **(Fig. 3.2.B)**. The compound also showed high chromatographic purity by HPLC **(Fig. 3.2.C)**

(A)

(B)

(C)

Fig. 3.2. A: PMR spectrum of 6-MNA **(1), B:** Mass spectrum of 6-MNA **(1),**
C: Chromatogram of 6-MNA **(1)**

3.1.2 Synthesis of BPA (2)

Fenbufen **(8)** is a potent anti-inflammatory agent that is metabolized into 4'-hydroxy-4-biphenylbutanoic acid and 4-biphenylacetic acid **(2)**. 4-Biphenylacetic acid **(2)** is an active metabolite of fenbufen **(8)** with three times more activity than the parent drug and has a long half life.[7-9]
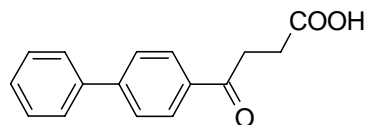
(8)

The NSAID 4-biphenylacetic acid **(2)** required for the preparation of liposomes was synthesized starting from biphenyl[9] **(9)** as shown in **Scheme-3.2.**
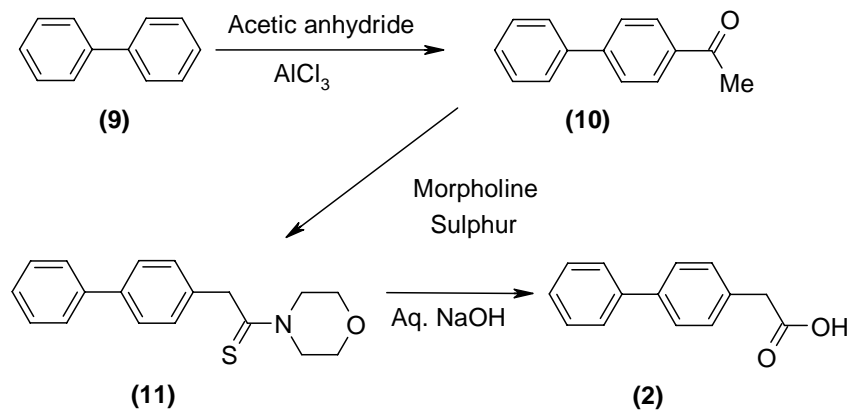
Scheme 3.2: Synthesis of BPA

251

Biphenyl **(9)** was reacted with acetic anhydride in the presence of anhydrous aluminium trichloride to yield 4-phenylacetophenone **(10)**. The compound **(10)** showed an intense peak at 1677cm^{-1} for the carbonyl (C=O) stretching in the IR spectrum. The ketone **(10)** was converted to 4-biphenylacetic acid **(2)** by the modified Willgerodt reaction which was carried out in two steps. The first step involved the conversion of ketone **(10)** to thiomorpholide **(11)** by reacting the ketone **(10)** with sulfur in presence of morpholine. In the second step, the thiomorpholide **(11)** was hydrolysed under basic conditions to obtain the required acid **(2)**.

Compound **(2)** showed the carbonyl stretching band at 1685 cm^{-1} and a broad peak for hydroxyl stretching at 3400 cm^{-1}in IR spectrum. The PMR spectrum **(Fig. 3.3. A)** showed broad signal at δ 8.84 due to carboxylic acid proton. A sharp singlet for the methylene protons (Ar-C*H*$_2$) appeared at δ 3.65 and signal for the aromatic protons appea-red as multiplet at δ 7.88-7.28.

(A)

(B)

252
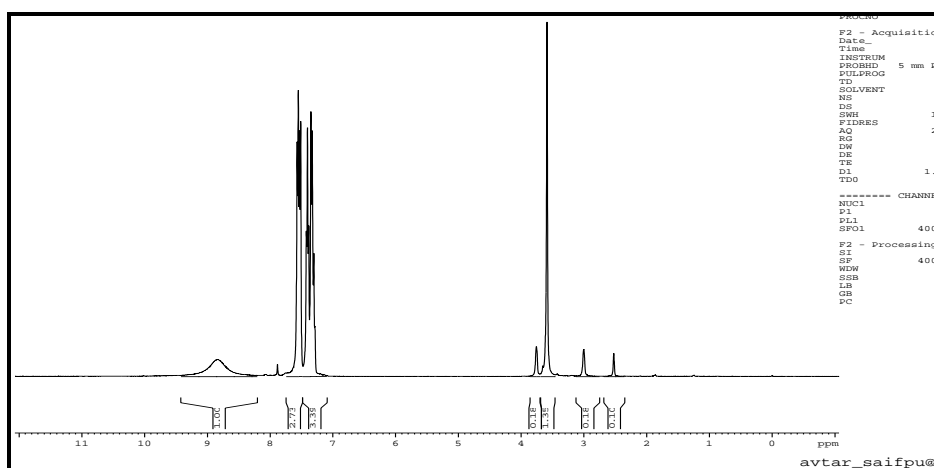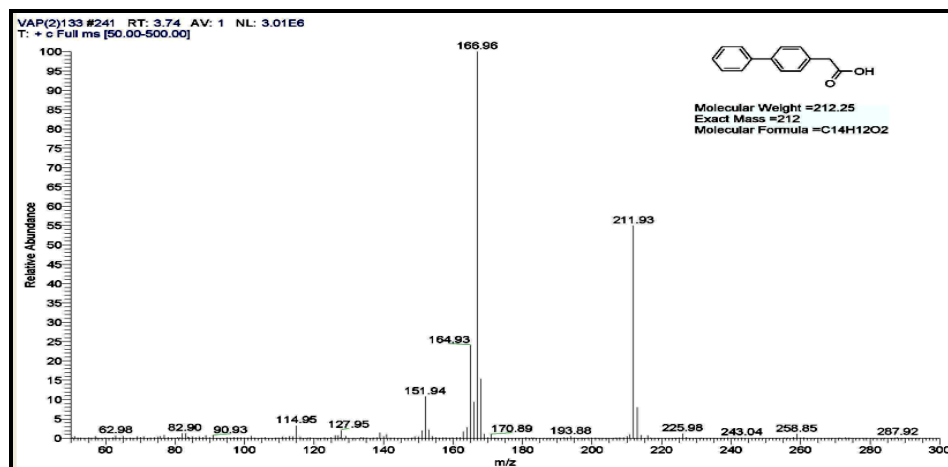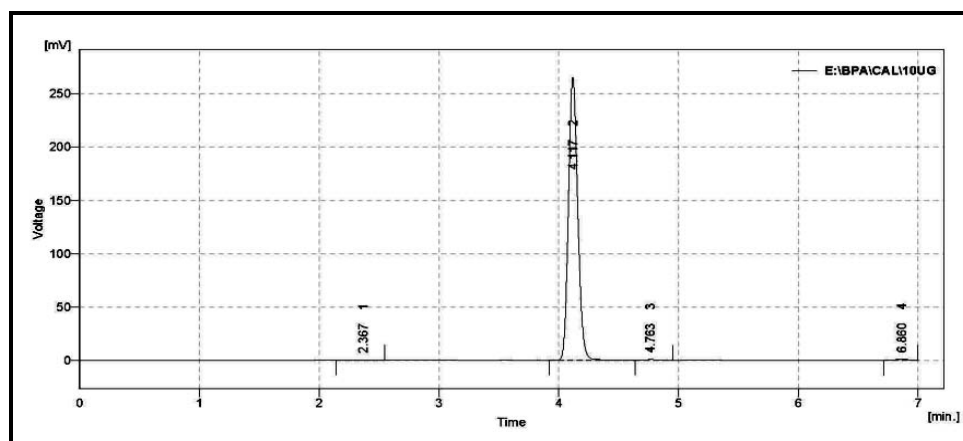
(C)

Fig. 3.3. A: PMR spectrum of BPA **(2)**, **B:** Mass spectrum of BPA **(2)**

C: Chromatogram of BPA **(2)**

Mass spectrum showed molecular ion peak at 211.93 (M^+) which was also the base peak **(Fig. 3.3. B)**. The compound also showed high chromatographic purity by HPLC **(Fig. 3.3. C)**

3.2 Preparation of salts and their characterization

3.2.2 Syntheses and characterization of NSAID-DSPE salts

Since the present work aims to prepare liposomes of NSAIDs mainly 6-MNA and BPA, literature survey was performed with respect to liposomal formulations of various NSAIDs. From the search it was revealed that liposomal formulations of naproxen, indomethacin and ketorolac tromethamine[10-12] have been developed to avoid side effects and control the *in vitro* release of the drugs. From the literature survey is was concluded that liposomal formulations of NSAIDs showed sustained release effect in comparison to the free drug and the said effect lasted for about 6-8 h. But for the IA drug delivery the requirement is that the drug should be released over a longer duration of time, ideally over a time period of >24 h. In order to achieve sustained and slow release of the active drug from liposomal formulation the NSAID must be physically entrapped in lipid membranes and also form ionic interactions with the lipids. So, it was achieved by salt formation with basic amino group containing lipids such as 1,2-distearoyl-*sn*-glycero-3-phosphoethanolamine (DSPE, **12**). Keeping this structure in mind and taking advantage of carboxylic acid functional group present in 6-MNA and BPA it was planned to prepare salts of these NSAIDs with DSPE and then prepare their liposomal formulations which could result in slow release of the drug.

(12)

(13)
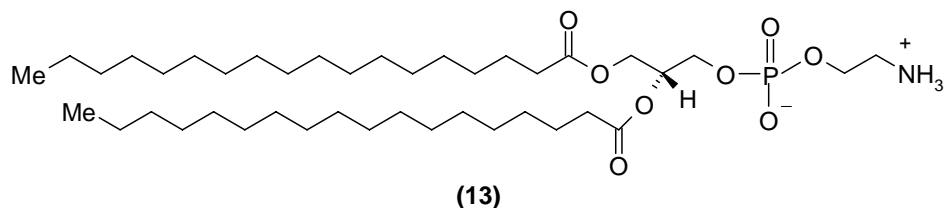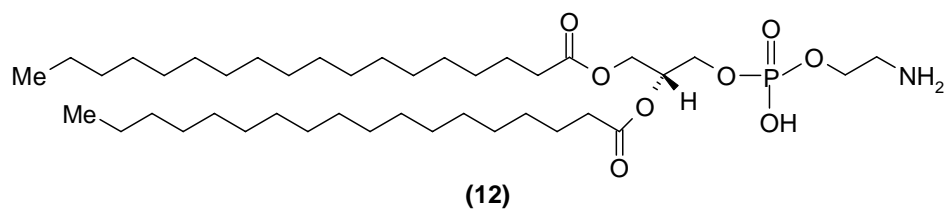
The required phospholipid was received as gift sample from lipoid GmbH (Germany) but we were not sure whether it was present as free base **(12)** or as a salt **(13)** due to intermolecular reaction. MSDS data disclosed structure **13** and showed its molecular formula as $C_{41}H_{82}NO_8P$ with molecular weight **748.07**. IR spectrum did not show broad peak for the presence of free amino group.

To solve this ambiguity it was planned to give it a base treatment to get sodium salt of DSPE **(14)** and generate free amino group which could further form salt with NSAIDs.

(13)

1. Methanolic NaOH
2. CHCl$_3$:MeOH
3. -5 to 2°C

(14)

R-COOH, **(1,2)**

(15a-15b)
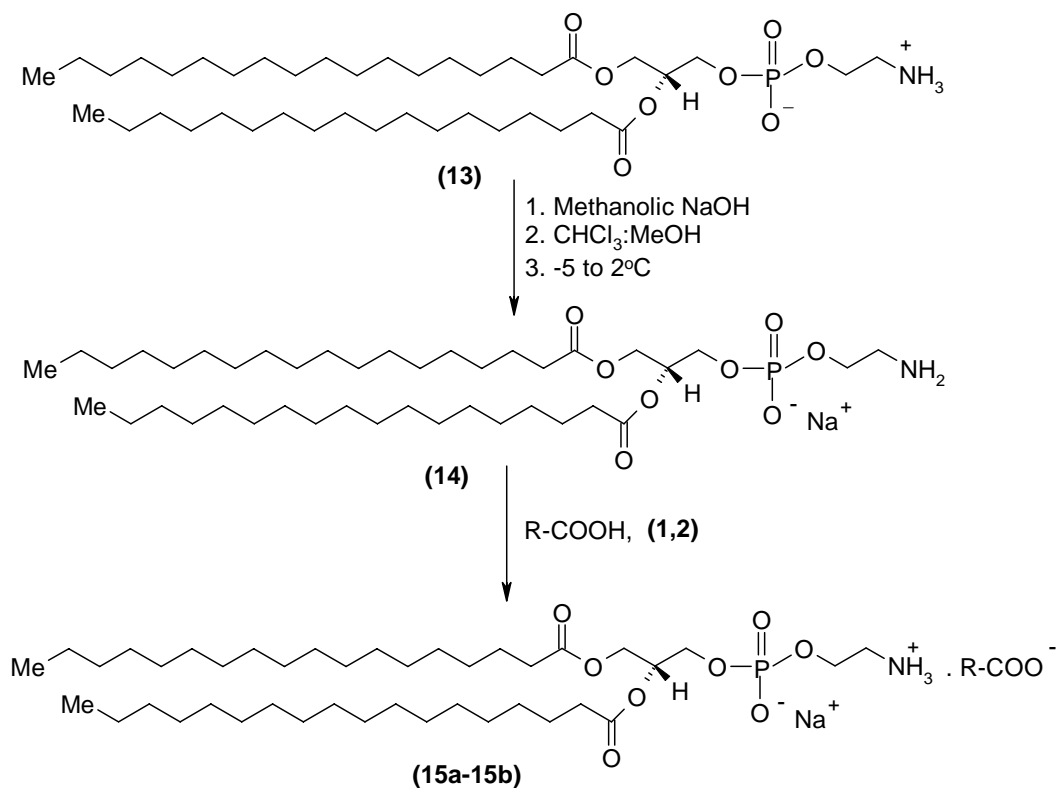
Scheme 3.3: Synthesis of salts of 6-MNA and BPA

The IR spectrum of DSPE-Na **(14)** showed carbonyl stretching due to presence of ester at 1741 cm^{-1} and N-H stretching of amine was observed at 3430 cm^{-1} (**Fig. 3.4**)

which was absent in IR spectrum of DSPE **(Fig. 3.5)** From this it could be concluded that ester functional group remained intact after salt formation and free amino group got generated due to breakdown of the internal salt and formation of sodium salt. Along with IR, mass spectrum also showed peaks at m/z 747 (negative mode) and 771 (positive mode) equivalent to DSPE (MW: 748) and its sodium salt (MW: 771) respectively **(Fig. 3.8)**
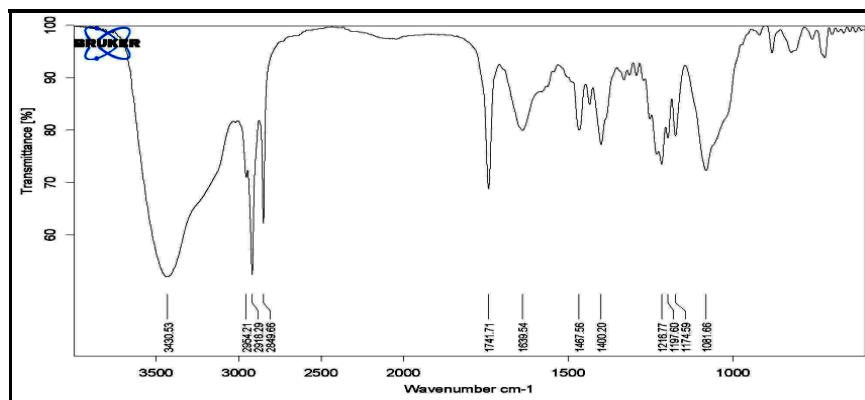
Fig. 3.4: IR Spectrum of DSPE-Na
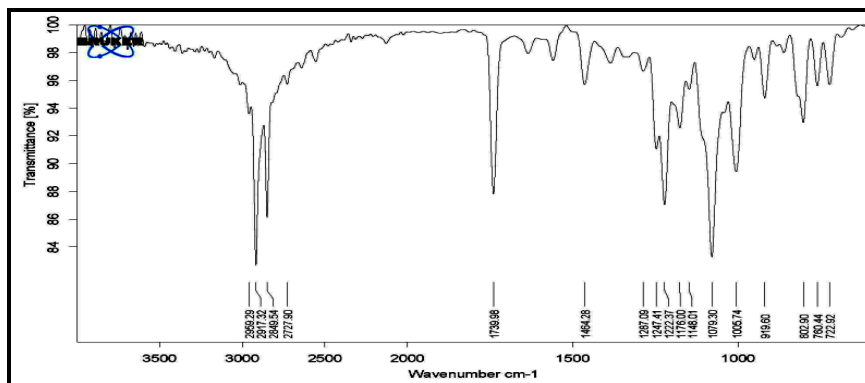
Fig. 3.5: IR Spectrum of DSPE
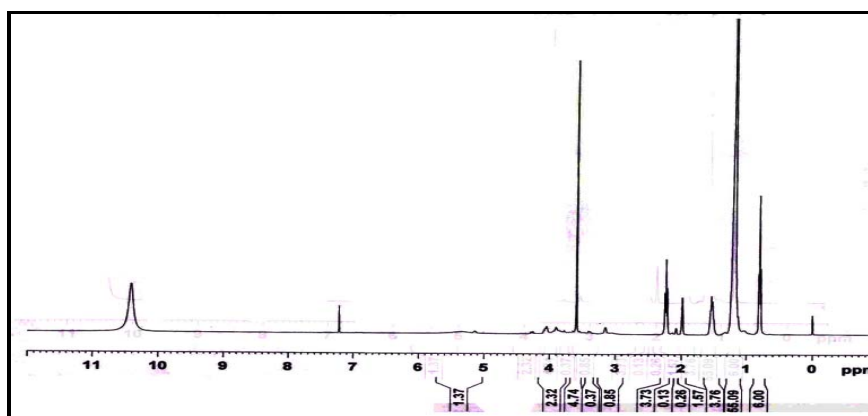
Fig. 3.6: PMR spectrum of DSPE-Na (Solvent-CDCl$_3$: acetic acid-d$_4$)
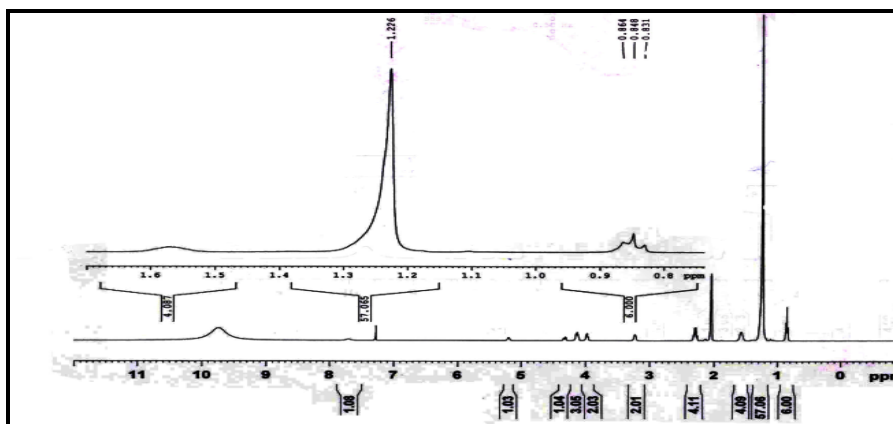
Fig. 3.7: PMR spectrum of DSPE (Solvent-CDCl$_3$: acetic acid-d$_4$)
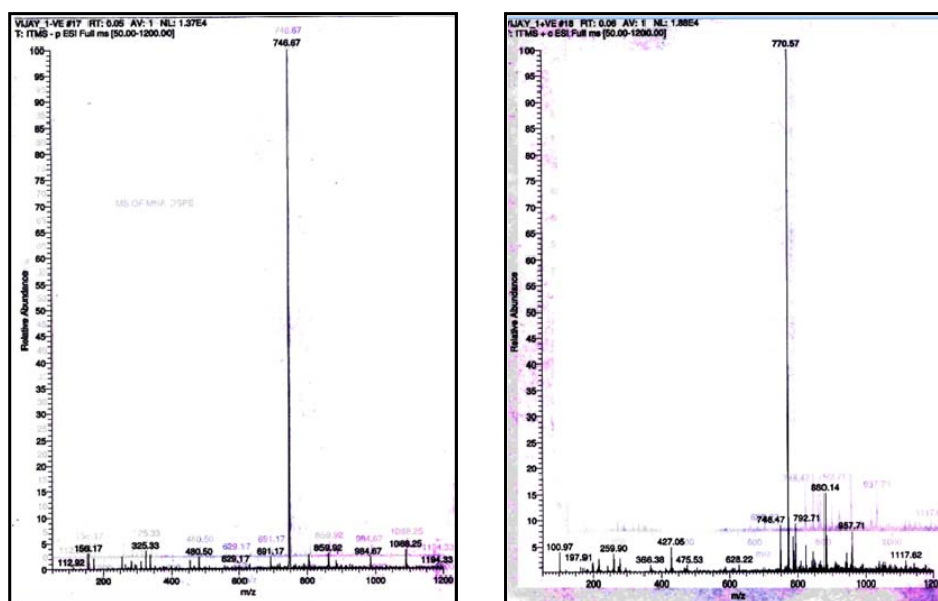
Fig. 3.8: Mass spectra of DSPE **(A)** and DSPE-Na **(B)**
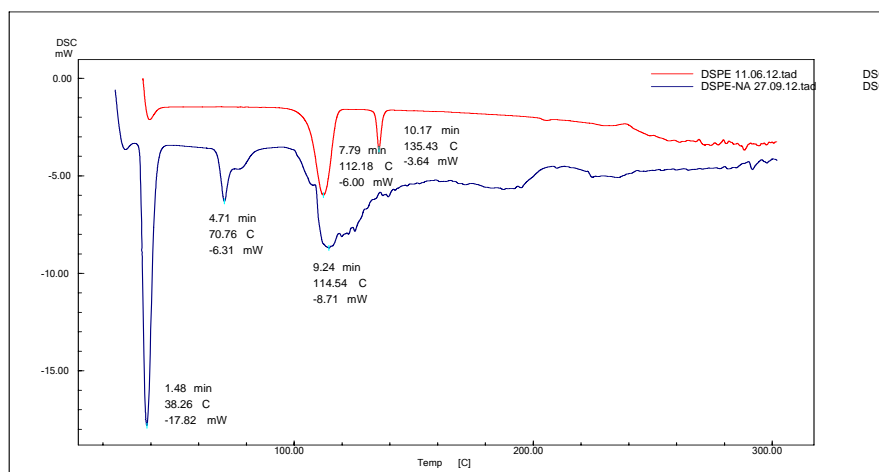
Fig. 3.9: DSC Thermogram of DSPE and DSPE-Na

(a)

(b)

(c)

(d)

(e)

(f)
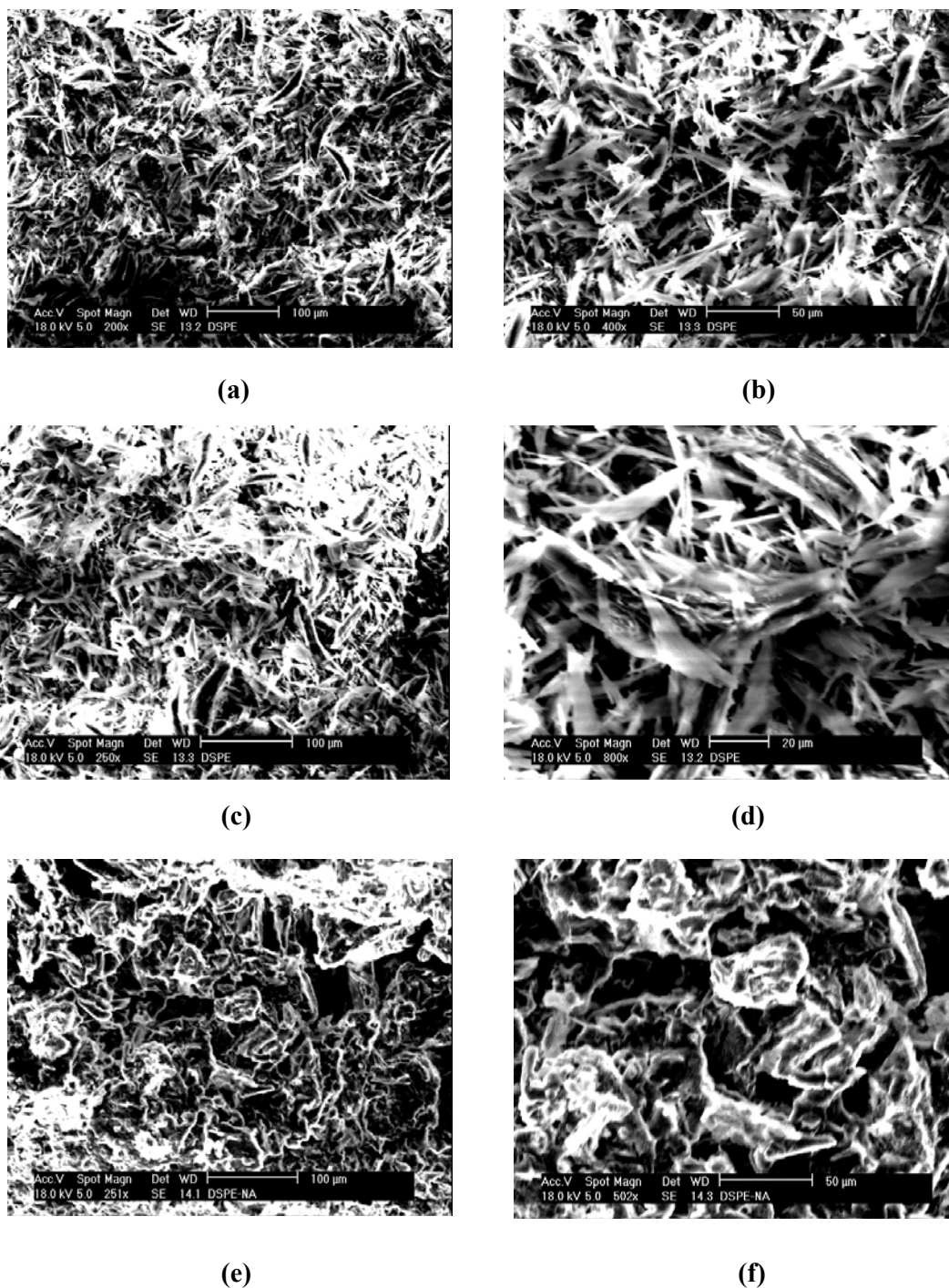
Fig. 3.10: Scanning electron microscope images of DSPE **(a-d)** and DSPE-Na **(e-f)**

Prepared DSPE-Na was characterized by using DSC. DSC showed endothermic peaks at 112.8 and 70.76^{o}C for DSPE and DSPE-Na respectively **(Fig. 3.9)** and these values are in good agreement with their melting points. DSC thermogram of DSPE-Na shows new endothermic peak at 70.76^{o}C which is absent in DSPE thermogram indicating

formation of sodium salt. Surface morphology was studied by SEM. SEM images also show changes in morphology when DSPE is converted to sodium salt (**Fig. 3.10**).

After successfully preparing sodium salt of DSPE containing free amine group, it was further treated with 6-MNA or BPA in chloroform and methanol mixture to get 6-MNA-DSPE or BPA-DSPE salts respectively. These salts were further characterized by various analytical techniques.
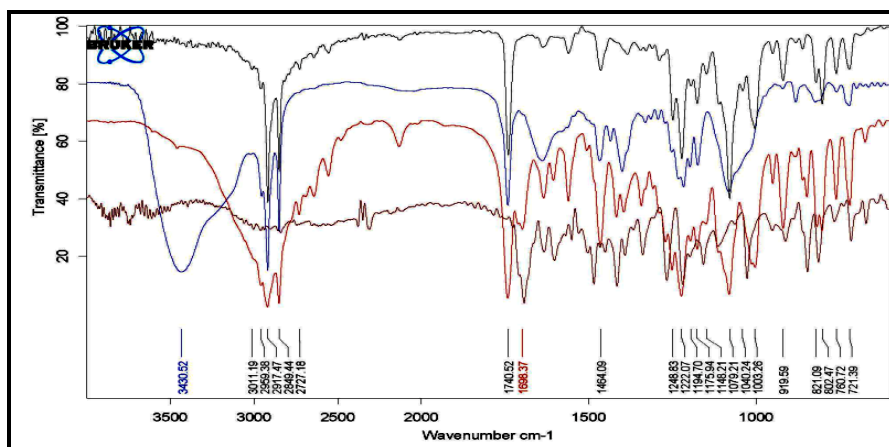
━━ DSPE, ━━ DSPE-Na, ━━ 6-MNA-DSPE ━━ 6-MNA

Fig. 3.11: Overlaid FT-IR Spectra of 6-MNA **(1)**, DSPE and its salt
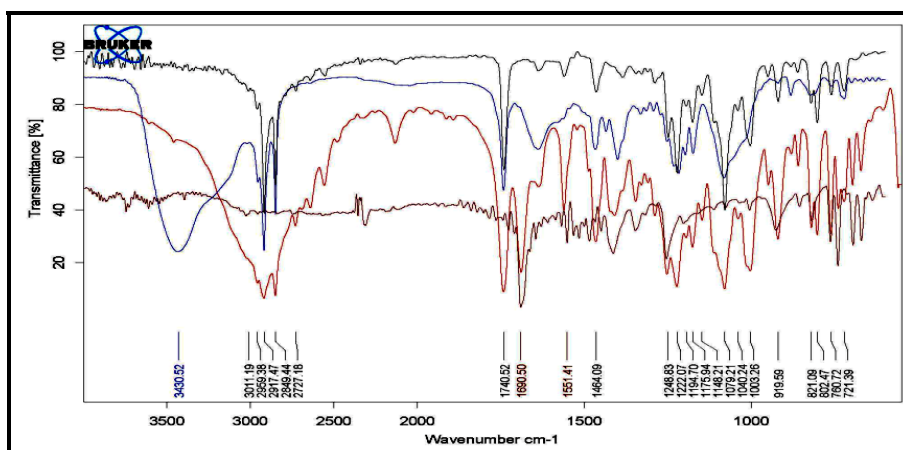
━━ DSPE, ━━ DSPE-Na, ━━ BPA-DSPE ━━ BPA

Fig. 3.12: Overlaid FT-IR Spectra of BPA **(2)**, DSPE and its salt

IR spectra of both 6-MNA-DSPE and BPA-DSPE show disappearance of peak at 3430 cm^{-1} of free amino group indicating formation of salt. PMR and CMR spectra of both the salts show protons or carbons equivalent to both the moieties of the salt. Salt formation and subsequent presence of both the moieties were also confirmed by mass spectra. Mass

spectrum of 6-MNA-DSPE salt showed single peak at 216.05 for 6-MNA but did not show peak of DSPE-Na using electron impact (EI) as ionization source **(Fig. 3.17)**. Similar results were observed when performed on LC-MS system having electrospray ionization (ESI) as ionization source **(Fig. 3.18)**.

Finally mass was performed on instrument having electrospray chemical ionization technique (ESCI=ESI+APCI). It showed peaks at 217.22 and 750.62 indicating presence of 6-MNA and DSPE-Na **(Fig. 3.19)**. Similar results were obtained with BPA and its salts. DSC thermograms also showed changes with respect to endothermic peaks when salt formation occurred **(Figs. 3.21-3.22)**.
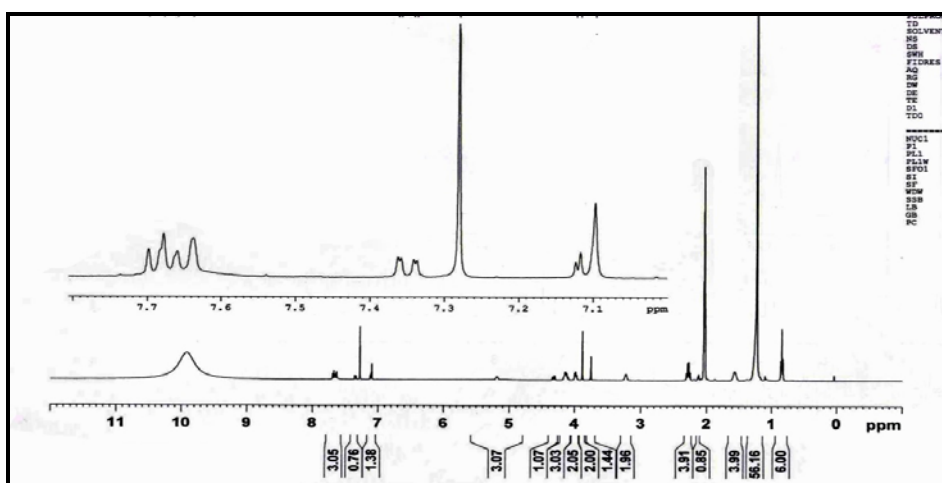
Fig. 3.13: PMR spectrum of 6-MNA-DSPE (CDCl$_3$: 1drop GAA-d$_4$)
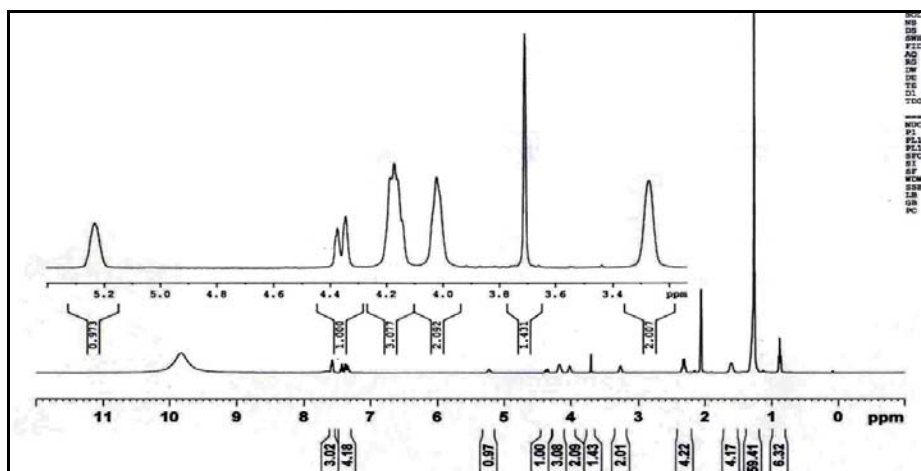
Fig. 3.14: PMR spectrum of BPA-DSPE (CDCl$_3$: 1drop GAA-d$_4$)
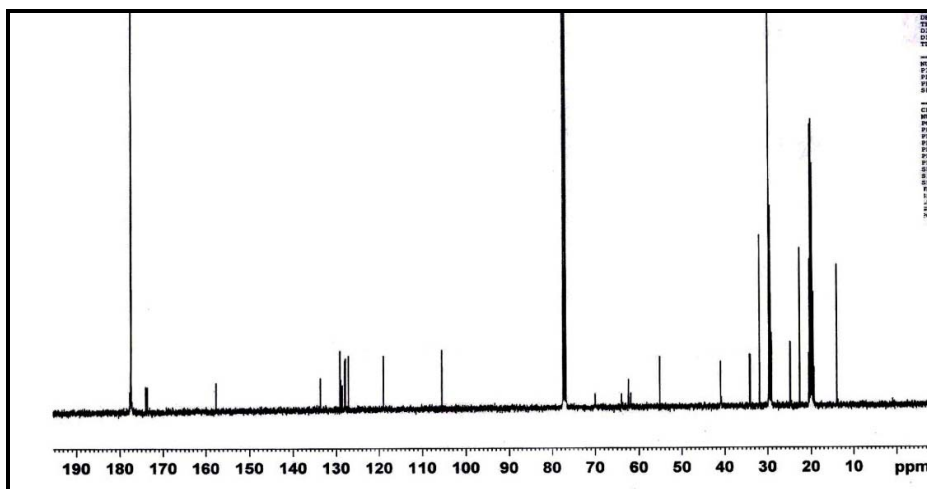
Fig. 3.15: ^{13}CMR spectrum of 6-MNA-DSPE (CDCl$_3$: 1drop GAA-d$_4$)
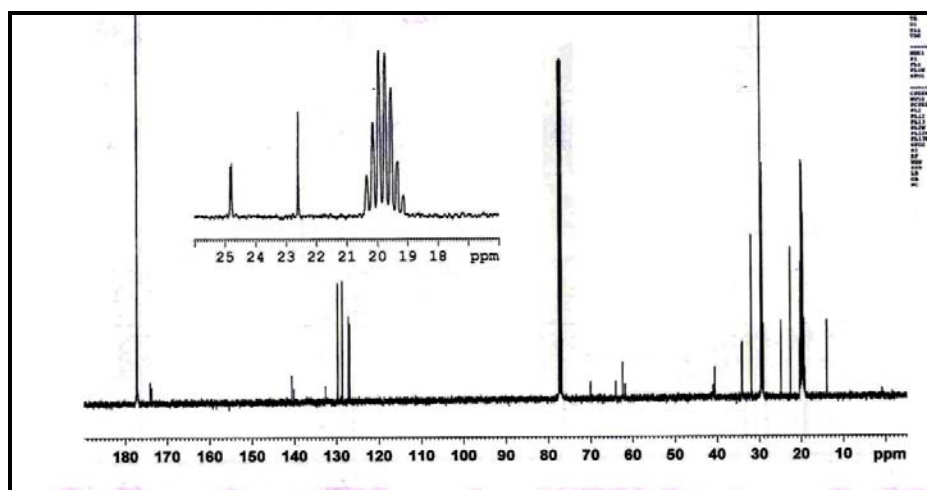
Fig. 3.16: ^{13}CMR spectrum of BPA-DSPE (CDCl$_3$: 1drop GAA-d$_4$)
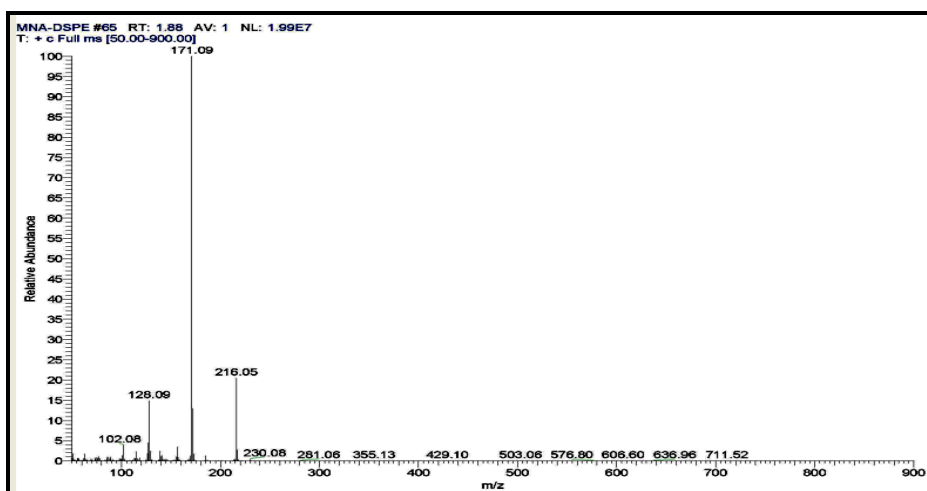
Fig. 3.17: Mass spectrum of 6-MNA-DSPE (Ionization: EI, DPI mode)
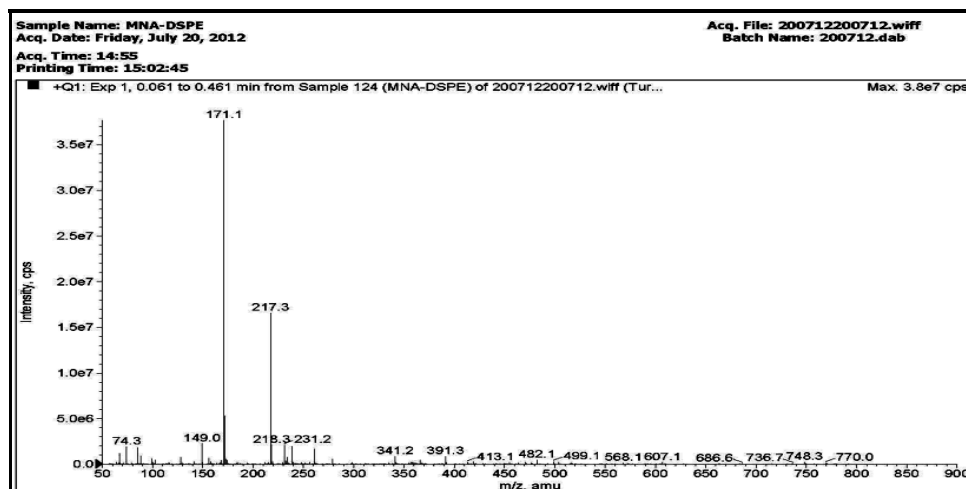
Fig. 3.18: Mass spectrum of 6-MNA-DSPE (Ionization: ESI)
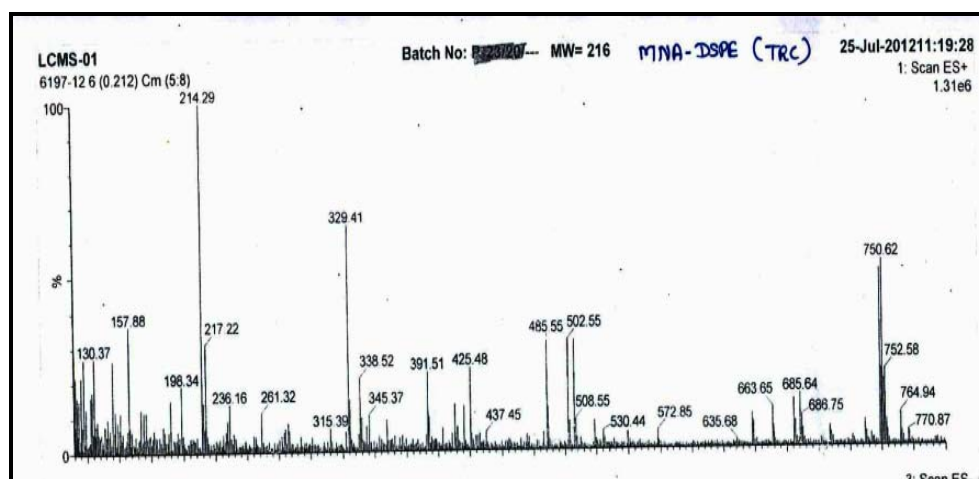
Fig. 3.19: Mass spectrum of 6-MNA-DSPE (Ionization: ESCI=ESI+APCI)
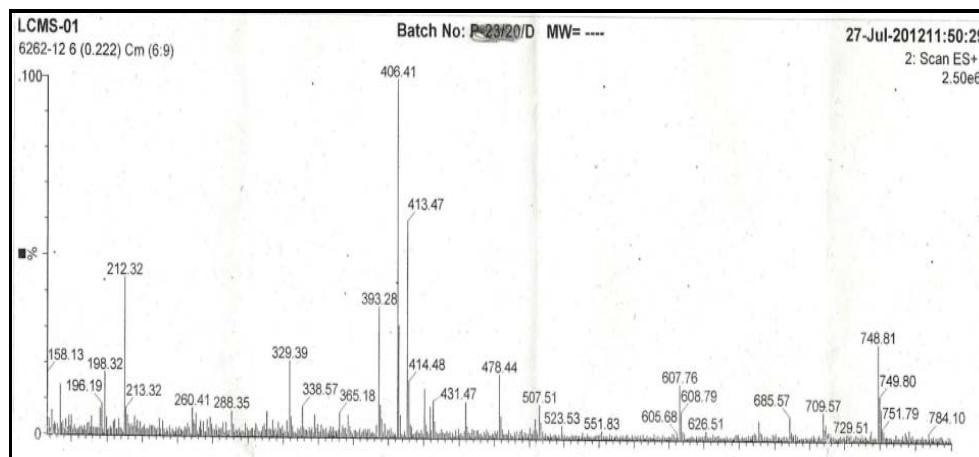
Fig. 3.20: Mass spectrum of BPA-DSPE (Ionization: ESCI=ESI+APCI)
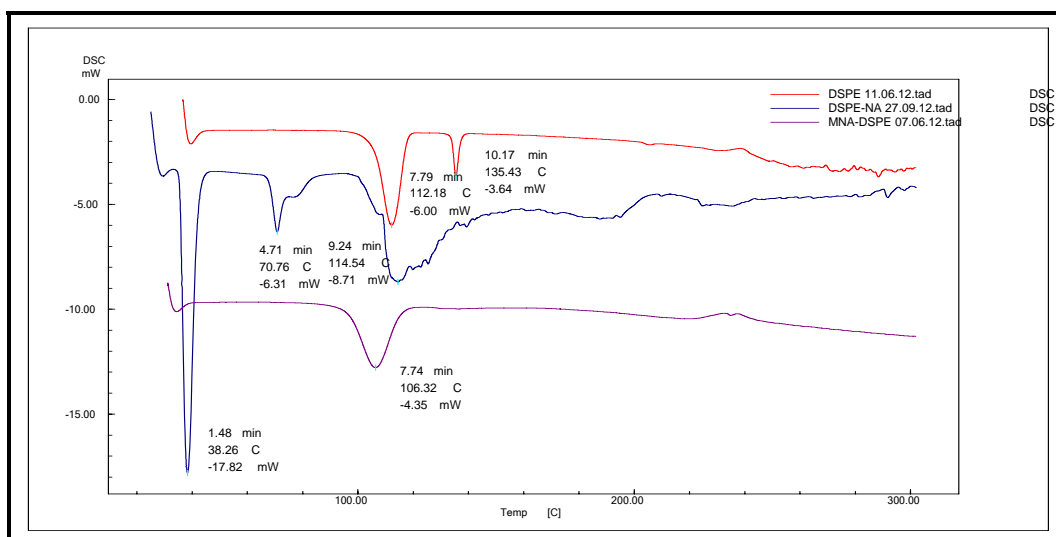
Fig. 3.21: DSC Thermograms of DSPE, DSPE-Na, 6-MNA-DSPE
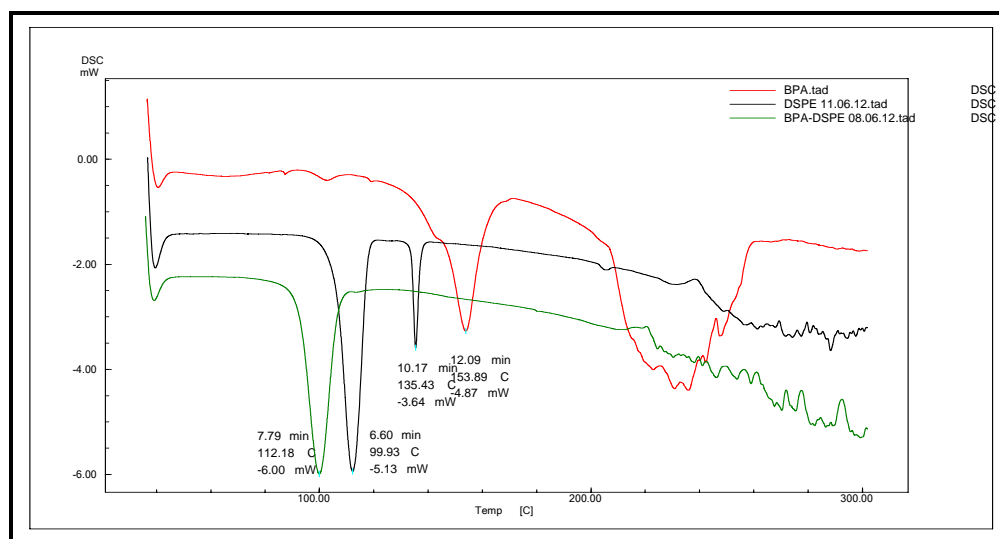
Fig. 3.22: DSC Thermograms of BPA, DSPE-Na, BPA-DSPE

3.3 Formulation of liposomes

3.3.1 Introduction

Liposomes are spherical lipid bilayers that serve as convenient delivery vehicles for biologically active compounds. The field of liposome research has expanded considerably over the last 35 years. It is now possible to engineer a wide range of liposomes varying in size, phospholipid composition and surface characteristics to suit the specific application for which they are intended. In comparison to other drug carriers, liposomes have some advantages like biological degradability and relative toxicological and immunological safety. It is not our intention to describe the details of such a vast field briefly and do injustice to all the relevant studies.

3.3.2 Preparation of liposomes

Liposomes containing NSAIDs were prepared by the lipid film hydration technique as it is simple and reproducible. Multilamellar vesicles (MLVs) were chosen for the entrapment of NSAIDs. Additional advantages of MLVs include ease of preparation and mechanical stability[13]. The requirement of mechanical stability and rigidity was further fulfilled by incorporating cholesterol, which is well documented to:

a) decrease the fluidity or micro viscosity of the bilayer by filling empty spaces among the phospholipid molecules.

b) reduce permeability of the membrane to water-soluble molecules due to the above effect and,

c) stabilize the membrane in the presence of biological fluids such as plasma.

A mixture of lipids, cholesterol and respective NSAID were dissolved in a mixture of chloroform and methanol (ratio 3:1) an RBF as the solubility of these lipids is higher in this solvent blend[13]. The flask was rotated in a rota evaporator at 65-75 rpm for 20 min in a thermostatically controlled water bath at 37 ^{o}C under vacuum (300 mm.Hg). The thin film so formed inside the RBF was further dried under vacuum for 6h. The thin dry lipid film was hydrated using purified water and the flask was rotated once again for 30 min at 50 ^{o}C. The liposomal suspension thus formed was then transferred to a suitable glass container for size measurement and it was found to be >1 μ. The liposomal suspension was incubated for 1-2 h at 75 ^{o}C (glass transition temperature of lipid) and the sample was sonicated for few seconds to reduce size and improve drug entrapment. The sonicated dispersion was then allowed to stand undisturbed for about 2h at room temperature for the annealing to be completed.

The next step in the preparation of the liposomes was the separation of unentrapped drug from the liposomes. Unentrapped drug was removed from the liposomal suspension by centrifugation at 4000-5000 rpm for 8-10 min at 0-5 ^{o}C temperature. The major process parameters were optimized using the percentage drug entrapment, size and zeta potential as the response parameters. The observations of the optimization processes are tabulated in **Table 3.1.**

3.3.3 Optimization of liposome formulation (Preliminary batches)

The following conditions were optimized for liposomes containing NSAIDs.

A. Composition of lipid mixture

Trials were initiated with a molar ratio of 1:4:0.15 (6-MNA: HSPC: Cholesterol, % EE=42.34±1.58 %, Table 3.1.). Increase in the proportion of HSPC, cholesterol in the lipid

mixture significantly enhanced the percentage of drug entrapped (Table 3.1). However further increase in HSPC, cholesterol proportion above 1:9 and 1:0.5 respectively did not lead to any significant improvement in the drug entrapment. This is probably due to saturation of the available space.

B. Hydration medium

Distilled water was used as the hydration medium for hydrating the dry lipid film. Trials using phosphate buffer or saline were not taken because solubility of 6-MNA/BPA in phosphate buffer might increase (due to salt formation) reducing drug entrapment, hence hydration medium was limited only to distilled water. The volume of distilled water was optimized to 8 ml for 6-MNA liposomes **(Batch: ML-7)**. Increase in the volume of water did not show any significant improvement in drug entrapment.

C) Hydration time

Increase in hydration time in the rotator flask from **15 min to 30 min** led to significant increase in drug entrapment. Further increase in hydration time did not lead to increase in drug entrapment. This indicated that the drug got incorporated in the lipid bilayer rather than aqueous compartment. A decrease in hydration time (<15 min) was associated with the incompletely formed liposomes when observed microscopically.

D) Sonication time

A sonication time of 15 sec was found to be sufficient for reduction in the particle size to around or less than 1μm without any significant change in the percent of drug entrapment. Sonication of liposomal suspension was optimized by altering time, cycle and amplitude according to the size requirements keeping in mind that sonication would not result in complete conversion of MLVs into LUVs and SUVs. Sonication was done at 60 % amplitude, 0.6 cycles for 15 sec to get mixture of MLVs, LUVs, and SUVs.

E) Zeta potential (DOTAP concentration)

Formation of liposome having positive zeta potential is important for this work hence cationic lipid DOTAP was used for this purpose and its concentration was optimized. DOTAP in low concentration (Drug: DOTAP=1:0.1) gave zeta potential in the range of 18-22 mV and it had no effect on liposome formation. To produce liposomes with zeta potential >25 mV higher concentrations of DOTAP (Drug: DOTAP=1:0.4 or 1:0.3) were used in formulation which resulted in increased zeta potential to >55.4 mV but the size of liposomes decreased significantly and initial size of liposomes without sonication was found to be <250 nm. This might be due to repulsion between charged lipids which leads to decreased drug entrapment. In order to get optimum zeta potential (25-35 mV)

and size of liposomes (>250 nm to <1.5 μm) with good entrapment efficiency (>70 %), DOTAP concentration was optimized to a ratio of 1:0.2 (Drug: DOTAP). It was found to be suitable to produce zeta potential in the range of 25-35 mV.

F) Entrapment efficiency

The percentage of drug entrapment of liposomes was calculated by estimating the drug in the liposomes. Liposomes were centrifuged at 6,000 RPM for 10-15 min at 2-8 ^oC the supernatant was removed off for estimating the entrapped drug in the liposome after lysis with methanol. Briefly, 0.1 mL of liposome was diluted upto 1.0 mL with methanol, sonicated for 5 min. and centrifuged at 3,000 RPM for 10 min at 2-8^oC. Supernatant was analyzed for respective drug contents after suitable dilution with mobile phase using HPLC. For the estimation of 6-MNA and BPA HPLC method was developed and the chromatographic conditions used for the assay are given in **Table 3.1.** Percentage of entrapment was calculated using the formula given below:

Table 3.1: Chromatographic conditions for the estimation of 6-MNA and BPA

NSAIDs	Linearity range (µg)	Mobile phase composition	Flow rate (ml/min.)	Retention time (R_t Min.)	λ_{max}
6-MNA	500 ng-20 ug	ACN:PB 15 mM (3:1)	1.0	3.60 ± 0.2	230
BPA	500 ng-20 ug	ACN:PB 15 mM (3:1)	1.0	4.10 ± 0.2	253

PB=Phosphate buffer (15 mM, *p*H 5.0), ACN=Acetonitrile
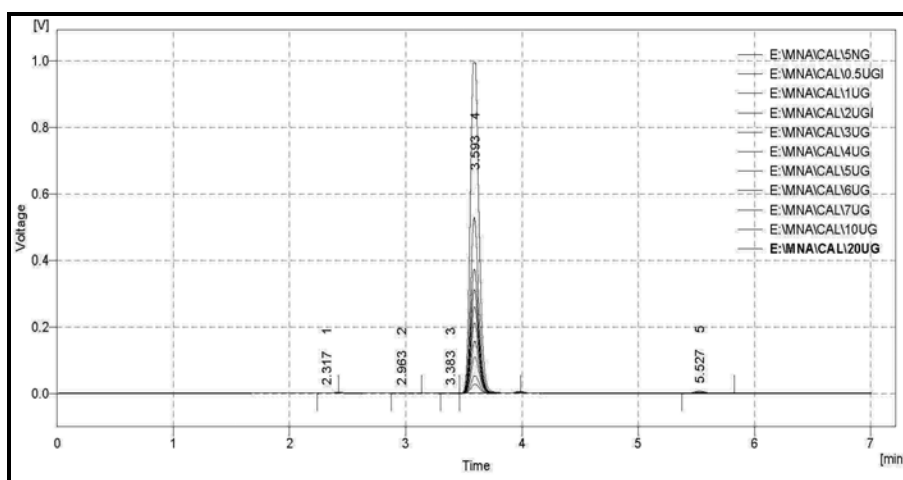
Fig. 3.23: Calibration and linearity chromatograms of 6-MNA **(1)**

265
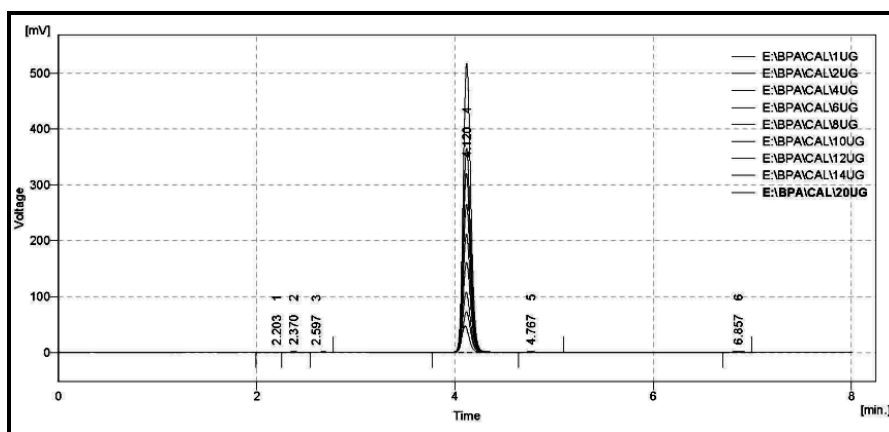
Fig.3.24: Calibration and linearity chromatograms of BPA **(2)**

$$\% \text{ Entrapment efficiency} = \frac{\text{Total drug added - Free drug}}{\text{Total drug added}} \times 100$$

$$= \frac{\text{Entrapped drug}}{\text{Total drug added}} \times 100$$

Table 3.2. shows preliminary batches used for optimization of liposomal formulation with their response parameters.

Table 3.2: Optimization of Drug: Lipid: DOTAP mixture ratio (6-MNA=10 mg)

Batch No.	MNA	HSPC	DOTAP	Volume†	% EE*	Size* (nm)	Zeta* (mV)
ML-1	1	4	0.1	6	42.34±1.58	1672±20.1	21.4±2.0
ML-2	1	6	0.1	6	56.12±2.04	1579±18.5	20.8±2.1
ML-3	1	8	0.1	8	67.96±2.56	1297±16.7	20.6±2.4
ML-4	1	8	0.3	8	62.89±1.98	239±12.6	65.3±4.3
ML-5	1	8	0.2	8	69.44±2.45	840±15.8	32.4±3.2
ML-6	1	10	0.2	8	71.66±3.04	914±17.4	31.8±2.3
ML-7	**1**	**9**	**0.2**	**8**	**74.23±3.22**	**722±18.9**	**29.8±2.4**
ML-8	1	9	0.2	9	74.56±3.41	761±14.8	38.44±3.1
ML-9	1	9	0.2	6	69.64±3.84	547±16.1	42.57±3.2
*=Mean±SD, n=3; †=Hydration volume (ml);							

3.3.4 Optimization of formulation variables by applying 3^2 factorial designs

Based on the results obtained in preliminary experiments, drug: lipid (HSPC) and drug: DOTAP ratio, were found to be the major variables affecting the percent drug content (PDC), zeta potential and mean particle size (MPS). To reduce the computational complexities, the above mentioned components were eased to 2 independent variables namely lipid (HSPC) and cationic carrier (DOTAP) concentrations. Approximate levels of these independent variables were chosen from the data available from literature as well as from the initial experimentation.

It was assumed that the independent variables would affect responses in linear or quadratic manner and the possibility of interaction effect of the independent variables was also taken in to consideration. This assumption was necessary to develop a mathematical model which could be tested for significance of contribution of various independent variables. Hence, it became essential to use a factorial design with three levels to estimate curvature of response (i.e. 3^2 factorial with total no. of experiments= 9). To save time, single block design with zero (0) replication has been preferred. The experimental grid was coded for ease of representation in **Table 3.3.**

Nine batches of different combinations were prepared by taking values of selective variables X1 and X2 at different levels as shown in **Table 3.3**. All other formulation and process variables were kept invariant throughout the study (Cholesterol concentration 0.023 mM (9.0 mg); hydration time 45 min; annealing time 2 h; hydration temperature 65±2 ^{0}C). The prepared batches were evaluated for drug entrapment/content, particle size and zeta potential as dependent variables, and the results are recorded in **Table 3.5. Table 3.4** summarizes the experimental runs and the employed factor combinations.

Table 3.3: Translation of experimental conditions into physical units for liposome formulation optimization.

Variables	Level		
	-1	0	1
X1 (lipid concentration)	294	314	334
X2 (DOTAP concentration)	3	6	9

Table 3.4: Factor combination as per the experimental design for optimization

Level	Batch								
	F1	F2	F3	F4	F5	F6	F7	F8	F9
X1	-1	0	1	-1	0	1	-1	0	1
X2	-1	-1	-1	0	0	0	1	1	1

Following parameters were kept constant for liposome formulation optimization process:

a) Cholesterol concentration=0.023 mM (9 mg), b) Hydration volume= 8 ml

The results obtained are given in **Table 3.5**. the obtained data was subjected to statistical analysis.

Table 3.5: 3^2 Full factorial design consisting of experiments for the study of two experimental factors in coded and actual levels with experimental results

Formulation	Actual value variables		Respone value		
	X1	X2	% Drug entrapment	Mean Particle size (nm)	Zeta potential (mV)
FML-1	294	3	68±2.14	1244±20.1	21.4±1.5
FML-2	314	3	71±3.44	1454±19.8	22.5±2.2
FML-3	334	3	75±1.89	1596±22.4	22.2±2.5
FML-4	294	6	72±2.56	550±18.4	25.9±3.1
FML-5	**314**	**6**	**74±3.08**	**774±14.66**	**30.5±3.2**
FML-6	334	6	76±2.7	582±12.58	44.7±4.7
FML-7	294	9	58±1.94	258±10.89	55.4±4.6
FML-8	314	9	62±1.74	269±11.44	66.4±6.7
FML-9	334	9	64±3.40	465±13.78	65.3±5.0

Values are Mean±SD, n=3

The effect of lipid and DOTAP concentration was statistically analyzed using Stat-Ease software (Design-Expert® 8), ANOVA for response surface quadratic model gives results as given in **Table 3.6.**

Table 3.6: ANOVA results for optimization of entrapment efficiency.

Source	F value	p-value, Prob>F
Model	63.67	0.0044
A-HSPC	45.37	0.0095
B-DOTAP	150.0	0.0017
AB	0.19	
A^2	0.011	
B^2	95.35	

The model F value of 49.47 implies that the model is significant. There is only a 0.44 % chance that a model f-value this large could occur due to noise. Values of prob >F less than 0.0500 indicate model terms are significant. In this case A, B and B^2 are significant model terms. The "Pred R-Squared" of 0.8556 is in reasonable agreement with the "Adj R-Squared" of 0.9680 "Adeq Precision, measures the signal to noise ratio, a ratio greater than 4 is desirable. Our ratio of 19.522 indicates an adequate signal, so this model can be used to navigate the design space.

Table 3.7: Statistical data for % entrapment

Parameter	Value	Parameter	Value
Std. Dev.	1.13	R-Squared	0.9880
Mean	68.94	Adj R-Squared	0.9680
C.V. %	1.65	Pred R-Sequared	0.8556
Press	46.54	Adeq Precision	19.522

Final equations in terms of coded factors is given below:

% Entrapment= $+74.22+2.75xA-5xB-0.25xAB-0.083xA^2-7.83B^2$

Where A= Conc. of HSPC, B=Conc. of DOTAP (ANOVA for response surface quadratic

model *p* <0.0044)

Zeta potential=+39.37+4.92xA+20.17xB (ANOVA for response surface linear model
$p<0.0008$)

Size= +799.11+98.50xA-550.33xB (ANOVA for response surface linear model $p<0.0007$)

When the relationship for the response is given as a function of two independent variables, it can be well represented by 3D plots. The surface responses show the 3D plot of two independent variables simultaneously. Graphically there are contour plots on which the axes represent the two independent variables; the counters represent a specific level of response and, we can select an optimum value. Graphically 3D surface response plot for % entrapment is shown in **Figure 3.25 A-C.**

Confirmatory report suggested batch-5 (FML-5) as the most appropriate batch with respect to % entrapment, size and zeta potential. This final batch was optimizd and evaluated thrice having composition of 6-MNA 0.046 mM (10 mg), HSPC 0.414 mM (314 mg), cholesterol 0.023 mM (9 mg), DOTAP 0.009 mM (6mg) and purified water 8 ml. Another objective of the present work was to develop sustained release liposomal formulations of NSAIDs, hence salts of these two NSAIDs with DSPE were used in the formulation to sustain the release. So, in order to develop liposomal formulations containing Drug-DSPE salts the above optimized batch (**FML-5)** was used for further
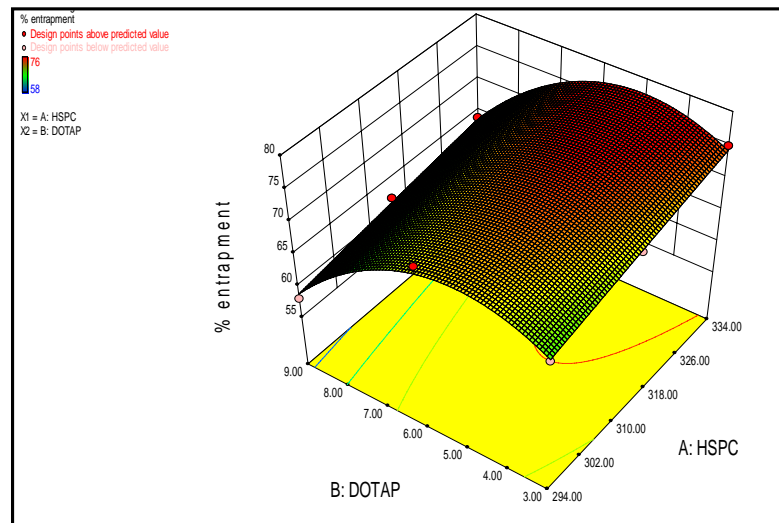
(A)
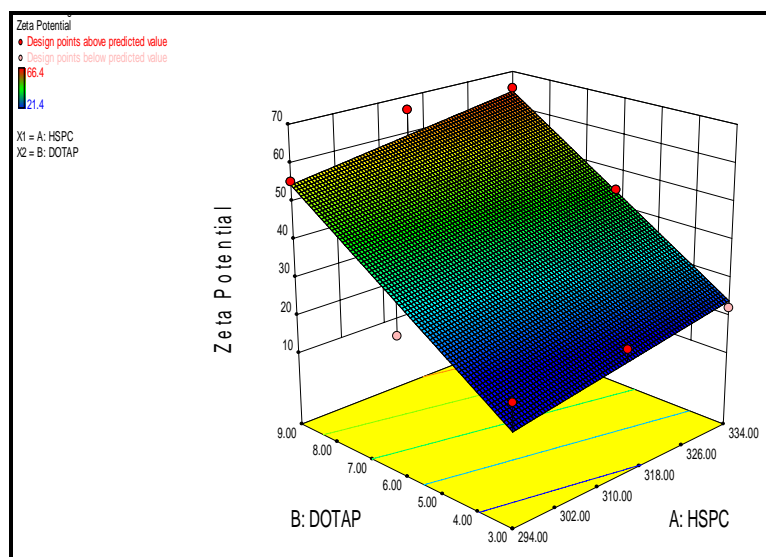
(B)
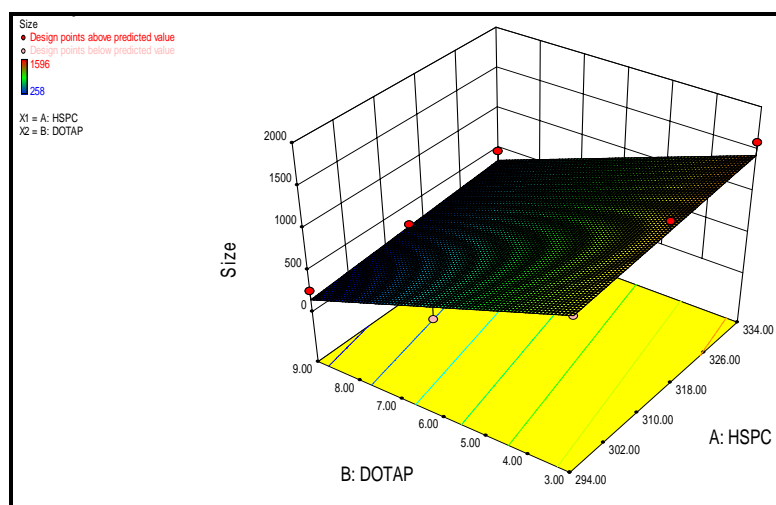
(C)

Fig. 3.25: 3D surface response plot for **A**: % entrapment, **B**: Zeta potential and
C: Size

development with varying mole ratio of the parent drug and Drug-DSPE **(Table 3.8)**. Four

batches with 6-MNA: 6-MNA-DSPE mole ratios of 9:1, 8:2, 7:3 and 6:4 were taken and

evaluated.

From the results it can be concluded that increasing the ratio of 6-MNA-DSPE salt

decreases the drug entrapment, and the optimum ratio was found to be 8:2. In order to

maintain optimum entrapment efficiency and susteined release we have chosen batch

(**CML-2)** which contains 6-MNA: 6-MNA-DSPE salt with mole ratio of 8:2. From the

previous studies it was conclude that plain 6-MNA batches have maximum drug

entrapment and it may be due to maximum space available in liposomes as shown in **Fig.**

3.26A. Incorporation of only 6-MNA-DSPE salt in liposome may result in very low

entrapment of the drug in liposomes but a higher sustained release effect **(Fig. 3.26B).**

271

Combining the advantages of both the approaches would give ideal drug delivery system having higher entrapement capacity and sustained release of drug **(Fig. 3.26C).**

Table 3.8: Optimization of the effect of ratios of 6-MNA: 6-MNA-DSPE on liposomes.

Formulation	Mole Ratio#	Respone value		
Formulation	6-MNA: 6-MNA-DSPE#	% Drug entepment	Mean Particle size (nm)	Zeta Potential (mV)
CML-1	9:1	73±2.10	864±12.78	31.5±4.2
CML-2	**8:2**	**72.55±4.25**	**695±10.89**	**33.4±5.3**
CML-3	7:3	64.88±5.17	680±11.33	28.7±3.8
CML-4	6:4	59.95±6.18	547±09.66	32.5±4.7

equivalent to 6-MNA
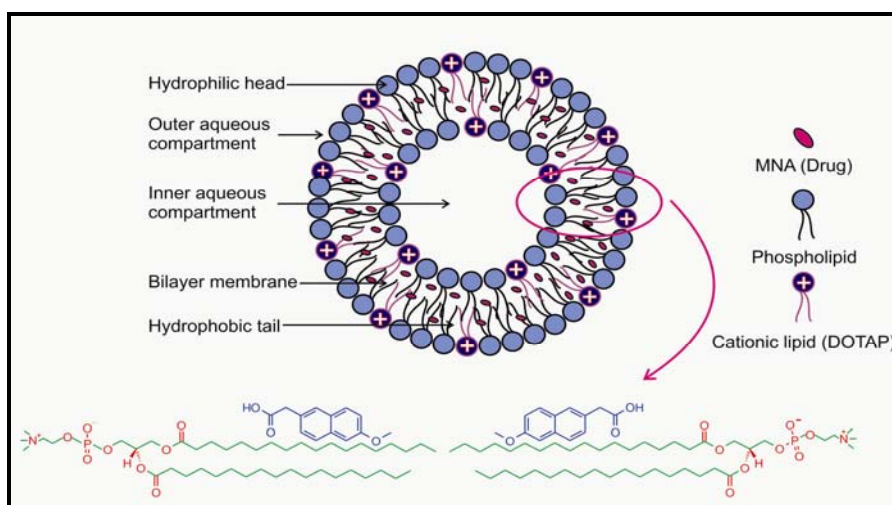
(A)
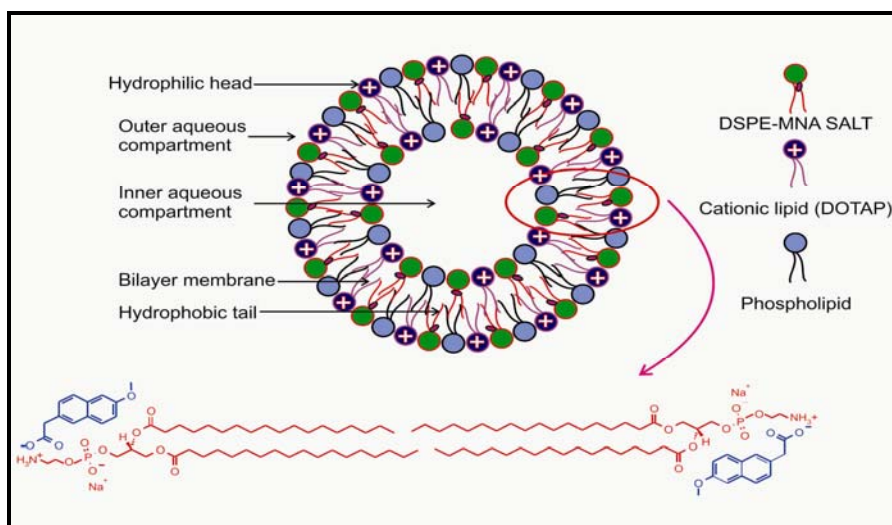
(B)
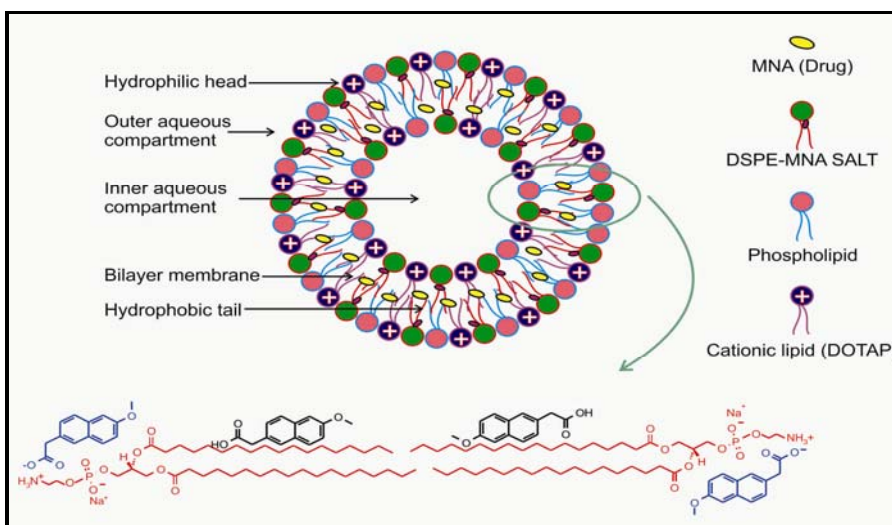
(C)

Fig. 3.26: A-C: Drug entrapment into liposomes

3.4 Characterization of liposomes

Both physical and chemical characterizations of liposomes influence their *in vivo* and *in vitro* behavior. Liposome characterization was performed immediately after preparation. The prepared liposomes were characterized for the following attributes:

A) Size

B) Morphology

C) Zeta (ς) potential

D) *In vitro* diffusion

A) Size

Size is an important parameter for IA drug delivery. Bonanomi *et al.* reported that increasing the size of liposomes, ranging from 160 nm to 750 nm in diameter, resulted in a 2.6-fold increase in retention to 48 h post-injection.[14-15] A similar observation was described for liposomes containing methotrexate, for which a mean diameter of 1.2 μm ensured a higher retention, and thus anti-inflammatory action, than the one with 100 nm size.[16-17] There is an upper limit (40-250 nm radius) to the size of particles that can escape freely from the joint cavity. So, >250 nm size of liposomes is an essential requirement of liposomal drug delivery.
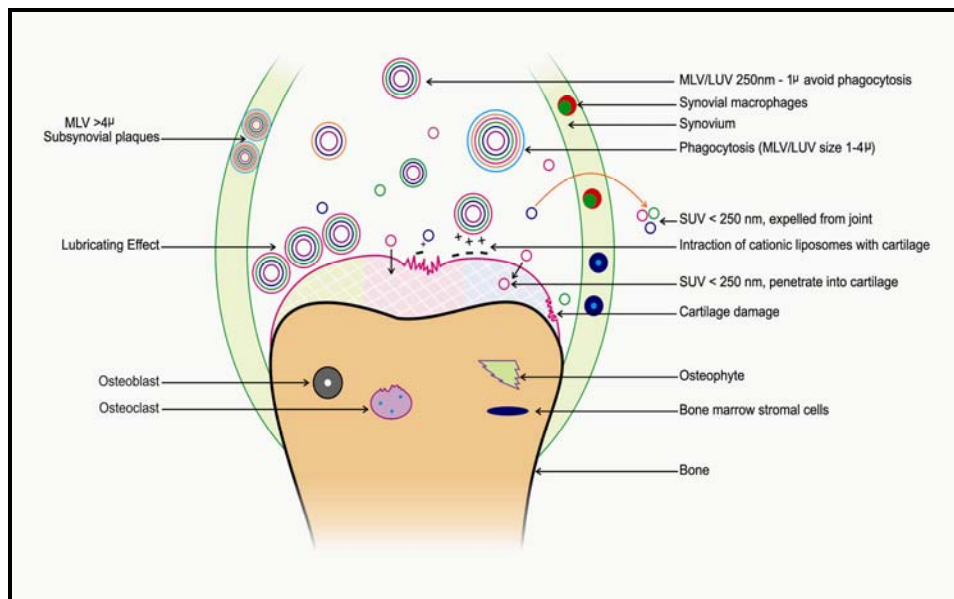
Fig. 3.27: Fate of IA administered liposomal drug delivery systems.

(A)
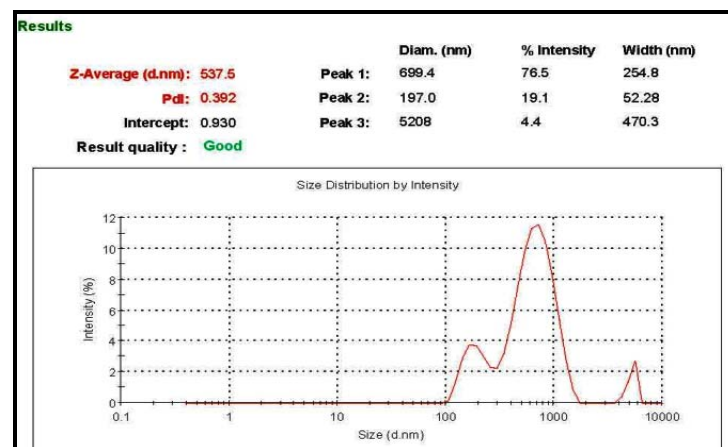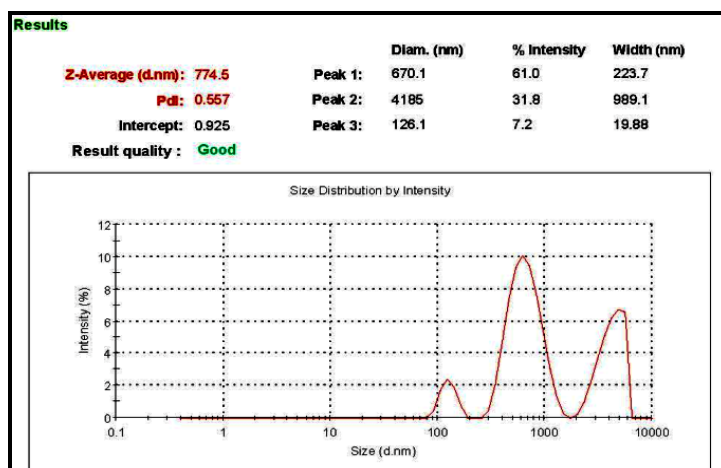
Fig. 3.28: Particle Size analysis of the optimized liposome batch, two readings **(A)** and **(B)**

Multilamellar as well as unilamellar liposomes with size range of 250-1000 nm will provide ideal drug delivery system. Small unilamellar vesicles would be expelled from the joint whereas large liposomes (>1 μ) would undergo phagocytosis as shown in **Fig. 3.27**. Considering all the above factors liposomes having size range of >250 nm but <1 μ have been prepared. The average particle size and PDI were calculated after performing the experiment in triplicate. PDI of 0.0 represents a homogenous particle population while 1.0 indicates a heterogeneous size distribution in the liposome. The particle size analysis results of liposomal formulation were shown in **Fig. 3.28A-B.**

Transmission electron microscopy (TEM)

The TEM images of the prepared liposomes are shown in **Fig. 3.29 A-D** below. Average size of the formed liposomes was found to be around 800 nm.
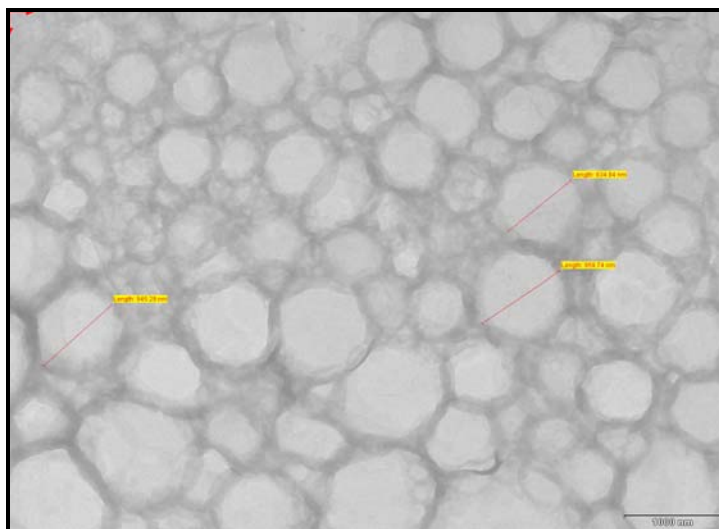
(A)
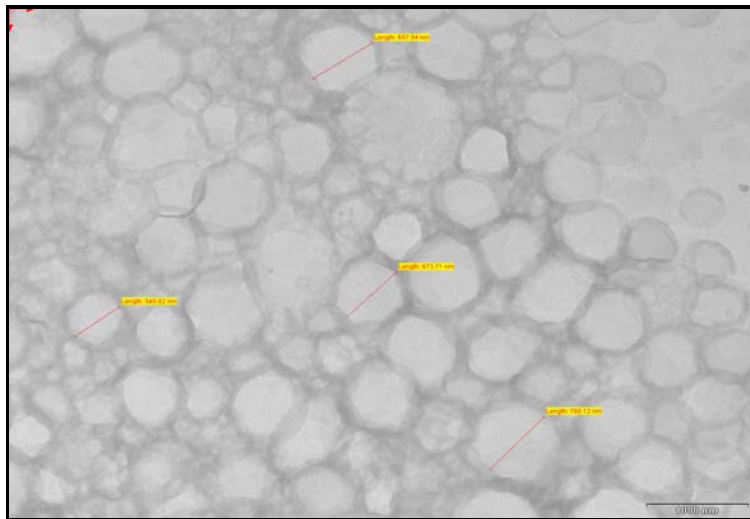
(B)
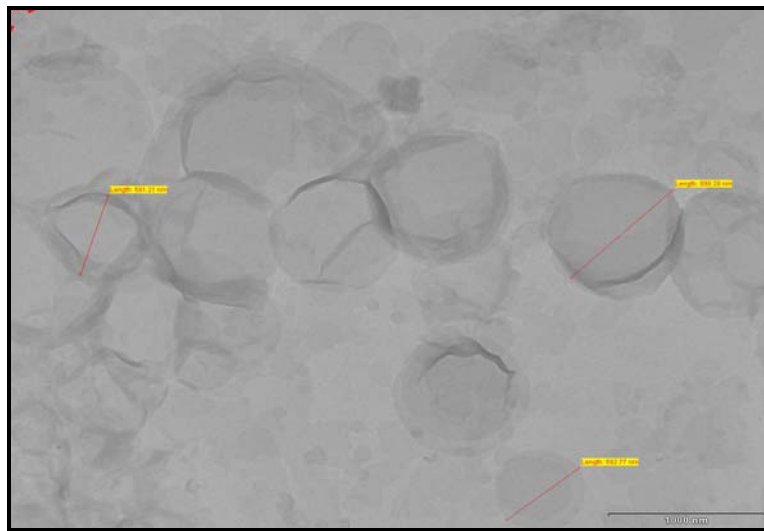
(C)
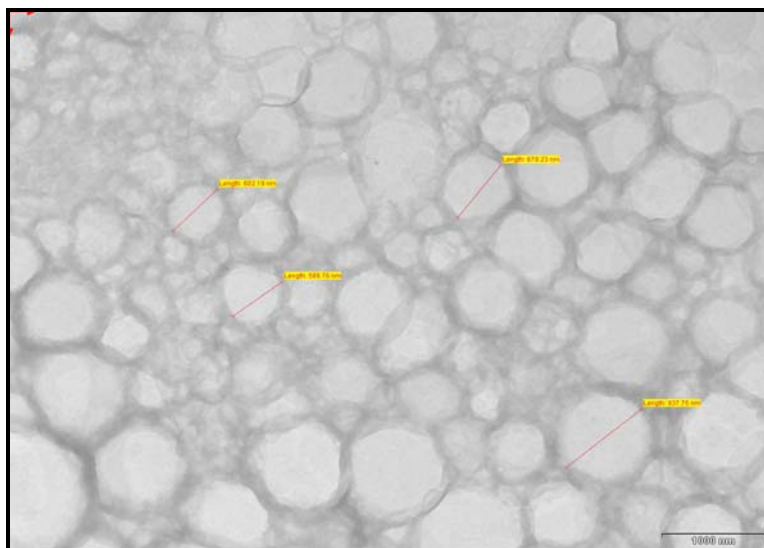
(D)

Figure 3.29: TEM of liposomes **A-D** (Scale 1000 nm)

Further, nature of the vesicles is also important as SUVs vesicles penetrate deep into cartilage whereas MLVs and LUVs are retained on cartilage surface and provide lubricating effect as well as adherence to cartilage via ionic interaction and slowly releases the drug over a long period of time as shown in **Fig 3.30.**
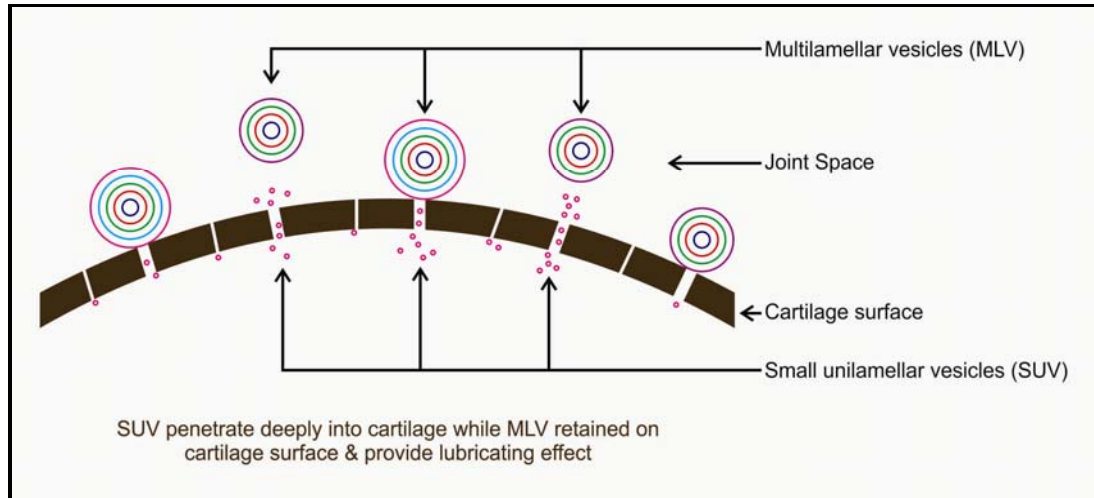
Fig. 3.30: Retention and penetration of liposomes having different sizes

B) Morphology

As discussed in detail in Section-I, not only the size but also the shape of the particles injected into the joint is important for triggering an immune response. Irregularly shaped microparticles have been demonstrated to promote tissue inflammation in comparison to the round shaped drug delivery systems. Hence shape is also important for drug delivery system for IA drug delivery.

(A)   (B)
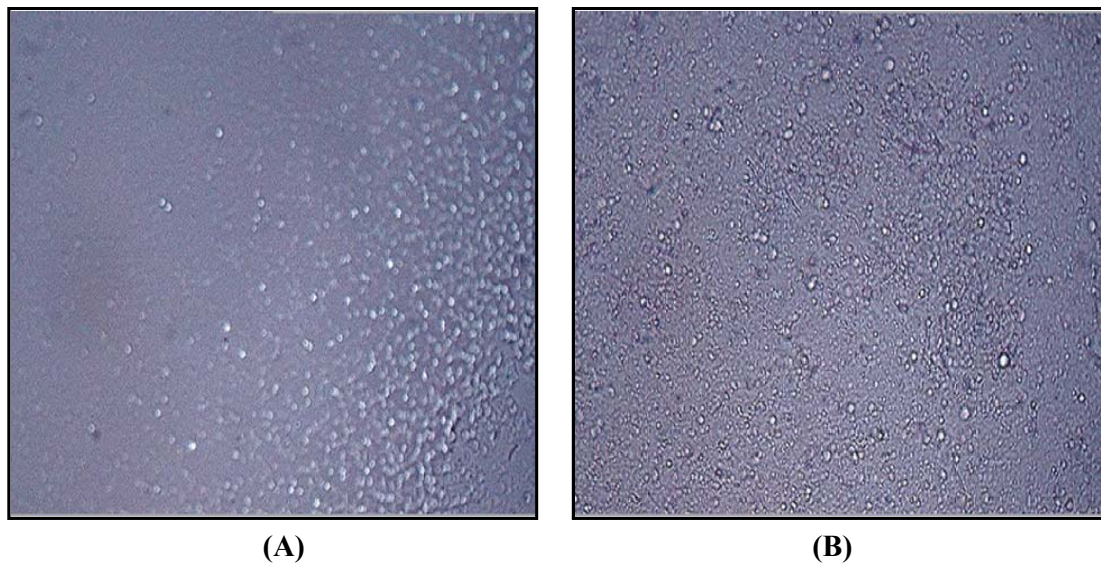
Fig. 3.31: Photograph of liposomes in Olympus microscopy **(A-B)**

(A)   (B)

(C)   (D)
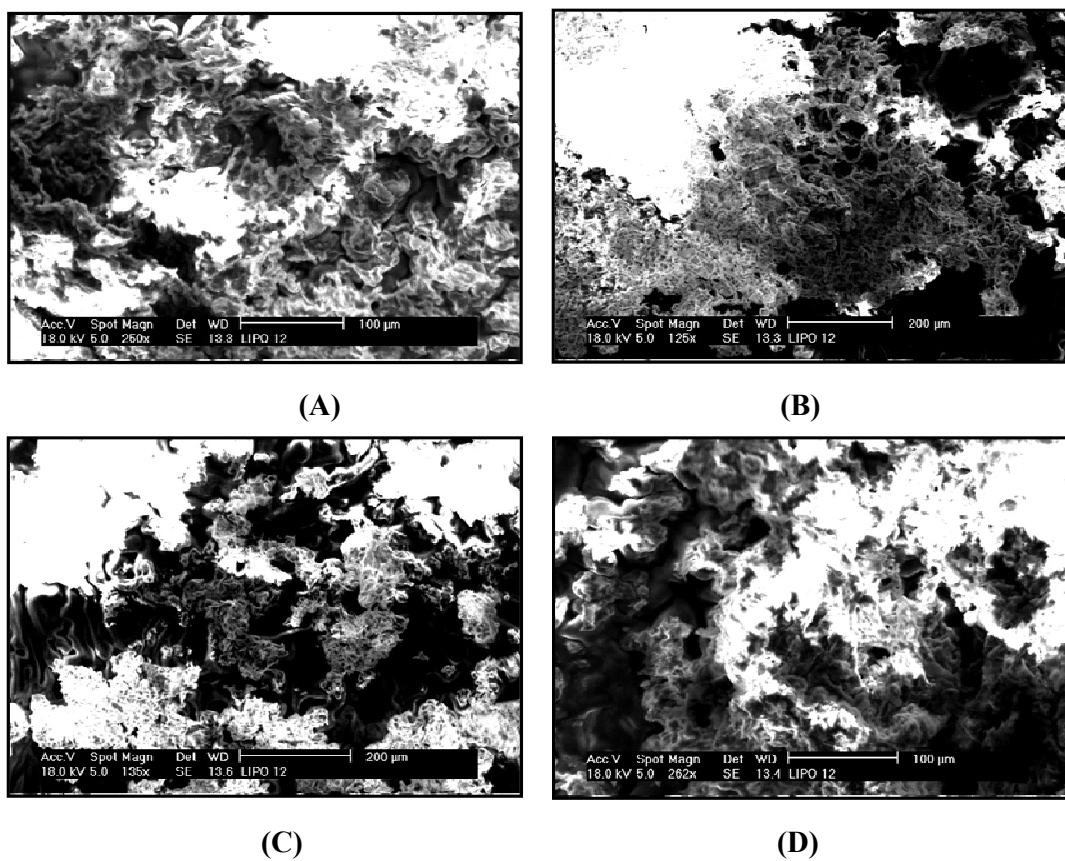
Fig. 3.32: Scanning electron microscope images of lyophilized liposomes.

Morphological evaluation was conducted using Optical microscopy, SEM and Cryo TEM. Photographs showed that all the liposomes (SUV/LUV/MLV) were round in shape with combination of MLV, LUV and SUVs as shown in **Fig. 3.31-3.34**

(A)   (B)
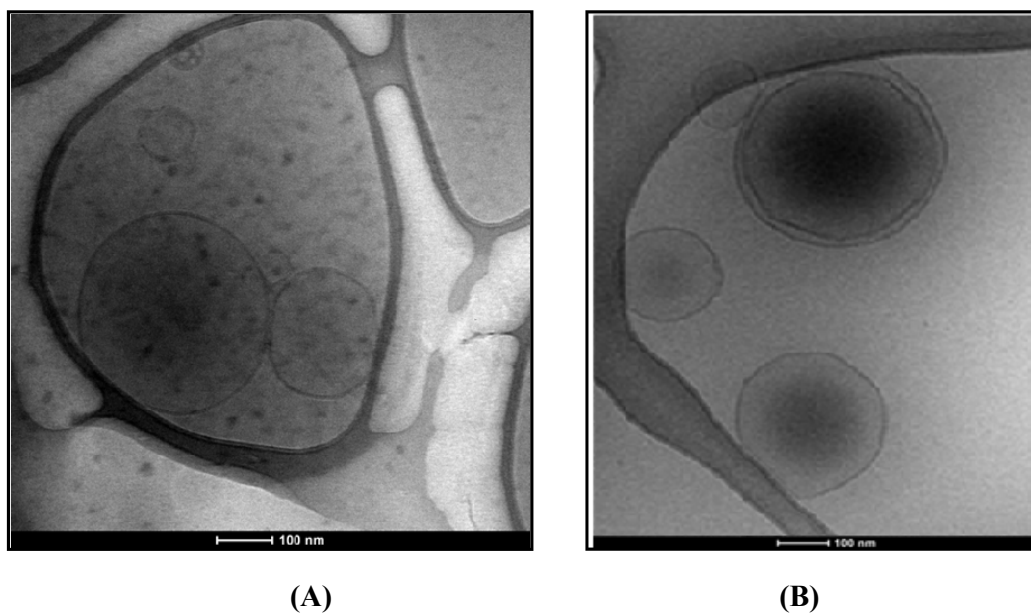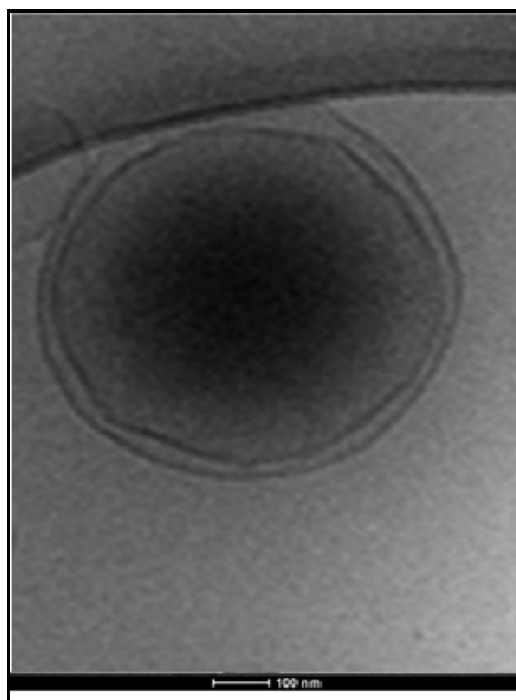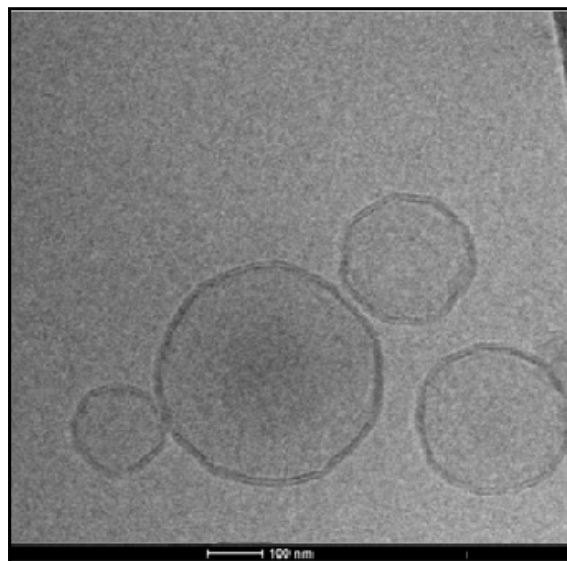
(C)   (D)

Fig. 3.33: Cryo-TEM images of liposomes **(A-E)**

C) Zeta (ς) potential analysis

Literature suggests that positively charged molecules interact with negatively charged sugars present in cartilage and may improve drug residence time within the joint cavity.[18-21]. Due to this aspect it is essential to prepare liposomes having positive zeta potential. The zeta potential (ς potential) of the prepared liposome suspensions was measured and was found to be dependent on concentration of DOTAP used in formulation. The obtained zeta potential was found to be around 30 mV as shown in **Fig 3.34 A-D**.
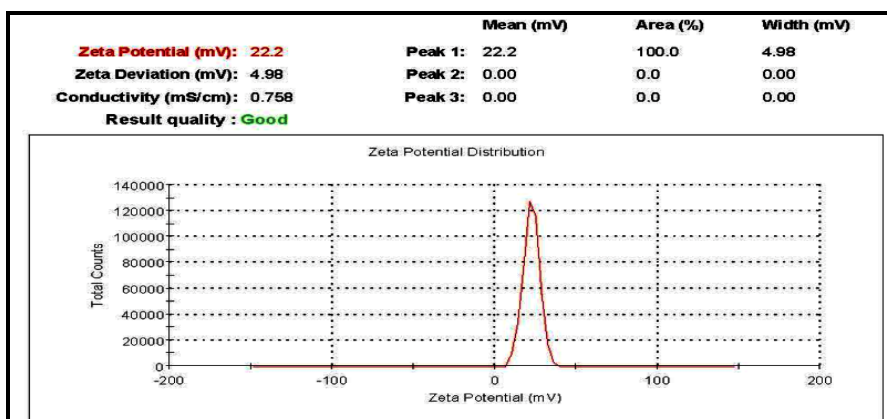
(A)
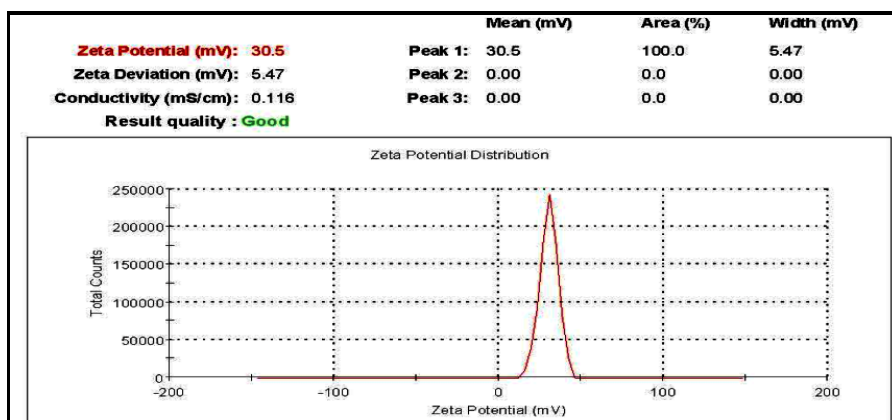
(B)
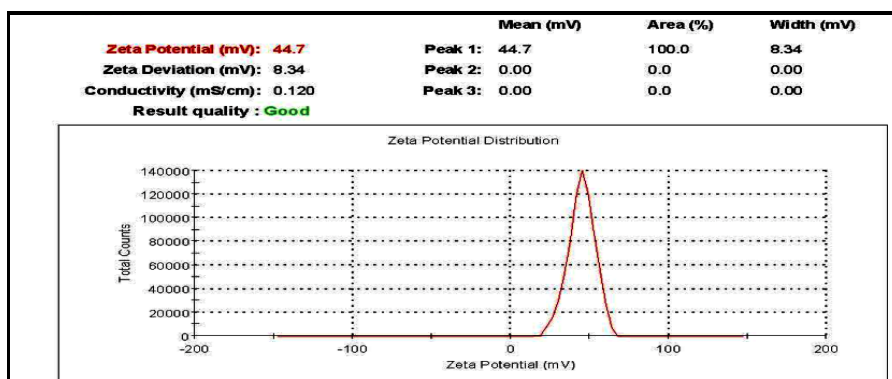
(C)
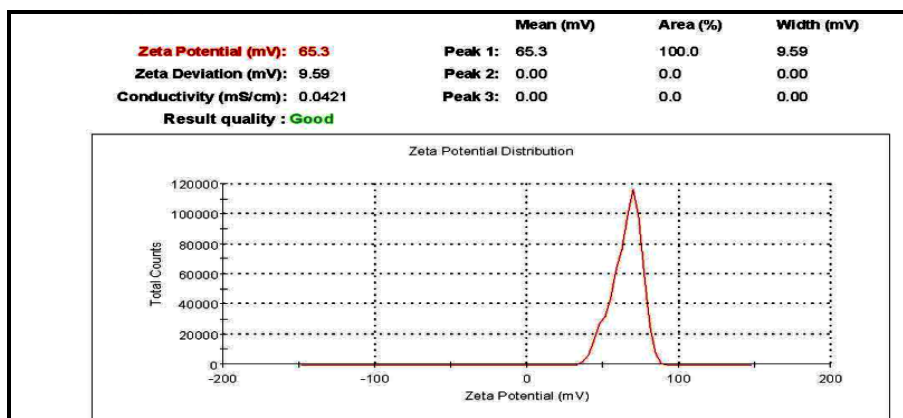
(D)

Figure 3.34: Zeta potential analysis data of the liposomes (samples **A-D)**

4.4.6 *In vitro* diffusion studies of liposomes

In vitro diffusion studies were performed on liposomal formulations and on plain MNA. Results of the release studies show **(Fig. 3.35)** that liposomes prepared with 6-MNA plus 6-MNA-DSPE salt in 8:2 ratio offered the slowest release (<45 %) over 12 h as compared to liposomal formulation containing 6-MNA in free form (~60 %). Studies

further showed that plain 6-MNA gave >85 % release within 30 min indicating that incorporation of drug into liposomal formulation coupled with salt retard drug release over a long period of time. The data of *in vitro* release studies is shown in **Table 3.9**
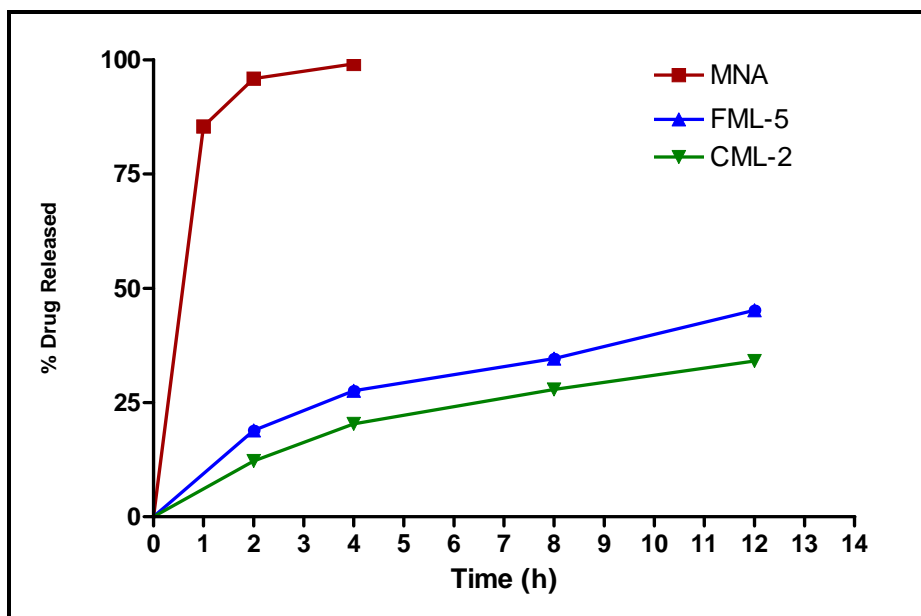
Fig. 3.35: *In vitro* release studies of GEM at *p*H 7.4 buffer (FML-5=Liposomes having MNA; CML-2=Liposomes having MNA and MNA-DSPE)

Table 3.9: *In vitro* release of **6-MNA** from liposomes at *p*H 7.4

Time (h)	% Cumulative Release at *p*H 7.4		
	6-MNA	**FML-5**	**CML-2**
30 min	85.41±0.38	--	--
1	95.88±0.75	18.89±0.68	12.22±0.78
2	99.08±0.49	27.55±0.54	20.33±0.94
4	--	34.62±0.94	27.88±0.55
8	--	45.18±0.43	34.08±0.81
12	--	58.74±0.87	42.77±0.56

3.5 Stability testing of liposomes

3.5.1 Introduction

The physical and chemical properties of the formulation must be maintained during storage and distribution, therefore stability studies of formulations are required to be performed. Physical and chemical data are generated as a function of time and storage conditions [e.g., temperature and relative humidity (RH)]. Stability testing provides evidence whether the quality of a drug substance or drug product under the influence of various environmental factors gets altered with time or not.

3.5.2 Stability of liposomes

The stability of liposomes depends upon conditions like temperature/humidity and is affected by processes like oxidation/hydrolysis etc. which lead to aggregation and leakage of the entrapped material from the vesicles affecting the shelf life of liposomes greatly. Liposomal formulations have been known to show poor stability and do not meet the required standards for long term stability of pharmaceutical preparations when stored as aqueous dispersions. Decrease in the entrapment efficiency, fusion and aggregation are the major stability problems associated with liposomal preparations. Lyophilization is considered as a promising means of extending the shelf-life of liposomes. However, both freezing and drying can induce structural and functional damage into the liposomes. Sugars are frequently used as the cryoprotectants in lyophilization for stability of liposomes[22]

The liposomal aqueous dispersions were evaluated for the effect of temperature on the particle size, zeta potential and percent entrapment efficiency of the drugs and for stability over a period of 2 months at refrigeration (2-8 ^{o}C) and room (30±5 ^{o}C) temperatures.

Table 3.10: Stability data of liposomal dispersion

Duration of storage	Particle Size (nm)	Zeta potential (mV)	% Entrapment Efficiency (EE)
0 Day	695±10.89	33.4±5.3	72.55±4.25
2-8 °C (Refrigerator conditions)			
15 Day	715±13.45	31.6±4.2	71.12±5.02
1M	704±11.66	34.2±3.8	70.33±4.14

2M	738±16.87	35.2±5.4	67.44±3.82
30 ± 5 ᵒC (Room temperature)			
15 Day	708±09.27	32.1±4.4	71.88±4.97
1M	752±12.71	34.8±5.2	65.11±5.07
2M	795±14.56	33.1±6.7	61.08±6.07

Liposomal formulations were found to be stable when stored at 2-8 °C as aqueous dispersions, whereas when stored at 30±5 ᵒC they showed increase in particle size after 2 months, compared to the initial samples **(Table 3.10)**, Saturated phospholipid (HSPC) was used in the preparation of liposomes. Higher positive zeta potential decreases vander Waals interactions (which is a major contributor to aggregation of electrostatically neutral complexes) in the liposomes, ultimately preventing liposomes from fusion and aggregation[23]. The entrapment efficiency of liposomal dispersions got lowered with time at all the storage conditions but maximum decrease in entrapment efficiency was observed for aqueous dispersions at 30±5 ᵒC **(Table 3.10)**.

Hence, it can be concluded that these liposomal dispersions can be stored at 2-8 ᵒC as aqueous dispersions for 2 months. Liposomal dispersion stored at 30±5 ᵒC shows a decrease in entrapment efficiency and increase in particle size.

3.6 Biodistribution and gamma imaging studies

The aim of the current study was to assess the residence time of the liposomes in the joint cavity upon IA administration. Little information is available in the literature on the effect of charge on residence time of drugs in joint cavity but our previous study has indicated that positively charged CDS possess improved drug residence time. To know the effect of positively charged liposomes, radiolabeling of the liposomes was required to be done for their localization/quantification in the joint cavity. To study these aspects, parent NSAID and the liposomes were labeled using ^{99m}Tc as per the details mentioned in **Section-I**. Radiolabeling parameters were optimized for liposomes and are shown in **Table 3.11**.

IA residence times of prepared liposomes and parent drug were studied in inflammatory condition. Animals were divided into three groups, Group-A (standard) was administered by IA the parent NSAID i.e 6-MNA **(1)**. Group-B (Test) was administered by IA the liposomes, 3 h after induction of inflammation in the rat paw. And the third

group was kept as control. Inflammation was induced in the right hind paw of the rats by injecting carrageenan (0.1 ml, 1 % w/v in normal saline) into the subplantar region of the paw. The animals were anaesthetized, fixed on a board and images were taken 1 h, 2 h, 6 h and 24 h after the administration of the radiolabeled complexes by IA route. Percentage radioactivity was calculated as given in **Table 3.12.**

Table 3.11: Optimization of radiolabeling of liposomes

No	Drug/Formulation	pH	Incubation Time (min)	SnCl$_2$.2H$_2$O (µg)	% Radiolabe-ling	% Stability (saline) 24 h
1	6-MNA	7.0	30	150	95.06±2.0	86.75±4.55
2	CML-2 (Liposome)	7.0	15	150	96.05±4.5	82.46±5.87

Table 3.12: Percentage of radioactivity in knee after IA administration

Time (h)	% Radioactivity in ROI*		
	6-MNA	Liposome	Q-CDS (7aI)
1	100±4.0	100±3.1	100±3.0
2	58.47±3.1	91.44±3.0	76.54±3.1
6	42.06±4.3	84.97±3.7	60.78±3.0
24	13.44±3.0	69.81±4.2	40.96±4.1

*Radioactivity counts converted in to percentage and initial counts taken as 100%

*ROI=Region of interest
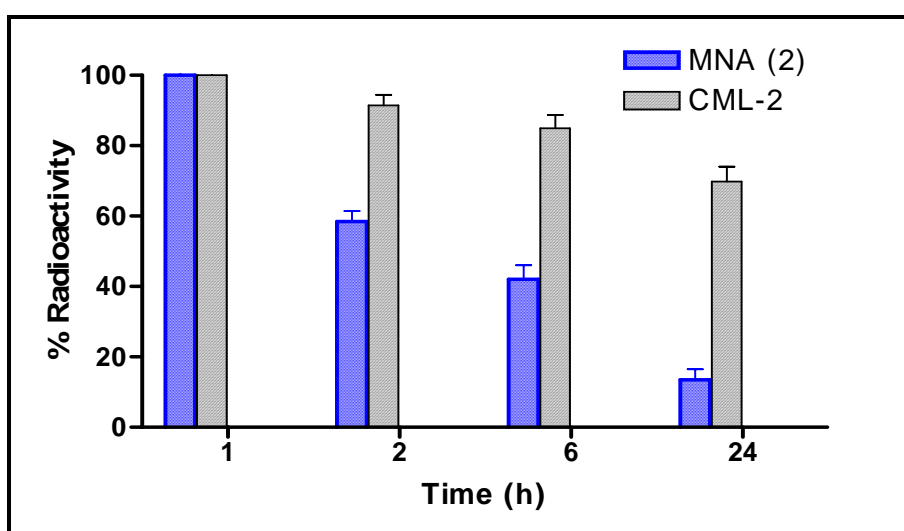
Fig. 3.37: % Radioactivity retained in rat knee ROI after IA injection of 6-MNA (1), Liposomal formulation CML-2, and quaternized CDS [(7aI) from section-I)] after 1, 2, 6 and 24 h (ROI=Region of interest)

From the obtained data and figures it is clear that liposomes showed higher retention in joints after IA administration as compared to parent drug **(2)** and quaternary ammonium chemical delivery system [(7aI) from section-I). Further, radioactivity obtained for the prepared liposomes after 24 h was about 5 times higher in ROI compared to the parent drug. So it could be concluded that liposomal drug delivery having cationic charge are retained for a longer period of time in joint cavity by ionic interaction. Hence it is clear that we can extend residence time of the drug by these drug delivery systems. Moreover, sustained release of the drug will give anti-inflammatory effect for a longer duration.
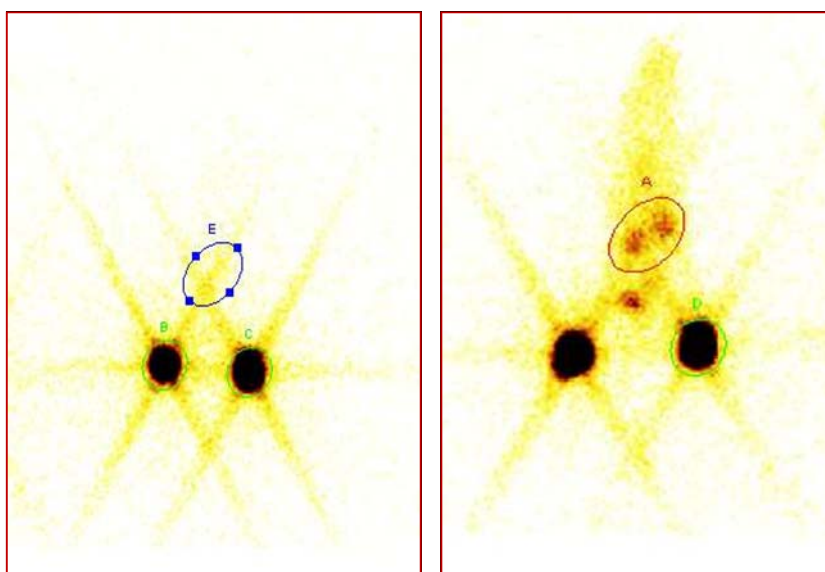
Fig. 3.38: Gamma camera image of rats after IA injection of **1** after 1 h **(A)** and 6 h **(B)**
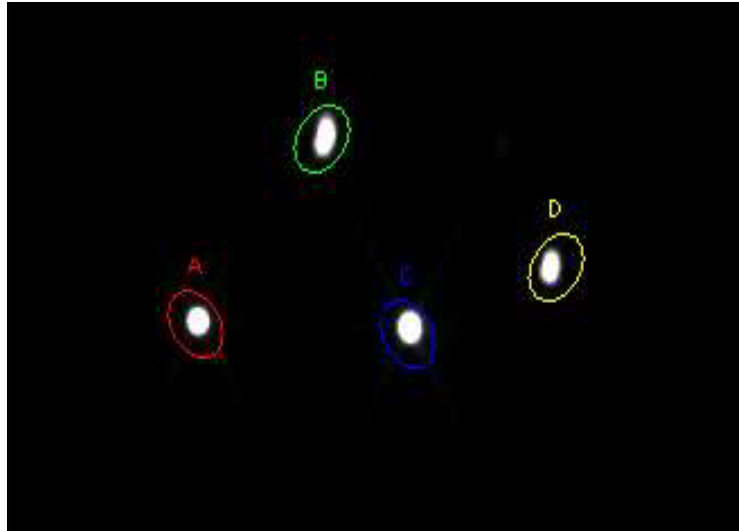
Fig. 3.39: Gamma camera image of rats after IA injection of **CML-2** after 1 h
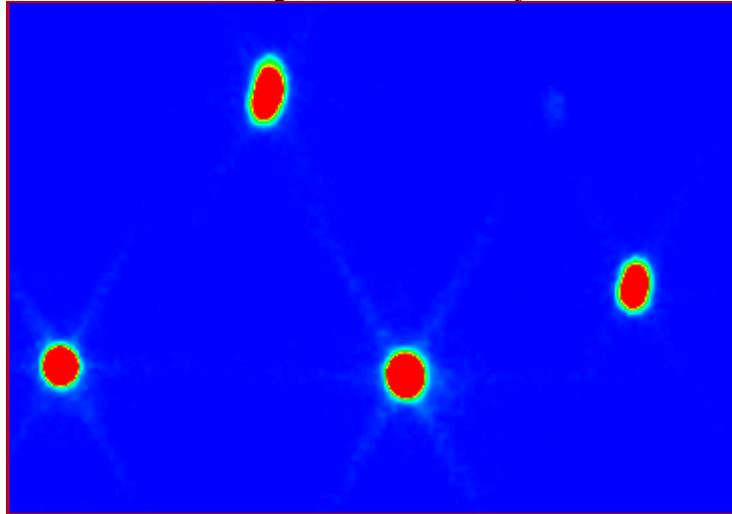
Fig. 3.40: Gamma camera image of rats after IA injection of **CML-2** after 6 h
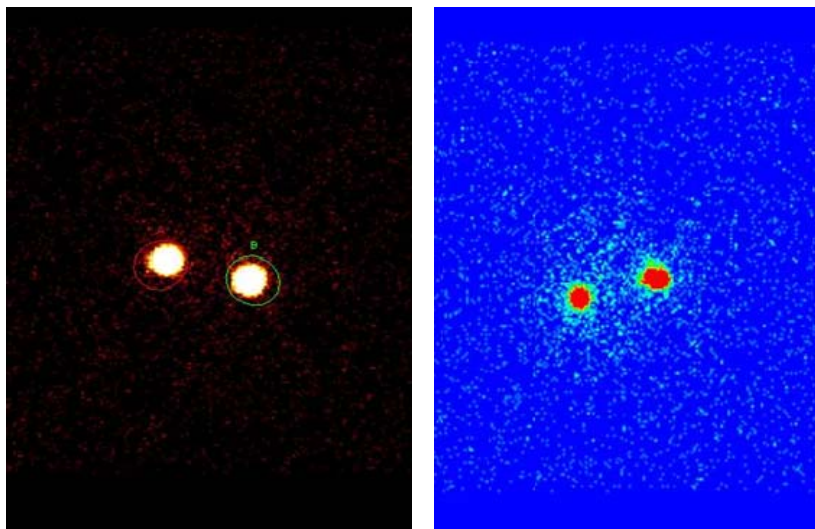
Fig. 3.41: Gamma camera image of rats after IA injection of **CML-2** after 12 h
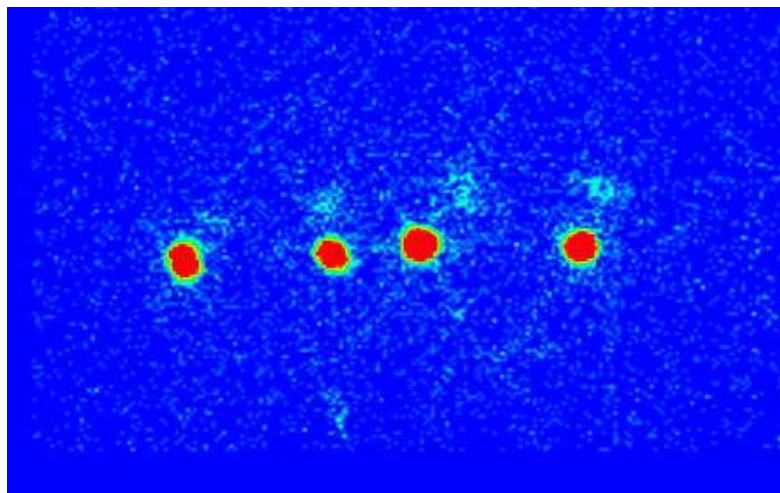
Fig. 3.42: Gamma camera image of rats after IA injection of **CML-2** after 24 h

3.7 *In vivo* studies in arthritis model

Adjuvant arthritis, an accepted and well established standard model was chosen for this purpose.[24-25] The parent NSAID 6-MNA **(1)** was used as standard for comparing the anti-inflammatory activity of the prepared liposomal formulation **(CML-2)**, which was administered on equivalent molar doses (4.27 mg/kg). Animals were dosed on day 1 with parent drug **(1)** and the liposomal formulation **(CML-2)** by IA route.

The phlogistic agent (Mycobacterium butyricum) suspended in heavy paraffin oil was injected into the subplantar region of the hind paws of the rats only on day 1. Paw volumes of all the test animals and controls were measured on days 0, 3, 7, 14 and 21. On day 21, liposome formulation exhibited significantly higher anti-inflammatory activity than the parent drug **(Table 3.9)**. The percent inhibition of inflammation exhibited by the parent drugs **(1)** declined on 21st day whereas, the percent inhibition of inflammation by the liposomal formulation increased on 21st day in comparison to that observed on 14th day. This could be due to the sustained release of 6-MNA from liposomal formulation in the body, which exhibited its normal anti-inflammatory activity over longer duration.

Table 3.9: Percent anti-inflammatory activity of liposomal formulation

Treatment with	Dose mg/kg	% Inhibition of paw edema (days)†			
		3rd	7th	14th	21st
6-MNA	4.27	32±2.33	41±2.98	45±3.60	40±2.88
CML-2	4.27	28±2.78	44±3.45	56±3.14	74±4.25

† mean±SD (n=6), $p<0.05$

The data obtained from the experiments was subjected to statistical analysis using the Student's t test and the chosen level of significance was $p < 0.05$

In vivo studies further indicate that there is decreased erythrocyte sedimentation rate (ESR), and C-reactive protein level (CRP) in test group administered IA with liposomal formulation compared to the control and standard group **(Table 3.10-3.13)**.

Table 3.10: Estimation of ESR and CRP levels in normal Rats.

No	Normal Group	Day 0		Day 21	
		ESR mm/hr*	CRP Quantitative†	ESR mm/hr*	CRP Quantitative†
1	N1	1	3.5	1	3.5
2	N2	7	2.2	5	2.0
3	N3	4	4.0	6	3.2
4	N4	3	3.2	2	4.2
5	N5	2	4.5	3	1.5

*Westergreen method, Normal range 1-15; †Normal range 1-10mg/L

Table 3.11: Estimation of ESR and CRP level in Control group rats

| No	Control Group	Day 0		Day 21	
		ESR mm/hr*	CRP Quantitative†	ESR mm/hr*	CRP Quantitative†
1	C1	2	11	11	06
2	C2	2	2	14	17
3	C3	4	4	16	19
4	C4	3	3	11	22
5	C5	6	4	18	10

Table 3.12: Estimation of ESR and CRP level in test group rats

No	Test Group	Day 0		Day 21	
		ESR mm/hr*	CRP Quantitative†	ESR mm/hr*	CRP Quantitative†
1	T1	9	13	2	14
2	T2	2	26	5	09
3	T3	8	11	4	05
4	T4	10	14	6	06
5	T5	9	12	2	08

*Westergreen method, Normal range 1-15; †Normal range 1-10mg/L

Table 3.13: Estimation of ESR and CRP level in standard group rats

No	Standard Group	Day 0		Day 21	
		ESR mm/hr*	CRP Quantitative†	ESR mm/hr*	CRP Quantitative†
1	S1	8	9	2	08
2	S2	6	3	8	10
3	S3	4	7	3	12
4	S4	9	8	9	09
5	S5	3	6	2	14

*Westergreen method, Normal range 1-15; †Normal range 1-10mg/L

Histological studies: Histopathological studies of cartilage tissue indicated less tissue damage in the test group than the control and standard groups. 21 Days after single IA injection of test and standard drug/delivery system, the joint capsule of the arthritic knee was removed, fixed in 10 % formalin and processed through routine paraffin embedding and sectioning to carry out histological studies. After staining by haematoxylin-eosin (HE), and Safranin-O, the sections were examined.[26-28]

Safranin-O and hematoxylin eosin (HE) stain articular cartilage and bone respectively as shown in **Fig. 3.43-3.47.** From this study it is concluded that IA

administration of anti-inflammatory drugs encapsulated in cationic liposomes provides better therapeutic effect in arthritic animal model.


(A)   **10x**   **(B)**

(C)   **20x**   **(D)**

(E)   **40x**   **(F)**

(G)

(H)

(I)

40x

(J)
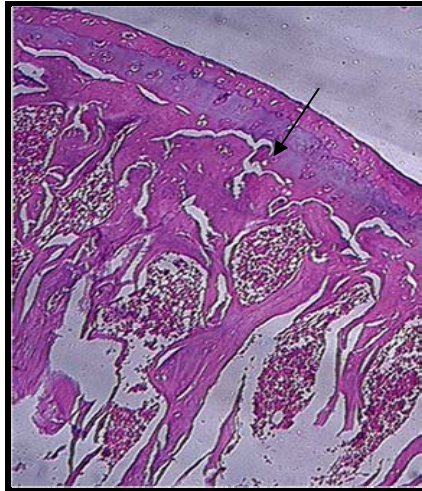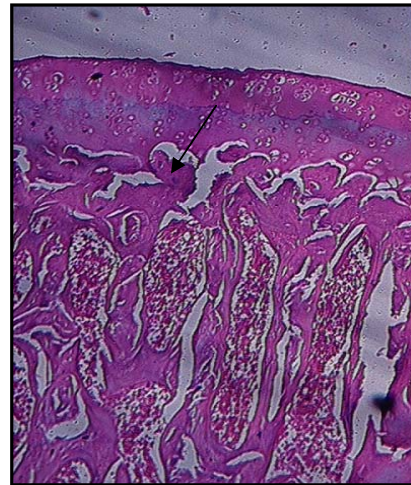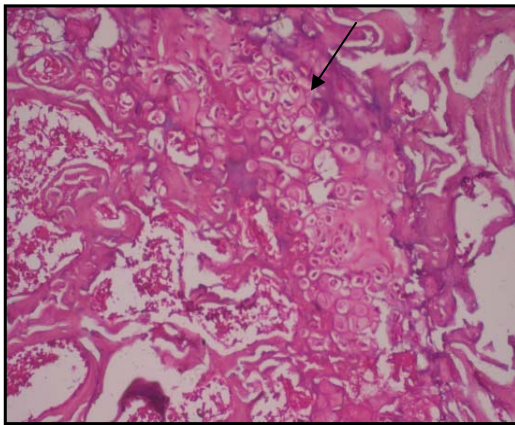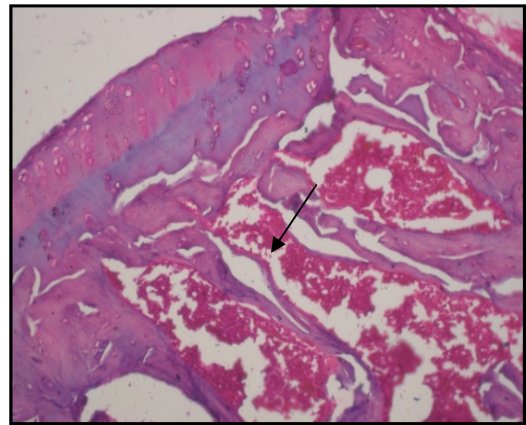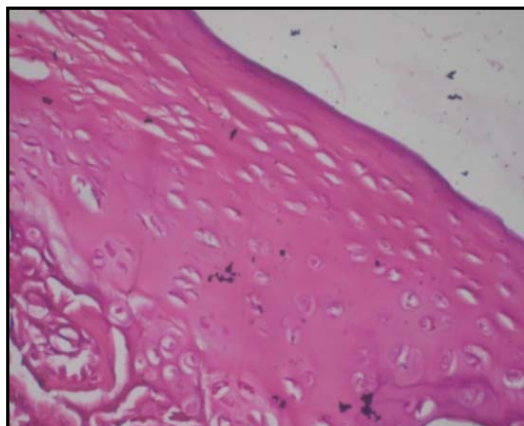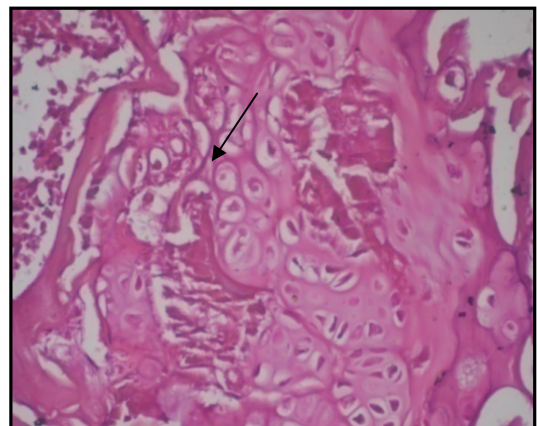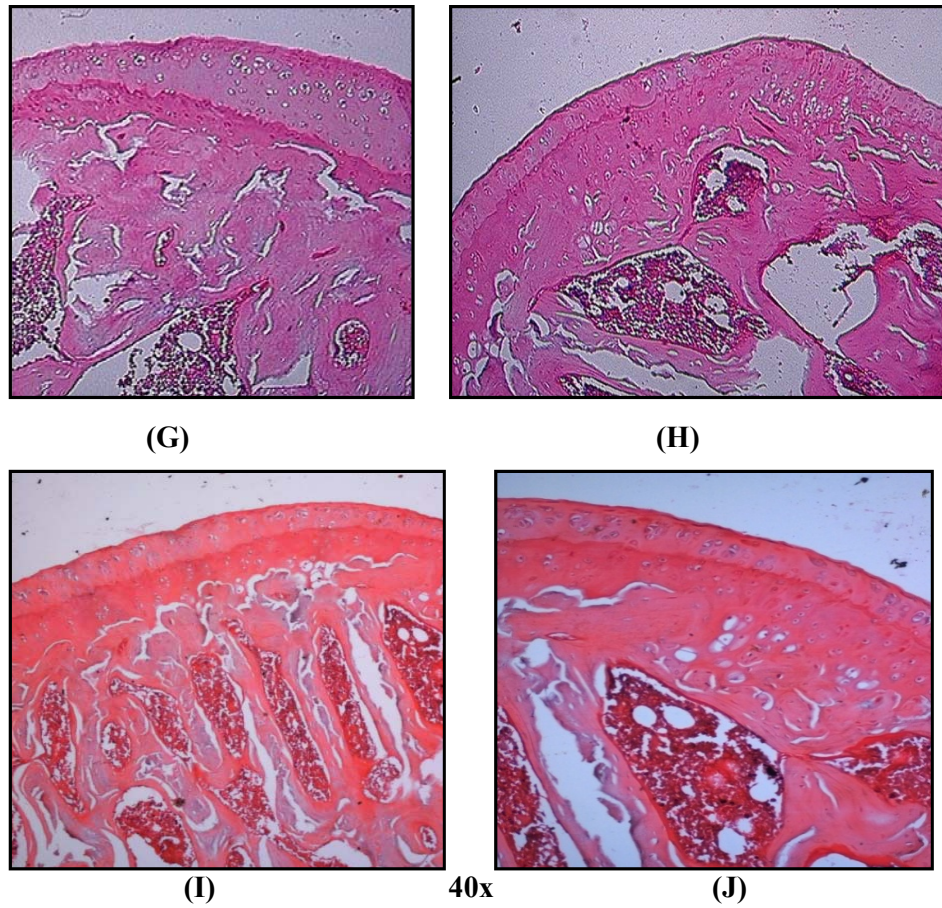
Fig. 3.43: A-F: Histopathological examination of normal knee haematoxylin and eosin
Staining (H/E). **A-B**: Normal cartilage; **C-F**: Chondrocytes; **D**: Bone
G-J: Safranin-O staining.

(A)

(B)
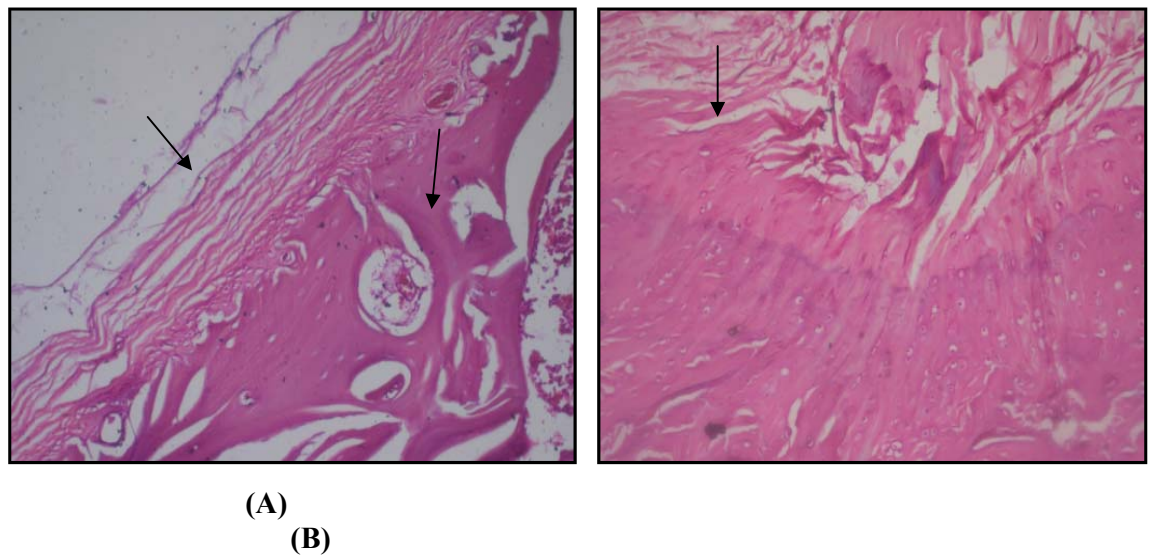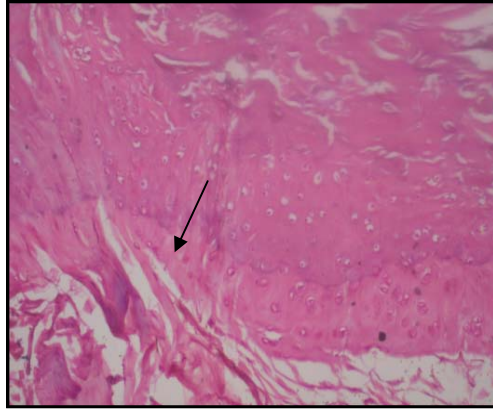
(C)
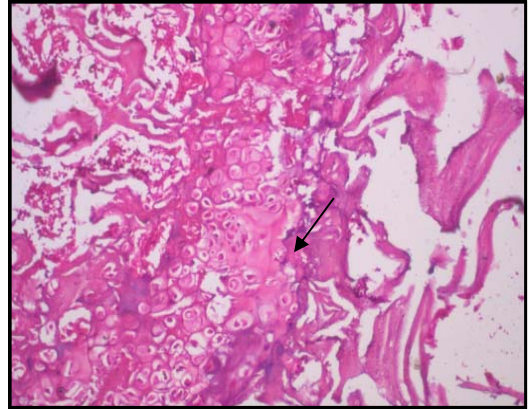
(D)
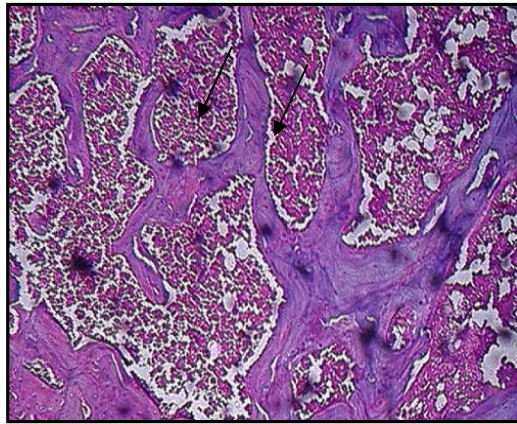
(E)
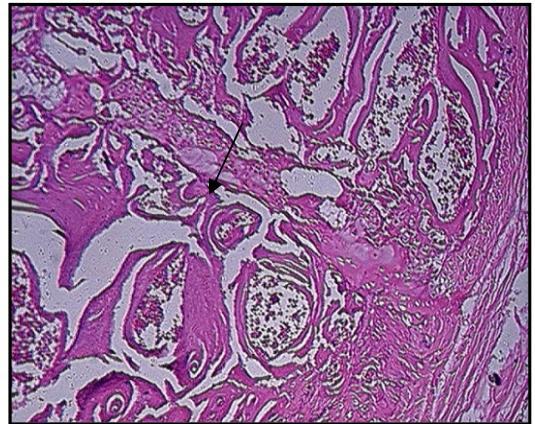
(F)
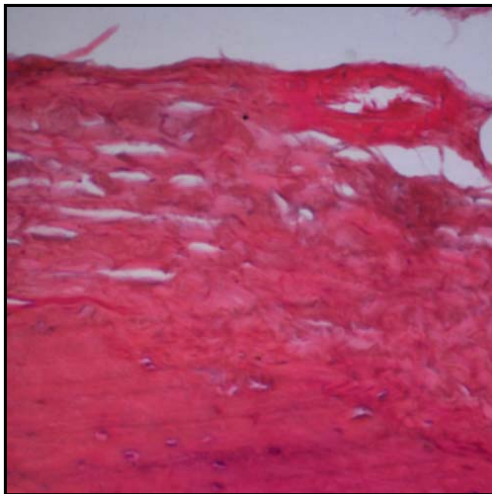
(G)
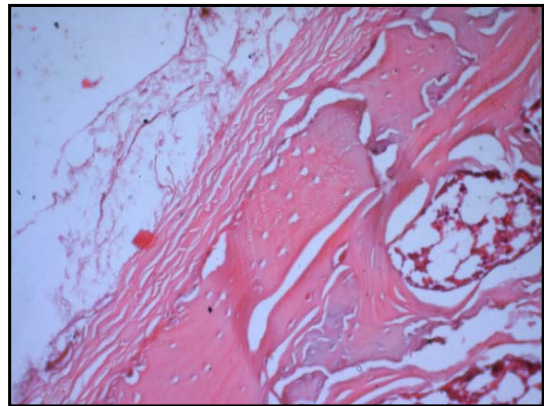
(H)

Fig. 3.44: **A-F**: Histopathological examination of knee treated with 6-MNA **(2)** haematoxylin and eosin staining (H/E). **A-D**: Cartilage and bone damage; **E**:Lymphocyte group; **F**: Polymorphonuclear leukocytes. **G-H:** Safranin-O

staining.

(A)   (B)

(C)   (D)

(E)   40x   (F)
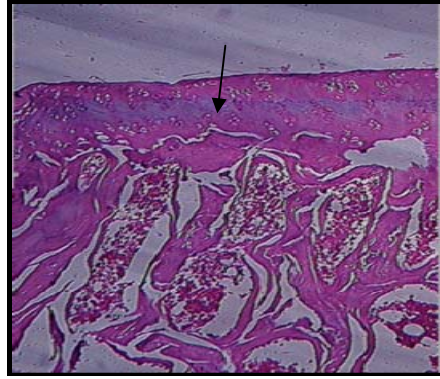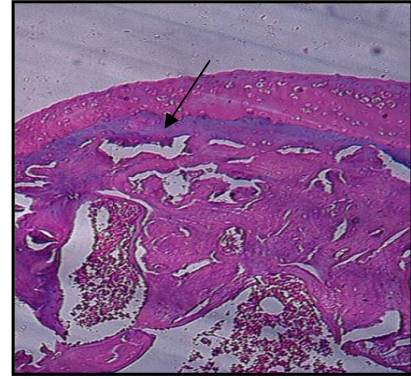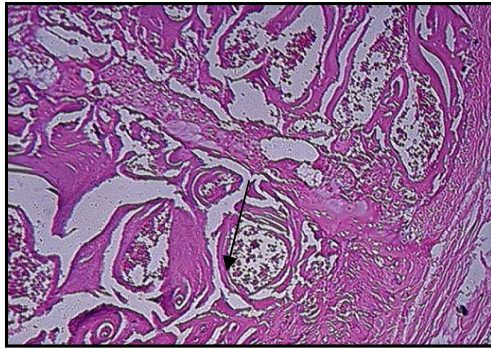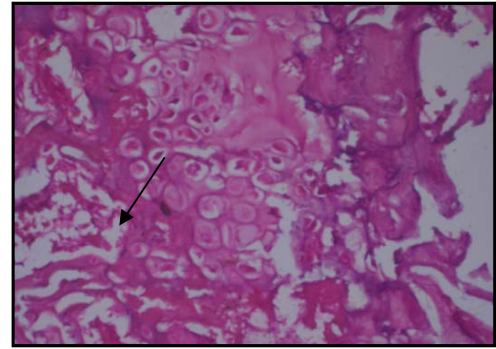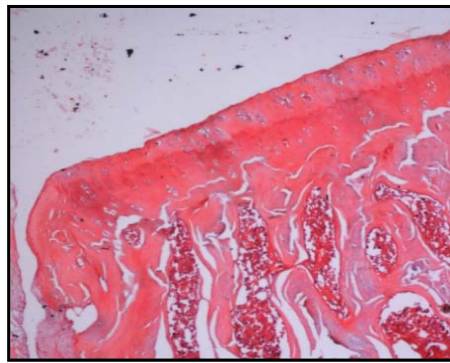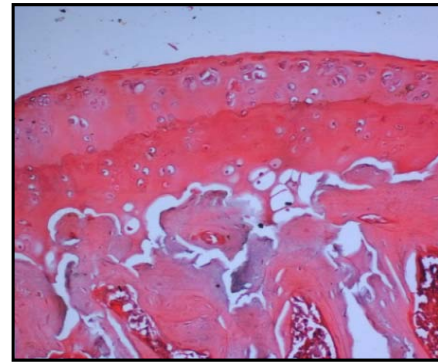
Fig. 3.45: A-F: Histopathological examination of knee treated with **CML-2**
haematoxylin and eosin staining (H/E). **A-B:** Normal cartilage; **C**: Bone;
**D**: Chondrocytes. **E-F:** Safranin-O staining.

(A) 10x **(B)**

(C) 20x **(D)**

(E) **(F)**

(G) **(H)**
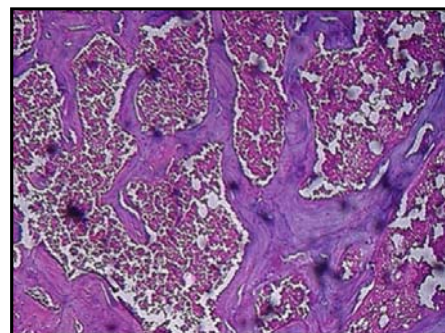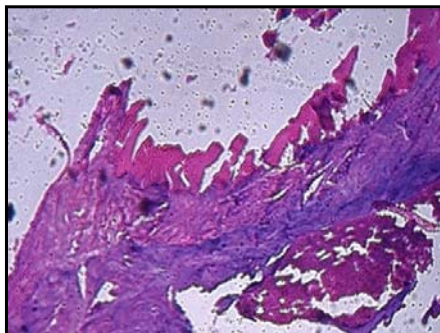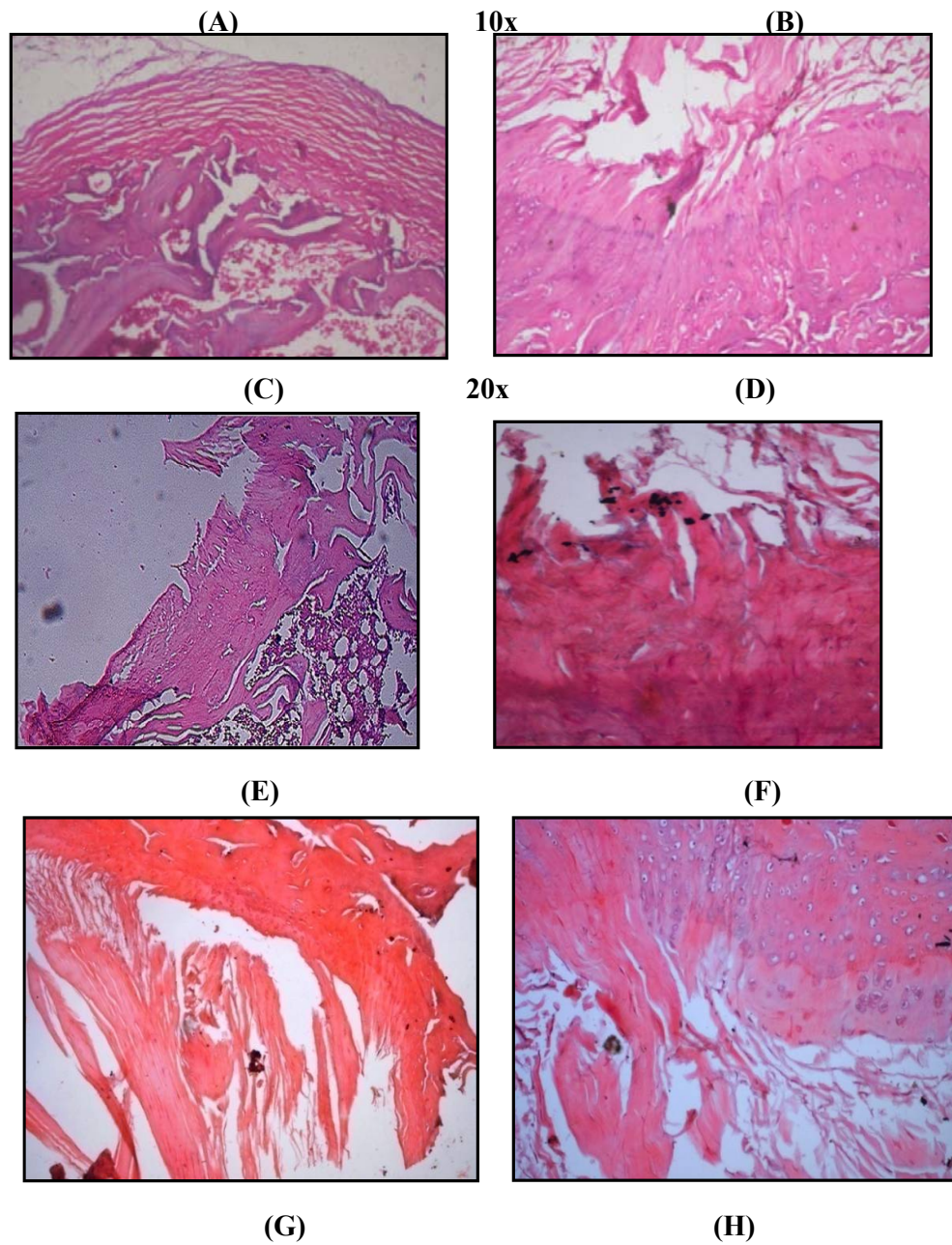
Fig. 3.46: **A-D**: Histopathological examination of knee **control group** haematoxylin and eosin staining (H/E). **E-H:** Safranin-O staining
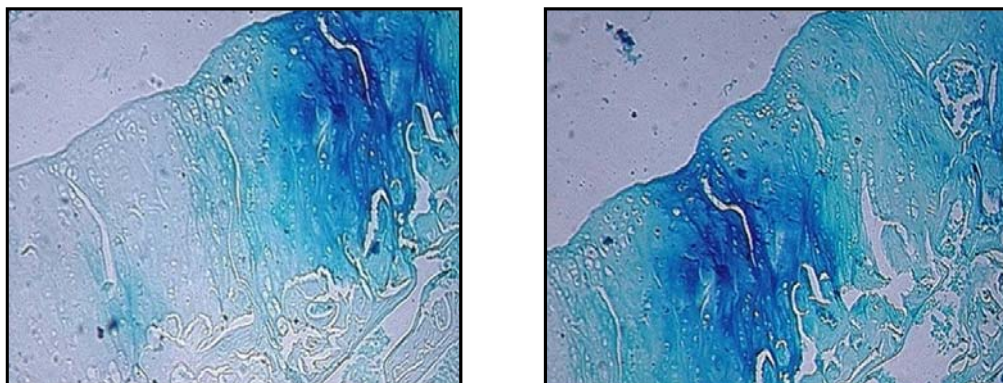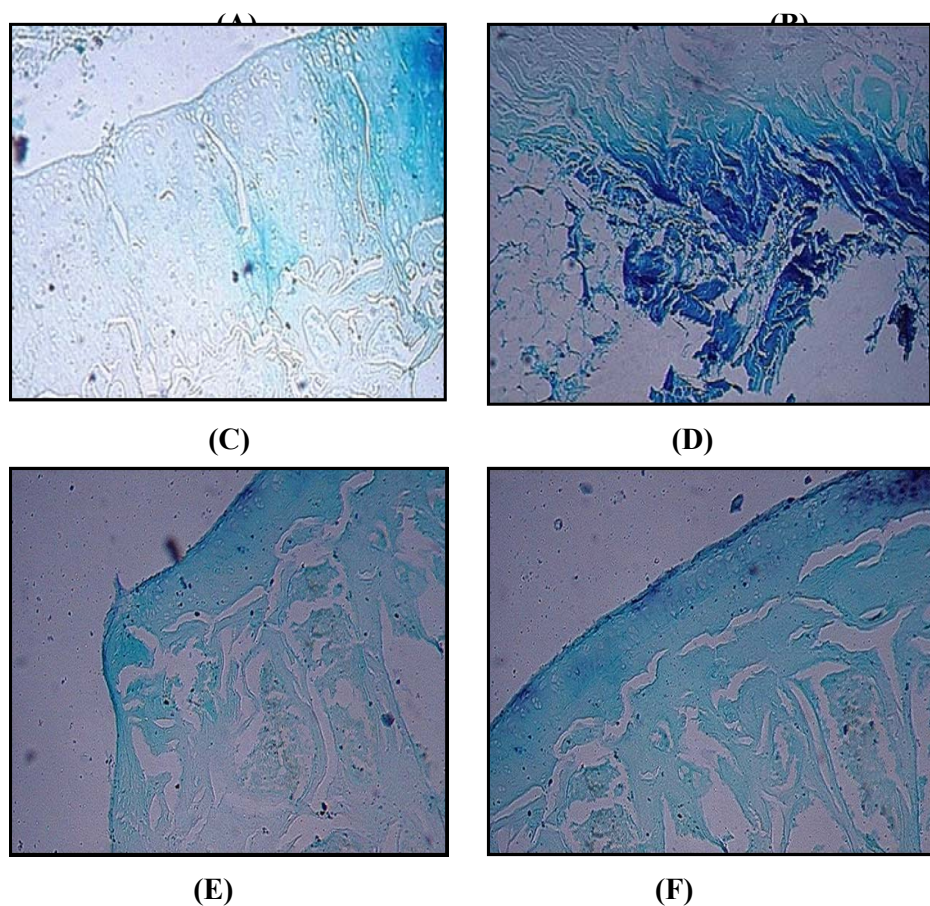
Fig. 3.47: A-F: Histopathological examination of knee toluidine blue staining;
A-B: Normal group; **C-D**: Control group; **E** and **F** Test and standard group.

It is concluded that retention time of a liposomal drug delivery system containing 6-MNA administered IA got extended significantly in this study. A drug carrier with a long half-life has great potential for the IA delivery of drugs used in the treatment of knee arthritis. The liposome dose was well tolerated by all animals indicating good biocompatibility. Additionally the liposomal formulation may provide lubricating effect due to presence of MLVs in liposome formulation along with SUV and LUVs.

A Coupled effect of positive charge and sustained release of drug from liposome formulation on retention time in joint cavity is responsible for the highest efficacy of liposomal formulation. *In vivo* studies further indicated that there is a decreased ESR, and CRP level, in test group administered with liposomal formulation compared to the control and standard groups. From this study it is concluded that IA administration of NSAIDs (having long half life) encapsulated in cationic liposomes prolong the residence time in the joint cavity. This type of drug delivery system will decrease frequency of IA drug administration and could provide good therapeutic option for the treatment of arthritis.

4. Experimental

All the reagents and solvents required for synthesis were purified by general laboratory techniques before use. Purity of the compounds and completion of reactions were monitored by thin layer chromatography (TLC) on silica gel plates (60 F_{254}; Merck). Melting points were determined using a Veego make silicon oil bath-type melting point apparatus and are uncorrected. The IR spectra were recorded using KBr disc method in cm^{-1} on a Bruker FT-IR, Model 8300. The PMR and ^{13}C-NMR (ppm) spectra were recorded in $CDCl_3$ or $CDCl_3$ plus one drop of glacial acetic acid-d_4 on a Bruker 400 MHz spectrometer (chemical shifts in δ ppm, coupling constant J in Hz). λ_{max} was determined on Shimadzu 1800 UV spectrophotometer.

HPLC analysis was performed by using Shimadzu prominence UV/VIS (pump LC-20AT, detector SPD 20 A), column purospher 5 μ (e) C-18, 5 X 250 mm (Merck), Column temperature was 25-28 °C. Chromatography was performed under isocratic conditions, at a flow-rate of 1.0 ml/min. The mobile phase consisted of acetonitrile-phosphate buffer (PB, 15 mM) in 3:1 ratio. Dialysis membrane-70 was procured from Himedia (Mumbai) with average diameter 17.5 mm and width 29.31 mm (Batch No: 0000116060), Confocal microscopy was performed on Carlzeiss LSM-710 model, made in Germany with 10x, 20x and 40x magnification. For optical microscopy Optical microscope with polarizer BX 40, Olympus Optical Co. Ltd., at a magnification of 40X was used. DSC was performed on Shimadzu DSC-60 model with thermal analyser TA 60WS. Mass of the compounds was determined in LC-MS or GC-MS using various ionization methods such as EI, ESI and ESCI (ESI+APCI). Scanning electron microscope (SEM) model ESEM-EDAX XL-30, Philips (Netherlands) was used for surface morphology study. TEM was performed on Holand Tecnai-20 model of Philips with operating accelerating voltage of 200 KV, line resolution 2.0 nm, and magnification of 25x to 750000x.

The work carried out has been discussed under the following heads:

4.1. Syntheses of NSAIDs

4.2. Salt formation and its characterization

4.3. Formulation of liposomes

4.4. Characterization of liposomes

4.5. Stability testing of liposomes

4.6. Biodistribution and gamma imaging studies

4.7. *In vivo* studies in arthritis model

4.1. Syntheses of NSAIDs

4.1.1.2-Methoxynapthene (nerolin) (5)

β-Naphthol **(4)** (3.6 g) was dissolved in an aqueous solution of sodium hydroxide (100 ml, 1.5%) and filtered. Dimethyl sulphate (2.35 ml) was added gradually to the above solution of β-naphthol with constant stirring at 10 °C. The reaction mixture was heated on water bath for two hours, cooled and poured into ice-cold water (200 ml). Precipitates so obtained were filtered, dried and the crude product crystallized from methanol to obtain white crystalline product[4] **(5)** (4.20 g, 76.55 %) m.p. 72-74 ^{0}C (lit.[4] 72-73°C).

Anal.:

TLC : R_f 0. 74 (Chloroform: methanol, 1:0.3)

UV (MeOH) : 270 nm

IR (KBr, cm^{-1}) : 1627, 1258, 1024 and 837

4.1.2. 2-Acetyl-6-methoxynaphthalene (6)

Anhydrous aluminium trichloride (4.30 g, 32 mM) was dissolved in nitrobenzene (20 ml) and the solution was cooled to 5 °C. Powdered nerolin **(5)** (3.95 g) was added to the above cooled solution with stirring. Acetyl chloride (2.3 ml, 32 mM) was added to it dropwise maintaining the temperature of the reaction mixture between 10.5 to 13 °C. The reaction mixture was stirred further in an ice-bath for two hours and left overnight at room temperature. The stored reaction mixture was poured into a mixture of ice (100 g) and conc. hydrochloric acid (10 ml) and extracted with chloroform (4 x 10 ml). The organic layer was washed with water (50 ml), dried and chloroform removed on rota evaporator. The solution so obtained was steam-distilled for about 3-4 h and the residue in the flask was allowed to cool. Residual water in the flask was decanted and the solid material extracted with chloroform and dried over sodium sulphate. The solvent was removed on rota evaporator yielding a solid mass which was vacuum-distilled at 140-60 °C/10 mm of Hg. The yellow distillate so obtained was crystallized from methanol to offer the white crystalline 2-acetyl-6-methoxynaphthalene[5] **(6)**. (2.1 g, 41.79 %) m.p. 106-108 ^{0}C (lit.[5] 104-105°C).

Anal.:

TLC : R_f 0.80 (Chloroform)

UV (MeOH) : 241 nm

IR (KBr, cm^{-1}): 1666, 1260, 855 and 666

Mass (m/z) : 199.91 (M$^+$)

4.1.3. 2-(6-Methoxy-2-naphthyl)-1-(4-morpholino)ethanethione (7)

A mixture of 2-acetyl-6-methoxynaphthalene **(6)** (5.0 g, 25 mM), and sulphur (2.40 g, 75 mM) in morpholine (6.52 ml, 75 mM) was refluxed for 18 h. The hot reaction mixture was poured into hot methanol and left overnight in a refrigerator. The precipitated material was filtered and washed with cold methanol (2 x 5 ml) to afford **7** as a brownish solid.[6] (5.5 g, 73.08 %) m.p. 130-132 ^{0}C (lit.[6] 131-133°C).

Anal.:

      TLC   : R_f 0.71 (Chloroform)

      UV (MeOH)   : 230 nm

      IR (KBr, cm^{-1}): 1601, 1492, 1103 and 854

      Mass (m/z)   : 300.92 (M$^+$)

4.1.4. 6-Methoxy-2-naphthylacetic acid (MNA) (1)

The thiomorpholide **(7)** was dissolved in methanol (20 ml) and aqueous sodium hydroxide (50 ml, 3.5%). The reaction mixture was refluxed for eighteen hours, excess of methanol recovered and the thick solution diluted further with water (100 ml), cooled and filtered. The clear filtrate was acidified with conc. hydrochloride acid (5 %) in cold and the precipitate so obtained was filtered, washed with water and dried. The dried residue was crystallized from methanol to afford the acid **(1)** as white solid[6] (2 g, 55.86 %) m.p.171-173 ^{0}C (lit.[6] 172-173°C).

Anal.:

      TLC   : R_f 0.89 (Chloroform: Methanol; 1:0.5)

      UV (MeOH)   : 230 nm

      IR (KBr, cm^{-1}): 1693, 1634, 1265 and 1216.

      NMR (DMSO-d$_6$): δ 7.67-7.07 (m, 6H, naphthalene-*H*), 3.87 (s, 3H, O-C*H*$_3$) and

                         3.68 (s, 2H, -C*H*$_2$)

      Mass (m/z)   : 215.91 (M$^+$)

      HPLC Purity : 99.6 %

4.1.5. 4-Phenylacetophenone (10)

In a 100 ml two necked round bottom flask provided with a dropping funnel and a reflux condenser with guard tube, biphenyl **(9)** (5.0 g, 32.46 mM), anhydrous aluminium trichloride (9.7 g, 72.40 mM) and anhydrous carbon disulphide (30 ml) were charged. The mixture was refluxed on a water bath for 20 minutes. Acetic anhydride (3.31 g/3.0 ml, 32.46 mM) in carbon disulphide (5 ml) was added dropwise over a period of 30 minutes

with efficient stirring at 30-35 ˚C. The reaction mixture was further refluxed for 3 hours and poured into crushed ice (100 g) containing concentrated hydrochloric acid (15 ml) and the residual carbon disulphide removed by air bubbling. The precipitate so obtained was filtered, dried and recrystallized from methanol to give[9] **10**, (4.30 g, 67.57 %), m.p. 118-120 °C. (lit.[9] 120-21°C).

Anal. :

TLC : R_f 0.74 (Benzene)

UV (MeOH) : 283 nm

IR (KBr, cm^{-1}) : 1677, 1262 and 763

Mass (m/z) : 195.84 (M^+)

4.1.6. 2-(4-Biphenyl)-1-(4-morpholino)ethanethione (11)

4-Phenylacetophenone (5.0 g, 25.5 mM), morpholine (6.7 ml, 76.5 mM) and sulphur (2.5 g) were refluxed for 18 h. The hot reaction mixture was poured into hot methanol (15 ml) and refrigerated overnight. The precipitated matter so obtained was filtered and washed with ice-cold methanol (5 ml) to get yellow colored thiomorpholide **(11)**.[9] (5.4 g, 71.27 %), m.p.138-140 °C (lit.[9] 137-139 °C).

Anal. :

TLC : R_f 0.74 (Benzene)

UV(MeOH) : 279 nm

IR (KBr, cm^{-1}) : 1677, 1262 and 763

Mass (m/z) : 296.93 (M^+)

4.1.7. 4-Biphenylacetic acid (BPA) (2)

The thiomorpholide **(11)** (7.6 g, 25.5 mM) was dissolved in a mixture of methanol (10 ml) and sodium hydroxide solution (50 ml, 6 %). The reaction mixture was refluxed for 16-18 h. Excess of the solvent was removed and the residue was dissolved in water and filtered. The filtrate so obtained was chilled and acidified with dilute hydrochloric acid to yield a buff colored precipitate which was filtered, dried and crystallized from methanol to yield 4-biphenylacetic acid **(2)**[9] (3.4 g, 62.67 %), m.p. 163-165 ºC (lit.[9] 164-165°C).

Anal. :

TLC : R_f: 0.61 (Chloroform: Methanol; 1:0.5)

UV (MeOH) : 253 nm

IR (KBr, cm^{-1}) : 1685, 1413, 1249 and 924

PMR (CDCl₃) : 8.84 (bs, 1H, -COOH), 7.88-7.28 (m, 9H, biphenyl-H) and 3.58 (s, 2H, Ar-CH_2)

Mass (m/z) : 211.93 (M$^+$)

HPLC Purity : 99.7 %

4.2. Synthesis of salts

4.2.1. Synthesis of DSPE-Na (14)

1,2-Distearoyl-*sn*-glycero-3-phosphoethanolamine (DSPE) was dissolved in cold chloroform-methanol (20 ml, 3:1). Cold methanol containing sodium hydroxide (equimolar ratio) was added slowly into above solution containing DSPE and the reaction was continued for 30 min. Then solvent was removed and the product so obtained was characterized.

Anal.:

IR (KBr, cm^{-1}) : 3430, 1741 and 1081

PMR (CDCl₃) : 5.34 (bs, 2H, NH_2), 4.28-4.25 (m, 2H, O-CH_2), 3.59-3.56 (m, 4H, (CH_2)₂), 3.15-3.05 (m, 1H, CH), 2.25-2.15 (m, 4H, (CH_2)₂), 1.99-1.98 (m, 2H, N-CH_2), 1.55-1.52 (m, 4H, (CH_2)₂), 1.17-1.15 (m, 56H, (CH_2)₁₄) and 0.81-0.78 (m, 6H, (CH_3)₂),

Mass (m/z) : 771 (M+Na)

4.2.2. Synthesis of MNA-DSPE salt (15a)

Equimolar amounts of MNA **(1)** and DSPE-Na **(14)** were dissolved in dichloromethane (25 ml) under stirring and the stirring was continued for 2-4 h till the salts precipitated out. Solvent was removed in *vacuo* and the residue was crystallized from methanol or ethyl acetate to get pure solid of the salt.

Anal.:

IR (KBr, cm^{-1}) : 1741, 1698 and 1080

PMR (CDCl₃) : 7.69-7.09 (m, 6H, Ar-H), 4.30-3.97 (m, 6H, (CH_2) NH_2), 3.88 (s, 2H, Ar-CH_2), 3.22 (s, 2H, CH_2), 2.31-2.25 (q, 4H, (CH_2)₂), 2.05-2.02 (m, 1H, CH), 1.56-1.52 (m, 4H, (CH_2)₂), 1.22-1.18 (m, 56H, (CH_2)₁₄) and 0.86-0.82 (m, 6H, (CH_3)₂)

Mass (m/z) : 217.22 (MNA) and 750.62 (DSPE)

4.2.3 BPA-DSPE salt (15b)

Equimolar amounts of BPA **(2)** and DSPE-Na **(14)** were dissolved in dichloromethane (25 ml) under stirring and the stirring was continued for 2-4 hour till the salts precipitated out. The solvent was removed in *vacuo* and the residue was crystallized from methanol or ethyl acetate to get pure solid of the salt.

Anal.:

IR (KBr, cm^{-1}) : 1741, 1689 and 1080

PMR (CDCl$_3$) : 7.66-7.32 (m, 9H, Ar-*H*), 5.23-5.20 (m, 1H, C*H*), 4.37-4.02 (m, 6H, (C*H$_2$*)$_2$, N*H$_2$*), 3.27 (s, 2H, Ar-C*H$_2$*), 2.35-2.29 (m, 4H, (C*H$_2$*)$_2$), 1.59-1.56 (m, 4H, (C*H$_2$*)$_2$), 1.26-1.20 (m, 56H, (C*H$_2$*)$_{14}$) and 0.89-0.86 (m, 6H, (C*H$_3$*)$_2$)

Mass (m/z) : 212.32 (BPA) and 748.81 (DSPE)

4.3 Formulation of liposomes

4.3.1 Formation of film: Thin film hydration method was used for the preparation of liposomes. All the lipids and the drug were mixed with cholesterol in different molar ratios separately in a 250 ml of round bottom flask (RBF) and dissolved in chloroform: methanol (3:1) mixture (40 ml). The organic solvent was evaporated using rotary flask evaporator under vacuum on a thermostatic water bath at 50±2 ºC at a speed of 60 rotations per minutes (RPM) of the rotor. This was continued till the complete evaporation of organic solvents leaving behind a dry thin lipid film deposited on the walls of the flask. This flask was further dried under vacuum in order to remove traces of organic solvent.[13]

4.3.2 Hydration of thin film: The film was hydrated using purified water (8 ml) in rotary flask evaporator under thermostatic water bath at 55±2 ºC at a speed of 60 RPM of the rotor. The multilamellar vesicles (MLVs) formed after hydration was kept at room temperature for 2 h for annealing. The liposomes were characterized for microscopic observation using Olympus microscope (BX40F4, Tokyo, Japan) at 40X magnification and photographed using digital camera.

Hydration Time

The film was hydrated with the hydration media for different time intervals from 30 min to 80 min and evaluated to optimize hydration time, for complete hydration of the lipid film. The above procedure was repeated three times. The effect of hydration time was shown in Table 4.2.

4.3.3 Size reduction (production of small unilamellar vesicles)

In order to get average liposome size below 1.5 μ, size reduction of the MLVs were carried out using probe sonicator (Labsonic, Sartoris, Germany) at 60 % amplitude 0.6 cycles for 15-20 sec. To convert large (>1.5 μ) MLVs into a mixture of MLV and SUVs, sonication of liposomal suspension was optimized by altering time, cycle and amplitude according to the size requirements. The procedure was repeated three times. The effect of sonication on liposomal formulation was shown in **Table 4.3.**

Table 4.2: Optimization of hydration time

Hydration time	Effect on Hydration of Lipid
20 min	Not properly hydrated leaves film behind.
30 min	**Complete hydration**
60 min	Complete hydration but loss of liposomal suspension

Table 4.3: Parameters for optimization of sonication

Sr.No.	Time (sec)	Cycle	Size (nm) *
1	10	60% Amplitude, 0.4 cycles ×2	1570±16.3
2	20	60% Amplitude, 0.4 cycles ×2	942±12.5
3	30	60% Amplitude, 0.4 cycles ×2	508±10.9
4	40	60% Amplitude, 0.4 cycles ×2	321±08.4
5	**50**	60% Amplitude, 0.4 cycles ×2	146±05.8
6	10	80% Amplitude, 0.6 cycles ×2	1290 ±24.1
7	20	80% Amplitude, 0.6 cycles ×2	859±18.1
8	30	80% Amplitude, 0.6 cycles ×2	498±14.5
9	40	80% Amplitude, 0.6 cycles ×2	275 ±10.6
10	**50**	80% Amplitude, 0.6 cycles ×2	110±6.50

* Mean±SD (n=3)

4.3.4 Determination of entrapment efficiency

The percent of drug entrapment in liposomes was calculated by estimating the entrapped drug in the liposomes after centrifugation at 8,000 RPM for 15 min at 4 °C

(Sigma 3K30). The supernatant was removed and discarded. The sedimented liposomes (0.2 ml) were diluted up to 1.0 ml with methanol and the supernatant was estimated for drug content after suitable dilution using HPLC. Liposomal batches were prepared by varying the process parameters like applying vacuum, changing of rotation per minute (rpm) and time. The films were prepared by keeping the lipid to cholesterol ratio constant. The films formation time was found to be dependent on applied vacuum and speed of rotation. Vacuum was kept constant at 300 mmHg and speed of rotation was varied between 50 to 120 rpm. The above procedure was repeated three times. The entrapment efficiency of the drug in liposomes was determined for each batch.

4.4 Characterization of liposomes
4.4.1 Size

The particle size (z-average) and polydispersability index (PDI) of the liposomes was analyzed by photon correlation spectroscopy (PCS) using a Malvern Zetasizer Nano (Malvern Instruments; UK). Liposome suspension (0.2 ml) was diluted to 1.0 ml with distilled water (DW) and the size distribution was measured after an equilibration time of 1 minute. The Zetasizer Nano is operating with a 4 mW He-Ne-Laser at 633 nm using non invasive back-scatter technique (NIBS) at a constant temperature of 25 °C. The measurements were conducted in the manual mode.

The size distribution by intensity and volume was calculated from the correlation function using the multiple narrow mode of the Dispersion Technology Software version 4.00 (Malvern, Herrenberg, Germany). The resulting size distribution shows the hydrodynamic diameter. The average particle size and PDI was calculated after performing the experiment in triplicate. PDI of 0.0 represents a homogenous particle population while 1.0 indicates a heterogeneous size distribution in the liposomes.

4.4.2 Morphology
Olympus microscopy

Morphological evaluation was conducted using optical microscope with polarizer BX 40, Olympus Optical Co. Ltd., at a magnification of 40X. On the basis of morphological evaluation it was concluded that the liposomes prepared by TFH method were spherical in nature.

TEM:

TEM is a microscopic technique wherein a beam of electrons is transmitted through an ultra thin specimen, interacting with the specimen as it passes through it. An

image is formed from the interaction of the electrons transmitted through the specimen. The image is magnified and focused onto an imaging device. To prevent charge build-up at the sample surface samples need to be coated with a thin layer of a conducting material, such as carbon, where the coating thickness is several nanometers. For negative-staining 5 µl of dilute liposome dispersion was placed on a 200 mesh copper grid (TAAB Laboratories Equipment, Berks, UK). The surplus dispersion was removed by filter paper and the suspension was, stained with 5 µl of 2.5 % uranyl acetate for 30 seconds. The surplus uranyl acetate was removed, and the sample was dried at room conditions before imaging the liposome with a transmission electron microscope operating at an acceleration voltage of 200 KV.

4.4.3 Zeta (ς) potential analysis

The zeta potential (ς potential) of prepared liposome suspension was measured by micro-electrophoresis using Malvern Zetasizer Nano ZS (Malvern, Instrument, U.K.). Zeta potential of the liposome was measured after separation of the free drug from the liposome. Liposomes (0.2 ml) were diluted to 1 ml with distilled water. The determination of the zeta potential was realized at 25 °C after injecting 1 ml of the sample into a standard sample cell.

4.4.4 *In vitro* diffusion studies of liposomes

The release studies were performed at 25±2.0 °C using the rotating dialysis cell model.[18] In this model, the donor compartment is separated from the acceptor compartment by a dialysis membrane (interfacial area: 22 cm^2, MW cut-off: 15000 Da). Experiments were conducted by applying the formulations to the donor compartment containing the phosphate buffer of *p*H 7.4 and tween 80 (1 %). At time zero, the dialysis cell containing the liposomes (2 ml) was placed inside a round-bottomed vessel containing 100 ml of preheated release medium (PBS). The revolution speed of the magnetic stirrer was 50 rpm. At appropriate times (1, 2, 4, 8, 12 h), samples were withdrawn (1 ml) from the acceptor phase and analyzed by HPLC. All release experiments were followed for a period of 10-12 h and repeated in triplicate. The cumulative amount of 6-MNA released was calculated.

4.5 Stability testing of liposomes

Stability studies of liposome were carried out to evaluate the change in particle size, zeta potential, percent drug loading, chemical stability of phospholipids and the drug over the period at different storage conditions. Change in the size of liposomes can take place over a period of time and these changes can be the result of aggregation and fusion.

Drug molecules can leak from the liposomes reducing the entrapment efficiency. The leakage of the drug form the liposome depends upon liposome composition and physicochemical nature of the drug. Various methods have been used in improving the stability of liposome, like incorporating saturated phospholipids to avoid oxidation process which is generally observed with unsaturated phospholipids, using charged phospholipids to reduce the possibility of aggregation and fusion, freeze drying of liposomes in presence of cryoprotectant to increase shelf life of the liposomes.[22-23]

The optimized formulations were studied for their stability and their potentials to withstand the atmospheric/environmental changes. These formulations were subjected to stability testing by evaluating parameters like particle size, zeta potential and percent entrapment efficiency.

4.6 Biodistribution and gamma imaging studies

6-MNA and the liposomal formulations were labeled using ^{99m}Tc as per the method mentioned in **Section-I**. Radiolabeling parameters such as pH, incubation time, stannous chloride concentration, and percentage of radiolabeling were optimized.

IA residence time of prepared liposomes and the parent drug were studied in inflammatory condition by injecting liposomal preparation IA in to rat knee. Animals were divided into two groups, Group-A (standard) was administered by IA the parent NSAID i.e 6-MNA **(1)**. Another group, Group-B (Test) was administered by IA the liposomal formulation, 3 h after induction of inflammation in the rat paw. Inflammation was induced in the right hind paw of the rats by injecting carrageenan (0.1 ml, 1 % w/v in normal saline) into the subplantar region of the paw. The animals were anaesthetized, fixed on a board and images were taken 1 h, 2 h, 6 h and 24 h after the administration of the radiolabeled complexes by IA route.

4.7 *In vivo* studies in arthritis model

For anti-inflammatory activity (arthritis model) Sprague-Dawley male rats with an initial body weight of 150-200 g were used. Rats were divided into groups of six each for test formulation, standard compound, control and normal group. On day 1, the animals were injected into the sub-plantar region of the left hind paw with 0.1 ml of complete Freund's adjuvant (6 mg/ml Mycobacterium butyricum suspended in heavy paraffin oil) except in the normal group.[24-25] On day 1 IA dose of 6-MNA and liposomal formulation **(CML-2)** were injected (4.27 mg/kg) on equivalent molar doses. Paw volumes of both

sides were measured plethysmographically. The paw volumes were measured on days 0, 3, 7, 14 and 21. Parent NSAID **(1)** dissolved in aqueous-DMSO as 'standard' was administered to the animals through IA route. Results are expressed as percentage inhibition of edema formation, calculated by the formula,

% Inhibition of paw edema = [1 – Ed (test)/Ed (control)] X 100

Where, Ed (test) and Ed (control) are the edema volumes in liposome/compound-treated and control groups, respectively.

On day 21 animals were sacrificed and cartilage tissue was removed and histological evaluation done. Blood samples were also tested on day 1 and 21 for the measurement of ESR and CRP levels.

4.7.1 Histology and haematology

Histological study of cartilage tissue was done by using three dyes namely Hematoxylin-Eosin (HE), Safranin-O and Toluidine blue.[26-28] Immature and mature bone show different staining characteristics; immature bone stains more with Hematoxylin and mature bone more with Eosin. Toluidine blue and Safranin-O are cationic stains (basic dyes) that stain acidic proteoglycan present in cartilage tissues. Toluidine blue, also called metachromasia dye, shows subtle color changes depending on the tertiary structure of the sample. Cytoplasm stains light blue, nuclear region dark blue and mast cell purple. Safranin-O, which binds to glucosaminoglycans and shows an orange color, is often used to stain articular cartilage. Fast green, the contrast stain of Safranin-O, is a sulfate-group containing acidic substrate, which binds strongly to the amino group in proteins and thereby strongly stains the non-collagen sites.

References

1. Goudie A.C., Gaster L.M., Lake A.W., Rose C.J., Freeman P.C., Hughes B.O. and Miller D., 4-(6-Methoxy-2-naphthyl)butan-2-one and related analogs, a novel structural class of antiinflammatory compounds. *J. Med. Chem.* **1978**, 21, 1260-64.

2. Friedel H.A., Langtry H.D. and Buckley M.M., Nabumetone: A reappraisal of its pharmacology and therapeutic use in rheumatic diseases. *Drugs* **1993**, 45, 131-56.

3. Davies N.M., Clinical Pharmacokinetics of Nabumetone. *Clin. Pharmacokinet.* **1997**, 33, 403-16.

4. Furniss B. S., Hannaford J. H., Smith P. W. G. and Tachell A. R., In: Vogel's Text book of Practical Organic Chemistry, 5th edition, Longman, Singapore, **1996**, 987

5. Arsenijevic L. Synthesis of 2-acetyl-6-methoxynaphthalene Organic synthesis Vol-6, 34

6. Furniss B. S., Hannaford J. H., Smith P. W. G. and Tachell A. R. In: Vogel's Text book of Practical Organic Chemistry, 5th edition, Longman, Singapore. **1996**, 1054.

7. Chalmers I. M., Bell M. A. and Bychanan W. W. Effect of flurbiprofen on the metabolism of antipyrine in man. *Ann. Rheum. Dis.* **1973**, 32, 58-61

8. Takase K., Masumoto S. and Okumura F. Anti-inflammatory studies of 2-(2-fluoro-4-biphenylyl) propionic acid (Flurbiprofen), *Folia Pharamcol.* **1975**, 71, 573

9. Schwenk E. and Papa D. Preparation of aryl aliphatic acids by the modified willgerodt reaction. *J. Org. Chem.*, **1946**, 11, 798

10. Puglia C., Bonina F., Rizza L., Cortesi R., Merlotti E., Drechsler M., Mariani P., Contado C., Ravani L. and Esposito E., Evaluation of Percutaneous Absorption of Naproxen from Different Liposomal Formulations. *J. Pharm. Sci.* **2010**, 99, 2819

11. Srinath P.P., Vyas S.P. and Diwan P.V., Preparation and Pharmacodynamic Evaluation of Liposomes of Indomethacin. *Drug. Dev. Ind. Pharm.* **2000**, 26, 313

12. Ruozi B., Tosi G., Forni F. and Angela V. M., Ketorolac Tromethamine Liposomes: Encapsulation and Release Studies. *J. lipo. Res.* **2005**, 15, 175

13. New RRC. Preparation of liposomes : A practical approach, New RRC ed. Oxford University Press, Oxford, **1990**, 33-104

14. Bonanomi M.H., Velvart M., Stimpel M., Roos K.M., Fehr K. and Weder H.G., Studies of pharmacokinetics and therapeutic effects of glucocorticoids entrapped in liposomes after intraarticular application in healthy rabbits and in rabbits with antigen-induced arthritis. *Rheumatol. Int.* **1987**, 7, 203-12.

15. Bonanomi M.H., Velvart M. and Weder H.G., Fate of different kinds of liposomes containing dexamethasone palmitate after intra-articular injection into rabbit joints. *J. Microencapsul.* **1987**, 4, 189-200

16. Williams A.S., Camilleri J.P., Goodfellow R.M. and Williams B.D., A single intraarticular injection of liposomally conjugated methotrexate suppresses joint inflammation in rat antigen-induced arthritis. *Br. J. Rheumatol.* **1996**, 35, 719-724.

17. Butoescu N., Jordan O. and Doelker E., Intra-articular drug delivery systems for the treatment of rheumatic diseases: A review of the factors influencing their performance. *Eur. J. Pharm. Biopharm.* **2009**, 73, 205-18

18. Larsen C., Ostergaard J., Larsen S.W., Jensen H., Jacobsen S., Lindegaard C. and Andersen P.H., Intra-Articular Depot Formulation Principles: Role in the Management of Postoperative Pain and Arthritic Disorders. *J. Pharm. Sci.* **2008**, 97, 4622-54.

19. Simkin P.A. and Pizzorno J.E. Transsynovial exchange of small molecules in normal human subjects. *J. Appl. Physiol.* **1974**, 36, 581-87

20. Nicolas C., Verny M., Giraud I., Ollier M., Rapp M., Maurizis J.C. and Madelmont J.C., New quaternary ammonium oxicam derivatives targeted toward cartilage: synthesis, pharmacokinetic studies, and anti-inflammatory potency. *J. Med Chem.* **1999**, 42, 5235-40.

21. De. Silva M., Hazleman B.L., Thomas D.P. and Wraight P., Liposomes in arthritis: a new approach. *Lancet.* **1979**, 1, 1320-22.

22. Lu D. and Hickey A.J., Liposomal Dry Powders as Aerosols for Pulmonary Delivery of Proteins. *AAPS Pharm Sci Tech.* **2005**, 6, E641-E648.

23. Maitani Y., Aso Y., Yamada A. and Yoshioka S. Effect of sugars on storage stability of lyophilized liposome/DNA complexes with high transfection efficiency. *Int. J. Pharm.* **2008,** 356, 69-75.

24. Saha, G. B. In Physics and Radiobiology of Nuclear Medicine; Saha, G. B., Ed., 5th ed.; Springer-Verlag: New York, **1993**, 100-106

25. Yadav M.R., Pawar V.A., Marvaniya S.M., Halen P.K., Giridhar R., Mishra A.K., Site specific chemical delivery of NSAIDs to inflamed joints: synthesis, biological activity and gamma-imaging studies of quaternary ammonium salts of tropinol esters of some NSAIDs or their active metabolites. *Bioorg. Med. Chem.* **2008**, 16, 9443-9.

26. Butoescu N., Seemayer C.A., Palmer G., Guerne P.A., Gabay C., Doelker E. and Jordan O., Magnetically retainable microparticles for drug delivery to the joint: efficacy studies in an antigen-induced arthritis model in mice. *Arthritis Res. Ther.* **2009**,11, R72

27. Butoescu N., Seemayer C.A., Foti M., Jordan O. and Doelker E., Dexamethasone-containing PLGA superparamagnetic microparticles as carriers for the local treatment of arthritis. *Biomaterials.* **2009**, 30, 1772-80

28. Türker S., Erdoğan S., Ozer A.Y., Ergün E.L., Tuncel M., Bilgili H. and Deveci S., Scintigraphic imaging of radiolabeled drug delivery systems in rabbits with arthritis. *Int. J. Pharm.* **2005**, 296, 34-43

Section-IV

ORAL DRUG DELIVERY

1. Introduction

Prolonged administration of NSAIDs in chronic diseases such as arthritis exhibits several undesired side effects; like GIT irritation and ulceration which still represent an unsolved therapeutic problem. The development of a GIT-friendly anti-inflammatory therapy for the treatment of disease of joints presents a unique challenge. Considerable attention has been focused on the development of bioreversible derivatives, such as prodrugs, to temporarily mask the acidic group of NSAIDs as a promising means of reducing or abolishing the GI toxicity due to the local action mechanism.

Different approaches used for prodrug designing of NSAIDs are as follows:

1. Ester and amide prodrugs

Most prodrugs of NSAIDs have been prepared by derivatization of the carboxyl group. The esters have dominated prodrug research because they have the ideal characteristic of exhibiting reasonable *in vitro* chemical stability which allows them to be formulated with adequate shelf-lives. Additionally, by virtue of their ability to function as substrates for esterases, esters are suitably labile, *in vivo*[1]. With this aim different pro-moieties have been taken into consideration to design new efficacious NSAID prodrugs.

2. Anhydride prodrugs of NSAIDs

Unlike the ester bond used in prodrugs, anhydride bond is more susceptible to hydrolysis and is less sensitive to enzymatic action than the ester and amides.

3. A mutual prodrugs of NSAIDs

A mutual prodrug is a kind of prodrug in which the carrier used is another biologically active drug instead of some inert molecule. Some of the mutual prodrug examples are as follow:

3.1. Benorylate: This was the first mutual prodrug of NSAID in which coupling of paracetamol with aspirin minimized ulceration.

3.2. Coupling with amino acids: It is a well known fact that amino acids have inherent anti-inflammatory and anti-arthritic activity. Amino acids like *L*-tryptophan, *L*-histidine and *L*-glycine are carriers that have marked activity of their own.

3.3. Glucosamine conjugate: The rationale behind use of glucosamine is to mask acidic functional group temporarily. Glucosamine is an amino sugar which is physiologically used by the body to produce natural joint components like joint lubricants and shock absorbers.

Despite extensive efforts for separating therapeutic effect from GI toxicity, the search for an ideal prodrug with a superior therapeutic advantage for clinical use still remains unmet for the NSAIDs. Further research is needed to design and identify prodrugs, which would be appropriate for clinical use in terms of stability, metabolism, toxicity and side effects. Instead of synthesizing new compounds which is a time consuming and costly affair, the designing of derivatives of existing clinically used NSAIDs is definitely an interesting and promising area of research. Moreover, as the metabolic profile of the liberated parent drug (after cleavage of the derivative in the body) would be already known, it could be advantageous to design derivatives of parent NSAIDs.[2]

It has been shown that quaternary ammonium compounds accumulated preferentially in certain avascular cartilaginous tissues on intramuscular injection.[3] It has been postulated that these quaternary ammonium compounds are localized in the cartilage tissues, probably by virtue of ionic interactions with cartilaginous tissues.[3-4]

The localization of these quaternary ammonium compounds in the articular and epiphyseal cartilage and joint spaces might be of significance in relation to the distribution of drugs to inflamed joints and lesions of articular cartilage, and raised the possibility of enhancing the duration and intensity of anti-inflammatory effect in the inflamed cartilaginous tissues by chemically designing the drug derivatives by combining the antiarthritic activity and the joint localizing property.

From the literature it was concluded that cationic group i.e. pyridinium or ammonium ion is essential in such derivatives to show tropism towards cartilage[3-4], but ionic compounds specially cationic, are repelled due to positive charge present on the outside wall of the gastrointestinal membrane[5], as a result cations with a high kinetic energy or small size only are able to penetrate the ionic barrier. Another means of penetration is via ion-pair transport mechanism or as some complex with endogenous substance using active transport. Thus, at a given *p*H the rate of permeation of different molecules is in the following order-*unionized moleculs > anions > cations.* [6-8]

Due to the above given reasons, ionic derivatives may have low to poor rate of absorption through GIT membrane, which adversely contributes to their oral bioavailability. So there is no alternative to administer these derivatives other than parenteral route. As per literature all such derivatives have been administered by parenteral route only, but from the pharmaceutical point of view this is not a convenient and safe route.

2. Aims and Objectives

Oral delivery of NSAIDs for the treatment of arthritis is a widely accepted delivery system but it produces side effects during the treatment due to local GIT irritation and widespread distribution of the drug throughout the body. So, in order to avoid these side effects, delivery systems with the ability to deliver the drug to the required site is essential.

All the NSAIDs have one or more of the side effects such as GIT toxicity, renal adverse drug reactions (ADRs), blockade of platelet aggregation etc. Conventional NSAIDs have short biological half life needing frequent dosing to maintain the therapeutic efficacy for an extended period of time, which results in exhalted side effects. Due to these reasons, the development of new NSAIDs without these side effects has long been awaited but unfortunately this has not happened. Hence, the present work was undertaken with the aim of developing oral drug delivery systems of conventional NSAIDs to give site specific delivery for the treatment of arthritis, mainly RA and OA.

It was evident from the literature that cationic molecules possess affinity towards cartilage tissue which is anionic in nature. But such molecules show poor bioavailability on oral administration. Hence it was planned to convert the conventional NSAIDs in to neutral chemical delivery systems which would be easily absorbed from the GIT. Once they enter in to systemic circulation they should be metabolized/converted in to cationic species. Having a specific affinity for the anions these cations could be targeted to the negatively charged cartilaginous tissues. Once bound to the cartilaginous tissue of the joints, they should get hydrolyzed slowly into the original parent NSAIDs exhibiting their known therapeutic effects in the joints.

To achieve the above described aim it was planned to prepare dihydropyridine derivatives of the NSAIDs. The dihydropyridine derivatives would show neutral characteristics in the intestine and hence would be absorbed due to their non-ionic characteristics. The dihydropyridine derivatives would be oxidized in to quaternary derivatives by NAD-NADH co-enzyme system and would be concentrated in to inflamed joints due to ionic interactions as shown in **fig. 2.1.**

Adopting the above described approach, the problem of poor oral bioavailability could easily be circumvented and after metabolic conversion site specificity of the NSAIDs to the cartilaginous tissue could be achieved. In nutshell, the newly synthesized derivatives could achieve the designed aims due to the following reasons:

- The free carboxylic group of the NSAIDs would be masked into ester/amide functional group avoiding local GIT irritation.

313

- The neutral ester/amide derivative would be easily absorbed from the intestine.

- The dihydropyridine grouping present in the derivative would be oxidized to quaternary pyridinium ions thus generating the cation bound NSAIDs having high affinity towards the inflamed joints.

- Random distribution of conventional NSAIDs would be minimized by selective delivery of NSAIDs to the site of action.

- Site specific delivery of the NSAIDs to the affected joints would reduce the effective dose of the NSAIDs leading to further reduction in the toxic side effects.

- Chemical/enzymatic hydrolysis of the derivatives in the inflamed area would lead to sustained specific release of the parent NSAIDs.
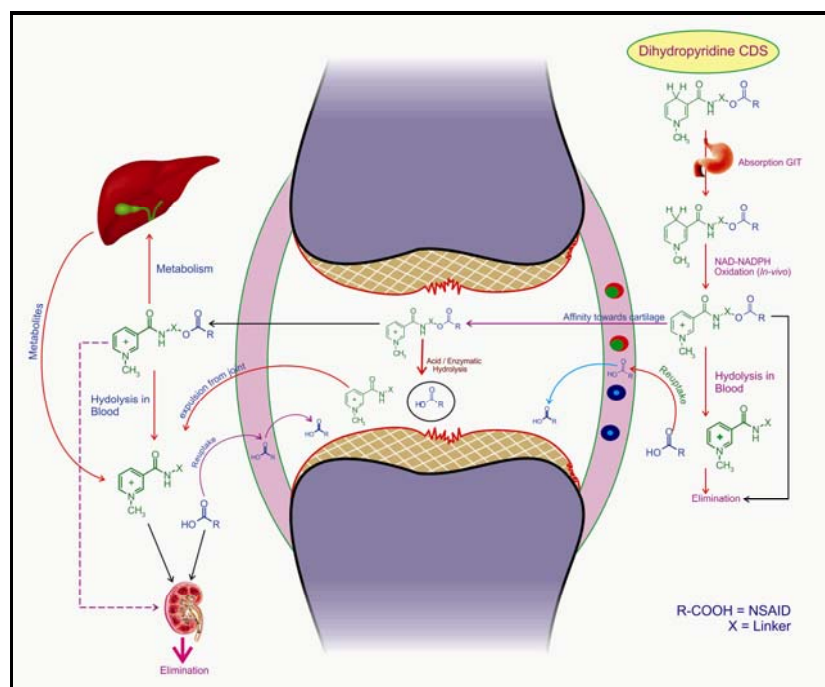
Fig. 2.1: Dihydropyridine Chemical delivery system

The following research activities were planned to be performed to achieve the laid down aims and objectives of the work:

I. To synthesize dihydropyridine derivatives of some common NSAIDs possessing ester or amide linkage.

II. To evaluate the synthesized derivative for their chemical/enzymatic susceptibility/stability.

III. To study the biodistribution of the quaternary derivatives using radiolabeling tags.

314

IV. Results and Discussion

The work carried out towards achieving the proposed plan has been discussed under the following three main headings:

    3.1. Chemical studies

    3.2. Hydrolyses kinetics

    3.3. Biodistribution and gamma imaging studies

3.1 Chemical studies

To synthesize the envisaged chemical delivery system (CDS), it was planned to couple the NSAIDs **(2)** with 3-aminopyridine **(1)** using EDC.HCl as the coupling agent to obtain the respective amide intermediate **(3)**. Quaternization of the pyridine nitrogen was planned by using methyl iodide. To obtain the desired dihydropyridine system **(7)** it was thought of using some mild reducing agent like sodium dithionite. To initiate the research work ibuprofen **(2I)** was used as the NSAID **(2)**. The planned **Scheme-1** for the synthesis of the desired CDS **(7)** went well up to the quaternization step to afford the ammonium derivative **(4)** but reduction of the quaternary ammonium derivative **(4)** to afford the desired CDS **(7)** could not be achieved using sodium dithionite.
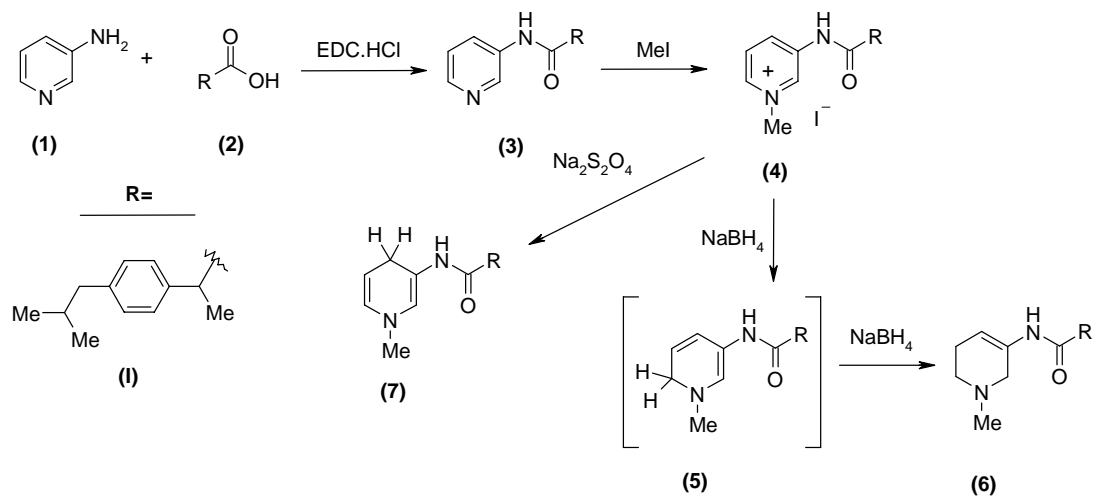

Scheme-1

The IR spectrum of compound **(3)** showed carbonyl stretching of amide group at 1693 cm^{-1} as sharp intense band. N-H stretching of amide was observed at 3282 cm^{-1}. The mass spectrum showed peak at 282.28 (M^{+}). This amide intermediate was quaternized using methyl iodide in acetonitrile or acetone as a solvent to obtain the quaternary ammonium derivative **(4)**. The IR spectrum **(Fig. 3.1. A)** of compound **(4)** showed

315

carbonyl stretching of amide group as sharp intense band at 1704 cm^{-1} and N-H stretching of amide was observed at 3453 cm^{-1}.

The PMR spectrum **(Fig. 3.1. B)** of the compound **(4)** showed singlet at δ 10.88 for single proton of pyridinium ring (-H_b), singlet at δ 9.75 due to amide-H_f, and a multiplet at δ 9.07-9.04 due to single proton of pyridinium ring (-H_e). Other protons of pyridinium ring appeared at δ 8.31-8.29 (-H_d) and δ 7.59-7.53 (-H_c) as multiplets.

(4)
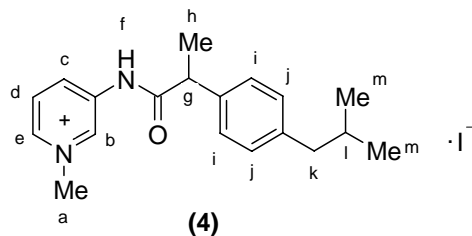
The protons of phenyl ring appeared at δ 7.51-7.08 as multiplet (Ar-$H_{i\text{-}j}$) and the methyl protons of quaternary nitrogen and -CH_g appeared at δ 4.36-4.30. The six methyl protons (-CH_{3m}) appeared at δ 0.87-0.85 as a doublet. The mass spectrum **(Fig. 3.1. C)** Showed peak at 297.1 (M$^+$).


(A)

(B)

MF: $C_{19}H_{25}N_2O$
MW: 297.2
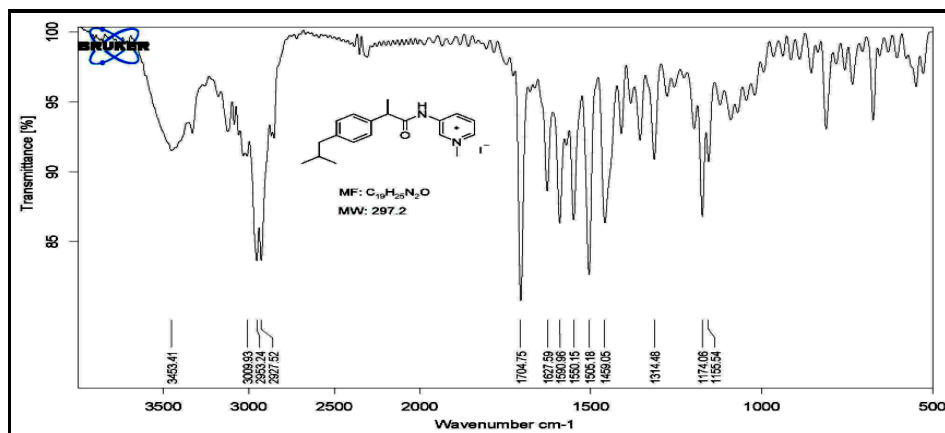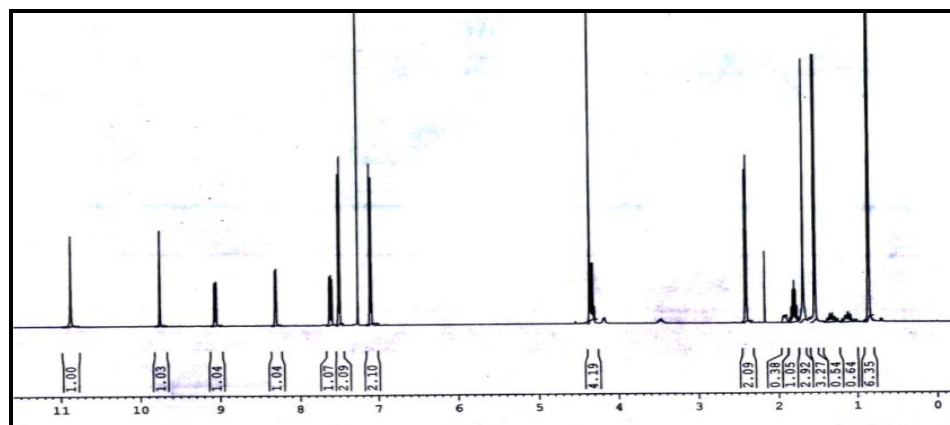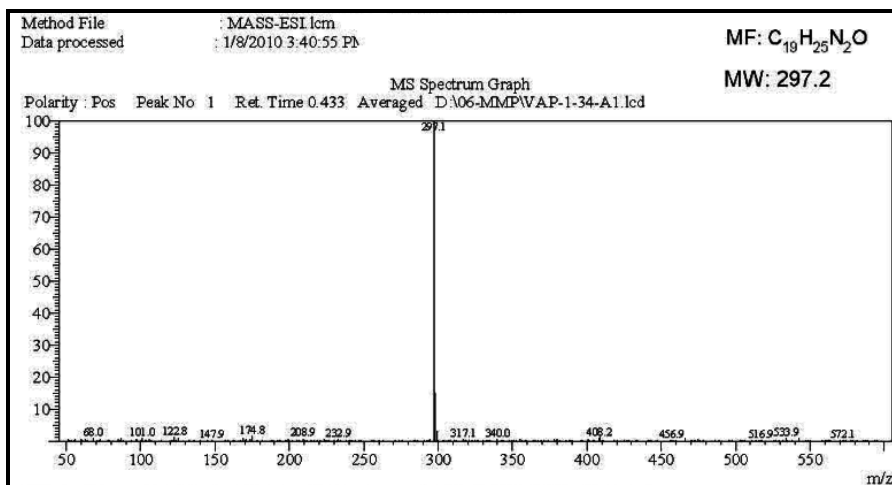
(C)

Fig. 3.1: Spectra of derivative **(4)**; IR spectrum **(A)**, ^{1}H-NMR **(B)** and Mass spectrum **(C)**

It was tried to reduce the quaternary derivative **(4)** using sodium dithionite under different experimental conditions but every time the starting material only was recovered back. After failing with dithionite it was thought of using a stronger reducing agent like sodium borohydride. After giving sodium borohydride treatment to the compound **(4)**, the product was isolated and characterized to be the 1,2,5,6-tetrahydro derivative **(6)** which was getting formed probably through the dihydro derivative **(5)** but even this dihydro derivative **(5)** could not be isolated.

The tetrahydro derivative **(6)** showed strong peaks at 1665 cm^{-1} and 3505 cm^{-1} for carbonyl and N-H stretching vibrations in its IR spectrum.
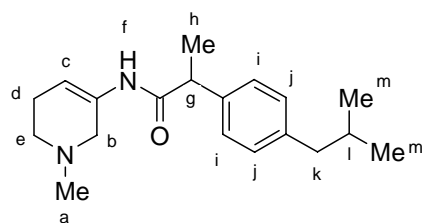
(6)

PMR spectrum **(Fig. 3.2. A)** of compound **(6)** showed the presence of aromatic protons at δ 7.19-7.11 (Ar-H_{i-j}), singlet at 6.23 due to N-H_f proton and the proton of cyclic alkene at 5.78 as multiplet (-H_c). Methyl protons on nitrogen appeared at δ 2.33 as a singlet (-CH_{3a}) and a doublet at δ 0.89-0.90 due to presence of dimethyl protons (-H_m). The mass spectrum **(Fig. 3.2. B)** showed peak at 300.1 (M$^+$). Its ^{13}C-NMR spectrum **(Fig. 3.2. C)** showed peaks at δ 172.7 for C=O carbon of amide groups, aromatic carbons at

140.96-110.23 and aliphatic carbons at 55.60-18.46. The H-H and C-H coupling was also confirmed using COSY and HETCOR spectra as shown in **Fig. 3.1. D-E**

(A)

(B)

(C)

318
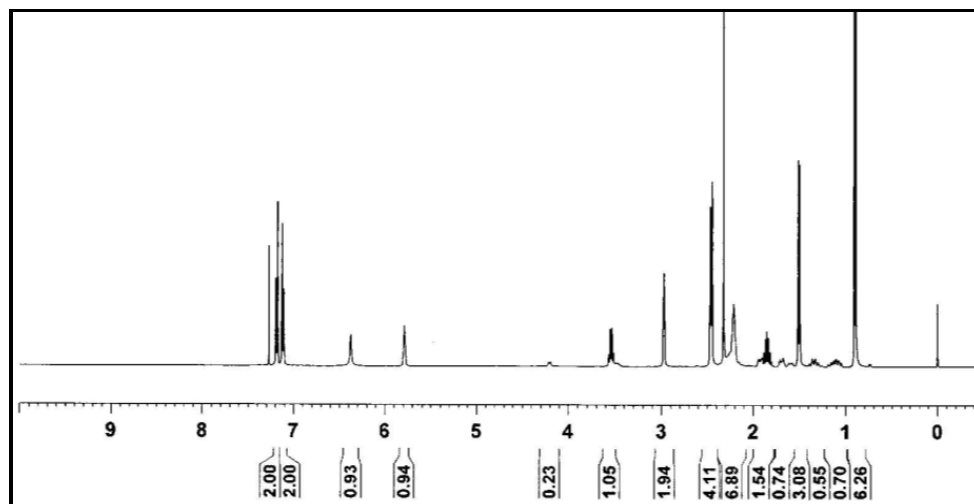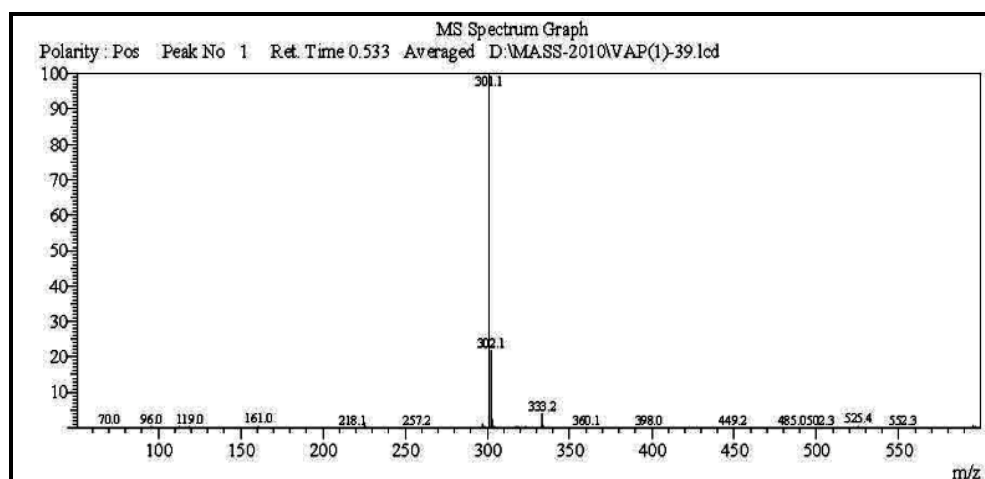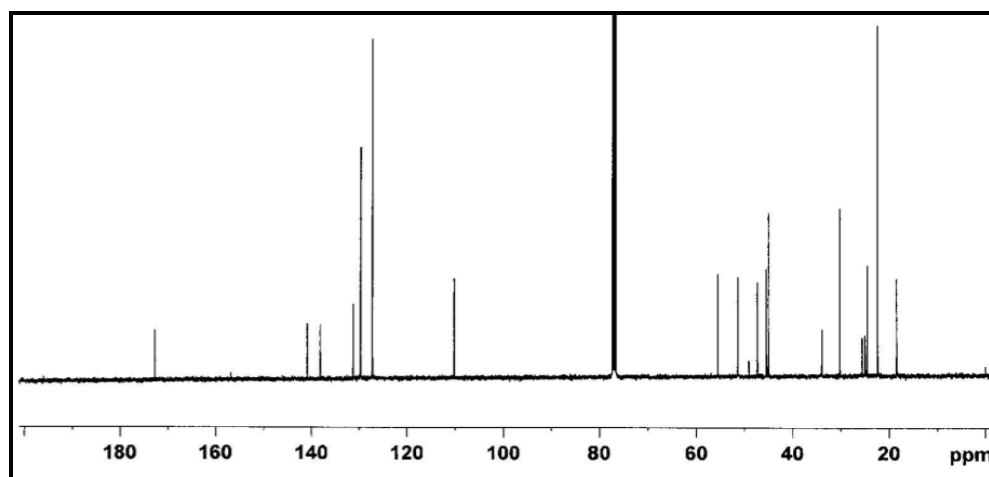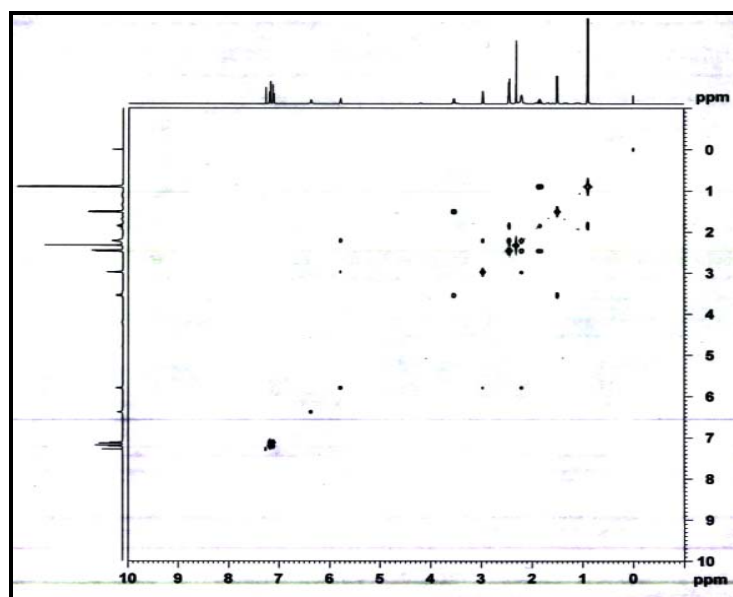
(D)
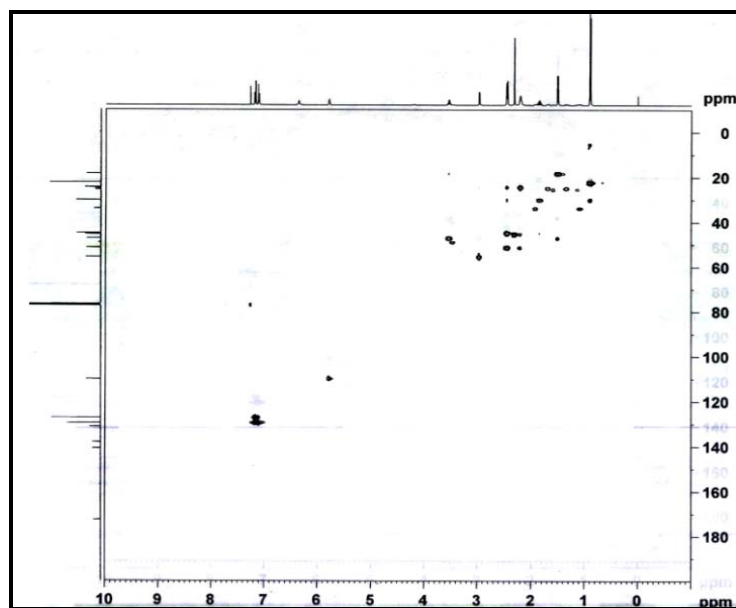
(E)

Fig. 3.2: Spectra of derivative **(6)**; ^{1}H-NMR **(A)**, ^{13}C-NMR **(B)**, Mass spectrum **(C)**, COSY **(D)** and HETCOR **(E)**.

From the literature it became known that reduction of substituted N-methyl pyridinium salts using sodium borohydride was easily achieved with regioselectivity. Pyridinium salts without electron withdrawing group **(4)** were reduced by sodium borohydride to give 1,2,5,6-tetrahydro derivatives, but not by sodium dithionite.[12] Reduction of these derivatives by sodium borohydride may take place in two ways, first direct reduction into 1,2,5,6-tetrahydro derivative **(6)** and the second one takes place

through two steps. First reduction offers 1,6-dihydopyridine derivative **(5)** followed by its further reduction in to 1,2,5,6-tetrahydro derivative **(6)**

Literature also revealed that substituents present on N-methyl pyridinium ring favor the regioselective reduction mediated by sodium borohydride as well as sodium dithionite. Electron withdrawing groups at position-3 on pyridine ring are necessary to give 1,4-dihydropyridine derivatives using dithionite as reducing agent while, derivatives without electron withdrawing groups are not reduced by dithionite at all but reduced by sodium borohydride to give tetrahydro derivatives[13-14]. So, it was planned to synthesize quaternary derivatives containing electron withdrawing group at position-3 which could be reduced by sodium dithionite to generate 1,4-dihydropyridine derivatives.

For the synthesis of the required derivatives containing electron withdrawing groups at position-3, nicotinic acid **(8)** was chosen as the starting material as shown in **Scheme-2**.
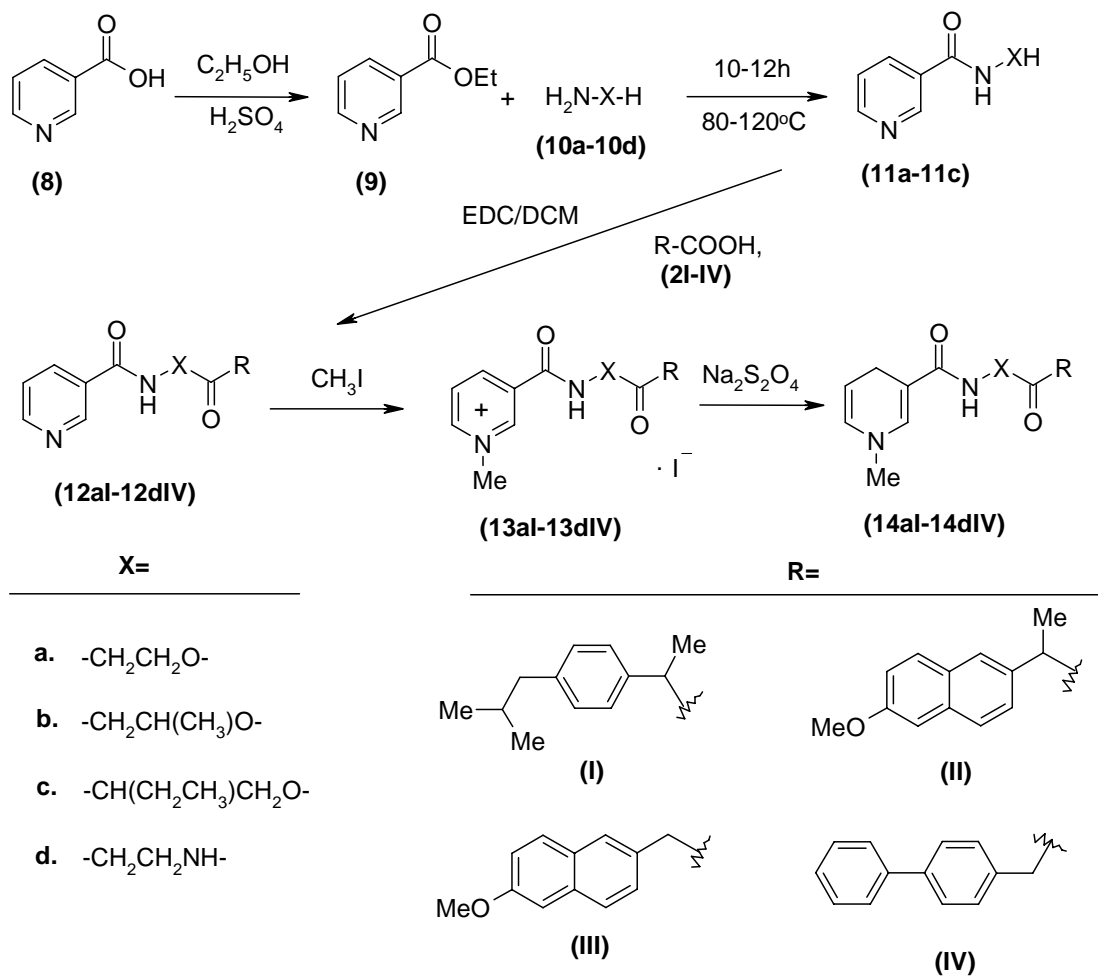
Scheme-2

Nicotinic acid was converted to ethyl nicotinate **(9)** and then treated with various aminoalcohols **(10a-10c)** or ethylenediamine **(10d)** at 100-120 ^{0}C to give the respective nicotinamide derivatives **(11a-11d)**. These intermediates were further coupled with various NSAIDs **(2I-2IV)** to offer the respective ester or amide derivatives **(12aI-12dIV)**. These derivatives were then quaternized by methyl iodide in acetonitrile to generate the quaternary derivatives (**13aI-13dIV**). The detailed synthesis and characterization of these derivatives has been described under **Section-I**

Reduction of the quaternary derivatives **(13aI-13dIV)** was planned to be carried out using Sodium dithionite $(Na_2S_2O_4)$ in an aqueous solution to afford 1,4-dihydropyridine derivatives **(14aI-14cIV).** From the NMR and mass data it became known that the synthesized dihydropyridine compounds were generally less stable than the corresponding quaternary derivatives.
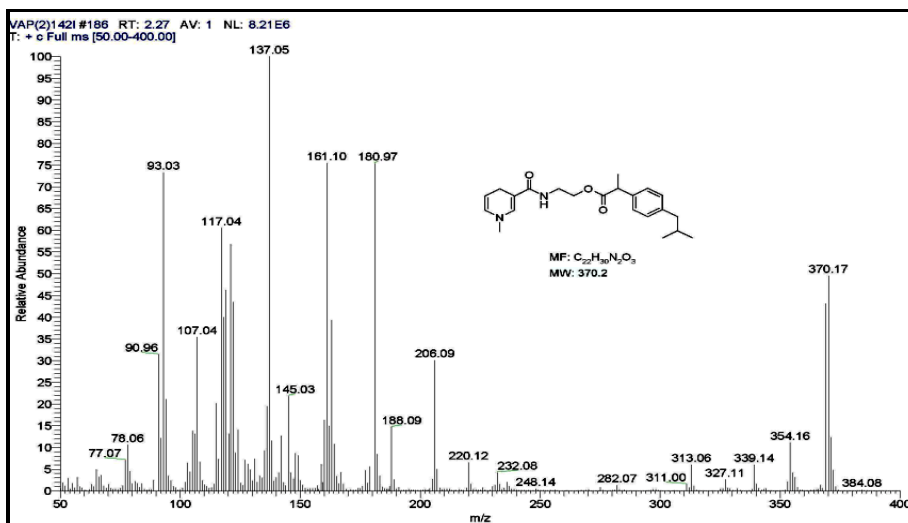

(A)
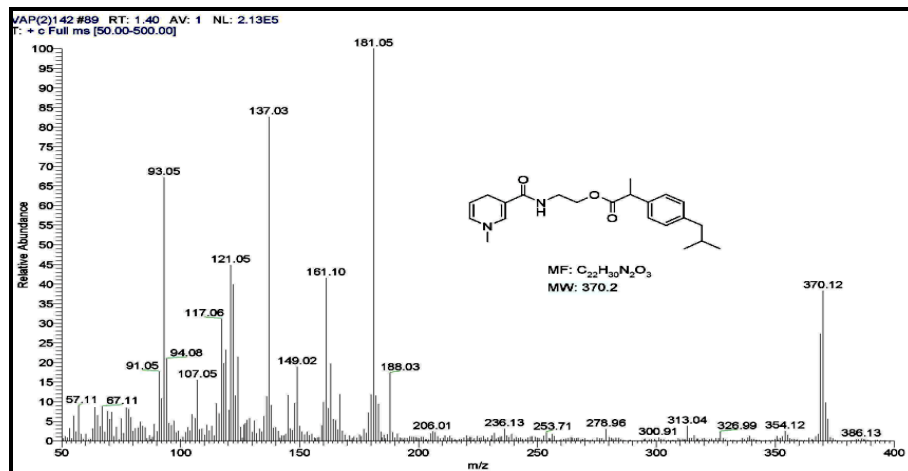
(B)
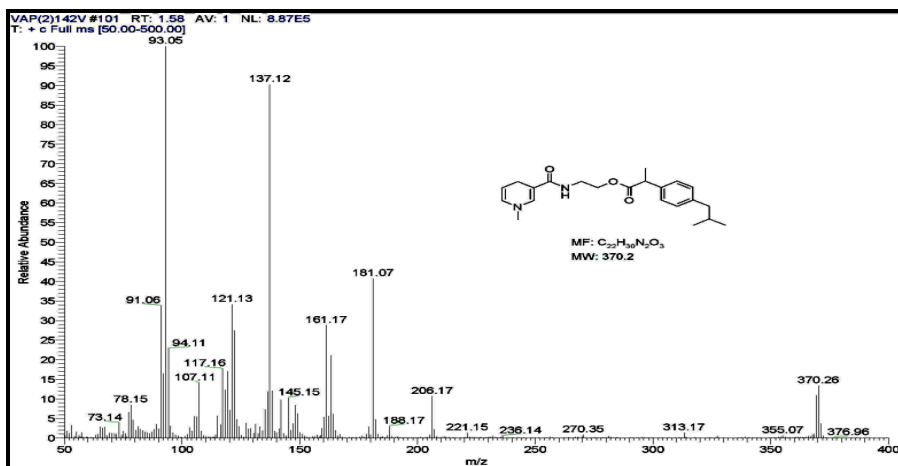
(C)
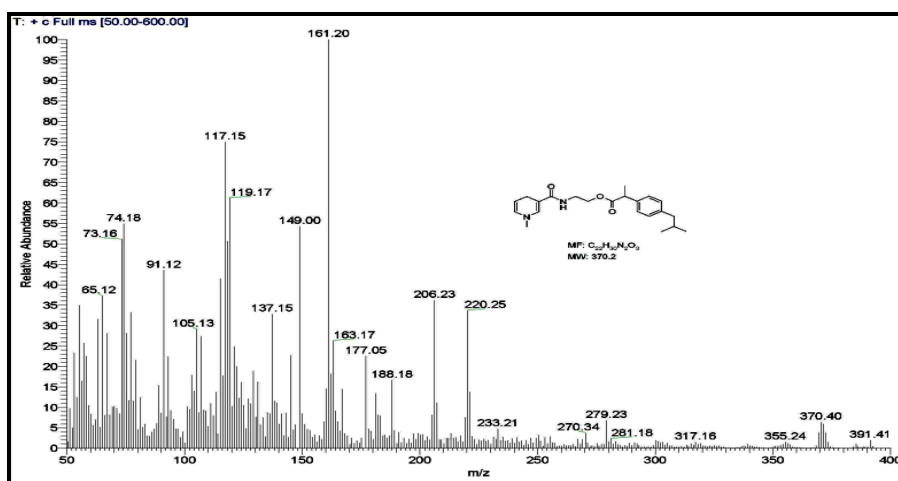
(D)

Fig. 3.3: A-D: Decrease in concentration of dihydropyridine derivative **(14aI)** with time.

The mass of the compounds showed gradual decrease in height of molecular ion peak and complete disappearance of the said peak occurred within 15-30 days. The decrease in peak height of mass spectrum with respect to time also confirmed instability of dihydropyridines as shown in **Fig. 3.3 A-D.** This instability of dihydropyridine derivatives was due to oxidation of the dihydropyridine ring system.[15]

Attempts to stabilize the dihydropyridine derivatives was made by salt formation approach using weak organic acids such as oxalic acid, succinic acid, as well as strong acids such as hydrochloric acid but without success.

It became evident from the literature that 1-alkyl 1,4-dihydropyridines are unstable and undergo facile oxidation (hydride loss) to the corresponding quaternary salts, but oxidation is not the only one process which is responsible for the instability of

dihydropyridines. It has been reported that 3-substituted-1,4-dihydropyridines such as **(15)** gets readily hydrated, especially in acidic media.[16-17] The mechanism of hydration involves a proton transfer from the acidic species to the C^5 position of the substrate, followed by a rapid attack by a hydroxy ion or other nucleophile at the C^6-position.[17-18]

**(15)**   **(16)**   **(17)**
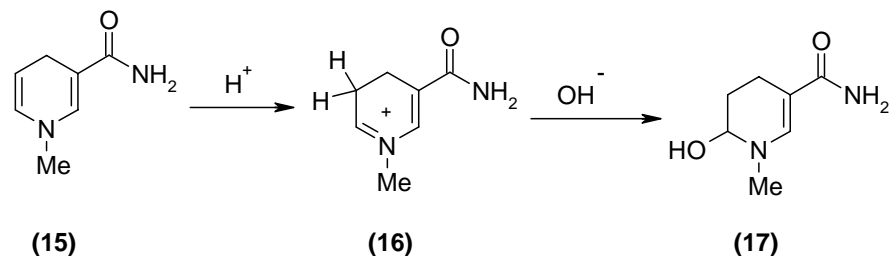
Fig. 3.4: Mechanism of water addition reaction to 1,4-dihydropyridines

Oxidation of dihydropyridines is the dominant process under physiological conditions (*p*H 7.4). Susceptibility of the enamines toward water may seriously limit the possibility of developing CDS in aqueous formulations with pharmaceutically acceptable shelf-life. Water is readily and irreversibly added to the 5,6-double bond of 3-substituted-1-alkyl-1,4-dihydropyridines **(Fig.3.4)**, and the resulting 6-hydroxy-1,4,5,6-tetrahydropyridine derivatives are no longer subject to the enzymatic oxidation that could convert them into the desired quaternary forms.[19]
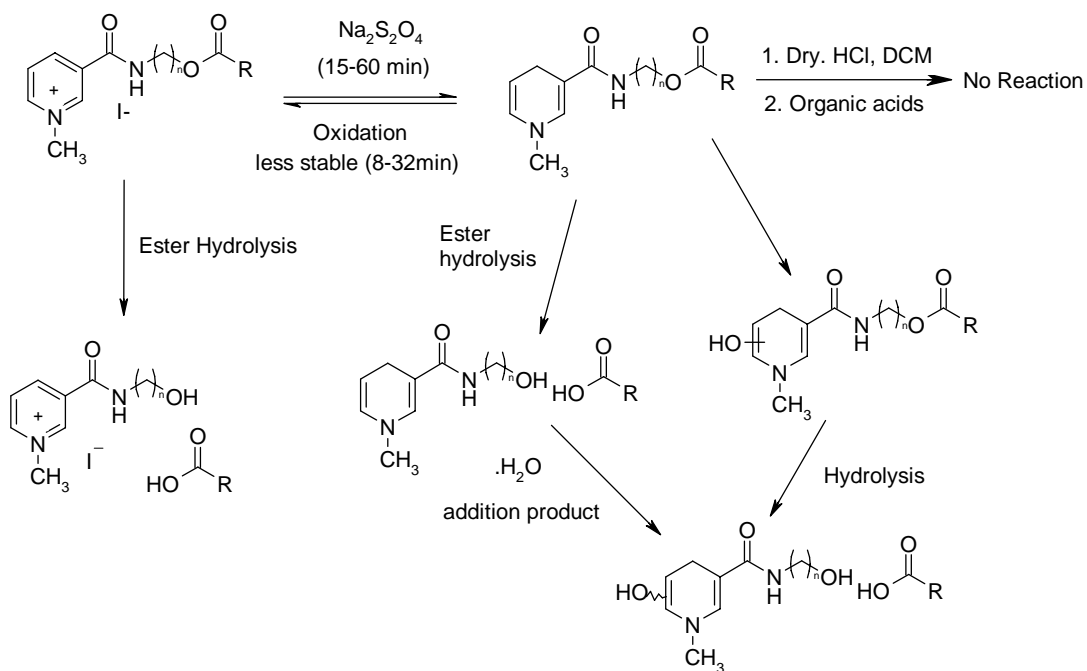

Fig. 3.5: Reduction of pyridinium salt and decomposition pattern of dihydropyridines

323

It was concluded that dihydropyridines followed much more complicated pattern than we imagined. [20] Dihydropyridines would show addition of water molecules to the 5,6-double bond, get oxidised to pyridinium salts, would exhibit hydrolysis of ester bond, and a combination of such processes. All these routes to liberate the parent drug are depicted in **Fig. 3.5.**

The possible protonation sites and mechanism of water addition in dihydropyridines is predicted by bodor *et al.*[21] as shown in **Fig. 3.6**. The addition of water to 1,4-dihydropyridines is chemically an enamine hydration type of reaction. It is known that electron donating (+*I*) substituents on the enamine nitrogen or carbon increase the reactivity of dihydropyridines towards hydration.[21]
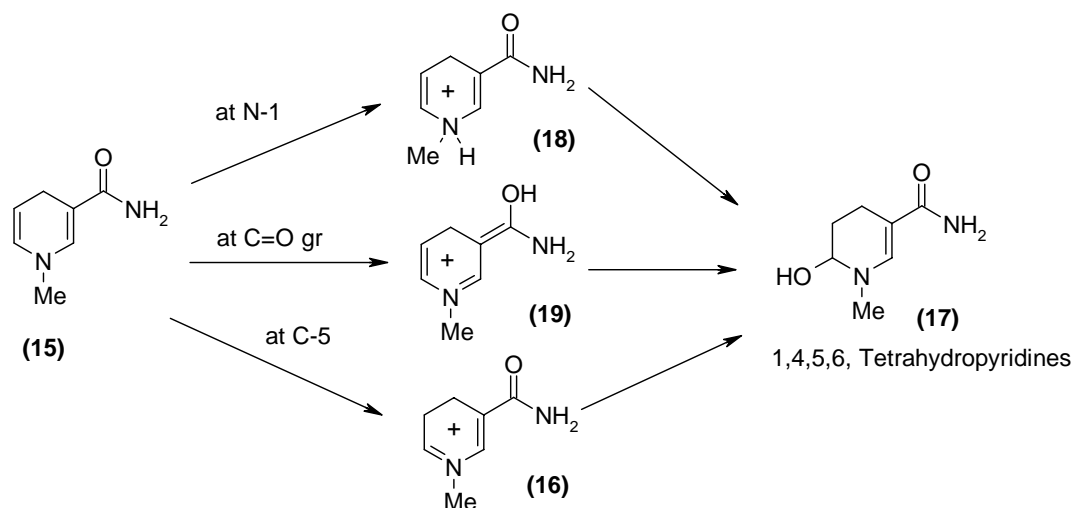

Fig. 3.6: Mechanisms of water addition in dihydropyridines

The possible protonation site was further confirmed by using AM1-based[22] semiempirical quantum chemical calculation. It show the C^5 position as the site with highest proton affinity in this moiety.[23] Furthermore, **Fig. 3.7** which represents the AM1-optimized structure of dihydropyridine derivative **(14aI)** covered with a soft surface, colored according to the electrostatic potential calculation based on AM1-charges. It shows a clear accumulation of electron density around the C^5-position, the site most susceptible to proton attack.[19]

Among the ibuprofen series, only one derivative **(14cI)** was found to be comparatively more stable. The IR spectrum of compound **(14cI)** showed carbonyl stretching of ester and amide groups as sharp intense bands at 1731 cm^{-1} and 1643 cm^{-1} respectively. N-H Stretching of amide was observed at 3301 cm^{-1}. Its mass spectrum **(Fig. 3.8.)** showed peak at 398.17 (M^+).

(A)
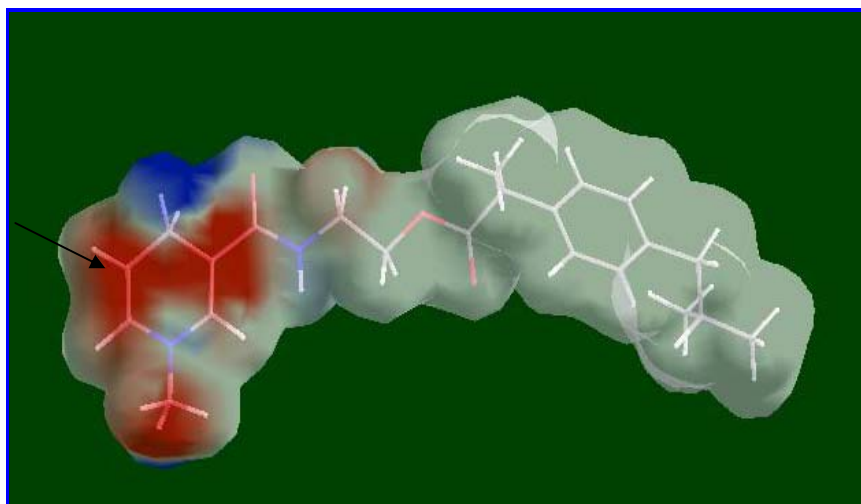
(B)
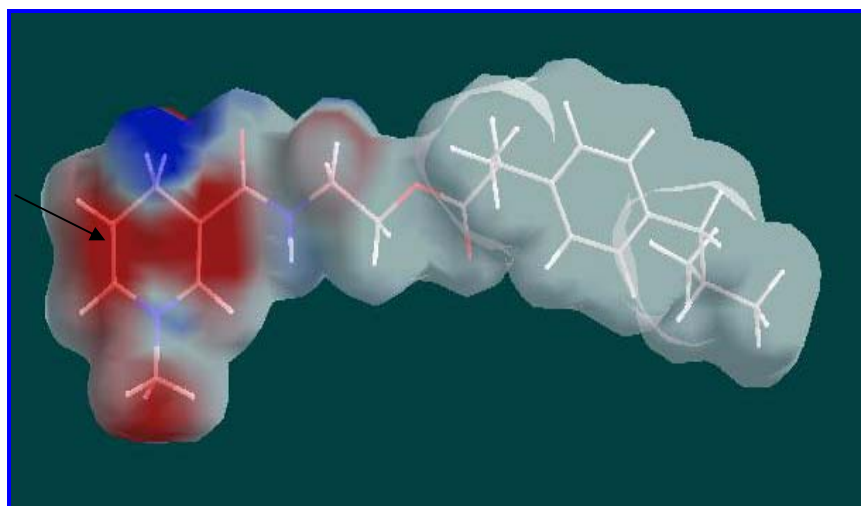
(C)
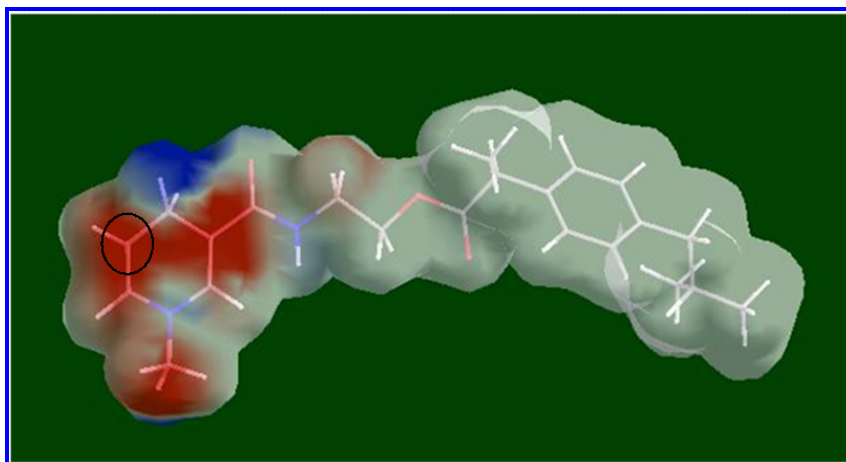
(D)

Fig. 3.7 A-D: AM1 optimized structure of dihydropyridine derivative **(14aI)** covered with a soft surface colored according to the electrostatic potential calculation based on AM1 charges. *(Region of increased electron density is found around C^5 even when compared to the basic N^1 atom)*
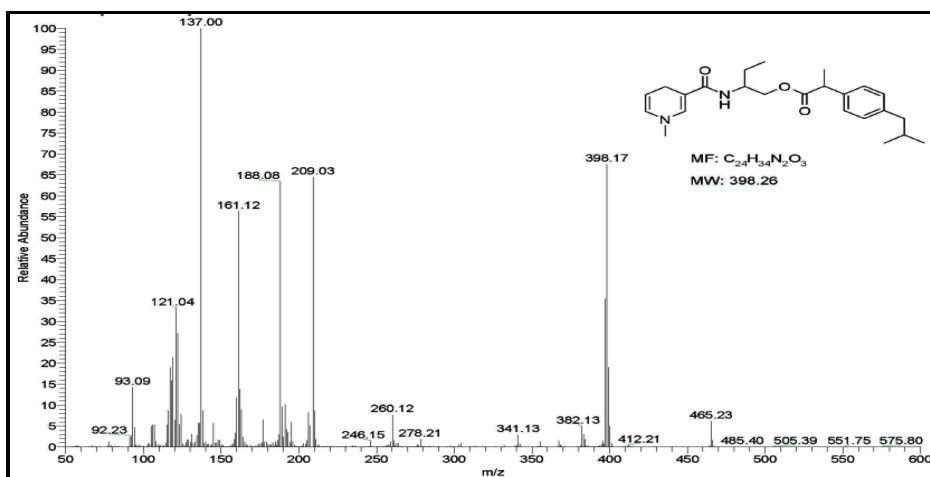

Fig. 3.8: Mass spectrum of **14cI**

Other dihydropyridine derivatives **(14bII-14dIV)** obtained in **Scheme-2** were also found to be unstable and slowly got oxidized or degraded in the same way as shown in **Fig. 3.5**. Out of all these synthesized derivatives three derivatives **(14aII-14aIV)** were having relatively higher stability. These were further characterized and evaluated. The IR spectrum of compound **(14aII)** showed carbonyl stretching of ester and amide groups as sharp intense bands at 1728 cm^{-1} and 1638 cm^{-1} respectively. N-H Stretching of amide was observed at 3330 cm^{-1}.

326

The PMR spectrum of the compound (14aII) showed multiplet at δ 7.64-7.0 for naphthalene protons equivalent to six protons (Ar-H_{k-m}). Singlet at δ 5.22 appeared due to the dihydropyridine proton (-H_b). Another proton of dihydropyridine ring was observed at δ 4.1-4.0 as a multiplet (-H_d) and a peak at δ 3.84 was due to methyl protons present on nitrogen. Its mass spectrum showed peak at 394.31 (M^+).
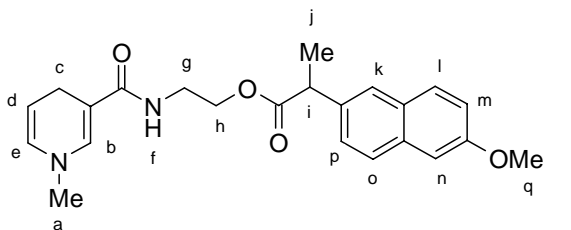
14aII

The IR spectrum of compound (14aIII) showed carbonyl stretching of ester and amide groups as sharp intense bands at 1731 cm^{-1} and 1684 cm^{-1} respectively. N-H Stretching of amide was observed at 3338 cm^{-1}.
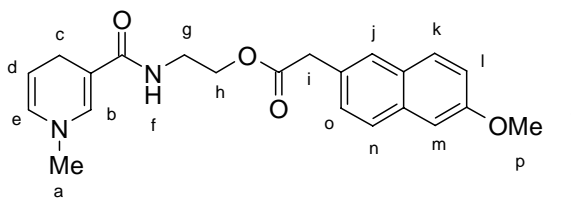
14aIII

The PMR spectrum of the compound (14aIII) showed multiplet at δ 7.64-7.28 for naphthalene protons equivalent to six protons (Ar-H_{j-o}). Singlet at δ 6.83 appeared due to dihydropyridine proton (-H_b) and another proton of dihydropyridine ring was observed at δ 4.42-4.38 as a multiplet (-H_d). Peak at δ 3.67 was due to methyl protons present on nitrogen. Singlet at δ 2.65 appeared due to methylene protons (Ar-CH_2).
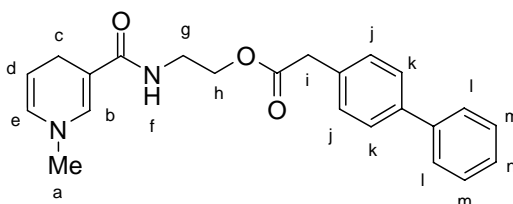
14aIV

The IR spectrum of compound (14aIV) showed carbonyl stretching of ester and amide groups as sharp intense bands at 1734 cm^{-1} and 1679 cm^{-1} respectively. N-H Stretching of amide was observed at 3223 cm^{-1}. The PMR spectrum of the compound (14aIV) showed multiplet at δ 7.52-7.19 for biphenyl protons equivalent to nine protons

(Ar-H_{j-n}). Singlet at δ 6.87 appeared due to dihydropyridine proton (-H_b) and another proton of dihydropyridine ring was observed at δ 5.56-5.54 as a multiplet (-H_d). Singlet at δ 2.65 appeared due to methylene protons (Ar-CH_2). Mass spectrum showed peak at 377.1 (M^+).

3.2 Hydrolyses kinetics study

All the synthesized CDS were evaluated *in vitro* for their stability at 37$\pm$1 °C in buffers of *p*H 2.0 and 7.4 which simulated the *p*H of the stomach and the blood. To get an idea about the enzymatic susceptibility of CDS towards serum esterase, in vitro hydrolyses studies were performed in pooled human serum (80/90 %) at 37$\pm$1 °C for all the CDS. HPLC methods were developed for the determination of half life of disappearance of the prodrugs over a definite period of time. The half life of disappearance of dihydropyridine CDS at various conditions are shown in **Table 3.1**.

Table 3.1: Half lives of disappearance of derivatives at various conditions

Derivative	Half life of disappearance of various CDS (min)		
	*p*H 2.0	*p*H 7.4	Human serum
14aII	12	18	54
14aIII	09	21	41
14aIV	11	14	46

From the above results it could be concluded that dihydropyridine CDS were quite unstable in phosphate buffer *p*H 2 as well as 7.4; the primary route of hydrolysis of these compound may be ester bond cleavage. All the synthesized CDS have undergone enzymatic hydrolysis in human serum to cleave ester bond present in CDS **(14aII-14aIV)**. From the table we can conclude that synthesized CDS were found to be comparatively more stable in human serum than in buffers of *p*H 2.0 and 7.4.

3.3 Biodistribution and gamma imaging studies

The radiolabeling of the compounds with reduced ^{99m}Tc was carried out as per the direct labeling method. The radiolabeling was optimized by taking three factors into account i.e. effect of *p*H on complex formation, incubation time and stannous chloride

concentration. The *in vitro* stability of radiolabeled complexes was tested in human serum and in saline.

Swiss albino mice were used for the biodistribution studies of the ^{99m}Tc-labeled compounds (**14aII-14aIV**). Site specificity of CDS was studied in inflammatory condition. Animals were divided into two groups. **Group-A** (standard) was administered by oral route the parent NSAID **(2I)**. Another group **Group-B** (Test) was administered by oral route the synthesized dihydropyridine CDS, 3 h after induction of inflammation in the rat paw. A 200 µl of the ^{99m}Tc- labeled complex was administered through the oral route in each mouse. Blood was obtained by cardiac puncture at different time intervals, animals (group of three mice for each time interval) were sacrificed, different organs were dissected out, washed with normal saline, made free from adhering tissues, weighed, and the radioactivity measured in a shielded-well gamma scintillation counter. The percent radioactivity for each organ was calculated, and considering 7.3% of the total body weight as whole blood, calculations were performed for determining the radioactivity for whole blood **(Table 3.2 to 3.3).**

Table 3.2: Biodistribution of compound (14aII) in mice

Organ/ Tissue	Percent injected dose/whole organ or tissue (±S.E.M.)	
	1 h	**4 h**
Blood	2.62 ± 0.19	2.08 ± 0.25
Heart	0.63 ± 0.10	0.93 ± 0.21
Lung	0.42 ± 0.09	0.38 ± 0.10
Liver	4.23 ± 0.34	10.47 ± 0.46
Spleen	0.68 ± 0.24	0.73 ± 0.29
Kidney	0.31 ± 0.08	0.34 ± 0.09
Intestine	4.61 ± 0.55	10.87± 1.45
Stomach	24.50 ± 3.25	17.33 ± 3.25

From the results obtained it could be conclude that stomach is the target site for dihydropyridine derivatives and free ^{99m}Tc in the body. The dihydropyridine derivatives may get converted to their water addition product and hence accumulate in stomach or passed in to intestine. The results of the biodistribution studies suggest that major fraction of the drugs is present in stomach or intestine and this may be due to oxidation of dihydropyridine ring to quaternary derivatives and or water addition product which will not be absorbed in to systemic circulation. Further, high radioactivity in stomach may be

due to instability of complexes of compounds (**14aII**) *in vivo* in stomach at pH 2.0. But the free NSAID **(2I)** gets absorbed from the stomach to a very high extent.

Table 3.3: Biodistribution of compound (14aIII) in mice

Organ/ Tissue	Percent injected dose / whole organ or tissue (±S.E.M.)	
	1 h	4 h
Blood	3.55 ± 0.21	2.37 ± 0.45
Heart	1.22 ± 0.15	1.17 ± 0.31
Lung	0.66 ± 0.11	0.48 ± 0.14
Liver	6.41 ± 0.36	16.98 ± 0.54
Spleen	0.71 ± 0.28	0.79 ± 0.22
Kidney	0.44 ± 0.12	0.54 ± 0.11
Intestine	5.23 ± 0.84	11.57± 2.45
Stomach	27.78 ± 2.89	12.10 ± 4.12

Table 3.4: Biodistribution of compound (2I) in mice

Organ/ Tissue	Percent injected dose / whole organ or tissue (±S.E.M.)	
	1 h	4 h
Blood	8.01 ± 0.18	2.34 ± 0.05
Heart	0.11 ± 0.02	0.08 ± 0.01
Lung	0.93 ± 0.12	0.54 ± 0.07
Liver	19.66 ± 1.21	15.98 ± 0.85
Spleen	2.55 ± 0.33	1.56 ± 0.13
Kidney	1.08 ± 0.14	1.09 ± 0.19
Intestine	0.82 ± 0.15	1.39 ± 0.12
Stomach	0.36 ± 0.003	0.15 ± 0.09

It could be concluded from the biodistribution studies that the designed CDS are not suitable for oral administration as these are not properly absorbed from the GIT, may be due to their fast conversion to various oxidation products which are not absorbed through oral route.

4. Experimental

The experimental work has been divided into three parts:

4.1. Chemical studies

4.2. Hydrolyses kinetics

4.3. Radiolabeling studies

4.1 Chemical studies

HPLC analysis was performed using Shimadzu prominence system (Kyoto, Japan) consisting of LC-20AT Pump, and SPD 20 A detector. The chromatographic column used was phenomenex C-18, 250 mm length X 4.6 mm diameter with 0.5 μ particle size and Column temperature was maintained at 25-28 °C. Separation of analytes was performed under isocratic conditions at a flow-rate of 0.5-1.0 ml/min. The mobile phase consisted of phosphate buffer (PB, 15mm)-acetonitrile. Chromatographic separations were performed on columns using silica gel 100–200 mesh and neutral alumina, activity grade I. All reagents used were of analytical reagent grade obtained from S. d. fine chemicals, Spectrochem, Qualigens and Sigma-Aldrich.

HPLC methods were developed for the determination of half life of disappearance of a prodrug over a definite period of time. The solutions and the buffers used in the study were prepared in triple distilled water. The buffers used were prepared according to the procedure as given in USP-2007. All the chemicals used were of analytical reagent grade. Anhydrous sodium sulphate was used as drying agent wherever required for the drying of organic solutions.

4.1.1. 2-(4-Isobutylphenyl)-*N*-(3-pyridinyl)propanamide (3)

Ibuprofen **(2I)** (2.41 g, 11.70 mM) and EDC (2.43 g, 12.77 mM) in dry dichloromethane (25ml) were stirred in an ice-bath at 0-5 °C. 3-Aminopyridine **(1)** (1 g, 10.64mM) dissolved in dry DCM (20 ml) was added drop-wise in to the above solution over a period of 10-15 min under stirring and the reaction mixture was stirred further for 6-8 h at room temperature. Glacial acetic acid (2-3 ml, 10 %) was added in to the reaction mixture and the stirring continued for further 30 min. The resulting reaction mixture was filtered through cotton and the filtrate washed twice with water, sodium carbonate solution (2 x 20 ml, 5%) and finally with water again (3 x 20 ml). The organic layer was separated and dried over sodium sulfate filtered and the solvent removed to get pure white colored oil. (2.4 g, 80 %).

Anal.:

TLC : R_f 0.71 (Chloroform: Methanol; 1:0.3)

UV (MeOH) : 221 nm

IR (Neat, cm^{-1}): 3282, 1693, 1167 and 802

MS (m/z) : 282.28 (M+1)

4.1.2. 3-[2-(4-Isobutylphenyl)propanamido]-*N*-methylpyridinium iodide (4)

2-(4-Isobutylphenyl)-*N*-(3-pyridinyl)propanamide **(3)** (1 g, 3.54 mM) was dissolved in to di-isopropyl ether (30 ml) and excess methyl iodide was added and the reaction mixture refluxed for 2 h. The solvent and excess reagent were removed to get a yellow residue which was crystallized using a mixture of water and methanol to get yellow crystals of the salt **(4)**, (1.2 g, 79.81 %, m.p. 166-168 ^{0}C)

Anal.:

TLC : R_f 0.61 (Chloroform: Methanol; 1:0.3)

UV (MeOH) : 220 nm

IR (Neat, cm^{-1}): 3453, 1704, 1627, 1174 and 750

PMR (CDCl$_3$): δ 10.88 (s, 1H, Ar-*H*), 9.75 (s, 1H, N*H*), 9.07-9.04 (d, 1H, Ar-*H*), 8.31-8.29 (d, 1H, Ar-*H*), 7.63-7.59 (t, 1H, Ar-*H*), 7.51-7.49 (d, 2H, Ar-C*H$_2$*), 7.10-7.08 (d, 2H, Ar-C*H$_2$*), 4.36-4.30 (q, 4H, -C*H$_3$*, CH), 2.41-2.39 (d, 2H, -C*H$_2$*), 1.83-1.77 (m, 1H -C*H*), 1.54-1.53 (d, 3H, -C*H$_3$*) and 0.87-0.85 (6H, d, (C*H$_3$*)$_2$)

MS (m/z) : 297.1 (M$^+$)

4.1.3. *N*-(1,2,5,6-Tetrahydro-1-methylpyridin-3-yl)-2-(4-isobutylphenyl)propanamide (6)

To a stirred ice cold solution of 3-[2-(4-isobutylphenyl)propanamido]-*N*-methylpyridinium iodide **(4)** (0.1 g, 0.23 mM) in demineralsed and degassed water (60 ml) under nitrogen purging was added potassium hydroxide (0.026 g, 0.47 mM) followed by sodium borohydride (0.009 g, 0.23 mM) . The mixture was stirred under nitrogen for 30 min at 0 ^{0}C maintaining the *p*H in alkaline range. Aqueous layer was extracted with degassed and cold ethyl acetate (3 x 20 ml) and the organic layer washed with cold demineralised water (3 x 20 ml) and dried over sodium sulphate. The solution was filtered through cotton and solvent removed under reduced pressure to give reduction product **(6)**

as white solid, which was further crystallized from ether to give a white solid. (0.046 g, 65.44 %, m.p. 114-116 ^{0}C)

Anal.:

TLC : R_f 0.61 (Chloroform: Methanol; 1:1)

UV (MeOH) : 220 nm

IR (Neat, cm^{-1}): 3505, 1665 and 835

PMR (CDCl$_3$): δ 7.19-7.17 (d, 2H, Ar-C*H*), 7.13-7.11 (d, 2H, Ar-C*H*), 6.23 (s, 1H, N*H*), 5.78 (s, 1H, -C*H*, cyclic), 3.56-3.51 (q, 1H, -C*H*), 2.98 (s, 2H, -C*H*$_2$, cyclic), 2.48-2.45 (t, 4H, (-C*H*$_2$)$_2$), 2.33 (s, 3H, -C*H*$_3$), 2.24-2.19 (d, 2H,-C*H*$_2$), 1.88-1.81 (m, 1H, -C*H*), 1.51-1.49 (d, 3H,-C*H*$_3$) and 0.90-0.89 (d, 6H, (C*H*$_3$)$_2$)

MS (m/z) : 301.1 (M$^+$)

4.1.4. 2-(1, 4-Dihydro-1-methylpyridine-3-carboxamido)ethyl 2-(4-isobutylphenyl) propanoate (14aI)

To a stirred ice cold solution of **13aI** (0.5 g, 1.0 mM) in demineralised and degassed water (60 ml) under nitrogen purging was added sodium bicarbonate (0.5 g, 6.0 mM) followed by sodium dithionite (0.88 g, 0.54 mM). The mixture was stirred under nitrogen for 20-30 min at 0-2 ^{0}C maintaining the *p*H at approximately 7 by addition of sodium bicarbonate. The aqueous layer was extracted with degassed and cold dichloromethane (3 x 20 ml) and the organic layer washed with cold demineralised water (3 x 20 ml) and dried over sodium sulphate. The solution was filtered through cotton and solvent removed under reduced pressure to give dihydropyridine derivative **(14aI)** as a yellowish semisolid. (0.25 g, 67.02 %)

Anal.:

TLC : R_f 0.78 (Chloroform: Methanol; 1:0.1)

UV (MeOH) : 221 nm

IR (Neat, cm^{-1}): 3316, 1730, 1645 and 1161

MS (m/z) : 370 (M$^+$)

4.1.5. 2-(1, 4-Dihydro-1-methylpyridine-3-carboxamido)ethyl 2-(6-methoxy-2-naphthyl)propanoate (14aII)

To a stirred solution of **13aII** (0.39 g, 0.75 mM) in demineralised and degassed water (150 ml) under nitrogen purging was added sodium bicarbonate (0.31 g, 3.75 mM) followed by sodium dithionite (0.39 g, 2.24 mM). The reaction was continued under

nitrogen for 20-30 min at RT. Then aqueous layer was extracted with degassed and cold dichloromethane or ether (3 x 20 ml) and the organic layer washed with cold demineralised water (3 x 20 ml) and dried over magnesium sulphate. The solution was filtered through Whatman filter and solvent removed under reduced pressure to give dihydropyridine derivative as a yellowish semisolid. The semisolid was further rinsed with ether and the solvent removed to get yellow oil which on standing got converted to yellow solid which was further purified by column chromatography to give dihydropyridine derivative **(14aII)** as a yellow semisolid. (0.20 g, 67.10 %).

Anal.:

TLC : R_f 0.78 (Chloroform: Methanol; 1:0.1)

UV (MeOH) : 221 nm

IR (Neat, cm^{-1}): 3316, 1728, 1638 and 1158

PMR (CDCl$_3$) : δ 7.64-7.0 (m, 6H, Ar-H), 5.22 (s, 1H, dihydropyridine-H_2), 4.1-4.0 (m, 2H, dihydropyridine-H_5, NH), 3.84-3.75 (m, 4H, N-CH_3), 3.43-3.36 (m, 3H, dihydropyridine-H_4), 2.94-2.73 (m, 3H, -CH_3), 2.0-1.97 (m, 2H, O-CH_2), 1.52-1.44 (m, 4H, O-CH_3, dihydropyridine-H_6) and 1.2-1.1 (q, 1H, -CH)

MS (m/z) : 394.31 (M$^+$)

4.1.6. 2-(1, 4-Dihydro-1-methylpyridine-3-carboxamido)ethyl 2-(6-methoxy-2-naphthyl)acetate (14aIII)

To a stirred solution of **13aIII** (0.50 g, 0.98 mM) in acetonitrile (5 ml) and demineralised and degassed water (150 ml) under nitrogen purging was added sodium bicarbonate (0.41 g, 4.90 mM) followed by sodium dithionite (0.51 g, 2.96 mM). The reaction was continued under nitrogen for 20-30 min at RT. Then aqueous layer was extracted with degassed and cold dichloromethane or ether (3 x 20 ml) and the organic layer washed with cold demineralised water (3 x 20 ml) and dried over magnesium sulphate. The solution was filtered through Whatman filter and solvent removed under reduced pressure to give dihydropyridine derivative **(14aIII)** as a yellowish semisolid. (0.25 g, 66.53 %)

Anal.:

TLC : R_f 0.78 (Chloroform: Methanol; 1:0.1)

UV (MeOH) : 221 nm

IR (Neat, cm^{-1}): 3338, 1731, 1684, 1168 and 852

PMR (CDCl$_3$): δ 7.64-7.28 (m, 6H, Ar-H), 6.83 (bs, 1H, dihydropyridine-H_2), 5.52-5.55 (d, 1H, dihydropyridine-H_6), 5.12 (bs, 1H, NH), 4.38-4.42 (m, 1H, dihydropyridine-H_5), 4.12-4.15 (m, 2H, dihydropyridine-H_5), 3.81-3.82 (m, 2H, N-CH_2), 3.83-3.84 (m, 2H, -CH_2), 3.66-3.67 (s, 3H, O-CH_3), 3.46-3.50 (m, 2H, O-CH_2), 2.81 (s, 3H, N-CH_3) and 2.64 (s, 2H, Ar-CH_2)

4.1.7. 2-(1, 4-Dihydro-1-methylpyridine-3-carboxamido)ethyl 4-biphenylacetate (14aIV)

To a stirred solution of **13aIV** (0.5 g, 0.99 mM) in acetonitrile (2-3 ml) and demineralsed and degassed water (150 ml) under nitrogen purging was added sodium bicarbonate (0.41, 4.90 mM) and sodium dithionite (0.51 g, 2.98 mM) once at a time. The reaction was continued under nitrogen for 30 min at RT. The aqueous layer was extracted with degassed and cold ethyl acetate (3 x 20 ml) and the organic layer washed with cold demineralised water (2 x 20 ml) and dried over magnesium sulphate. The solution was filtered through Whatman filter and solvent removed under reduced pressure to give dihydropyridine derivative **(14aIV)** as a yellowish solid (0.30 g, 80.15 %).

Anal.:

TLC : R$_f$ 0.71 (Chloroform: Methanol; 1:0.1)

UV (MeOH) : 221 nm

IR (Neat, cm^{-1}): 3060, 1734, 1679, 835 and 753

PMR (CDCl$_3$): δ 7.52-7.19 (m, 9H, biphenyl-H), 6.87 (s, 1H, dihydropyridine-H_2), 5.56-5.54 (d, 1H, dihydropyridine-H_6), 5.21 (bs, 1H, NH), 4.50-4.47 (m, 1H, dihydropyridine-H_5), 4.33 (s, 2H, dihydropyridine-H_4), 4.17-4.15 (m, 3H, N-CH_3), 3.69-3.63 (t, 2H, O-CH_2), 3.53-3.51 (m, 2H, N-CH_2) and 2.85 (s, 2H, Ar-CH_2)

MS (m/z) : 377.1 (M$^+$)

4.2 Hydrolyses kinetics

All the synthesized CDS were evaluated *in vitro* for their stability at 37±1 °C in buffers of *p*H 2.0 and 7.4 which simulated the *p*H of the stomach and the blood. To get an idea about the enzymatic susceptibility of CDS towards serum esterases, *in vitro* hydrolyses studies were performed in pooled human serum (80/90 %) at 37±1 °C for all

the CDS. HPLC methods were developed for the determination of half life of disappearance of the prodrugs over a definite period of time.

Solutions and Buffers

1. Sodium hydroxide (0.2 M): Sodium hydroxide (0.8 g) was dissolved in distilled water and the volume made to 100 ml with distilled water.

2. Phosphate buffer (0.2 M): Potassium dihydrogen phosphate (2.722 g) was diossolved in water and made the volume up to 100 ml with distilled water.

3. Potassium chloride (0.2 M): Potassium chloride (1.491 g) was dissolved in distilled water and diluted to 100 ml.

4. Hydrochloric acid (0.2 N): Concentrated hydrochloric acid (1.7 ml) was diluted to 100 ml in a standard volumetric flask with distilled water.

5. Phosphate buffer *p*H 7.4: Potassium dihydrogen phosphate solution (0.2 M, 50 ml) was placed in a 200 ml volumetric flask and sodium hydroxide solution (0.2 M, 39.1 ml) added and the volume made up to 200 ml with distilled water.

6. Hydrochloric acid buffer *p*H 2.0: Potassium chloride solution (0.2 M, 50 ml) was placed in a 200 ml volumetric flask and hydrochloric acid (0.2 N, 13 ml) was added and the volume made with distilled water up to 200 ml.

Chromatographic conditions

Chromatography was performed under isocratic conditions, at a flow-rate of 0.75 ml/min. The mobile phase consisted of phosphate buffer (15 mM): acetonitrile (8:2). The solution was filtered through Whatman filter paper (0.2 μ) and degassed for 10 min in an ultrasonic bath. The column effluent was monitored at respective λmax. An aliquot of sample solution (20 μl) was injected onto the analytical column with a manual injection.

Calibration

An aliquot (20 μl) of each solution was then injected into the analytical column. All the measurements were performed in duplicate for each concentration The peak areas were measured and plotted against the respective concentration of the derivatives. Least square linear regression analysis was used to determine the slope, *y*-intercept and the correlation coefficients of the standard plots.

4.3 Radiolabeling studies

Swiss albino mice (a group of 3 animals for each time interval) were used for the biodistribution studies of the ^{99m}Tc-labeled compounds. The ^{99m}Tc-labeled complex (0.2 ml), prepared as described above, was administered through oral route to each mouse. At different time intervals (1 h and 4 h) the animals (group of three mice for each time interval) were anaesthetized and the blood obtained by cardiac puncture.

Blood was weighed and radioactivity measured in the gamma counter for each sample. The animals were sacrificed and tissues (heart, lung, liver, spleen, kidney, stomach and intestine) were dissected, washed with normal saline, made free from adhering tissues, weighed and their radioactivity measured. To correct for physical decay and to calculate radiopharmaceutical uptake in each organ as a fraction of the injected dose (% activity), aliquots (2.0 ul) of the complex solution, containing 2 % of the injected dose, were counted simultaneously at each time point. The percent activity for the whole organs and whole blood was determined for each time interval. The above described procedure was followed for studying the biodistribution of the complexes of compounds (**14aII-14aIII**).

References

1. Bundgaard H., The Double Prodrug Concept and its Applications. *Adv. Drug Deliv. Rev.*, **1989**, 3, 39-65.

2. Halen P.K., Murumkar P.R., Giridhar R. and Yadav MR., Prodrug Designing of NSAIDs *Mini-Reviews in Medicinal Chemistry*, 2009, 9, 124-39

3. Khursheed A. and Lloyd J.R., Distribution of hexamethonium and other quaternary ammonium compounds in cartilage. *J. Pharmacol. Exp. Ther.* **1971**, 176, 83-92

4. Giraud I., Rapp M., Maurizis J.C. and Madelmont J.C., Application to a Cartilage Targeting Strategy Synthesis and in Vivo Biodistribution of ^{14}C-Labeled Quaternary Ammonium-Glucosamine Conjugates. *Bioconjugate Chem.* **2000**, 11, 212-18

5. Brahmankar D.M. and Jaiswal S.B., Biopharmaceutics and Pharmacokinetics a Treatise, Chapter: 2 Absorption of Drugs, Vallabh Prakashan, Delhi. First edition. **1995,** 5-75

6. Higuchi T. and Wagner J.G., "Biopharmaceutics and Relevant Pharmacokinetics",. Drug Intelligence Publication, Hamilton. III, **1971,** 28.

7. Levine R.R. and Pelkin E.W., The influence of experimental procedures and dose on the intestinal absorption of an onium compound, benzomethamine. *J. Pharmacol. Exp. Ther.* **1961**, 131, 319-27

8. Levine R.R. and Spencer A.F., Effect of a phosphatido-peptide fraction of intestinal tissue on the intestinal absorption of a quaternary ammonium compound. *Biochem. Pharmacol.* **1961**, 8, 248-50

9. Roberts L.J. and Morrow J.D., In the Pharmacological Basis of Therapeutics, 9th edition, MC Graw hill, New York. **1996,** 617

10. Robert K.M., Daryl K.G., Peter A.M. and Victor W.R., Biological oxidation. Harpers illustrated Biochemistry, Lange Medical Books/McGraw-Hill New York, Twenty sixth edition, **2000**, chapter-2. 86-91

11. Bodor N., Shek E. and Higuchi T., Improved delivery through biological membranes. Synthesis and properties of 1-methyl-1, 6-dihydropyridine-2-carbaldoxime a pro-drug of N-methylpyridinium-2-carbaldoxime chloride. *J. Med. Chem.* **1976**, 19, 102-107

12. Zilong T. and Joelle M., Synthesis of piperidine derivatives by reduction of pyridinium salts. *Synthetic communications.* **2007**, 37, 3367

13. Kwanghee K.P., et.al. Reduction of N-aryl pyridinium compounds by sodium borohydride and dithionite. *Bull. Korean Chem. Soc*. **1986**, 7, 201

14. Lavilla R., Bernabeu M.C., Brillas E., Carranco I., Díaz J.L., Llorente N., Rayo M. and Spada A., Productive trapping of NAD type radicals. Non-biomimetic reduction of pyridinium salts. *Chem. Commun.* **2002**, 850-51

15. Michael J.P., Improved Delivery through biological membranes XXXVII. Synthesis and stability of novel redox derivatives of Naproxen and Indomethacin. *Pharmaceutical Res.* **1989**, 6, 667

16. Anderson A.G. and Berkelhammer G., "A study of the primary acid reaction on model compounds of reduced diphosphopyridine nucleotide", *J. Am. Chem. Soc.* **1985**, 80, 992–99.

17. Bodor N. and Kaminski J.J., "Correlation between hydride transfer and one-electron oxidation of dihydropyridines and heterocycles" *J. Mol. Struct. (Theochem)*, **1988**, 163, 315-30.

18. Jordan F., "Direct determination of C-protonation and hydrolysis rates in enamines application to ethyl cyanomethylaminocrotonate" *J. Am. Chem. Soc.* **1974**, 96, 825-28.

19. Bodor N., Farag H.H., Barros M.D., Wu W.M. and Buchwald P., *In Vitro* and *In Vivo* Evaluations of Dihydroquinoline and Dihydroisoquinoline-based Targetor Moieties for Brain-specific Chemical Delivery Systems. *Journal of Drug Targeting* **2002**, 10, 63-71

20. Delmas P.D., Biochemical markers of bone turnover in Paget's disease of bone. *J. Bone Miner. Res. 1999,* 14, 66-69

21. Dewar M.J.S., Zoebisch E.G., Healy, E.F. and Stewart J.J.P., "AM1: a new general purpose quantum mechanical molecular model", *J. Am. Chem. Soc.* **1985**,107, 3902–3909.

22. Pop E., Brewster M.E., Huang M.J. and Bodor N., "Substituent effects on the stability of 1,4-dihydropyridines" *J. Mol. Struct. (Theochem)*, **1995**, 337, 49-55

SUMMARY AND CONCLUSION

Summary and Conclusion

Arthritis is a group of conditions involving damage to the <u>joints</u> of the body. Rheumatic diseases are estimated to affect up to 1.1 % of world's population and these patients are often treated with steroids, NSAIDs, DMARDs and/or immunosuppressive drugs. Currently available therapy for the arthritis focuses on reducing inflammation of the joints with NSAIDs and steroids.

After studying the various options for the treatment of arthritis it was felt that it should be possible to deliver therapeutic agents with improved therapeutic efficacy, longer duration of action with minimal side effects which is very essential in chronic diseases such as arthritis. It was planned to adopt the following four strategies to achieve the above defined goals:

5. Intra-Articular Chemical Delivery Systems (IA-CDS)
6. Percutaneous Drug Delivery Systems (PDDS)
7. Intra-Articular Liposomal Drug Delivery Systems (IA-LDDS)
8. Oral Drug Delivery Systems (ODDS)

1. Intra-Articular Chemical Delivery Systems (IA-CDS)

Literature survey revealed that a drug in solution form is rapidly expelled from the joint cavity upon IA administration; so various drug delivery systems such as suspensions, liposomes, microspheres etc. have been developed and tested but till date no drug delivery system having longer duration of action without side effects has been developed. Hence there is a need to develop delivery system with improved drug residence time in joints on IA administration. CDS of various NSAIDs have been designed, synthesized and evaluated as shown below:
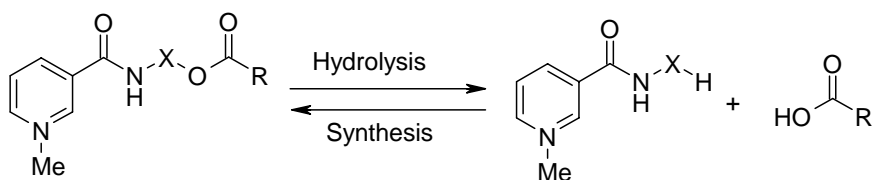
From the obtained data it is clear that the synthesized CDS **(7aI-7gV)** showed high retention time in joints after IA administration as compared to the parent drug **(5IV)**. Further, radioactivity obtained for the synthesized CDS after 24h was about 4 times higher in Region of Interest (ROI) compared to the parent drug.
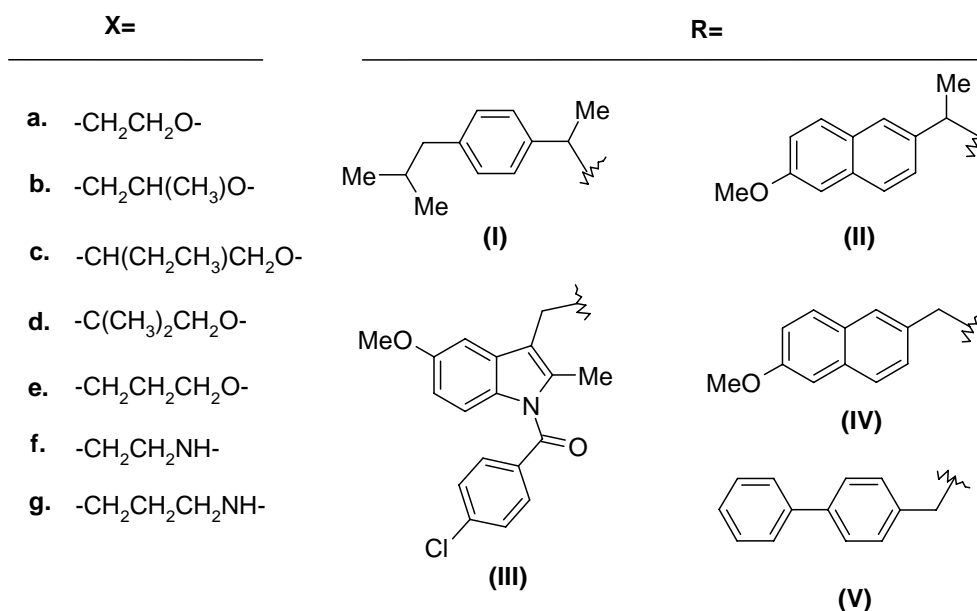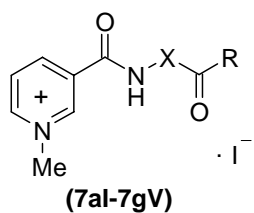
(7aI-7gV)

| X=		R=
a.	-CH$_2$CH$_2$O-	
b.	-CH$_2$CH(CH$_3$)O-	
c.	-CH(CH$_2$CH$_3$)CH$_2$O-	
d.	-C(CH$_3$)$_2$CH$_2$O-	
e.	-CH$_2$CH$_2$CH$_2$O-	
f.	-CH$_2$CH$_2$NH-	
g.	-CH$_2$CH$_2$CH$_2$NH-	

So, it can be concluded that cationic molecules are retained for a longer period of time in joint cavity by ionic interaction and hence in the initial phase we can extend residence time of the drug by these CDS.

2. Percutaneous Drug Delivery Systems (PDDS)

The bioavailability of topically applied NSAIDs is only up to 1-2 % in humans. To improve the percutaneous delivery of NSAIDs the usefulness of the salt formation and prodrug approach for NSAIDs has been evaluated.

Amongst all of the synthesized salts of NSAIDs, the ethanolamine salts of MNA and BPA **(18b, 19b)** displayed 9-10 times higher flux than the parent NSAIDs. The result also showed that salts with higher flux have a balance between solubility and partition coefficient. Further, except for sodium salt all the salts have shown lower melting points than the parent drugs and higher permeability through the skin, which support previous reports indicating that a decrease in melting point or conversion of solid state to liquid state improves the permeability of drugs through skin.

MeO—[naphthalene]—CH₂COO⁻ X⁺

(18a-18e)

[biphenyl]—CH₂COO⁻ X⁺

(19a-19e)

$X^+ =$
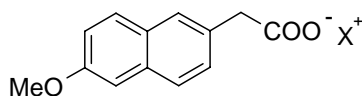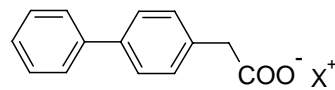
a. Na^+
b. H_3N-CH_2CH_2OH
c. $H_2N(CH_2CH_2OH)_2$
d. $HN(CH_2CH_2OH)_3$
e. $H_2N(CH_2CH_3)_2$

In case of prodrugs the diffusion experiments showed that both 6-MNA and its prodrugs were able to permeate rat abdominal skin *in vitro*. The steady-state flux (*J*ss) of prodrugs showed higher flux values than the parent NSAID.
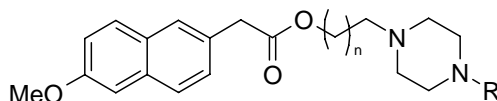
R=

a= -CH₃
b= -CH₂CH₃
c= -COCH₃
d= -Phenyl

(25a-25d): n=1
(26a-26d): n=2

Among all of the prodrugs, prodrug **(26b)** has exhibited the highest steady state flux while **25b** the lowest. Prodrugs **(25a** and **26a)** have shown intermediate flux values but still both the values were 5-fold and 7-fold higher than the parent NSAIDs. Prodrug **(26b)** having the highest flux was 12-fold higher than the parent NSAID. The result indicated that lipophilic piperazinyl prodrugs with adequate aqueous solubility increased the flux of 6-MNA.

3. Intra-Articular Liposomal Drug Delivery Systems (IA-LDDS)

Another objective of the present work was to develop cationic liposomal formulations of NSAIDs having long half life, selectivity towards COX-II enzyme and affinity towards joint cavity producing less gastrointestinal side effects.
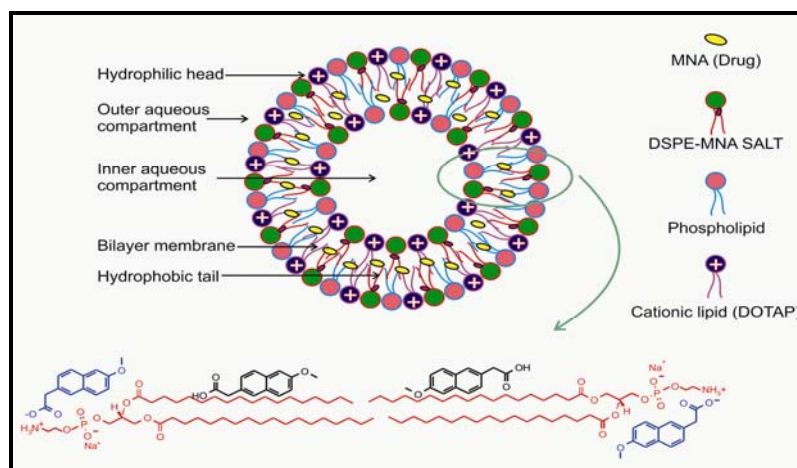
The encapsulation of an NSAID possessing all these ideal features into liposomes with further modifications of liposomal properties such as size, lammelarity, charge etc. could improve the overall therapeutic efficacy of the agent after IA injection in patients with OA. As shown in the above figure cationic liposomes were prepared and evaluated.

From the obtained data it was clear that liposomes showed higher retention in joints after IA administration as compared to the parent drug and the quaternary ammonium chemical delivery system. Further, radioactivity obtained for the prepared liposomes after 24 h was about 5 times higher in ROI compared to the parent drug. So it could be concluded that liposomal drug delivery systems having cationic charge are retained for a longer period of time in joint cavity by ionic interaction. Hence residence time of the drug in the joint can be extended by these drug delivery systems. Moreover, sustained release of the drug will give anti-inflammatory effect for still longer duration reducing frequency of administration of IA injections.

4. Oral Drug Delivery Systems (ODDS)

It was evident from the literature that a cationic molecule possesses higher affinity towards cartilage tissue. But such molecules show poor bioavailability on oral administration. Hence it was planned to convert the conventional NSAIDs into neutral chemical delivery systems which could be easily absorbed from the GIT.

Once the CDS enters into the systemic circulation it should be metabolized/converted into a cationic species. The designed CDS was synthesized and evaluated. From the results it could be concluded that dihydropyridine CDS were quite unstable in phosphate buffer pH 2 as well as 7.4; the primary route of hydrolysis of these

compounds was ester bond cleavage. All the synthesized CDS have undergone enzymatic hydrolysis in human serum to cleave the ester bond present in CDS.
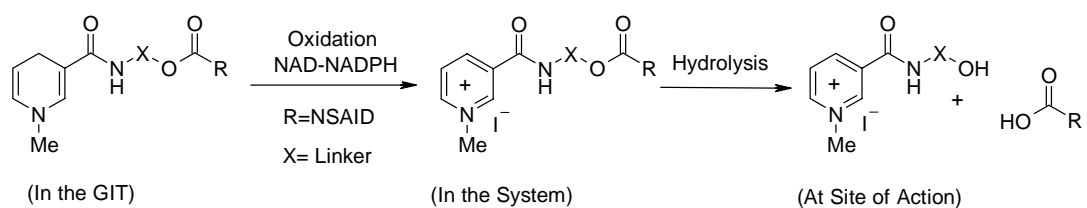
Further, it could be concluded that the synthesized CDS were found to be comparatively more stable in human serum than in buffer of *p*H 2.0 and 7.4. It may be due to protonation of dihydropyridine ring which might stabilize the dihydropyridine ring. Biodistribution studies clearly indicated that the designed dihydropyridine CDS were not suitable for oral administration as these were not properly absorbed from the GIT, may be due to their fast conversion to various oxidation products which were not absorbed through oral route.